10 August 2007 | $10

Science

Attosecond SPECTROSCOPY

AAAS

Same people. Same support. New possibilities.

If you work with proteins, you've relied on Pierce reagents. For gene silencing, you've depended on Dharmacon innovations. In cell culture, HyClone is likely a good friend. For PCR, ABgene has helped you along the way. And for high content screening, you've trusted Cellomics and BioImage.

Now these top names in life science are sold under the Thermo Scientific brand. You'll still find the same technical support and application expertise that you've come to expect. Only now, we can develop new ways to integrate technologies to accelerate and improve your results even further.

So yes, there's a new brand name – Thermo Scientific. But you can keep your trusted relationships and high level of service as we unite to help you pursue new possibilities.

Moving science forward

Learn more at www.thermo.com/LSR.

Part of Thermo Fisher Scientific

Thermo SCIENTIFIC

What if staying up to date with the latest technology published in journals and patents were as easy as pushing a button?

It is.

With the "Keep Me Posted" alerting feature, SciFinder sends you automatic updates on areas you—and your competitors—are interested in.

You can monitor specific research topics, companies, authors, substances, or sequences, and choose how frequently you receive notifications: daily, monthly, or weekly.

The service isn't just convenient, it's incredibly current. Journal article records often appear in SciFinder before they're even in print. New references, substances, and sequences are added daily. Patents from all the major offices are added within two days of issuance.

As with all SciFinder features, Keep Me Posted is integrated with your workflow. At any point in a search (including the beginning), simply click on the Keep Me Posted button. SciFinder tracks your steps and will generate the appropriate alert—even for complex topics. When you receive a notification, you can follow each reference as you would in a search: find citing or cited articles (with links to the electronic full text), and follow referenced substances and reactions for further information.

Comprehensive, intuitive, seamless—SciFinder doesn't just alert you, it's part of the process. To find out more, call us at 800-753-4227 (North America) or 614-447-3700 (worldwide) or visit www.cas.org/SCIFINDER.

SciFinder®

Part of the process.™

GE Healthcare

Drop. Measure. Done.

NanoVue, the easy-to-use spectrophotometer.

The new NanoVue™ spectrophotometer, with its special "drop and measure" feature, couldn't be any easier to use in getting accurate results for DNA, RNA, oligos, and proteins.

NanoVue allows sensitive measurements of very small (< 2 µl) samples. Simply pipette onto the sample plate, and in 3 seconds you'll have your results. NanoVue also offers quick and easy cleaning, which reduces the risk of cross-contamination.

Through innovations that save time and make your research easier, we're bringing science to life. We call it **Life Science Re-imagined.**

Be one of the first to experience NanoVue for yourself, register for a trial at:
www.gelifesciences.com/tryNanoVue

imagination at work

Volume 317, Issue 5839

COVER

An array of multilayer mirrors compresses ultrabroadband laser pulses (orange beam) to 1.5 wave cycles. The attosecond x-ray pulses produced with them allow the control and real-time observation of atomic-scale electron motion. See the special section on attosecond spectroscopy beginning on page 765.

Photo: Thorsten Naeser for Max Planck Institute for Quantum Optics/Laboratory for Attosecond and High-Field Physics

DEPARTMENTS

EDITORIAL

SPECIAL SECTION

Attosecond Spectroscopy

INTRODUCTION

PERSPECTIVES

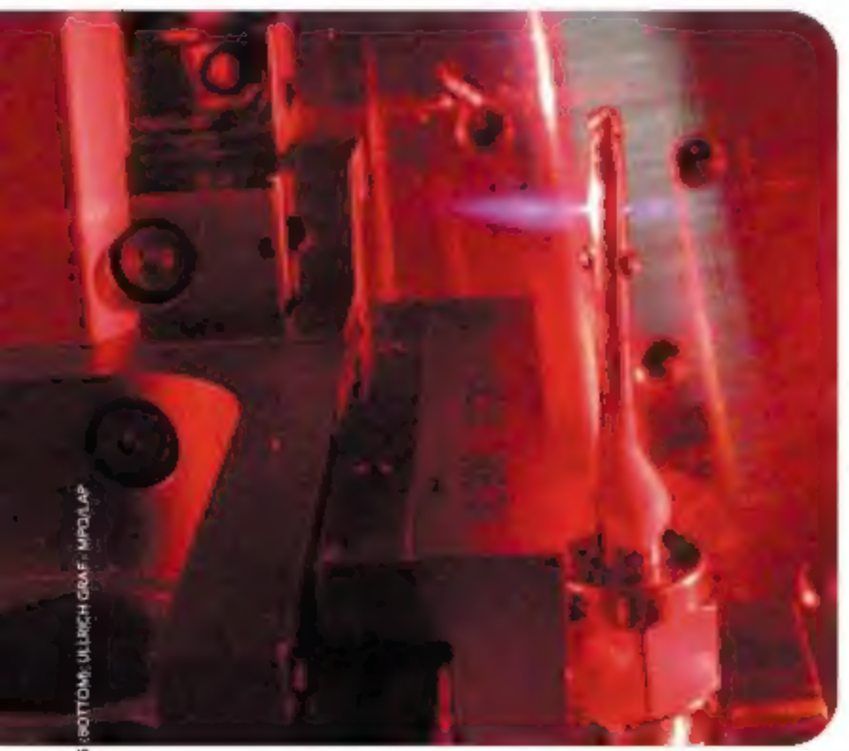

CREDITS: (BOTTOM) ULRICH GRAF, MPQ/LAP

NEWS OF THE WEEK

NEWS FOCUS

CONTENTS continued >>


HEALTH & FAMIL
Life Expectancy Reaches 126
of advanc
The future l
Someday, researchers will fully unravel the genetic mysteries that define human life. When that day arrives, we hope to have played a part. To learn about scientists making significant discoveries today, visit www.promega.com/today
TODAY COULD BE THE DAY.
Promega
©2007 Promega Corporation

Science

SCIENCE EXPRESS

www.sciencexpress.org

ECOLOGY

Land-Use Allocation Protects the Peruvian Amazon
P. J. C. Oliveira et al.
Fine-scale satellite monitoring of deforestation and logging in Peruvian rainforest suggests that land-use and conservation policies are effective in reducing forest losses.
10.1126/science.1146324

NEUROSCIENCE

BREVIA: Leptin Regulates Striatal Regions and Human Eating Behavior
I. S. Farooqi, E. Bullmore, J. Keogh, J. Gillard, S. O'Rahilly, P. C. Fletcher
A brain-imaging study of two leptin-deficient individuals suggests that this appetite-suppressing hormone acts to diminish the perception of food's rewarding properties.
10.1126/science.1144599

GENETICS

Common Sequence Variants in the *LOXL1* Gene Confer Susceptibility to Exfoliation Glaucoma
G. Thorleifsson et al.
A genome-wide study reveals that a syndrome that is found in 10 to 20 percent of the world's population over 60 and leads to a form of glaucoma is associated with variation in a gene that modifies elastin fibers.
>> *News story p. 735*
10.1126/science.1146554

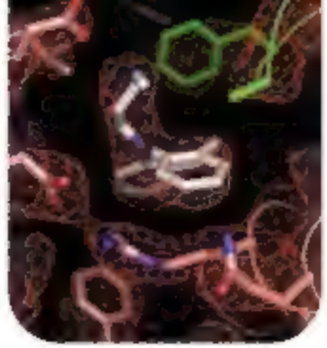

STRUCTURAL BIOLOGY

LeuT-Desipramine Structure Reveals How Antidepressants Block Neurotransmitter Reuptake
Z. Zhou et al.
The structure of an antidepressant drug bound to a bacterial transporter reveals how these drugs may work on neurotransmitter transporters in humans.
10.1126/science.1147614

CLIMATE CHANGE

20th-Century Industrial Black Carbon Emissions Altered Arctic Climate Forcing
J. R. McConnell et al.
A Greenland ice core shows that black carbon particles have altered snow reflectivity and Arctic climate and were particularly abundant in the atmosphere from 1850 to 1950.
10.1126/science.1144856

PERSPECTIVE: "C"ing Arctic Climate with Black Ice
R. B. Alley
10.1126/science.1147470

LETTERS

BOOKS *ET AL.*

POLICY FORUM

PERSPECTIVES

BREVIA

REPORTS

754

CONTENTS continued >>

REPORTS *CONTINUED...*

CREDIT: LARRY PARKER, WYOMING GAME AND FISH DEPARTMENT

AAAS
ADVANCING SCIENCE, SERVING SOCIETY

SCIENCE (ISSN 0036-8075) is published weekly on Friday, except the last week in December, by the American Association for the Advancement of Science, 1200 New York Avenue, NW, Washington, DC 20005. Periodicals Mail postage (publication No. 484469) paid at Washington, DC, and additional mailing offices. Copyright © 2007 by the American Association for the Advancement of Science. The title SCIENCE is a registered trademark of the AAAS. Domestic individual membership and subscription (51 issues): $142 ($74 allocated to subscription). Domestic institutional subscription (51 issues): $710. Foreign postage extra: Mexico, Caribbean (surface mail) 65%; other countries (air assist delivery) 185. First class, airmail, student, and canadian rates on request. Canadian rates with GST available upon request, GST #1254 88122. Publications Mail Agreement Number 1069624. **Printed in the U.S.A.**

Change of address: Allow 4 weeks, giving old and new addresses and 8-digit account number. **Postmaster:** Send change of address to AAAS, P.O. Box 96178, Washington, DC 20090-6178. **Single-copy sales:** $10.00 current issue, $15.00 back issue prepaid includes surface postage; bulk rates on request. **Authorization to photocopy** material for internal or personal use under circumstances not falling within the fair use provisions of the Copyright Act is granted by AAAS to libraries and other users registered with the Copyright Clearance Center (CCC) Transactional Reporting Service, provided that $30.00 per article is paid directly to CCC, 222 Rosewood Drive, Danvers, MA 01923. The identification code for Science is 0036-8075. *Science* is indexed in the Reader's *Guide to Periodical Literature* and in several specialized indexes.

CONTENTS continued >>

New Electroporation Buffer!
Check out our new Gene Pulser® electroporation buffer for improved transfection efficiency and cell viability.

Bio-Rad and RNAi. Come have a look.

From design to detection, Bio-Rad supports your RNAi research.

With a broad range of proven delivery technologies, award-winning detection systems, and a suite of high-quality support products, it's clear that Bio-Rad has a vision for RNAi.

- High-performing, potent Dicer-substrate siRNAs that produce ≥85% knockdown with as low as 5 nM siRNA
- Broad selection of delivery technologies
- RNA and protein purification products
- Automated microfluidic system for nucleic acid analysis
- Sensitive, optimized cDNA synthesis kits
- Systems for both protein and mRNA detection and analysis

For a close look at Bio-Rad's tools for RNAi, visit us on the Web at **www.bio-rad.com/rnai/**

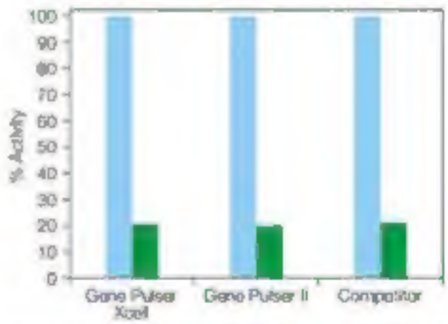

Electroporation with Gene Pulser electroporation buffer in different instruments. The Gene Pulser Xcell™, Gene Pulser II, and a competitor instrument were used to demonstrate the Gene Pulser electroporation buffer's flexibility across various instrument platforms. CHO cells were transfected in 0.4 cm cuvettes with a scramble siRNA (■) or a luciferase siRNA (■). Similar transfection efficiencies were observed across all platforms.

To find your local sales office, visit **www.bio-rad.com/contact/**
In the U.S., call toll free at 1-800-4BIORAD (1-800-424-6723)

Visit us on the Web at discover.bio-rad.com

BIO-RAD

SCIENCENOW

www.sciencenow.org

Life From the Oldest Ice?
Team claims to have resurrected microbes from 8-million-year-old Antarctic samples.

Turning on the Female Brain
New work in mice suggests a simple genetic switch is all that separates male and female behavior

Red Bean Revenge
Undercooked legumes can be a source of food poisoning

Poverty makes an impact later in life.

SCIENCECAREERS

www.sciencecareers.org

U.S.: Opportunities—The Power of Poverty
P. Fiske
The lessons Peter Fiske learned as a starving student have served him well in his professional life

U.S.: The Post-Bac—One or Two Years That Make Careers
S. Webb
A short hiatus before graduate school, say many students and faculty members, is almost always time well spent

ITALY: An Astrophysicist at La Città della Scienza
E. Pain
Alessandra Zanazzi turned astrophysics training and communications skills into a career at Italy's first interactive science museum

FROM THE ARCHIVES: U.S. Academic Scientists at Work—Where'd My Day Go?
J. Bass and S. Eckert
If you want to accomplish what you need to accomplish each day, you need to take control of your time

GLOBAL: *Science Careers* Blog
Science Careers Editors
Career development news and highlights, updated daily

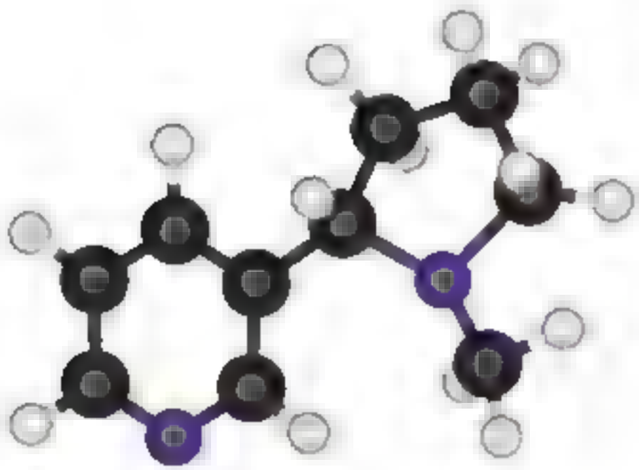

Nicotine alters neuronal plasticity

SCIENCE'S STKE

www.stke.org

PERSPECTIVE: Nicotine and Synaptic Plasticity in Prefrontal Cortex
D. S. McGehee
Nicotine's modulation of synaptic plasticity in prefrontal cortex may contribute to its effects on memory and reward circuitry.

CONNECTIONS MAP: TGF-β Signaling in Development
K. Kitisin et al.
This pathway highlights the role of the TGF-β signaling pathway in key aspects of mammalian development.

SCIENCEPODCAST

Listen to the 10 August *Science* Podcast to hear about soot and Arctic climate, a controversial treatment for trauma, the limits of human visual awareness, and more.
www.sciencemag.org/about/podcast.dtl

Separate individual or institutional subscriptions to these products may be required for full-text access.

In every successful paper you'll find a beginning, middle and

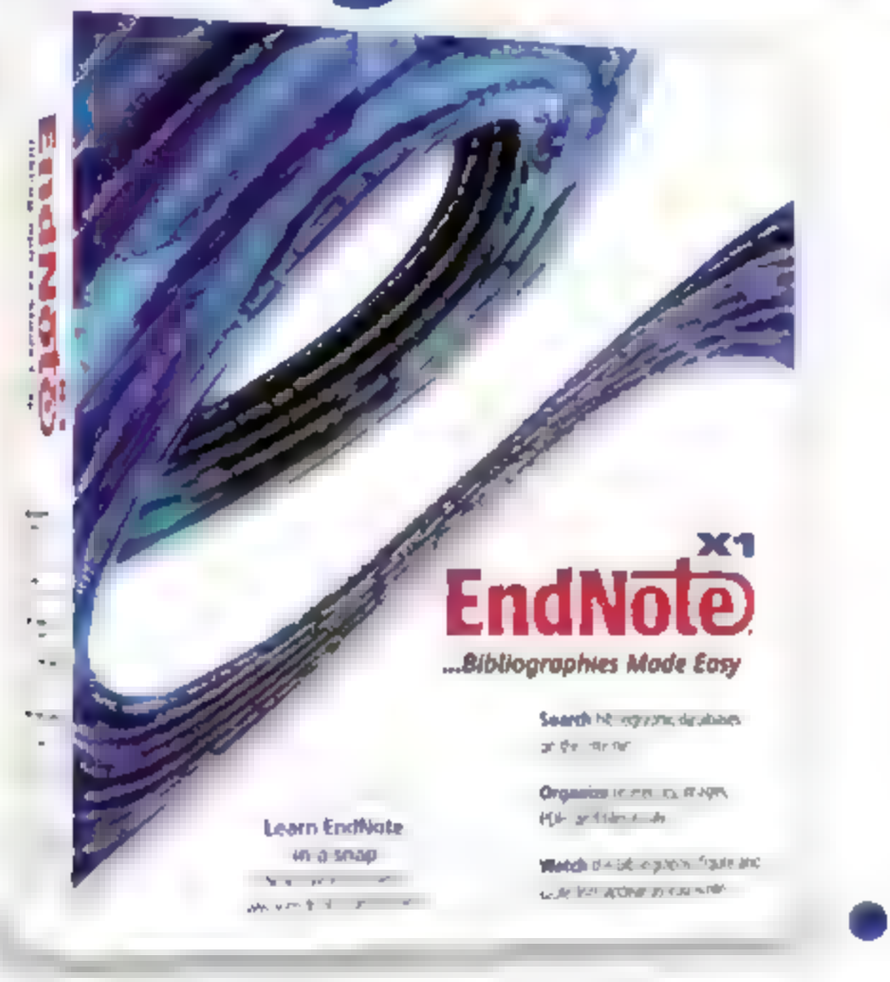

Anyone who has ever written a paper knows all too well the steps required for it to become a success. That's where EndNote® comes to the rescue. EndNote is there as you start your research and collect references. And, it continues to support you as you cite references in your paper. By listening to writers and researchers like you, and delivering ways to simplify your work, EndNote remains the favored, time-saving solution for organizing references and creating instant bibliographies. The newest release, EndNote X1, allows you to create custom groups of references using a simple drag and drop action, manage associated files with your references easily and more. EndNote X1 libraries can be shared across Windows® and Mac® OS X platforms and with all your colleagues via EndNote Web. Learning EndNote is easy with online tutorials that you can watch any time of day or night. All this put together means more productivity with less effort, which ultimately means a successful paper.

800-722-1227 • 760-438-5526 • rs.info@thomson.com

Download your free demo or buy online today
www.endnote.com

THOMSON

EDITED BY STELLA HURTLEY AND PHIL SZUROMI

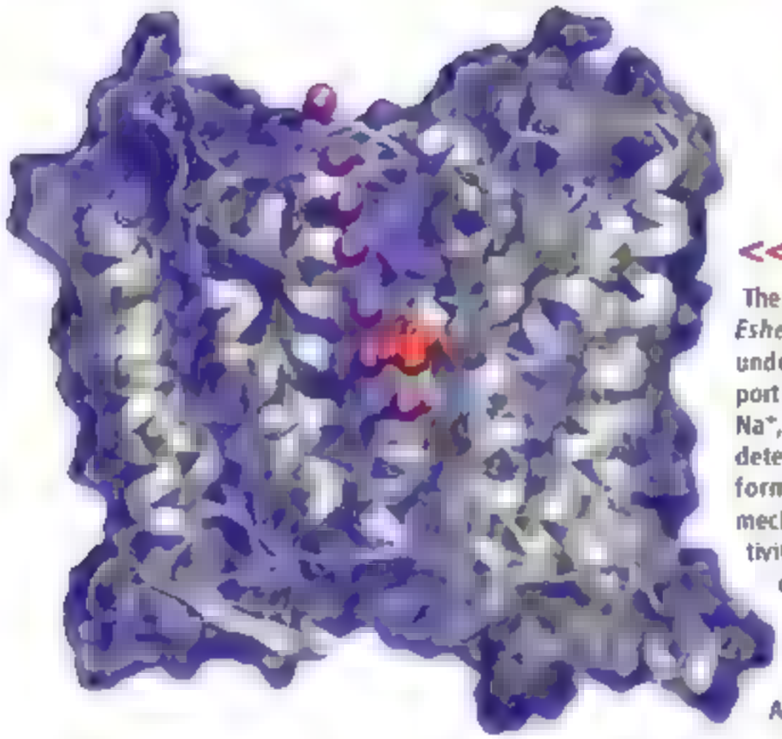

<< High-Salt Survival Tactics

The Na^+/H^+ antiporter NhaA is an inner-membrane protein in *Escherichia coli* that is required for survival in high salt or under alkaline stress. NhaA uses energy from proton transport down an electrochemical gradient into the cell to excrete Na^+, but not K^+, from the cytoplasm. Starting from a recently determined structure of NhaA, **Arkin *et al.*** (p. 799) performed molecular dynamics simulations to examine the mechanism of ion transport, pH regulation, and cation selectivity. The simulations, together with existing experimental data and mutagenesis experiments, indicate that three aspartates are essential to NhaA function: Asp^{164} is the Na^+ binding site, Asp^{163} controls alternating cytoplasmic or periplasmic access to the binding site, and Asp^{133} is involved in pH regulation.

A Layered Response

Actuators convert energy into mechanical force, and **Masmanidis *et al.*** (p. 780; see the Perspective by **Blencowe**) present a method for the actuation of nanomechanical resonators based on piezoelectric semiconductors, in this case, cantilevers of epitaxially grown GaAs that form a pin diode (an intrinsic layer, which is charge depleted and an active piezoelectric material, sandwiched between p-type and n-type layers). The strength of the mechanical resonance induced by an applied ac voltage can be controlled by a dc bias, which alters the charge depleted layer. The actuation can be tailored by altering the device's band structure, geometry, and crystallographic direction.

Heating a Monolayer

Heat is carried through crystalline solids via very low frequency acoustic vibrations. In contrast, the rates and mechanisms whereby isolated molecules transport heat are more obscure, but are potentially important for applications such as molecular electronics. **Wang *et al.*** (p. 787; see the Perspective by **Nitzan**) have used coherent vibrational spectroscopy to quantify the rate of heat conduction from a flash-heated gold substrate to the top of an alkanethiol monolayer assembled on its surface. The technique is sensitive to the disordering of terminal methyl groups that spreads across the ensemble in picoseconds as heat flows through the hydrocarbon chains. A theoretical analysis is consistent with ballistic heat transport at an effective rate of ~1 kilometer per second.

CREDITS (TOP TO BOTTOM): D. E. SHAW RESEARCH; ADAPTED FROM NITZAN

Straight to Amides

The prevalence of amides in biomolecules and commercial polymers places high value on a flexible and efficient synthetic route to molecules bearing this C(=O)N motif. In general, oxidative coupling of available alcohols and amines to amides requires the use of wasteful quantities of stoichiometric activators or corrosively strong acids and bases. **Gunanathan *et al.*** (p. 790) show that a ruthenium complex catalyzes the direct coupling of a wide range of primary alcohols and amines to the corresponding amides, with the endothermic reaction driven by liberation of H_2 as the sole by-product. High yields were obtained from boiling toluene solutions in less than 10 hours.

Ice Through 11 Glacial Cycles

The ice core drilled at Dome C, Antarctica, provides the longest continuous record of climate and atmospheric composition of any polar ice site, encompassing 11 glacial cycles. **Jouzel *et al.*** (p. 793, published online 5 July) present the deuterium isotopic profile for the entire 3260-meter length of the core, which allows the construction of a climate record that extends back to 800 000 years before the present. The high resolution of this record allows the relation between shorter, millennial-scale climate events in the northern and southern high latitudes to be examined. The authors also used an atmospheric General Circulation Model to calculate an improved temperature record for the entire interval, finding temperatures during warm intervals as much as 4.5°C warmer, and during cold intervals as much as 10°C lower, than preanthropogenic Holocene values.

Looking Within

Global climate models have been criticized as being overly simple representations of an extremely complex system; for example, they include only natural and anthropogenic external forcing terms (like those for solar radiation, atmospheric aerosols, and the concentrations of greenhouse gases) and neglect to incorporate the effects of nonanthropogenic internal climate variability that could have a significant effect on predictions. **Smith *et al.*** (p. 796; see the news story by **Kerr**) report model hindcast results that include the effects of that internal variability. They found that surface temperature can be predicted with substantially more skill over a decade, both globally and regionally. Their forecast of global, annual mean surface temperature for the decade beginning in 2005 indicates a reduced rate of warming for the next few years, followed by continued and more rapid warming, with at least half of the years after 2009 predicted to be warmer than the warmest year currently on record.

Activity of the Depressed Brain

To try to understand how brain circuits malfunction during depression, **Airan *et al.*** (p. 819,

Continued on page 719

PreCR™ Repair Mix from New England Biolabs

REPAIRS A BROAD RANGE OF DNA DAMAGE PRIOR TO PCR

Increase your chances for success in PCR with the PreCR™ Repair Mix. This novel enzyme mix of [illegible] protocols to restore intact, damaged DNA prior to amplification. PCR can also be performed directly on the repair reaction. Adding a simple 20 minute reaction to prepare a wide range of DNA damage due to [illegible] low pH, oxygen, and UV light.*

*Not recommended for highly fragmented DNA or for damage due to DNA crosslinks

Proven Repair with the PreCR Repair Mix

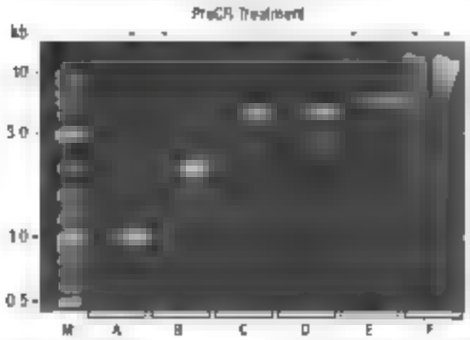

A: UV exposure (- DNA)
B: heat treatment (- DNA)
C: oxidation (plasmid)
D: UV exposure (human genomic DNA)
E: hydrolysis & UV exposure (- DNA)
F: hydrolysis (- DNA)
M: 2 Log DNA Ladder (NEB #N3200)

Advantages:

- Suitable for PCR, microarrays and other DNA technologies
- Does not harm DNA template
- Can be used in conjunction with any thermostable polymerase
- PCR can be done directly on repair reaction
- Easy to use protocols included

[illegible]

PreCR™ Repair Mix M0309S/L

For more information and our international distribution network, please visit www.neb.com

New England Biolabs Inc. 240 County Road Ipswich, MA 01938 USA • 1-800-NEB-LABS Tel. (978) 927-5054 Fax (978) 921-1350 info@neb.com
Canada Tel. (800) 387-0915 info@ca.neb.com • **China** Tel. 010-82378266 beijing@neb-china.com • **Germany** Tel. 0800/246 527 info@de.neb.com
Japan Tel. +81 (0)3 5669-6191 info@neb-japan.com • **UK** Tel. 0800 318486 info@uk.neb.com

NEW ENGLAND BioLabs® Inc.
the leader in enzyme technology

Continued from page 717

published online 5 July, see the Perspective by **Insel**) tracked neural activity within the hippocampus with voltage-sensitive dyes in brain slices from rats experiencing depression-like states. Certain aspects of neural activity predicted the degree of "depression" exhibited by the animal, including behavioral improvements after administration of antidepressant drugs. This indication that hippocampal neural activity reflects the behavioral state of these animals provides a starting point for further understanding of the malfunctioning circuits in depression and suggests an approach for the study of other mental illnesses.

Wnt, the Fountain of Youth?

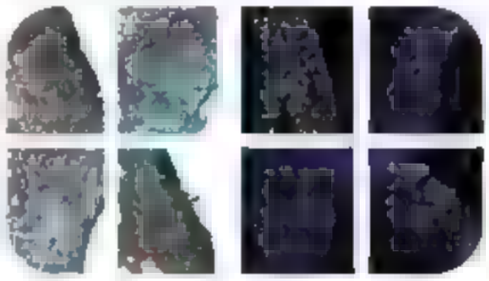

Wnt proteins are secreted ligands that bind to cell surface receptors and have important effects during development, which it now seems may also contribute to phenotypes of stem and progenitor cells associated with aging. **Liu *et al.*** (p. 803) examined stem cell properties in mice carrying a mutation in the Klotho protein, which show characteristics of accelerated aging. They observed increased senescence of stem cells in the mutant mice and found that the Klotho protein physically interacted with and inhibited Wnt proteins in transfected cells. Exposure of mouse embryo fibroblasts in culture to excessive Wnt signaling enhanced senescence, and in transgenic mice also promoted senescence of skin cells. **Brack *et al.*** (p. 807) found that Wnt signaling appeared to be more active in aging animals. Injection of Wnt3A into young regenerating muscle reduced proliferation and increased deposition of connective tissue. Thus, antagonizing Wnt signals could provide a strategy to ease the effects of aging and age-related diseases.

Birds of a Feather

The European Union's Birds Directive was a pioneering international policy instrument that was enacted in 1979 with the aim of providing a framework for the conservation of bird species considered to be rare or vulnerable. **Donald *et al.*** (p. 810) evaluate the effectiveness of the directive in terms of the population response of all the species at which it is targeted. As was hoped, positive population changes were observed between 1990 and 2000 for listed species compared to nonlisted species. Such international initiatives are indeed capable of delivering measurable conservation benefits.

Regulatory Change and Phenotypes

Phenotypic changes between related species are thought to arise from changes in gene composition and alterations in their mode of regulation. **Borneman *et al.*** (p. 815, see the Perspective by **Kruglyak and Stern**) have studied the divergence in transcription networks across four yeast species by directly determining the binding site distribution of orthologs of the transcription factors Ste12 and Tec1. Gene regulatory binding sites were considerably more variable than the genes themselves, suggesting that such changes may drive phenotypic variation.

Flu Variations

A major question in the transmission of the H5N1 strain of influenza between humans is how mutations might influence the ability of the virus to enter human cells and how this might affect detection by our immune systems. **Yang *et al.*** (p. 825) reveal that specific mutations in the influenza hemagglutinin gene can alter host receptor binding and the recognition of the virus by neutralizing antibodies. However, new neutralizing antibodies specific to the mutants could be elicited by immunization, which will be important in the design of vaccines to combat the virus.

What You See and What You Don't

What are the limits to the visual information that can be consciously accessed by a human being at any one time? **Huang *et al.*** (p. 823) analyzed single momentary acts of conscious perception specifically with respect to location and color of briefly presented visual stimuli. They found that we can be aware of more than one location, but not more than one color, per visual scene. The results are interpreted within the framework of "labeled Boolean maps," which postulates that people can attend to multiple locations simultaneously, but only a single feature.

CREDIT: BRACK *ET AL.*

NIH DIRECTOR'S

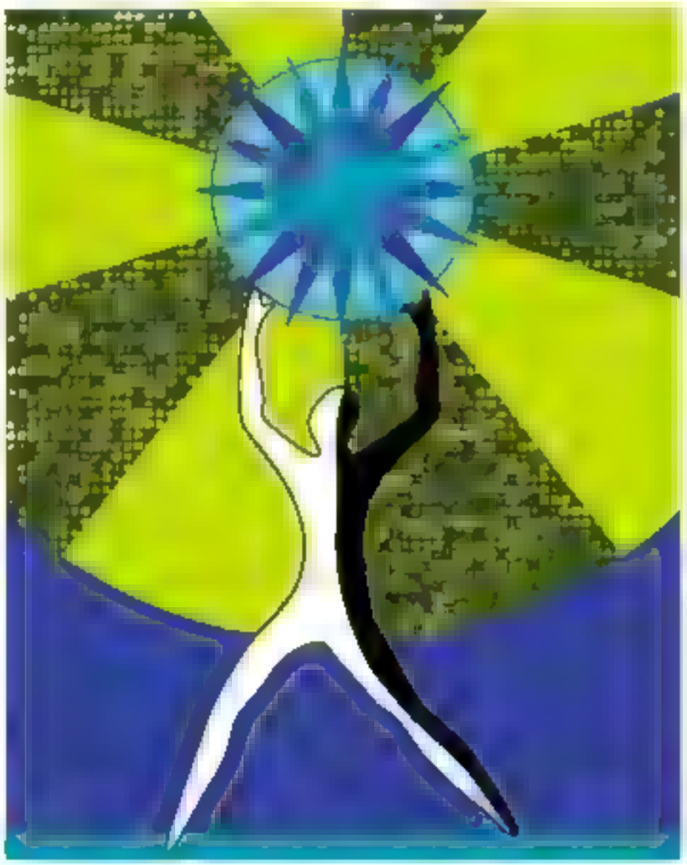

PIONEER A·W·A·R·D

SYMPOSIUM

WEDNESDAY, SEPTEMBER 19, 2007
8:15 A.M.–5:30 P.M.

NATCHER CONFERENCE CENTER (BUILDING 45)
NATIONAL INSTITUTES OF HEALTH
BETHESDA, MARYLAND

Attendance [illegible]

[illegible] will be videocast [illegible]

For more information, visit [illegible]
symposium2007

FEATURING

TALKS BY THE 2006 PIONEER AWARD RECIPIENTS

- **Kwabena A. Boahen, Ph.D.**
  Stanford University
- **Arup K. Chakraborty, Ph.D.**
  Massachusetts Institute of Technology
- **Lila M. Gierasch, Ph.D.**
  University of Massachusetts Amherst
- **Rebecca W. Heald, Ph.D.**
  University of California, Berkeley
- **Karla Kirkegaard, Ph.D.**
  Stanford University School of Medicine
- **Thomas J. Kodadek, Ph.D.**
  University of Texas Southwestern Medical Center at Dallas
- **Cheng Chi Lee, Ph.D.**
  University of Texas Health Science Center at Houston
- **Evgeny A. Nudler, Ph.D.**
  New York University School of Medicine
- **Gary J. Pielak, Ph.D.**
  University of North Carolina at Chapel Hill
- **David A. Relman, M.D.**
  Stanford University
- **Rosalind A. Segal, M.D., Ph.D.**
  Dana-Farber Cancer Institute
- **James L. Sherley, M.D., Ph.D.**
  Massachusetts Institute of Technology (through June 2007)
- **Younan Xia, Ph.D.**
  University of Washington, Seattle

ANNOUNCEMENT OF THE 2007 PIONEER AWARD RECIPIENTS

POSTER SESSION BY THE 2004, 2005, AND 2006 AWARDEES AND LAB MEMBERS

Donald Kennedy is Editor-in-Chief of *Science*

Dan Koshland: A Retrospective

AS I WALK AROUND AT THE AMERICAN ASSOCIATION FOR THE ADVANCEMENT OF SCIENCE where the journal *Science* has its home, I encounter one framed cover after another. Many of them are from issues published between 1985 and 1995, when Dan Koshland was at work as its editor, creating the journal's process infrastructure and bringing aboard many of the Editorial and News staff with whom I am privileged to work today. Pick your way through this issue and explore it; in substantial part, it is the magazine Dan created.

Two weeks ago, a few days after Dan's death, many of his colleagues spoke about his passionate enthusiasm for good science of all kinds. Because he had come to *Science* as its first nonresident editor, trailing extraordinary scientific credentials, it would not have been surprising had his new staff been intimidated. They gave that up upon discovering that he liked to manage by walking around and that he relished productive argument. He was a regular contributor to the journal himself; indeed, a posthumous contemporary essay classifying strategies of scientific discovery is on p. 761 of this issue.

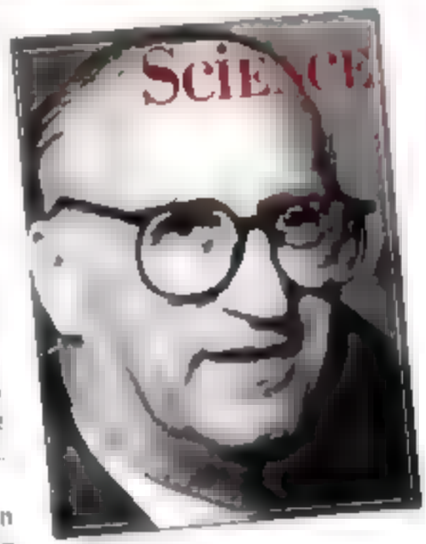

Readers may recall one occasional persona of Dan's, the self-confident Dr. Nontall Well; he may have been Dr. Nontall for that audience, but in house he was Dr. Letsdebate. The memories disclosed by his former staff colleagues are as varied as they are rich. Dan's love for a novel piece of science, his thoughtful holiday habit of bringing a box of Godiva chocolates to each editor and assistant, and his outrageous sense of humor. My colleague Monica Bradford, who was there for much of Dan's editorship, describes him as a "transformationist." He changed procedures, people, and projects wherever he thought it might do some good; one innovation (among many) was the first Science International office in Cambridge, UK, where many of our Editorial and News colleagues work.

Dan's teacher Wendell Latimer brought him to Glenn Seaborg, an extraordinary project manager with whom he worked on the Manhattan Project. He later underwent a conversion to biochemistry that brought him through the University of Chicago, Brookhaven National Laboratory, and eventually to the University of California, Berkeley. Much of this history is given in a 1996 personal account in the *Annual Review of Biochemistry* (http://arjournals.annualreviews.org/toc/biochem/65/1), entitled "How to Get Paid for Having Fun." At Brookhaven and later at Berkeley, he performed a stunning series of experiments demonstrating that protein conformation was flexible, and these findings led him away from the lock-and-key model to the now widely accepted "induced-fit" model of enzyme-substrate interactions. Dan's experience in breaking a paradigm was an example for his editors. Understanding that exceptional results require exceptional evidence, he nevertheless encouraged them not to overlook surprises simply because they seemed improbable.

After his first wife Marian Koshland passed away, Dan made a very large gift to the National Academy of Sciences, of which Dan and Marian (aka Bunny) were both members. It honored her by creating a museum that illustrates the value of basic science and its importance to society. A committee was assigned to monitor the process of exhibit development, with Dan as chairperson; as his nominal co-chair, I soon figured out that I was expected to support him and, if necessary, calm him down when things weren't suiting him. Dan had views, and a way of expressing them forcefully (that was fair, it was, after all, his money). It was an enjoyable exercise. Dan was right more often than not, and the Marian Koshland Science Museum is a jewel that teaches visitors—adults and kids—in a participatory way about matters such as climate change and genomics.

I am grateful to Dan for his wisdom, his friendship, and his legacy, and for encouraging me as I considered coming to *Science*. The legacy is shared by a dozen present News and Editorial staff who served in Dan's decade, and by the young staff who later fell to his persuasiveness as a recruiter. "Dan's people" in turn created an institution strong and exciting enough to attract a new crop of colleagues to continue *Science*'s growth. We owe Dan much for his role in shaping the place, the conditions, and many of the people with whom we work.

– **Donald Kennedy**

10.1126/science.1148461

FUJIFILM

Highly sensitive luminescent image analyzer with a full choice of light sources for your needs

LUMINESCENT IMAGE ANALYZER

LAS-4000

- Large-aperture F0.65 lens
- 3.2 megapixels Super CCD chip
- Remote control from a computer
- Quick(er response to reduce stress)

Chemi / Bioluminescence

Fluorescence

Digitizing (Gel documentation)

LAS-4000 (with any Epi-Illuminator) is categorized as the class 1 laser (JIS) (IEC60825-1+A2:2001).

Notice: With regard to patents owned by third parties related to, among other things, sample preparation, we recommend that you consult with a lawyer or patent attorney about obtaining a license from the third parties.

http:// lifescience.fujifilm.com [Download Brochures and Application notes in PDF form]

FUJIFILM Corporation Life Science Products Div. 7-3, Akasaka 9-Chome Minato-ku, Tokyo 107-0052 Japan Tel: +81-3-6271-2158 Fax: +81-3-6271-3136 E-mail: lsprod@fujifilm.co.jp
FUJIFILM Medical Systems U.S.A., Inc. 419 West Avenue Stamford CT 06902 USA Tel: +1-866-902-3654 Fax: +1-203-327-8485 E-mail: dor.sales@fujimed.com
FUJIFILM Europe GmbH Heesenstr. 31 40549 Düsseldorf Germany Tel: +49-211-5089-74 Fax: +49-211-5089-8744 E-mail: lifesciences@fujifilm.de
FUJIFILM UK Ltd. Unit 12 St Martins Way St Martins Business Centre, Bedford, MK42 0LF U.K. Tel: +44-1234-245291 Fax: +44-1234-245753 E-mail: lifesciences@fujifilm.co.uk
富士胶片(中国)投资有限公司 31st floor, Hong Kong New World Tower, No.300 Huai Hai Zhong Road, Shanghai P.R.China. Tel: +86-21-3302-4666 ext.363 Fax: +86-21-6384-3322 E-mail: wangyq@fujifilm.com.cn

EDITED BY GILBERT CHIN AND JAKE YESTON

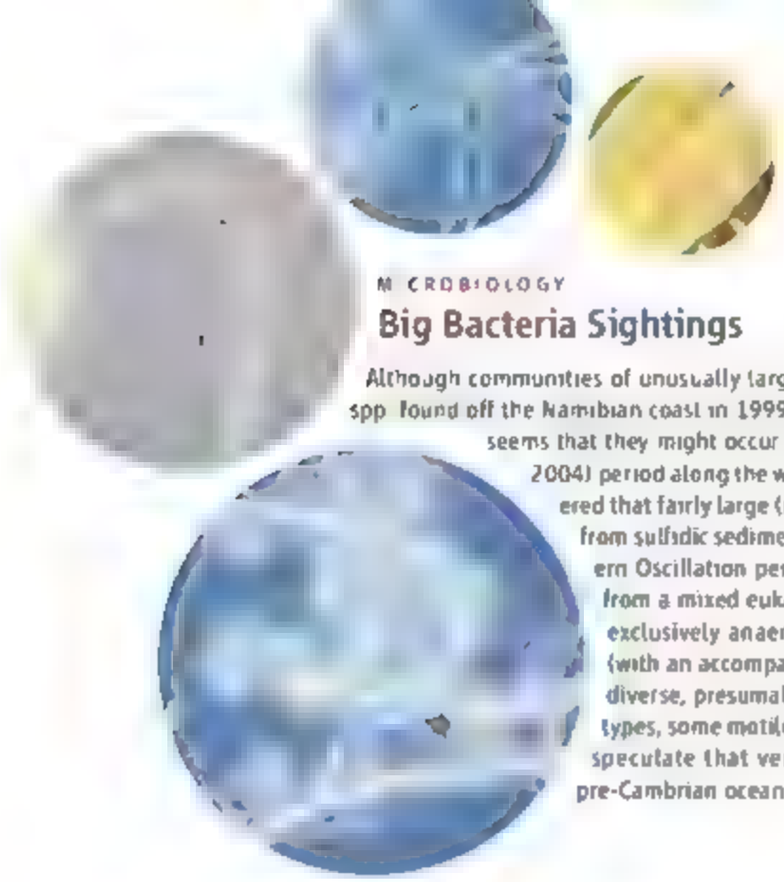

MICROBIOLOGY

Big Bacteria Sightings

Although communities of unusually large bacteria, like the gigantic 1 mm-diameter *Thiomargarita* spp. found off the Namibian coast in 1999, have only recently been discovered in marine sediments, it seems that they might occur widely in the benthos. During a long inter–El Niño (1998 to 2004) period along the western coast of South America, Gallardo and Espinoza discovered that fairly large (roughly 1 x 100 mm) filamentous bacteria could be recovered from sulfidic sediments overlain by oxygen-deficient water. As the El Niño–Southern Oscillation persisted, repeat sampling showed that the community shifted from a mixed eukaryote plus megabacteria (*Thioploca* spp.) composition to an exclusively anaerobic complex of the newly discovered filamentous bacteria (with an accompanying loss of megafauna). These macrobacteria appear to be diverse, presumably representing many ecotypes, and there are several phenotypes, some motile and some containing refractive sulfur granules. The authors speculate that very similar assemblages may have been present in anoxic pre-Cambrian oceans. — CA

Int. Microbiol. **10**, 97 (2007).

PHYSIOLOGY

Ensuring Milk Quality

In discussions of diet and health, fat generally gets a bad rap. One notable exception is the case of newborn babies, who require substantial quantities of milk lipids for normal growth and development. Indeed, to meet this need, the mammary glands of new mothers secrete nearly 6 kg of fat during a typical 6 month lactation period.

In a study of genetically manipulated mice, Wan *et al.* show that the quality of fat in milk is as important to neonatal health as the quantity, and they begin to dissect the mechanism by which quality control is achieved. The authors noticed that nursing pups of female mice that were genetically deficient in the transcription factor PPARγ (peroxisome proliferator–activated receptor γ) exhibited growth delays and hair loss. These abnormalities were not related to the genotypes of the fathers or the pups, nor were they related to maternal parenting behaviors. Instead, they could be traced to a nutritional defect in the milk produced by the mutant mothers—namely, the presence of proinflammatory lipids, which were the products of aberrantly overexpressed lipid oxidation enzymes in the maternal mammary glands. One confirmatory piece of evidence that hair loss in the pup was a consequence of inflammatory responses was that treatment with aspirin effectively prevented the alopecia. Thus, maternal PPARγ appears to protect nursing newborns by suppressing the production of "toxic" fats in milk. Interestingly, the source of the PPARγ mediating this protective effect is not the mammary epithelium but appears to be hematopoietic or endothelial cells. — PAK

Genes Dev. **21**, 10.1101/gad.1567207 (2007).

ENVIRONMENTAL SCIENCE

Silver and Its Surroundings

Silver has been prized throughout human history for its sheen and more recently for its exceptional electrical conductivity and its chemical applicability to photographic processing. Although its toxicity is only moderate in comparison with that of other heavy metals, its antimicrobial properties point to the utility of a more thorough understanding of its environmental impact, particularly in light of the steadily increasing stream of electronics waste. In this vein, Eckelman and Graedel have analyzed the worldwide anthropogenic release of silver to air, land, and water. Their analysis spanned 64 countries for the year 1997 and compared releases from the mining stage through manufacturing and waste disposal (they note that more than half of processed silver is recycled). The plurality of the 13 million kg of discarded silver (~44%) went to landfills, with the next highest category (~30%) being composed of tailings released during mining. Regional toxicological impact was estimated based on a previously established hazard ranking of various silver compounds. — JSY

Environ. Sci. Technol. **41**, 10.1021/es062970d (2007).

EVOLUTION

An Early Use of Androstenedione

Sex hormones such as estrogen, progesterone, and androgen exert their physiological effects by binding to proteins of the steroid hormone receptor family. Studies with basal vertebrates have mapped out the evolution of these signaling pathways, which are important in regulating reproduction. Prior work has suggested that the estrogen receptor was the first steroid receptor and that other steroid receptors arose later, probably through gene duplication. Although androgens are generally traced back to gnathostomes, Bryan *et al.* now identify an androgen receptor in the sea lamprey *Petromyzon marinus*, a jawless vertebrate. The specific androgen, androstenedione, is a precursor of testosterone, and when androstenedione was implanted into male lampreys, the development of the testis and secondary male characteristics was accelerated. Hence, by showing that a functional androgenic hormone and its receptor are present in jawless vertebrates, this work argues against the claim that androgen receptors evolved after agnathan-gnathostome divergence. — BAP

Petromyzon marinus.

Biol. Reprod. **77**, 10.1095/biolreprod.107.061093 (2007).

Continued on page 725

AAAS & NPA

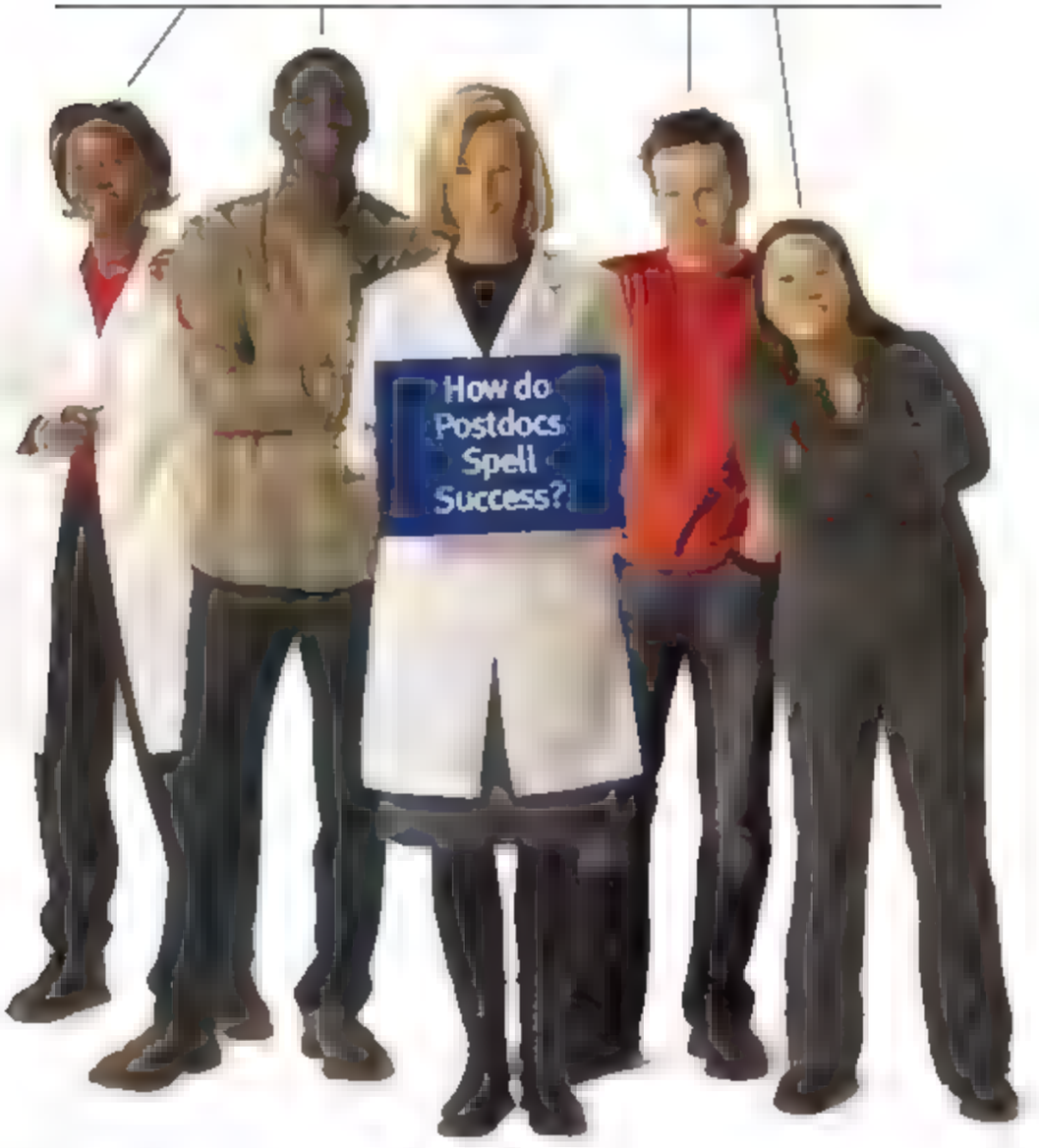

Here's your link to career advancement

AAAS is at the forefront of advancing early-career researchers offering job search, grants and fellowships, skill-building workshops, and strategic advice through ScienceCareers.org and our Center for Careers in Science & Technology.

NPA, the National Postdoctoral Association, is providing a national voice and seeking positive change for postdocs partnering with AAAS in career fairs, seminars, and other events. In fact, AAAS was instrumental in helping the NPA get started and develop into a growing organization and a vital link to postdoc success.

If you're a postdoc or grad student, go to the AAAS-NPA link to find out how to spell career success.

AAAS.org/NPA

NATIONAL POSTDOCTORAL ASSOCIATION

Science

AAAS

Continued from page 723

ASTROPHYSICS

The Red and the Blue

All galaxies can be built up from two major components, a central spherical bulge and a surrounding flattened disk of stars. The relative size of each has been widely used to classify galaxies, so that a variety of types can be identified with disks of varying size and when there is no disk, the galaxy is classified as elliptical. Complementing this picture, galaxies tend to favor one of two colors, either red or blue. Ellipticals are mostly red and spirals blue, leading to suggestions that this color preference is simply due to the relative contributions of stars in the bulge and disk to the galaxy's overall light.

Drory and Fisher have found that this simple view is inadequate, however. Decomposing the shapes of tens of galaxies selected from the Sloan Digital Sky Survey using images taken by the Hubble Space Telescope, they find that some particular galaxies do not follow the expected relationship between color and brightness expected from their bulge-to-disk ratio. The galaxies in question instead have

CREDIT: DRORY AND FISHER, *ASTROPHYS. J. LETT.* 664 (2007)

so-called "pseudobulges," or central puffed up concentrations of stars whose properties are more similar to those in the disks than in ellipticals or normal bulges. Such differences imply that it is the type of central bulge that is important, not its size, in characterizing a galaxy. Also, the characteristics ultimately depend on the environment in which the galaxy first formed, so that pseudobulges are indicative of later, less violent formation in comparison with the conditions that give rise to normal bulges. — JB

Astrophys. J. **664**, 640 (2007)

CHEMISTRY

Strong Solvent Imprint

The optical rotation of polarized light caused by chiral molecules dissolved in solution is usually attributed to the interaction of the light field with the electron distribution of the solute. However, the solvent shell around the molecule can also exert strong effects, for example, the sign of the optical rotation of (*S*)-methyloxirane switches from positive to negative when the solvent is changed from water to benzene. Previous theoretical work has shown that the interaction of (*S*)-methyloxirane with water accounts for most of the optical rotary dispersion (ORD) in aqueous media. Mukhopadhyay *et al.* now present time-dependent density functional theory calculations of ORD for Monte Carlo simulations of (*S*)- and (*R*)-methyloxirane solvated with benzene. They show that for an explicit solvent model, the dissymmetric benzene solvent shell, rather than the solute itself, dominates the ORD. This effect was not seen with implicit solvent molecules or with an achiral solute (ethylene oxide). — PDS

Angew. Chem. Int. Ed. **46**, 10.1002/anie.200702273 (2007)

CELL BIOLOGY

A Needle in a Haystack

Primary cilia are composed of a stereotypical arrangement of microtubules that are anchored to a basal body and extend within a membrane sheath from many animal cells. Primary cilia act as microscopic sensory organs in sampling the extracellular environment and play a role during development in morphogen sensing, as well as contributing to sight and smell and other functions in multiple organs. Defects in primary cilium formation are associated with several diseases, such as retinal degeneration and neural tube defects. Primary cilium initiation and function require the coordination of both membrane trafficking and microtubule assembly pathways.

Yoshimura *et al.* wanted to define the mechanisms involved in primary cilium formation and undertook a systematic approach to identify which members of the multitudinous Rab GTPase family of membrane traffic regulators were important. Only one of them, Rab8a, localized to the primary cilium. It interacted specifically with cenexin, a microtubule- and basal body–binding protein known to be involved in primary cilium production. Two other family members, Rab17 and Rab23, and their partnered GTPase activators also participated in primary cilium generation, whereas other Rabs and their activators were not required. This study paves the way for an understanding of the requirements for the specific recruitment of membrane trafficking and microtubule assembly machineries during primary cilium biogenesis, and how deficiencies lead inexorably to disease. — SMH

J. Cell Biol. **178**, 363 (2007)

www.sciencemag.org

Science

1200 New York Avenue, NW
Washington, DC 20005
Editorial: 202-326-6550, FAX 202-289-7562
News: 202 326-6501, FAX 202 371-9227

Unit 4, Hodgkin House, 82-88 Hills Road
Cambridge, UK CB2 1LQ
+44 (0) 1223 326500, FAX +44 (0) 1223 326501

Subscription Services For change of address, missing issues, new orders and renewals, and payment questions: 866-434-AAAS (2227) or 202 326-6417, FAX 202 842 2065. Mailing addresses: AAAS, P.O. Box 96178, Washington, DC 20090-6178 or AAAS Member Services, 1200 New York Avenue, NW, Washington, DC 20005

Institutional Site Licenses please call 202 326-6755 for any questions or information

Reprints: Author inquiries 800-635-7181
Commercial inquiries 803 359-4578

Permissions 202 326-7074, FAX 202 682-0816

Member Benefits Bookstore: AAAS/BarnesandNoble.com bookstore, www.aaas.org/bn, Car purchase discount: Subaru VIP Program 202 326 6417; Credit Card: MBNA 800-847-7378, Car Rentals: Hertz 800-654-2200 CDP#343457, Dollar 800-800-4000 #AA1115, AAAS Travel: Betchart Expeditions 800-252-4910; Life Insurance: Seabury & Smith 800-424-9883, Other Benefits: AAAS Member Services 202 326-6417 or www.aaasmember.org.

science_editors@aaas.org (for general editorial queries)
science_letters@aaas.org (for queries about letters)
science_reviews@aaas.org (for returning manuscript reviewers)
science_bookrevs@aaas.org (for book review queries)

Published by the American Association for the Advancement of Science (AAAS). *Science* serves its readers as a forum for the presentation and discussion of important issues related to the advancement of science, including the presentation of minority or conflicting points of view, rather than by publishing only material on which a consensus has been reached. Accordingly, all articles published in *Science*—including editorials, news and comment, and book reviews—are signed and reflect the individual views of the authors and not official points of view adopted by the AAAS or the institutions with which the authors are affiliated.

AAAS was founded in 1848 and incorporated in 1874. Its mission is to advance science and innovation throughout the world for the benefit of all people. The goals of the association are to foster communication among scientists, engineers and the public; enhance international cooperation in science and its applications; promote the responsible conduct and use of science and technology; foster education in science and technology for everyone; enhance the science and technology workforce and infrastructure; increase public understanding and appreciation of science and technology; and strengthen support for the science and technology enterprise.

Information for Authors

See pages 120 and 121 of the 5 January 2007 issue or access www.sciencemag.org/feature/contribinfo/home.shtml

HotStart-IT
Less Heat. No DNA Damage.
We couldn't be more specific.

USB's novel hot start PCR method requires no extensive heat denaturation step. The result is no damage to precious samples with increased specificity and yield. HotStart-IT™ highly sensitive to all your critical PCR applications.

HotStart-IT™ Taq DNA Polymerase

- Based on primer sequestration—a novel method developed by USB scientists
- Unique proprietary antibodies to prevent mispriming
- Primers activated during heat denaturation

Benefits

High Specificity

- Detects 1 to 10 copies
- Linear dynamic range of 7–8 orders of magnitude. $R^2 \geq 0.95$

Ease of Use

- Multiple instrument compatibility

Increased specificity of HotStart-IT™ Taq DNA Polymerase

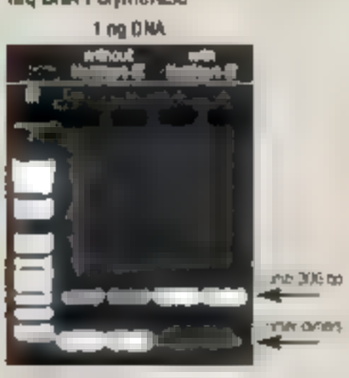

Results clearly demonstrate a shift from predominantly primer-dimers to the specific target when HotStart-IT™ is included in the reactions.

Real-time PCR from 10^5 copies down to a single copy target using HotStart-IT™

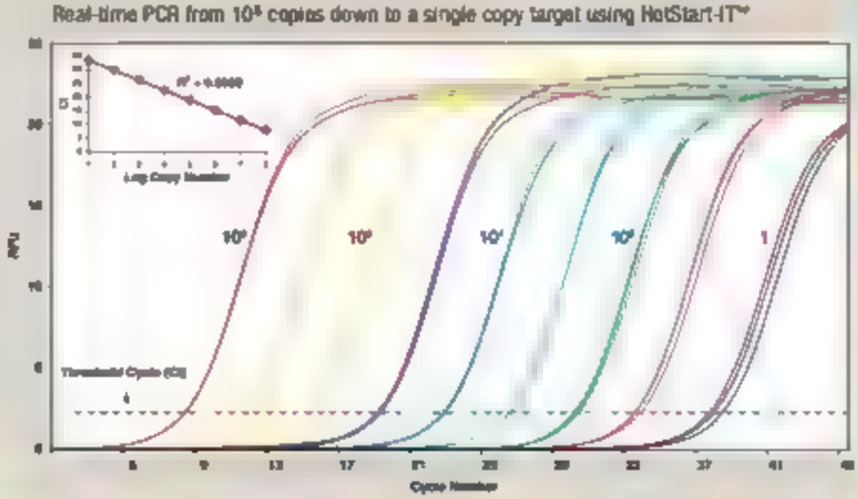

For more information on HotStart-IT™
call 800.321.9322 or visit www.usbweb.com/hotstart
In Europe: +49(0)76 33-933 40 8 or visit www.usbweb.de/hotstart

usb
Fueling Innovation in Life Science

Pass the Salt

Since ancient times, people have been salting meat for storage. Now Iranian archaeologists are using the same trick to preserve the body of a man who mined some of that salt millennia ago.

The body is the sixth found since modern mining operations resumed in the Chehr Abad mine in Zanjan province in 1992. The other five are on display in museums in Tehran and Zanjan, but Iran's Cultural Heritage, Handicrafts, and Tourism Organization says the museum specimens are degrading. So when the most recent body was unearthed this year, archaeologists decided to reinter it. Iranian, German, and British experts will meet in Iran this autumn to plan long-term preservation.

University of Oxford archaeologist Mark Pollard, who has studied samples from the remains, says the six bodies most likely belonged to miners who died in cave-ins. Pollard hopes to find out where the miners came from by comparing strontium isotopes in their bones with the isotopes in nearby areas, which the miners would have absorbed from their food and drinking water. Field surveys show no sign of habitation within 30 kilometers of the mine during the Achaemenid (550–330 B.C.E.) and Sassanid (224–651 C.E.) dynasties, when the miners lived.

DEBRIS (TOP TO BOTTOM): A. M. POLLARD; COURTESY ZANJAN MUSEUM; CHRISTOPHER PALA; MIRAMAR FILM; COLLECTION

Call the Hose Brigade!

This month in Hawaii's scenic Kaneohe Bay, scientists fighting an infestation of alien seaweed will unleash a pair of new weapons: vacuum cleaners. Their target is an ugly, gristly alga the color of canned peas. Called *Eucheuma*, it smothers and kills coral, creating underwater devastation worthy of a horror movie. "I've never seen algal growth with such lethal capabilities," says Celia Smith, a professor of marine botany at the University of Hawaii, Manoa, involved in fighting it.

Smith's late predecessor, Max Doty, imported *Eucheuma* to his Kaneohe Bay lab from its native Philippines in the 1970s to study its potential as a source of the food additive carrageenan. Methods he developed made *Eucheuma* the world's most widely farmed seaweed, cultivated in 23 countries. But the alga began spreading across Kaneohe Bay and now covers nearly half the fringe reef. So the state, the university, and The Nature Conservancy teamed up to create Super Sucker and Super Sucker Jr., barge-mounted vacuum cleaners capable of cleaning up to 350 kilograms of seaweed an hour. Eric Conklin of The Nature Conservancy says the battle is winnable in Hawaii, but that little is known about how much damage *Eucheuma* has wreaked in the remote, impoverished areas where most of the farming takes place.

Keeping Tabs on Tabloid Science

The *Weekly World News*, the supermarket tabloid that once claimed 12 U.S. senators were space aliens, is ending publication this month. But there are enough purveyors of pseudoscience, anti-science, and quackery to keep the following three Web sites in business.

Crank Dot Net* furnishes a taxonomy of crackpot Web sites. Erik Max Francis, a computer programmer in San Jose, California, rates the entries on how far they've strayed from reality. For instance, a page on the possibility that the sun has an unobserved twin merits only a "fringe" classification, whereas a site that dispenses advice on conducting diplomacy with aliens earns the highest ranking.

Homeopaths, advocates of untested herbal remedies, and credulous reporters who promote them take a beating at British doctor Ben Goldacre's Bad Science blog.† Pharmacologist David Colquhoun of University College London hammers similar targets at DC's Improbable Science.‡ Although both sites have a British emphasis, the quackery they expose is often international.

* www.crank.net

† www.badscience.net

‡ dcscience.net

DÉJÀ VU ON DEMAND?

Time travel is possible, and you can do it without exotic particles or short-cut wormholes. Normal matter, a vacuum, and a spaceship are enough.

The good news comes from theoretical physicist Amos Ori of the Technion–Israel Institute of Technology in Haifa. In July's issue of *Physical Review D*, Ori shows how gravitational fields could twist space-time into a hollow doughnut. By zipping around the tube, a time traveler could shake hands with her younger self or with future presidents without breaking any laws of physics. Other theorists have proposed similar models, but they all required matter with exotic properties such as negative mass. Ori's tube, by contrast, is immersed in a sphere of normal matter—"like dust from under your bed," says J. Richard Gott III, a theoretical physicist at Princeton University who has written a popular book on time travel.

Ori's ideas are "quite promising," Gott says, but both men agree that at present time travel is strictly fiction. And even if it becomes possible, Ori says, his time machine won't be able to take you into the past before it was invented. You could visit your great-great-grandchildren or vice versa, but the family won't get front-row seats at the signing of the Magna Carta.

EDITED BY YUDHIJIT BHATTACHARJEE

In the Media

CREATIONIST SPIN. Dutch evolutionary biologist Gerdien de Jong doesn't like how the EO, an evangelical public broadcasting group, has been editing the work of BBC documentary maker David Attenborough. So she's put on YouTube and on a Dutch evolution blog a sample of what she considers egregious examples from Attenborough's series *The Life of Mammals*.

In the Dutch version, a voice-over translates "100 million years ago" as "long ago" and "our closest relatives" as simply "apes." Entire scenes are removed, including one in which Attenborough, brandishing a flashlight, wanders through a dark forest to explain mammals' modest place before the dinosaurs died out, and another in which he explains how marsupials ended up in Australia and South America thanks to continental drift. And his episode on human evolution is entirely excluded. "I want the EO to stop censoring," says De Jong.

A spokesperson says the station has the right to edit the documentaries to avoid contradictions with the biblical account of creation, which the BBC confirms. Attenborough himself seems unperturbed. The list of omissions faxed to him by a reporter "seemed fairly innocuous to me," he told *Science*.

HONORS

INDELIBLE. The government of Greece has issued a postal stamp in honor of Greek neurophysiologist George Cotzia, who pioneered the use of L-dopa—a chemical similar to dopamine—for the treatment of Parkinson's disease. Cotzia was a "rare intellectual with a high consciousness of his mission," says Spyros Markelos, a biologist at the University of Athens Medical School in Greece. The stamp marks the 30th anniversary of Cotzia's death.

EMBO PRIZE. Jan Löwe of the Medical Research Council's Laboratory of Molecular Biology in Cambridge, U.K., is the winner of this year's Gold Medal from the European Molecular Biology Organization. Löwe wins the prize—which includes a cash award of $14 000—for his studies on the structure and function of proteins involved in bacterial cell division.

MOVERS

YOUNG AT HEART. The head of one of the largest biomedical philanthropies in the United States has announced her retirement after 13 years on the job. Enriqueta "Queta" Bond, 68, will step down as president of the Burroughs Wellcome Fund (BWF) next year, but she intends to remain "involved in science policy and philanthropy."

Bond oversaw a doubling of BWF's endowment to $800 million and led a movement to improve opportunities for young biomedical researchers. Under her leadership, BWF launched several initiatives to help early-career scientists become independent, which became a model for the National Institutes of Health's Pathway to Independence Awards that were set up last year.

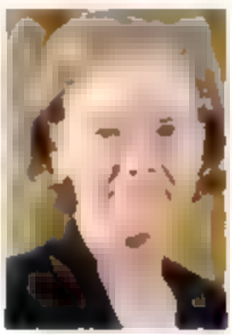

In addition to fellowships, BWF has supported scientific career development by co-sponsoring lab management courses with the Howard Hughes Medical Institute and by supporting the AAAS/*Science* career-development site, *Science* Careers. "We need to continue to invest in people and take risks on young scientists," she says.

CAMPAIGNS >>

TESTING HIS MEDAL. Nobelist Torsten Wiesel has spent a lifetime championing human rights around the world. Last month, the neuroscientist and former university administrator made his case directly to President George W. Bush during a White House ceremony to honor the winners of the 2005 and 2006 National Medals of Science and Technology.

After receiving his medal, Wiesel handed Bush a letter expressing concern about the government's treatment of prisoners at Guantanamo Bay and its policy of "not giving full recognition" to the Geneva Convention. Wiesel says Bush put the letter in the inside pocket of his jacket without comment.

Wiesel, who along with David Hubel did pioneering research on how the visual system works, says he was inspired by a similar act by a group of high school students visiting Washington, D.C., this summer as Presidential Scholars. "I am not a publicity seeker, but I thought to say nothing would be shameful," says the Swedish-born Wiesel, a former president of Rockefeller University who served as chair of the National Academies' Committee on Human Rights from 1994 to 2004. "The United States has lost its standing as a beacon of freedom. It is much more difficult for us today to lecture other countries about human rights because they can turn around and ask, 'What are you doing in Guantánamo?'"

Genes and glaucoma 735

Congress's prescription for innovation 736

BIOSECURITY

U.K. Labs Suspected as Source Of Foot-and-Mouth Outbreak

In what could prove an eerie replay of a 1960 incident, U.K. officials and scientists this week were investigating what looks like an accidental but potentially highly embarrassing release of foot-and-mouth disease (FMD) in the county of Surrey. Tests had indicated that the virus—which by Tuesday had hit two farms—belonged to a strain that has not recently circulated in animals but is present at the Institute for Animal Health (IAH) in Pirbright, close to the affected farms, and at Merial, a vaccine company housed on the same premises.

Officials at IAH and Merial have said they are unaware of any safety breaches, but biohazard teams quickly visited both labs to look for signs of a viral escape, and scientists were further analyzing the outbreak's strain to shed more light on its origins. A government report released Tuesday night as *Science* went to press concluded that "there is a strong probability that the FMDV strain involved in the farm outbreak originated from the IAH or the Merial sites." Scientists were already expressing concern that the episode could undermine public support for high-containment labs, especially a new one planned in the United States.

In the U.K., this week's images of cordoned-off farms and culling teams revived memories of the catastrophic FMD outbreak of 2001. During that episode, the government ordered the destruction of some 6 million sheep, cattle, and pigs to stamp out the disease, which also spread to the Netherlands, Ireland, and France. This time, the government response has been much swifter, and the virus may be thwarted before more than a handful of farms are affected, says Neil Ferguson of Imperial College London, one of several scientists who helped guide policy in 2001 by building models of the virus's spread. Ferguson and other modelers have been enlisted again, but with only two farms affected, "there's not a whole lot of modeling we can do," he says.

Even if major losses to U.K. agriculture and tourism can be averted—the European Union has already imposed a ban on U.K. meat exports—the limited data so far suggest that a biosafety breach occurred. On Saturday, the U.K.'s Department for Environment, Food and Rural Affairs announced that tests at IAH had shown the virus to be very close to a strain called O1 BFS67, which was isolated in Great Britain in 1967. Merial, a joint venture between Merck and Sanofi-Aventis, grows that strain to create vaccines, primarily for countries outside the European Union. IAH also has that strain for research and diagnostic purposes; as the global FMD reference center, it maintains a large collection of strains.

Several groups are investigating the outbreak, including an independent panel led by Imperial College molecular epidemiologist Brian Spratt; researchers familiar with the effort say Spratt's panel is awaiting the full genome sequence of the virus found on the farms. Comparing that to strains at IAH and Merial should help pinpoint the culprit, says Martin Hugh-Jones of Louisiana State University in Baton Rouge. But Ferguson says if both labs happened to have the exact same strain and if there aren't other signs of biosafety problems—such as virus outside high-containment areas—"we may never find the smoking gun."

Pirbright has been the source of an FMD outbreak before. In January 1960, animals at a single farm close to what was then called the Animal Virus Research Institute became infected with a South African strain of the virus, "which had apparently escaped through the Institute's ventilation system," according to a 1969 report on FMD by a panel of experts. Improvements in containment technology and procedures were supposed to make such accidents a thing of the past, however. At the safety level required for FMD work, labs operate under negative pressure so that air flows in, not out, through any leaks. All outgoing air is filtered twice, wastewater is sterilized, and garbage incinerated. Workers must shower and scrub before going home.

A 2001 review did raise questions about the state of facilities at IAH, however. Although the review didn't specifically warn about safety, it did conclude that "some of the laboratories and other areas of the Pirbright estate are not close to the standard expected of a modern biomedical facility." The report helped pave the way for an expansive building project that started in 2003; construction of a new high-containment lab is still under way, an IAH spokesperson says.

On Monday, U.K. Chief Veterinary Officer Debby Reynolds said that the recent floods may have carried the virus to the farm after it was released through a drain. Even that scenario would still imply a technical or human error, however, and some infectious-disease researchers worry that the incident will cause public distrust. In the United States, for instance, the FMD outbreak could trigger worries among the five communities that may host the new National Bio and Agro-Defense Facility, which will also be home to FMD work. "It's obviously a concern. It's a situation we're going to monitor very closely," says David Lee, vice president for research at the University of Georgia, Athens, one of the five sites being considered.

—MARTIN ENSERINK

With reporting by John Travis and Jocelyn Kaiser.

Under suspicion. The U.K.'s Institute for Animal Health is a possible source of the virus that caused foot-and-mouth disease among cattle on two nearby farms.

CREDIT: JANE MINGAY/PA PHOTOS/LANDOV

HUMAN EVOLUTION

New Fossils Challenge Line of Descent in Human Family Tree

Ever since the famous fossil hunter Louis Leakey found a skull of *Homo habilis* in Olduvai, Tanzania, in 1960, researchers have thought that this 2-million-year-old hominid was the first member of our own genus, *Homo*. This "handyman's" relatively big brain and association with flake tools eventually convinced many paleoanthropologists that *H. habilis* gave rise to *H. erectus* between 2 million and 1.6 million years ago, in a neat line of descent that led to modern humans.

Now, this gradual succession that dominated textbooks for decades is being challenged by none other than Leakey's daughter-in-law and granddaughter, Meave and Louise Leakey. This week in *Nature*, the Leakeys and their international collaborators describe the discovery of a surprisingly recent upper jawbone of *H. habilis* in Kenya that persisted until 1.44 million years ago. The team also found an older skull of *H. erectus* in the same region, which, taken together with earlier discoveries of this species, extends the time that the two types of humans lived in the same Lake Turkana basin to half a million years. "Their coexistence makes it unlikely that *H. erectus* evolved from *H. habilis*," says paleontologist Meave Leakey, an associate of the National Museums of Kenya in Nairobi.

Some other researchers agree. "Half a million years suggests that we are dealing with two lineages, not one with a bit of overlap," says paleoanthropologist Bernard Wood of George Washington University in Washington, D.C. But others question the identification of the jawbone as *H. habilis*, given that it depends on three worn teeth. When it comes to possible ancestors, "*Homo habilis* is all we've got," says paleoanthropologist Philip Rightmire of Harvard University. "I don't see any compelling reason to reject this species as the antecedent to *Homo erectus*."

H. habilis arose during a time, 2 million to 3 million years ago, when there is a gap in the fossil record. As a result, no one knows where it came from or how it is related to the smaller-brained, more apelike australopithecines such as the fossil Lucy, whose species *Australopithecus afarensis* lived 3 million to 3.6 million years ago.

H. erectus appeared about 1.8 million years ago in Africa and Asia, in both places with a larger brain and other more modern features. The lineage of *H. habilis* to *H. erectus* had seemed straightforward, even though earlier discoveries showed overlap between them. But the new discoveries on the east side of Lake Turkana in Kenya suggest the two coexisted for so long that they must have adapted to different niches, says Leakey. If so, the team concludes, it's unlikely that *H. habilis* gave rise to *H. erectus*. "The unilineal picture, where you start with this smaller, more primitive thing and it gradually gets bigger brains, bodies, and limb proportions—that really doesn't work," says co-author Susan Anton of New York University.

Gender gap? A tiny *Homo erectus* skull found in Kenya shows that the species had a huge variation in brain size, possibly due to sex differences.

CREDIT: NATIONAL MUSEUMS OF KENYA; PHOTO BY F. SPOOR AND J. READER

A more likely scenario, Leakey says, is that both species arose from another, yet-to-be-identified ancestor. Several other fossils have been proposed as candidates for that role, but so far the evidence is "not satisfactory" to nail down a connection, says paleoanthropologist William Kimbel of Arizona State University in Tempe.

But Rightmire defends an early "*habilis*-like creature" as the most likely ancestor of early *H. erectus*. Fossils of early *H. erectus* that date to 1.7 million years from Dmanisi, Georgia, show affinities with *H. habilis* and lack some traits that appeared later in *H. erectus* in Africa, suggesting that *H. erectus* arose from one group of *H. habilis* in Asia and later migrated to Africa, Rightmire says (*Science*, 5 July 2002, p. 26).

Meanwhile, the new skull of *H. erectus* from the Ileret area east of Lake Turkana is revealing that this ancestor came in many sizes. "What is truly striking about this fossil is its size," says co-lead author Fred Spoor, a paleontologist at University College London. With a cranial capacity of just 691 cubic centimeters, it is the smallest *H. erectus* ever found and is almost as small as some skulls of *H. habilis*. Yet it is not primitive or transitional from *H. habilis*. The new skull dates to 1.55 million years ago, which "nicely shows that there were big *H. erectus* and little ones for a long time," says Anton. Because the worldwide variation is greater than that between living male and female humans or chimpanzees but less than that between male and female gorillas, some researchers suspect that male *H. erectus* might have been significantly larger than female *H. erectus*.

The skull also shows features that had previously been seen only in Asian fossils of *H. erectus*, such as a keel (or ridge) on its frontal and parietal bones. These traits had persuaded a growing number of researchers in recent years to split the fossils of *H. erectus* into two species, with *H. erectus* from Asia and *H. ergaster* from Africa. But the skull's mix of traits shows *H. erectus* cannot be "easily divided between two species from Africa and Asia," says Spoor. Kimbel and Arizona State graduate student Claire Terhune reached a similar conclusion after studying the temporal bones of 15 *H. erectus* skulls, in a paper published in the July issue of the *Journal of Human Evolution*.

Others who have championed *H. ergaster* are taking note. "The new cranium blurs the distinction between *H. erectus* and *H. ergaster*," says Wood. "I am not willing to sell my shares in *H. ergaster* just yet, but I am not relying on them for my retirement!"

–ANN GIBBONS

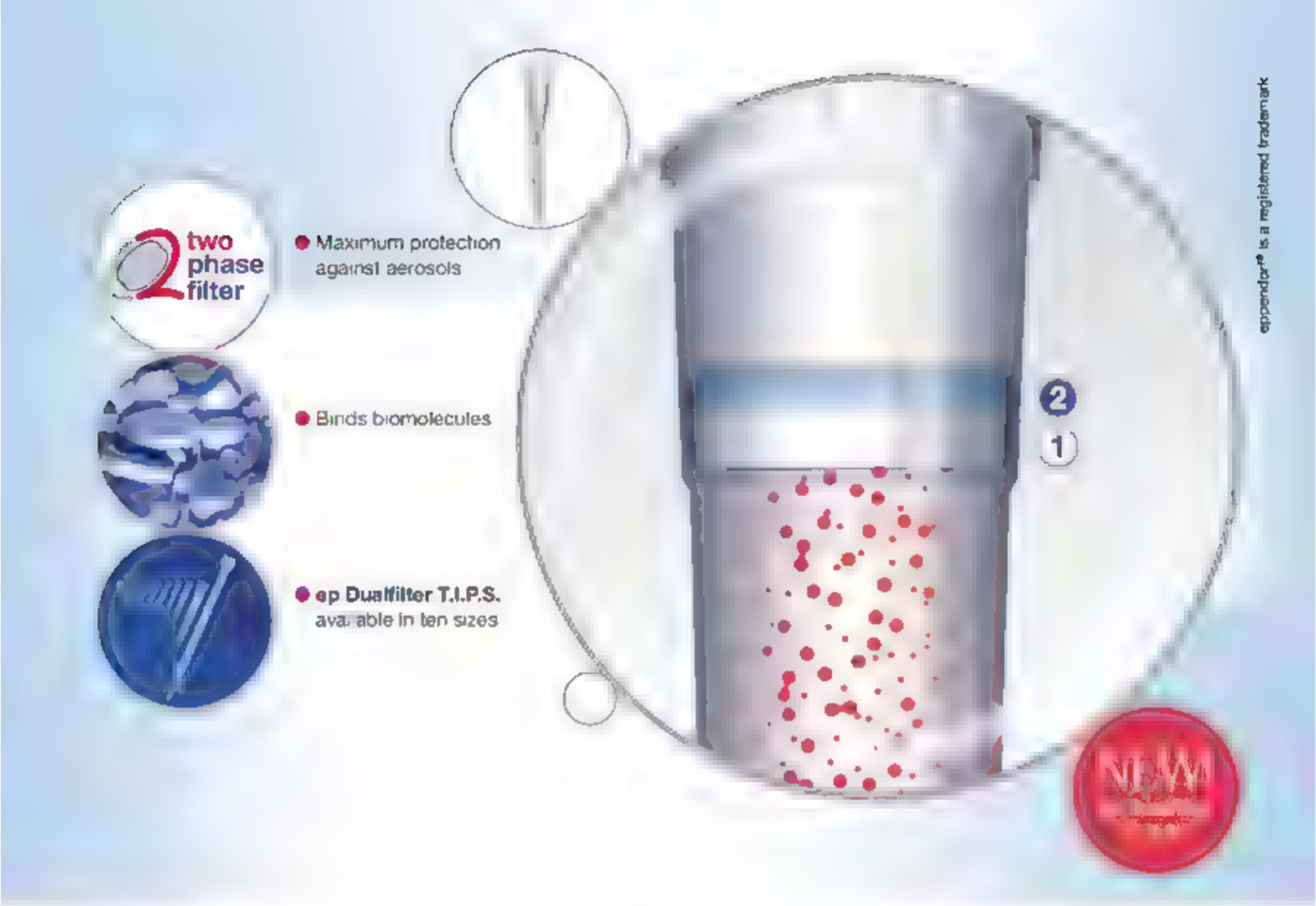

Stop aerosols!

Unique two phase filter protection with ep Dualfilter T.I.P.S.™

The new Eppendorf ep Dualfilter T.I.P.S., with their unique two-phase filter, provide the perfect shield against contamination.

The filter consists of two visible phases, each with a different pore size. This two-phase filter protection ensures ultimate absorption of aerosols ❷ and biomolecules ❶, outmatching all conventional filters. Rely on it.

For more information go to
www.eppendorf.com/dualfilter

Features of the ep Dualfilter T.I.P.S.
Double protection provided by the two phase filter
- Provides maximum protection for both pipette and sample
- Ultimate absorption of aerosols and biomolecules
- Free from PCR inhibitor additives
- Patent pending two phase filter technology
- Supplied sterile, Eppendorf PCR clean and pyrogen-free
- IvD conformity
- Batch-related certificates available

eppendorf
In touch with life

Your local distributor: www.eppendorf.com/worldwide · Application Support: +49 180-3 66 67 89
Eppendorf AG · Germany · +49 40 538 01-0 · Eppendorf North America, Inc. 800-645-3050

GENETICS

High-Risk Glaucoma Gene Found in Nordic Studies

Glaucoma can be an insidious disease. It often develops painlessly, robbing its victims of their sight so gradually that they barely notice at first. Conventional wisdom holds that a buildup of pressure in the anterior chamber of the eye causes the vision loss by damaging the optic nerve. But why that pressure increases for the most part remains a mystery. Now, researchers have a new clue to the cause of a common form of the eye disease, one that's particularly tough to treat.

In work published online this week in *Science* (www.sciencemag.org/cgi/content/abstract/1146554), a team led by Kari Stefansson of deCODE Genetics Inc. in Reykjavik, Iceland, and Fridbert Jonasson of the University of Iceland reports the discovery of a gene variant that confers an extremely high risk of developing exfoliation glaucoma. This form of glaucoma accounts for perhaps as many as 10% of all cases in the United States, yet it responds poorly to the current treatment of eye drops that lower pressure in the eye. The genetic find might lead to better ways to diagnose and prevent the slow descent into blindness. "I think it's a great paper. ... People with this glaucoma have a much higher risk of going blind," says Mary Wirtz, an expert in glaucoma genetics at Oregon Health and Science University in Portland.

Stefansson and his colleagues found the gene using a genomewide association study, a method that is fast becoming the standard way to track down disease genes (*Science*, 11 May, p. 820). This technique identifies small variations in gene sequences known as single-nucleotide polymorphisms (SNPs) that occur in greater frequency in people with the disease under study—in this case 195 Icelandic glaucoma patients—than in unaffected persons. One SNP variant stood out as being associated with glaucoma, but only in the 75 people who had the exfoliation type. A subsequent study of a Swedish population confirmed the association.

This particular SNP turned out to be only indirectly related to glaucoma risk, however. It's located in a gene that makes an enzyme called lysyl oxidase–like protein 1 (LOXL1), but the SNP is in a so-called intron that doesn't encode any part of the enzyme. Still, the enzyme made sense as a possible contributor to exfoliation glaucoma, which develops when tiny flakes slough off the lens and iris of the eye. These eventually deposit in the trabecular meshwork, a small structure that allows fluid to drain from the anterior eye chamber. Blocking this drainage presumably produces the very high intraocular pressures. The exfoliated material contains tiny fibrils of a protein called elastin, which may be where LOXL1 comes into play. The enzyme helps form elastin fibrils, so its malfunction might well lead to exfoliation glaucoma.

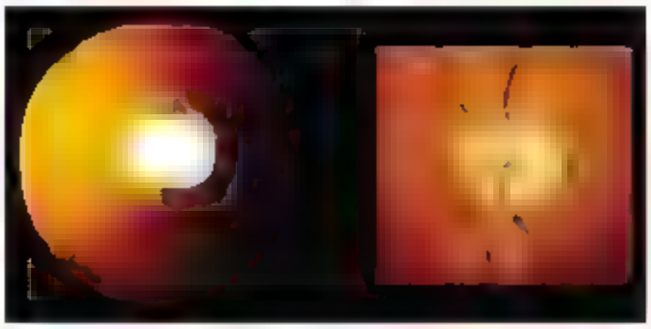

Damage signs. Exfoliation deposits appear as a rough peripheral ring around the anterior chamber of the eye (*left*), whereas in the view at right, the light central region indicates a deteriorating optic nerve.

CREDIT: G. THORLEIFSSON ET AL., SCIENCE

In a closer look at the gene, Stefansson and his colleagues turned up two more SNPs associated with exfoliation glaucoma, neither of which was examined in the original screen. These two do appear to play a role in glaucoma risk. They reside in the protein-coding portion of LOXL1, and a person carrying both of the highest risk variants is up to 700 times more likely to develop exfoliation glaucoma as persons with low-risk variants. The analysis showed, Stefansson says, that "the variant accounts for ... all or most cases of exfoliation glaucoma."

Exactly how the changes to the LOXL1 gene lead to exfoliation glaucoma remains to be determined. Studies of animals genetically engineered to have the high- and low-risk versions of the gene should help clarify this issue, Stefansson says. Once that issue is resolved, it might be possible to develop ways to correct the problem given that the eye is so accessible to treatment. And that could mean a brighter day for some glaucoma patients.

–JEAN MARX

SCIENCESCOPE

Educating India

Over the next 7 years, India plans to invest roughly $33 billion in new universities and institutes. The plan, announced last week, will add eight elite Indian Institutes of Technology and 20 regional engineering colleges, along with scores of new research, computing, and management campuses. Indian Prime Minister Manmohan Singh said the system will be a "symbol of excellence" and emphasized his commitment to offer scholarships to increase the gross enrollment rate at the college level; of India's 1.1 billion population, only 9.2 million are higher education students. The government has ordered a 50% hike in the starting stipends for grad students and postdocs.

–PALLAVA BAGLA

A Western Slant?

Young scientists from Western Europe were about three times more likely than Eastern European researchers to make the first cut in a grants competition in all disciplines from the new European Research Council (ERC). Last month, the ERC announced 559 finalists for the 250 so-called Starting Grants it plans to award before the end of the year, and only 21 work in the mostly Eastern European countries that have joined the E.U. since 2004. Although some politicians might complain that their country is being slighted, Pavel Exner, a physicist at the Czech Academy of Sciences in Prague and a member of the ERC Scientific Council, thinks that the peer review process did its job in sifting through the 9167 applications. "The point is not fairness, the point is excellence," he says.

–GRETCHEN VOGEL

Sonar Tests Halted

The U.S. Navy plans to appeal a decision this week by a federal judge to halt use of so-called active sonar during naval exercises planned through December in the southern Pacific off the California coast. "Plaintiffs have established to a near certainty that use of [active] sonar during the ... exercises will cause irreparable harm to the environment," wrote Judge Florence-Marie Cooper of the Central District of California, mentioning the Navy's own forecasted losses of beaked and ziphid whales. The Navy says the 3 August decision, in favor of the Natural Resources Defense Council and allied plaintiffs, will disrupt important antisubmarine training. The judge did not address the plaintiffs' contention that the sonar is illegal under environmental laws.

–ELI KINTISCH

Preaching to the choir. Representative Bart Gordon speaks at a rally of business, university, and legislative supporters of the innovation bill, that includes Norm Augustine (*left*) and Rep. Vern Ehlers (*far right*).

CREDIT: COURTESY OF HOUSE COMMITTEE ON SCIENCE AND TECHNOLOGY

U.S. SCIENCE POLICY

Congress Passes Massive Measure To Support Research, Education

In 2005, a U.S. National Academies' panel drew up a blueprint for sustaining economic growth by strengthening the country's research and educational systems (*Science*, 21 October 2005, p. 423). Last week, Congress adopted nearly all of its recommendations in a bill that prescribes new policies and programs at six federal agencies.

The academies' report, titled *Rising Above the Gathering Storm*, named 20 priorities, putting more and better science and math teachers at the top of the list. It also called for a sustained boost in federal spending on research, especially for the physical sciences and engineering, and increased support for those planning to become scientists. Congress folded most of those proposals into the America COMPETES (Creating Opportunities to Meaningfully Promote Excellence in Technology, Education, and Science) Act, a 407-page leviathan that authorizes $43 billion over 3 years for dozens of research and training programs. It passed the House by a vote of 367–57 on 2 August and, a few hours later, the Senate by unanimous consent.

Part of the reason for the overwhelming support was that America COMPETES is not a spending bill that appropriates money for the next, or any, fiscal year. Instead, it's an authorization bill that describes broad policies an agency should follow, specifies programs to achieve those goals, and endorses a desired spending level. It is the job of the appropriations committees to decide how much money will be spent in any particular year.

Appropriators are still working on the 12 spending bills for the 2008 fiscal year that begins 1 October. The preliminary signs are good for the three agencies—the National Science Foundation (NSF), the Department of Energy's Office of Science, and the National Institute of Standards and Technology (NIST)—that are included in the president's American Competitiveness Initiative (ACI), itself a response to the academies' report. Still, the new legislation gives appropriators lots of suggestions.

It puts NSF on a 7-year doubling track, for example, compared with 10 years under ACI, and increases many of its education programs, including a huge jump in a $10-million-a-year program to give scholarships to science, math, and engineering undergraduates who promise to teach. It declares that an NSF program partnering universities and local school districts is complementary to one at the Department of Education, rather than redundant, as the Bush Administration has argued. It greatly expands DOE's role in elementary and secondary school education, giving it the authority to create new science and math academies affiliated with its network of national labs. It authorizes a new version of an industrial research program at NIST that Republicans have long sought to eliminate, converting the Advanced Technology Program to the Technology Innovation Program and starting it off with $100 million. It also creates grants for young scientists who have failed in their first NSF submission, in hopes of bolstering their chances of success the next time around. The most controversial element is a new agency within DOE (see sidebar p. 737).

In addition to beefing up current efforts and creating a cornucopia of new programs, the legislation ties up some loose policy ends. It enshrines the social and behavioral sciences as an essential element in NSF's research portfolio, a rebuff to attempts last year by Senator Kay Bailey Hutchison (R–TX) and others to downplay their importance. And it orders the White House Office of Science and Technology Policy (OSTP) to come up with a standard policy for all agencies on the dissemination of research results, a reaction to a spate of reports that federal scientists have been hindered in publicizing studies that appear to contradict Administration policies on global warming and other hot-button issues. That will happen, promises OSTP director and presidential science adviser John Marburger, "We're a science policy shop, and we'll do what Congress tells us to do," he says.

Legislators portray the bipartisan support for science as a matter of enlightened self-interest. "This bill will help us keep our brainpower advantage," trumpeted Senator Lamar Alexander (R–TN), who shepherded the bill through three Senate panels. "Securing a brighter future for our children is simply not a partisan issue," noted Alexander's Tennessee colleague, Representative Bart Gordon (D–TN), who as chair of the science committee played a similar role in the House. Even so, only three Republicans voted in favor of moving the measure to the House floor, expressing their ire over how the Democratic majority handled the procedural steps leading to the final vote.

Why was the academies' report so influential when similar proposals to bolster science have fallen short in the past? The trick this time around, says Norman Augustine, former CEO of Lockheed Martin and chair of the panel that produced the report, was to argue in terms that the public would understand. "We quit talking about the virtues of science in the abstract and started talking about its impact on jobs," he explained about the 2-year lobbying effort by university and industry leaders. "Everybody understands jobs."

Even one-time critics say that the final legislation provides a useful road map for managing the country's scientific ▶

enterprise. "It's good for Congress to say that STEM [science, technology, engineering and mathematics] education and research are important," says Marburger. "But we have to pay for this stuff, and this bill is way over the top in terms of authorized spending and the number of new programs. My concern is that when the time comes for Congress to appropriate the money for each of these agencies, what will they choose to support?"

Gordon praised university and business leaders for being effective "cheerleaders" for the new legislation. But Augustine cautioned that their work is far from over. "Our biggest challenge is to sustain this coalition for the next 10 to 15 years, because it will take that long for the new jobs to appear," he predicts. "Still, you can't finish if you don't start, and that's what this bill does."

–JEFFREY MERVIS

New DOE Agency Sparks an Energetic Debate

Can a new agency within the Department of Energy (DOE) give the country a technological boost to develop new energy sources?

Last week, as part of a mammoth innovation bill (see main text, p. 736), Congress created the Advanced Research Projects Agency–Energy (ARPA-E) that would, as the legislation explains, identify and fund "transformational technological advances that industry by itself is not likely to undertake." To do that, the new agency's rotating program managers will fund risky projects with aggressive performance targets and timetables, an approach modeled on the Pentagon's DARPA.

Supporters say that it's important to keep ARPA-E at arm's length from the rest of the department by keeping its funding separate from the $4 billion Office of Science. But critics say the new agency will be at best a redundant layer of bureaucracy and at worst a drain on the agency's ability to fund basic research in the physical sciences.

Representative Bart Gordon (D–TN), who as chair of the House Science and Technology Committee has pushed hard for the new agency, hopes ARPA-E will catalyze partnerships among universities, companies, and national laboratories. "ARPA-E will foster a much more distributed base of energy researchers and technology developers than you see today, with the result being a vibrant domestic energy technology industry and workforce," Gordon explained shortly after last week's successful vote. Last year, Steve Chu, director of DOE's Lawrence Berkeley National Laboratory in California, said the new agency could improve DOE science by funding "activities more applied than DOE basic research programs and too basic for its applied research programs."

But others, noting current DOE efforts to patch such holes, are skeptical that ARPA-E is needed. "It's completely pointless," says Joseph Romm, head of DOE's renewable energy office during the Clinton Administration and no fan of the agency's current performance. "I don't know what DOE isn't doing that ARPA-E would be doing." Some observers also doubt that the new agency will help bring new discoveries to the market. "What it can do to further commercialization is harder to see," says Robert Fri, a former deputy secretary of energy who has led several National Academies' studies of DOE's activities. "DOE's skills in managing large science programs and large applied technology programs are not necessarily the right ones for the [new] job."

The COMPETES Act authorizes up to $300 million for the new agency in 2008 and "such sums as are necessary" for the next 2 years. But congressional appropriators haven't been enthusiastic about making more money available, and the current Administration may well drag its feet appointing a director, who must then be confirmed by the Senate. Earlier this year, President George W. Bush objected to a smaller and less independent entity that was part of the Senate bill (S. 761), expressing "serious doubts about the applicability of the national defense model to the energy sector."

–ELI KINTISCH

Growing pains. Many hopes ARPA-E will advance these and other [illegible]

CREDITS (LEFT AND MIDDLE PHOTOS COMBINED): JOVELAND WATER AND POWER; WWW.D.JOVELAND.CO.US

Breaking the Ice on Icebreakers

A campaign to build two new U.S. icebreakers is picking up steam. Last fall, a report from the National Academies said the ships are needed to preserve full and timely access to the region for a host of missions, including the National Science Foundation's Antarctic research station (*Science*, 6 October 2006, p. 33). And last week, a key Senate panel, as part of a reauthorization of the U.S. Coast Guard, ordered the agency "to acquire or construct" the new icebreakers as part of its current fleet, which includes two aging icebreakers in need of major repairs.

With melting ice promising to increase activity in the Arctic, the Bush Administration thinks the icebreakers are needed to maintain a U.S. presence for economic and national security reasons. "I think a bill such as this makes a lot of sense," presidential science adviser John Marburger told *Science*. Observers say the Coast Guard would welcome such a directive, although it has not formally requested the funds from Congress.

–JEFFREY MERVIS

Progress on Virus Deadlock

Indonesia threw global health officials into a panic last January when it stopped sharing H5N1 avian influenza samples with the World Health Organization (WHO), which has centers run by the governments of the United Kingdom, the United States, Japan, and Australia for virus analysis. Indonesia called unfair WHO's policy of passing viral samples on to pharmaceutical firms, as the resulting vaccines developed are likely to be too expensive for developing nations to use.

Last week, at a meeting of technical experts from 23 countries held in Singapore, a solution was proposed: having WHO itself assume ownership of donated biological materials, better positioning the organization to negotiate how those samples are used. The idea drew the support of "almost all countries," says Masato Tashiro, director of the WHO Collaborating Centre for Reference and Research on Influenza in Tokyo. He cautions that the details have yet to be worked out.

WHO's David Heymann says that even if WHO assumed ownership, it would still provide viruses freely to vaccine manufacturers. He adds that WHO is working on mechanisms to ensure vaccines would be available to developing countries during a pandemic, but he doesn't foresee a move to link virus sharing with virus benefits. The issue will be taken up at a meeting of WHO member states in early November.

–DENNIS NORMILE

AIDS RESEARCH

Feud Over AIDS Vaccine Trials Leads Prominent Italian Researchers to Court

Impassioned debates have swirled around several AIDS vaccines, with proponents aggressively pushing for larger trials in humans and detractors contending that little evidence suggests that the given approach will succeed. If no serious safety concerns exist, the issue typically comes down to money, peer-review committees, blue-ribbon panels, or deep-pocketed pharmaceutical companies ultimately decide whether the trial receives the many millions of dollars needed. But a dispute about the merits of an AIDS vaccine being developed by a leading Italian researcher, Barbara Ensoli of the Istituto Superiore di Sanità (ISS) in Rome, has wound up in a different venue: the courtroom. Ensoli is suing another prominent Italian investigator, immunologist Fernando Aiuti of the University of Rome "La Sapienza," for what she contends is damage to her reputation. Aiuti, a former collaborator of Ensoli's, has assailed what he sees as critical flaws in the early clinical trials of the vaccine.

The feud raises serious questions about the boundaries of academic debate and the conduct of clinical trials, as well as how the Italian government sets its HIV/AIDS research priorities. HIV co-discoverer Robert Gallo, in whose lab Ensoli worked for many years, says her battle with Aiuti has caught the attention of many Italian AIDS researchers who are frustrated that their government has committed tens of millions of euros to Ensoli's project while they struggle to find funding for their own work. "It's disproportionate to the money available to other scientists," says Gallo, who now directs the Institute of Human Virology at the University of Maryland School of Medicine in Baltimore. "That's the background to all of this."

And there's a dash of soap opera in the mix, too, given that Aiuti was once Ensoli's mentor, employed her brother, collaborated with her former husband and former sister-in-law, and ran one of the centers that helped test her AIDS vaccine. "It's a classic Roman infight," says one Italian AIDS researcher who did not want to be quoted by name. "We are all refusing to be dragged into this."

Ensoli has taken an unusual approach to developing an AIDS vaccine. Most AIDS vaccines in development combine several HIV genes or their proteins, but Ensoli has focused on one HIV protein, Tat, that helps the virus produce more copies of itself. Ensoli hopes that bolstering the immune response to Tat can prevent infections and also help people who are already infected. Although Ensoli has reported some success in monkey studies with her Tat vaccine, studies by several other labs that used different conditions have not had the same success. "There's no body of data that suggests this vaccine will work," says retrovirologist Genoveffa Franchini of the U.S. National Cancer Institute (NCI) in Bethesda, Maryland. Franchini, who collaborated on a monkey study of a Tat vaccine that failed and once worked with Ensoli in Gallo's lab, adds, "I don't think it has any chance." Gallo, who says Ensoli was a useless worker in his lab, similarly believes her Tat vaccine has dim prospects, and he has long cautioned that the form of Tat in her vaccine could potentially suppress some immune responses.

> If you're in science, you're very well used to getting criticisms. **But scientific criticisms based on science is one thing and defamation is another."**
>
> Barbara Ensoli

The saga began in January 2004 when ISS launched phase I trials of Ensoli's Tat vaccine to test for toxicity in both HIV-infected and uninfected people. Researchers conducting the two studies aimed to recruit 88 volunteers in 3 months. Few people initially volunteered, and Aiuti and investigators running other sites were allowed to continue enrolling until the end of the year. But in November 2004, over Aiuti's objections, ISS decided to stop enrolling people into both trials, which then had a total of only 47 participants. Although the trials were placebo-controlled and the investigators were not told who received the actual vaccine, Ensoli backed the decision, she says, because ISS determined that the trial had met its endpoints. No serious safety issues had surfaced, and blood tests showed that a significant number of participants had developed immune responses to Tat. "When you reach the endpoint, it's not ethical to continue the trial," says Ensoli.

On 11 July 2005, inspectors at the Agenzia Italiana del Farmaco (AIFA)—Italy's equivalent of the U.S. Food and Drug Administration—wrote a harsh report about the conduct of the clinical trials, highlighting several "critical deviations" from the original protocol. In addition to noting that researchers had not enrolled the number of people specified and had failed to seek amendments to change the protocols, AIFA's inspectors reported that clinicians had difficulty removing all of the vaccine solution from the vials, making it technically impossible in 70% of the cases to administer the specified dose.

Aiuti, who says he received a copy of the document from several

CREDIT: REUTERS

sources including the hospital he works with, raised the issues identified by the AIFA investigators in letters to several university and government officials. Ensoli charges in her lawsuit that he had no right to share this confidential document with them. Aiuti counters that no one told him it was confidential and that it was his duty to report the serious findings to officials.

In a 26 July 2005 letter, AIFA Director Nello Martini accepted ISS's explanations, writing in a letter addressed to Ensoli, ISS officials, and a company hired to oversee the studies that neither the change in enrollment nor the problem with the vaccine itself compromised the trials, which he wrote indeed hit their endpoints.

Aiuti stepped up his efforts to inform the media, public officials, and colleagues about what he saw as the shortcomings of the trials. "It's not enough to say there are no problems," insists Aiuti, who says he believes that Martini too readily dismissed the deviations that his inspectors found. "Just the word of the AIFA director is not enough. All the data of the four inspectors were very specific. There is not a single reply from any of the inspectors." Ensoli says the assertion that Martini does not speak for his inspectors is ludicrous. "It's totally untrue," she says. Martini did not respond to e-mailed questions about Aiuti's allegation.

Ensoli was particularly perplexed that Aiuti suggested in a letter to the health minister that conflicts of interest compromised the study. Ensoli's brother was appointed to run the core lab, and her brother's ex-wife helped run the clinical trial. "We all come from Aiuti's] lab, which is funny," says Ensoli. "When we were all working in his lab, everything was okay. When we left, it was a conflict of interest, which is totally crazy."

Despite Aiuti's complaints, Italy's Ministry of Health and, separately, Ministry of Foreign Affairs decided to invest heavily in staging larger phase II studies of the vaccine in both Italy and Africa. In a December 2005 press release quoted in Ensoli's lawsuit, Italy's then minister of health claimed "there has never been an AIDS vaccine, as we can see in research from the whole world, which has seen such success during research." In all, the Italian government committed €21 million for expanded trials in Italy and another €31 million for an extensive AIDS program in South Africa that includes phase II trials of Ensoli's vaccine. None of this funding was subject to peer review, though Ensoli notes that the decisions were based on results from the phase I studies and that a scientific committee at ISS reviewed the data. Aiuti, not surprisingly, thinks the funding is a mistake. "I don't think this vaccine should move to phase II trials," he says.

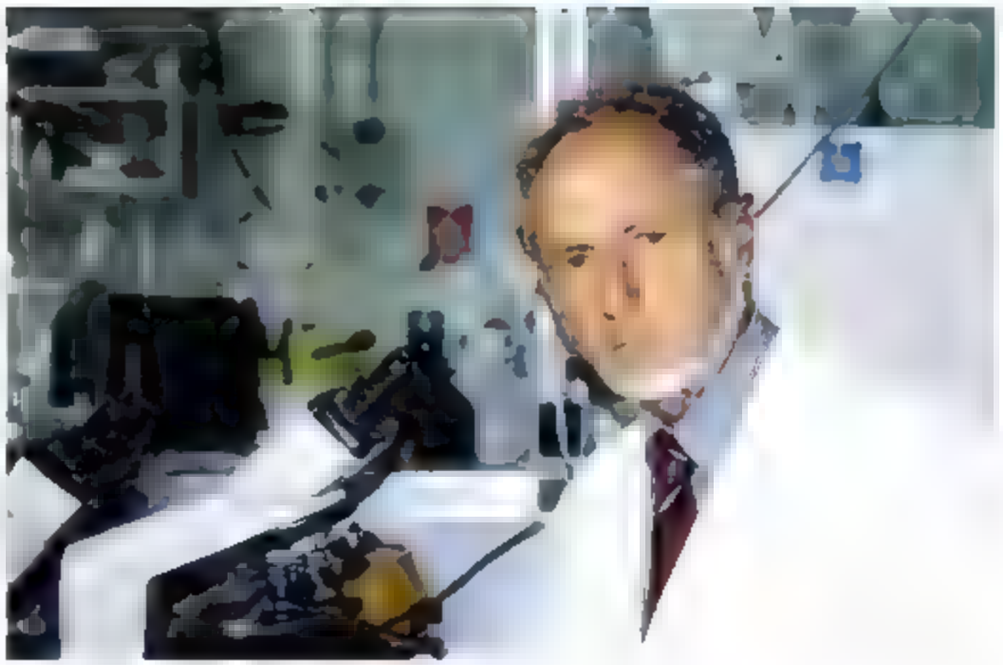

CREDIT: COURTESY OF FERNANDO AIUTI

> Criticism is less tolerant" in the Italian scientific community than elsewhere
> **"I don't think this vaccine should move to phase II trials."**
>
> Fernando Aiuti,
> University of Rome "La

Ensoli filed suit against Aiuti this May. She alleges that he "went beyond the limits of his legitimate right to criticize" and damaged her reputation, citing a newspaper article that is headlined "Aiuti: AIDS Vaccine a Trick to Find Funding." (Aiuti denies he said any such thing, and the article does not directly quote him making that statement.) Ensoli further charges that Aiuti "overstepped the line in criticism" in other statements to the press that derided the decision to stop enrollment. She alleges that his "inappropriate use" of the AIFA report was a "malicious diffusion of false information," and she charges that he spread "false information about her supposed use of privilege to involve members of her family in the research program." The suit concludes with an allegation that Aiuti, in a "wholly arbitrary and unlawful fashion," wrote the ministries of health and foreign affairs to "denigrate" her work.

Ensoli is seeking €2.5 million for damages to her reputation and the resultant loss of income from speaking engagements. "If you're in science, you're very well used to getting criticisms," says Ensoli. "But scientific criticism based on science is one thing and defamation is another." Aiuti, she charges, is not making a good-faith attempt to critique these studies. "There was an intention to sabotage here," claims Ensoli.

Aiuti says he has "nothing personal" against Ensoli and was surprised that she sued him, but he emphasizes that he has not changed his opinions. "Criticism is less tolerant" in the Italian scientific community than elsewhere, he says. "The Latin mentality is in part responsible."

Glenda Gray, who heads a unit at Chris Hani Baragwanath Hospital in Soweto, South Africa, that is considering conducting phase II studies of the vaccine, contacted Ensoli after learning of Aiuti's concerns to inquire about enrollment and other issues. Ensoli replied in an e-mail that she thought Gray was "acting like a court of law." Gray wrote back that she construed this as "threats of legal action" and decided to forward the matter to her institutional review board, which she told *Science* will now try to get to the bottom of what she sees as the biggest outstanding question: Why was enrollment stopped so abruptly?

Ensoli says phase II therapeutic studies will start in Italy during the next few months, and she's now making a second-generation preventive vaccine that will contain the HIV envelope protein as well as Tat. The court case against Aiuti is slated to come to trial in October, and ISS leaders urged its board of directors in a 17 July memo to file a separate suit against Aiuti to "defend its own image and professional reputation and seek payment of the damages it has suffered." Aiuti says he may countersue.

–JON COHEN

The Fellowship Of the Hobbit

Adversaries join debate with momentous implications: whether a tiny human fossil found in Indonesia is a new species—mulled fresh data on followed hunt. But the hobbit remains an enigma.

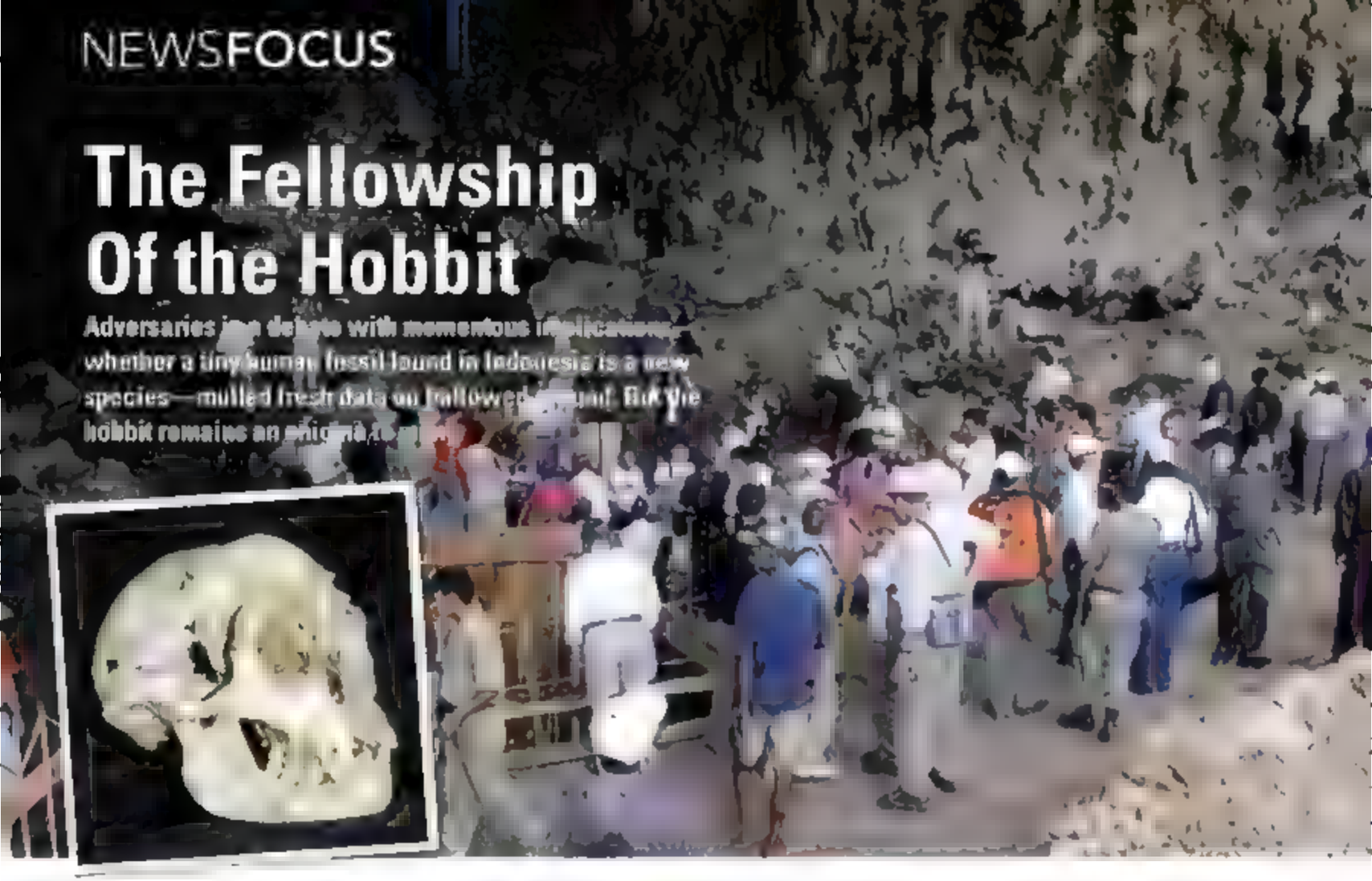

FLORES, INDONESIA—Liang Bua cave, as big as a concert hall with a domed ceiling and a giant stalactite for a chandelier, thrums with the din of a portable generator and excited conversation in many languages. Fifty anthropologists plus a retinue of villagers, police, and curious children mill about in cool air that smells faintly of damp rock and cigarettes. The researchers are on a pilgrimage to ground zero of one of the most contentious debates in human evolution. Here, in 2003, the skull and skeleton of a meter-tall adult woman were unearthed. Ever since, experts have sparred over the "hobbit": Is it an astonishingly primitive species with a tiny head, dubbed *Homo floresiensis*, or a diseased member of our species, *H. sapiens*?

The stakes are high. A new species shakes to the core ideas about the defining role of big brains in our genus and about relations among hominids. The hobbit bones are dated to as recently as 12,000 years ago, so the diminutive hominid must have lingered on Flores for thousands of years while modern humans colonized nearby islands. The tiny human suggests that big brains aren't required for making tools—and, according to a theory proposed by the hobbit's discoverers, may imply that the first hominid migrated out of Africa far earlier than anyone had thought. "Flores is the thorn in the flesh. [It implies] that we have to rethink everything," says anthropologist Maeta Ponce de Leon of the University of Zurich in Switzerland.

The visit to Liang Bua cave was the culmination of an unprecedented gathering* of the hobbit's discoverers and their critics, several of whom had battled fiercely in print and on film but had never met in person. For the most part, adversaries were on their best behavior, like feuding relatives gathered for a reunion. Conference organizer Teuku Jacob of Gadjah Mada University in Yogyakarta has argued that the hobbit is a diseased *H. sapiens*. Two years ago, he borrowed the bones for study over the objections of co-discoverer Mike Morwood of the University of Wollongong, Australia, some of the bones were broken upon return (*Science*, 25 March 2005, p. 1848). But Jacob was unfailingly smiling and polite to all, and Morwood made a point of speaking to each critic. Still, divisions run deep among both Indonesians and foreigners.

At the meeting, funded generously by businessman and philanthropist Hashim Djojohadikusumo, who paid for the travel and five-star accommodations for all presenters, researchers heard much of the latest thinking on crucial aspects of hobbit science and lore, from cave geology to an unsuccessful hunt for living "orang pendek," mythical humanlike creatures that legends say once roamed Flores. The critics, most of whom were in attendance, were unshaken in their belief that the hobbit is a pathological modern human, perhaps one who suffered from microcephaly, a disorder that results in a tiny head, or from a growth hormone insensitivity called Laron syndrome.

Meanwhile, a growing number of those working on the bones, several of whom were not invited or chose not to attend, are

*Joint national Seminar on Southeast Asian Paleoanthropology, 22–29 July, Yogyakarta, Indonesia.

Field captain. Co-discoverer Mike Morwood defended his team's view of *Homo floresiensis*.

CREDITS (TOP TO BOTTOM): A. TALAS/REAL PICTURES; D. ARGUE/AAAS; A. TALAS/REAL PICTURES

Cave exploration. Liang Bua, home of the "hobbit" (*inset*), swarms with researchers.

convinced that they are dealing with a new phenomenon in human evolution. "This is a different species for sure," says William Jungers of Stony Brook University in New York, who is working on the skeletal bones but was not invited. "There is no pathology that recapitulates early hominid morphologies and proportions." Others haven't made up their minds, perhaps in part because the bones themselves were deemed by the Archaeological Institute in Jakarta to be too fragile to send to the conference for viewing. "It was a pity we didn't see the fossils," said Zhao Lingxia of the Institute of Vertebrate Paleontology and Paleoanthropology in Beijing, as she picked up her baggage after the last trip. "I am not sure what (the hobbit) is."

Reading the bones

Even for scientists steeped in the mysteries of the hobbit, the seminar offered surprises. One was from archaeologist Carol Lentfer of the University of Queensland in Brisbane, Australia, who analyzed residues and polish on the edges of stone tools found in Liang Bua. Under the microscope, substances such as animal hide, wood, and plant materials leave telltale traces on stone. Because the tools were found near animal bones, especially baby pygmy elephants called *Stegodon*, researchers had inferred that the little people used the tools to process meat. But to Lentfer's surprise, most of the tools she examined were used for working with woody and fibrous plants, perhaps to craft spear shafts of wood or bamboo or items like traps. "It looks like a tool kit for making other tools," she said in her talk.

Whatever the tools were for, some experts aren't sure that hobbits made them. James Phillips of the Field Museum in Chicago, Illinois, has argued that long, narrow blades removed sequentially from blade cores are too sophisticated to have been made by anyone other than a member of our species. That means that the hobbit must have been part of a *H. sapiens* population, he said. Harry Widianto of the Centre for Archaeology in Jakarta also believes that the tool kit belonged to our species. The tools were made with "very high skill," he said, and resemble artifacts found in other Indonesian caves, including those occupied more recently.

But every shred of hobbit evidence has conflicting interpretations. Morwood and two colleagues—hobbit excavator Thomas Sutikna of the Centre for Archaeology and archaeologist Mark Moore of the University of New England in Armidale, Australia, who did his Ph.D. on the artifacts—don't agree that they are sophisticated. Moore, who was not invited to the meeting, told *Science* that although "blades"—flakes twice as long as they are wide—are found at Liang Bua, there is no evidence that they were flaked deliberately, as seen in classic *H. sapiens* tools. "These are simple stone artifacts," agrees Sutikna.

When it was Morwood's turn at the podium, he emphasized the evidence against the theory that the hobbit was a modern human. His voice crackling with intensity, Morwood reminded colleagues that the famous skull and skeleton known as LB1 is not alone. To date, the team has found an additional jaw bone plus various bones of the leg, arm, and shoulder, all petite, from different layers. "We have a minimum of 12 individuals going back to 95 000 years ago," he said. "That's twice the accepted date for *H. sapiens* in Southeast Asia and Australia. Twice the accepted date, okay?" He adds that the hobbit layers show no traces of pigments, ornaments, or formal burial—all signs of *H. sapiens* that are found in the cave's upper levels.

Morwood also underscored the similarities among the hobbit bones. "The radius and leg bones in the deeper deposits have the same unique characters as seen in the higher levels," he said. Because it's highly unlikely that only diseased individuals died in the cave over thousands of years, the additional specimens rule out pathology, he said. But critics have argued that, except for the tiny brain, some hobbit traits are also seen in living Southeast Asians and so aren't signs of either pathology or a new species (*Science*, 25 August 2006, p. 1028).

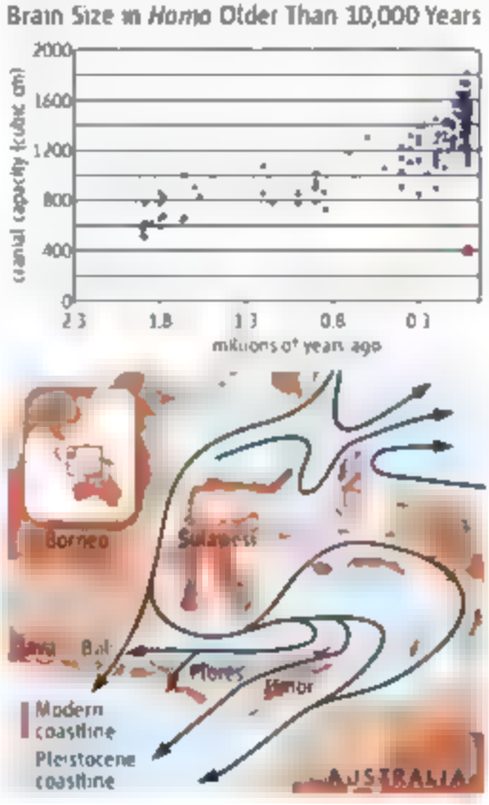

Misfit? The hobbit's tiny brain (in red, *top*) stands out when plotted with those of other hominids, discoverers say it evolved on Flores thanks to currents that isolated the island (*bottom*).

Not the brainiest

For others, no trove of skeletal bones can compensate for the puzzle of that puny brain. Short stature alone does not mean that it is a distinct species, as small stature is known from living pygmies, including those in the village of Rampasasa near Liang Bua, say Jacob and others. But pygmies have brains nearly the same size as those of other modern humans. The minute brain that would have fit inside LB1's skull was only 400 cubic centimeters, compared to the roughly 1350 cubic centimeters seen on average in living humans (see graph). "Flores falls outside the range of anything I have seen before," said Robert D. Martin, a paleoanthropologist at the Field Museum.

Martin and other presenters suggested that LB1 was diseased, perhaps suffering from microcephaly, Laron syndrome, or both. The Laron's hypothesis debuted in the hobbit debate on 27 June, in a paper published online in the *American Journal of Physical Anthropology* by a trio from Tel-Aviv University who were not at the meeting: Israel Hershkovitz, Liora Kornreich, and Zvi Laron, discoverer of the disease. Their paper lists Laron's symptoms—although with few measurements—that are also seen in hobbits, including pillars of bone near the nose, a short clavicle, a curved tibia, and an upper arm bone whose top end is not twisted. Some of these traits have been considered signs of a primitive ancestry for *H. floresiensis*. "All [Laron's] patients share a battery of traits, which they also share with *Homo floresiensis*," Hershkovitz and Laron told *Science*.

At the meeting, Dean Falk of Florida State University in Tallahassee, who has concluded from computed tomography (CT) scans of the skulls of LB1 and microcephalics that the hobbit is a new species, tackled the Laron's hypothesis head-on. Hershkovitz and colleagues note that many Laron's patients also lack the sinuses of a normal human head. And although in most people the texture of the mastoid process—the bony bump behind the ear—is spongy and air-filled, in Laron's patients this bone is dense. CT scans of LB1's skull show that it has normal sinuses and a porous mastoid process, Falk said. "We don't

SOURCE (TOP TO BOTTOM): AFTER DE MIGUEL AND HENNEBERG, 2001; AFTER MORWOOD AND VAN OOSTERZEE, 2007

think LB1 comes close to looking like their description of Laron's," she said firmly. Hershkovitz responds that some Laron's patients do have normal sinuses, and so their presence does not disprove the hypothesis.

Island living

If the hobbit is a new species, who were its ancestors? Morwood's team once postulated that *H. floresiensis* evolved from *H. erectus*, the first human ancestor known to have left Africa. Dozens of *H. erectus* specimens have been unearthed on the nearby island of Java. But the team now argues for a more radical idea of the hobbit's origins: a "pre-*erectus* ancestor"—a small-bodied, small-brained, primitive hominid, which shrank further once on Flores. In her talk analyzing the skull and jawbones, Debbie Argue of Australian National University in Canberra proposed that the hobbit shared an ancestor with 2-million-year-old *H. habilis* (see p. 733).

When asked by colleagues, Morwood referred to unpublished work presented at recent meetings that unites *H. floresiensis* with early *Homo* or with the even more ancient australopithecines. He ticked off a few key features: an odd shoulder joint (*Science*, 19 May 2006, p. 983), a wrist like that of an ape (*Science*, 6 April, p. 34), and primitive feet. Jungers agrees that the hobbit "has australopithecine limb proportions and australopithecine ape wrists and tarsals." Given these primitive traits, Morwood argues for a very ancient ancestor. "I believe now that they split from as 2 to 3 million years ago," he said. That would imply that an australopithecine or very early *Homo*, rather than *H. erectus*, was the first hominid to leave Africa.

Skeptics are unimpressed. For starters, they point out that there is no evidence of the hobbit lineage for those millions of years. "If you go back that far, where are all the intermediates?" asks Martin.

Other scientists, including those convinced that the hobbit is a new species, think it may be premature to eliminate *H. erectus* as a possible ancestor. To date, the most complete *H. erectus* skeleton published is much larger than *H. floresiensis*, but there are other, smaller skulls of the species, particularly from the 1.7-million-year-old site of Dmanisi, Georgia.

And evolving into a smaller form on an island is a common phenomenon in other mammals. In his talk, paleontologist John de Vos of the National Museum of Natural History in Leiden, the Netherlands, gave a whirlwind tour of such island dwarfing. On islands from the Mediterranean to Southeast Asia, some large species such as elephants and hippos shrank, while others such as rats and hedgehogs evolved into giant forms, depending on the available ecological niches. "On islands, we get relict lineages," de Vos added—lineages that hark back to primitive ancestors. In his view, animal and hominid bones from Flores fit this pattern.

Dwarf island forms are also often pedomorphic, in that they retain childlike traits into adulthood, de Vos said. Thus on islands, adult elephants, hippos, and deer retain short snouts and short legs. This could be what happened to a *H. erectus*–like ancestor on Flores, he speculated, for many of *H. floresiensis*'s peculiarities appear to be pedomorphic: the lack of twisting at the top of the arm and leg bone, a flat face, and short legs. Christoph Zollikofer of the University of Zurich, who works with Ponce de Leon on the *H. erectus* fossils from Dmanisi, compared them to the Flores bones and independently came to the same idea. "*Homo floresiensis* can be understood as a pedomorphic, dwarf *erectus*," Zollikofer said. Some degree of island dwarfing makes sense, even if starting from a smaller ancestor, said Morwood.

Meeting of the minds. Excavator Thomas Sutikna (*bottom, left*) showed off artifacts in Liang Bua; conference organizer Teuku Jacob (*top*) did not visit the cave.

Yet skeptics aren't swayed by the dwarfing evidence. Martin argues that mammalian brains are unlikely to shrink to the same degree as their bodies during dwarfing. "Weird things happen on islands, but not that weird," he said. He and de Vos are considering a joint project to probe dwarfing and brain size.

The controversy may rage until more fossils emerge—and new specimens may not all come from Liang Bua. Given ocean current patterns, Morwood thinks that *H. floresiensis* might have originally been swept to Flores from Sulawesi, and he's planning to dig there to find out. On many Southeast Asian islands, says de Vos, excavations stopped at layers dated to the beginning of our current Holocene Epoch, about 11,000 years ago. Morwood found the hobbit "because he dug deep," says de Vos. "The message for the future is, dig a very deep hole." Luzebio Dizon of the National Museum of the Philippines in Manila, for one, is eager to excavate. "In the Philippines, we have the right fauna—*Stegodon*, giant rats, and turtles," he said. "It is perhaps just a matter of time until such species [as the hobbit] appear."

Researchers on both sides are also pinning their hopes on DNA. Genetic data could establish or rebut the existence of a new species, test the Laron's hypothesis, and perhaps even identify a mechanism of dwarfing. Previous attempts at retrieving DNA from hobbit bones failed, but clean sampling will be done immediately at the site if more bones are found, Morwood says. "The issues won't be resolved here at the meeting," he adds.

Nor were they resolved on the brief visit to Liang Bua cave, where Morwood and Sutikna recounted this year's excavations to a handful of colleagues, pointing to two pits the size of telephone booths, shored up with wood and with stratigraphic layers neatly revealed on the sides. In one excavation, the team had just struck a layer of a whitish volcanic tuff dated to 12,000 years ago that they say runs through the cave. Yet skeptics such as the Field Museum's Phillips say cave stratigraphy is notoriously hard to decipher, and they aren't ready to accept the dates.

Later, after the visiting scientists troop out of the cave, Sutikna and other excavators welcome one more group: a priest and a few dozen of his flock who have come to sing and pray for the excavation's success. After the last hymn, the worshippers file out, and Sutikna and the crew clean up. The next day they will dig deeper, continuing their quest for more tiny bones with big implications.

—ELIZABETH CULOTTA

CREDITS: (TOP TO BOTTOM) A. TALAS/REAL PICTURES; E. CULOTTA/SCIENCE

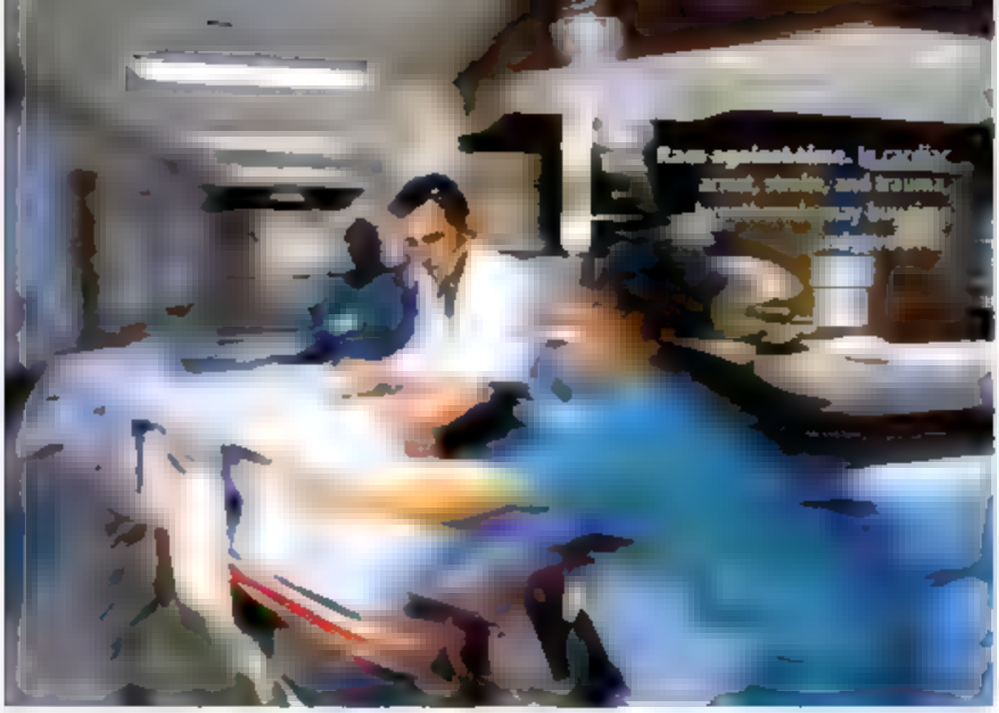

CREDIT: CHARLES THATCHER/GETTY IMAGES

MEDICINE

The Big Chill

Lowering the body's temperature improves the chances of surviving a cardiac arrest and other types of trauma, but as cold therapy expands, researchers are struggling to understand why and for whom it works

PITTSBURGH, PENNSYLVANIA—In the first frantic minutes after a trauma victim rolls through the emergency room double doors at the University of Pittsburgh Medical Center, the medical team employs an arsenal to keep the patient's temperature up. The trauma rooms hold warm blankets and heated saline fluid in a small silver cabinet. Blood often runs through a warming device before a transfusion. Heat lamps glow next to a bulky x-ray machine.

Keeping warm helps protect the immune system and sustain blood clotting, but for the most grievously wounded, that's often not enough. More than 90% of patients with massive bleeding who lose a pulse will die—a figure that has remained stubbornly high. "What we do doesn't work" to save these people, says Samuel Tisherman, a soft-spoken, goateed surgeon at the medical center. And so, as a last-ditch effort, Tisherman, who has spent nearly all his life in this industrial city, wants to try something radical. Jettison warming, and put the critically injured who have lost circulation into a deep freeze of sorts, giving surgeons time to repair the wound. Infusing and draining up to 20 liters of cold saline fluid will plunge a patient's body temperature from 37°C to less than 10°C, "pickling" him, in the words of one researcher, in order to bring him back to life.

As drastic as it sounds, hypothermia—albeit not normally this profound—has had a lengthy, bumpy history in emergency medicine. At its core, the aim is to push the outer limits of survival. "When I was training, I learned [that] after 4, 5 minutes [without oxygen], the brain would die," says Lance Becker, director of the Center for Resuscitation Science at the University of Pennsylvania. With hypothermia, he says, "many of us are beginning to think it's possible to shift that" to 10 minutes and beyond. "We don't really have a fix on what death is" or when it's irreversible, says Becker. Although it's still not clear exactly how and why hypothermia works, physicians are using it against an assortment of maladies.

Mild hypothermia improves survival of people experiencing cardiac arrest and infants deprived of oxygen before birth. Clinical trials are testing it in head injury and stroke, and a vast European study is gearing up to refine hypothermia's effects in cardiac arrest victims. Tisherman hopes that his much colder, profound-hypothermia trial will open within a year or so.

But there have also been high-profile failures and some safety concerns, a reminder of how much is left to learn. Once considered especially promising for those with brain trauma, hypothermia has proven unexpectedly fickle in this population. It has also proven exceptionally difficult to test in people, especially in the United States, where strict informed-consent guidelines mean that emergency-medicine trials are developed at what researchers contend is a glacial pace.

Beginnings

"I remember as a resident, we had patients in hypothermia for a week or longer," says Patrick Kochanek, a pediatric critical care specialist who directs the Safar Center for Resuscitation Research at the University of Pittsburgh. In those days in the early 1980s, Kochanek was at Children's Hospital San Diego in California, and youngsters with devastating head injuries were routinely cooled to 30°C, and sometimes less, for days, a trend that began in the 1950s. Pediatricians led the hypothermia charge, inspired by stories of children who had drowned in ice-cold water and been revived. "Everyone had their one miracle case of an amazing recovery," says Kochanek.

But cooling in brain injury was largely abandoned after life-threatening complications surfaced, including pneumonia, cardiac arrhythmias, and blood-clotting problems. Hypothermia continues to be used in many heart and brain surgeries to protect cells. But in the operating room, "we apply cooling before we deprive the system of oxygen," not after, which has different effects, says Hasan Alam, a trauma surgeon at Massachusetts General Hospital in Boston. The controlled conditions in surgery are also a world apart from the chaos in the emergency room.

The hypothermia field revived when a number of labs made a fortuitous discovery. For neurosurgeon Guy Clifton, now at the University of Texas Health Science Center in Houston, the insight came one winter in the mid-1980s while he was testing drugs in gerbils to prevent cell death during stroke. Animals in the control group, whose brains ought to have been seriously damaged, kept throwing off the experiments by staying healthy. The building in which Clifton was working was 100 years old and drafty. He found that the gerbils' body temperature had dipped 2°C—enough, it turned out, to protect them. "It was better than any drug we ever looked at," he says now.

A group in Miami made the same chance observation in rats, and another in Pittsburgh found similar responses in dogs. It dawned on the community that hypothermia need not be deep to be potent. "It wasn't just one laboratory showing that this works, it was almost everybody," says W. Dalton Dietrich, a neuroscientist at the University of Miami in Florida, one of the discoverers. Cooling a few degrees kept brain cells from dying.

It's far from clear why. Hypothermia slows metabolism and lowers the body's demand for oxygen, which is especially useful in cases of ischemia, in which blood supply stops and there's little oxygen to be had. Hypothermia may also inhibit a destructive cascade of molecules that surge through brain cells after someone is resuscitated. Starting the heart up after a minutes-long pause can do serious harm to the brain, causing inflammation and damage from free radicals—a process called reperfusion injury. Reperfusion "adds a great insult to the injury" of ischemia in cardiac arrest and stroke, killing brain cells over many days, says Stephen Bernard, a critical-care specialist at Alfred Hospital in Melbourne, Australia. It is precisely this type of cellular death some scientists believe hypothermia can prevent.

But scientists are now finding that mild hypothermia, defined in humans as cooling from 37° to about 33°C, has more nuanced effects. "The assumption for many years was that hypothermia was primarily downregulating metabolism" and downregulating gene expression, says David Berger, an emergency-medicine physician and biomedical engineer at the University of Chicago in Illinois. "But there's another aspect of this that is kind of puzzling." In a survey of 45,000 genes, Berger and his colleagues found that when cooling clumps of cells or mice in shock from massive bleeding, just as many genes increased expression as decreased it. Berger presented his findings at a June meeting and is preparing them for publication.

When the heart stops

As happens often in medicine, clinicians are concentrating more on how to use hypothermia than on understanding why it might work. "Our focus has always been on outcomes, not on what various molecules are doing," says Tisherman. This goal-driven mentality runs deep in the field, in part because of the man who shaped it: Peter Safar, widely considered the father of CPR and a believer in hypothermia long before it was in vogue.

The animal studies showing benefits from mild hypothermia immediately prompted clinical trials. One of the first was led by Fritz Sterz, a paramedic turned emergency-medicine doctor who had spent 3 years at Pittsburgh with Safar.

Cooling at Vienna General Hospital in Austria, where Sterz returned after his Pittsburgh sojourn, was a decidedly low-tech enterprise. Sterz invited over the local firefighters, who agreeably carted mammoth ventilators into his emergency room and blasted ice-cold air onto unconscious cardiac-arrest victims. That lowered body temperature 2° to 3°C. Sterz later graduated to a mattress blowing cold air, which dropped temperature by up to 5°C for 24 hours.

Simple as it was, the technique saved lives. In a clinical trial run by Sterz with 273 patients, 41% of those in the hypothermia group died within 6 months, compared with 55% in the control group. A second cardiac-arrest trial in Australia led by Bernard found that 49% of patients given hypothermia survived with minimal disability, compared with 26% in the control group. (Bernard wedged ice packs around his patients.) Both studies appeared in 2002 in *The New England Journal of Medicine*.

A 2005 study described equally compelling outcomes for babies deprived of oxygen before birth—a condition that affects the body much like a cardiac arrest. Among more than 200 newborns in the study, half were cooled to 33°C for 72 hours. Forty-four percent of those treated with hypothermia died or survived with significant disabilities. As grim as that sounds, the number was worse in the group that received standard treatment: 62%, or a difference of 19 babies.

"I was astonished that they were able to show a beneficial effect," says Kochanek. Some of the infants could have been deprived of oxygen for a day or two before birth. The cardiac-arrest studies, furthermore, suggested that doctors had been wrong in thinking brain damage was inevitable after more than 5 minutes without oxygen.

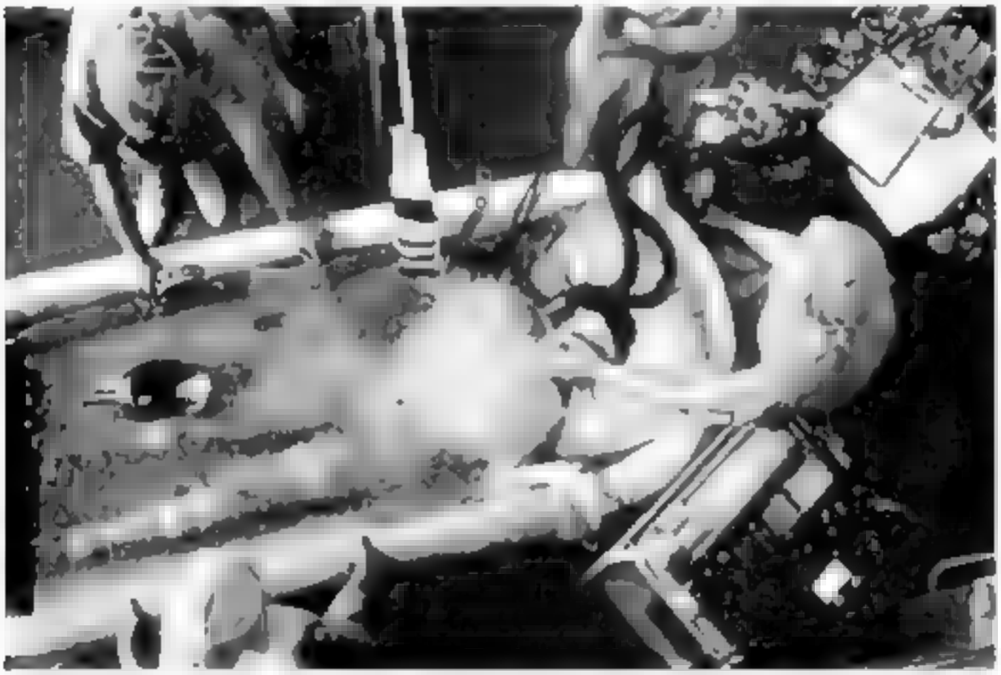

Crude beginnings. A bathtub full of ice was one of the earliest ways doctors induced hypothermia in the 1950s.

A knottier test

The next frontier, treating brain injury, has been far more difficult to cross. This is surprising, because it's brain cells that seem to benefit most when hypothermia is used against ischemia. Pediatric critical-care specialist Jamie Hutchison of the Hospital for Sick Children in Toronto, Canada, concedes disappointment that his trial of 225 children with serious head injuries detected no benefit from hypothermia, a finding he first presented at a June meeting in Switzerland. This is consistent with an earlier head-injury trial of almost 400 adults, led by Clifton, which also flunked the hypothermia test.

The failures are of special concern because hypothermia is not harmless. The larger of the two cardiac-arrest trials, for example, saw more sepsis among treated patients (hypothermia depresses the immune system), more bleeding, and more cardiac arrhythmias. These were not considered significant, but they have long been associated with cooling. Perhaps the greatest risk comes not from cooling itself but from rewarming, which can sink blood pressure to life-threatening lows.

Why the dispiriting results in the head-injury trials? One possibility is that, whereas ischemia from a cardiac arrest briefly shuts down oxygen to the entire brain, "trauma's a dirty disease," says pediatric neurosurgeon P. David Adelson of Children's Hospital of Pittsburgh. Traumatic brain injury can mean multiple injuries to different parts of the brain, or be combined with trauma elsewhere in the body. That variability is not reflected in

CREDIT: W. DALTON DIETRICH/UNIVERSITY OF MIAMI

lab studies, in which hypothermia has performed so impressively. There, "you hit a group of animals in the same place with exactly the same force," says Hutchison.

Another theory is that different injuries provoke different forms of cell death, and hypothermia may be more suited to preventing one form than it is another. For example, the apoptotic death of cells observed after a cardiac arrest, in which cells "self-destruct," may be more amenable to hypothermia than the necrotic cell death seen in head injury, says Kochanek.

None of these ideas persuaded Clifton, who was baffled by hypothermia's lackluster showing in his head-injury trial. But parsing the data, he noticed that younger people whose bodies cooled spontaneously right after injury—a common effect of head trauma—and who then received hypothermia fared better. This suggested that early cooling could be key.

Narrowing his focus, Clifton has launched a second head-injury trial with $15 million in funding from the National Institutes of Health (NIH) in Bethesda, Maryland. He aims to enroll 240 people under age 45 and cool them within 2 hours of injury. Where possible, paramedics infuse chilly IV fluids in the helicopter en route to the hospital.

This time constraint presents a sticky problem: It's rarely possible to obtain informed consent so quickly from a patient's family. Relatives might be difficult to locate, or, in the worst case scenario, they might have died or been badly injured in the same accident. Many countries allow researchers to waive consent in emergency situations, though to do so in the United States, researchers must alert the community to their trial in advance. Clifton ran newspaper advertisements and met with community groups to describe the potential benefits and risks of cooling and how his study would be conducted. One man he met in Houston asserted that "only a Nazi would do this," says Clifton, adding, "but the majority of people ask a lot of questions and don't have a problem with it."

In Pittsburgh, Adelson also received an emergency waiver of informed consent from the university's Institutional Review Board (IRB) for a $15 million hypothermia study on head injuries in children also funded by NIH. Although Hutchison's trial in Canada failed, Adelson says his trial, which he hopes to start this fall, will cool patients for longer—48 hours instead of 24. And it will treat children within 6 hours rather than 8 hours of injury. Adelson is heartened by hints from a pilot trial he published 2 years ago that found that 44% of children treated with hypothermia were still showing improvements in cognition and behavior 6 months later, compared to 36% of those given standard care.

Tisherman is working toward approval and funding for his trial of trauma victims, the first that will cool injured patients dramatically, to 7° or 10°C. Alam of Mass General hopes to participate as well. Some consider this strategy especially risky because hypothermia is known to inhibit blood clotting, and these patients are already enduring massive internal bleeding. But "there really is no good alternative" treatment, says Jeannie Barone, assistant director of the Pittsburgh IRB.

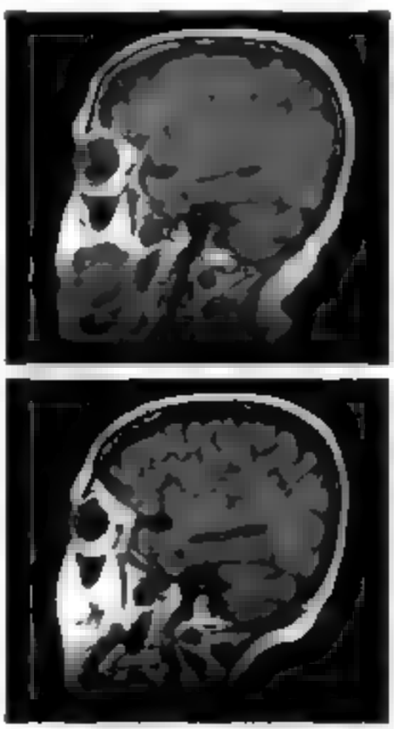

SOURCE: CLINICALTRIALS.GOV; CREDIT: ELANA BONFANTE

A view of the brain. Half of this stroke victim's brain is healthy (*top*), but the other half is damaged by the loss and restoration of blood flow—harm that might be reduced by hypothermia.

Spotty execution

Clinicians say that trials like these, as well as at least a half-dozen others in Europe, Asia, North America, and Australia, are crucial to learning how hypothermia might help. But the field is fragmented. Already the treatment is being used in situations not backed by clinical data and not used in situations that are. Frustration creeps into Adelson's voice as he describes how some centers refused to join his head-injury trial because they are reluctant to randomize their young charges. Instead, physicians are treating brain-injured patients as they come in, without the rigors of a clinical trial, says Adelson. "That's despite data showing it's not effective in probably 65% of patients."

Trial by Ice: A Sampling of Hypothermia Studies

Condition	Patients	Home of Lead Center	Status
Head injury, adults	240	Houston, Texas	Ongoing
Head injury, children	225	Toronto, Canada	Complete, not published
Head injury, children	340	Pittsburgh, Pennsylvania	Opens in fall
Shock from bleeding	100	Pittsburgh, Pennsylvania	Seeking funds
Stroke	50	San Diego, California	Ongoing
Cardiac arrest	2000	Vienna, Austria, and Lund, Sweden	Seeking funds
Cardiac arrest, children	40	Toronto, Canada	Ongoing

Meanwhile, hypothermia's impressive ability to boost survival after a cardiac arrest prompted professional societies, beginning in late 2002, to recommend its use. Yet a 2006 survey of more than 2200 physicians in the United States, the United Kingdom, and England found that 74% in the United States and 64% in Europe had never used hypothermia to treat patients after a cardiac arrest. Often, hospitals don't adopt hypothermia unless it's foisted upon them. In Norway, Kjetil Sunde, an anesthesiologist at Ullevaal University Hospital in Oslo, spent 2 years pressing for the treatment. At first, many doctors, he says, "didn't believe in this." Now more than 90% of the country's hospitals use hypothermia in cardiac-arrest cases, he notes.

One reason hypothermia hasn't caught on is money, says James Grotta, director of the Stroke Program at the University of Texas Health Science Center. Drug companies don't develop it. The pharmaceutical industry provides "a substantial impetus for teaching, education, and practice patterns," says Grotta, who is studying hypothermia in stroke. When it comes to cooling, "nobody's pushing this. ... There's nothing really patentable here."

Still, "it's almost to me scandalous" that the treatment remains so rare, says Clifton. "There are not that many cities where a patient can expect to get it."

–JENNIFER COUZIN

CLIMATE CHANGE

Humans and Nature Duel Over the Next Decade's Climate

Pitting greenhouse forecasts against natural variability, researchers are trying to predict how the next few decades' natural climate variations will play out against a backdrop of human-induced warming

For a century or more, meteorologists have known the secret to weather forecasting. To glimpse tomorrow's weather, one must know today's. And lately they have realized that the same precept applies to predicting climate years or decades ahead. Stirrings in the North Atlantic Ocean today that have nothing to do with the strengthening greenhouse—just natural joshings of the climate system—could lead to drought in Africa's Sahel in a decade or two, they recognized. Ignore today's ocean conditions, and your 2020 global-warming forecast could be a bust. And such natural variability can be far-reaching. In a recent study, researchers found that when the Atlantic Ocean swung from one state to another, it apparently helped trigger a decade-long climate shift in the late 1960s that sprang from the Atlantic and reached as far as Australia.

But until now, climate forecasters who worry about what greenhouse gases could be doing to climate have ignored what's happening naturally. Most looked 100 years ahead, far enough so that they could safely ignore what's happening now. No more. In this week's issue, researchers take their first stab at forecasting climate a decade ahead with current conditions in mind. The result is a bit disquieting. Natural climate variability driven by the ocean appears to have held greenhouse warming at bay the past few years, but the warming, according to the forecast, should come roaring back before the end of the decade.

"This is a very valuable step forward," says meteorologist Rowan Sutton of the University of Reading, U.K. "It's precisely on the decadal time scale and on regional scales that natural variability and anthropogenic effects have comparable magnitudes." So improved climate forecasting of the next few decades could help decision-makers focus on where and when the most severe climate change will be happening. Or conversely, they could recognize when the looming threat of global warming will be masked—temporarily—by natural variability.

Jiggly climate

No one ever said Earth's atmosphere was a boring place. Air is in continually shifting motion, from the wafting of innumerable summer breezes to a few roaring jet streams. But forecasters have long recognized that certain parts of the chaotic atmosphere are better behaved than others. Over the North Atlantic, for example, atmospheric pressure over Iceland and Portugal tends to "seesaw" over the weeks and months, rising at one site while it falls at another. This North Atlantic Oscillation (NAO) in turn switches winds to and fro across the Atlantic, guiding storms into or away from western Europe. Other modes of natural variability—atmospheric jigglings that lack an external cause such as added greenhouse gases—tend to cause atmospheric reorganizations over the North Pacific and the high latitudes of both hemispheres. The tropical warmings and coolings of the El Niño–La Niña cycle can also hold sway in various regions around the globe.

Once meteorologists recognized that natural variability offered hope of predicting out a few months, climate researchers began to see that the same or similar modes might improve forecasting a decade or more ahead. On a regional scale, the NAO seesaws over the decades as well. Its dramatic strengthening in winter between the 1960s and 1990s pumped extra heat into Northern Europe on top of greenhouse warming, according to a new analysis in press at the *Journal of Geophysical Research* by climate researcher

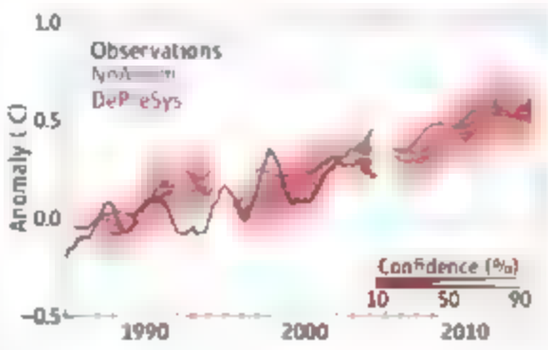

Better. A model starting from current conditions (white) came closer to reality (black) than one without (blue).

CREDIT: JASON EDWARDS/NATIONAL GEOGRAPHIC. SOURCE: D. M. SMITH ET AL./SCIENCE

David Parker of the Hadley Centre for Climate Prediction and Research in Exeter, U.K., and his colleagues.

On a broader scale, natural variability over decades is clearly rooted in the oceans. A warm-cool cycle that spans the Pacific, both North and South, has lately swung back and forth on a time scale of 30 to 50 years. By Parker and his colleagues' data and model analysis, this so-called Interdecadal Pacific Oscillation seems to be driven by interactions between the tropical ocean and atmosphere much like those that drive El Niño. the IPO could be the multidecadal expression of the El Niño cycle, they say.

Over in the Atlantic, there's the Atlantic Multidecadal Oscillation (AMO) of sea surface temperature. It is apparently driven by the acceleration and slowing of the great ocean conveyor that carries warm surface water into the northern North Atlantic (*Science*, 1 July 2005, p. 41). The AMO's vacillations have been linked to everything from triggering drought in the Sahel and the central United States to alternately suppressing and—in the past decade—firing up hurricanes (*Science*, 10 November 2006, p. 910).

A global reach

Lately, researchers are finding that the AMO may have a stronger influence and a longer reach than they once thought. They knew that the oscillation affected climate around the Atlantic, but some suspected it had also caused a mid-century warming of the Northern Hemisphere or even the globe.

This past January in *Geophysical Research Letters*, climate modeler Rong Zhang and colleagues at the Geophysical Fluid Dynamics Laboratory in Princeton, New Jersey, showed how the AMO might have warmed at least the one hemisphere. They varied the warmth of the North Atlantic in their model to mimic the way the temperature of the real North Atlantic varied under the AMO during the 20th century. In the model, the Northern Hemisphere warmed to mid-century and then cooled slightly through the 1950s and 1960s, as it did in the real world.

In work accepted at the *Journal of Climate*, climate researchers Sergey Kravtsov and Christopher Spannagle of the University of Wisconsin, Milwaukee, extract what looks like an AMO temperature signal from not just the hemispheric but the global record as well. To gauge the effect of natural variations, they took 20th century temperature records from around the globe and subtracted the warming due to rising greenhouse gases, as simulated by 16 climate models. The difference—a strong warming over southern Greenland, a warming North Atlantic, a cooling South Atlantic, and a weak warming in the far North Pacific—looks like the pattern and timing attributed to the AMO. Kravtsov and Spannagle conclude that the shifting ocean circulation behind the AMO has global effects on global warming.

The AMO may have had a hand in a more dramatic global climate event, according to meteorologist Peter Baines of the University of Melbourne, Australia, and climatologist Chris Folland of the Hadley Centre, writing in the 15 June issue of the *Journal of Climate*. Their climate shift rattled the circum-Atlantic region over a decade starting in the early 1960s and reached around the globe.

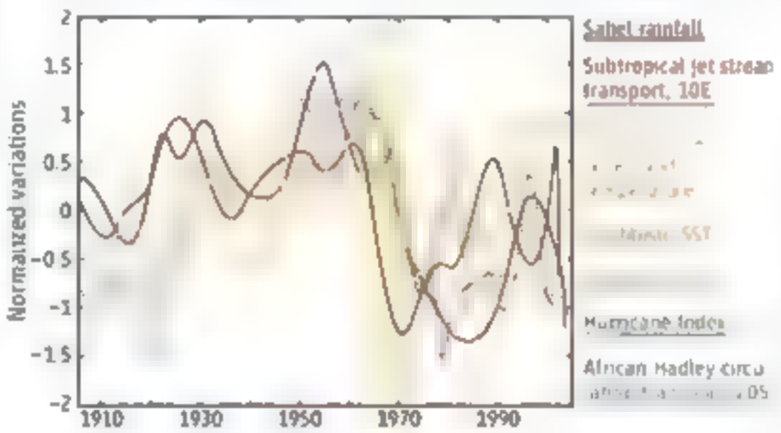

Doin' the shift. All sorts of regional climate—from African rainfall to hurricane activity—changed in the late 1960s, especially around the Atlantic.

First, Baines and Folland pulled together a range of regional changes in temperature, rainfall, and atmospheric circulation around the Atlantic that could all be tied back to a cooling of the North Atlantic. The AMO presumably cooled the ocean—perhaps with the help of sun-shielding pollutant hazes—as the warm conveyor slowed. Greenland cooled, Brazilian rainfall swelled, hurricane activity dropped, and the Sahel dried to the most catastrophic drought in more than a century. These changes, which are most evident in the northern summer, can all be linked to the reduction and relocation of the ocean's transfer of heat into the atmosphere, Baines and Folland say. Those shifts, in turn, led to changes in atmospheric circulation and precipitation over adjacent continents.

Searching for the most remote limits of this climate shift, Baines and Folland looked out along the atmospheric circulations ultimately driven by tropical ocean heating in the Atlantic. There they found changes in subtropical jet streams in both hemispheres and poleward shifts in storm paths. In southwest Australia, for example, the shift reduced the rains and brought long-term drought. Baines and Folland's explication of a globe-girdling late-'60s climate shift only reinforces the view that "the AMO does affect global climate," says meteorologist Mojib Latif of the University of Kiel, Germany. "It's not just regional climate."

Anticipating nature

Appreciating the power and reach of natural climate variations is a major step. To put that information to use, however, climate forecasters must find a way to model the future course of the variations themselves, starting from current conditions. Climate researchers from the Hadley Centre, led by Douglas Smith, are the first to try that, as they report on page 796.

The Hadley group tested the usefulness of their new prediction model by "hindcasting" the climate of two past decades. Starting from the observed distribution of ocean heat content, the model outperformed its own forecasts that lacked observed [illegible] conditions. Errors in predicting global temperature declined by 20% or 36%, depending on the type of error. The model successfully predicted the warming of El Niño and the effect of unusually warm or cold waters around the world. An actual forecast starting in June 2005 correctly predicted that natural variability—the appearance of cooler water in the tropical Pacific and a resistance to warming in the Southern Ocean—would offset greenhouse warming until now. But beyond 2008, warming sets in with a vengeance. "At least half of the 5 years after 2009 are predicted to be warmer than 1998, the warmest year currently on record," the Hadley Centre group writes.

"Smith *et al.* is an important first step in setting out the method," says meteorologist Tim Palmer of the European Centre for Medium-Range Weather Forecasts in Reading, U.K. Now researchers need to amass more computing power, more past observations to test the method better, and more future observations to feed the models, he says. And time is of the essence. If the AMO in fact played a substantial role in the rapid warming and enhanced hurricane activity of the past decade or two, says Sutton, "there will in all probability be a turnaround [of the AMO], possibly in the next decade." It would be nice to know for sure.

—RICHARD A. KERR

SOURCE: P. G. BAINES AND C. K. FOLLAND, JOURNAL OF CLIMATE

LETTERS

edited by Etta Kavanagh

Retraction of an Interpretation

IN THE REPORT "STRUCTURE OF THE 8200-YEAR COLD EVENT REVEALED BY A SPELEOTHEM trace element record" (*1*) we presented a 7762-μm-long ion probe trace element traverse chosen to include the 8200-year event as detected in a previously published laser ablation oxygen isotope study from the same stalagmite (*2*). The oxygen isotope anomaly was distinct and dropped $\delta^{18}O$ values to a low value for the entire Holocene of −12‰ and was reproducible on a reverse track. However, recent reanalysis of the calcite believed to contain the oxygen isotope anomaly suggests that the anomaly was probably an analytical artifact possibly caused by laser ablation–induced fracturing during the original analysis (*3*). Consequently, without the original $\delta^{18}O$ "marker," the precise location in the stalagmite of calcite deposited during the 8200-year event is uncertain.

The trace element data in this Report, previously believed to correspond precisely with the entire 8200-year event, are now believed to represent the hydrological and bioproductivity response in western Ireland to a cold dry event of uncertain provenance and intensity. The U-Th–derived dates of the event correspond approximately with the 8200-year event in Greenland ice cores, but without the additional presence of the $\delta^{18}O$ anomaly, the precise timing in relation to the 8200-year event is now somewhat ambiguous. Unfortunately, it is now unlikely that the approximately 114-year duration ion probe track coincides with the entire 8200-year event (if at all); thus, the ~37-year estimate derived for its duration is probably no longer accurate. However, the trace element data remain robust and are interpreted as reflecting colder and drier conditions in western Ireland, followed by the return to more maritime conditions at the end of the first-order trace element anomaly. Additionally, the novel application of annual trace element cycles to build a high-resolution chronology and reconstruct paleoseasonality remains unchanged.

JAMES U. L. BALDINI,[1] FRANK MCDERMOTT,[2] IAN J. FAIRCHILD[3]

[1]Department of Earth Sciences, Durham University, South Road, Durham DH1 3LE, UK. [2]Department of Geology, University College Dublin, Dublin 4, Ireland. [3]School of Geography, Earth and Environmental Science, University of Birmingham, Birmingham B15 2TT, UK.

References

1. J. U. L. Baldini, F. McDermott, I. J. Fairchild, *Science* **296**, 2203 (2002).
2. F. McDermott, D. P. Mattey, C. Hawkesworth, *Science* **294**, 1328 (2001).
3. J. U. L. Baldini *et al.*, *Earth Sci. Rev.* **75**, 105 (2006).

The Dangers of Advocacy in Science

IN MATTERS OF POLICY, MANY SCIENTISTS view "advocacy" as a dangerous word. In peer-reviewed literature, many scientists practice a subtler form of advocacy in pushing their methods, results, and conclusions. Call this IMRAD (Introduction, Methods, Results, and Discussion) advocacy. Once bold claims about a poorly tested method or weak result are published, their sins are forgiven and they can be worked into future introductions and discussions at will. IMRAD advocates often stretch available data, gloss over uncertainties in their evidence, and ignore contrary results.

This occurs throughout the hierarchy of journals. One would hope that it would be least common in prestigious journals. On the other hand, top journals have limited space; they emphasize papers with broad, seemingly decisive conclusions but passively encourage readers not to worry about methods (or rebuttals). Often, this form of advocacy is obvious only to the small percentage of any journal's readers that have scientific expertise in a specialized area—a small pool of appropriate reviewers (*1*).

As with policy advocacy, there is a gray area between objective justification and flagrant, half-supported promotion. Somewhere in the middle sits the honest, often acrimonious debate necessary for scientific progress. Would anyone disagree that publishing overly liberal conclusions is poor science, that the personal rewards of doing so far outweigh risks, or that the peer-review process should strip papers of this garbage? Humiliation could assist rebuttals and time in the self-correcting process of science. For example, each professional society should survey members at year's end to decide on the five papers in their field with the most overly inflated claims. The authors, approving reviewers, and subject editors could receive suitable prizes.

> **"Would anyone disagree** that publishing overly liberal conclusions is poor science...?"
>
> —Gitzen

ROBERT A. GITZEN

Department of Fisheries and Wildlife Sciences, University of Missouri, Columbia, MO 65211, USA.

Reference

1. R. Hilborn, *Fisheries* **31**, 554 (2006).

Controversy Over EmrE Structure

TWO X-RAY STRUCTURES OF EMRE, THE SMALLest ion-coupled multidrug transporter, have provided a cautionary tale about the difficulty of determining the three-dimensional structures of membrane proteins and the dangers of ignoring biochemical results. The structures have since been retracted (*1*, *2*) but the intriguing and controversial idea that the

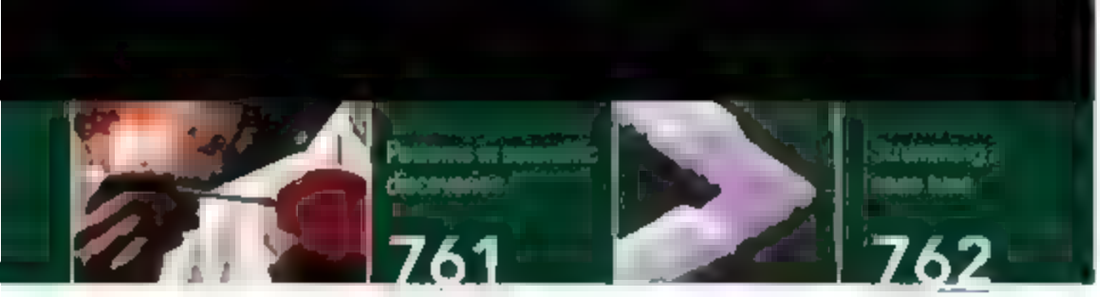

proteomers in the EmrE homodimer adopt an antiparallel transmembrane orientation continues to have support. In their Report "Emulating membrane protein evolution by rational design" (2 March, p. 1282), M. Rapp *et al.* describe results that seem to support such an antiparallel arrangement and that are thought to provide the missing link in membrane protein evolution. However intriguing the results may be, the starting point is too fuzzy and ignores biochemical results. The interpretation is based on the assumption that EmrE displays a dual topology. However, the x-ray structures have been retracted, and the results that support such an assumption in Rapp *et al.* cannot be taken at face value as the authors admit because the large fusion proteins they used to determine the topology of a protein two to four times smaller seem to bias the results. This is unfortunate and it would be helpful to apply alternative approaches, which may be more time-consuming but less ambiguous.

In their Perspective "A missing link in membrane protein evolution" (2 Mar, p. 1229), B. Poolman *et al.* claim that our rigorous demonstration that EmrE with a parallel topology of the protomers is fully functional was based on the now obsolete structural model. On the contrary, our work showed that this model was incorrect, rather than being based on it (3).

There is suggestive evidence that some homologs of EmrE that function as heterodimers or a properly mutated EmrE display an antiparallel topology of the protomers relative to each other. If the case can be made for antiparallel heterodimers, what makes it so different for a homodimer? If antiparallel homodimers exist, researchers would be faced with fascinating questions about the insertion and assembly of these proteins in the membrane (*4*). Do the protomers insert with a random topology and wait for the next randomly inserted one? To our knowledge the existence of homodimers with an antiparallel orientation of the monomers has not yet been biochemically demonstrated.

SHIMON SCHULDINER

Biological Chemistry, Silberman Institute of Life Sciences, Hebrew University of Jerusalem, Givat Ram, Jerusalem, 91904 Israel

References

1. G. Chang *et al.*, *Science* **314**, 1875 (2006).
2. C. Ma, G. Chang, *Proc. Natl. Acad. Sci. U.S.A.* **104**, 3668 (2007).
3. M. Soskine, S. Mark, N. Tayer, R. Mizrachi, S. Schuldiner, *J. Biol. Chem.* **281**, 36205 (2006).
4. S. Schuldiner, *Trends Biochem. Sci.* **32**, 252 (2007).

Response

IN RECENT MONTHS, EMRE HAS TAKEN CENter stage in the world of membrane proteins because there are opposing views on its

membrane topology (*1*) and because two x-ray structures of EmrE were recently retracted (*2*, *3*).

EmrE is an unusually intriguing protein. It is by far the most well-studied representative of the bacterial small multidrug-resistance (SMR) proteins, a family of potential drug targets, and it may be the first example of a "dual topology" protein, i.e., a homodimeric protein composed of two identical monomers with opposite orientations in the membrane (*4*).

The final proof for a dual topology for EmrE is still lacking. So, what is the evidence? First, the dual topology idea was originally proposed on the basis of an early electron crystallography structure (*5*, *6*). This structure, albeit of rather low resolution, is still the gold standard, since the two-dimensional crystals bind substrate with nM affinity.

Second, a steadily increasing number of SMR proteins have been shown to be heterodimers composed of two homologous monomers [e.g., (*7*)]. In at least one case (the EmrE homologs YdgE:YdgF in *E. coli*), the two monomers have been shown to adopt opposite orientations in the membrane (*8*), and topology predictions suggest that this is the general rule for heteromeric SMR proteins (*9*). By extension, a dual topology for homodimeric EmrE seems likely.

Third, by mutating positively charged residues in the loops connecting the transmembrane helices, we have constructed two EmrE variants that insert with either N_{in}-C_{in} or N_{out}-C_{out} orientations. These variants are nonfunctional when expressed alone, but make cells resistant to ethidium bromide when coexpressed (*10*), as does wild-type EmrE. The complementation between the two oppositely oriented EmrE variants suggests that they form an antiparallel heterodimer, like other heteromeric SMR proteins.

On the other hand, the Schuldiner lab has reported that a chemically cross-linked EmrE dimer is active after reconstitution in vitro (*11*). With the cross-linked residues chosen such that they should not be able to form a cross-link in an antiparallel dimer (according to the now retracted x-ray structure), this result provides an argument against a dual topology. But is this biochemical finding with solubilized, cross-linked protein compelling enough to override the structural, coexpression, and evolutionary arguments that support a dual topology for EmrE? We think not. In any case, given its current "15 minutes of fame" (*12*), EmrE will no doubt attract enough attention for the debate over its topology to be resolved in the normal scientific way—by more and better experiments.

MIKAELA RAPP, SUSANNA SEPPÄLÄ, ERIK GRANSETH, GUNNAR VON HEIJNE

Center for Biomembrane Research, Department of Biochemistry and Biophysics, Stockholm University, SE 106 91 Stockholm, Sweden.

References

1. S. Schuldiner, *Trends Biochem. Sci.* **32**, 252 (2007).
2. G. Chang *et al.*, *Science* **314**, 1875 (2006).
3. C. Ma, G. Chang, *Proc. Natl. Acad. Sci. U.S.A.* **104**, 3668 (2007).
4. G. von Heijne, *Nat. Rev. Mol. Cell. Biol.* **7**, 909 (2006).
5. I. Ubarretxena-Belandia, J. M. Baldwin, S. Schuldiner, C. G. Tate, *EMBO J.* **22**, 6175 (2003).
6. S. J. Fleishman *et al.*, *J. Mol. Biol.* **364**, 54 (2006).
7. Z. Zhang *et al.*, *Biochemistry* **46**, 5218 (2007).
8. O. O. Daley *et al.*, *Science* **308**, 1321 (2005).
9. M. Rapp, E. Granseth, S. Seppälä, G. von Heijne, *Mol. Struct. Mol. Biol.* **13**, 112 (2006).
10. M. Rapp, S. Seppälä, E. Granseth, G. von Heijne, *Science* **315**, 1282 (2007).
11. M. Soskine, S. Mark, N. Tayer, R. Muracchi, S. Schuldiner, *J. Biol. Chem.* **281**, 36205 (2006).
12. Warhol photo exhibition, Stockholm, 1968, in *Bartlett's Familiar Quotations*, J. Kaplan, J. Justin, Eds. (Little Brown, New York, 1992).

Response

THE QUESTION OF THE MEMBRANE ORIENTATION of the two subunits in the multidrug efflux protein EmrE is befuddled by two separate issues. First, there are the x-ray crystallography studies of EmrE that were recently retracted (*1*, *2*). Clearly, invalid structural models cannot be used as a lead in any study. Second, there are biochemical data that lead to different conclusions on the subunit orientation of EmrE. Von Heijne and colleagues have provided evidence for an antiparallel orientation of the subunits (*3*), whereas Schuldiner and colleagues support a parallel orientation (*4*).

Conflicting models are proposed all the time in the process of scientific progress, and to choose which model is most probable, we have to scrutinize the available data and interpretations. Which studies are at hand? First, there is the only piece of structural information left: the 3D model of EmrE-based electron crystallography experiments (*5*), which provides a reliable structural model of EmrE. Unfortunately, the resolution is too low to reach definitive conclusions on the orientation of the subunits.

Second, there are the biochemical studies of the Schuldiner group (*6*–*8*). Soskine *et al.* (*8*) argue in favor of a parallel orientation of the subunits because their cross-linking data are inconsistent with the antiparallel orientation of the subunits observed in the now-obsolete x-ray crystallographic structural model. Both the design of their experiments (the positions of the engineered cysteines and the calculated intermolecular distances between the residues) and the interpretation of their data were based on the structural model that has since been shown to be incorrect (*1*). Moreover, the combination of high concentrations of detergent in the experiments, possibly leading to increased conformational flexibility of the protein, and the relatively large span of the applied cross-linker severely limit the validity of the approach. Consequently, we feel that the cross-linking data are not necessarily in conflict with an antiparallel orientation of the subunits (*9*).

CORRECTIONS AND CLARIFICATIONS

Reports: "Synthesis of ultra-incompressible superhard rhenium diboride at ambient pressure" by H. Y. Chung *et al.* (20 April, p. 436). After publication, the original authors concluded that Robert W. Cumberland (Department of Chemistry and Biochemistry and the Department of Materials Science and Engineering, University of California, Los Angeles, CA 90024, USA; current address: HRL Laboratories, Malibu, CA 90265, USA), who was acknowledged, contributed sufficiently to the work to be listed as an author. This change was approved by the Vice Chancellor for Research at UCLA. The authors should now be:

Hsiu-Ying Chung,* Michelle B. Weinberger,* Jonathan B. Levine, Robert W. Cumberland, Abby Kavner, Jenn-Ming Yang, Sarah H. Tolbert, Richard B. Kaner

(*These authors contributed equally to this work).

Reports: "Causal reasoning in rats" by A. P. Blaisdell *et al.* (17 February 2006, p. 1020). There are three minor typos in the Supporting Online Materials. First, test sessions for Experiments 1, 2a, and 2b were 60 minutes. Second, the number of background nose pokes in Experiment 1 were 2793 ± 571 (Condition Intervene-T), 3051 ± 991 (Condition Observe-T), 2885 ± 823 (Condition Intervene-N), and 2849 ± 514 (Condition Observe-N). Third, in Experiment 1, the F value for the planned comparison between condition Intervene-T versus Observe-T was 9.07, $p < 0.05$. A reanalysis of the data from Experiment 2b revealed that the test-trial data for one subject from group Unpaired-Observe was inadvertently counted twice in the statistical analyses. A reanalysis on the corrected data results in a change of three F values by a tenth of a point or less, and thus has no effect on the outcome of the analyses. The authors failed to revise the caption in the corrected Fig. 1 (*Science* **314**, 595 (2006)). The F values were slightly different from those reported. Corrected values show the main effect of inference type = $F(1, 21) = 4.57$, $P < 0.05$, and the interaction = $F(1, 21) = 5.69$, $P < 0.05$.

Third, there are the studies of von Heijne and colleagues (*3*). Contrary to Schuldiner's suggestion, the interpretation of the data of Rapp *et al.* is not dependent on the prior assumption that EmrE displays a dual topology. The experiments were designed to discriminate between two alternative scenarios: parallel versus antiparallel orientation of the subunits. Schuldiner is correct in arguing that fusing a large reporter domain to a protein like EmrE may influence its orientation in the membrane. However, von Heijne and colleagues clearly recognize this point, and in a series of in vivo complementation studies with the EmrE protein subtly mutated to obtain a unique orientation, they showed that only an antiparallel arrangement of the EmrE subunits is functional. Schuldiner has proposed an alternative evolutionary model, but the scenario presented in (*4*) depends on many chance assumptions and is not very likely. The antiparallel topological model proposed by von Heijne and colleagues is also supported by the recent data of Zhang *et al.* (*10*).

We believe that both groups performed solid experiments. Our view (*9*) is that the experiments from the Schuldiner group do not sufficiently discriminate between a dual topology model and a parallel model. Their evidence for parallel topology is based on cross-linking results with protein in the detergent-solubilized state, a nonnatural environment. In contrast, the von Heijne group used the native lipid membrane to study the function of EmrE. We therefore consider the dual topology model of EmrE more compelling — for now.

BERT POOLMAN, ERIC GEERTSMA, DIRK-JAN SLOTBOOM

Department of Biochemistry, Groningen Biomolecular Sciences and Biotechnology Institute, and Zernike Institute for Advanced Materials, University of Groningen, Nijenborgh 4, 9747 AG Groningen, The Netherlands. E-mail: b.poolman@rug.nl

References

1. G. Chang *et al.*, *Science* **314**, 1875 (2006).
2. C. Ma, G. Chang, *Proc. Natl. Acad. Sci. U.S.A.* **104**, 3668 (2007).
3. M. Rapp *et al.*, *Science* **315**, 1282 (2007).
4. S. Schuldiner, *Trends Biochem. Sci.* **32**, 252 (2007).
5. M. Ubarretxena-Belandia *et al.*, *EMBO J.* **22**, 6175 (2003).
6. S. Rimo *et al.*, *FEBS Lett.* **562**, 193 (2004).
7. M. Soskine *et al.*, *Proc. Natl. Acad. Sci. U.S.A.* **99**, 12043 (2002).
8. M. Soskine *et al.*, *J. Biol. Chem.* **281**, 36205 (2006).
9. B. Poolman *et al.*, *Science* **315**, 1229 (2007).
10. Z. Zhang *et al.*, *Biochemistry* **46**, 5218 (2007).

A Clarification on Centrifugal Force

THE ARTICLE "SPINNING A NUCLEAR COMEback" (News Focus, 30 March, p. 1782) contains an erroneous statement about centrifugal force. The article states that "centrifugal forces pushed the gas outward, against the spinning wall." There is, in fact, no force pushing the gas outward. Instead, as covered in Newton's first and second laws, a force is required to prevent the gas from going in a straight line (and thereby accelerating the gas due to its constant change in direction). This force (termed centripetal force) acts inward toward the center of rotation and is provided by contact of the gas with the spinning wall.

ALLEN ZIMMERMAN

Ohio State University, 1328 Dover Road, Wooster, OH 44691, USA.

HISTORY OF SCIENCE

Fame, Philosophy, and Physics

Jeroen van Dongen

In 1921 when the earliest Einstein biography, by the Berlin publicist Alexander Moszkowski (2), was about to appear, Einstein tried to halt its publication, because seeking the limelight was frowned upon in the German academic milieu of his day. His name had been widely publicized following the 1919 British eclipse expedition that had confirmed central predictions of the theory of relativity. In its aftermath, a group of right-wing physicists and agitators had started to publicly protest the clamor about relativity and its Jewish, liberal, and pacifist creator.

Despite Einstein's initial resistance, his fame has far from diminished. This year, a great many biographies later, two new books try to capture again his science, politics, and private life. Walter Isaacson's *Einstein: His Life and Universe* and Jürgen Neffe's *Einstein: A Biography*. Isaacson and Neffe, both successful journalists, shared a privilege that their predecessors lacked: access to Einstein's most private correspondence that had remained closed in the Einstein Archives at the Hebrew University in Jerusalem until the summer of 2006. New perspectives on Einstein's personal life might therefore be expected from their books.

Indeed, Neffe discusses at length Einstein's divorce from his first wife, Mileva Marić, and the troubled relationship with his two sons. Einstein could at times be harsh and selfish toward his family, as when he presented Marić (who desperately wanted to remain married) with exacting terms under which he might agree to endure living together with her; she would practically have been reduced to his maid. Although bad endings to bad marriages happen to good people, others too have observed a lack of empathy on Einstein's part [e.g., Thomas Levenson (3)]. Neffe, however, seems to be short of sympathy for his subject and consistently portrays Einstein in the darkest light imaginable. He even mentions an unnamed diary that is supposed to state that Einstein was beating Mileva. Neffe does not shy away from sensationalism or simplistic explanations: He offers as a matter of course the presumption that Einstein's talent had to be accompanied by some form of autism. And when Einstein's second wife (and cousin), Elsa, passed away after close to 20 years of marriage, Neffe claims that her "enstatured husband" exhibited barely any emotion and simply started to work harder. Isaacson's account is better informed. Einstein wept when Elsa died. He did delve into his work, but "ashen with grief," as his collaborator Banesh Hoffmann recalled.

Neffe interviewed a number of leading (mostly German) researchers whose work reflects themes of Einstein's physics. This effort nicely connects Einstein's science to today's laboratories. Yet the explanations Neffe offers vary from muddled to simply incorrect. His account of relativity has an observer who "moves away from his frame of reference," and according to him Max Planck held that "light is a mass divisible in any number of ways." Nor is Neffe's book the source to turn to for accounts of Einstein's fundamental discussions about quantum mechanics with Niels Bohr.

Isaacson presents Einstein's ideas with greater clarity. In fact, it is a pleasure to read his discussions of Einstein's philosophy and the philosophers of science that influenced Einstein: David Hume, Ernst Mach, and Immanuel Kant. Most physicists will know that the ideas of the empiricist Mach were instrumental to Einstein's formulation of his relativity theory, which did away with the unobserved ether. According to Einstein, who studied Hume's work in his early twenties with a group of friends, Hume "saw clearly that certain concepts ... cannot be deduced from our perceptions of experience by logical methods." Einstein had read Kant when he was just a schoolboy, and Kant had found that there was nonetheless a category of propositions the truth of which was "grounded in reason itself." Einstein contended that relativity theory had proven Mach and Hume right and Kant wrong. One of the latter's a priori truths had been that space had to be three-dimensional and adhere to the ancient geometric axioms of Euclid. This clearly conflicted with the dynamic and curved spacetime perspective of Einstein's theory.

Eventually, the biggest influence on Einstein's philosophy was undoubtedly his own discovery of the relativistic theory of gravity. Recent historical research has shown that this was the result of an intricate interplay between mathematical and physical considerations (*4*). In Einstein's later recollections, he held that eventually mathematics had given him the final theory. He derived a methodological maxim from this experience—"nature is the realization of the simplest conceivable mathematical ideas (*5*)"—that was to stay with him in his decades-long search for theories that should unify all of nature's forces (*6*).

Isaacson's book is to be recommended, not only because it presents us with a philosophically coherent picture of Einstein (Isaacson was educated as a philosopher at Oxford) but foremost for the balanced and humane account of its protagonist's life and work.

In the limelight. During their 1931 visit to the United States, the Einsteins accepted Charlie Chaplin's invitation to attend the premiere of his film *City Lights*.

Nevertheless, one exception needs to be noted after an extensive discussion of Einstein's strong opposition to McCarthyism, Isaacson finds that "Einstein was not used to self-righting political systems." When McCarthy's influence waned, and Einstein saw parallels with the rise of Nazism fall away, he "finally discovered what was fundamental about America: it can be swept by waves of what may seem, to outsiders, to be dangerous polit-

The reviewer is with the Einstein Papers Project, California Institute of Technology, and at the Institute for History and Foundations of Science, Utrecht University, Princetonplein 5, Utrecht, 3584 CC, Netherlands. E-mail: J.vanDongen@phys.uu.nl

tical passions but are instead passing sentiments that are absorbed by its democracy and righted by its constitutional gyroscope.

Following the Nazi takeover in Germany, Einstein relocated to the United States in 1933 and became an American citizen in 1940. Few Americans have had their opinions as closely followed by the press, or as warmly sought by their compatriots, as Einstein. Yet to Isaacson, Einstein apparently remained an "outsider." America's own version of Voltaire's *ingenu*. This is an awkward qualification in light of Isaacson's own discussions of Einstein's public role, both in Europe and the United States. But it resonates with that of many Einstein contemporaries, who found Einstein's opinions naïve. Such judgment was usually passed by those who disagreed with him. It might be the case that Isaacson—who in his introductory chapter stresses the need for creativity in education so that his country could "in the face of global competition" reach a "competitive advantage" (not very Einsteinian words)—recoiled from Einstein's harsh judgment of the Red Scare.

Nevertheless, Isaacson's book is a welcome addition to the literature on Einstein, because it is an accessible overview that any student of the subject will appreciate. Unlike what Einstein's reaction to Moszkowski may suggest, Isaacson believes that Einstein loved publicity as much as he loved to complain about it. He points out, persuasively, that those who truly dislike the attention of journalists (Einstein's "natural enemies" according to Nettl) do not turn up with Charlie Chaplin at a movie premiere, as the Einsteins eventually did. Both then and now, one can be surprised by the scale of Einstein's celebrity. Yet, as he himself said, "it is a welcome symptom in an age which is commonly denounced as materialistic, that it makes heroes of men whose ambitions lie wholly in the intellectual and moral sphere" (*7*).

References

1. J. Nettl, *Einstein. Eine Biographie* (Rowohlt, Reinbek, Germany, 2005)
2. A. Moszkowski, *Einstein, the Searcher: His Work Explained from Dialogues with Einstein*, H. L. Brose, Transl. (Methuen, London, 1921)
3. T. Levenson, *Einstein in Berlin* (Bantam, New York, 2003)
4. J. Renn, Ed., *The Genesis of General Relativity* (Springer, Dordrecht, 2007)
5. A. Einstein, *On the Method of Theoretical Physics* (Oxford Univ. Press, Oxford, 1933)
6. J. van Dongen, *Arch. Hist. Exact Sci.* **58**, 219 (2004)
7. A. Einstein, "My First Impressions of the U.S.A.," *Nieuwe Rotterdamsche Courant*, 4 July 1921, reprinted in *Ideas and Opinions* (Random House, New York, 1954), pp. 3–7

10.1126/science.1145120

SYSTEMS BIOLOGY

How Central Is the Genome?

Eric Werner

Traditionally the genome DNA is seen as the dominant force in living systems. In *The Music of Life*, Denis Noble criticizes this view. Challenging the foundations of current biological sciences, he questions the central dogma, its unidirectional view of information flow, and its imposition of a bottom-up methodology for research in the life sciences. Behind the scenes, a conceptual revolution is transforming biology and medicine: systems biology applies the methods of mathematics, computer science, engineering, physics, and, even, philosophy to understanding living systems.

Noble, an emeritus professor of physiology at the University of Oxford (and colleague of mine), is one of the founders of systems biology, and his work on modeling of the heart is a paradigm in the field. *The Music of Life* offers an excellent informal introduction to the concepts and issues that form the bedrock of systems biology. Noble orchestrates a coherent symphony of ideas spanning genes, embryology, evolution, and consciousness.

A provocative theme recurring throughout the book is that there is no program (or, using the author's musical metaphor, conductor) that controls a biological system neither in its development nor its functioning. Noble states, "There are no privileged components telling the rest what to do." The genome he holds, is not a program but a passive database, one of many equal contributors to the development and dynamics of a living organism. The interaction of many components produces the result. Although I am sympathetic to Noble's critique of reductionism, his sidelining of the genome—considering it to be only a passive participant or resource—seems problematic.

At the heart of the issue are two questions: Where does the complexity of a developing embryo come from? How is the development of organisms controlled? Many developmental biologists, like Eric Davidson, assume that the information required to generate the complexity of organisms lies in the genome, in particular its regulatory networks, and that these networks control the development of the organism (*1*). In contrast, Noble questions both that the genome is the source of complexity and that it functions like a central controller.

Noble appears to identify centrality of control with the existence of a central program (or score). Centrality of control is an ambiguous concept. It can either mean that the genome contains most of the control information necessary for development or it can mean that the control is centralized in one agent controlling the rest. The conductor metaphor that Noble uses and attacks suggests the image of one agent controlling a group. However, even though the genome is the same in all cells, its control is local. There is no single conductor genome. Rather there are many copies, each in different activation states, each influencing the activity of the cell in which it resides. It is as if each cell had its own conductor, with the same score (the genome), but the individual conductors direct independently, reading from different parts of the score. The multiple conductors are autonomous but can also react, interact, and cooperate (coordinating their activity by communication or signaling). Thus, there are two separate issues: the source of the complexity of organisms and the locality of control.

The view of developmental biology that Noble presents in the book is influenced by Enrico Coen (*2*), who holds that the process of copying is fundamentally different from creative processes like development. For Coen, the creative actions of an artist and, analogously, embryological development are self-reflexive

No conductor necessary. A New Orleans jazz band

The reviewer is at the Department of Physiology, Anatomy, and Genetics, University of Oxford, Parks Road, Oxford OX1 3PT, UK. E-mail: eric.werner@dpag.ox.ac.uk

processes that involve extensive interaction with the results of previous actions. Coen claims there is no central program, but he fails to see that such interactions might well be controlled by distributed networks, which are, in effect, programs that run separately in each cell in a vast multicellular system. In essence, genomes function as strategies that guide the cell agents as the system develops (*3*). Such strategies or programs can also interact with their environment (including other cell agents) at each stage of development. Hence they can also be self-reflexive in Coen's sense.

Coen has a restrictive view of programs akin to John von Neumann's conception of a self-reproducing automaton, which involves a printerlike process generating a copy of itself line by line, based on a set of instructions (which are also copied) (*4*). In contrast, living cells with their genomes, rather than emulating the von Neumann architecture for self-reproducing automata, are more like distributed strategic agents.

Because Coen and Noble do not consider distributed programs as the source of developmental control, they are forced to rely on the problematic notions of interactionism and emergence—in which organisms are generated by the interactions of simpler parts. Yet, the problem of the source of information for the generation of the complex space-time event we call embryogenesis cannot be avoided by stating that embryogenesis is the result of a complex interaction—doing so does not help us understand the process. Rather, we need to link control information in the genome with the process of development (*1*, *2*).

According to Noble, the egg contains analog information whereas the genome contains digital information. Because analog information is continuous, the egg carries potentially infinite amounts of information that overwhelm the finite digital information present in the genome. One must, however, consider the relevance of the information (*5*, *6*). At detailed levels of resolution (approximations of the continuous state), the molecular state of the egg is virtually random and, in that sense very complex. An enormous amount of information would be required to characterize the egg's state. But such random information does not make a relevant contribution to the generation in space and time of the morphology of a multicellular organism. Most of the information at the lower level of ontology, namely, the protein state of the egg, is irrelevant to the development of the organism. Indeed, the random fluctuations in the egg and its environs have to be damped or avoided in some way for the process of development to work.

Suppose we inserted a dinosaur's genome into a chicken egg. If the egg then developed into a dinosaur, we would have to conclude that the genome and not the information in the egg was responsible for the ontogeny. Undoubtedly, we would have needed to provide maternal dinosaur transcription factors to bootstrap the developmental process. And there may be other relevant factors such as the size, nutrients, and thickness of the egg shell. But it would be clear that they do not contain the crucial control information required to generate the dinosaur. Although this thought experiment verges on science fiction, it makes the point that the genome, rather than the egg or the maternal matrix, contains the information necessary for the generation of multicellular organisms. For Noble, the developmental process—not being controlled by any program—is the result of a mysterious interaction of equal partners. I am simply saying they are far from equal in information content.

Thought-provoking, *The Music of Life* is a surprisingly, if deceptively, easy read. One learns as much, if not more, on a second reading as on the first. Noble presents his case for the systems approach with elegance and a simplicity that hides unnecessary detail. His conversational style together with personal vignettes give readers the feeling they are with him sharing in an active process of discovery. The book can be recommended to anyone—novice or professional, interested in systems biology and the foundations of life.

BROWSINGS

Marshes. The Disappearing Edens. William Burt. Yale University Press, New Haven, CT, 2007. 192 pp. $35, £25. ISBN 9780300122299.
For more than three decades, Burt has been stalking shy inhabitants (especially rails, bitterns, grebes, and gallinules) of North America's grassy wetlands with his camera. Here he presents 90 photographs of marsh birds, wildflowers (right, perennial salt marsh asters, Old Lyme, Connecticut), and scenes. He also reflects on the marshes he has explored—their riches, their pasts, and the threats they now face.

Sippewissett. Or, Life on a Salt Marsh. Tim Traver. Chelsea Green, White River Junction, VT, 2006. 260 pp. $22.50. ISBN 9781933392141.
Biologists (including Louis Agassiz and Rachel Carson) have long been drawn to the patch of Cape Cod marsh where Traver spent his boyhood summers and to which he still returns. His reflections on the fauna, flora, habitats, and human culture eloquently weave together ecology, history, and memory. He offers enticing discussions of tidal flows, spawning runs, eelgrass beds, clam hunts, and even the microbial communities in the muds. His treatment of sometimes contentious conservation issues demonstrates his recognition of the challenges facing those who wish to sustain their sense of home.

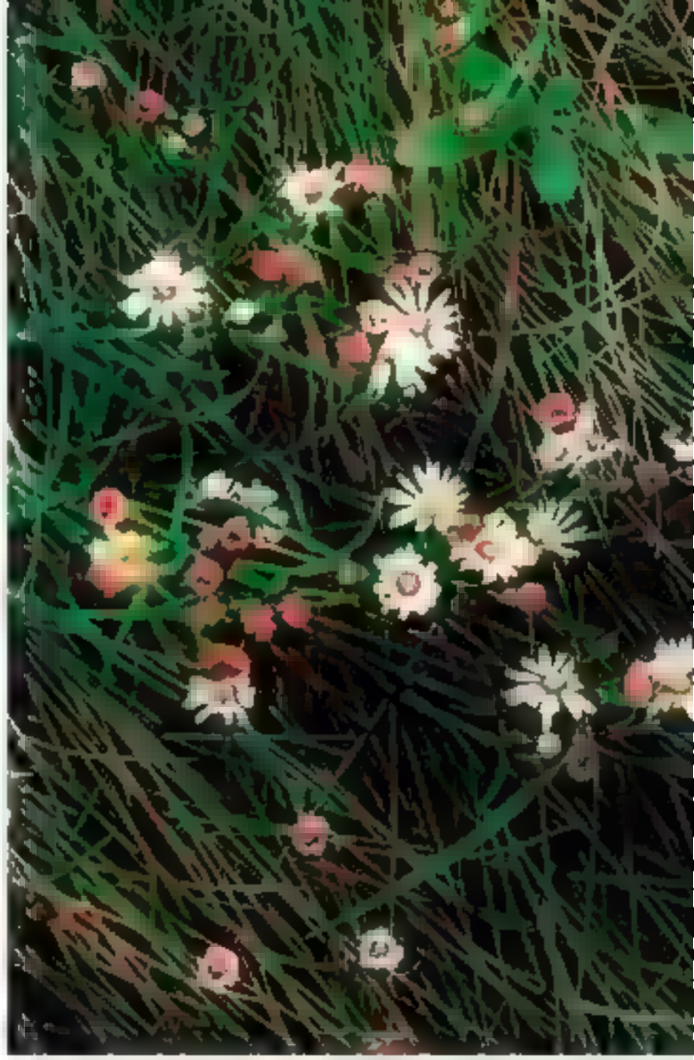

CREDIT: WILLIAM BURT/COURTESY YALE UNIVERSITY PRESS

References

1. E. H. Davidson, *The Regulatory Genome: Gene Regulatory Networks in Development and Evolution* (Academic Press, Burlington, MA, 2006); reviewed by D. Arendt, *Science* **314**, 1085 (2006).
2. E. Coen, *The Art of Genes: How Organisms Make Themselves* (Oxford Univ. Press, Oxford, 1999).
3. E. Werner, in *Proceedings of the Second Conference on Theoretical Aspects of Reasoning About Knowledge*, M. Y. Vardi, Ed. (Morgan Kaufman, San Francisco, 1988), pp. 129–143.
4. J. von Neumann, *The Neumann Compendium*, F. Brody, T. Vámos, Eds. (World Scientific, Singapore, 1995).
5. M. Gellman, S. Lloyd, *Complexity* **2**, 44 (1996).
6. E. Werner, in *Distributed Software Agents and Applications*, J. W. Perram, J. P. Müller, Eds. (Springer Verlag, Berlin, 1996), pp. 19–39.

10.1126/science.1141807

ENVIRONMENT

Globalization of Conservation: A View from the South

Successful global strategies for biodiversity conservation require increasing reliance on local leadership and major investment in local capacity.

J. P. Rodriguez,[1] A. B. Taber,[2]* P. Daszak,[2,3] R. Sukumar,[4,5] C. Valladares-Padua,[6] S. Padua,[6] L. F. Aguirre,[7,8] R. A. Medellín,[9] M. Acosta,[10] A. A. Aguirre,[2] C. Bonacic,[11] P. Bordino,[12] J. Bruschini,[2] D. Buchori,[13] S. González,[14] T. Mathew,[5] M. Mendez,[12,15] L. Mugica,[16] L. F. Pacheco,[8,16] A. P. Dobson,[17] M. Pearl[2]

Large international nongovernmental organizations (INGOs) are increasingly setting the global conservation agenda. These INGOs have developed a range of tools, e.g., Biodiversity Hot Spots (*1*), Global 200 Ecoregions (*2*), and others (*3*) to set priorities and to compete with each other. They often use a corporate "branding" strategy to help raise funds and to define and communicate their niches in a crowded and competitive market. This corporate model has been very successful for fundraising: Conservation International's "Hot Spots" strategy accompanied an increase in overall annual expenditures from U.S. $27.8 million in 1998 to U.S. $89.3 million by 2004, and World Wildlife Fund U.S.A.'s "Ecoregions" program accompanied a rise in expenditures from U.S. $80 million to U.S. $121.7 million between 1997 and 2005 (*4*). This helped offset declines of ~50% in government and multilateral agency investment in biodiversity conservation over the past decade (*5*) while expanding the influence of these INGOs globally. These factors have led some to equate the operations of large INGOs with transnational corporations (*6*).

Although these brands are derived from conservation science, they are vulnerable to scientific criticism (*7*). For example, priority-setting plans that target fixed areas for conservation (e.g., Hot Spots and Ecoregions) are insufficient to deal with fast-moving threats such as pathogens or invasive species (*8*), the alteration of species' ranges due to climate change (*9*), or spatially dynamic marine ecosystems (*10*). Furthermore, large-scale international development initiatives, designed centrally and top-down, have rarely met expectations (*11*). This does not bode well for globalized conservation approaches, which require that the often inadequately evaluated strategies of developed country INGOs be adopted by developing countries (*12*, *13*). Such top-down approaches can fail to link agendas of a broad constituency of local communities, scientists, conservation practitioners, and policy-makers (*14*, *15*).

CREDIT: ILLUSTRATION BY JOE BUTLER

In some cases, the investments of foreign conservationists are seen as a threat to sovereignty and an imposition on local peoples. For instance, in Bolivia where INGOs like Wildlife Conservation Society and Conservation International have helped establish and manage national parks, there have been calls for the "nationalization" of protected areas. Although protected areas have never been out of government control, foreign organizations are seen by some Bolivians as usurping control of national territory and as having disempowered grassroots efforts. Here it has proven difficult to convince government and local communities that conservation INGOs are free of hidden intentions (*16*–*18*). Similarly, calls made by international conservationists to remove tribal people from parks in India to better protect tigers may have further polarized positions, making the search for workable solutions even more difficult (*19*).

It can be argued that INGOs are fundamentally different from globalizing corporations. What leads to success in commerce is profit, whereas success in developing country conservation typically hinges on local support to sustain results. Globalization of industry followed three phases (*20*): first the 19th-century "international model," with companies selling goods through overseas sales offices, then the 20th-century classic multinational corporation, where the parent created smaller versions of itself overseas, and finally, the 21st-century globally integrated enterprise, where the corporation acts as a single global entity able to place people and operations anywhere around the world. The most effective modern multinationals recognize the importance of local knowledge, e.g., for product sales. However, generalized global approaches fail for biodiversity conservation at local scales, because solutions must integrate extremely diverse natural, socioeconomic, and cultural systems and usually require a sense of community ownership.

[1]Instituto Venezolano de Investigaciones Científicas and PROVITA, Caracas, Venezuela. [2]Wildlife Trust, New York, NY, USA. [3]Consortium for Conservation Medicine, New York, NY, USA. [4]Indian Institute of Science, Bangalore, India. [5]Asian Nature Conservation Foundation, Bangalore, India. [6]IPÊ - Instituto de Pesquisas Ecológicas, Nazaré Paulista, São Paulo, Brazil. [7]Centro de Biodiversidad y Genética, Universidad Mayor de San Simón, Cochabamba, Bolivia. [8]BIOTA—Centro de Estudios en Biología Teórica y Aplicada, La Paz, Bolivia. [9]Instituto de Ecología, Universidad Nacional Autónoma de México and BioConciencia, Mexico City, Mexico. [10]Universidad de la Habana, Cuba. [11]Fauna Australis and Pontificia Universidad Católica de Chile, Santiago, Chile. [12]AquaMarina—Centro de Estudios en Ciencias Marinas, Pinamar, Argentina. [13]Bogor Agricultural University and PEKA Indonesia Foundation, Bogor, Indonesia. [14]NBCE, Facultad de Ciencias, Universidad de la República, Montevideo, Uruguay. [15]Columbia University, New York, NY, USA. [16]Universidad Mayor de San Andrés, La Paz, Bolivia. [17]Princeton University, Princeton, NJ, USA.

*Author for correspondence. E-mail: taber@wildlifetrust.org.

One trend in the globalization of conservation is that INGOs are increasingly registering in developing countries. For example, Conservation International and The Nature Conservancy are now legally registered in at least 18 and 23 developing world countries, respectively (*21*, *22*). This provides greater accountability to national governments and donors, but also enables them to compete for funds with local NGOs, which may decrease efforts to strengthen local institutions. This can result in developing-world conservationists, with locally tuned priorities but lacking donor connections, being obliged to obtain funds from INGOs pushing global agendas. Ultimately, this can lead to INGOs edging out local institutions essential for sustaining long-term conservation (*19*). It also means that changes in donor or INGO priorities can lead to abrupt withdrawals of support. Conservation efforts then fail if local conservationists have not been trained or local institutions have not been developed with their own programs and funding. Training is usually insufficiently supported: e.g., only 4% of the U.S.$3.26 billion invested in Latin American biodiversity conservation between 1990 and 1997 was specifically spent on capacity building (*23*). Similarly the U.S. Agency for International Development, a key supporter of international conservation, has cut back university scholarships in all fields for developing world students to 900 per year from a previous 20,000 (*24*). Furthermore, the lack of long-term career structures often results in scarce local practitioners migrating to developed countries, weakening conservation infrastructure in front-line countries.

Biodiversity conservation continues to require improved integration with human welfare concerns. This has been central to a long-standing debate among environmentalists stretching back at least to the 1970s when the Club of Rome think tank in its "Limits to Growth," emphasized the global risk to humanity and ecosystems from natural resource depletion, greatly influencing the modern environmental movement (*25*). At the same time, developing-world scientists from the Bariloche Foundation in Argentina produced the "Latin American World Model," which stressed the need to address socioeconomic concerns to build what we would now call a sustainable society (*26*).

Investment will be most effective where such issues (as well as social justice and governance regimes) are addressed adequately and where local capacity exists, however, conservationists need not abandon countries that score poorly on development criteria. Here, support can be targeted and managed so that local capacity is built and marginalized indigenous peoples and other local stakeholders become equal partners to maximize prospects for success (*5*). Part of the solution is to increase local pools of practitioners at all levels, from community parabiologists to university professors and government officials (*27*). INGOs could provide funds for salary and staff retention at local organizations. Investment in scholarships for first-world universities could be matched with funds for strengthening developing country universities and technical programs where studentships typically cost much less.

Bolstering independent local institutions (e.g., civil society organizations, universities, and local government agencies) is key to keeping conservation on national agendas in developing countries. Small, locally focused organizations working at the front lines of biodiversity loss are often the most effective—witness the rise of community-based conservation projects across the developing world with examples including the Mamiraua Sustainable Development Reserve and the Pontal do Parapanema area in Brazil, the Kaa-Iya del Gran Chaco National Park in Bolivia, and other similar areas in Africa (*28*, *29*). In these cases, although international assistance sometimes provided essential help, key to success has been the existence of strong local organizations to take the lead in implementing management. This may hold true even in developed countries, where local chapters of national conservation NGOs are often the groups that effect change (e.g., regional chapters of the Audubon Society in the U.S.A.). Although such institutions are weak in much of the developing world (*30*), they are critically important, because they can adapt the conservation agenda for local implementation, working collaboratively with government institutions and policy-makers. The bottom line is that biodiversity will only be conserved if local people and interests want to save it for ethical and broadly utilitarian purposes. This level of support has to be large enough to resist a minority that may seek alternative land uses for narrowly selfish utilitarian reasons.

Some INGOs have fostered collaboration by setting up egalitarian networks of local conservation organizations that are mutually supporting, around the world. Examples include Birdlife International (*31*) and the Wildlife Trust Alliance (*32*). In these cases, developed country NGOs help raise funds for agendas set by local partners. We recognize that INGOs have efficiencies of scale and operation as well as an important role in influencing global policy. However, we argue that leadership in conservation has to be decentralized and better integrated into local conditions. Locally produced strategies and agendas, implemented by strong local institutions and individuals are key to success.

References and Notes

1. N. Myers *et al.*, *Nature* **403**, 853 (2000).
2. D. M. Olson, E. Dinerstein, *Ann. Missouri Bot. Gard.* **89**, 199 (2002).
3. T. M. Brooks *et al.*, *Science* **313**, 58 (2006).
4. Capital Research Center, www.capitalresearch.org.
5. M. Chapin, *World Watch* **17**, 17 (2004).
6. D. Ransom, *New Int.* **383**, 2 (October, 2005).
7. C. D. L. Orme *et al.*, *Nature* **436**, 1016 (2005).
8. J. R. Mendelson III *et al.*, *Science* **313**, 48 (2006).
9. C. D. Thomas *et al.*, *Nature* **427**, 145 (2004).
10. E. A. Norse, L. B. Crowder, Eds., *Marine Conservation Biology: The Science of Maintaining the Sea's Biodiversity* (Island Press, Washington, DC, 2005), 496 pp.
11. W. Easterly, *The White Man's Burden: Why the West's Efforts to Aid the Rest Have Done So Much Ill and So Little Good* (Penguin Press, New York, 2006), 436 pp.
12. P. J. Ferraro, S. K. Pattanayak, *PLoS Biol.* **4**, 482 (2006).
13. B. S. Halpern *et al.*, *Conserv. Biol.* **20**, 56 (2006).
14. S. Aswani, M. Lauer, *Hum. Org.* **65**, 81 (2006).
15. S. Schwartzman, B. Zimmerman, *Conserv. Biol.* **19**, 721 (2005).
16. "Gobierno recupera hoy propiedad y soberanía de áreas protegidas," *El Diario* (La Paz, Bolivia), 26 August 2006 [in Spanish]; www.eldiario.net/noticias/nt060826/nal.php?pag=5_01nal.html
17. R. M. Ruiz, *J. Sustain. Forest.* **17**, 7 (2003).
18. "An interview with Bernardo Peredo: Indigenous communities, biodiversity, natural resources, and sustainable development in Bolivia." *In Motion Magazine* (10 June 2007); www.inmotionmagazine.com/global/bp_int.html.
19. V. Saberwal, M. Rangarajan, Eds., *Battles over Nature: Science and the Politics of Conservation* (Permanent Black, Delhi, 2003), 412 pp.
20. Anonymous, *Economist* **383**, 67 (7 April 2007).
21. Conservation International, www.conservation.org.
22. The Nature Conservancy, www.tnc.org.
23. G. Castro, I. Locher, *Mapping Conservation Investments: An Assessment of Biodiversity Funding in Latin America and the Caribbean* (Biodiversity Support Program, Washington, DC, 2000), 79 pp.
24. *The U.S. Response to East African Famines and the Future Outlook for Food Aid in Africa, Hearing before the House Committee on International Relations*, 108th Congress, 1st session (U.S. GPO, Washington, DC, 2003), 89 pp.
25. D. H. Meadows, D. L. Meadows, J. Randers, W. W. Behrens III, *The Limits to Growth: A Report for the Club of Rome's Project on the Predicament of Mankind* (Universe Books, New York, 1972), 205 pp.
26. A. O. Herrera *et al.*, *Catastrophe or New Society? A Latin American World Model* (International Development Research Centre, Ottawa, Canada, 1976), 108 pp.
27. J. P. Rodriguez, J. A. Simonetti, A. Premoli, M. A. Marini, *Conserv. Biol.* **19**, 969 (2005).
28. D. Hulme, M. Murphree, Eds., *African Wildlife and Livelihoods: The Promise and Performance of Community Conservation* (Heinemann, Portsmouth, NH, 2001), 344 pp.
29. K. M. Silvius, R. E. Bodmer, J. M. V. Fragoso, Eds., *People in Nature* (Columbia Univ. Press, New York, 2004), 463 pp.
30. C. B. Barrett, K. Brandon, C. Gibson, H. Gjertsen, *Bioscience* **51**, 497 (2001).
31. Birdlife International, www.birdlife.org.
32. Wildlife Trust Alliance, www.wildlifetrust.org.

10.1126/science.1145560

NEUROSCIENCE

Shining Light on Depression

Real-time, high-speed optical imaging is a promising approach for elucidating networks of brain activity associated with depression

Thomas R. Insel

Just as research during the Decade of the Brain (1990–2000) forged the bridge between the mind and the brain, research in the current decade is helping us to understand mental illnesses as brain disorders. As a result, the distinction between disorders of neurology (e.g., Parkinson's and Alzheimer's diseases) and disorders of psychiatry (e.g., schizophrenia and depression) may turn out to be increasingly subtle. That is, the former may result from focal lesions in the brain, whereas the latter arise from abnormal activity in specific brain circuits in the absence of a detectable lesion. As we become more adept at detecting lesions that lead to abnormal function, it is even possible that the distinction between neurological and psychiatric disorders will vanish, leading to a combined discipline of clinical neuroscience (*1*).

But before we can understand depression as a brain disorder, we need information on the specific neuronal circuits that contribute to the hopeless despair that forms the core of this illness. Neuroimaging studies of people with depression might be helpful for identifying brain regions of interest, but the temporal and spatial resolution of current functional magnetic resonance imaging and positron emission tomography may not capture the real-time dynamics of brain function that are most relevant to mood and cognition. In a new approach, Airan *et al.* report on page 819 of this issue the use of optical imaging to capture cellular activity at millisecond resolution in brain slices (*2*). Their study, which uses rodents with some of the behavioral features of depression, does not define the neurobiology of depression in humans, but it demonstrates how optical imaging—in this case, using voltage-sensitive dyes—can identify changes in brain activity, enabling correlations between real-time cellular activity and changing affective state.

The findings of Airan *et al.* are consistent with other results that implicate the hippocampus in rodent studies of depression. Chronic or intense stressors, such as social defeat, result in behaviors that resemble human depression, and these stressors have been reported to reduce hippocampal neurogenesis (*3*). They also down-regulate the hippocampal expression of brain-derived neurotrophic factor (*4*), a molecule that promotes neuron survival, proliferation, and differentiation. Clinically effective antidepressants increase hippocampal neurogenesis (*5*), and blocking neurogenesis during treatment prevents the antidepressant effect in rodents (*6*).

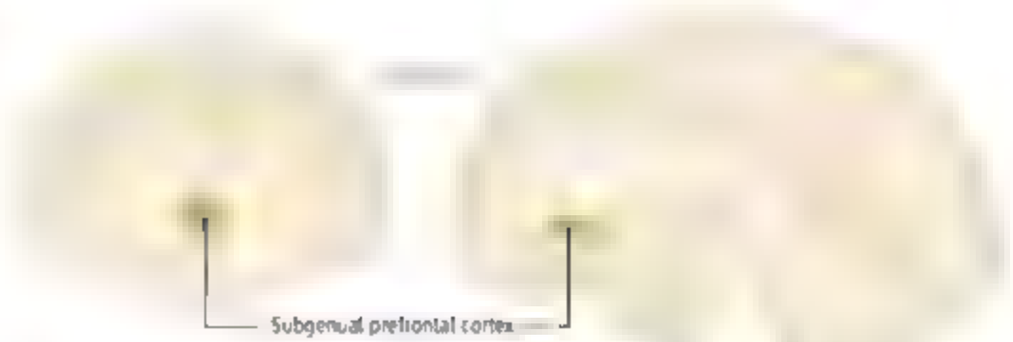

In search of the core of depression. Imaging brain activity in human patients suffering from depression or in animal models of the disease will help to link brain activity in regions such as the hippocampus and prefrontal cortex to behavioral disorders (*10*, *11*).

What about the hippocampus and human depression? Major depressive disorder is associated with cognitive deficits and dysregulation of the hypothalamic-pituitary-adrenal (HPA) axis, part of the neuroendocrine system that controls the stress response. Because the hippocampus is involved in both forming new memories and regulating the HPA axis, one might expect a link between depression and the hippocampus. Indeed, some human neuroimaging studies have reported a subtle reduction in the size of the hippocampus in patients with depression (*7*), and postmortem studies have reported alterations in hippocampal gene expression (*8*). But the evidence thus far is unconvincing. Humans with hippocampal lesions have memory deficits but not mood disorders (*9*). And none of the imaging or postmortem findings have been shown to be specific to the hippocampus or to major depressive disorder. Although the absence of evidence is hardly evidence of absence, most recent clinical studies of the neurobiology of depression have been following a different lead.

Neuroimaging studies of humans with major depressive disorder have largely pointed to prefrontal sites, especially implicating an area in the midline subgenual anterior cingulate cortex, often denoted as area 25 (see the figure) (*10*, *11*). Not only does this region appear abnormal on structural and functional scans (*10*, *11*), but also it is enriched with the serotonin transporter, a target for many antidepressant drugs. Individuals inheriting a risk allele within the promoter of the serotonin transporter gene have reduced volume of area 25 and reduced functional coupling of this region to the amygdala, a subcortical region implicated in the regulation of emotion (*12*). An initial study of treatment-resistant depressed patients reports that deep brain stimulation adjacent to area 25 relieves the symptoms of major depressive disorder (*13*).

How do we resolve the differences between rodent studies that implicate the hippocampus and human studies that implicate the midline prefrontal cortex? Of course, the discrepancies might be attributed to neuroanatomical differences between rodent and human brains. Rodents have at most a primitive subgenual anterior cingulate cortex, whereas this region in the primate brain shows extensive connections with subcortical and cortical targets (*14*). But other fundamental issues should be kept in mind when jumping from studies of rodent behavior to human psychopathology. Human psychiatric disorders are complicated amalgams of affective, cognitive, and behavioral abnormalities. We might model aspects of one of these dimensions, such as helplessness or memory loss, in rodents, but we are then studying an aspect of the disorder, not the disorder itself.

Major depressive disorder, the result of an unfortunate convergence of genetic and environmental factors, is certainly more than the

The author is at the National Institute for Mental Health, Room B235, 6001 Executive Boulevard, Bethesda, MD 20892, USA. E-mail: tinsel@mail.nih.gov

sum of its observable parts. Identifying brain regions correlated with "the parts" will be an important next step for human imaging studies, but the field will need to avoid high-tech phrenology. Understanding the neurobiology of abnormal mood regulation will not be accomplished through the identification of a focal lesion or a single explanatory hot spot. The task will be to define altered activity within a functional neuronal network that might well include both the ventral hippocampus and midline prefrontal cortex (*15*). The importance of the new report by Airan *et al.* is the demonstration of abnormal network dynamics in a defined circuit through the use of a technique with combined spatial and temporal resolution that we have not even begun to consider for human studies. We are not able to apply voltage-sensitive dye imaging to people with major depressive disorder, but studies in model animals that help us to link behavior to real-time circuit information will be the foundation for understanding depression as a brain disorder.

References

1. T. R. Insel, R. Quirion, *J. Am. Med. Assoc.* **294**, 2221 (2005).
2. R. D. Airan *et al.*, *Science* **317**, 819 (2007); published online 5 July 2007 (10.1126/science.1144400).
3. R. M. Sapolsky, *Arch. Gen. Psychiatry* **57**, 925 (2000).
4. N. Tsankova *et al.*, *Nat. Neurosci.* **9**, 519 (2006).
5. R. S. Duman, *Biol. Psychiatry* **56**, 140 (2004).
6. I. Santarelli *et al.*, *Science* **301**, 805 (2003).
7. A. Neumeister *et al.*, *Biol. Psychiatry* **57**, 935 (2005).
8. A. L. Lopez-Figueroa *et al.*, *Biol. Psychiatry* **55**, 225 (2004).
9. L. R. Squire, C. E. L. Stark, R. E. Clark, *Annu. Rev. Neurosci.* **27**, 279 (2004).
10. W. C. Drevets *et al.*, *Nature* **386**, 824 (1997).
11. H. S. Mayberg *et al.*, *Neuroreport* **8**, 1057 (1997).
12. L. Pezawas *et al.*, *Nat. Neurosci.* **8**, 828 (2005).
13. H. S. Mayberg *et al.*, *Neuron* **45**, 651 (2005).
14. D. Drevets, J. L. Price, *Cereb. Cortex* **10**, 206 (2000).
15. J. Houenou *et al.*, *Mol. Psychiatry* 10.1038/sj.mp.4002010 (2007).

10.1126/science.1147565

EVOLUTION

An Embarrassment of Switches

A surprising abundance of evolutionary changes in transcription factor binding sites may obscure the causes of phenotypic divergence.

Leonid Kruglyak and David L. Stern

What makes a human different from a chimpanzee or a mouse? Of course, we know the answer in broad outline. Mutations in the genome, sifted by natural selection, cause changes in appearance, physiology, and behavior—what geneticists call the phenotype. But we have only a vague picture of a more detailed answer. Precisely which mutations generate phenotypic evolution? It's not that we can't find the mutations. Today's DNA sequencing technology readily identifies all differences between two genomes. There are simply too many differences—tens of millions between human and chimp, for example (*1*). An unknown fraction of these mutations alter the phenotype. Nonetheless, the molecular effects of mutations provide a rough guide to their phenotypic effects. Some mutations change the amino acid sequence of proteins, thereby altering their functions, and some change so-called cis-regulatory regions, altering when and where proteins are produced. We know a lot about the first class, but much less about the second. Several recent papers, including one by Borneman *et al.* on page 815 of this issue (*2*), demonstrate a surprising abundance of cis-regulatory changes between closely related species.

It is easy to identify mutations that alter proteins, because of the simplicity of the genetic code. Linear strings of DNA nucleotide triplets encode proteins, and each triplet always specifies a particular amino acid. Thus, mutations that alter a protein can be immediately read off from the DNA sequence. By contrast, we are only beginning to understand how the cis-regulatory code works (*3*). Cis-regulatory regions contain short strings of nucleotides, from 6 to 20 nucleotides in length, scattered irregularly in the vicinity of the protein-coding DNA. Proteins called transcription factors bind to these short DNA strings—transcription factor binding sites—to regulate the production of messenger RNA and thus the synthesis of proteins. In 1975, King and Wilson found that only about 1% of amino acids differed between a set of human and chimpanzee proteins (*4*). They thus proposed that changes in cis-regulatory regions—evolutionary switching of transcription factor binding sites—might cause the majority of phenotypic differences between species. This hypothesis has gained support from studies over the past decade (*5*).

Recent computational studies across species illustrate that many transcription factor binding sites have evolved quickly. That is, binding sites present in one species are often absent in another (*6–8*). New findings provide experimental evidence for this conclusion.

Man or mouse? Both the presence and absence of transcription factor binding sites in a genome, as well as the binding of transcription factors to sites that are present, can differ between species and may account for differences in gene expression and phenotype.

The authors are in the Department of Ecology and Evolutionary Biology, and L. Kruglyak is also at the Lewis-Sigler Institute for Integrative Genomics, Princeton University, Princeton, NJ 08544, USA. E-mail: leonid@genomics.princeton.edu; dstern@princeton.edu

These studies use a technique called chromatin immunoprecipitation to capture from cells a particular transcription factor along with its bound short DNA strings. These DNA strings are then identified by hybridization to DNA microarrays (*9*, *10*).

Using this approach, Borneman *et al.* examined binding of two transcription factors in three yeast species. In only about 20% of cases did a transcription factor bind to the same site (meaning, approximately the same position with respect to the target gene) in all three species. In some cases, the absence of binding corresponded to a loss of the appropriate binding site. Surprisingly, in other cases, the absence of binding in one species occurred despite conservation of the DNA sequence. In a similar study that compared transcription factor binding between human and mouse genomes, Odom *et al.* (*11*) found that 41 to 89% of cis-regulatory regions bound in one species were not bound in the other. Even when the same gene region was bound by a particular transcription factor in both species, the precise position of the bound site with respect to the target gene often differed between species.

Do all of these evolutionary switches in transcription factor binding sites cause phenotypic differences? For two reasons, it seems likely that many do not. First, change of a single site may not alter gene expression. Transcription factors often bind to multiple sites within the same cis-regulatory region and act synergistically to regulate gene expression (*3*) (see the figure). Thus, individual binding sites may be gained and lost during evolution while the phenotype remains the same (*12*, *13*). Second, the phenotype is robust to some changes in gene expression (*14*). For example, changes in enzyme concentration often have little effect on the output of a metabolic pathway (*15*).

Thus, while the new results support a major role for cis-regulatory mutations in evolution, they leave us little closer to the question we first posed: Which DNA changes make species different? The definitive way to identify the mutations causing phenotypic differences is to perform a genetic cross between species, and then trace the association between genomic locations and phenotypes in offspring. But most species pairs are too diverged to mate and produce viable offspring, and this approach is morally untenable for humans and chimpanzees. Therefore, the discovery of the specific genomic changes that make species different will rely largely on computational and experimental searches for putative functional differences.

The experimental approach discussed here begins to identify the DNA differences that may influence gene expression. The large number of changes discovered, however, emphasizes the difficulty of the problem. Distinguishing between DNA changes that merely alter transcription factor binding and those that actually alter the phenotype requires innovative approaches for inferring the phenotypic consequences of molecular switches.

References

1. The Chimpanzee Sequencing and Analysis Consortium, *Nature* **437**, 69 (2005).
2. A. R. Borneman *et al.*, *Science* **317**, 815 (2007).
3. R. J. White, *Gene Transcription: Mechanisms and Control* (Blackwell Science, Oxford, 2001).
4. M. C. King, A. C. Wilson, *Science* **188**, 107 (1975).
5. G. A. Wray, *Nat. Rev. Genet.* **8**, 206 (2007).
6. S. W. Doniger, , C. Fay, *PLoS Comput. Biol.* **3**, e99 (2007).
7. A. M. Moses *et al.*, *PLoS Comput. Biol.* **2**, e130 (2006).
8. The ENCODE Project Consortium, *Nature* **447**, 799 (2007).
9. V. R. Iyer *et al.*, *Nature* **409**, 533 (2001).
10. B. Ren *et al.*, *Science* **290**, 2306 (2000).
11. D. T. Odom *et al.*, *Nat. Genet.* **39**, 730 (2007).
12. M. Z. Ludwig, C. Bergman, N. H. Patel, M. Kreitman, *Nature* **403**, 564 (2000).
13. A. P. McGregor *et al.*, *Evol. Dev.* **3**, 397 (2001).
14. J. L. Hartman IV, B. Garvik, L. Hartwell, *Science* **291**, 1001 (2001).
15. H. Kacser, J. A. Burns, *Genetics* **97**, 639 (1981).

10.1126/science.1146921

CHEMISTRY

Molecules Take the Heat

Advances in understanding how heat is transported through molecules will help to guide the development of molecular electronic devices

Abraham Nitzan

Problems of heating and heat transfer are ubiquitous in everyday life, from planning efficient air conditioners to dealing with overheated car engines. Such heat transfer is also of critical importance for the stability and performance of the extremely small systems considered in nanotechnology applications. In this regime, new scientific questions arise. In particular, advances in molecular electronics (where molecules are active components in nanometer-scale electronic circuits) require heating and heat transport to be understood and controlled on the molecular scale. On page 787 of this issue, Dlott and co-workers (*1*) report an important step in this direction. The authors describe and apply a novel method for measuring heat conduction through a monomolecular layer.

The author is in the School of Chemistry, Tel Aviv University, Tel Aviv 69978, Israel. E-mail: nitzan@post.tau.ac.il

Heat flow into or out of a macroscopic system can easily be monitored by measuring the change in the system temperature with a conventional thermometer. Carrying out such measurements on the molecular scale is much more difficult. First, in a heat-conducting molecular wire, local temperature may change along the molecule, requiring temperature to be gauged with submolecular resolution. Second, the thermal response may need to be detected at the picosecond (1 ps = 10^{-12} s) time scale that characterizes molecular relaxation processes. Finally, researchers have to guard against artifacts associated with noise and cope with competing energy transfer processes to and from the surrounding macroscopic environment.

Schwab *et al.* have previously scaled thermal measurements down to a few micrometers (*2*), and Kim *et al.* have measured the heat transport properties of carbon nanotubes of similar length (*3*). Dlott and co-workers now take a bottom-up approach, studying heat transport through monomolecular hydrocarbon layers of varying chain lengths with 6 to 24 carbon atoms. In these insulating systems, heat transport is dominated by vibrational motions.

R. Y. Wang *et al.* have previously reported experiments in which a monomolecular layer connects gallium arsenide and gold surfaces via sulfur end groups. They inferred the thermal conduction of the layer from the electrical resistance to an oscillatory driving current on the gold (*4*). Dlott and co-workers use a different approach: They attach the molecules at one end via sulfur bonds to a gold layer deposited on glass; the other ends, terminated by methyl groups, point outward. These methyl ends form a two-dimensional surface, situated above the gold substrate at a distance determined by the length of the molecular

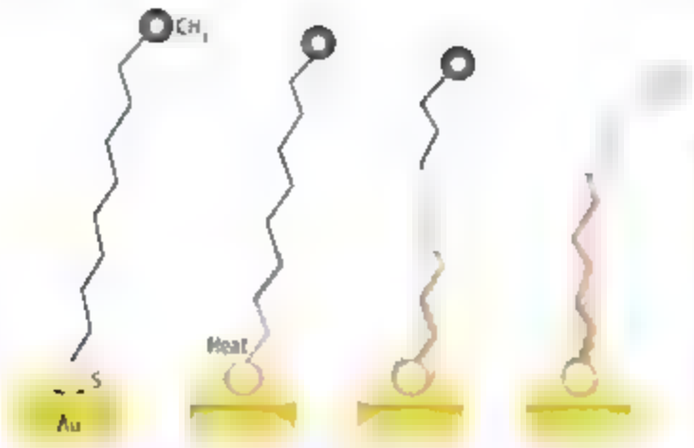

How molecules heat up. In the experiments reported by Dlott and co-workers, heat is transferred from the heated gold substrate along the molecular chain, causing the chain to become increasingly disordered.

chain and its tilt with respect to the surface. The authors use a short laser pulse to heat the gold substrate to an estimated temperature of 800 K and measure the rate at which thermal energy reaches the methyl end of the molecules (see the first figure). They do so by using a method called sum-frequency generation to follow the disorder that develops as the methyl groups heat up.

Analysis of the observed time evolution yields two characteristic times, both proportional to the molecular chain length. Dlott and co-workers interpret the time delay, t_0, between the heating laser pulse and the onset of disorder at the methyl end of the monomolecular layer as the time it takes for the heat pulse to travel between the hot gold substrate and that methyl end. Its linear dependence on chain length indicates the ballistic (that is, interruption-free) nature of this travel. The other time, τ, governs the relaxation of this energy pulse and the evolution of thermal disorder; its dependence on molecular length reflects the fact that the rate of temperature increase in the monomolecular layer is inversely proportional to its heat capacity and, therefore, to its thickness.

The ballistic heat transfer observed in (*1*, *4*) is similar to the free propagation of energy along a chain of beads connected by harmonic springs after the first bead is pushed (see the second figure, bottom panel). In contrast, macroscopic heat conduction is an energy-diffusion process (see the second figure, top panel), governed by collisions with impurities and anharmonic interactions, in which heat spreads like a drop of ink inserted into water.

Dlott and co-workers find that t_0 and τ extrapolate to essentially zero at chain lengths shorter than four carbon atoms. If we think of the molecule as a collection of ballistics pathways for energy transfer (called normal modes), most of these pathways appear to be operational for chains shorter than four atoms but become blocked (localized) beyond this length. These observations are consistent with calculations (*3*) and earlier observations (*6*) of chain-length dependence of vibrational energy transfer in alkane molecules.

These studies (*1*, *4*) continue a string of recent exciting experiments on heat transport in nanojunctions, which demonstrated the existence of a fundamental quantum unit of heat transport (that is, a limit on the maximum conductance per pathway) (*2*, *7*), thermal rectification (that is, preferred conduction in one direction) (*8*) and a transistor-like nanorefrigerator (*9*). These experiments raise important issues regarding the nature of heat conduction in such junctions, including molecular junctions.

First is the analogy between energy transfer and electronic transport in such systems. In their ballistic regimes, both of these transport phenomena can be described by Landauer's theory for electronic conduction. For example, the quantum unit of heat conduction has the same origin as the analogous unit in electronic conduction. Considerations of molecular heat rectification (*8*, *10*) were motivated by earlier studies of rectification in molecular-conduction junctions. Ge *et al.* (*11*) have reported first steps toward addressing the relation between structure and function in molecular heat conduction, a problem much studied in electronic conduction.

Second is the realization that a full description of molecular conduction junctions requires consideration of both electronic and heat conduction, which together determine the temperature rise in such systems under operating conditions. Theoreticians have only recently targeted this important problem (*10*), and a first attempt to determine junction temperature was recently made (*12*). The same framework can be used to discuss the thermoelectric effect in molecular junctions (*13*, *14*), whose first experimental manifestation was recently published (*15*).

Next is the observation that molecular (vibrational) heat transport is closely related to the long-studied problem of molecular vibrational energy redistribution, which determines the amount of energy available to the reaction in many chemical processes. Future efforts to elucidate energy transfer pathways and identify efficient carrier modes in molecular heat conduction will benefit from experience gained in these earlier studies.

Finally, the ballistic heat transport on the molecular scale must become diffusive in larger systems, where anharmonic interactions and external collisions become effective. The role played by such interactions and the nature of this change are other important issues for future studies.

Thermometry, heat conduction, and thermoelectricity are old problems that pose new fundamental questions and experimental challenges when studied on the molecular scale. Heating issues in molecular electronics and visions of future applications to molecular heat engines and nanorefrigerators add a strong technological motivation for these studies. The experiment of Dlott and co-workers and other recent advances (*4*, *7*–*9*, *11*, *12*, *15*) are first important steps in what promises to be an exciting endeavor.

References

1. Z. Wang *et al.*, *Science* **317**, 787 (2007).
2. K. Schwab, E. A. Henriksen, J. M. Worlock, M. L. Roukes, *Nature* **404**, 974 (2000).
3. P. Kim, L. Shi, A. Majumdar, P. L. McEuen, *Phys. Rev. Lett.* **87**, 215502 (2001).
4. R. Y. Wang, R. A. Segalman, A. Majumdar, *Appl. Phys. Lett.* **89**, 173113 (2006).
5. D. Segal, A. Nitzan, P. Hanggi, *J. Chem. Phys.* **119**, 6840 (2003).
6. D. Schwarzer, P. Kutne, C. Schroder, J. Troe, *J. Chem. Phys.* **121**, 1754 (2004).
7. M. Meschke, W. Guichard, J. P. Pekola, *Nature* **444**, 187 (2006).
8. C. W. Chang, D. Okawa, A. Majumdar, A. Zettl, *Science* **314**, 1121 (2006).
9. O.-P. Saira *et al.*, *Phys. Rev. Lett.* **99**, 027203 (2007).
10. M. Galperin, M. A. Ratner, A. Nitzan, *J. Phys. Cond. Mat.* **19**, 103201 (2007).
11. Z. Ge, D. G. Cahill, P. V. Braun, *Phys. Rev. Lett.* **96**, 186101 (2006).
12. Z. F. Huang, B. Q. Xu, Y. C. Chen, M. Di Ventra, N. J. Tao, *Nano Letters* **6**, 1240 (2006).
13. M. Paulsson, S. Datta, *Phys. Rev. B* **67**, 241403 (2003).
14. D. Segal, *Phys. Rev. B* **72**, 165426 (2005).
15. P. Reddy, S.-Y. Jang, R. A. Segalman, A. Majumdar, *Science* **315**, 1568 (2007).

10.1126/science.1147011

CREDIT (TOP): P. HUEY/SCIENCE

PHILOSOPHY OF SCIENCE

The Cha-Cha-Cha Theory of Scientific Discovery

Dividing the discovery process into three categories can aid in understanding the genesis of small, everyday advances as well as breakthroughs that appear in history books.

Daniel E. Koshland Jr.

Scientific discoveries are the steps—some small, some big—on the staircase called progress, which has led to a better life for the citizens of the world. Each scientific discovery is made possible by the arrangement of neurons in the brain of one individual and as such is idiosyncratic. In looking back on centuries of scientific discoveries, however, a pattern emerges which suggests that they fall into three categories—Charge, Challenge, and Chance—that combine into a "Cha-Cha-Cha" Theory of Scientific Discovery. (Nonscientific discoveries can be categorized similarly.)

"Charge" discoveries solve problems that are quite obvious—cure heart disease, understand the movement of stars in the sky—but in which the way to solve the problem is not so clear. In these, the scientist is called on, as Nobel laureate Albert Szent-Gyorgyi put it, "to see what everyone else has seen and think what no one else has thought before." Thus, the movement of stars in the sky and the fall of an apple from a tree were apparent to everyone, but Isaac Newton came up with the concept of gravity to explain it all in one great theory.

Challenge discoveries are a response to an accumulation of facts or concepts that are unexplained by or incongruous with scientific theories of the time. The discoverer perceives that a new concept or a new theory is required to pull all the phenomena into one coherent whole. Sometimes the discoverer sees the anomalies and also provides the solution. Sometimes many people perceive the anomalies, but they wait for the discoverer to provide a new concept. Those individuals, whom we might call "uncoverers," contribute greatly to science, but it is the individual who proposes the idea explaining all of the anomalies who deserves to be called a discoverer.

"Chance" discoveries are those that are often called serendipitous and which Louis Pasteur felt favored "the prepared mind." In this category are the instances of a chance event that the ready mind recognizes as important and then explains to other scientists. This category not only would include Pasteur's discovery of optical activity (D and L isomers), but also W. C. Roentgen's x-rays and Roy Plunkett's Teflon. These scientists saw what no one else had seen or reported and were able to realize its importance.

There are well-known examples in each one of the Cha-Cha-Cha categories (see the figure). Two conclusions are immediately apparent. The first is that the original contribution of the discoverer can be applied at different points in the solution of a problem. In the Charge category, originality lies in the devising of a solution, not in the perception of the problem. In the Challenge category, the originality is in perceiving the anomalies and their importance and devising a new concept that explains them. In the Chance category,

D. E. Koshland Jr. passed away on 23 July 2007. He was a professor of biochemistry and molecular and cell biology at the University of California, Berkeley, since 1965. He served as *Science*'s editor-in-chief from 1985 to 1995.

CREDITS: NASA; JUPITER IMAGES

CATEGORIES OF DISCOVERY

Problem that needed solving	Discovery	Discoverer	Category of discovery
Movement of stars, Earth, and Sun	Gravity	Newton	Charge
Structure of C_6H_6	Benzene structure	Kekulé	Challenge
Clear spots on petri dish	Penicillin	Fleming	Chance
Constant speed of light	Special relativity	Einstein	Challenge
Preventing heart attacks	Cholesterol metabolism	Brown & Goldstein	Charge
Crystals of D- and L-tartaric acid	Optical activity	Pasteur	Chance
Atomic spectra that could not be explained	Quantum mechanical atom	Bohr	Challenge
How DNA replicates and passes on coding	Base pairing in double helix	Watson & Crick	Challenge
Reagent "stuck" in storage cylinder	Teflon	Plunkett	Chance
Why offspring look like their parents	Laws of heredity	Mendel	Charge

the original contribution is the perception of the importance of the accident and articulating the phenomenon on which it throws light.

Second, most important discoveries are usually not solved in one "Eureka" moment, as movie scripts sometimes suggest. True, there are moments in which a scientist has been mulling over various facts and problems and suddenly puts them all together, but most major discoveries require scientists to make not one but a number of original discoveries and to persist in pursuing them until a discovery is complete. Thus, to solidify his theory of gravity, Newton developed calculus and laws of physics that he described in his *Principia*. In a modern example, Michael Brown and Joseph Goldstein not only studied the metabolism of cholesterol but also discovered the role of lipoprotein receptors and the movement of key proteins from the outside to the interior of cells. Great discoveries are frequently covered in textbooks with a single word or phrase, but the concepts actually become solidified as scientific understanding by a series of discoveries.

It is also pertinent to define "the prepared mind" that is required for all of these innovations. Such a mind must be curious and knowledgeable. Curious refers to the fact that the individual is interested in phenomena and is constantly seeking to understand and explain them. Knowledgeable means that the individual has a background of facts and theories as a fertile incubator into which the new facts can fall.

The Cha-Cha-Cha Theory pertains to small everyday findings by scientists as well as the big discoveries that appear in history books. When, for example, a researcher discovers a new chemical isolated from a plant, there is so much understood today that the "charge" to that scientist is to find the formula and structure of the compound. There are now many ways to find the structure of an unknown chemical. Along the way there may be anomalous results that present challenges to the scientist and unexpected findings that must be interpreted by the prepared mind. So each of these represent real discoveries, not as big as a theory of gravity, but important just the same.

Finally, scientific discoveries are not that different from nonscientific discoveries. In the earliest days, there was an obvious "charge" for a set of rules to guide conduct in the close environment of a village that led to social customs and religious guidelines such as the Ten Commandments. As more complex societies emerged, the idea of a democratic vote probably resulted from a "charge" that saw the importance of getting consensus. The Magna Carta and the Bill of Rights came out of "challenges" to an entrenched social system. So when Einstein said that scientific thinking and general thinking were not that different, he probably meant that the patterns of thought of those with "prepared minds" in government and law operated by some of the same general principles as science, even though the methods of science and law are very different.

Someday we may understand the arrangement of neurons in the brain enough to understand how originality can arise. A wild guess would be that the brain of a discoverer has a greater tendency than the average individual to relate facts from highly separate compartments of the brain to each other. As a step to making that Herculean problem tractable, we can at least follow the traditions of scientific reductionism and use the Charge, Challenge, and Chance categories to make the interpretation of brain imaging experiments easier to analyze.

10.1126/science.1147166

APPLIED PHYSICS

How to Strum a Nanobar

A method for vibrating a nanocantilever may yield much more sensitive measurement tools and computers based on mechanical logic devices.

Miles Blencowe

Nanotechnologists are increasingly interested in using mechanical vibrating structures as fast, sensitive detectors of such properties as electric charge (*1*), magnetism (*2*), and mass (*3*). These devices make good detectors because, just as a bit of sealing wax changes the frequency of a tuning fork, the properties of a nanoresonator will change in response to external forces. Nanomechanical resonators may also be suitable as ultracompact, high-frequency filters and mixers for electromagnetic signals (*4*). That is, by tailoring the vibrational properties of the structure, only select frequencies are detected. For these applications to be feasible, it is crucial that we have the ability to drive the nanomechanical resonator into motion with an electromagnetic force (i.e., "actuate" the resonator) in an efficient and controllable way. At the same time, the delicate quivering of a nanomechanical resonator as it responds to a local stimulus must be efficiently transduced into an electromagnetic signal that can be amplified to measurable levels. These requirements of efficiency, compactness, and speed favor methods of actuation and transduction that are part of the nanomechanical resonator itself.

On page 780 of this issue (*5*), Masmanidis *et al.* demonstrate an intrinsic actuation method ideally suited to nanoscale mechanical resonators. The method relies on a property of some crystals called piezoelectricity (*6*), deriving from the Greek *piezein*, meaning "to press." As the name suggests, stressing such a crystal will produce a corresponding voltage between certain faces of the crystal. Conversely, applying a voltage between the same faces will generate a corresponding mechanical deformation or strain of the crystal. Masmanidis *et al.* use both singly clamped cantilevers and doubly clamped bridge resonators (see the micrograph) that are fashioned from gallium arsenide (GaAs) (*7*). The underlying GaAs crystal orientation is chosen such that applying a voltage between the top and bottom faces will cause it to either elongate or shorten, depending on the polarity of the applied electric field.

To understand better how the motion is produced, consider a GaAs cantilever and suppose that an ac voltage source is applied between its top and bottom faces. If the frequency of the ac voltage matches that of one of the cantilever's longitudinal vibration modes (i.e., stretching modes along the direction of the cantilever), then the cantilever will ring at this frequency. However longitudinal modes are difficult to detect because of their relatively high frequencies and small displacement amplitudes. As with stringed musical instruments, it is preferable to excite the lower frequency, bending modes of the cantilever, especially the fundamental mode. The method of actuation should also be internal to the cantilever and not require external electrodes attached to its top and bottom faces.

Masmanidis *et al.* elegantly meet both of

The author is in the Department of Physics and Astronomy, Dartmouth College, Hanover, NH 03755, USA. E-mail: blencowe@dartmouth.edu

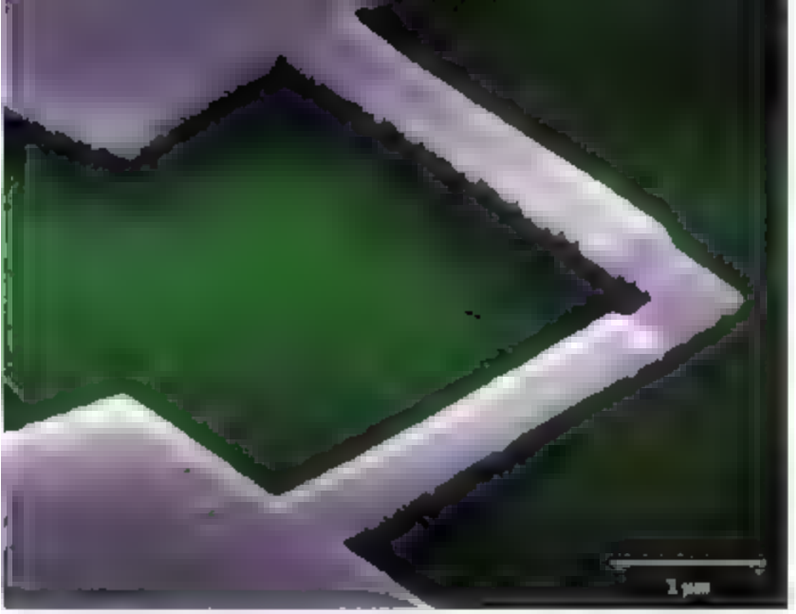

Cantilever logic. A nanomechanical logic device studied by Masmanidis *et al.* (6) is the analog of a conventional logic element called the "exclusive-OR" (XOR) gate. The three different doping densities of the 200-nm-thick PIN diode arms have been shaded for clarity (purple to blue). The inputs to the logic gate are represented by the two cantilevers, which are isolated electrically but connected mechanically. The output is represented by the collective motion of the T-shaped structure. There is appreciable vertical deflection only when a signal is applied to either one of the two inputs, but not both simultaneously.

these challenges by selectively doping the top and bottom regions of the cantilever crystal with negatively and positively charged donor impurity atoms (see the diagram), respectively. The n-type impurity atoms contribute excess negative charge carriers (electrons) to the top layer, whereas the p-type impurity atoms contribute excess positive charge carriers (holes) to the bottom layer. The conducting charge layers function as built-in electrodes, sandwiching a much higher resistance middle layer called the depletion region, where most of the piezoelectrically induced stress occurs. The combined layer structure of p-type, intrinsic, and n-type materials is called a "PIN" diode. If the n- and p-type layers are made with different thicknesses, the depletion region can be located off center with respect to the cantilever's axis. Thus, an induced stress is not applied evenly across the cantilever cross section, causing it to bend or flex as desired.

This method of actuation is remarkably efficient and sensitive at the nanoscale. With a resonant ac driving voltage having an amplitude equivalent to varying the charge on the electrode by just a single electron, it was still possible to measure a piezoelectric displacement of the cantilever. In this case, the sensitivity was only limited by the random thermomechanical jiggling of the cantilever.

An unanticipated function was the ability to control the ac voltage actuation strength of cantilevers. Applying a separate reverse-biased dc voltage such that the electrons in the top n-type layer and holes in the bottom p-type layer are pulled away from the depletion region causes the latter to increase in width and also to shift relative to the cantilever's center axis. Depending on the initial location of the depletion region in the unbiased case, the associated flexing amplitude could be made either larger or smaller as the dc voltage was increasingly reverse-biased. This method of actuation strength control is uniquely suited to the nanoscale, where variations in the depletion width are comparable to the beam cross sections themselves. In contrast, cantilevers larger than nanoscale (that is, devices larger than a few hundred nanometers) would show marginal actuation efficiency control.

Masmanidis *et al.* achieved additional control by applying a separately adjustable dc voltage to the top and bottom electrodes of a doubly clamped bridge resonator. The resulting induced piezoelectric strain is converted into a stress that changes the fundamental mechanical frequency of the resonator in much the same way that a stringed instrument can be tuned by either tightening or loosening its pegs.

Transduction is at least as important as actuation in nanomechanical sensing and signal processing applications. It would be most natural to transduce the motions of the GaAs resonators via the same piezoelectric mechanism as used for actuation (*6*). However, large stray capacitances at the input stages of the electron amplifiers can effectively short out the tiny piezoelectric signals at the MHz and higher radio frequencies of interest.

If such problems can be overcome and the methods of transduction and actuation further refined, then we might look forward one day to machines with all mechanical nanoscale logic elements (*9*), which are both electrically controlled and electrically monitored. We will then have come full circle, emulating the ideas of full mechanical control and computation invented by individuals such as Jacquard (*10*) and Babbage (*11*) in the 18th and 19th centuries, only now nearly six orders of magnitude smaller in design.

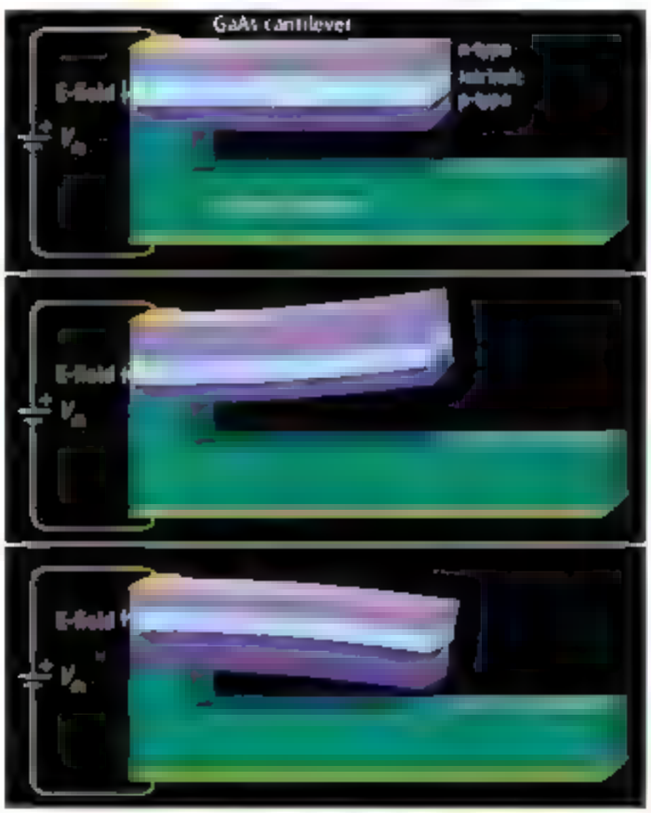

Gaining leverage. (**Top**) A voltage V_{dc} is applied between the top and bottom faces of a cantilever via metal electrodes (yellow) and the p-doped substrate (green). The E-field in the intrinsic depletion region (blue) induces a longitudinal strain. Depending on the doping profile and hence the depletion region location with respect to the cantilever's center axis (dashed line), the cantilever can be engineered to bend either upward (**center**) or downward (**bottom**) for the same electric field direction. When the applied dc voltage is increasingly reverse biased (that is, the polarity shown), the ac voltage-actuated amplitude of the cantilever bending can be controlled.

CREDITS: FROM M. L. ROUKES AND S. MASMANIDIS/CALIFORNIA INSTITUTE OF TECHNOLOGY; BOTTOM: P. HUEY/SCIENCE

References and Notes

1. A. N. Cleland, M. L. Roukes, *Nature* **392**, 160 (1998).
2. D. Rugar, R. Budakian, H. J. Mamin, B. W. Chui, *Nature* **430**, 329 (2004).
3. Y. T. Yang, C. Callegari, X. L. Feng, K. Ekinci, M. L. Roukes, *Nano Lett.* **6**, 583 (2006).
4. A.-C. Wong, C. T.-C. Nguyen, *J. Microelectromech. Syst.* **13**, 100 (2004).
5. S. C. Masmanidis *et al.*, *Science* **317**, 780 (2007).
6. W. G. Cady, *Piezoelectricity* (Dover, New York, 1978).
7. J. Söderkvist, K. Hjort, *J. Micromech. Microeng.* **4**, 28 (1994).
8. Z. L. Wang, J. Song, *Science* **312**, 242 (2006).
9. A. Knoll, L. Durig, D. Zuger, H. J. Güntherodt, *Microelect. Eng.* **83**, 1261 (2006).
10. J. Essinger, *Jacquard's Web* (Oxford Univ. Press, Oxford, 2004).
11. D. Swade, *The Difference Engine* (Viking, New York, 2001).
12. I thank the NSF (grant CMS0404031) for their support.

10.1126/science.1146803

Q

Who's working to increase support for science?

Top quality research depends on comprehensive support. AAAS is present at every stage of the process – from advising on funding policy initiatives to tracking the US Federal R&D budgeting process. As the experts, we brief Congressional staffers and representatives from governments around the world. And only AAAS Funding Updates – sent out monthly – provide continual coverage of R&D appropriations. By actively working to increase support for research, AAAS advances science.
To see how, go to **www.aaas.org/support**

AAAS

ADVANCING SCIENCE. SERVING SOCIETY

Attosecond Spectroscopy

CONTENTS

Reviews

INTRODUCTION

The Electron Stopwatch

THE PRECISION ATTAINABLE IN TIMING EVENTS ONCE DEPENDED ON HOW fast a human being could press the button on a stopwatch. More recently, pulsed laser sources have taken the place of those hand-held devices for measuring the fastest phenomena. The technology for tracking the time scale of nuclear motion in free molecules and solids was limited by the duration of a single cycle of visible light (approximately 0.000000000000001 second, or 1 femtosecond). Electrons move even faster than that, and for a long time, scientists could only watch their rearrangements as an indiscrete blur. Over the past several years, however, laser technology has crossed the threshold into the attosecond regime (a thousandth of a femtosecond). This series of three Reviews highlights the methods underlying this advance and the science its prospects they have enabled.

Bucksbaum (p. 766) lays out the essential physics of high harmonic generation, a technique whereby an intense laser field pulls an atomic electron away from the nucleus like a loaded slingshot and then sends it careening back, giving rise to the emission of an attosecond light pulse. The Review also describes in general terms what events such light pulses can be used to track, ranging from electron rearrangements in chemical bonding to conduction dynamics in metallic solids.

Goulielmakis *et al.* (p. 769) take a more in-depth look at the laser techniques that create and detect attosecond pulses. Their Review also details the prospects not only of passively probing electron motions, but of actively manipulating and controlling them.

In keeping with the uncertainty principle, compressing a light pulse's duration must also broaden its spectral bandwidth. Thus, attosecond pulses extend into the x-ray region of the electromagnetic spectrum. Kapteyn *et al.* (p. 775) describe efforts to harness this feature of the technology in diffraction and imaging experiments, which would otherwise depend on much more elaborate x-ray generation apparatus.

Optical technology continues to evolve. It seems that just as events at the atomic scale are at last observed with precision, they bring into view a new series of blurs, previously unappreciated. Then the quest begins for an even faster stopwatch.

– IAN OSBORNE AND JAKE YESTON

Science

REVIEW

The Future of Attosecond Spectroscopy

Philip H. Bucksbaum

Attoscience is the study of physical processes that occur in less than a fraction of a cycle of visible light, in times less than a quadrillionth of a second. The motion of electrons inside atoms and molecules that are undergoing photoionization or chemical change is within this time scale, as does the plasma motion that causes the reflectivity of metals. The techniques to study motion on this scale are based on careful control of strong-field laser-atom interactions. These techniques and new research opportunities in attosecond spectroscopy are reviewed.

Time is measured in human-scale units with 1 s equivalent to a heartbeat, more or less, but the physical world encompasses enormous ranges of time, from the origin of the universe some 14 billion years ago (~400 quadrillion seconds, or 4×10^{17} s), to times that are as short compared to a second as a second is short compared to the age of the universe. These brief instants, a few billionths of a billionth of a second, or 10^{-18} s, are called attoseconds (as).

Attosecond-scale phenomena have been studied indirectly for years. For example, the neutral pion (π_0) particle, which appears when high-energy electrons, protons, or γ-rays collide with matter in cosmic rays or in particle accelerator experiments, has a measured lifetime of 82.0 as, plus or minus 2.4 as (*1*). Yet, despite this precision, the time interval between the production and decay of a neutral pion has never been observed. The lifetime is inferred from careful measurement of the kinematics of colliding particles and the decay debris, which in the case of the π_0 is quite simple: It decays into two photons emitted back-to-back with equal energy in the rest frame of the particle. These measurements show that the rest energy of the π_0 is indefinite by a few electron volts, which yields the lifetime through the quantum mechanical uncertainty principle. In more complex systems, such as the electrons in a molecule rearranging after the scattering of an x-ray, indirect observations cannot reveal many details of the process. There is really no substitute for direct observation. The techniques to perform these ultrafast measurements and the science they enable have come to be known as "attoscience."

If we use the oscillations of light waves as a clock, the shortest time that we can measure with a beam of visible light depends on how fast we can turn the light on and off. Lasers have been developed over the past two decades that have special features to produce extremely short optical pulses. These technical innovations, such as light valves inside the laser based on the nonlinear Kerr effect (*2*), and external spectral broadening based on the intensity dependence of the index of refraction of gases (*3*, *4*), can now produce pulses nearly as short as a single optical cycle (*5*, *6*). These shortest pulses are on the scale of the laser wavelength λ divided by the speed of light *c*, about 2×10^{-15} s, or 2 fs, for a red laser (λ = 600 nm). A single optical cycle seemed until recently to be a natural lower bound on direct measurement of short intervals of time.

Recently, scientists have broken this femtosecond barrier of the single optical cycle by using a new kind of nonlinear optical phenomenon that can create pulses of light substantially briefer than 1 fs (*7*) because the wavelength is a factor of 10 or more shorter than a cycle of visible radiation. These "attosecond" pulses of vacuum ultraviolet (VUV) radiation have led in recent years to laboratory demonstrations of previously unobserved dynamics in atomic and molecular processes. The time evolution of collisions between electrons in atoms, such as occurs in Auger relaxation or two-electron ionization, has been recorded in the laboratory with the new tools of attosecond science. These tools may also help to reveal the earliest steps in chemical reactions, or help us to see in real-time the processes responsible for the optical properties of materials.

What Happens in Less Than a Femtosecond?

Before discussing how subfemtosecond pulses are made and used, we should summarize the science motivating research at this time scale. It turns out that this case is quite strong.

The atomic unit of time is $\tau_{atomic} = \hbar/2R_y$, where $\hbar$ is Planck's constant divided by 2π and R_y is the Rydberg constant, the binding energy of hydrogen, equal to 13.6 eV. The value of τ_{atomic} is ~24 as. This time has a dynamical significance in the old Bohr theory of the atom. It is the time it takes for a Bohr electron to complete 1 rad of its orbit in the ground state of hydrogen. So attoscience is fundamentally the study of electron motion inside atoms, or on the atomic scale.

In modern quantum theory, the electron in the ground state of hydrogen does not orbit the proton like a moon around a planet. The wave function that describes its position is stationary even though the electron still has momentum due to quantum confinement. That is, the uncertainty principle guarantees that an electron confined to an atomic radius a_0 has a momentum uncertainty on the order of $\hbar/a_0$, so the electron's state contains a distribution of momenta and positions, but the average values of these quantities do not evolve. In an excited atom, however, the electrons need not be stationary. The average positions and momenta of excited electrons can evolve on many time scales, from attoseconds to microseconds. This motion gives rise to a number of phenomena and applications, including multiple ionization, atomic clocks, and quantum tunneling. These phenomena inside the atom have been studied carefully over the past century, but the fastest motion has not been directly observed before because science has not had the measurement tools to capture such short intervals of time until now.

A common example of an attosecond-scale atomic process is the phenomenon of Auger relaxation, which occurs when multiple-electron atoms are ionized by photons with energy far above the atomic binding energy. When kilovolt x-rays ionize such atoms, the ions almost never remain in their ground state. The x-ray is very likely to remove a deeply bound electron, leaving the ion in an excited state with a vacancy in an inner electron shell, which must relax through subsequent motion of the electrons. Auger relaxation accomplishes this task by moving two electrons from a more weakly bound outer shell. One electron fills the hole, the other is ejected, so that the whole process can conserve energy. The evolution of the atom from a neutral ground state before the x-ray absorption, to a doubly charged ion following the Auger process, is a challenge for theory, and until now it has been impossible to observe. All we know about it comes from examining the debris, the electrons and ions following the event. The electron energies tell us that the process is very fast; that the two electrons ejected from the atom can affect each other during the ejection event, and that there are sometimes a number of different electron states that can participate. What we would like to see is the evolution of the process itself, on its own time scale.

When atoms are bound into molecules, we must consider the interplay between the motion of the electrons and the nuclei. Ultimately this is the basis for all chemistry. The characteristic vibrational motion of atoms in chemical bonds occurs on the time scale of tens to hundreds of femtoseconds, and the importance of femtosecond processes in chemistry has been widely recognized, including by award of a Nobel Prize (*8*), but there are critical intervals during a chemical reaction when the outcome is determined by dynamics that are still faster, on the

PULSE, Stanford Linear Accelerator Center, Stanford University, 2575 Sand Hill Road, Menlo Park, CA 94025, USA. E-mail: phb@slac.stanford.edu

time scale of a few femtoseconds or less. These are moments when the atoms involved in the reaction are in transition-state configurations, and the electrons rapidly rearrange to guide the nuclear motion into the final state.

It is convenient to imagine the electron-driven dynamics between the atoms as motion of the atoms on potential energy surfaces, like marbles rolling around on a curved landscape of many dimensions, guided by gradient forces and their own inertia. This picture comes naturally out of the Born-Oppenheimer approximation, which states that the electron motion and nuclear motion occur on such different time scales that they may be considered separately in seeking solutions to the quantum mechanical equations of motion for the molecular system. In this picture, the transition states occur at high points in the potential energy landscape, or at intersections between two different potential energy surfaces, known as "conical intersections" (Fig. 1). Conical intersections are points where the Born-Oppenheimer approximation breaks down, and the many-body quantum dynamics is no longer simple. Naturally, these are regions of intense interest in physical chemistry, and these are areas that might be addressed by attosecond-scale probes of the molecules.

Fig. 1. Conical intersections describe the connection between two electronic states, represented by the two conjoined cones, and nuclear motion, represented by a dotted arrow trajectory along lines on the cone surface, during nonradiative molecular transitions in the Born-Oppenheimer approximation. This standard and powerful picture is no longer valid when the viewing time is so short that the Heisenberg uncertainty in the electron energy is larger than the difference between two potential energy surfaces. Attosecond science requires a reconsideration of these ideas.

Solids are also held together by electrons which are typically delocalized over many atomic sites and form continuous bands of energies separated by energy gaps, rather than sharp energy levels in single atoms. To get an idea about the ultrafast time scales in solids, consider the physics of optical reflection from a metal mirror. A metal mirror can be treated as a dense plasma of free electrons, moving in a background of atomic ions to neutralize the overall charge. A light field on the surface of the mirror drives electrical currents that produce the reflected light beam.

There are several related time scales that control the physics of optical reflection, and they are all in the range of femtoseconds to attoseconds for typical mirrors, which seems instantaneous to a visual observer. A central concept is the plasma frequency $\omega_p/2\pi$. The inverse of this frequency is just the natural period of oscillation of an electron density perturbation in the solid, due to the restoring force created by the charge imbalance. In a typical metal like aluminum, that period is about 200 as. The value of ω_p is related to the electron density N and its effective mass m^* in the solid:

$$\omega_p^2 = \frac{Ne^2}{\varepsilon_0 m^*}$$

If the incident-light frequency is lower than ω_p, then the electrons in the plasma can respond to the force of the light fields in time to produce the reflected radiation; but if the light frequency is higher than the plasma frequency, then the oscillating electrons cannot respond to cancel the light field in the material. This condition is called "ultraviolet transparency," because light waves at frequencies higher than this limit can travel through the metal without reflecting from the surface.

A still faster time scale is connected to the electrical conductivity σ of the metal. The conductivity relates the current $\mathbf{J}$ (charge per time per area) produced by an applied field $\mathbf{E}$ (units of charge per area) through Ohm's Law:

$$\mathbf{J} = \sigma\mathbf{E}$$

The quantity $1/\sigma = \rho$, the resistivity, evidently has units of time. The common unit for ρ, the Ω-cm, is approximately equal to 1 ps (10^6 as). The resistivity of aluminum, a common mirror material, is about 2.7 $\mu\Omega$-cm, or about 3 as. The physical importance of this extremely short time is the establishment of the conditions for Ohm's law–like behavior in the metal. When an electron first feels an electric field, it does not instantly move with a velocity proportional to the force. Instead, it accelerates in the field and only reaches its terminal velocity by a balance between the driving force, which speeds it up, and plasma scattering forces, which slow it down. The resistivity sets the time scale for this balance.

How Do We Make Attosecond Pulses?

The technology for producing and for measuring attosecond pulses of light (i.e., pulses with a duration between 1 as and 1 fs (1000 as)) is based on the interaction of strong visible or infrared (i.e., long-wavelength) laser pulses with atoms. The use of infrared lasers to produce attosecond pulses may seem counterintuitive, because an optical period of 1 fs corresponds to light with a wavelength of 300 nm, in the near-ultraviolet range, and a period of 1 as implies a wavelength of 0.3 nm, which is considered an x-ray. The connection is made because of the strength of the laser field.

Focused pulsed lasers can concentrate all of their power into an area only a few laser wavelengths across, or a few micrometers for a red or infrared laser. This concentration increases the electric field in the laser inversely to the diameter of the focus. Typical fields available in even a modest modern atomic physics lab are 100-fs pulses with 100 μJ of energy and wavelength 800 nm, focused to 30 μm. In this case, the peak field is 3 V/Å. The typical binding energy Φ_0 of an electron in an atom is only on the order of 10 eV, and the size of the atom is an ångstrom, so it is clear that a 3 V/Å field can distort the electron trajectories. A simple calculation based on these ideas, which is well verified in experiments (9), shows that the electron orbit becomes unstable, and the electron is pulled out of the atom altogether, when the applied laser field reaches a small fraction of the average magnitude of the Coulomb field felt by the bound electron. We can also put this critical field amplitude E_{Crit} in terms of Φ_0:

$$E_{Crit} = \frac{\Phi_0^2}{4e^3}\left(\frac{4\pi\varepsilon_0}{}\right)^{1/2}$$

So atoms field-ionize in the presence of high-powered focused lasers. Furthermore, because the laser oscillation period is 2 fs or more, which is very long compared to the electron orbital period of a few tens of attoseconds, we can picture the electron leaving the influence of the ion in much less than a laser field cycle.

After ionization, the electron still feels the laser field. It accelerates away from the atom, but soon (after about a quarter of a laser cycle)

the field reverses, and the electron starts to decelerate, stop, and accelerate in the other direction. The trajectory of the electron is therefore a wiggly drifting motion, and most of the phenomena that have been observed in strong-field atomic ionization can be traced back to the properties of the drifting electron (*10*). The wiggle itself can be quite energetic on an atomic scale. The average wiggle energy, called the ponderomotive energy (U_p), can be many times greater than the binding energy of the atom.

The ponderomotive energy for an electron in an oscillating field is given by the following expression

$$U_p = \frac{e^2 E^2}{(4\pi\varepsilon_0)4m\omega^2} = \frac{e^2 E^2 \lambda^2}{(4\pi\varepsilon_0)16\pi^2 mc^3}$$

U_p has a value of ~3 eV in the case of the modest focused laser field ionization experiment considered above. The trajectory of the electron depends sensitively on the precise instant of ionization over the laser cycle. If the atom ionizes just when the electric field cycle is reaching its peak, the electron will first move away, and then return back to its starting point at the atom just as it comes to rest at the end of one full cycle of oscillating field. If the electron departs a bit early, before the peak field, then the period of acceleration is slightly longer, and the electron cannot return to its starting point; it drifts slowly away.

The most interesting case is for electrons that depart a bit after the field peak. They do not travel as far from the atom, and when they return they still have quite a bit of ponderomotive energy. These electrons can return to their original state in the atom, and when they recombine with the ion they give up their kinetic energy in the form of a high-energy photon.

This phenomenon is known as "high harmonics generation" (HHG), because the emission spectra can consist of a series of nearly equally intense discrete frequencies at the position of the odd harmonics of the laser (*11*, *12*). We now understand that separation of the emission spectrum into a series of high harmonics is due to interference among many recombination photons emitted by many different atoms over several different cycles of the laser pulse. On the single-cycle time scale, the spectrum is continuous and follows the spread of recombination energies. The peak return energy is for an electron ionized at about 17° past the peak of the oscillating field. Its energy is $3.17U_p + \Phi_0$ (*10*).

This electron recombination process, known as the "rescattering picture," does not by itself appear to lead to the production of attosecond pulses. The HHG spectrum is composed of radiation produced by recombination over a range of electron energies, distributed over the entire 3-fs duration of the optical cycle of the drive laser, and repeated over many cycles. For example, according to both the quantum and semiclassical formulations of the rescattering process, different parts of the HHG spectrum are caused by recombination of the itinerant electron at different times during an optical cycle, so the entire spectrum appears to have a frequency sweep, or "chirp" (*13*). Actually, there are two different chirps. Electrons that ionize near the peak of the cycle execute relatively long trajectories, and their recombination radiation appears chirped from high to low frequency. Electrons that ionize after 17° of phase past the peak of the field execute short trajectories, and the radiation is chirped from low to high frequency. To make the shortest attosecond pulse, all of the frequencies must be in phase, i.e., they must all appear at the same time.

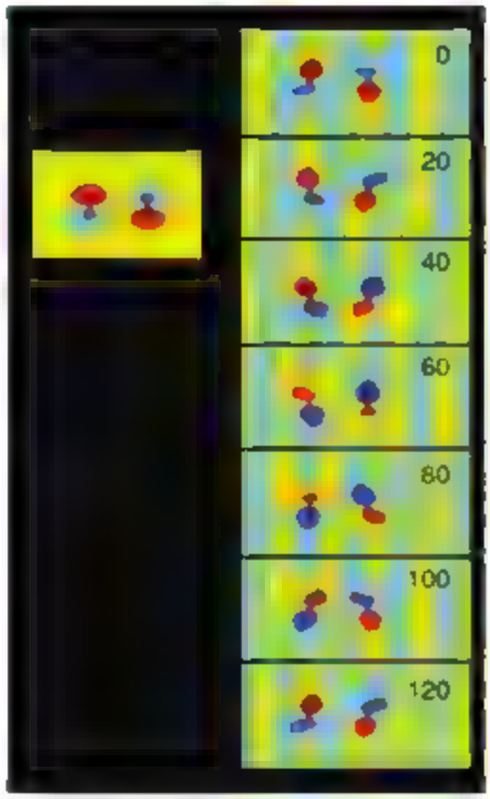

Fig. 2. (Left) Wave function simulating the most weakly bound electron in carbon dioxide, consisting of two p_π orbitals separated by 2.32 Å. Red and blue parts of the wave function are π radians apart in quantum phase. (Right) Coherent scattering of a 25-eV electron from the carbon dioxide orbital out of which it was recently ejected by a strong laser field. The returning electron is incident from the right, and several views are shown over a 120-as time interval. The relative time (in attoseconds) is shown in the top right of the frames. Motion of the wave function is due to interference with the incoming electron.

This frequency chirp can be removed after the light leaves the atom, by a variety of clever techniques. When VUV radiation from HHG passes through a very thin film of aluminum a few thousand angstroms thick, for example, the lower frequencies have a lower velocity, which is a direct consequence of the ultraviolet transparency described above. This removes the chirp from the radiation for short trajectories, which can lead to short, nearly perfect attosecond pulses (*14*).

To date (mid-2007), the only sources of attosecond coherent radiation use the technique described above. However, there are more ideas about how to do this in the future.

For example, as mentioned above, laser light reflected from a metal mirror has a characteristic delay of a few attoseconds because of the nonzero resistivity of the metal. But consider what happens if the laser intensity is increased to more than 1×10^{20} W cm^{-2}. Such focused intensities have been achieved in the laboratory. The optical electric fields in this case are hundreds of times higher than the atom's binding field, and they accelerate the electrons in the metal to nearly the speed of light in a fraction of an optical cycle. The electrons form a terrifically hot plasma that starts to expand away from the surface of the metal. The plasma is a moving mirror, and the light bouncing off it experiences a severe Doppler shift and pulse-length contraction. Simulations show conversion factors and frequency shifts of 10 times or more, so that ultrafast visible pulses could reflect from the mirror as VUV attosecond pulses (*15*).

The most powerful sources of x-rays will be the new x-ray free-electron lasers (XFELs), under construction in the United States, Germany, and Japan. XFELs can in principle produce attosecond pulses, but the technology to do this has not yet been demonstrated (*16*).

Viewing and Using Attosecond Pulses: Creating Attoscience

Attosecond pulses are so recent and unusual that new techniques are required to make full use of their resolving power. For example, the HHG spectrum itself, the source of attosecond radiation, is also a sensitive detector of attosecond processes in the atomic or molecular nonlinear medium (*17*). Recent experiments that delve into this issue using HHG in molecules have found that the harmonic spectrum is rich in features that relate directly back to the attosecond physics of the electron evolution in the molecule (*18*, *19*). There have been recent suggestions that this information permits tomographic reconstruction of the active electron orbitals inside the molecule. If this concept can be developed, it may be possible in the future to watch the electrons in molecules as they form and break bonds during isomerization, ionization, or other chemical processes.

This ability to detect the shape of a quantum orbital in HHG depends on the electron's quantum coherence. The electron that is pulled away from the atom or molecule and then recollides a femtosecond later has wavelike features. These are not waves of charge, but rather oscillations in quantum phase, a nonclassical quality of electrons

that is responsible for such quantum-mechanical phenomena as electron diffraction through crystals. Likewise, the bound electron state possesses a quantum phase, which can change sign from place to place in the molecule. The quantum phases of the returning electron wave interfere with the different parts of the molecular bound state wave function, creating attosecond modulation of the electronic structure that is recorded in the shape of the HHG spectrum (Fig. 2).

The physics of HHG is still under active discussion, and this coherent scattering picture has many subtleties that are still unresolved. Nonetheless, the effect of molecular shape on the HHG spectrum is genuine and dramatic. For example, two simple molecules O_2 and N_2 are similar enough in their gross structure, each consisting of two atoms separated by about an angstrom, and a difference of only two electrons out of more than a dozen, but their highest occupied orbitals, the ones that will field-ionize in an intense laser field, have very different symmetries. HHG spectra reveal this difference, and recent experiments have used the spectra to perform tomographic reconstructions of the wave function responsible for ionization.

Conclusion

Only a few years ago, the direct measurement of transient phenomena lasting less than an optical cycle seemed a supreme challenge. Now scientists have brought together techniques from atomic and laser physics to make these measurements possible, if not yet routine. Attoscience is a new field, with the promise to reveal some of the fastest processes of chemistry and atomic physics, or to freeze motion that will allow us to view the structure of matter under extreme conditions. The subject is still dominated by attempts to understand and improve the sources, and to interpret the data, and there are still frontiers in source development. For example, attosecond pulses at subangstrom wavelengths have not been demonstrated. There are even more challenges in the theory of attosecond molecular dynamics. One of the most difficult issues yet to be resolved in attoscience is how we should describe the structure and motion of electrons and nuclei in physical chemistry and molecular physics to accommodate processes that are so fast that cherished concepts such as potential energy surfaces or the Born-Oppenheimer approximation are no longer valid. Despite these difficulties, the rapid progress in attoscience over the past few years is not abating, and we may anticipate new physical insights in the coming decade.

References and Notes

1. W.-M. Yao *et al.*, *J. Phys. G: Nucl. Part. Phys.* **33**, 1 (2006); http://meetings.aps.org/link/BAPS.2007.APR.B2.1.
2. D. E. Spence, P. N. Kean, W. Sibbett, *Opt. Lett.* **16**, 42 (1991).
3. M. Nisoli, S. De Silvestri, O. Svelto, *Appl. Phys. Lett.* **68**, 2793 (1996).
4. C. P. Hauri *et al.*, *Appl. Phys. B* **79**, 673 (2004).
5. R. L. Fork, C. H. Brito Cruz, P. C. Becker, C. V. Shank, *Opt. Lett.* **12**, 483 (1987).
6. E. Matsubara *et al.*, *J. Opt. Soc. Am. B* **24**, 985 (2007).
7. M. Hentschel *et al.*, *Nature* **414**, 509 (2001).
8. Ahmed Zewail received the 1999 Nobel Prize in Chemistry for his studies of the transition states of chemical reactions using femtosecond spectroscopy.
9. S. Augst *et al.*, *Phys. Rev. Lett.* **63**, 2212 (1989).
10. P. B. Corkum, *Phys. Rev. Lett.* **71**, 1994 (1993).
11. M. Y. Li *et al.*, *Phys. Rev. A* **39**, 5751 (1989).
12. J. L. Krause *et al.*, *Phys. Rev. A* **45**, 4998 (1992).
13. K. J. Schafer, K. C. Kulander, *Phys. Rev. Lett.* **78**, 638 (1997).
14. R. López-Martens *et al.*, *Phys. Rev. Lett.* **94**, 033001 (2005).
15. M. M. Naumova, J. A. Nees, G. A. Mourou, *Phys. Plasmas* **12**, 056707 (2005).
16. A. A. Zholents, G. Penn, *Phys. Rev. ST Accel. Beams* **8**, 050704 (2005).
17. M. Lein, N. Hay, R. Velotta, J. P. Marangos, P. L. Knight, *Phys. Rev. A* **66**, 023805 (2002).
18. J. Itatani *et al.*, *Nature* **432**, 867 (2004).
19. T. Kanai, S. Minemoto, H. Sakai, *Nature* **435**, 470 (2005).

20. This paper was written at the Stanford PULSE Center, with support from the NSF and from the Stanford Linear Accelerator Center, a national laboratory operated by Stanford University on behalf of the U.S. Department of Energy, Office of Basic Energy Sciences. We acknowledge useful discussions with M. Gaarde, who also provided Fig. 2 for this article.

10.1126/science.1142135

REVIEW

Attosecond Control and Measurement: Lightwave Electronics

E. Goulielmakis,[1] V. S. Yakovlev,[2] A. L. Cavalieri,[1] M. Uiberacker,[2] V. Pervak,[2] A. Apolonski,[2] R. Kienberger,[1] U. Kleineberg,[2] F. Krausz[1,2]*

Electrons emit light, carry electric current, and bind atoms together to form molecules. Insight into and control of their atomic-scale motion are the key to understanding the functioning of biological systems, developing efficient sources of x-ray light, and speeding up electronics. Capturing and steering this electron motion require attosecond resolution and control, respectively (1 attosecond = 10^{-18} seconds). A recent revolution in technology has afforded these capabilities. Controlled light waves can steer electrons inside and around atoms, marking the birth of lightwave electronics. Isolated attosecond pulses, well reproduced and fully characterized, demonstrate the power of the new technology. Controlled few-cycle light waves and synchronized attosecond pulses constitute its key tools. We review the current state of lightwave electronics and highlight some future directions.

Quantum mechanics predicts the characteristic time scale for the rapidity of microscopic dynamics as $\Delta t \sim h/\Delta W$, where ΔW is the spacing between the relevant energy levels of the microscopic system and h is Planck's constant. The milli–electron volt and multi–electron volt energy spacing of vibrational and electronic energy levels, respectively, imply that structural dynamics of molecules and solids as well as related chemical reactions and phase transitions evolve on a femtosecond time scale, whereas electronic motion on the atomic scale is to be clocked in attoseconds.

Before the invention of the laser, the resolution of time-resolved spectroscopy was limited by the nanosecond duration of pulses of incoherent light. The laser and the successive technological developments for the generation and measurement of ultrashort laser pulses improved the resolving power of pump-probe spectroscopy from several nanoseconds to several femtoseconds (*1*). The birth of femtosecond technology permitted real-time observation of the breakage and formation of chemical bonds (*2*).

We review the recent developments in the optical technology that have led to the breaking of the femtosecond barrier and provided real-time access to intra-atomic electron dynamics. Consequences include the observation of electronic motion deep inside (i.e., in inner shells of) atoms (*3*) and its control in real time (*4*). We address the underlying physical concepts and highlight the current status as well as future prospects of attosecond technology (*5*).

Femtosecond Technology: Control and Measurement with the Amplitude and Frequency of Light

Control and measurement of dynamics are intertwined. Time-resolved measurement relies on a physical quantity varying in a controlled, reproducible fashion on the relevant time scale.

[1]Max-Planck-Institut für Quantenoptik (MPQ), Hans-Kopfermann-Straße 1, D-85748 Garching, Germany. [2]Department für Physik, Ludwig-Maximilians-Universität, Am Coulombwall 1, D-85748 Garching, Germany.
*To whom correspondence should be addressed. E-mail: krausz@lmu.de

Femtosecond technology is the result of controlling the nonlinear polarization of matter with the amplitude of light. Controlling the absorption and/or refractive index in this way has yielded, along with group delay dispersion control, femtosecond pulses from laser oscillators by means of passive mode locking (*1*). Measurement of the pulses relies on the same physical effect: control of the nonlinear polarization of matter by a replica of the pulse in the presence of the pulse to be characterized (*6*, *7*).

The controlled, well-characterized evolution of the amplitude envelope and carrier-frequency sweep (chirp) of ultrashort laser pulses permits measurement (*2*) and control (*8*) of quantum transitions on a femtosecond time scale. Reliance on these cycle-averaged quantities implies that measurement resolution and control speed are ultimately limited by the carrier wave cycle. The carrier wave cycle period is about 3 fs in the near infrared, where low dispersion favors the generation of the shortest laser pulses.

Toward Attosecond Technology: X-ray–Pump/X-ray–Probe Spectroscopy?

Femtosecond measurement and control techniques utilizing nonlinear material response could, in principle, be extended into the attosecond time domain by using intense attosecond pulses of extreme ultraviolet (XUV) or x-ray light. Unfortunately, in these regions of the optical spectrum, the probability of two-photon absorption is prohibitively low. X-ray pump/x-ray probe spectroscopy and x-ray quantum control therefore rely on x-ray intensities that can be attained only with large-scale free-electron lasers (*9*). Even though these sources are expected to eventually deliver their radiation in subfemtosecond pulses (*10*) and XUV sources pumped by large-scale, high energy lasers have already pushed the frontiers of nonlinear optics to the range of several tens of electron volts (*11*, *12*), proliferation of attosecond technology and its widespread applications call for another approach—one that relies on light sources suitable for small laboratories.

An Alternative Route: Light-Induced Electronic Motion Within the Wave Cycle of Light

The electric field of visible, near-infrared or infrared (henceforth, referred to collectively as NIR) laser light, $E_L(t)$, exerts a force on electrons that varies on a subfemtosecond scale. The use of this gradient for initiating and probing the subsequent dynamics with attosecond timing precision and resolution has led to the emergence of an attosecond technology that does not rely on the existence of intense x-ray pulses.

According to theory, strong-field induced ionization of atoms is confined to subfemtosecond intervals near the peaks of the oscillating NIR field (Fig. 1A), setting a subfemtosecond electron wave packet $\psi_{free}(t)$ free: this prediction was recently confirmed by real-time observation (*13*). The subfemtosecond ionization process, locked to the peak of NIR field oscillation with corresponding precision, may serve as a subfemtosecond "starter gun" for a wide range of dynamics (including electronic and subsequent nuclear motion and related dynamics of molecular structure).

The energetic radiation concurrent with optical-field ionization in a linearly polarized laser field (*14*) provides a means of triggering motion in a more gentle way, without applying an intense field. The broadband XUV light building up during the propagation of the driving pulse through an ensemble of atoms was predicted to emerge in a subfemtosecond burst within every half optical cycle that is sufficiently intense for ionization (*15*). In this Review, we focus on these photonic tools of attosecond technology, noting that the recolliding electron wave packet itself can also be used to explore dynamics (*16*–*18*).

The electronic (and concurrent) phenomena following the attosecond trigger can be tracked with comparable resolution with the use of the generating NIR field, the oscillations of which are synchronized with the trigger event (tunnel ionization, recollision, or XUV burst from recollision). Let us consider an electron ejected during the unfolding evolution of the system under scrutiny. In the presence of a linearly polarized NIR field, outgoing electrons collected along the direction of the laser electric field $E_L(t)$ (Fig. 1B) suffer a momentum change $\Delta p(t) = e\int_t^\infty E_L(t')dt' = eA_L(t)$. Here, e is the charge of the electron, t is the instant of its emission, and $A_L(t)$ is the vector potential of the laser field. This change varies monotonically within a half wave cycle of the laser field, mapping the temporal evolution of the emitted subfemtosecond electron wave packet to a corresponding final momentum and energy distribution of the emitted electrons. We recognize here a new embodiment of the basic concept of streak imaging, with the streaking controlled by the NIR field in this case. The electrons can gain or lose an energy of several electron volts depending on whether they have been emitted some hundred attoseconds sooner or later than the peak of the field cycle (Fig. 1B), endowing this light-field–driven streak camera with attosecond resolution (*19*, *20*).

The physical concepts and mechanisms outlined above have opened a realistic prospect of measuring and controlling electron dynamics on an attosecond time scale. However, full exploitation of the potential offered by this conceptual framework requires precise control over the applied laser field.

Steering Electrons with the Electric Field of Controlled Light Waves

In a laser pulse comprising many field cycles, the subfemtosecond electron and photon bursts born in the ionizing field emerge every half cycle, resulting in a train of subfemtosecond bursts (*21*). Its spectrum consists of equidistant lines that represent high-order odd harmonics of the driving field (*22*). The subfemtosecond pulse train and its multicycle driver constitute powerful tools for controlling and tracking electron dynamics that terminate within the NIR field oscillation cycle (*23*–*25*). The characteristics of the individual bursts in the train can be difficult to control and measure. Extension of attosecond control and metrology to a wide range of electronic phenomena (including all those extending in time over more than half an optical cycle) calls for the isolation of one to several attosecond pulses and precise control of their properties (*26*).

Isolation was predicted to be achievable by manipulating the polarization state (polarization gating) of the driving field (*27*) or shortening its duration to nearly a single cycle of the carrier wave (*28*). In fact, intense few-cycle laser pulses lasting several femtoseconds (*1*) led to the first observation of light lasting for less than 1 fs (*29*). Full control of the number and properties of bursts isolated, however, requires precise control of the driving electric-field waveform $E_L(t)$.

Intense few-cycle laser pulses with controlled waveform (*4*)—along with careful bandpass filtering of the highest-energy (cutoff) harmonics—have indeed permitted the reproducible generation of single and twin subfemtosecond pulses with cosine- and sine-shaped electric field waveforms, respectively, as well as their reliable measurement by means of attosecond streaking (*30*, *31*) (fig. S1). The series of streaked electron spectra shown in Fig. 1C yields complete information about the driving laser field and allows determination of the temporal shape, duration, and a possible chirp of the emitted subfemtosecond XUV pulse (Fig. 1D) as well as the degree of its synchronism with its driver (*31*–*33*). These experiments reveal that few-cycle light with controlled waveform permits reproducible generation and complete characterization of subfemtosecond light. Owing to the attosecond synchronism between them, these tools allow attosecond metrology without the need for high-intensity x-rays.

Lightwave Electronics: Versatile Technology for Control and Chronoscopy on the Electronic Time Scale

Controlled light fields permit control of microscopic electric currents at the atomic scale just as synthesized microwave fields permit control of currents at the mesoscopic scale in semiconductor chips. By analogy to microwave electronics, we propose to name this new technology lightwave electronics. In marked contrast with previous quantum control through controlling transitions between quantum states with the amplitude and frequency of light (*8*), lightwave electronics gives way to controlling dynamics directly by the force that the electric field of intense light exerts on

electrons. This new approach is powerful in that (i) it provides a direct way of affecting the position and momentum of electrons and (ii) control is matched in speed to the electronic time scale.

The first notable manifestations of the power of lightwave electronics include controlling subfemtosecond XUV emission (*4*, *25*, *31*–*35*); molecular dissociation (*36*); measuring subfemtosecond XUV and electron pulses (*21*, *31*–*33*, *35*); and imaging dynamic changes in molecular structure (*16*–*18*) by means of steering electron wave packets with light fields. Sub–wave cycle (i.e., subfemtosecond) control of electron wave packet motion can be accomplished by mixing multicycle fields (*25*, *35*). However, full control over the entire system evolution from attosecond to femtosecond time scales—and, consequently, precision attosecond measurements—relies on optical waveforms that can be accurately controlled in shape and polarization state (*4*, *37*) and confined to several cycles. Exploitation of the full potential of lightwave electronics for attosecond control and metrology requires waveform-controlled broadband light.

The attosecond streaking spectrogram shown in Fig. 1C yields the complete history of photoelectron emission induced by a subfemtosecond XUV pulse as well as of the streaking optical field (*38*). Similar spectrograms can also be recorded with secondary (Auger) electrons, which uncover the history of a quantum transition of an electron deep inside an atom in real time (*3*). Attosecond streaking is not the only way of observing the temporal evolution of atomic-scale electron motion. Energetic excitation of atoms, molecules, or solids is often accompanied by the promotion of valence electrons to excited states (referred to as a shake up). The transient population of these states provides information about the instantaneous (electronic) state of the system. This population can be probed by means of attosecond tunneling induced by the time-delayed waveform-controlled, few-cycle laser field (*13*).

In attosecond streaking and tunneling spectroscopy, the subfemtosecond XUV pulse serves as a pump and the controlled optical wave as the probe. Their roles can be interchanged. The optical field may—by means of tunnel ionization (*13*)—initiate an electronic process and control the unfolding dynamics (*36*), and the subfemtosecond XUV pulse may probe this process by, for example, photoelectron spectroscopy (*39*).

Attosecond technology based on a controlled optical wave and a synchronized subfemtosecond

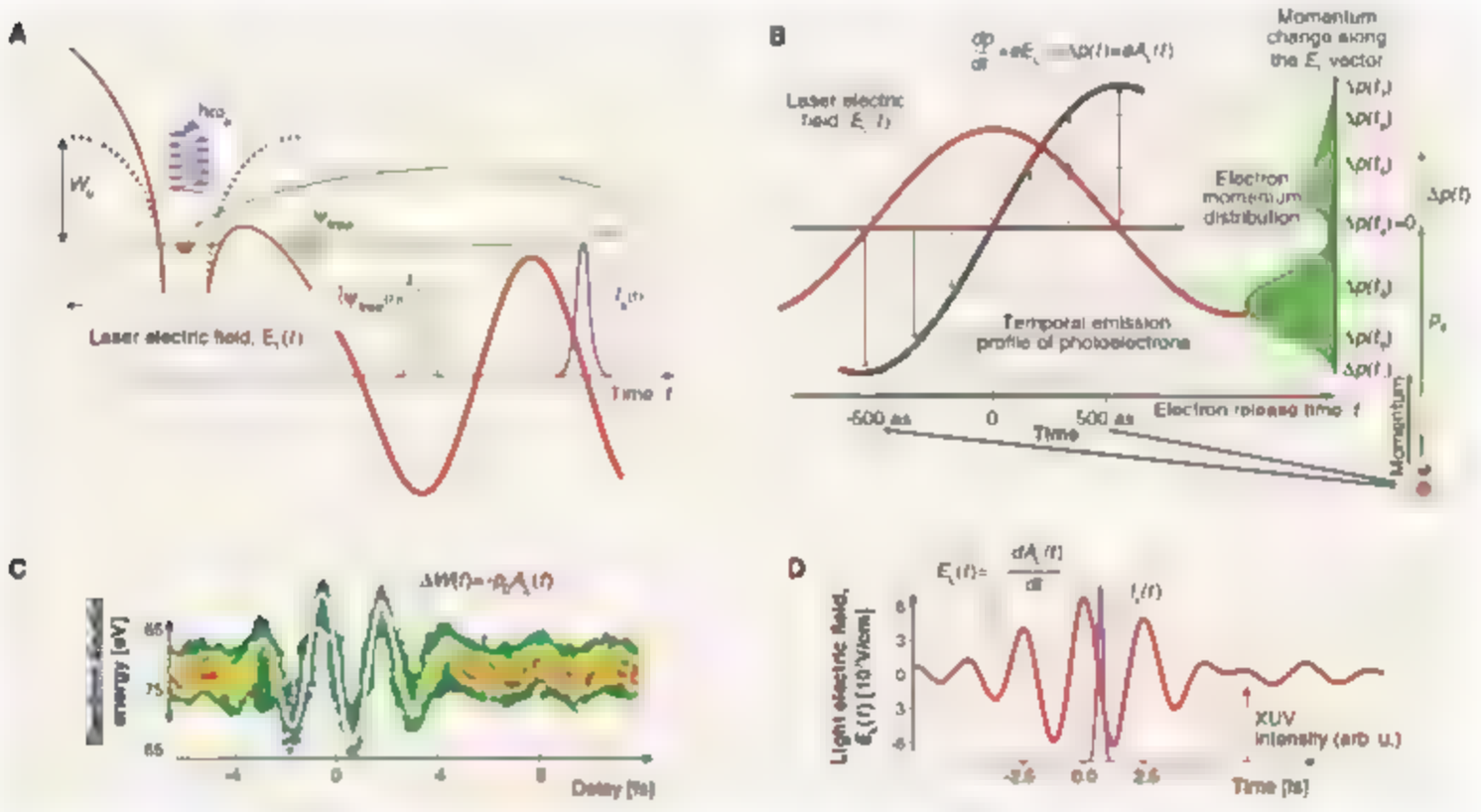

Fig. 1. The birth and measurement of a subfemtosecond (XUV) light pulse. (**A**) The field of a femtosecond NIR laser pulse, $E_L(t)$, is able to suppress the Coulomb potential in atoms sufficiently to allow a valence electron to tunnel through the narrow barrier and release a subfemtosecond wave packet, $\psi_{free}(t)$, near the peaks of its most intense oscillations. The wave packet is subsequently removed from the vicinity of the atomic core and less than a period later pushed back by the reversed field (green trajectory). Upon recollision, it interferes with the bound-state portion of the electron wave function. This interference results in high-frequency oscillations, emitting broadband XUV light. The highest-frequency portion, with intensity $I_X(t)$, is temporally confined to a small fraction of the optical period. (**B**) Concept of optical-field–driven streak imaging of electron emission from atoms. Electrons released by an XUV pulse parallel to the direction of electric field (red line) suffer a change in their initial momenta that is proportional to the vector potential of the field (black line) at the instant of release, mapping the intensity profile of the emitted electron and hence of the ionizing subfemtosecond XUV pulse into a corresponding final momentum and energy distribution of electrons. (**C**) Streaked spectra of photoelectrons released from neon atoms by a single subfemtosecond XUV pulse ($\hbar\omega_X \approx 95$ eV) recorded for a series of delays between the XUV pulse and NIR field (streaking spectrogram). The laser field causes only a moderate broadening (streaking) of the electron spectra; its main effect is the shift of the center of mass of the electron spectrum. In the limit of large initial kinetic energy of the electrons, this shift is linearly proportional to the vector potential of the field at the instant of impact of the XUV pulse (see white line). (**D**) Electric field of the NIR wave and intensity of the XUV pulse as retrieved from the streaking spectrogram shown in (C). The measurement confirms that the few-cycle waveform must be near cosine-shaped to warrant the production of a single subfemtosecond pulse and reveals a near-Fourier–limited XUV pulse of a duration of 250 attoseconds. arb. u., arbitrary units.

pulse is both versatile and sufficiently compact and affordable to allow proliferation in small laboratories. The core infrastructure required is sketched in Fig. 2. The scope of the technology largely depends on the characteristics and flexibility of its key tools: synthesized fields of laser light and attosecond pulses synchronized to them.

From Controlled Light Waveforms Toward Optical Waveform Synthesis

Lightwave electronics benefits from ever-broader optical bandwidth in several ways. Superposition of spectral components beyond an octave permits subcycle shaping of the light waveform and hence sculpting of the electric force on the electronic time scale for steering electrons in atomic systems. The increased bandwidth and improved dispersion control also lead to shorter optical pulses, which allow advancing subfemtosecond XUV pulse generation in terms of all relevant parameters: duration, intensity, and photon energy.

Intense few-cycle optical pulses (~5 fs) were first generated (*40*) by spectral broadening of femtosecond pulses (initially ~25 fs) in a hollow-core waveguide, and the resultant supercontinuum was compressed by reflection off of chirped multilayer dielectric mirrors (*41*) (Fig. 3A). Combined with waveform control (*4*), this technology matured to become a workhorse for attosecond science. Its current state is represented by the results summarized in Fig. 3, B and C. The spectrum of near 20-fs, 800-nm pulses is first broadened by self-phase modulation in a gas-filled capillary to a supercontinuum reaching from 400 to 1000 nm, followed by compression of the ~400-μJ pulses to ~3.5 fs with octave-spanning chirped mirrors (*42*). These pulses constitute the shortest controlled optical waveforms demonstrated to date.

Figure 3D shows how a single subfemtosecond XUV pulse can emerge from an atom ionized by a linearly polarized few-cycle light field. The green lines depict the kinetic energy, W_{kin}, with which different portions of the freed electron wave packet (v_{free} in Fig. 1B) return to the core as a function of return time, determining the energy of the emitted harmonic photon, $\hbar\omega = W_{kin} + W_b$, where W_b is the binding energy of the electron. For the optimum (near-cosine) waveform (Fig. 3D), we can estimate—in the limit of $\hbar\omega_C \gg W_b$—the bandwidth over which photons of the highest energy (near the cutoff of the emitted spectrum depicted in violet) are emitted from one recollision only as

$$\frac{\Delta W_{single\ pulse}}{\hbar\omega_C} \approx 0.6\left(\frac{T_{osc}}{T_{FWHM}}\right)^2$$

where T_{osc} and T_{FWHM} stand for the oscillation period (osc) of the carrier wave and the full width at half maximum (FWHM) duration of the laser pulse ionizing the atoms, respectively (*43*). Equation 1 underscores the importance of minimizing the number of cycles within the driver pulse. The intense sub–1.5 cycle ($T_{FWHM} < 1.5T_{osc}$) laser pulses that can now be produced with commercially available ingredients of ultrafast laser technology (Fig. 3, A to C) constitute a promising tool for pushing the frontiers of attosecond-pulse technology.

Advancing femtosecond technology to its ultimate limit is the key to extending the frontiers of both measuring and controlling dynamics with attosecond precision. Metrology benefits from broader spectral coverage and shorter duration of subfemtosecond pulses. The scope of control crucially depends on the variety of waveforms, which is determined by the available bandwidth of intense coherent radiation. The shortest intense laser pulses also provide ideal conditions for generating the broadest supercontinua of coherent light, extending over more than three octaves (*44*). Advanced chirped multilayer mirror technology holds promise for versatile and scalable (multichannel) implementation of optical waveform synthesis. A prototypical three-channel synthesizer operational over the 1- to 3-eV band indicates the vast variety of possibilities for steering electrons in atomic systems with synthesized optical waves (fig. S2).

From Subfemtosecond Toward Attosecond Pulses

Equation 1 suggests that femtosecond technology must approach the monocycle limit to push the frontiers of XUV pulse generation toward and below 100 as. However, there are other options. Modulation of the polarization state of the ionizing NIR pulse (*33*, *37*, *45*) or of its amplitude by coherent addition of second harmonic radiation (*46*, *47*) can efficiently increase $\Delta W_{single\text{-}pulse}$ even by using several-cycle NIR driver pulses. Implementation of polarization gating with waveform-controlled, approximately two-cycle NIR pulses (*37*) has recently led to a spectacular achievement: the generation of isolated XUV

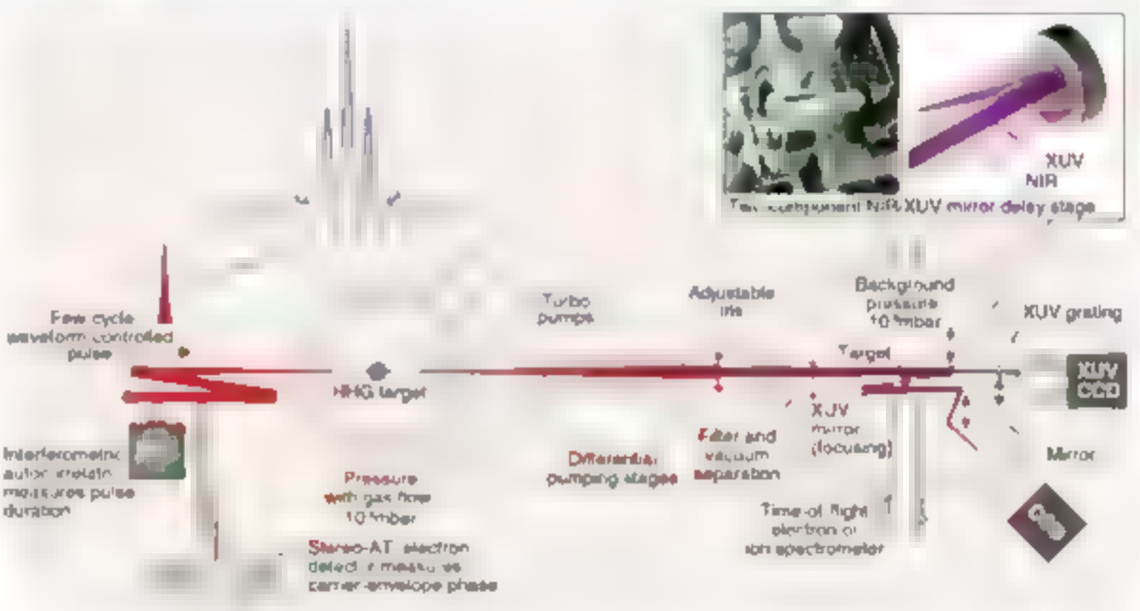

Fig. 2. Schematic of an experimental setup for attosecond-pulse generation and attosecond metrology as well as spectroscopy: the AS-1 attosecond beamline at MPQ. The intense, waveform-controlled few-cycle NIR laser pulse generates a subfemtosecond XUV pulse in the first interaction medium (jet of noble gas). The collinear XUV and NIR beams then propagate into a second vacuum chamber, where they are focused by a two-component XUV multilayer mirror into a gas target. The inner and outer part of the two-component mirror reflects and focuses the XUV and the (more divergent) NIR beam, respectively. By positioning the internal mirror with a nanometer-precision piezotranslator, the XUV pulse can be delayed with respect to the NIR pulse with attosecond accuracy. Analysis of the generated electrons and/or ions as a function of delay between the subfemtosecond XUV and the waveform-controlled NIR pulse permits characterization of the attosecond tools (Fig. 1) as well as real-time observation of atomic-scale electron dynamics in all forms of matter by means of attosecond streaking spectroscopy (*3*) and attosecond tunneling spectroscopy (*13*) with the same apparatus. In the former case, the final energy distribution of the outgoing electron is analyzed with a time-of-flight spectrometer; in the latter case, the observables measured as a function of delay are multiple-charged ions. ACF, auto-correlation function; CCD, charged-coupled device.

pulses at $\hbar\omega_{carrier}$ = 36 eV with a bandwidth of $\Delta W_{single\text{-}pulse}$ = 15 eV. Along with dispersion control and trajectory selection (*49*), these isolated pulses resulted in near single-cycle XUV pulses that had a duration of 130 as (*33*) (see the low-energy streaking spectrogram in Fig. 4A).

The increased $\Delta W_{single\text{-}pulse}$ with several-cycle pulses comes, however, at the expense of efficiency because (i) only a small temporal fraction of the driver pulse participates in the generation process and (ii) the cycles preceding the generation moment pre-ionize the atoms, causing substantial depletion of the ground state before the XUV pulse can be emitted. The unprecedented confinement of electromagnetic energy into a single well-controlled oscillation of light in sub-1.5-cycle NIR pulses (Fig. 3) avoids these shortcomings and offers several more benefits. Indeed, the high contrast between the wave crests at $t = T_{osc}/2$ and earlier ones in Fig. 3D permits, thanks to the exponential scaling of ionization probability with the field strength, adjustment of the pulse intensity so as to allow the electron to survive with a high probability in its ground state until $t = T_{osc}/2$ (in Fig. 3D) and then to be set free with a high probability near this instant through tunneling. The resulting wave packet, ψ_{free} (Fig. 1A), is launched with unprecedented amplitude. Upon its return to the core at about $t = T_{osc}/4$, it interferes with the ground state portion of the wave function causing

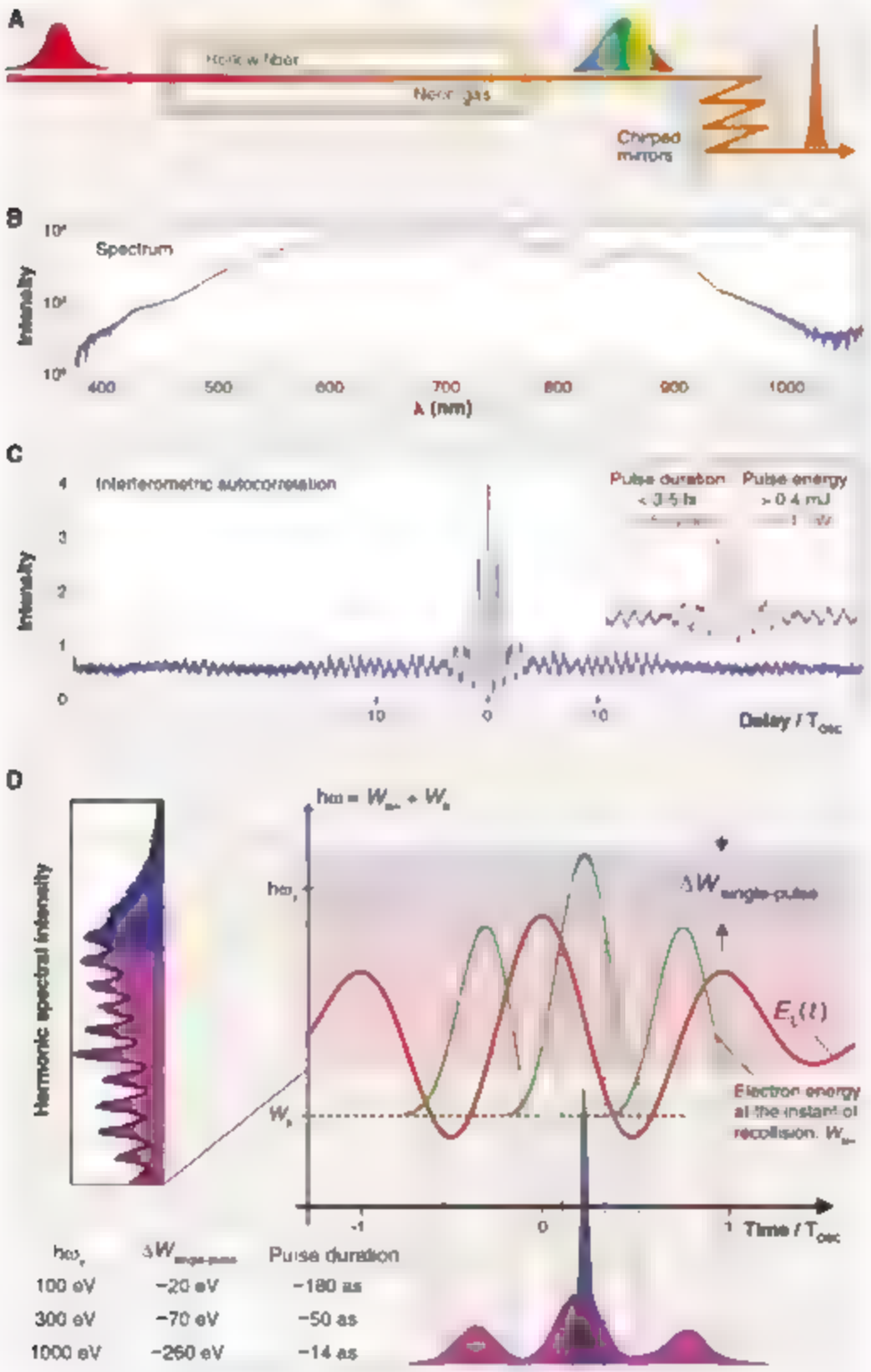

Fig. 3. Toward intense, monocycle optical pulses. (**A**) Hollow-fiber/chirped-mirror optical pulse compressor for the generation of intense, few-cycle laser pulses. (**B**) The spectrum of millijoule-energy near–20-fs, phase-controlled near-infrared laser pulses delivered at a repetition rate of 3 kHz from a Ti:sapphire laser (Femtopower, Femtolasers GmbH) is first broadened to more than an octave (~450 to 950 nm) in a neon-filled capillary (pressure ~ 2 bar, length ~ 1 m, bore diameter 250 μm). (**C**) The spectrally broadened pulses are compressed by octave-spanning chirped multilayer mirrors. The interferometric autocorrelation trace indicates a near–bandwidth-limited ~3.5-fs pulse carried at $\lambda_0 \approx$ 720 nm. (**D**) Energies of XUV photons emitted from an atom exposed to a linearly polarized 3.5-fs, 720-nm Gaussian laser pulse that is sufficiently intense for efficient tunnel ionization. The photon energies (green lines) are depicted as a function of the return time of the electron to the atomic core and have been obtained by analyzing classical electron trajectories (*43*). The width of the energy band within which only one recollision contributes to XUV emission determines the bandwidth $\Delta W_{single\text{-}pulse}$ available for the generation of an isolated attosecond pulse. Based on the classical trajectory analysis, $\Delta W_{single\text{-}pulse}$ is found to be maximum for a near–cosine-shaped waveform, $E_L(t) = E_0 s(t)\cos(\omega_0 t + \varphi)$, with the carrier-envelope phase φ varying between $\pi/12$ and $\pi/6$ depending on the pulse shape and intensity. Here, E_0 and ω_0 stand for the amplitude and angular frequency of the oscillations of the laser electric field, with $s(t)$ being the amplitude envelope function. The table summarizes bandwidths over which the sub–1.5-cycle pulses are predicted to support the emergence of an isolated attosecond pulse at different XUV photon energies. The estimated pulse durations derive from the conservative assumption that no spectral components are available for the pulse synthesis outside the given spectral window.

high-frequency (soft x-ray) dipole oscillations with unprecedented amplitude. Hence, the intense near single-cycle waveforms appear to constitute ideal tools for the pursuit of powerful soft x-ray pulses with pulse durations approaching the atomic unit of time (see table in Fig. 3D) and photon energies approaching the kilo–electron volt frontier.

A first indication of the potential that near single-cycle NIR pulses offer for attosecond-pulse generation is provided by the high-energy streaking spectrogram in Fig. 4A. It has been recorded with sub two-cycle (near 4-fs) NIR (750-nm) pulses and XUV pulses filtered by a molybdenum-silicon chirped multilayer mirror with a high-reflectivity band of ~16 eV (FWHM) centered at 93 eV (Fig. 4B). The bandwidth (FWHM) of the bandpass–filtered XUV light amounts to ~13 eV. The streaking spectrogram indicates isolated sub-170-as pulses that are near bandwidth-limited (*49*). The pulses contain more than 10^8 photons, which are delivered at a repetition rate of 3 kHz, implying a photon flux of $>3 \times 10^9$ photons per second transported in a near diffraction-limited beam. With the Mo/Si mirror, which has a 10-cm focal length, used in the MPQ attosecond beamline AS-1 (Fig. 2), this beam can be focused to a spot diameter of several micrometers.

The recently demonstrated, waveform-controlled sub 1.5-cycle NIR pulses are capable of producing $\Delta W_{\text{single-pulse}} > 30$ eV at $\hbar\omega_X \approx 120$ eV (Fig. 4D), offering the potential for generating sub 100-as pulses at a wavelength of ~10 nm (*47*). To exploit this potential, researchers must develop ultrabroadband soft x-ray multilayer mirrors with precisely controlled group-delay (GD) dispersion. Figure 4C plots the reflectivity and GD of the first chirped multilayer mirror design that supports sub 100-as pulses. Chirped multilayer mirror technology (both metallic and dielectric) is likely to play as important a role in advancing attosecond technology as it has played in advancing femtosecond technology to its ultimate limits.

Prospects

New research tools allow scientists to seek answers to questions that, in the absence of a means of addressing them, have never been posed before. Grand questions serve as a compass providing directions for research that promises the most extensive return. We pose a few questions across disparate areas of science connected by the fundamental role that atomic-scale electronic motion plays in physical, chemical, and biological processes.

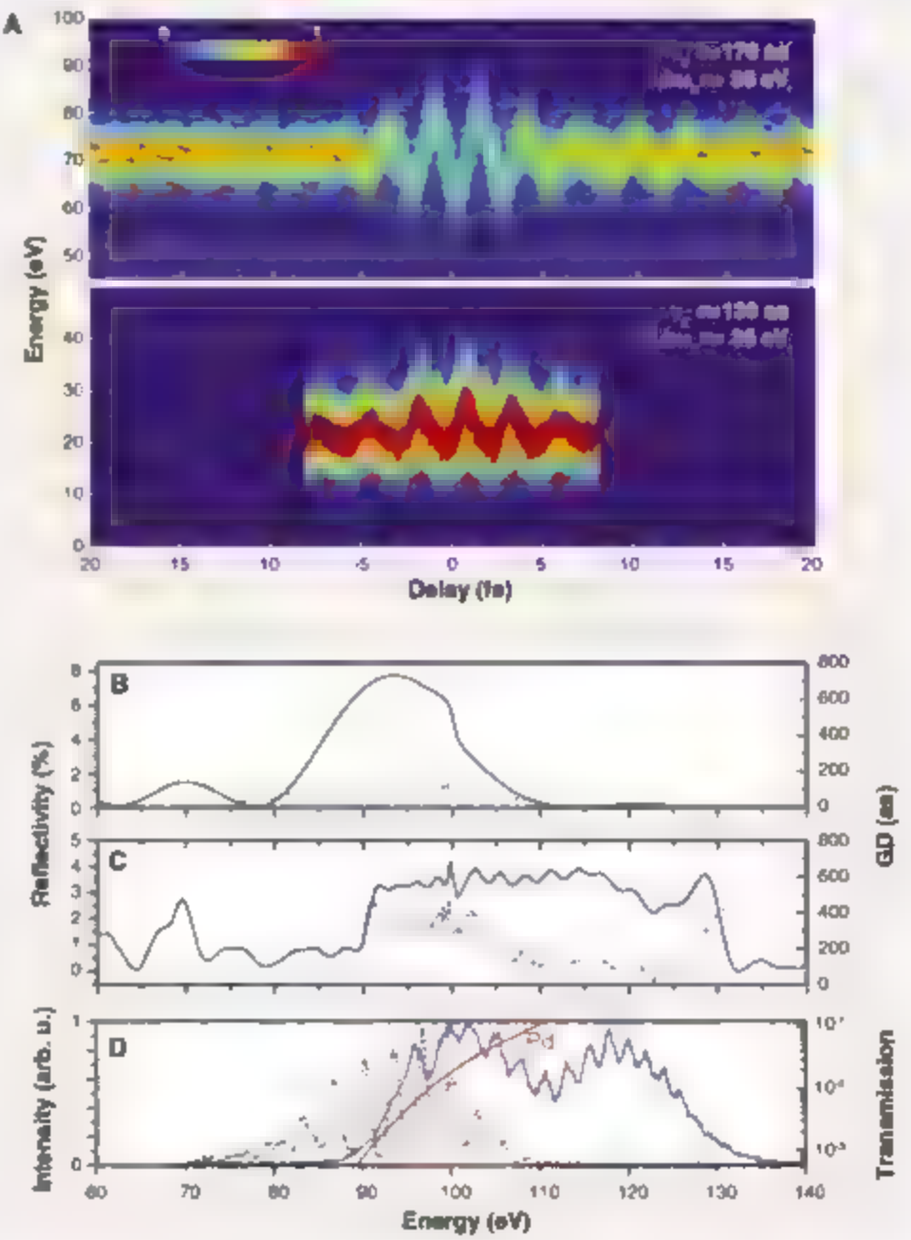

Fig. 4. Current frontiers of attosecond technology. **(A)** Attosecond streaking spectrograms recorded with few-cycle NIR pulses ($\lambda_L \approx 750$ nm). The low-energy spectrogram (bottom) shows the carrier photon energy of an XUV pulse, $\hbar\omega_X = 36$ eV, with argon target atoms (courtesy of M. Nisoli). The high-energy spectrogram (top) shows $\hbar\omega_X = 93$ eV, with neon target atoms (*49*). **(B)** Computed reflectivity and group delay of the chirped Mo/Si multilayer mirror used for filtering and focusing the isolated sub–170-as, 93-eV pulses. **(C)** Computed reflectivity and group delay of an ultrabroadband chirped multilayer Mo/Si mirror designed for compensating the chirp carried by an attosecond pulse filtered near cutoff from short-trajectory emission (group delay dispersion ~ −0.007 fs^2) and for reflecting a band sufficient for sub–100-as pulse generation (bandwidth > 35 eV). **(D)** Spectrum of high-order harmonics emitted from neon ionized by ~4-fs–duration NIR (~720-nm) pulses near cutoff as transmitted through a high-pass filter (150-nm palladium). The transmission of the Pd foil is shown by the red curve. The spectrum has been recorded with the carrier-envelope phase φ of the waveform-controlled NIR pulse set to provide the broadest continuum. Variation of φ reshapes the overall distribution of the continuum (*42*) rather than introducing a pronounced harmonic-like structure, as observed with several-cycle driver pulses for appropriate phase setting (dashed line). The smooth continuum with a bandwidth of >30 eV suggests the feasibility of sub–100-as XUV pulse generation without manipulation of the driving pulse (e.g., superimposing its second harmonic or gating its polarization).

Atomic physics and x-ray science. How is the energy of an x-ray photon distributed between electrons upon its absorption by an atom? Can electronic transitions deep inside atoms be affected by controlled ultrastrong external fields rivaling in strength the internal Coulomb fields, e.g., for opening up novel routes to efficient, compact x-ray lasers?

Physical chemistry, molecular biology, bioinformatics, and photovoltaics. Can controlled light fields offer a fundamentally new way of modifying the structure and/or composition of molecules by driving electron wave packets across molecules with synthesized optical fields? What are the microscopic mechanisms underlying biological information transport? Can charge-transfer in host-guest systems (e.g., dye-semiconductor assemblies) be exploited for developing solar cells with unprecedented efficiency?

Information technology. Can electron-based information processing and storage be downscaled to atomic dimensions and sped up to the atomic time scale (i.e., to optical frequencies)? Can these ultimate limits be reached by exploiting electric interactions (electronics) or magnetic interactions (spintronics) or collective electron motion (plasmonics)? Which incarnation of light-wave electronics will be the ultimate electron-based information technology?

The answers to these questions will rely on exploring and controlling the microscopic motion of electrons, on atomic scales in space and time. Attosecond technology now offers the tools for tackling these and many other exciting questions. The importance of the answers being sought will drive its proliferation.

References and Notes

1. T. Brabec, F. Krausz, *Rev. Mod. Phys.* **72**, 545 (2000).
2. A. H. Zewail, *J. Phys. Chem. A* **104**, 5660 (2000).
3. M. Drescher *et al.*, *Nature* **419**, 803 (2002).
4. A. Baltuška *et al.*, *Nature* **421**, 611 (2003).
5. For a comprehensive historical review, see P. Agostini, L. F. DiMauro, *Rep. Prog. Phys.* **67**, 813 (2004).
6. R. Trebino *et al.*, *Rev. Sci. Instrum.* **68**, 3277 (1997).
7. C. Iaconis, I. A. Walmsley, *IEEE J. Quantum Electron.* **35**, 501 (1999).
8. P. W. Brumer, M. Shapiro, *Principles of the Quantum Control of Molecular Processes* (Wiley, New York, 2003).
9. W. Ackermann *et al.*, *Nature Phot.* **1**, 336 (2007).
10. A. A. Zholents, W. M. Fawley, *Phys. Rev. Lett.* **92**, 224801 (2004).
11. P. Tzallas, D. Charalambidis, N. A. Papadogiannis, K. Witte, G. Tsakiris, *Nature* **426**, 267 (2003).
12. T. Sekikawa, A. Kosuge, T. Kanai, S. Watanabe, *Nature* **432**, 605 (2004).
13. M. Uiberacker *et al.*, *Nature* **446**, 627 (2007).
14. P. B. Corkum, *Phys. Rev. Lett.* **71**, 1994 (1993).
15. P. Antoine, A. L'Huillier, M. Lewenstein, *Phys. Rev. Lett.* **77**, 1234 (1996).
16. H. Niikura *et al.*, *Nature* **417**, 917 (2002).
17. F. Kanai, S. Minemoto, H. Sakai, *Nature* **435**, 470 (2005).
18. S. Baker *et al.*, *Science* **312**, 424 (2006).
19. The first implementation of the basic concept of a light-field-driven streak camera has drawn on an orthogonal detection geometry (electrons collected along a direction orthogonal to the electric field vector of the streaking NIR field (*29*).
20. The laser field needed to induce this change in electron energy is orders of magnitude less intense than that required for strong-field ionization. Hence, this streaking field has negligible influence on the atomic or molecular processes under study, unless its oscillations happen to be in resonance with a transition from an occupied to an unoccupied quantum state of the system.
21. P. M. Paul *et al.*, *Science* **292**, 1689 (2001).
22. M. Ferray *et al.*, *J. Phys. B* **21**, L31 (1988).
23. K. J. Schafer, M. B. Gaarde, A. Heinrich, J. Biegert, U. Keller, *Phys. Rev. Lett.* **92**, 023003 (2004).
24. F. Remetter *et al.*, *Nature Phys.* **2**, 323 (2006).
25. J. Mauritsson *et al.*, *Phys. Rev. Lett.* **97**, 013001 (2006).
26. Experiments that can be performed with subfemtosecond pulse trains (including those described in (*23*–*25*)) would benefit from using a small number of well-controlled and characterized subfemtosecond pulses.
27. P. B. Corkum, N. H. Burnett, M. Yu. Ivanov, *Opt. Lett.* **19**, 1870 (1994).
28. I. P. Christov, M. M. Murnane, H. C. Kapteyn, *Phys. Rev. Lett.* **78**, 1251 (1997).
29. M. Hentschel *et al.*, *Nature* **414**, 509 (2001).
30. J. Itatani *et al.*, *Phys. Rev. Lett.* **88**, 173903 (2002).
31. R. Kienberger *et al.*, *Nature* **427**, 817 (2004).
32. E. Goulielmakis *et al.*, *Science* **305**, 1267 (2004).
33. G. Sansone *et al.*, *Science* **314**, 443 (2006).
34. I. P. Christov, R. Bartels, H. C. Kapteyn, M. M. Murnane, *Phys. Rev. Lett.* **86**, 5458 (2001).
35. N. Dudovich *et al.*, *Nature Phys.* **2**, 781 (2006).
36. M. F. Kling *et al.*, *Science* **312**, 246 (2006).
37. I. J. Sola *et al.*, *Nature Phys.* **2**, 319 (2006).
38. F. Quéré, Y. Mairesse, J. Itatani, *J. Mod. Opt.* **52**, 339 (2005).
39. A. D. Bandrauk, S. Chelkowski, H. S. Nguyen, *Int. J. Quantum Chem.* **100**, 834 (2004).
40. M. Nisoli *et al.*, *Opt. Lett.* **22**, 522 (1997).
41. R. Szipőcs, K. Ferencz, C. Spielmann, F. Krausz, *Opt. Lett.* **19**, 201 (1994).
42. A. L. Cavalieri *et al.*, *New J. Phys.* **9**, 242 (2007).
43. The electron kinetic energies have been calculated in terms of the classical description of the center-of-mass motion of the freed electron wave packet (Fig. 2), under the assumption of a Gaussian pulse shape and by using the strong-field approximation. The factor of ~0.6 in Eq. 1 depends on the pulse shape and intensity but varies less than 15% in the relevant parameter range.
44. M. Aidarbek *et al.*, *New J. Phys.* **8**, 177 (2006).
45. Z. Chang, *Phys. Rev. A* **70**, 043802 (2004).
46. I. Pfeifer *et al.*, *Phys. Rev. Lett.* **97**, 163901 (2006).
47. Y. Oishi, M. Kaku, A. Suda, F. Kannari, K. Midorikawa, *Opt. Exp.* **14**, 7230 (2006).
48. R. Lopez-Martens *et al.*, *Phys. Rev. Lett.* **94**, 033001 (2005).
49. M. Schultze *et al.*, *New J. Phys.* **9**, 243 (2007).

50. We apologize that many original research papers could not be cited because of space limitations. This work is supported by the Max-Planck-Society and the Deutsche Forschungsgemeinschaft through the DFG Cluster of Excellence Munich-Centre for Advanced Photonics (www.munich-photonics.de). E.G. acknowledges support from a Marie Curie Intra-European Fellowship. We thank B. Feuerstein, M. Hofstetter, B. Horvath, and M. Schultze for their support in the preparation of this manuscript.

Supporting Online Material

www.sciencemag.org/cgi/content/full/317/5839/769/DC1
Figs. S1 and S2
References

10.1126/science.1142855

REVIEW

Harnessing Attosecond Science in the Quest for Coherent X-rays

Henry Kapteyn, Oren Cohen, Ivan Christov, Margaret Murnane*

Modern laser technology has revolutionized the sensitivity and precision of spectroscopy by providing coherent light in a spectrum spanning the infrared, visible, and ultraviolet wavelength regimes. However, the generation of shorter-wavelength coherent pulses in the x-ray region has proven much more challenging. The recent emergence of high harmonic generation techniques opens the door to this possibility. Here we review the new science that is enabled by an ability to manipulate and control electrons on attosecond time scales, ranging from new tabletop sources of coherent x-rays to an ability to follow complex electron dynamics in molecules and materials. We also explore the implications of these advances for the future of molecular structural characterization schemes that currently rely so heavily on scattering from incoherent x-ray sources.

Next year, 2008, will mark the 50th anniversary of the revolutionary paper by Schawlow and Townes that proposed the laser (*1*). This paper extended concepts first used to demonstrate the maser in the microwave region of the spectrum into the visible spectrum. Soon after the laser was demonstrated, scientists discovered how to control laser light to generate extremely short nanosecond, picosecond, and even femtosecond pulses. Given the origin of the laser, it was also natural to attempt to generate coherent light at shorter and shorter wavelengths. However, this effort proved very challenging because of the punishing power scaling inherent in lasers. Basic physics dictates that the energy required to implement a laser scales roughly as $1/\lambda^5$, that is, a laser at a 10 times shorter wavelength (λ) requires ~100,000 times the input power. Thus, the first x-ray lasers implemented in the 1980s used the bunding-sized Nova fusion laser at Lawrence Livermore National Laboratory as a power source to generate soft (relatively long-wavelength) x-rays. Since that initial x-ray laser, considerable progress has been made in downscaling the laser needed as the power source

JILA and the National Science Foundation Center for Extreme Ultraviolet Science and Technology, University of Colorado at Boulder, Boulder, CO 80309–0440, USA.

*To whom correspondence should be addressed. E-mail: murnane@jila.colorado.edu

(2). Nevertheless, the generation of coherent hard x-rays from x-ray lasers remains a daunting prospect.

Fortunately, in recent years scientists have found a way to make rapid progress toward generating coherent light at very short wavelengths by using alternative techniques. Large-scale free-electron lasers promise to produce high-energy pulses of coherent x-rays using, for example, the 2-km-long electron accelerator at the Stanford Linear Accelerator Center. Extreme nonlinear optical techniques have succeeded in upconverting visible laser light into x-rays, making a tabletop source of coherent x-rays possible. This ability has given us a new coherent light source that spans such a large region of the spectrum that we can now access processes that occur on subfemtosecond or attosecond (1 as 10^{-18} s) time scales. Equally intriguing is the fact that we have learned how to use femtosecond laser light to coherently manipulate electrons in atoms and molecules on their fundamental attosecond time scales. The richness and complexity of attosecond science and technology are only just beginning to be uncovered. As we discuss here, attosecond science can capture the complex interwoven dance of electrons in molecules and materials. Attosecond science also shows great promise for developing new ultrasensitive molecular imaging and spectroscopic techniques. Finally, attosecond science represents the most promising avenue to achieve what had seemed hopelessly impractical until now: the generation of bright, coherent, hard x-ray beams using a tabletop-scale apparatus.

The Birth of Attosecond Science

Attosecond science began with the discovery of high harmonic generation: an extreme nonlinear process that remains to date perhaps the best example of complex attosecond dynamics. When driven by a strong femtosecond laser, atoms can emit coherent light at frequencies much higher than that of the incident laser. This high harmonic generation process is a result of an electron rescattering process (Fig. 1). When an atom or molecule is exposed to a strong electric field that is comparable to the field binding the electron to the nucleus, the most loosely bound electron can be ripped from the atom. The laser intensities required (10^{13} to 10^{15} W cm^{-2}) are easily accessible with tabletop femtosecond lasers. Once free, the electron will follow a trajectory controlled by the laser field, first moving away from the parent ion and then reversing its motion as the laser field oscillates in time.

Upon returning to the vicinity of its parent ion, this electron has some probability of recombining with it and giving up its excess kinetic energy as a photon, with energy corresponding to dozens or hundreds of visible laser photons. Each time this recollision happens, a burst of attosecond-duration x-rays is emitted. This burst generally occurs twice during each cycle of the driving laser field, or every 1.3 fs for a driving laser at 800 nm wavelength (because the ionizing laser field peaks twice each optical cycle). A classical picture of high harmonic generation (Fig. 1, top left) gives a simple expression for the maximum energy of the photons that can be generated ($h\nu_{max}$), which is simply the energy that the electron possesses when it recollides with the ion (Eq. 1)

$$h\nu_{max} = I_p + 3.17 U_p = I_p + 3.17 \times I_{laser} \lambda^2 \quad (1)$$

where I_p is the ionization potential of the atom, U_p is the ponderomotive potential (or the average kinetic energy of an electron oscillating in response to the driving laser field), and I_{laser} and λ are the intensity and wavelength of the driving laser at the time of the ionization (3, 4). From this simple picture, one can see that high harmonic generation corresponds to the coherent version of the x-ray tube first demonstrated by Roentgen, where electrons accelerated by an electric field collide with atoms in a target. In high harmonic generation, the randomly phased electron impact that occurs in an x-ray tube is replaced by the coherent impact of an electron driven by a coherent laser field. Each electron starts in a bound state of the atom and is ripped from the atom and accelerated by the same coherent laser field. Therefore, under the correct conditions, the re-radiated x-ray waves are identical for each atom and add together to generate a fully coherent laserlike x-ray beam (5). Moreover, the linear intensity scaling law given by the cutoff relation of Eq. 1 (for high recollision energies >> I_p) is remarkably favorable; the intensities required to generate hard x-rays of ~1 to 10 keV are readily accessible using current tabletop lasers.

Much of the beauty and complexity that have sparked long-term interest in high harmonic generation originate because of its quantum or wavelike properties (3, 6). During its trajectory as a free particle, the electron wave evolves with a deBroglie wavelength corresponding to $\lambda = h/p$ (where p is the electron momentum and h is Planck's constant) (Fig. 1, bottom). The total quantum phase advance of the electron during its free trajectory between ionization and recombination is quite large, corresponding to dozens to hundreds of radians. Moreover, the quantum phase accumulated by the electron depends on the exact shape of the electromagnetic field of the laser that guides it during the suboptical cycle time interval between ionization and rescattering. This same quantum phase accumulated by the electron is then acquired by the high harmonic x-ray wave that is emitted when the electron recombines with the ion. The surprising end result is that the phase of the x-ray waves is thus not rigidly related to the phase of the driving laser, but rather depends on the light field that guides the electron in its boomerang-like journey first away from, and then back to, the ion. This property is very different from those pertaining to any other type of nonlinear optical process and opens up many exciting possibilities. For example, during the attosecond time interval between when the electron is ejected and when it recombines with the ion, its wave function can be manipulated in useful ways (7–9). This can be accomplished by shaping the driving laser field itself or by imposing another external light field.

Several remarkable scientific and technological opportunities have emerged as a result of the interaction of strong light fields with matter—a property of matter that is intimately associated with attosecond science and was discovered only 20 years ago (10, 11). Most current research in attosecond science falls into three broad categories: (i) understanding how to control electron rescattering in order to manipulate electrons on attosecond time scales in useful ways, (ii) learning how to use the rescattering electrons as a probe of molecular dynamics, and (iii) using the attosecond time

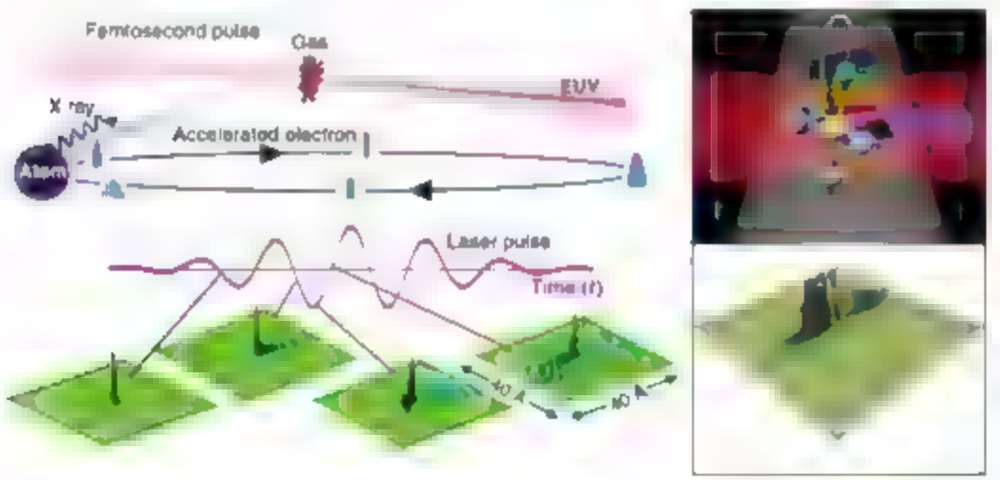

Fig. 1. Attosecond coherent electron rescattering from atoms and molecules. Classical (**top**) and quantum (**bottom**) pictures of high harmonic generation. A strong laser field plucks an electron from an atom (**left**) or molecule (**right**). After evolving as a free electron for a fraction of a femtosecond, the electron can recombine with the ion, emitting a coherent x-ray. The quantum wave functions of the ionizing electrons (shown in green) have many modulations that rapidly change in time as the electron is accelerated by the laser field.

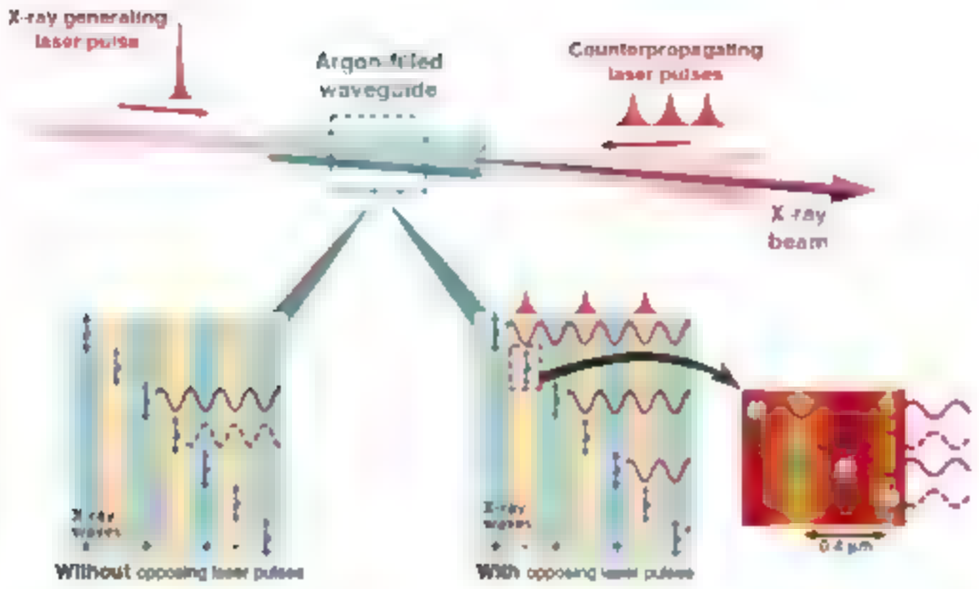

Fig. 2. Crystals made from light by manipulating electron rescattering. Shining a light pattern on a gas can control where in the gas the coherent x-rays are generated (bottom left). X-rays are generated throughout the medium, but emissions from the orange regions cancel out emissions from the blue regions, because the driving laser field and x-ray waves slip in phase by π after traveling through each region (corresponding to one L_c or a few hundred micrometers at 70-eV photon energies). This results in a weak x-ray output from the medium. (Bottom right) A light pattern is used to scramble and disrupt the electron and x-ray phases in regions where the forward- and backward-propagating laser beams overlap. In these overlapping regions (shown in the inset, and indicated by the horizontal black arrow), the laser intensity is modulated on short distances (0.4 μm) that are much shorter than L_c. The modulated laser intensity modulates and scrambles the electron phase, shown in green in the inset. This eliminates x-ray emission from the orange regions, so that emission from the blue regions can now add constructively to generate a bright x-ray output.

structure of x-rays generated by high harmonic generation as a probe of complex electron dynamics in molecules and materials. We briefly discuss the exciting scientific opportunities in each area.

Manipulating Electrons on Attosecond Time Scales

In exciting recent experimental and theoretical developments (*9*, *12*), the concept of manipulating coherent electrons on attosecond time scales has been used to overcome one of the major outstanding problems in nonlinear optics: the efficient generation of coherent high-energy x-rays from lasers. The major challenge in generating a usable flux of x-rays from high-order harmonic generation is in phase-matching the process. As the driving laser beam propagates in the gas, the harmonic signal wave will build up constructively over a long distance only if the driving laser wave and the generated harmonic wave travel with the same crest or phase velocity throughout the medium. In conventional nonlinear optics, this is achieved using birefringence, that is, a nonlinear crystal structure is chosen specifically to equalize the propagation phase velocities of the two disparate colors. This approach of structuring the medium will not work for high harmonic generation, where a gas must be used as the medium because it is literally ripped apart by the strong laser field. Moreover, free electrons act like highly dispersive prisms, causing a severe phase-velocity slip between the laser and the x-ray waves. This effect greatly reduces the distance over which the x-ray waves build up constructively [called the coherence length (L_c)] to millimeters or micrometers for photon energies between 150 eV and 1 keV. (Photon energies below 130 eV can be generated before the gas is fully ionized. Under these conditions, the dispersion of the neutral gas and the free-electron plasma can balance, resulting in perfect phase-velocity matching of the laser and x-ray waves.)

The propagating phase-velocity slip that occurs as the laser and harmonic x-ray waves travel through the gas will add to any quantum phase accumulated by the electron during its trajectory away from the ion. So an intriguing question arises: Is there a way to compensate for the propagation phase slip using the quantum phase accumulated by the electron during its attosecond excursion from the ion? Fortunately, the answer is yes. The phase-matching challenge for high harmonic generation at high energies can be overcome by patterning the laser field driving the process rather than by structuring the medium, as is the case in visible nonlinear optics. This is because high harmonic generation is a purely electronic process that nevertheless does not respond instantly but rather has a subfemtosecond response time (*13*). The quantum phase resulting from the recollision process can be influenced by the driving laser field or by any other field that is simultaneously applied to the atom or molecule (*14*). This provides a way to control electrons at angstrom spatial dimensions and on attosecond time scales (*15*).

Two approaches for using a patterned light field to correct for the propagation phase-velocity slip between the laser and x-rays have been demonstrated experimentally to date. In one approach, the driving laser propagates through a periodically modulated, gas-filled waveguide (*16*). The x-ray emission is brightest where the waveguide diameter is smallest and the laser intensity is highest. By limiting the x-ray generation to certain regions in the waveguide where the laser intensity is highest, the laser and x-ray waves can slip back into perfect phase alignment in the regions in between, where no x-rays are generated. This quasi phase-matching (QPM) scheme therefore automatically ensures that in-phase spatial regions contribute most to the x-ray signal, while the out-of-phase regions are suppressed.

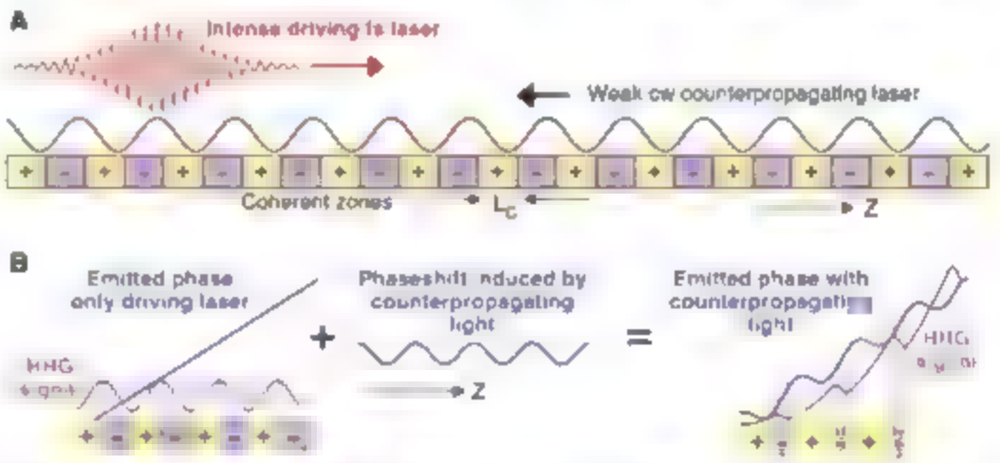

Fig. 3. Coherent hard x-rays produced by manipulating electron rescattering. (**A**) An intense laser pulse (red) generates harmonic x-rays as it travels through a gas. Most of the emitted x-rays interfere with each other from the different out-of-phase zones shown in yellow and purple, because the driving laser and generated x-ray waves slip in phase by π over each zone. (**B**) Shining a continuous wave laser whose wavelength matches the coherent zone widths, can manipulate the phase of the recolliding electron on attosecond time scales, to adjust its phase so that x-ray emissions from the entire medium can add constructively. This scheme is ideally suited for hard x-rays around 1 keV and higher, where the coherent zone widths are in the micrometer range.

In more recent experiments, the quantum phase of the recolliding electron was manipulated using a second, independent, patterned light field (9). While the electron is away from the ion, it is essentially free of its Coulomb field. Remarkably, very small changes in the light field can result in large changes in the phase of the recolliding electron, because this phase is approximately proportional to the applied laser intensity. Any change in the laser intensity will therefore change the quantum phase of the electron, and this phase shift is then directly mapped into the phase of the x-ray emission as a result of quantum mechanics. As illustrated in Fig. 2, a sequence of weak counterpropagating pulses can interfere with the driving laser pulse that generates the coherent x-rays. In any spatial region where the two pulses collide, an interference pattern is created between the forward- and backward-going pulses. This modulated laser intensity scrambles the recolliding electron phase on very short spatial lengths (~400 nm), and as a result, will also scramble the x-ray phase effectively preventing any x-ray wave buildup. In regions where the forward- and backward-propagating pulses do not intersect, the x-ray signal grows over distances as great as L_{abs}, and the x-ray signal from the different regions can add in-phase under the correct conditions. Such light sequences were used recently to selectively enhance a single harmonic order by almost three orders of magnitude (9).

How far can we go with these attosecond manipulation techniques? Is it possible to generate bright, coherent, hard x-rays using high harmonic generation for applications in crystallography, biology, materials science, and medical imaging? In theory, the answer is yes. As shown in Fig. 3, instead of using sequences of pulses to eliminate harmonic emission from wide (a fraction of a millimeter) regions of the medium that would otherwise contribute destructively, the oscillating field of a continuous-wave laser can be used to continually adjust the phase of the recolliding electron and x-rays (12). This approach shows great promise for generating bright coherent beams at very high photon energies well above 1 keV, where the phase-slip distance is extremely short, on the order of micrometers, and is well matched to infrared wavelengths. Even more complicated light patterns could be used to manipulate x-ray wave fronts, for example, to focus them.

Attosecond Electron Recollisions with Molecules

Another exciting frontier of attosecond science is to exploit attosecond electron recollisions with molecules. In these experiments, an electron is plucked from a molecule and returns to the same molecule a fraction of an optical cycle later (Fig. 1) while emitting a coherent x-ray. As the electron accelerates in the laser field, it gains energy ranging from tens to hundreds of electron volts, corresponding to a characteristic electron deBroglie wavelength of ~1 Å. This electron wavelength is well matched to the spacing between atoms in a molecule. What is intriguing about this electron recollision is that the electron is coherent with its parent ion and can be used as an in situ probe of molecular dynamics—essentially using a molecule's own electrons for a new type of electron diffraction experiment. X-ray harmonics generated from molecules are very sensitive to the orientation (17), structure (18), and dynamic motion (19, 20) of the electrons and atoms in a molecule. To date, this technique has been used to map the valence electron orbital in a diatomic molecule and to observe simple shape changes and vibrational dynamics in molecules.

As a method for observing molecular dynamics, high harmonic generation also conveniently probes motions of the molecules in their ground electronic state, which is particularly relevant to chemistry. Moreover, the time resolution is high enough to decouple the electronic and nuclear motions. In the future, high harmonic generation from molecules could become a broadly applicable probe of chemical dynamics, combining ultrahigh time resolution with the potential for obtaining structural information, complementary to techniques such as femtosecond electron diffraction.

Probing Attosecond Electron Dynamics in Atoms, Molecules, and Materials

The x-ray high harmonic bursts generated by recolliding electrons represent the fastest strobe light in existence (21–23), fast enough to capture the fleeting motion of electrons in atoms, molecules, and solids. No other probe has succeeded in this endeavor to date. Moreover, their average brightness compares well with bending magnet synchrotron sources and will increase further as more powerful lasers are developed. Single, isolated, attosecond x-ray bursts can be produced with a laser pulse lasting only a few optical periods (~5 fs) (22, 23). In this case, the time-varying few-cycle field ensures that the highest harmonics are emitted only during one half-cycle of the laser field. Trains of attosecond bursts of x-rays are generated if a longer driving laser pulse is used. These attosecond bursts of x-rays (whether isolated or in a train of pulses, depending on the experiment) are ideal probes of complex correlated electron dynamics in atoms, molecules, and materials.

To date, attosecond pulses have been used to follow some of the fastest electron dynamics, such as Auger decay in atoms (24) or laser-assisted photoemission from solids (25). In some cases, these experiments have confirmed information already available from spectral studies. More sophisticated current experiments are just beginning to probe electron dynamics in molecules and solids that cannot be examined in other ways, such as the dynamics of multi-electron processes, highly excited and strong field processes, and correlated electron dynamics at surfaces or in nanomaterials.

Looking Forward

The attosecond physics of high-order harmonic generation is one of the great success stories of nonlinear optics in the past 20 years. The first experiments were little more than a physics curiosity, with limited apparent use. Since that time, many exciting applications of attosecond bursts of coherent x-rays have been demonstrated, including high-resolution coherent x-ray imaging, femtosecond holography for studying nanothermal transport, real-time observation of molecular motion on surfaces, ultrasensitive molecular spectroscopies and imaging, and capturing the motion of electrons in atoms, molecules, and materials (26–29). As we look forward, attosecond science is poised to revolutionize how we understand and control electron dynamics in matter, whereas attosecond technology may revolutionize crystallography, x-ray spectroscopy, and biological, materials, and medical imaging.

References and Notes

1. A. L. Schawlow, C. H. Townes, *Phys. Rev.* **112**, 1940 (1958).
2. J. J. Rocca, *Rev. Sci. Instrum.* **70**, 3799 (1999).
3. J. L. Krause, K. J. Schafer, K. C. Kulander, *Phys. Rev. Lett.* **68**, 3535 (1992).
4. P. B. Corkum, *Phys. Rev. Lett.* **71**, 1994 (1993).
5. R. A. Bartels *et al.*, *Science* **297**, 376 (2002).
6. M. Lewenstein, P. Balcou, M. Y. Ivanov, A. L'Huillier, P. B. Corkum, *Phys. Rev. A* **49**, 2117 (1994).
7. R. Bartels *et al.*, *Nature* **406**, 164 (2000).
8. I. P. Christov, R. Bartels, H. C. Kapteyn, M. M. Murnane, *Phys. Rev. Lett.* **86**, 5458 (2001).
9. X. Zhang, A. L. Lytle, H. C. Kapteyn, M. M. Murnane, O. Cohen, *Nat. Phys.* **3**, 270 (2007).
10. A. McPherson *et al.*, *J. Opt. Soc. Am. B* **4**, 595 (1987).
11. M. Ferray *et al.*, *J. Phys. B* **21**, L31 (1988).
12. O. Cohen *et al.*, *Phys. Rev. Lett.* **99**, 53902 (2007).
13. Initial experiments validated the quantum electron-rescattering picture by observing how the harmonic beam characteristics (spectrum and beam shape) changed with the driving laser characteristics (*30*, *31*).
14. J. Peatross, M. V. Fedorov, K. C. Kulander, *J. Opt. Soc. Am. B* **12**, 863 (1995).
15. The first experiment to achieve coherent attosecond electron manipulation adjusted the shape of the driving laser pulse using pulse shaping. This made it possible to control the phase of the recolliding electrons, on a cycle-to-cycle basis of the driving laser field, to a precision of ±12 as. Using a learning algorithm, an optimal laser pulse shape was found so that for a selected harmonic, each attosecond burst of x-rays interfered constructively because x-rays emitted in adjacent harmonics interfered destructively, a single harmonic order was selectively enhanced (*7*, *8*).
16. A. Paul *et al.*, *Nature* **421**, 51 (2003).
17. R. Velotta, N. Hay, M. B. Mason, M. Castillejo, J. P. Marangos, *Phys. Rev. Lett.* **87**, 183901 (2001).
18. J. Itatani *et al.*, *Nature* **432**, 867 (2004).
19. M. L. Wagner *et al.*, *Proc. Natl. Acad. Sci. U.S.A.* **103**, 13279 (2006).
20. S. Baker *et al.*, *Science* **312**, 424 (2006); published online 1 March 2006 (10.1126/science.1123904).
21. P. M. Paul *et al.*, *Science* **292**, 1689 (2001).
22. I. P. Christov, M. M. Murnane, H. C. Kapteyn, *Phys. Rev. Lett.* **78**, 1251 (1997).
23. A. Baltuška *et al.*, *Nature* **421**, 611 (2003).
24. R. Kienberger *et al.*, *Nature* **427**, 817 (2004).
25. L. Miaja-Avila *et al.*, *Phys. Rev. Lett.* **97**, 113604 (2006).
26. H. C. Kapteyn, M. M. Murnane, I. P. Christov, *Phys. Today* **58**, 39 (2005).
27. H. N. Chapman *et al.*, *Nat. Phys.* **2**, 839 (2006).
28. R. L. Tobey *et al.*, *Opt. Lett.* **32**, 286 (2007).
29. M. Bauer *et al.*, *Phys. Rev. Lett.* **8702**, 5501 (2001).
30. Z. Chang *et al.*, *Phys. Rev. A* **58**, R30 (1998).
31. P. Balcou, P. Salières, A. L'Huillier, M. Lewenstein, *Phys. Rev. A* **55**, 3204 (1997).

32. The authors gratefully acknowledge support for their research from NSF and the U.S. Department of Energy.

10.1126/science.1143679

Rapid Population Growth of a Critically Endangered Carnivore

M. B. Grenier,[1,2]* D. B. McDonald,[1] S. W. Buskirk[1]

Endangered species taken captive for breeding and then reintroduced to the wild commonly fail to produce self-sustaining populations (*1*). Such costly failures result from the persistence of the environmental factors that caused the species to become endangered, the effects of inbreeding in small populations, and the behavioral and physiological consequences of a captive environment. However, the first reintroduced population of the most endangered mammal species in North America, the black-footed ferret (*Mustela nigripes*), is recovering rapidly in the Shirley Basin of Wyoming after a lag that seemed to portend population extinction.

The population recovery is notable because the bottleneck of the 1980s reduced genetic variability (*2*) and captive breeding affected various phenotypic traits (*3*). Further, endangered vertebrates commonly exhibit slow life history strategies (*4*, *5*) producing low rates of population increase, unlike the 35% annual increase estimated by our matrix population model for the period 2003–2006. Remarkably, an even higher annual rate of increase (69% (r = 0.47), was estimated from an exponential fit to the minimum number alive for the period 2000–2006 (Fig. 1). Also, two potentially devastating infectious diseases, plague and canine distemper, occurred shortly after the releases. Notably, the primary prey at this site is the white-tailed prairie dog (*Cynomys leucurus*), which is considered suboptimal because it hibernates for extended periods and has low population densities (*5*).

The last known wild population of ferrets discovered in 1981 near Meeteetse, Wyoming formed the basis for the captive breeding program (*5*). From seven genetic founders in 1987, over 4800 juveniles have been produced, and many were reintroduced to sites in the ferret's historical range. Shirley Basin received 228 captive-born animals during 1991–1994 (Fig. 1). There, diseases triggered a decline; fewer than 25 ferrets were observed in 1996. By 1997, only five ferrets were found, and monitoring efforts were intermittent over the next 5 years, population extinction seemed imminent. In 2003, however, surveys revealed a surprising increase to 42 animals, and monitoring intensified. Three seasons of demographic data now permit a mark-recapture estimate of population size [N = 223, 95% confidence interval (CI) is 192 to 401] within the 8100-ha study area, which includes only about 14% of the contiguous prairie dog habitat.

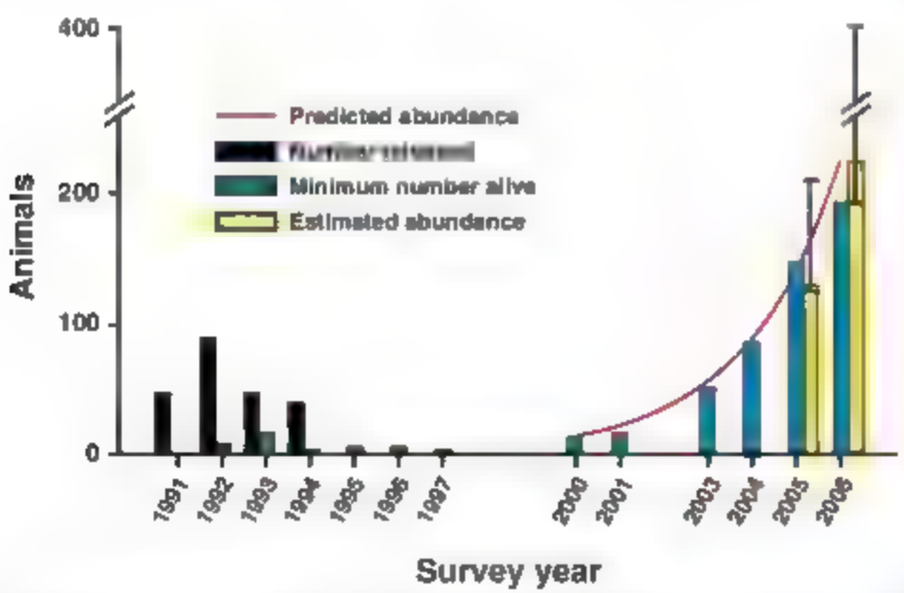

Fig. 1. Rapid population growth of black-footed ferrets in Shirley Basin, Wyoming, since 2000. Releases of captive-born animals ended in 1994, and abundance was so low by 1997 that monitoring was intermittent during 1998–2002 (no data for 1998–99 or 2002). Since 2003, more-intensive monitoring has revealed a rapidly growing population [223 animals in 2006 (95% CI 192 to 401)], which has expanded beyond the study area boundaries. The predicted abundance is exponential growth fitted to the minimum number alive (r = 0.47). The estimated population growth rate (λ), from our matrix population model, is 1.35.

The species' potential for rapid population growth seems to contradict the slow life history strategy common to endangered vertebrates: low fecundity, high longevity, and high age at first reproduction (*4*). A matrix population model (*6*) based on our estimates of vital rates (including birthrates, survival rates, and mortality rates) revealed unexpected attributes (*7*). Matrix-based elasticity analysis showed that success in the first year of life is the key to demographic success. Elasticities assess the impact on the population growth rate (λ) of proportional changes in the vital rates (*6*): for the black-footed ferret, more than half of the total elasticity is attributable to survival (e_{S1} = 0.27) and fertility (e_{1F} = 0.31) through the first year of life (fig. S1). Thus, early survival and recruitment are the crucial factors in this animal's life history, rather than the later adult survival that commonly matters to endangered species (*4*).

Black-footed ferrets have bred successfully in the wild for 7.5 (±3.8 SD) generations (fig. S1), largely obviating fears that inbreeding depression or captive propagation would impair population establishment or short-term persistence (*3*). Vulnerabilities to infectious diseases and potential declines of prairie dog populations remain serious concerns. We suggest, however, that management could include more opportunistic and widespread reintroduction attempts without short-term postrelease monitoring. Although some attempts may not yield immediate success, the Shirley Basin example shows that species recovery is possible, given the ferret's capacity to persist at low population levels and to increase rapidly in favorable environments.

References and Notes

1. B. Griffith, J. M. Scott, J. W. Carpenter, C. Reed, *Science* **245**, 477 (1989).
2. S. M. Wisely, S. W. Buskirk, M. A. Fleming, D. B. McDonald, E. A. Ostrander, *J. Hered.* **93**, 231 (2002).
3. S. M. Wisely *et al.*, *Anim. Conserv.* **8**, 321 (2005).
4. A. Purvis, J. L. Gittleman, G. Cowlishaw, G. M. Mace, *Proc. R. Soc. London Ser. B* **267**, 1947 (2000).
5. J. M. Lockhart, E. T. Thorne, D. R. Gober, in *Recovery of the Black-Footed Ferret: Progress and Continuing Challenges*, J. E. Roelle, B. J. Miller, J. L. Godbey, D. E. Biggins, Eds. (U.S. Geological Survey, Reston, VA, 2006), pp. 6–19.
6. H. Caswell, *Matrix Population Models* (Sinauer Associates, Sunderland, MA, 2001).
7. Materials and methods are available on *Science* Online.
8. We thank C. Martinez del Rio and M. Kaufman for helpful reviews. The project was supported by the Wyoming Game and Fish Department, the U.S. Fish and Wildlife Service, and private landowners.

Supporting Online Material

www.sciencemag.org/cgi/content/full/317/5839/779/DC1
Materials and Methods
Fig. S1
References

4 May 2007; accepted 19 June 2007
10.1126/science.1144648

[1]Department of Zoology and Physiology, University of Wyoming, 1000 East University Avenue, Laramie, WY 82071, USA. [2]Wyoming Game and Fish Department, 260 Buena Vista Drive, Lander, WY 82520, USA.
*To whom correspondence should be addressed. E-mail: martin.grenier@wgf.state.wy.us

Multifunctional Nanomechanical Systems via Tunably Coupled Piezoelectric Actuation

Sotiris C. Masmanidis,[1] Rassul B. Karabalin,[1] Iwijn De Vlaminck,[2] Gustaaf Borghs,[2] Mark R. Freeman,[3] Michael L. Roukes[1]*

Efficient actuation is crucial to obtaining optimal performance from nanoelectromechanical systems (NEMS). We employed epitaxial piezoelectric semiconductors to obtain efficient and fully integrated NEMS actuation, which is based on exploitation of the interaction between piezoelectric strain and built-in charge depletion. The underlying actuation mechanism in these depletion-mediated NEMS becomes important only for devices with dimensions approaching semiconductor depletion lengths. The induced actuation forces are controlled electrically, and resonant excitation approaching single-electron efficiency is demonstrated. The fundamental electromechanical coupling used can be programmed by heterostructure band engineering, externally controllable charge depletion, and crystallographic orientation. These attributes are combined to realize a prototype, mechanically based, exclusive-or logic element.

The dominant theme in nanoscale science presents new opportunities for realizing electromechanical transducers with ultralow power consumption, high sensitivity, integrated large-scale array architecture, and coupling to mesoscopic phenomena (*1*). As an advancement of microelectromechanical systems, which have become mainstream devices such as optical switches, ink jets, and accelerometers, nanoelectromechanical systems (NEMS) have shown great promise as highly sensitive detectors of mass (*2*, *3*), displacement (*4*), charge (*5*), and energy (*6*). However, as electromechanical devices are scaled downward, transduction becomes increasingly difficult, hampering efforts to create finely controlled integrated systems. In spite of substantial progress in the field (*7*), an efficient, integrated, and customizable technique for actively driving and tuning NEMS resonators has remained elusive. Conventional approaches such as magnetomotive, electrostatic, and electrothermal techniques (*7*, *8*) suffer from either low power efficiency, limited potential for integration, or poor nanoscale control over electromechanical coupling. In contrast, one of the earliest and most straightforward actuation methods, based on the piezoelectric effect, provides a means of directly converting an electric field into mechanical strain. Discovered by the Curie brothers in 1880 (*9*), it has since been widely applied in a multitude of systems ranging from clocks to microwave electromechanical filters and biosensors. However, new nanoscale functionality enabled by piezoelectric coupling has not yet been systematically explored with top-down NEMS devices.

We investigated the use of piezoelectric semiconductors as active structural materials for NEMS resonators. The active region of our nanomechanical devices consists of a 200-nm-thick epitaxially grown GaAs p-type intrinsic n-type (pin) diode (*10*). The clamped ends of the suspended structures lie on top of a sacrificial $Al_{0.8}Ga_{0.2}As$ layer, which is doped along with the substrate to allow the back side of the wafer to be used as a ground electrode. An n-doped layer serves as the top electrode, and finally, the charge-depleted high-resistance region in the middle forms the piezoelectrically active layer. Details on the pin junction doping profile and device fabrication are presented in (*11*). We first focused on NEMS cantilevers, as depicted in Fig. 1A, which we used to gauge the efficiency of piezoelectric excitation. To ensure that the mechanical readout scheme was decoupled from charge-depletion effects, we employed optical interferometry (*12*) to sense motion so that unnecessary complications were not introduced into our analysis. During a typical measurement (Fig. 1B), an ac signal applied across the pin junction actuates the device at or near its resonance frequency, while the addition of dc voltage tunes the depletion-region width. Within the device, a transverse electric field, E_z, produces a longitudinal strain $e_y = d_{31}E_z$, where d_{31} is the anisotropic piezoelectric coefficient (*13*). A bending moment develops when the strain is asymmetrically distributed around the beam's neutral axis, which results in mechanical resonance under a suitable range of driving frequencies. The particular cantilever shown in Fig. 1 is found to have a resonance frequency of 8 MHz and a quality factor (Q) of 2700 (Fig. 1C). Our measurements are in agreement with the expected value for this structure's first out-of-plane vibrational mode. The piezoelectric effect is capable of driving the device with ac signals as low as 5 μV before the onset of thermomechanical fluctuations (Fig. 1C, inset), corresponding to approximately a single electronic charge on the cantilever itself. Assuming a maximum current flow of 1 nA at 5 μV of ac drive (*14*), the minimum required power consumption of this device approaches 5 fW, with ~1 nW being more representative of typical operating conditions (an ac drive of 10 mV) during actuation. Further improvement is expected from semiconductor band-structure optimization.

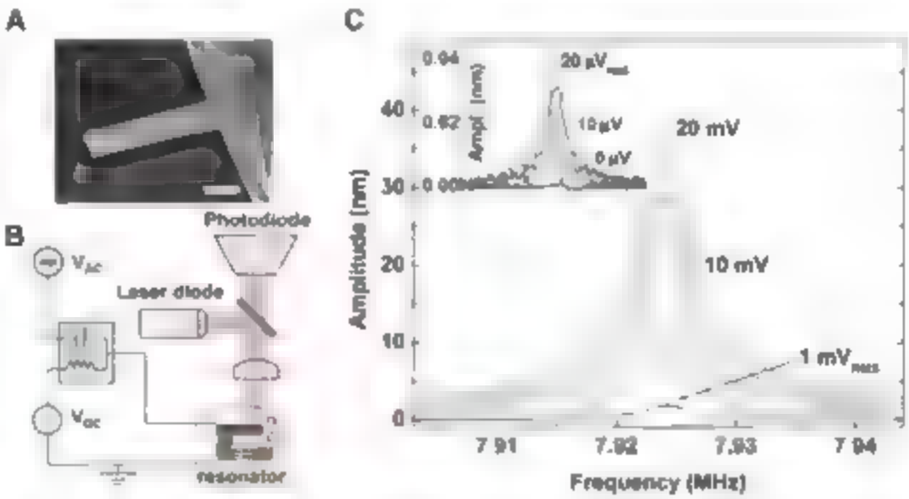

Fig. 1. Nanomechanical piezoelectric actuation. (**A**) GaAs cantilever with embedded pin diode structure. The dimensions are: length, 4 μm; width, 0.8 μm; and thickness, 0.2 μm. Scale bar, 1 μm. (**B**) Measurement setup. The bias T allows both dc and ac signals to be applied. All measurements were performed at room temperature and a pressure of 5 millitorr. (**C**) Frequency response around the resonance of a diode-embedded cantilever (pin 1) under 0 dc bias. Each line corresponds to a different amplitude ac driving signal across the diode junction. (Inset) Response to drive signals of a few microvolts. (Each line, in order of increasing amplitude, corresponds to the addition of 5 μV.) The black line labeled "0 μV" corresponds to thermomechanical noise at a 10-Hz bandwidth and sets a lower limit on the ac driving signal that is required to generate an observable response. RMS, root mean squared.

[1]Kavli Nanoscience Institute, California Institute of Technology, Pasadena, CA 91125, USA. [2]IMEC, Kapeldreef 75, B-3001 Leuven, Belgium. [3]Department of Physics, University of Alberta, and National Institute for Nanotechnology, Edmonton, Alberta, Canada.

*To whom correspondence should be addressed. E-mail: roukes@caltech.edu

These measurements demonstrate the efficiency of this integrated excitation technique, both in terms of charge and of power required. For comparison, magnetomotive and electrothermal NEMS actuation schemes are not easily realizable with comparable power efficiency, because their comparatively low impedance results in substantial current flow. Moreover, many alternative actuation schemes rely on external electromagnetic fields mediated by gates (electrostatic), solenoids (magnetomotive), or lasers (optothermal); hence, they are not readily incorporated into the active vibrating structure of a nanoscale device.

The strain generated by an electric field is concentrated within the highly resistive charge-depletion region. This allows us to adjust the piezoelectric actuation efficiency by altering the depletion width with an applied voltage, in much the same way as capacitance is systematically altered in varactor diodes. This actuation effect, however, is unique to nanoscale semiconductor structures, where the characteristic device length scale (i.e., the thickness of the pin heterostructure) can become comparable to the depletion width. To verify this form of electromechanical coupling, we measured the performance of the cantilever under different dc bias conditions (Fig. 2A). As expected, the mechanical amplitude of the device's response strongly depends on the dc voltage. We developed a simple analytical model that combines two competing mechanisms that control actuation (*11*): (i) depletion-mediated strain (Fig. 2B and fig. S1) and (ii) variable resistance of the pin diode junction (fig. S2). Because strain is proportional to the voltage across the junction, lowering the resistance via excessive forward or reverse biasing of the diode leads to a reduction of actuation efficiency. However, this effect is not evident as long as the diode bias value lies below its "on" state and above breakdown, which are respectively determined to be ~0.7 and −3 V. To validate our predictions, we fabricated identical cantilevers from three pin diode junctions and measured their resonance amplitudes as a function of dc voltage. The diodes' doping profiles were designed to demonstrate three qualitatively different effects of depletion-mediated strain on actuation: (i) increasing resonance amplitude under decreasing voltage (pin-1), (ii) constant amplitude (pin-2), and (iii) decreasing amplitude (pin-3). We found good agreement between the observed and predicted mechanical response of these devices (Fig. 2C).

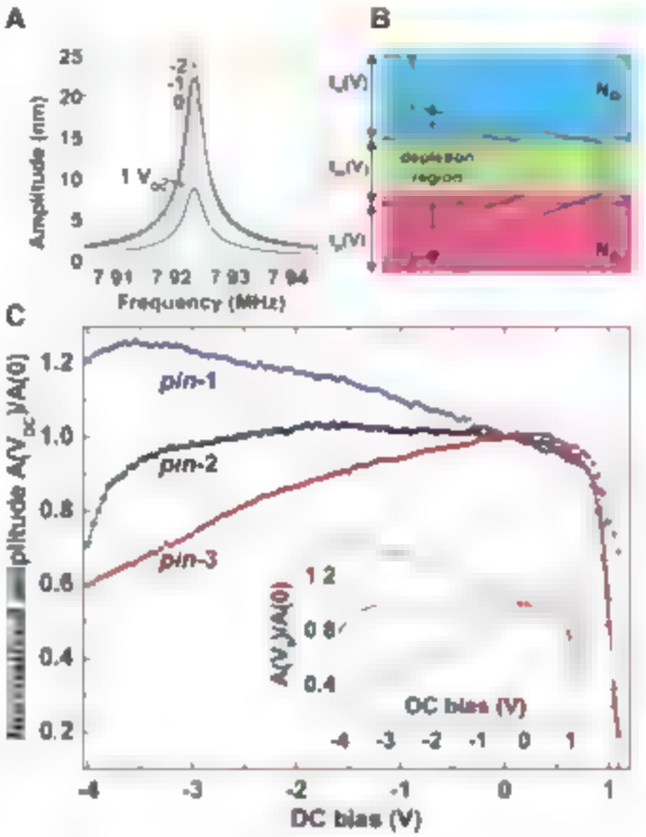

Fig. 2. Voltage-tunable depletion-mediated strain manifests itself as a change in actuation efficiency. (**A**) Frequency response of the same device as in Fig. 1, but with a fixed ac drive (10 mV) and a different dc bias. (**B**) Model electric-field distribution in a stereotypical pin junction. The colored lines correspond to the field under increasing applied voltage. The field lines are skewed toward the lower-doped side (in this case, the pink p-type layer), resulting in a different piezoelectric strain distribution that alters the actuation efficiency. (**C**) Normalized resonance amplitude versus dc bias voltage for three different pin diodes embedded in identically shaped cantilevers. For ease of comparison, the response of each device was normalized to its own amplitude at 0 dc volts. The ac driving signal was fixed at 10 mV. (Inset) Predicted behavior of the diodes (*11*).

Another remarkable feature of NEMS fabricated from piezoelectric materials is voltage-induced resonance-frequency control. To demonstrate this, we patterned doubly clamped beams such as those shown in Fig. 3A. These structures are driven to resonance in the same fashion as are cantilevers. Shifts in resonance are clearly observed upon the de-biasing of the device (Fig. 3B), because piezoelectric strain is converted into stress as a result of clamped-clamped boundary conditions (*15*). In the case of small perturbations, this behavior can be quantitatively described by the following expression (*16*)

$$\Delta f = \sqrt{3}\, t\rho\, d_{31} E' / (2\pi l^2) \qquad (1)$$

The elastic Young's modulus E is 101 GPa, the density ρ is 5.3 g/cm^3, t is the total device thickness (200 nm), Δf is the change in frequency, and l is the voltage. The above expression implies linear frequency-voltage dependence. In addition, because of the anisotropic nature of the piezoelectric coefficient, we expect to be able to control the slope of Δf by fabricating the beam along a prescribed direction. Both predictions are verified by the measurements displayed in Fig. 3C. The equal and opposite tuning slope of devices aligned along the [110] and [−110] direc-

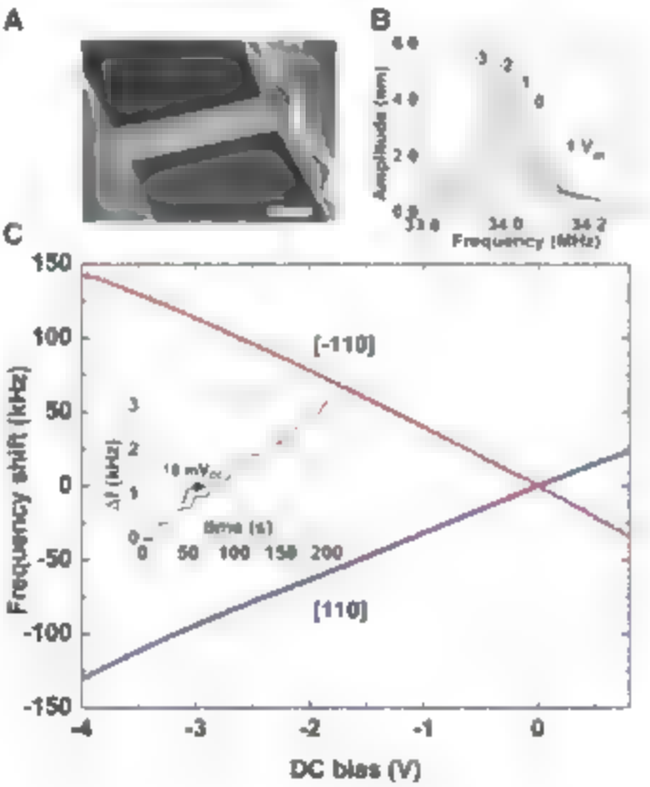

Fig. 3. Piezoelectric resonance-frequency control. (**A**) Doubly clamped beam structure with the same dimensions as in Fig. 1A. Scale bar, 1 μm. (**B**) Frequency response near the beam's fundamental out-of-plane resonance mode. Each line corresponds to a different dc bias applied across the diode junction. The ac driving amplitude is fixed at 70 mV. (**C**) Phase-locked–loop measurements of resonance-frequency shift as a function of voltage. The blue and red lines correspond to beams fabricated along the [110] and [−110] crystallographic directions, respectively. Their slopes have opposite signs because of piezoelectric anisotropy. (Inset) Time-dependent frequency shift under the stepwise addition of 10 mV. About 500 electronic charges were added to the beam at each step.

tions is characteristic of the opposite sign of d_{31} along these directions. Fitting the slope of the steepest line to Eq. 1 yields a value of d_{31} = 1.33 pm/V, in excellent agreement with the accepted measured value along the [110] direction (*13*). Because stresses in cantilevers can relax by expanding or contracting, their frequency tunability is substantially lower than that of beams, as is evident by comparing Figs. 2A and 3B. The combination of integration, linearity, voltage efficiency, and crystallographic anisotropy of piezoelectric frequency tuning presents an advantage over other tuning mechanisms that rely on electrostatic force (*5*) or thermal stress (*17*). Devices that may benefit from the added functionality include parametric amplifiers (*18*), intrinsically cooled nanomechanical resonators (*19*), and voltage-controlled mechanical oscillators in frequency standards or sensing applications.

As a further example of the potential application of voltage-dependent frequency tuning, we demonstrated piezoelectric nanomechanical charge sensing. The inset of Fig. 3C shows the time progression of frequency during stepwise 0-mV increases in DC bias. Each step corresponds to the addition of ~2 kV/cm of field across the depletion region or ~500 electronic charges on the resonant device (*20*). The highest achievable resolution at room temperature is ~100 electrons, and it may be possible to approach single-electron resolution by using enhanced readout techniques, an optimized quality factor, and higher aspect-ratio beams (*21*). This suggests that, unlike other NEMS resonator sensors, which typically measure only mass accretion, tunable piezoelectric transducers could also serve as detectors of ionic species, making them attractive candidates for mass spectrometry applications (*3*).

Our ability to finely control the mechanical response of NEMS devices in a variety of ways raises the intriguing possibility of creating elements for nanomechanical logic and computation. It is worth recalling that some of the earliest computers were mechanical, and interest in this concept has resurfaced with the advent of nonvolatile carbon-nanotube memory elements (*22*). As an initial implementation of piezoelectric NEMS logic, we took advantage of the crystallographic anisotropy of d_{31}. The prototype device (pictured in Fig. 4A) consists of an L-shaped cantilever with two separately addressable inputs for actuation. The top conducting portion of the structure was removed at the tip, resulting in a pair of mechanically bound but electrically isolated actuators. When driven from only input A or B, the entire structure resonates with a fundamental frequency of 10 MHz and a Q of 2000 (Fig. 4B). Because the two halves of the structure are aligned along crystallographically orthogonal directions, we observed that a stimulus at input A results in an equal-magnitude but opposite-phase mechanical response as the same stimulus applied at input B (Fig. 4, B (inset) and C) (*23*). Thus, when the a driving stimulus of the same magnitude was simultaneously applied to both inputs through a 0-degree power splitter, the response of the device was found to be substantially attenuated, as one would expect from a cancellation of motion. This device represents a prototype radio-frequency nanomechanical analog to an exclusive-or (XOR) logic gate with a demonstrated on/off ratio of 8:1. We envision the integration of NEMS logic in large-scale arrays that could carry out preliminary computations in the electromechanical domain before conventional digital processing (*24*). Potential advantages of this approach include lower net power consumption and greater functionality in computation.

We have demonstrated an approach to designing nanoelectromechanical systems from piezoelectric semiconductors with tailored band structure, geometry, and crystallographic direction. The resulting electromechanical coupling phenomena, which rely entirely on intrinsic material properties, facilitate the creation of compact, tunable NEMS arrays for multidimensional sensing (*25*) and nanomechanical computing applications (*24*). The ability to regulate actuation efficiency through depletion-mediated strain in the semiconductor heterostructure's low operating-power regime raises the prospect for developing efficient, high-speed electromechanical switches. Such devices may play an important role in selectively addressing individual elements in large-scale arrays of NEMS. Furthermore, the integration of a reliable and customizable frequency-tuning method adds a useful layer of functionality that has so far been absent in NEMS. Although not explored here, the reversibility of piezoelectric phenomena offers the potential for ultrasensitive electrical measurement of nanomechanical motion (*26*–*29*). Finally, all of the concepts presented here are transferrable to a wide variety of other materials beyond GaAs (such as AlN, SiC, or ZnO), which may provide enhanced electrical and mechanical properties.

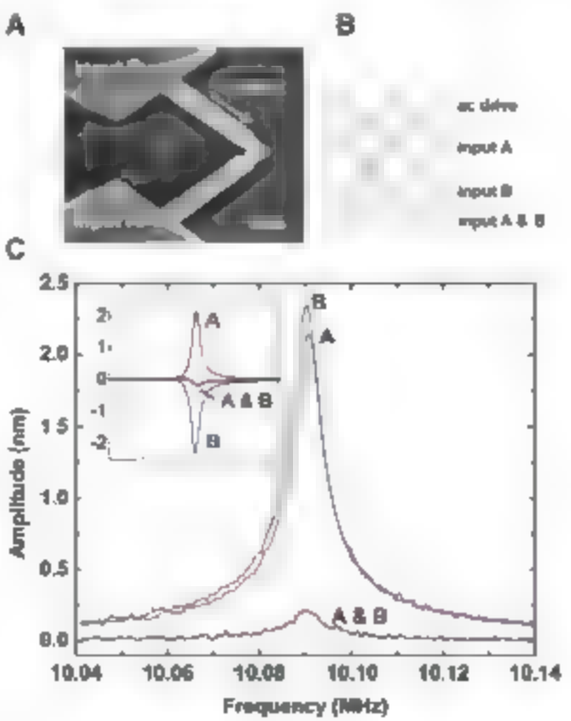

Fig. 4. Radio-frequency nanoelectromechanical analog of an XOR logic gate. (**A**) L-shaped cantilever with electrically isolated but mechanically connected inputs. Scale bar, 1 μm. (**B**) Measured frequency response to a 5-mV ac driving signal applied to the inputs: A not B, red; B not A, blue; and A and B, black (Inset) The real component of the response signal, indicating the 180° phase shift between the response due to driving at input A and that due to driving at input B. (**C**) Schematic illustration of the mechanical XOR logic gate's operational principle, exploiting piezoelectric anisotropy. When an ac drive was applied across only one of the inputs, the device responded with equal mechanical amplitude but opposite phase (the "on" state). This resulted in an effective cancelation of motion ("off" state) when the drive was simultaneously applied to the two inputs.

References and Notes

1. M. L. Roukes, *Phys. World* **14**, 25 (2001).
2. J. Fritz *et al.*, *Science* **288**, 316 (2000).
3. Y. T. Yang, C. Callegari, X. L. Feng, K. L. Ekinci, M. L. Roukes, *Nano Lett.* **6**, 583 (2006).
4. M. D. LaHaye, O. Buu, B. Camarota, K. C. Schwab, *Science* **304**, 74 (2004).
5. A. N. Cleland, M. L. Roukes, *Nature* **392**, 160 (1998).
6. W. C. Fon, K. C. Schwab, J. M. Worlock, M. L. Roukes, *Nano Lett.* **5**, 1968 (2005).
7. K. L. Ekinci, *Small* **1**, 786 (2005).
8. I. Bargatin, I. Kozinsky, M. L. Roukes, *Appl. Phys. Lett.* **90**, 093116 (2007).
9. P. Curie, J. Curie, *Bull. Soc. Minéral. Fr.* **3**, 90 (1880).
10. Pin diode junctions were used because of their high electrical resistance, which is required for efficient actuation, and convenience in modeling voltage-dependent charge-depletion effects.
11. Materials and methods are available as supporting material on *Science* Online.
12. D. W. Carr, H. G. Craighead, *J. Vac. Sci. Technol.* **B15**, 2760 (1997).
13. K. Focke, *J. Appl. Phys.* **70**, 914 (1991).
14. The actual measured current in the low-bias regime was typically between 0.001 and 1 μA per 20 mV, which would lead to an even lower estimate of power consumption.
15. B. Piekarski, D. DeVoe, M. Dubey, R. Kaul, J. Conrad, *Sens. Actuat. A* **91**, 313 (2001).
16. S. Timoshenko, D. H. Young, W. Weaver *Vibration Problems in Engineering* (Wiley, New York, ed. 4, 1974).
17. S. C. Jun *et al.*, *Nanotechnology* **17**, 1506 (2006).
18. D. Rugar, P. Grütter *Phys. Rev. Lett.* **67**, 699 (1991).
19. C. H. Metzger, K. Karrai, *Nature* **432**, 1002 (2004).
20. It is important to distinguish the total induced charge, which is dominated by the parasitic capacitance of the gold-wire–bond contact pads (and is much greater than 500 electronic charges per 20 mV of bias), from the charge on the NEMS device. The phase-locked–loop sampling rate was set to 10 Hz.
21. One would ideally like to make devices as thin as possible to maximize charge sensitivity (see Eq. 1). However, surface-depletion effects in GaAs place practical constraints on this dimension.
22. T. Rueckes *et al.*, *Science* **289**, 94 (2000).
23. The small disparity between the response to a drive at input A and the response to input B is believed to be due

to symmetry-breaking device inhomogeneities introduced during fabrication.
24. M. L. Roukes, *Electron Devices Meeting, 2000. IEDM Technical Digest. IEEE International* (Institute of Electrical and Electronics Engineers, Piscataway, NJ, 2000) pp. 539–542.
25. M. C. Lonergan *et al.*, *Chem. Mater.* **8**, 2298 (1996).
26. D. Devoe, *Sens. Actuat. A* **88**, 263 (2001).
27. R. G. Beck, M. A. Eriksson, R. M. Westervelt, K. L. Campman, A. C. Gossard, *Appl. Phys. Lett.* **68**, 3763 (1996).
28. Y. Zhang, M. P. Blencowe, *J. Appl. Phys.* **92**, 7550 (2002).
29. K. Knobel, A. N. Cleland, *Appl. Phys. Lett.* **81**, 2258 (2002).
30. This work was supported by the Defense Advanced Research Projects Agency Microsystems Technology Office Micro Gas Analyzer through Department of Interior contract no. NBCH1050001. We thank W. van de Graaf and S. Degroote for the epitaxial crystal deposition and P. Van Dorpe and J. M. Choi for discussions.

Supporting Online Material

www.sciencemag.org/cgi/content/full/317/5839/780/DC1
Materials and Methods
SOM Text
Figs. S1 and S2
References

8 May 2007; accepted 6 July 2007
10.1126/science.1144793

Label-Free, Single-Molecule Detection with Optical Microcavities

Andrea M. Armani,[1] Rajan P. Kulkarni,[2] Scott E. Fraser,[1,2]* Richard C. Flagan,[3]* Kerry J. Vahala[1]

Current single-molecule detection techniques require labeling the target molecule. We report a highly specific and sensitive optical sensor based on an ultrahigh quality (*Q*) factor ($Q > 10^8$) whispering-gallery microcavity. The silica surface is functionalized to bind the target molecule; binding is detected by a resonant wavelength shift. Single-molecule detection is confirmed by observation of single-molecule binding events that shift the resonant frequency, as well as by the statistics for these shifts over many binding events. These shifts result from a thermo-optic mechanism. Additionally, label-free, single-molecule detection of interleukin-2 was demonstrated in serum. These experiments demonstrate a dynamic range of 10^{12} in concentration, establishing the microcavity as a sensitive and versatile detector.

Single-molecule fluorescence experiments have improved our understanding of many fundamental biological processes, such as protein folding kinetics (*1*), molecular transport (*2*, *3*), and aspects of DNA replication (*4*). However, all of these breakthrough experiments required labeling of the target molecules (*5*, *6*). In the case of surface-enhanced Raman spectroscopy (SERS), total internal reflection fluorescence microscopy (TIRF) and confocal microscopy, this label behaves as an amplifier for an otherwise undetectable single-molecule signal; however, it also restricts an experiment's scope, because there must be prior knowledge of the target's presence and the target molecule must be modified to incorporate the label (*7*–*12*). There have been several attempts to overcome this need to label the analyte by developing label-free sensing technologies, ranging from fiber-optic waveguides (*13*) and nanowires (*14*) to nanoparticle probes (*15*), biochips (*16*), and mechanical cantilevers (*17*), but none has achieved single-molecule sensitivity.

Optical microcavities have been proposed as a powerful method to achieve label-free detection of single molecules because the resonant recirculation of light within a microcavity allows the light to sample target molecules many more times (*18*–*21*). For example, in a simple optical waveguide sensor, the input light has only one opportunity to interact with the target molecule. In contrast, by using a planar microcavity with a quality (*Q*) factor of 10^6 (Fig. 1A), the molecule is sampled more than 100,000 times. This increased sampling manifests itself both as a shift of the resonant wavelength and as a decrease in the *Q* factor as the target molecules directly change the optical path length and or the cavity loss of the sensor (*18*, *19*). The current work extends these ideas by adding a new mechanism through which molecules can induce a resonant wavelength shift. In particular, it will be shown that a thermo-optic mechanism greatly enhances detection sensitivity. Biochemically functionalizing the surface of the resonator to recognize the target molecule should provide an excellent platform for ultrasensitive detection and specific identification of dissolved, unlabeled target molecules (*22*, *23*).

We fabricated planar arrays of silica microtoroid whispering-gallery resonators (Fig. 1A) using a simple three-step process: (i) circular oxide pads were lithographically defined, (ii) the silicon wafer was selectively etched with xenon difluoride, forming arrays of silica microdisks, and (iii) the microdisks were reflowed with a CO_2 laser (*24*, *25*). Microtoroids offer *Q* factors in excess of 100 million for enhanced detection sensitivity, and their silica surfaces are readily functionalized for specific detection of biomolecules (*23*). The microtoroids were coupled to a tunable laser and detector by a tapered optical fiber waveguide and were immersed in water with a microaquarium with syringe inlets for introducing samples (*26*). The tapered optical fiber waveguide handles light into the whispering-gallery mode at the periphery of the microtoroid. The resonant whispering-gallery mode is partially confined inside the silica microtoroid, but it evanesces into the liquid environment (Fig. 1B). Thus, the light interacts strongly with the molecules once they are captured on the toroidal surface, in a manner similar to the way that a surface plasmon resonance (SPR) sensor interrogates a sample (*27*). The silica surfaces were sensitized either with biotin or antibodies to capture specific molecules, avidin or the target antigen, respectively (*26*)]. This binding interaction creates red shifts of the resonant wavelength that can be monitored in real time (*26*). In the static condition without the presence of biological molecules, the opposing thermo-optic

Fig. 1. The microtoroid resonator biological sensor. (**A**) A scanning electron micrograph (SEM) image of the UHQ microtoroid optical resonator. The silica microtoroid is fabricated on a silicon wafer using planar lithography and reflowed using a CO_2 laser. The typical microtoroid diameter used in this work was 80 μm. (**B**) A finite element mode [FEMLAB (COMSOL, Burlington, Massachusetts, USA)] of a 4-μm minor diameter microtoroid resonator immersed in water. Although the majority of the optical field resides in the silica toroid, a portion of the field evanesces into the environment (indicated by a white arrow). The interaction of the whispering-gallery mode with the environment, specifically molecules bound on the surface of the toroid, enables the ultrasensitive detection.

[1]Department of Applied Physics, MC 128-95, California Institute of Technology, Pasadena, CA 91125, USA. [2]Division of Biology, MC 139-74, California Institute of Technology, Pasadena, CA 91125, USA. [3]Division of Chemistry and Chemical Engineering, MC 210-41, California Institute of Technology, Pasadena, CA 91125, USA.
*To whom correspondence should be addressed. E-mail: sefraser@caltech.edu (S.E.F.); flagan@caltech.edu (R.C.F.)

effects of water and of silica balance to stabilize the conventional thermally induced shift (26).

The working range of this device was determined with interleukin-2 (IL-2), a cytokine released in response to immune system activation to extrinsic and intrinsic stimuli. Concentrations ranging from 1×10^{-19} M to 1×10^{-6} M were controllably flowed past the microtoroid resonator using a syringe pump (26). For IL-2, the highest sensitivity occurred in the lower concentration range. The dose-response curve (Fig. 2) is sigmoidal, as would be expected from antibody-antigen binding if there were a finite number of binding sites. An easily detectable response was obtained at 5×10^{-18} M, with greater than 10:1 signal-to-noise ratio (Fig. 2, inset A). With increasing concentration, the responsivity diminished; however, wavelength shifts were detectable for concentrations as large as 10^{-6} M (Fig. 2, inset B). This working range is a 12-decade concentration range (10^{12}). This can be compared with that for other label-free room-temperature detection techniques, such as nanowire sensors (10^{3}) (28) and microcantilevers (10^{3}) (29) and is comparable to or greater than fluorescent or luminescent assays such as chemiluminescence (30).

For the lowest concentrations where shifts are observed, small numbers of molecules would be expected to interact with the toroid, which suggests that the sensor might accomplish label-free single-molecule detection. To investigate this regime further, a data acquisition system was used to measure resonant wavelength versus time at fixed concentrations and flow rates. Figure 3A shows shift responses versus time at three concentrations of IL-2 (26). By optimizing solution concentration, solution injection rate, and data acquisition rate, shifts caused by individual molecules binding to the surface of the toroid were resolved. We observed stepwise shifts, and their frequency scaled linearly with concentration. Using raw data like that presented in Fig. 3A, we plotted a histogram of the distribution of shifts over a given period of time for several concentrations of IL-2 (bin size is 0.001 pm) (Fig. 3C). In each case, the histogram has a maximum shift value that is independent of the concentration. This behavior is expected because wavelength shifts will depend on the strength of interaction between the bound molecule and whispering-gallery optical mode. The interaction will be strongest for binding at the equatorial plane and diminish rapidly as molecules bind even a few micrometers offset from this plane. Hence, these histogram plots are consistent with somewhat uniform binding of molecules over the toroid surface, thereby creating a distribution of shifts with a maximum given by molecules at the equatorial plane (26).

To further verify the single-molecule nature of these binding events, the statistics in time were studied in (26) and confirmed a Poissonian behavior for binding events. A single-molecule photo-bleaching experiment was also designed using a Cy5-labeled antibody (31). The experimental details and the results demonstrating single-molecule bleaching using the toroid as the excitation source are contained in (26).

The single-molecule shifts observed here are large based on previously proposed detection mechanisms (18, 19). However, at the fundamental level, these theories assume that biological molecules have only a direct effect on either optical path length or Q factor by way of their complex polarizability. In such cases, it is straightforward to show that sensitivity scales linearly with microcavity Q factor and that wavelength shifts produced by single-molecule binding events are several orders of magnitude too small to explain the current observations. We propose instead, and verify through a series of measurements, a mechanism of detection that attains a greatly enhanced sensitivity by leveraging the high Q factor of the silica microtoroid twice (i.e., quadratic dependence of sensitivity with Q factor). This mechanism, not previously considered in a microresonator sensor, results when the high circulating intensities within the resonator locally heat molecules attached to the whispering gallery. This temperature increase results in a red shift of the resonant wavelength through the thermo-optic effect, when the whispering-gallery material itself (in this case, silica) is heated by the molecule. Contrasting this mechanism with the conventional method of microcavity detection based on directly induced changes in optical path length of the whispering-gallery resonant mode shows that the optical path length in the present case is varied indirectly and in proportion to the intensity-induced heating of the molecule. This mechanism therefore receives a double benefit (i.e., quadratic) from the ultrahigh Q factor (UHQ): first, from the narrow linewidth (i.e., improved resolution in measuring shifts), and second, from an increase in the intrinsic shift by way of the thermo-optic effect.

The expected thermo-optic wavelength shift is straightforward to predict. Beginning with the wave equation and adding a perturbing thermal contribution to the susceptibility, the theoretical wavelength shift produced by a single molecule (bound at the intensity maximum) by the thermo-optic mechanism can be shown to be given by (32):

$$\left(\frac{\delta\lambda}{\lambda}\right)_{TO} = \frac{\sigma}{\kappa}\frac{\lambda^{2} n_{eff}}{8\pi^{2} n^{2} \kappa_{t}} QP \int \frac{|\psi(r)|^{2}}{r^{3} + r_{p}^{3}} dr \qquad (1)$$

where λ is the wavelength, σ is the absorption cross section of the molecule, dn/dT is the optothermal constant of silica (1.3×10^{-5} K^{-1}), κ is thermal conductivity, n is the effective refractive index of the silica toroid, V is the optical mode volume, Q is cavity Q factor, and P is the coupled optical power. The integral in this expression accounts for the spatial overlap of the whispering-gallery mode field $|\psi(r)|$, with the temperature profile created by the nearly pointlike molecular heat source. The parameter r_p is on the order of the physical radius of the molecule (33) and, as shown below, has a negligible role in determining the magnitude of predicted shifts. As noted above, the strength of the thermo-optic effect depends on the circulating intensity within the toroidal whispering gallery, as evident in Eq. 1 by the dependence of the resonance shift on the coupled optical power, cavity Q, and modal volume.

Using this expression, we can establish the absorption cross section required to create a shift equal to one-cavity linewidth (34),

$$\sigma_{1} = \frac{1}{Q^{2} P} \frac{8\pi^{2} n_{eff}^{2} \kappa_{t} \lambda}{dn/dT} \left[\int \frac{|\psi(r)|^{2}}{r^{3} + r_{p}^{3}} dr \right]^{-1} \qquad (2)$$

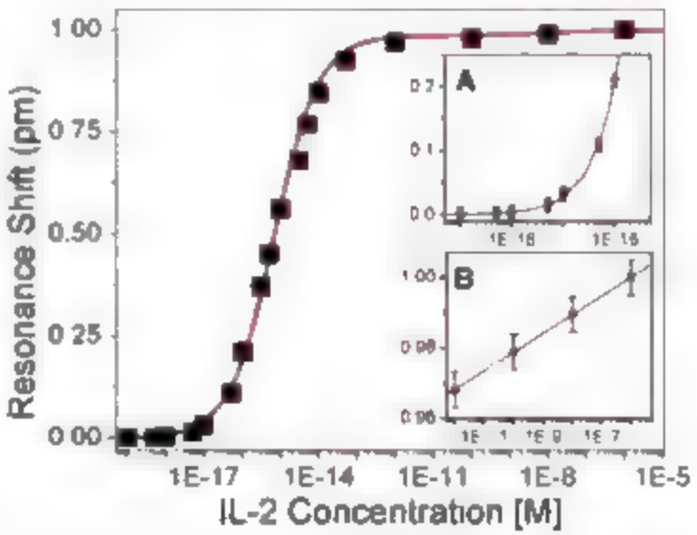

Fig. 2. The working range and dose response of the microtoroid sensor was investigated using a series of IL-2 solutions ranging from 10^{-19} M to 10^{-6} M. The Q of the cavity used in this study was 1.83×10^{8}. This response is sigmoidal, as would be expected from antibody-antigen binding if there were a finite number of binding sites. The first reliable signal was obtained at 5×10^{-18} M. The total working range of the sensor is from 5 aM (5×10^{-18}) to 1 μM (1×10^{-6}); the response of the sensor is not linear over this entire concentration range. The error bars are smaller than the symbols in the main graph and are shown in the insets. (**A**) Enlarged view of the low concentration response. The first concentration that has a detectable response is 5 aM. The error in this data is ± 0.005 pm. (**B**) Enlarged view of the higher concentration response (after considerable site saturation has occurred). The error in this data is ± 0.005 pm.

This figure of merit illustrates how the sensitivity benefits quadratically from the cavity Q factor. As an example, for a cavity Q factor of 250 million, a coupled power of 1 mW, a molecular radius in the range of 3 to 50 nm (*34*), a wavelength of 680 nm, a toroid of diameter 80 μm, and the optical and thermal constants of silica, σ_I is between 1.1×10^{-17} cm^2 and 1.5×10^{-17} cm^2. This value is well below the values for many biomolecules and does not represent a fundamental limit of detection because, in principle, detection of sub-linewidth shifts is possible provided that the signal-to-noise ratio is adequate (*34*). Conversely, if a cross section of 2×10^{-16} cm^2 is assumed (typical of several molecules used in this study), then a single-molecule wavelength shift of between 50 and 33 fm is predicted, which is easily detected for a UHQ microcavity. We note that the thermo-optic mechanism is not limited to UHQ silica resonant cavities and can be generalized to other lower-Q resonant cavities, provided that power levels are substantially boosted to overcome the reduced Q.

We verified the proposed thermo-optic detection mechanism and investigated its universality by performing a series of single-molecule detection experiments using molecules of varying absorption cross sections, ranging from 10^{-16} to 10^{-13} cm^2 at low concentrations (*35*). The dependence of the resonant shift on Q was verified by using cavities with Q factors of either $\sim 1 \times 10^8$ or $\sim 2 \times 10^8$ (*26*). The lowest cross section molecules used were the IL-2 antigen (Fig. 3), protein G, and streptavidin. Two different polyclonal antibodies were also used and served as intermediate absorption cross section molecules. Two high cross section fluorescent dye molecules were also used: Cy5-labeled antibody (fluorescent dye) and QSY-21 (a quencher molecule designed to absorb light like a fluorescent dye but not to re-emit photons) to provide further cross-sectional dynamic range in the test. If we assume that the largest shift in the histogram corresponds to the case of a single-molecule binding event at the region of highest intensity (i.e., the equatorial plane of the whispering gallery), this maximum shift can be plotted versus the molecular cross sections to verify Eq. 1.

Figure 4 summarizes the theoretical predictions and experimental results by plotting the

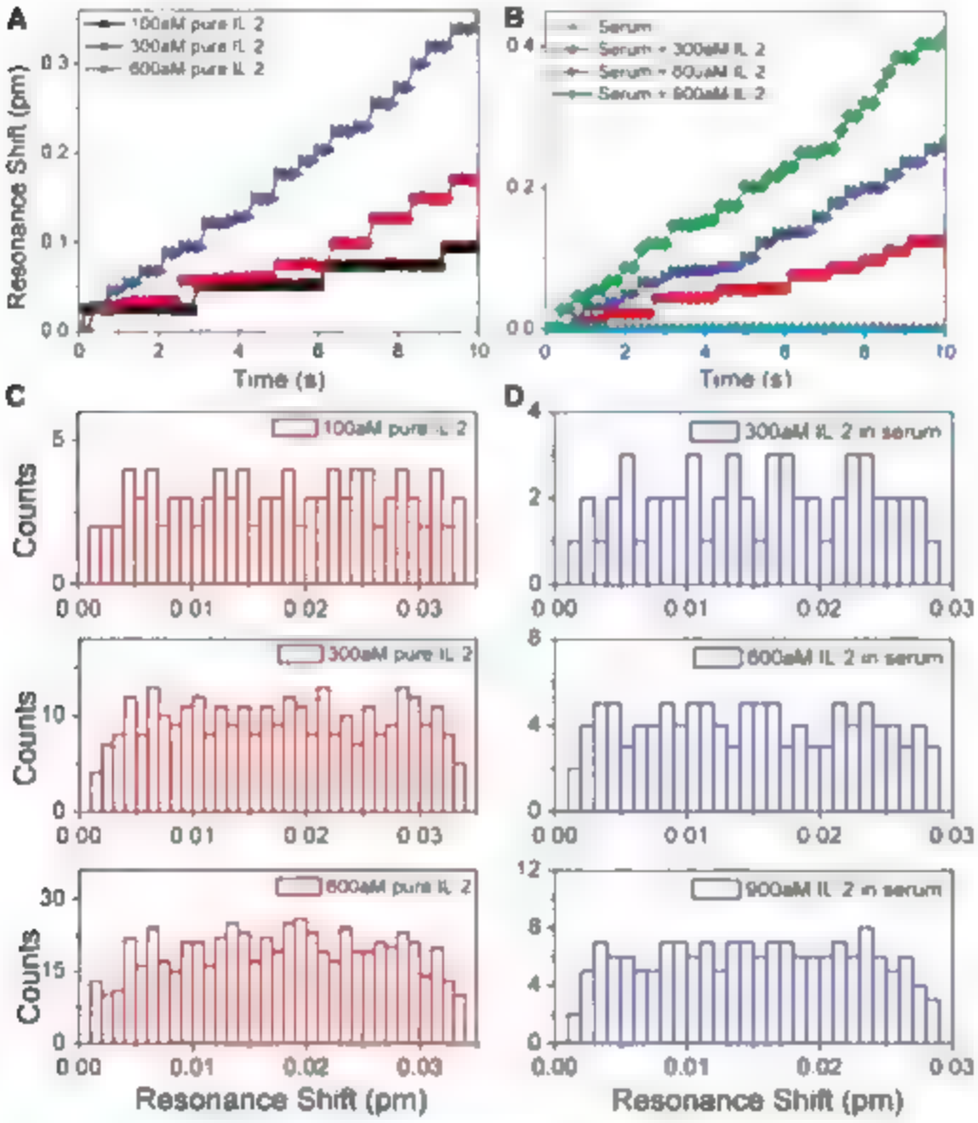

Fig. 3. (**A**) The position of the resonance wavelength as a function of time at three different interleukin-2 concentrations. As molecules bind to the surface, the resonant wavelength position jumps, creating the steps seen. When the concentration is increased, the general slope of the trace increased because the binding rate increased. It is important to note that discrete binding events can be resolved at this data acquisition rate. (**B**) The position of the resonance wavelength as a function of time at three different IL-2 concentrations in fetal bovine serum. Also shown is the case of pure serum. As molecules bind to the surface, the resonant wavelength position shifted, creating the steps seen. Similar to the data shown in (A), the slope is related to the concentration, and individual events are resolved. (**C**) A series of histograms formed from steps like those in (A), showing the relation between total resonant wavelength shift and number of molecules that bound to the surface of the toroid. As the concentration increased, the number of binding events increased; however, the largest shift remained constant. This shift is a result of molecules binding at the highest intensity region on the surface of the toroid. The largest shift achieved agrees very well with the expected shift from the thermo-optic theory based on the Q factor of the microcavity used in this experiment (1.20×10^8). This histogram is formed from 5 min of data, and the bin size is 0.001 pm. (**D**) Histogram showing single-molecule binding events like those in (C). Two features are noteworthy. The largest shift is independent of concentration, and the number of binding events increases in proportion to concentration. The largest shift achieved agrees very well with the expected shift from the thermo-optic theory based on the Q factor of the microcavity used in this experiment (1.05×10^8). This histogram is formed from 1 min of data, and the bin size is 0.001 pm.

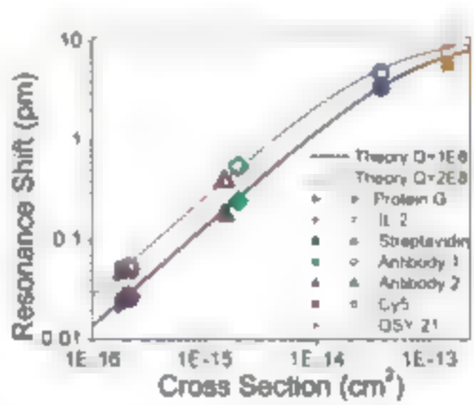

Fig. 4. The expected theoretical relation between absorption cross section and maximum resonance shift is confirmed experimentally for IL-2, streptavidin, protein G, two different IL-2 antibodies, and two synthetic fluorophores (Cy5 and QSY-21). These shifts are determined using the method described in (*26*). The solid symbols were taken using microresonators with $Q \sim 1 \times 10^8$; the hollow symbols were taken using microresonators with $Q \sim 2 \times 10^8$. The two solid curves are the theoretically predicted dependence based on Eq. 1.

largest measured single-molecule resonance shift versus absorption cross section. For small cross sections (that do not lower cavity Q), a linear dependence is expected based on the thermo-optic model presented above (we assume a negligible impact of the size parameter ε). The coupled input power and toroid diameter were constant throughout the measurements. With the exception of the shift data for QSY-21, single-molecule data were obtained for multiple binding events on a single toroid. QSY-21 appreciably lowers the Q factor, which made multiple single-molecule measurements untenable. From Fig. 4, it is apparent that there is excellent alignment of the data across all of the distinct molecules and for both Q factors. Furthermore, it should be noted that the higher Q factor provides a proportionally larger shift, as expected from the proposed mechanism. The solid lines in Fig. 4 are the theoretical predictions based on the previously outlined thermo-optic model, using a single ε value of 35 nm.

The detection mechanism is not purely linear in cross section because a single molecule that is highly absorbing can decrease the cavity Q factor (*26*). This phenomenon occurs both with Cy5 and QSY-21, which impact the Q factor even at the single-molecule level. Because the Q factor is decreased, the circulating intensity is reduced, and the thermo-optic induced heating is also decreased. Thus, the linear fit for smaller cross section molecules (which assumes a constant Q and hence constant circulating power) is expected to break down in these cases in precisely the manner observed.

To verify the application of the microtoroid sensor as a diagnostic tool for medical applications, detection of IL-2 in fetal bovine serum was chosen. As mentioned previously, IL-2 is a cytokine which is released in response to immune system activation. However, the concentration of IL-2 in serum has been shown to change in patients with childhood leukemia and to be an indicator of an impaired immune system (*36*). However, IL-2 is present at very low concentrations (10^{-12} to 10^{-15} M) and, therefore, it can be difficult to detect these changes quickly.

To demonstrate detection of IL-2 in serum, three serum solutions were made that contained 300 aM, 600 aM, or 900 aM of IL-2 (*26*). Additionally, pure serum was flowed over the functionalized toroid (*26*). Figure 3B shows the resonant wavelength shifts that resulted from these detection events. Several features of this data are significant. First, the total resonant wavelength shift increases as a direct function of the concentration, and the individual binding events can be resolved, as in the previous detection events in pure solution (Fig. 3A). Second, the shift from the pure serum is negligible, which indicates that none of the additional components in the serum interferes appreciably with the detection (*26*).

From this resonant shift data, a histogram is created for each of the IL-2 concentrations. Figure 3D shows the distribution of wavelength shifts for all of the single-molecule binding events. The largest shift that occurred (which, as noted before, corresponds to binding at the highest intensity region of the microtoroid) was the same at all three IL-2 concentrations. This value agrees very well with the theoretically predicted value based on the cavity Q for the toroid used in this experiment and the absorption cross section of IL-2. Additionally, the number of molecules that bind increases as a function of the concentration, as would be expected (*26*).

Although there are many other single-molecule detection schemes possible, this (UHQ) optical microcavity does not require specific labeling of the analyte or antigen in question. This method of detection functions at room temperature and is capable of performing both label-free single-molecule measurements and higher concentration measurements on a single platform. It will enable a new class of biological experiments, including monitoring growth factors that are emitted from living cells in vivo. Because our device is biocompatible and can operate in aqueous environments, it can be used for direct detection of proteins within biological samples without labeling, or even separation, and it should be applicable for the detection of tumor markers present at low concentration in a serum sample or rare growth factors secreted from cells in culture.

References and Notes

1. B. Schuler, E. A. Lipman, W. A. Eaton, *Nature* **419**, 743 (2002).
2. Y. Sako, S. Minoghchi, T. Yanagida, *Nat. Cell Biol.* **2**, 168 (2000).
3. J. K. Jaiswal, S. M. Simon, *Nat. Chem. Biol.* **3**, 92 (2007).
4. M. J. Lang, P. M. Fordyce, A. M. Engh, K. C. Neuman, S. M. Block, *Nat. Methods* **1**, 133 (2004).
5. B. Huang *et al.*, *Science* **315**, 81 (2007).
6. J. Eid, G. W. Li, X. S. Xie, *Science* **316**, 1191 (2007).
7. R. P. Kulkarni, K. Castelino, A. Majumdar, S. E. Fraser, *Biophys. J.* **90**, 142 (2006).
8. B. D. Moore *et al.*, *Nat. Biotechnol.* **22**, 1133 (2004).
9. T. Funatsu, Y. Harada, M. Tokunaga, K. Saito, T. Yanagida, *Nature* **374**, 555 (1995).
10. W. P. Ambrose *et al.*, *Chem. Rev.* **99**, 2929 (1999).
11. S. Myong, I. Rasnik, C. Joo, T. M. Lohman, T. Ha, *Nature* **437**, 1321 (2005).
12. Y. W. C. Cao, R. C. Jin, C. A. Mirkin, *Science* **297**, 1536 (2002).
13. R. C. Hughes, A. J. Ricco, M. A. Butler, S. J. Martin, *Science* **254**, 74 (1991).
14. Z. H. Zhong, D. L. Wang, Y. Cui, M. W. Bockrath, C. M. Lieber, *Science* **302**, 1377 (2003).
15. J. M. Nam, C. S. Thaxton, C. A. Mirkin, *Science* **301**, 1884 (2003).
16. W. S. Yeo, D. H. Min, R. W. Hsieh, G. L. Greene, M. Mrksich, *Angew. Chem. Int. Ed.* **44**, 5480 (2005).
17. T. P. Burg *et al.*, *Nature* **446**, 1066 (2007).
18. S. Arnold, M. Khoshsima, I. Teraoka, S. Holler, F. Vollmer, *Opt. Lett.* **28**, 272 (2003).
19. R. W. Boyd, J. E. Heebner, *Appl. Opt.* **40**, 5742 (2001).
20. E. Krioukov, D. J. W. Klunder, A. Driessen, J. Greve, C. Otto, *Opt. Lett.* **27**, 512 (2002).
21. A. Ksendzov, Y. Lin, *Opt. Lett.* **30**, 3344 (2005).
22. It is possible to perform single-molecule detection without first sensitizing the surface. This type of detection is shown in Fig. 4 where single-molecule detection experiments of Protein G and QSY-21 were successfully demonstrated without first sensitizing the surface. However, this type of detection has limited applications in biology because specificity is often as important as sensitivity. This surface sensitization is distinct from a label because the antibody is attached to the surface of the microtoroid and not to the molecule of interest (e.g., antigen or streptavidin), whereas a label is attached to the molecule of interest.
23. R. A. Vijayendran, D. E. Leckband, *Anal. Chem.* **73**, 471 (2001).
24. D. K. Armani, T. J. Kippenberg, S. M. Spillane, K. J. Vahala, *Nature* **421**, 925 (2003).
25. A. M. Armani, D. K. Armani, B. Min, K. J. Vahala, S. M. Spillane, *Appl. Phys. Lett.* **87**, 151118 (2005).
26. Materials and methods are available as supporting material on *Science* Online.
27. K. Nakatani, S. Sando, I. Saito, *Nat. Biotechnol.* **19**, 51 (2001).
28. G. F. Zheng, F. Patolsky, Y. Cui, W. L. Wang, C. M. Lieber, *Nat. Biotechnol.* **23**, 1294 (2005).
29. G. H. Wu *et al.*, *Nat. Biotechnol.* **19**, 856 (2001).
30. Turner BioSystems, www.turnerbiosystems.com.
31. L. Fweder Kitzmuller, J. Hesse, A. Ebner, H. J. Gruber, G. J. Schutz, *Chem. Phys. Lett.* **404**, 13 (2005).
32. The majority of the optical field intensity (over 90%) resides within the toroidal boundary. This fact and the similar magnitudes of the thermal conductivity of water and silica (0.6 and 1.38 W/mK) make it possible to attribute all thermal tuning in (*2*) (and, indeed, the shape of the thermal plume) to the silica. The resulting error in the calculated tuning shift is estimated to be about 5%. We also note that the indicated shift is in steady state, and the response time of the system is set by the thermal response (on the order of microseconds).
33. The actual form of the temperature plume in the vicinity of the molecule is likely complex and has been combined into a single empirical parameter ε. In contrasting a perfect point source of heat with a molecule, this parameter captures the essential fact that the temperature profile is not singular at the source and instead rises steadily until reaching some radius on the order of the molecular size. This approximation is justified, first, because the thermal transport process itself rapidly smoothes nanoscale spatial variations created by molecular shape and, second, because the ensuing temperature field created by the molecular hot spot is long-range (i.e., $1/r$ dependence). For this reason, the tuning shift is only a weak function of the parameter ε. Along these lines, it is the optical cross section σ, as opposed to the physical radius r, that is of far greater relevance to the thermal-induced tuning. However, the size of ε strongly suggests a maximum temperature in the vicinity of the molecule; therefore, on physical grounds (i.e., molecules are not denaturing in the present work), we expect ε to be many times the actual physical size of the molecule.
34. A cavity linewidth measurement is the minimum sensitivity measurement that can be performed without requiring additional equipment or employing more complex techniques (such as locking onto the resonant wavelength). The primary assumption in this measurement is that the resonant wavelength shifts an entire linewidth upon the binding of a molecule. For example, a cavity with a Q of 100 million operating at 680 nm would need to shift 6.8×10^{-6} nm. As mentioned, this limit is not fundamental but can be viewed as what is detectable by methods that do not enable detection of sub-linewidth shifts. Thus, this limit is the most desirable one to consider when balancing detection limits and experimental complexity.
35. The absorption cross sections of the IL-2, protein G, streptavidin, and the two different IL-2 antibodies were determined with an ultraviolet-visible spectrophotometer (Shimadzu BioSpec-1601, San Diego, CA, USA), whereas the absorption cross section of the Cy5-labeled antibody and the QSY-21 quencher were determined from absorption spectra available from the manufacturer (Invitrogen, Carlsbad, CA, USA). The absorption spectra of the Cy5-labeled antibody and of the bleached Cy5-labeled antibody were verified with the spectrophotometer.

36. B. Mazar, A. Mertas, D. Sonta-Jakimczyk, T. Szczepanski, A. Jamik-Moszant, *Hematological Oncology* 22, 27 (2004)

37. We thank O. Painter for useful discussions, B. Min for FEMLAB simulations, N. Pierce for spectrophotometer measurements, and D. Armani for microtoroid fabrication. A.M.A. is supported by the Clare Boothe Luce Postdoctoral Fellowship. This work was supported by the Defense Advanced Research Projects Agency's Center for Optofluidic Integration and the Biological Imaging Center of the Beckman Institute at the California Institute of Technology.

Supporting Online Material
www.sciencemag.org/cgi/content/full/1145002/DC1
Materials and Methods
Figs. S1 to S11
References

11 May 2007; accepted 14 June 2007
Published online 5 July 2007;
10.1126/science.1145002
Include this information when citing this paper

Ultrafast Flash Thermal Conductance of Molecular Chains

Zhaohui Wang,[1]* Jeffrey A. Carter,[1]* Alexei Lagutchev,[1]* Yee Kan Koh,[2] Nak-Hyun Seong,[1]* David G. Cahill,[2,3] Dana D. Dlott[1,3]†

At the level of individual molecules, familiar concepts of heat transport no longer apply. When large amounts of heat are transported through a molecule, a crucial process in molecular electronic devices, energy is carried by discrete molecular vibrational excitations. We studied heat transport through self-assembled monolayers of long-chain hydrocarbon molecules anchored to a gold substrate by ultrafast heating of the gold with a femtosecond laser pulse. When the heat reached the methyl groups at the chain ends, a nonlinear coherent vibrational spectroscopy technique detected the resulting thermally induced disorder. The flow of heat into the chains was limited by the interface conductance. The leading edge of the heat burst traveled ballistically along the chains at a velocity of 1 kilometer per second. The molecular conductance per chain was 50 picowatts per kelvin.

Heat transport is central to the operation of nearly all electronic machines, but at the level of individual molecules, the familiar concepts of heat diffusion by phonons in bulk materials no longer apply. Heat is transported through a molecule by discrete molecular vibrations. An emerging area in which vibrational energy transfer becomes crucial is the field of molecular electronics, where long-chain molecules attached to tiny electrodes are used to transport and switch electrons. When an electron is transported through a molecule, a portion of the electron's kinetic energy can be lost, appearing as molecular vibrational energy (*1*). In studies such as this one, in which molecular energy levels are not individually resolved, it is conventional to call such processes "heat dissipation" or "nanoscale thermal transport" (*2*), even though an equilibrium Boltzmann distribution is not necessarily achieved. Nitzan and co-workers (*3*) have estimated that 0 to 50% of the electron energies could be converted to heat, so that a power of 10^{11} eV/s may be dissipated on a molecular electronic bridge carrying 10 nA under a bias of 1 eV. Using classical and quantum mechanical methods, they and others (*1*) have calculated steady-state temperatures resulting from such dissipation. Steady-state calculations, however, do not entirely capture the essence of this phenomenon. The energy lost when electrons are transported through a molecular wire in a fraction of a picosecond appears as staccato bursts, up to 1 eV per burst. On a 10-carbon alkane molecule, for instance, 1eV is enough energy to produce a transient temperature jump ΔT = 225 K. At the temperatures associated with these ultrafast energy bursts, Nitzan and co-workers (*3*) suggest that, instead of the usual phonon mechanisms prevalent in ordinary thermal conduction processes (*1*), much of the heat is carried by higher-energy molecular vibrations such as carbon-carbon bending and stretching and carbon-hydrogen bending, which are delocalized over a few carbon segments (*3*).

To study molecular energy transport in the regime of short distances, short time intervals, and large temperature bursts, we have used an ultrafast flash thermal conductance apparatus to study densely packed self-assembled monolayers (SAMs) of long-chain hydrocarbon molecules anchored to metal substrates. Laser flash-heating increased the temperature of the metal substrate to ~800°C in 1 ps. Heat flowed from the metal layer into the base of the molecular chains and then through the chains. A vibrational spectroscopy method was used that selectively probed the thermal-induced disorder of the methyl groups at the ends of the chains. The alkane chain lengths yielded a ballistic velocity for heat flow through the chains, and the measured thermal conductance plus the area per chain yielded a molecular thermal conductance.

The concept of the thermal conductance apparatus is illustrated in Fig. 1A. A femtosecond laser pulse flash-heated an ~300-μm-diameter region of an Au layer coated for a fast time response of ~1 ps. The SAMs were formed from *n*-alkanethiol molecules $HS(CH_2)_nCH_3$ with an even number of carbon atoms from C 6 to C 24 (i.e., *n* from 5 to 23). A novel near-concentration spectroscopic method (*4*) termed broadband multiplex vibrational sum-frequency generation spectroscopy (SFG) probed an ensemble of 10^{11} alkane chains at the center of the heated region. We determined an overall rate for heat transport from Au into the alkane chains, and a

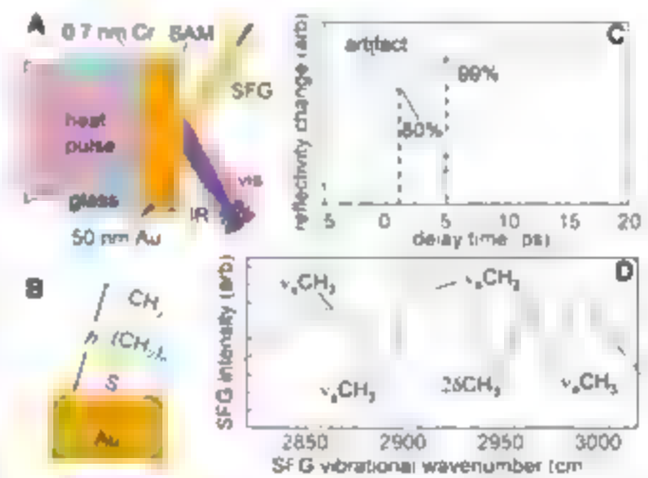

Fig. 1. (**A**) Concept of the ultrafast flash thermal conductance measurements. IR and visible pulses combine to generate SFG in an ~200-μm-diameter region containing ~10^{11} alkane chains. SFG is sensitive to thermal disordering of the alkane terminal methyl groups of SAMs, which occurs when heat propagates from the Au surface to the ends of the alkane chains. (**B**) Alkanethiol molecule of length *h* bound to Au surface. (**C**) Ultrafast thermal reflectance measurements show that the Au layer heats up to 80% of its final temperature in 1 ps. (**D**) SFG spectra of alkane thiol (n = 17) SAM at ambient temperature (blue) and after an ultrafast temperature increase to 800°C (red).

[1]School of Chemical Sciences, University of Illinois at Urbana-Champaign, Urbana, IL 61801, USA. [2]Department of Materials Science and Engineering, University of Illinois at Urbana-Champaign, Urbana, IL 61801, USA. [3]Frederick Seitz Materials Research Laboratory, University of Illinois at Urbana-Champaign, Urbana, IL 61801, USA.

*These authors contributed equally to this work.
†To whom correspondence should be addressed. E-mail: dlott@scs.uiuc.edu

time for heat to propagate from the base to the ends of the chains, as a function of the length h of the alkane molecules.

An 800-nm, 500-fs-duration laser pulse from an amplified titanium-doped sapphire laser (5) incident on the Au-glass interface (the back side) of the 50-nm-thick Au layer generated hot electrons within a skin depth of ~15 nm (6). Because the hot electrons have a large diffusion coefficient, the electron temperatures at the front and back of the Au layer equalized even before electron-phonon coupling brought the hot electrons into equilibrium with the lattice (6). Within ~1 ps, the Au layer was in thermal equilibrium and uniformly heated throughout (6). To improve the adhesion of Au to glass it was necessary to add a Cr layer beneath the Au. Unfortunately, heat transfer from a Cr layer to Au is relatively slow; to minimize this effect, we made the Cr layer just 0.8 nm thick. An ultrafast thermoreflectance apparatus (2, 7) was used to characterize the temperature rise of the Au layer. As shown in Fig. 1C, there is a fast increase of the Au surface temperature to 80% of the final temperature within 1 ps. There is also a slower (1.5 ps time constant) rise to the final temperature due to the Cr layer. The same transient response was observed with either front-side or back-side flash-heating and with or without a SAM. The Au layer remained at an approximately constant high temperature for several nanoseconds, subsequently cooling by heat diffusion into the glass. In the SFG experiments, the intensity of the heating pulse was varied to locate the threshold for melting the Au, and then the pulse was attenuated by 20%. Because the melting temperature of Au T_m = 1064°C, this procedure resulted in flash-heating of the Au layer to ~800°C.

SAMs have been studied extensively by SFG since 1991 (8), but ultrafast probing of a flash-heated SAM requires some elaboration. In the SFG technique we used, a femtosecond infrared (IR) pulse at 3.3 μm with a bandwidth of ~50 cm^{-1} is incident on the SAM, coherently exciting all the alkane CH-stretch transitions in the 2850 to 3000 cm^{-1} range, along with electrons in the Au skin layer, producing an oscillating polarization in both the Au and the SAM layers. At the same time, a picosecond-duration 800-nm pulse (visible) with a bandwidth of 7 cm^{-1} is incident on the sample. The visible pulse interacts with this oscillating polarization through coherent Raman scattering to create a coherent output pulse at the IR + visible frequency. This combined IR-Raman interaction is forbidden (in the dipole approximation) in centrosymmetric media because the second-order susceptibility $\chi^{(2)}$ vanishes in such media. Because the methylene CH_2 groups of the alkane SAM form a nearly centrosymmetric sound, the SFG signal that we observed originated predominantly from the Au surface and the terminal methyl CH_3 groups. The well-known SFG spectrum obtained in *ppp* polarization (9) from a SAM with n = 17 (i.e., an 18-carbon or C18 SAM), is shown in Fig. 1D. Molecular vibrational transitions appear as dips against a broad nonresonant background from Au. These methyl transitions have a spectral width $\Delta\nu$ = 15 cm^{-1}, corresponding to a coherence decay time constant T_2 = 0.7 ps, which indicates that SFG signals are emitted during an ~1 ps time window. Thus the time resolution of these SFG measurements is ~1 ps.

Three intense vibrational transitions were observed, originating from the symmetric $\nu_s CH_3$ and antisymmetric $\nu_a CH_3$ methyl stretching vibrations and from the δCH_3 bending overtone transition, which draws intensity from a 2:1 Fermi resonance with the CH stretches (*4*, *8*). All methylene transitions are weak, which is indicative of a high degree of order (*4*). Figure 1D shows the spectrum of a C18 SAM ~400 ps after flash-heating, where the SAM is in equilibrium with Au at ~800°C. All three methyl transitions have lost intensity as a result of thermal disordering of the methyl groups. The $2\delta CH_3$ band evidences a red shift. The red shift is caused by thermal excitation of the ~1500 cm^{-1} ν = 1 state, which introduces an additional contribution from the anharmonically red-shifted ν = 1 ⟶ ν = 3 transition. It is notable that methylene transitions remain weak at high temperature and that the transient intensity loss is reversible once the SAM returns to ambient temperature. This indicates that chains remain upright and remain bonded to their original sites. Under ordinary circumstances, alkane SAMs on Au desorb to form the disulfide CH_3-$(CH_2)_n$-S-S-$(CH_2)_n$-CH_3 at 175 to 225°C (*9*, *10*), which displays enhanced methylene SFG transitions, so the unexpected stability of these SAMs at 800°C must be attributed to the brief duration of the temperature increase.

We performed molecular simulations of a C16 SAM on Au (27 molecules with periodic boundary conditions) to better understand thermal disordering of the terminal methyl groups. When the SAM was equilibrated at 300 K, the well-known (*11*) all-trans structure with a chain tilt of ~35° and a zenith angle (angle between surface normal and final C-C bond) of ~25° was obtained. The $\nu_s CH_3$ transition has an IR transition dipole moment of mag-

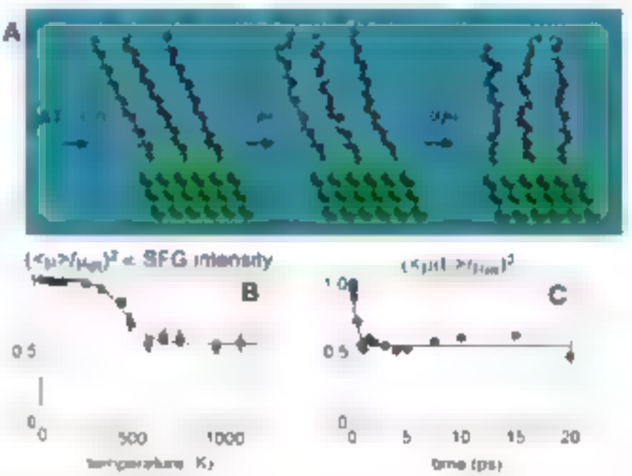

Fig. 2. Results of molecular simulations of alkanethiol SAMs. **(A)** Structure of alkanethiol SAM (n = 15). Simulations were performed on a unit cell of 27 alkanes with periodic boundary conditions. When T is increased to a high temperature, the methyl head groups become orientationally disordered. **(B)** The SFG intensity for the $\nu_s CH_3$ transition is approximately proportional to the square of the normalized ensemble-average IR dipole moment $(\mu_z/\mu_{all})^2$, which is temperature dependent. **(C)** With an instantaneous temperature jump to 1100 K, the methyl head groups become orientationally disordered in less than 2 ps.

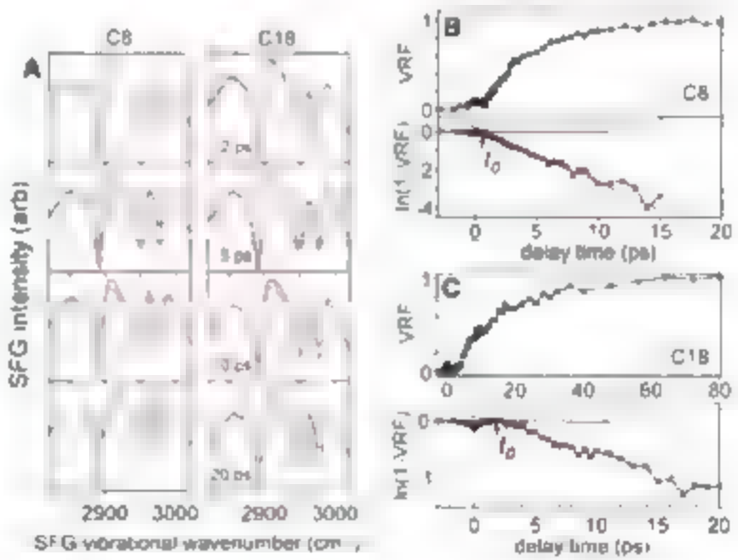

Fig. 3. **(A)** SFG spectra of C8 (n = 7) and C18 (n = 17) SAMs without heating pulses (blue) and with flash-heating to 800°C (red). **(B)** VRF for a C8 monolayer. **(C)** VRF for a C18 monolayer.

nitude, μ_{IR}, which is parallel to this final C-C bond. Because polarized Raman scattering from a methyl group is not very sensitive to methyl orientation, the SFG intensity of the $v_s CH_3$ transition would be expected to be approximately proportional to the square of the normalized ensemble-averaged IR transition dipole moment,

$$\mu^2 \mu_{IR}^2 \quad \left[\left(\frac{1}{n}\sum_{j=1}^{n} \mu_j\right) \cdot \mu_{IR}\right]^2$$ As temperature

was increased in the simulation, the methyl groups became orientationally disordered, which decreased the magnitude of $\langle\mu\rangle^2$. As shown in Fig. 2B, the SFG intensity in the 300 K > T > 600 K regime can be used as a molecular thermometer, and this molecular thermometer is approximately 1.5 Å thick, the width of a single CH_3 group. Above 600 K, SFG becomes insensitive to T; in our experiments, this helped to smooth out the effects of nonuniformity in laser heating. Figure 2, A and C, shows how thermal disordering progresses after a simulated fast temperature increase to 1100 K. On the <1-ps time scale, the labile terminal methyl groups undergo orientational fluctuations. On the ~2-ps time scale, multiple gauche defects are created below the surface (*12*, *13*). On a metal surface in *ppp* polarization, these gauche defects do not enhance methylene SFG intensities significantly as long as the chains remain upright (*12*, *13*).

Figure 3A shows a time series of SFG spectra after flash-heating of the Au to 800°C for C8 and C18 chains. SFG intensity loss is clearly faster with the shorter chains. The intensity-loss time dependence was similar for all three methyl vibrational transitions, so we now consider only $v_s CH_3$, the most intense transition. To quantify the intensity loss, we define a normalized vibrational response function (VRF) (*5*, *13*) as

$$VRF(t) = [I(T_{cold}) - I(t)]/[I(T_{cold}) - I(T_{hot})]$$

where $I(T_{cold})$ is the $v_s CH_3$ vibrational intensity at ambient temperature and $I(T_{hot})$ the intensity after a few hundred picoseconds when Au and SAM have equilibrated. The VRFs for C8 and C18 chains are shown in Fig. 3, B and C, where $t = 0$ denotes arrival of the flash-heating pulse. Near $t = 0$, there is a coherent artifact caused by interactions between the SFG pulses and the small portion of flash-heating pulse that leaks through the Au layer. This artifact is a fiducial time marker that locates $t = 0$. For all alkane chains, the VRFs increased exponentially toward unity with time constant τ. However, the VRF increase did not begin at $t = 0$. There was a time delay t_0 before this buildup. As a result of the delayed buildup, we fit the data to the function, $VRF(t) = 0$ for $t < t_0$ and $VRF(t) = [1 - \exp[-(t - t_0)/\tau]]$ for $t > t_0$. To extract the parameters t_0 and τ from the data, we plotted $\ln(1 - VRF)$ versus t as in Fig. 3, B and C, and used linear least-squares fitting in the $t > t_0$ region. The slope gave τ, and the abscissa intercept gave t_0. In Fig. 4, A and B, we plot t_0 and τ versus chain length. The chain length h, based on conventional molecular bonding parameters (*11*), obeys the relation h(nm) = 0.127 n + 0.4. Both t_0 and τ increased linearly with chain length.

The delay time t_0 emerges from the ability of SFG to selectively probe alkanes at the terminal methyl groups. The heat burst from the Au substrate travels along the chains, but only after the leading edge of this heat burst reaches the terminal methyl groups does the SFG optical thermometer began to register an effect. Thus, t_0 is interpreted as the time for heat to travel from the Au surface to the ends of the alkane chains. The linear dependence of t_0 on chain length indicates that the leading edge of the heat burst propagates ballistically along the chains, and the slope of the data in Fig. 4A gives a velocity of 0.95 (±0.1) nm/ps = 0.95 km/s.

The parameter τ is the time constant for SAM thermal disordering. Our simulations with infinitely fast heating indicate that thermal disorder can be created in about 2 ps, much faster than observed values of τ. Figure 2B indicates that the VRF stops increasing after the SAM reaches a temperature of ~600 K. Thus we interpret τ as the time for a SAM in contact with a hot surface to attain a temperature of ~600 K.

In Fig. 4, both t_0 and τ go to zero at a finite chain length of ~0.8 nm. This indicates that the hot Au layer does not transfer its heat to an individual atom at the base of the SAM, but instead Au transfers energy to a region at the base of the SAM 0.8 nm in length, which is about four carbon segments. This result is in good agreement with the predictions of Segal *et al.* (*3*), which find that the heat-carrying vibrations of short-chain alkanes are delocalized over four to five carbon segments.

The linear dependence of τ on chain length h is indicative of a heat-transfer process dominated by interface thermal conductance (*2*, *14*). In this case, heat transfer from Au to alkane chains is the rate-limiting step, the rate is controlled by the strength of coupling between Au phonons and alkane vibrations, and the interface thermal conductance $G = \rho h C_p/\tau$, where ρ is the SAM density and C_p the SAM-specific heat. G is independent of chain length, but longer chains need more heat to reach the same temperature, so longer chains heat up more slowly. To estimate G, we need to correct the value of τ to account for the insensitivity of the SFG thermometer above 300°C and to estimate the specific heat C_p of the SAM layers up to 300°C, as described in the supporting online material. Because τ represents the time to heat to 300°C, a linear extrapolation would give the time to heat to 800°C as 2.8τ. We estimate, an average specific heat $\bar{C}_p$ = 3000 J Kg^{-1} K^{-1} in the 25 to 300°C range, based on a high-temperature extrapolation of low-density polyethylene data. Using the results in Fig. 4B, we obtained G = 220 (±100) MW m^{-2} K^{-1}. This value of G is similar to what was previously obtained in studies of SAM-decorated nanoparticles in aqueous solutions (*15*).

The SFG probe technique can be seen to confer two important advantages. In the past, thermal conductance measurements of SAMs were based on measuring heat flow across two interfaces (*16*, *17*); the ability to probe the SAM itself eliminates one interface. Even though the flow of energy into the SAM is determined largely by interface effects, the ability to selectively probe the atomic groups that terminate the chains, rather than the thermal expansion of the entire chain (*18*), allows us to investigate energy transport through the chain molecules themselves.

The quantum mechanical models of Nitzan and co-workers (*1*, *3*) show that 700°C heat transport along alkane chains attached to a pair of metal electrodes involves molecular vibrations ranging up to 1500 cm^{-1}. The ballistic velocity of 1 km/s for heat transport along alkane chains should be understood as resulting not from acoustic phonons, which in polyethylene propagate at ~2.3 km/s, but instead from a mix of intramolecular vibrations with slower velocities. The calculated values of thermal conductances at 700°C (*3*) were found to be approximately chain-length independent for n > 7 and slightly less than 100 pW K^{-1}. Using our value of G and an area per alkane chain of 2.2 10^{-19} m^2 (*11*), we obtain a single-molecule thermal conductance of 50 pW K^{-1} = 0.3 eV ns^{-1} K^{-1}. Thus, our measurements are in good agreement with quantum mechanical calculations that preceded our work.

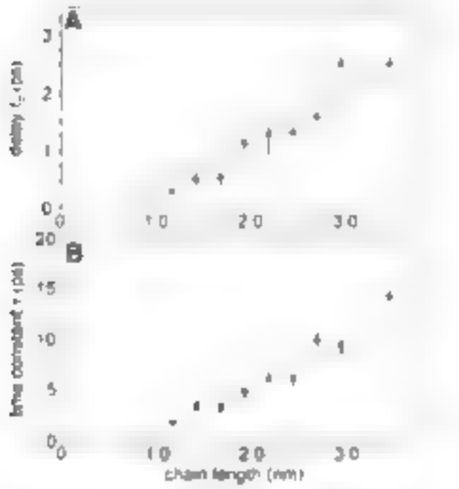

Fig. 4. (**A**) Dependence on chain length of the delay time t_0 between the flash-heating pulse and the arrival of the initial burst of heat at the methyl head groups. (**B**) Dependence on chain length of the time constant τ for thermal equilibration between flash-heated Au and alkane chains.

References and Notes

1. M. Galperin, M. A. Ratner, A. Nitzan, *J. Phys. Condens. Matter* **19**, 103201 (2007).
2. D. G. Cahill *et al.*, *J. Appl. Phys.* **93**, 793 (2003).
3. D. Segal, A. Nitzan, P. Hänggi, *J. Chem. Phys.* **119**, 6840 (2003).

4. L. J. Richter, T. P. Petralli-Mallow, J. P. Stephenson, *Opt. Lett.* **23**, 1594 (1998).
5. A. S. Lagutchev, J. E. Patterson, W. Huang, D. D. Dlott, *J. Phys. Chem. B* **109**, 5033 (2005).
6. S. D. Brorson, J. G. Fujimoto, E. P. Ippen, *Phys. Rev. Lett.* **59**, 1962 (1987).
7. D. G. Cahill, *Rev. Sci. Instrum.* **75**, 5119 (2004).
8. C. D. Bain, P. B. Davies, T. H. Ong, R. N. Ward, *Langmuir* **7**, 1563 (1991).
9. N. Nishida, M. Hara, H. Sasabe, K. Wolfgang, *Jpn. J. Appl. Phys.* **35**, 5866 (1996).
10. H. Kondoh, C. Kodama, H. Sumida, H. Nozoye, *J. Chem. Phys.* **111**, 1175 (1999).
11. C. D. Bain *et al.*, *J. Am. Chem. Soc.* **111**, 321 (1989).
12. J. E. Patterson, D. D. Dlott, *J. Phys. Chem. B* **109**, 5045 (2005).
13. J. E. Patterson, A. S. Lagutchev, W. Huang, D. D. Dlott, *Phys. Rev. Lett.* **94**, 015501 (2005).
14. H. K. Lyeo, D. G. Cahill, *Phys. Rev. B* **73**, 144301 (2006).
15. Z. Ge, D. G. Cahill, P. V. Braun, *J. Phys. Chem. B* **108**, 18870 (2004).
16. Z. B. Ge, D. G. Cahill, P. V. Braun, *Phys. Rev. Lett.* **96**, 186101 (2006).
17. R. Y. Wang, R. A. Segalman, A. Majumdar, *Appl. Phys. Lett.* **89**, 173113 (2006).
18. S. Chen, M. T. Seidel, A. H. Zewail, *Angew. Chem. Int. Ed.* **45**, 5154 (2006).

19. This material is based upon work supported by the U.S. Department of Energy (DOE), Division of Materials Sciences under award DEFG02-91ER45439, through the Frederick Seitz Materials Research Laboratory at the University of Illinois at Urbana-Champaign. Thermal reflectance measurements were carried out in the Frederick Seitz Materials Research Laboratory Central Facilities, University of Illinois, which are partially supported by the DOE under grant DEFG02-91-ER45439. D.D.D. acknowledges additional support from the National Science Foundation under award DMR 0504038 and from the Air Force Office of Scientific Research under award FA9550-06-1-0235.

Supporting Online Material

www.sciencemag.org/cgi/content/full/317/5839/787/DC1
Materials and Methods
SOM Text
References

16 May 2007; accepted 27 June 2007
10.1126/science.1145220

Direct Synthesis of Amides from Alcohols and Amines with Liberation of H_2

Chidambaram Gunanathan, Yehoshoa Ben-David, David Milstein*

Given the widespread importance of amides in biochemical and chemical systems, an efficient synthesis that avoids wasteful use of stoichiometric coupling reagents or corrosive acidic and basic media is highly desirable. We report a reaction in which primary amines are directly acylated by equimolar amounts of alcohols to produce amides and molecular hydrogen (the only products) in high yields and high turnover numbers. This reaction is catalyzed by a ruthenium complex based on a dearomatized PNN-type ligand [where PNN is 2-(di-*tert*-butylphosphinomethyl)-6-(diethylaminomethyl)pyridine], and no base or acid promoters are required. Use of primary diamines in the reaction leads to bis-amides, whereas with a mixed primary-secondary amine substrate, chemoselective acylation of the primary amine group takes place. The proposed mechanism involves dehydrogenation of hemiaminal intermediates formed by the reaction of an aldehyde intermediate with the amine.

Amide formation is a fundamental reaction in chemical synthesis (*1*). The importance of amides in chemistry and biology is well recognized and has been studied extensively over the past century (*2*–*4*). Although several methods are known for the synthesis of amides, preparation under neutral conditions and without the generation of waste is a challenging goal (*1*, *5*). Syntheses of amides is mostly based on activated acid derivatives (acid chlorides and anhydrides) or rearrangement reactions induced by an acid or base, which often produce toxic chemical waste and involve tedious procedures (*5*). Transition metal catalyzed conversion of nitriles into amides was reported (*6*–*8*). Catalytic acylation of amines by aldehydes in the presence of a stoichiometric amount of oxidant and a base is known (*9*, *10*). Recently, oxidative amide synthesis was achieved from terminal alkynes (*11*). Cu(I)-catalyzed reaction of sulfonyl azides with terminal alkynes is a facile method for the synthesis of sulfonyl amides (*12*, *13*). A desirable goal is the direct catalytic conversion of alcohols and amines into amides and dihydrogen (Eq. 1).

$$RNH_2 + R'CH_2OH \xrightarrow[\text{(R = alkyl, aryl)}]{\text{catalyst, } \Delta} RNHCOR' + 2H_2 \quad (1)$$

This unknown, environmentally benign reaction (*14*–*18*) might lead to a diverse library of amides from very simple substrates, with high atom

Department of Organic Chemistry, Weizmann Institute of Science, Rehovot 76100, Israel.

*To whom the correspondence should be addressed. E-mail: david.milstein@weizmann.ac.il

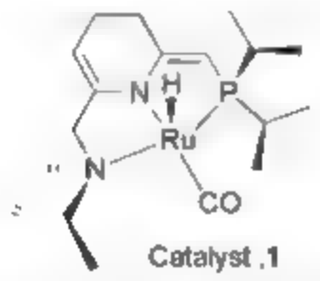

Fig. 1. Structure of dearomatized PNN pincer complex **1**.

Fig. 2. Proposed mechanism for the direct acylation of amines by alcohols catalyzed by complex **1**.

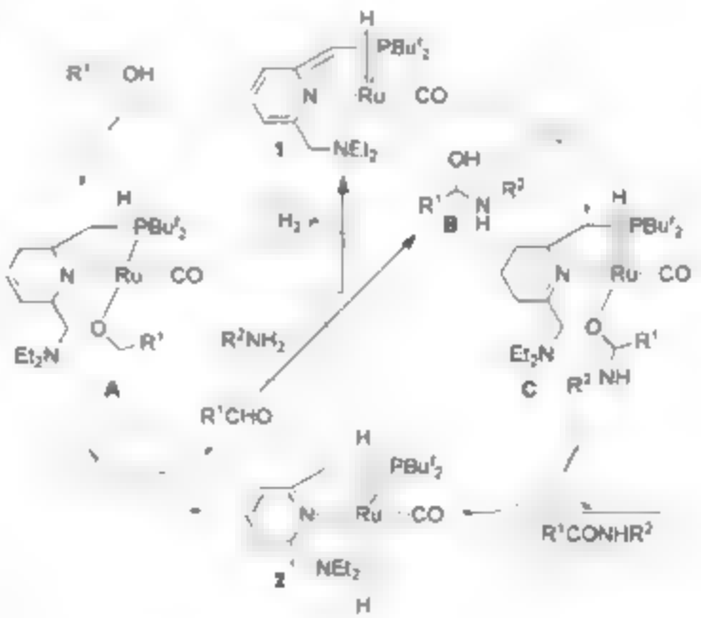

economy and no stoichiometric activating agents, generating no waste. Although such a reaction is expected to be thermodynamically uphill, it is envisioned that the liberated hydrogen gas (valuable in itself) will shift the equilibrium and drive the reaction.

We recently reported the dehydrogenation of alcohols catalyzed by 2,6-bis-(di-*tert*-butylphosphinomethyl)pyridine (PNP) Ru(II) and PNN-Ru(II) hydride complexes (*19*). Whereas secondary alcohols lead to ketones (*20*, *21*), primary alcohols are efficiently converted into esters and dihydrogen (*19*, *21*). The dearomatized PNN pincer complex **1** (Fig. 1) is particularly efficient (*19*, *22*); it catalyzes this process in high yields under neutral conditions, in the absence of acceptors or promoters. We have now discovered that complex **1** catalyzes the reaction of alcohols with amines to form amides and H_2, leading to a variety of amides (Table 1).

At the outset, when a toluene solution of complex **1** (0.2 mole percent) with benzylamine and 1-hexanol (1:1 ratio) was refluxed in a closed system for 6 hours, 63% conversion of 1-hexanol to *N*-benzylhexanamide was observed. Continuing the reaction up to 40 hours resulted in a mixture of products. In order to facilitate formation of the product amide by hydrogen removal, we heated 1-hexanol and benzylamine with complex **1** (0.1 mol %) under a flow of argon in refluxing toluene for 7 hours. This setup resulted in the formation of *N*-benzylhexanamide in 96% yield and a trace of *N*-benzyl-hexyl-1-amine (1%). We observed no formation of hexyl hexanoate, which forms quantitatively in the absence of amine (Table 1, entry 1). Repeating the reaction with 1-pentanol under identical conditions led to selective direct amidation, providing *N*-benzylpentanamide in 97% yield (Table 1, entry 2). 2-Methoxyethanol underwent clean dehydrogenative acylation by reaction with the primary amines benzylamine, pentylamine, and cyclohexylamine to give methoxyacetylated amides in almost quantitative yields (Table 1, entries 3, 8, and 10).

The amidation reactions are sensitive to steric hindrance at the α positions of either the alcohol or the amine. Thus, when 2-methyl-1-butanol reacted with benzylamine, the corresponding amide was obtained in 70% yield, with the rest of the alcohol being converted to the ester 2-methylbutyl 2-methylbutanoate (Table 1, entry

Table 1. Direct dehydrogenative acylation of amines with alcohols catalyzed by the ruthenium complex **1**. Catalyst **1** (0.01 mmol), alcohol (10 mmol), amine (10 mmol), and toluene (3 ml) were refluxed under Ar flow (*33*). Conversion of alcohols was 100% [by gas chromatography (GC) analysis]. The following reaction illustrates the transformation: $R^1CH_2OH + R^2{-}NH_2 \xrightarrow[\text{Toluene, Reflux, -2H}_2]{1\ (0.1\ \text{mol}\ \%)} R^2NHCOR^1$

Entry	R^1CH_2OH	R^2NH_2	Time (hours)	Amide	Yield* (%)
1			7	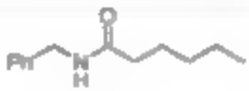	96
2			7		97
3			9	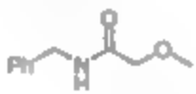	99
4			12	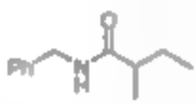	70†
5			8	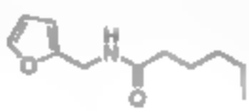	78†
6		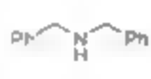	8	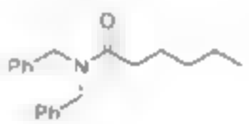	0†
7		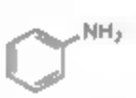	8	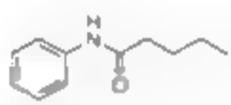	58†
8			8	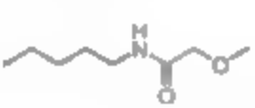	99
9		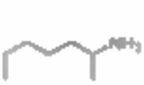	8	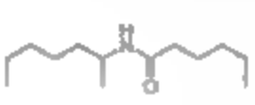	72†
10		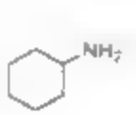	8	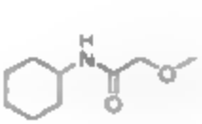	99

*Isolated yields. †The remaining alcohol was converted into the corresponding ester. In the reactions involving hexanol and pentanol, trace amounts of the corresponding secondary amines were detected (GC–mass spectrometry).

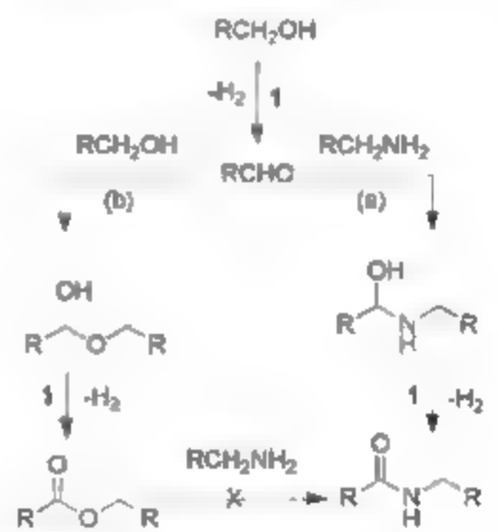

Scheme 1.

Table 2. Bis-acylation of diamines with alcohols catalyzed by complex **1**. Catalyst **1** (0.01 mmol), alcohol (10.5 mmol), diamine (5 mmol), and toluene (5 ml) were refluxed under Ar flow (*33*).

Entry	Diamine	Time (hours)	Bis-amide	Yield (%)
1	Ethylenediamine	9		99
2	Diethylenetriamine	8	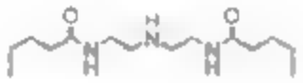	88
3	Hexamethylenediamine	9		95

4). A similar pattern was also observed when 2-methylhexylamine reacted with hexanol, leading to 72% yield of the corresponding amide (Table 1, entry 9). 1-(2-Furyl)methylamine provided 78% yield of amide when it reacted with 1-hexanol (Table 1, entry 5). When aniline was subjected to acylation with 1-pentanol, the amide was obtained in 58% yield (Table 1, entry 7). The lower reactivity of aniline may be attributed to its lower nucleophilicity as compared with that of the alkylamines. Secondary amines do not react. Thus, heating dibenzylamine with 1-hexanol under the experimental conditions resulted in a quantitative yield of hexyl hexanoate (Table 1, entry 6).

We have also examined the scope of this method with respect to bis-acylation processes with diamines. Upon refluxing a slight excess of a primary alcohol and catalyst **1** with diamines (>100 equivalents relative to catalyst **1**) in toluene under argon, we produced bis-amides in high yields. Thus, reaction of 2-methoxyethanol with ethylenediamine, and 1-hexanol with hexamethylene diamine, resulted in quantitative yields of the corresponding bis-amides (Table 2, entries 1 and 3). The high selectivity of the dehydrogenative amidation reaction to primary amine functionalities enabled the direct bis-acylation of diethylenetriamine with 1-hexanol to provide the bis-amide in 88% yield without the need to protect the secondary amine functionality (Table 2, entry 2).

The direct acylation of amines to amides with H_2 liberation may in principle proceed in two ways, as shown in Scheme 1: ("a") dehydrogenation of the alcohol to the aldehyde followed by its reaction with a primary amine to form a hemiaminal that is subsequently dehydrogenated to the amide and ("b") formation of a hemiacetal (from the aldehyde and alcohol) that is subsequently dehydrogenated to the ester (*19*), which reacts with the amine to form the amide (*23*). The latter possibility was ruled out because refluxing a toluene solution of hexyl hexanoate (1.25 mmol) and benzylamine (2.5 mmol) under argon for 8 hours, either in the presence or absence of catalyst **1**, did not result in the formation of *N*-benzylhexanamide. Thus, the reaction probably proceeds via the hemiaminal pathway.

On the basis of the above results and the known chemistry of PNN-type and PNP-type pincer complexes (*19*, *22*, *24*), we tentatively propose the mechanism depicted in Fig. 2. After a catalytic cycle for dehydrogenation of the alcohol to the corresponding aldehyde, reaction with the amine can form the hemiaminal **B**, which (upon reaction with complex **1**) can lead to the aromatic intermediate **C**. β-H elimination from **C** can form the observed product amide and generate the known *trans*-Ru dihydride complex **2** (*19*, *22*). Elimination of dihydrogen from complex **2** (*19*, *22*) would regenerate catalyst **1**, completing the catalytic cycle. The dehydrogenation of the hemiaminal **B** to the amide prevails relative to the expected facile water elimination to give an imine, which on hydrogenation would provide the secondary amine (*25*–*27*), that was observed in our system only in trace amounts.

These results highlight the substantial scope for the preparation of the fundamental amide motif by direct acylation of amines with alcohols, which is a clear departure from the conventional synthetic procedures.

References and Notes

1. R. C. Larock, *Comprehensive Organic Transformations* (Wiley-VCH, New York, ed. 2, 1999).
2. M. Sewald, H.-D. Jakubke, *Peptides: Chemistry and Biology* (Wiley-VCH, Weinheim, Germany, 2002).
3. A. Greenberg, C. M. Breneman, J. F. Liebman, Eds. *The Amide Linkage: Selected Structural Aspects in Chemistry, Biochemistry, and Materials Science* (Wiley-Interscience, New York, 2000).
4. B. L. Bray, *Nat. Rev. Drug Discov.* **2**, 587 (2003).
5. M. B. Smith, *Compendium of Organic Synthetic Methods* (Wiley, New York, vol. 9, 2001), pp. 100–116.
6. C. J. Cobley, M. van den Heuvel, A. Abbadi, J. G. de Vries, *Tetrahedron Lett.* **42**, 2467 (2000).
7. S.-I. Murahashi, T. Naota, E. Saito, *J. Am. Chem. Soc.* **108**, 7846 (1986).
8. S.-I. Murahashi, S. Sasao, E. Saito, T. Naota, *J. Org. Chem.* **57**, 2521 (1992).
9. Y. Tamaru, Y. Yamada, Z. Yoshida, *Synthesis* **1983**, 474 (1983).
10. A. Tillack, I. Rudloff, M. Beller, *Eur. J. Org. Chem.* **2001**, 523 (2001).
11. W.-K. Chan, C.-M. Ho, M.-K. Wong, C.-M. Che, *J. Am. Chem. Soc.* **128**, 14796 (2006).
12. S. H. Cho, E. J. Yoo, I. Bae, S. Chang, *J. Am. Chem. Soc.* **127**, 16046 (2005).
13. M. P. Cassidy, J. Raushel, V. V. Fokin, *Angew. Chem. Int. Ed.* **45**, 3154 (2006).
14. M. Hudlicky, *Oxidations in Organic Chemistry* (ACS Monograph 186, American Chemical Society, Washington, DC, 1990).
15. 1-Butanol was acylated with amines by means of stoichiometric amount of imidazole (via carbonyl imidazole). Reaction time and yield were not reported (*28*).
16. For a procedure based on three separate reactions, involving aldehyde synthesis by alcohol dehydrogenation, reaction of the aldehyde with hydroxylamine hydrochloride to form an oxime, and rearrangement of the oxime to an amide, see (*29*).
17. In the presence of an excess of a sacrificial hydrogen acceptor, ruthenium-catalyzed lactamization of amino alcohols with a total of 16 turnovers was reported (*30*).
18. Rhodium-catalyzed lactamization of aryl amino alcohols in the presence of base and hydrogen acceptor with a total of 20 turnovers was reported (*31*).
19. J. Zhang, G. Leitus, Y. Ben-David, D. Milstein, *J. Am. Chem. Soc.* **127**, 10840 (2005).
20. J. Zhang, M. Gandelman, L. J. W. Shimon, D. Milstein, *Dalton Trans.* **2007**, 107 (2007).
21. J. Zhang, M. Gandelman, L. J. W. Shimon, D. Milstein, *Organometallics* **23**, 4026 (2004).
22. J. Zhang, G. Leitus, Y. Ben-David, D. Milstein, *Angew. Chem. Int. Ed.* **45**, 1113 (2006).
23. Intermolecular formation of amides from esters and amines catalyzed by aluminum and tin reagents are known (*5*).
24. E. Ben-Ari, G. Leitus, L. J. W. Shimon, D. Milstein, *J. Am. Chem. Soc.* **128**, 15390 (2006).
25. Ruthenium-catalyzed alkylation of amines by alcohols was reported (*32*).
26. Y. Watanabe, Y. Tsuji, H. Ige, Y. Ohsugi, T. Ohta, *J. Org. Chem.* **49**, 3359 (1984).
27. R. A. T. M. Abbenhuis, J. Boersma, G. van Koten, *J. Org. Chem.* **63**, 4282 (1998).
28. S. P. Rannard, N. J. Davis, *Org. Lett.* **2**, 2117 (2000).
29. M. A. Ointon, A. J. Parker, J. M. J. Williams, *Org. Lett.* **9**, 73 (2007).
30. T. Naota, S.-I. Murahashi, *Synlett* **1991**, 693 (1991).
31. K. Fujita, Y. Takahashi, M. Owaki, K. Yamamoto, R. Yamaguchi, *Org. Lett.* **6**, 2785 (2004).
32. M. H. S. A. Hamid, J. M. J. Williams, *Chem. Commun.* **2007**, 725 (2007).
33. Materials and methods are available as supporting material on *Science* Online.

34. This project was supported by the Israel Science Foundation, the programme for Deutsch-Israelische Partnerschaft, and the Helen and Martin Kimmel Center for Molecular Design. C.G. is the recipient of Deans of Faculties Postdoctoral Fellowship. D.M. is the Israel Matz Professor of Organic Chemistry.

Supporting Online Material

www.sciencemag.org/cgi/content/full/317/5839/790/DC1
Materials and Methods
References

17 May 2007; accepted 13 June 2007
10.1126/science.1145295

Orbital and Millennial Antarctic Climate Variability over the Past 800,000 Years

J. Jouzel,[1]* V. Masson-Delmotte,[1] O. Cattani,[1] G. Dreyfus,[1] S. Falourd,[1] G. Hoffmann,[1] B. Minster,[1] J. Nouet,[1] J. M. Barnola,[2] J. Chappellaz,[2] H. Fischer,[3] J. C. Gallet,[2] S. Johnsen,[4,5] M. Leuenberger,[6] L. Loulergue,[2] D. Luethi,[6] H. Oerter,[3] F. Parrenin,[2] G. Raisbeck,[7] D. Raynaud,[2] A. Schilt,[6] J. Schwander,[6] E. Selmo,[8] R. Souchez,[9] R. Spahni,[6] B. Stauffer,[6] J. P. Steffensen,[2] B. Stenni,[10] T. F. Stocker,[6] J. L. Tison,[9] M. Werner,[11] E. W. Wolff[12]

A high-resolution deuterium profile is now available along the entire European Project for Ice Coring in Antarctica Dome C ice core extending this climate record back to marine isotope stage 20.2, 800,000 years ago. Experiments performed with an atmospheric general circulation model including water isotopes support its temperature interpretation. We assessed the general correspondence between Dansgaard-Oeschger events and their smoothed Antarctic counterparts for this Dome C record, which reveals the presence of such features with similar amplitudes during previous glacial periods. We suggest that the interplay between obliquity and precession accounts for the variable intensity of interglacial periods in ice core records.

The European Project for Ice Coring in Antarctica (EPICA) has provided two deep ice cores in East Antarctica, one (EDC) at Dome C (*1*), on which we focus here, and one (EDML) in the Dronning Maud Land area (*2*). The Dome C drilling (fig. S1 and supporting online material (SOM) text) was stopped at a depth of 3260 m, about 15 m above the bedrock. A preliminary low-resolution δD record was previously obtained from the surface down to 3139 m with an estimated age at this depth of 740,000 years before the present (740 ky B.P.), corresponding to marine isotope stage (MIS) 18.2 (*1*). Other data, such as grain radius, dust concentration, dielectric profile, and electrical conductivity, as well as chemical data (*3*), are available down to this depth, and analyses of the entrapped air have extended the greenhouse gas record (i.e., CO_2, CH_4, and N_2O) back to MIS 16, ~650 ky B.P. (*4*, *5*).

[1]Laboratoire des Sciences du Climat et l'Environnement/Institut Pierre Simon Laplace, CEA-CNRS–Université de Versailles Saint-Quentin en Yvelines, CE Saclay, 91191, Gif-sur Yvette, France. [2]Laboratoire de Glaciologie et Géophysique de l'Environnement, CNRS/Université Joseph Fourier, Boîte Postale 96, 38402 Saint Martin d'Hères, France. [3]Alfred Wegener Institute for Polar and Marine Research, Columbusstrasse, D27568 Bremerhaven, Germany. [4]Department of Geophysics, Juliane Maries Vej 30, University of Copenhagen, DK-2100, Copenhagen, Denmark. [5]Science Institute, University of Reykjavik, Dunhaga 3, Reykjavik 107, Iceland. [6]Physics Institute, University of Bern, Sidlerstrasse 5, CH 3012 Bern, Switzerland. [7]Centre de Spectrométrie Nucléaire et de Spectrométrie de Masse/CNRS, Bat 108, 91405, Orsay, France. [8]Department of Earth Sciences, University of Parma, 43100 Parma, Italy. [9]Département des Sciences de la Terre et de l'Environnement, Université Libre de Bruxelles, Brussels, Belgium. [10]Department of Geological, Environmental and Marine Sciences, University of Trieste, 34127 Trieste, Italy. [11]Max Planck Institute for Biogeochemistry, 100164, 07701 Jena, Germany. [12]British Antarctic Survey, High Cross, Madingley Road, Cambridge, CB3 0ET, UK.

*To whom correspondence should be addressed. E-mail: jean.jouzel@lsce.cea.fr

We completed the deuterium measurements, δD_{ice}, at detailed resolution from the surface down to 3259.7 m. This new data set benefits from a more accurate dating and temperature calibration of isotopic changes based on a series of recent simulations performed with an up-to-date isotope model. In turn, this very detailed Antarctic surface temperature record sheds light on climate analyses in four ways. (i) It allows reliable extension of the climate record back to MIS 20.2 (~800 ky B.P.); (ii) it resolves Antarctic millennial variability over eight successive glacial periods; (iii) it allows quantifiable comparison of the strengths of the successive interglacial and glacial periods; and (iv) the improved time scale allows more accurate investigation of the links between Antarctic temperature and orbital forcing.

This detailed and continuous δD_{ice} profile is shown as a function of time in Fig. 1 and on a depth scale in figs. S2 and S3. For our analysis, we adopted a more precise time scale (SOM text), in which EDC3 has a precision of ~5 ky on absolute ages and of ~20% for the duration of events (*6*, *7*). This scale clearly indicates that the Antarctic counterpart of MIS 15.1 was too long by about a factor 2 in EDC2 (*1*), as already suggested from the comparison with the deep-sea core record (*8*), whereas the scale confirms the long duration of MIS 11.3 (*1*).

The deep-sea benthic oxygen-18 record (*8*) and the δD_{ice} Dome C record are in excellent overall agreement back to ~800 ky B.P. (MIS 20.2), which suggests that our extended EPICA Dome C record now entirely encompasses glacial stage MIS 18 and interglacial MIS 19. This agreement does not hold true for the earlier part of the record below ~3200 m, and we have strong arguments that the core stratigraphy has been disturbed over its bottom 60 m (SOM text). In contrast, the stratigraphic continuity of the record above ~3200 m is supported by all available data, including preliminary CO_2 and CH_4 measurements performed along the transition between MIS 20.2 and 19 (SOM text). We are thus confident that the Dome C δD record provides an ~800-ky-old reliable climatic record.

Results derived from a series of experiments performed with the European Centre Hamburg Model General Circulation Model implemented with water isotopes (*9*) for different climate stages (SOM text) allowed us to assess the validity of the conventional interpretation of ice core isotope profiles (δD or $\delta^{18}O$) from inland Antarctica, in terms of surface temperature shifts (fig. S4). We inferred that the change in surface temperature (ΔT_s) range, based on 100-year mean values, was 15°C over the past 800 ky, from −10.3°C for the coldest 100-year interval of MIS 2 to +4.5°C for the warmest of MIS 5.5 (Fig. 2). Despite some differences, the three long East Antarctic isotopic records, Dome C, Vostok (*10*, *11*), and Dome F (*12*), show a very high level of similarity over their common part, and the EDC temperature record is expected to be representative of East Antarctica. All glacial stages before 430 ky B.P. are warmer than MIS 2, by ~1°C for MIS 12, 16, and 18 and by 2°C for MIS 14 (Fig. 2).

We confirm that the early interglacials periods, now including MIS 19, were characterized by less pronounced warmth than those of the past four climate cycles (*1*). Whereas peak temperatures in the warm interglacials of the later part of the record (MIS 5.5, 7.5, 9.3, and 11.3) were 2° to 4.5°C higher than the last millennium, maximum temperatures were ~1° to 1.5°C colder for MIS 13, 15.1, 15.5, and 17, reaching levels typical of interstadials, such as 7.1 and 7.3. MIS 19 shows the warmest temperature for the period before T_s (~ −0.5°C). For MIS 11 to MIS 17, with the exception of MIS 15.1, peak warmth occurred at the end of the warm periods in contrast with the more recent interglacials for which earlier peak warmth was typical (Fig. 2).

Although isotopic records from Antarctica do not exhibit the rapid and large climate variability observed in Greenland records for the so-called Dansgaard-Oeschger (DO) events of the last glacial period (*13*–*15*), they clearly exhibit millennial-scale variability with muted and more symmetrical events. Synchronization based on gas indicators unambiguously showed that large DO events have Antarctic counterparts (*16*, *17*), and there were indications that shorter events also have such counterparts both from Vostok and Dome C cores (*18*–*20*).

The recent high-resolution EDML isotopic profile over the last glacial period has unambiguously revealed a one-to-one correspondence between all these Antarctic Isotope Maxima (AIM) and DO events (*2*), which with a few exceptions holds true for the EDC core over the entire last glacial period back to DO 25 (Fig. 2 and fig. S5). At Dome C, the typical amplitude of larger events is ~2°C, much lower than for corresponding DO warmings in Greenland, which are often larger than 8°C and as high as 16°C (*21*, *22*).

Although some AIM events are more prominent in one of the two EPICA sites (fig. S5), they record millennial variability of comparable magnitude (SOM text), despite the fact that EDML is situated in the Atlantic sector whereas Dome C is facing the Indo-Pacific Ocean. Atmospheric circulation and/or efficient circumpolar oceanic currents can contribute to distribute such climatic signals around Antarctica. This detailed comparison between EDC and EDML records further supports the thermal bipolar seesaw hypothesis (*23*), which postulates that abrupt shutdowns and initiations of the Atlantic meridional overturning circulation produce slow warmings and coolings in the Southern Ocean and Antarctic region.

Our record exhibits quite similar millennial climate variability during the past three glacial periods, in terms of both magnitude and pacing (fig. S5), suggesting this was also the case in the North Atlantic, as indicated by sediment data (*24*) and inferred from CH_4 data from Antarctic cores (*5*, *25*). Our lower temporal resolution prevents clear detection of small AIM for earlier glacials, but the amplitude of large AIM, thus presumably of large DO events, does not appear to be substantially influenced by the smaller extent of Northern Hemisphere ice sheets before Termination V. In particular, a very well featured sequence is displayed by the additional cycle provided by the extension of the core from 740 and 800 ky B.P. (Fig. 2 and fig. S5) with three well-marked oscillations that have not yet had counterparts identified in the MIS 18 ocean record (*8*). Finally, our record shows that during each glacial period, AIM events appear once Antarctic temperatures have dropped by at least 4°C below late Holocene temperature (Fig. 2). We suggest that decreases in Antarctic temperature over glacial inceptions modified the formation of Antarctic bottom waters and that the associated reorganization in deep ocean circulation is the key for the onset of glacial instabilities.

Obliquity changes were previously invoked to explain the change in amplitude between glacial and interglacial periods at the time of the Mid-Brunhes Event (MBE), ~430 ky B.P. (*1*). This key characteristic of the EDC δD record is now fully supported by our 800-ky detailed temperature record and its improved EDC3 time scale (Fig. 3). Dominated by a periodicity of ~100 ky, the power spectra of ΔT_z (fig. S6) also reveal a strong obliquity component and point to the influence of the precession, at least for 0 to 400 ky. The relative strength of the obliquity and 100-ky components increases when going from past to present, which is consistent with the increasing amplitude of obliquity variations over the past 800 ky due to a 1.2-million-year modulation (*26*). The 40-ky component is particularly strong, accounting for one-third (4.3°C) of the total range of temperature in the 800-ky record (Fig. 3). Also noticeable are its strong coherency with 65°N summer insolation in the obliquity range (0.97) and its substantial ~5-ky lag with respect to obliquity (fig. S7).

Intermediate-complexity climate models indeed capture a high-latitude signature in annual mean temperature in response to extreme configurations of obliquity, albeit half of that observed here (*27*). With respect to the strong linear relationship between δD and obliquity, the link may be local insolation changes, which at 75°S vary by ~8‰ up to 14 W m^{-2} (*28*). Such changes in high-latitude insolation may be amplified by associated changes in heat and moisture transport in the atmosphere (including water vapor and sea-ice feedbacks at high latitudes). They can thus generate changes in the density of ocean surface waters and therefore in ocean thermohaline circulation; such processes involve deep ocean heat storage with constants of millennia. Notably, the obliquity components of temperature records from the tropical Pacific and from Antarctica are in phase (*29*) within age scale uncertainties. They are thus in phase with the mean annual insolation at high latitude but out of phase with the obliquity component of the mean annual insolation in the tropics. This indicates that mechanisms transferring the high-latitude effect of obliquity

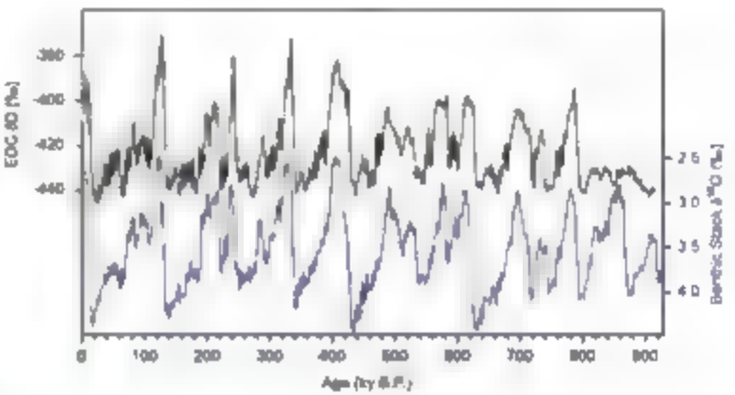

Fig. 1. Comparison of the δD Dome C record on the EDC3 time scale (with all data points in light gray and a smoothed curve in black) with the benthic oxygen-18 record (blue) on its own time scale (*8*). The 3259.7-m δD record, which includes published results down to 788 m (*38*), benefits from an improved accuracy (1σ of ± 0.5‰) and a much more detailed resolution of 55 cm all along the core, whereas the previously published record was based on 3.85-m samples (*1*). The agreement between the two time series back to ~800 ky B.P. justifies the use of oceanic sediment nomenclature (MIS) for describing the ice core record.

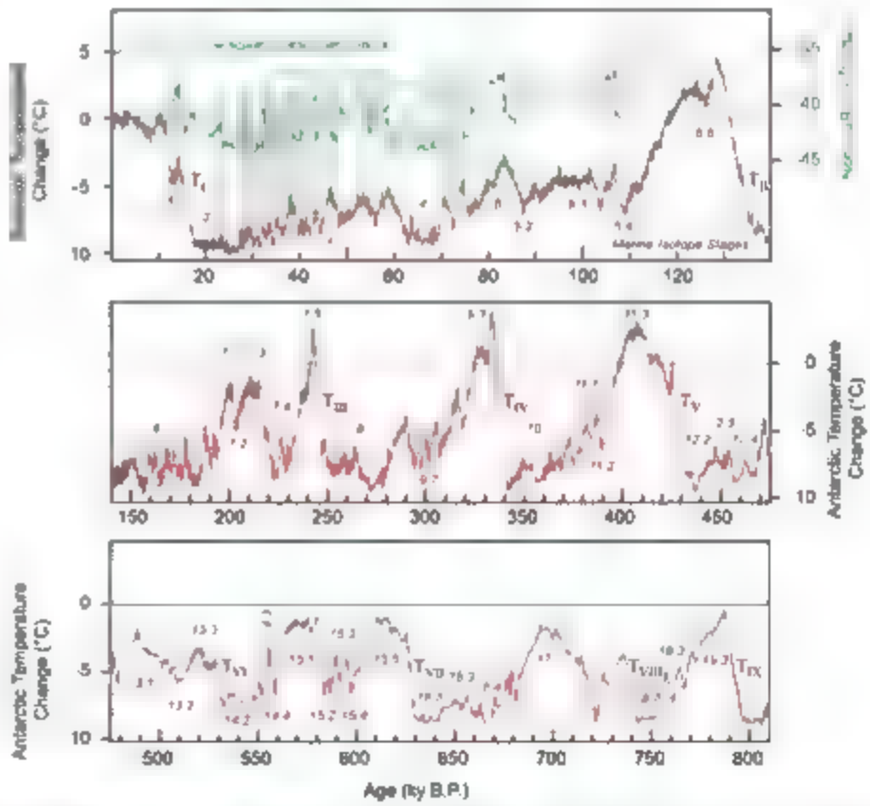

Fig. 2. Dome C temperature anomaly as a function of time over the past 810 ky. Back to 140 ky B.P., we report 100-year mean values, whereas for earlier periods (middle and lower traces), ΔT_z is calculated from 0.55-m raw data; a smooth curve using a 700-year binomial filter is superimposed on this detailed record. In the upper trace (which is plotted on a more highly resolved time axis), we show the correspondence between the DO events as recorded in the North Greenland Ice Core Project isotopic record (*2*, *15*) and AIM events recorded in the EDC temperature record during the last glacial period and the last deglaciation. We have indicated the successive MIS, and the transitions are labeled from T_I to T_{IX}.

toward the tropics may involve changes in heat export from the tropics.

Our EDC ice core shows no indication that greenhouse gases have played a key role in such a coupling. Not only does the obliquity component of the radiative forcing (calculated accounting for both CO_2 and CH_4 changes (*30*)) have a small amplitude over the past 650 ky (~0.5 W m^{-2}, Fig. 3) but it also seems to lag Antarctic and tropical temperature changes. Nor can this in-phase temperature behavior be explained by local insolation, given that this parameter is in antiphase between low and high latitudes. Rather than assuming that this is caused by greenhouse coupling, we suggest that it results from a transfer of the high-latitude obliquity signal to the tropics through rapid processes involving atmospheric circulation or intermediate oceanic waters, possibly linked, as documented from present-day climates (*31*) and examined for past climates (*32*), with changes in sea-ice around Antarctica. The amplitude of the radiative greenhouse forcing, however, is very important in the 100-ky band (~2.5 W/m^2 comparable to the additional greenhouse forcing due to anthropogenic activities). This points to a strong carbon-cycle feedback involved in the magnitude and possibly duration of ice ages (*33*) and to a global character of the Antarctic temperature record.

One key question in this frequency band concerns the relative role of the different orbital parameters in driving terminations. Some authors suggest that terminations occur at multiples of obliquity (*34*, *35*) or precession cycles (*36*). The latter includes the insolation canon hypothesis that calls upon the interplay of precession and obliquity with considerations of total energy input and threshold effects (*37*). With our current age scale, the insolation canon approach works well for T_I to T_{IV} but not for earlier terminations. We support the view of combined effects of precession and obliquity in driving ice age dynamics but suggest that the role of obliquity is underestimated by this approach [e.g., high-latitude insolation should not be considered for mid-month but integrated over several months (*35*)].

The strength of interglacials is highly variable along the record. We suggest that this variation results from an interplay between obliquity and precession (Fig. 3). When 65°N summer insolation (or the inverted precession parameter) and obliquity changes peak in phase (within 5 ky), their combined effects induce strong interglacial periods (MIS 1, 5, 9, 11, and 19). When they are in antiphase, compensating effects induce weak interglacial intensities (MIS 13, 15, 17, and 7.3). In this line, we calculated for each interglacial the cumulative warmth defined with respect to a temperature threshold; we then explored the relationship between this index and insolation. This analysis accounts for the effects of both precession (in the timing of glacial-interglacial transitions) and obliquity (through the mean annual high-latitude insolation). The most robust result is obtained when comparing the cumulative warmth with the cumulative high-latitude insolation (above its average value and taking into account the phase lag of 5 ky). Whereas for small changes in insolation, there is no clear relationship between these two, a linear relationship is observed when the cumulative insolation is larger than ~1700 GJ/m^2 (fig. S8). In turn, we suggest a causal link between the change of amplitude observed in the EDC temperature record and the modulated amplitude of obliquity.

Our new high-resolution Antarctic climate record is able to resolve systematic long-term as well as millennial changes over the past 800,000 years. Whereas the former may be controlled by local insolation changes largely induced by the obliquity cycle, the latter are induced by changes in North Atlantic deep water formation through the thermal bipolar seesaw. Clearly shown for the last glacial cycle, this is also suggested for earlier glacial periods. Overall, our Antarctic temperature record points to an active role for high southern latitudes in the dynamics of climate change both at orbital and millennial time scales, rather than to a picture of these polar regions simply recording variability originating from other parts of the climate system. This climate record will now serve as a benchmark for exploiting the many properties that are, or will be in the near future, measured on the Dome C core both in the ice (elemental and isotopic composition of dust and of chemical compounds) and in the gas phase (records of greenhouse gases, other atmospheric compounds, and their isotopic signatures).

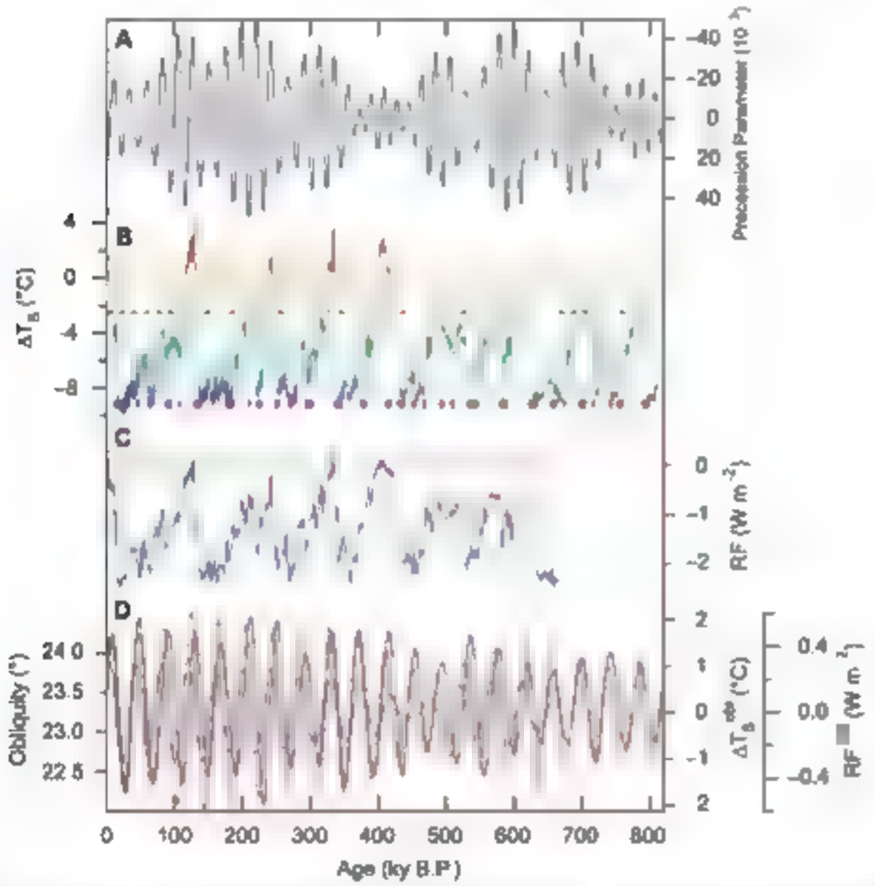

Fig. 3. (**A**) Precession parameter displayed on an inversed vertical axis (black line). (**B**) EDC temperature [solid line, rainbow colors from blue (cold temperatures) to red (warm temperatures)] and its obliquity component extracted using a Gaussian filter within the frequency range 0.043 ± 0.015 ky^{-1} [dashed red line, also displayed in (D) as a solid red line on a different scaling]. Red rectangles indicate periods during which obliquity is increasing and precession parameter is decreasing. (**C**) Combined top-of-atmosphere radiative forcing due to CO_2 and CH_4 (solid blue) and its obliquity component (dashed blue, also displayed in (D) as a solid blue line on a different scaling). (**D**) Obliquity (solid black line), obliquity component of EDC temperature (red line), and obliquity component of the top-of-atmosphere radiative forcing due to CO_2 and CH_4 (blue). Insolations were calculated using the Analyseries software (*39*).

References and Notes

1. EPICA Community members, *Nature* **429**, 623 (2004).
2. EPICA Community members, *Nature* **444**, 195 (2006).
3. E. W. Wolff *et al.*, *Nature* **440**, 491 (2006).
4. U. Siegenthaler *et al.*, *Science* **310**, 1313 (2005).
5. R. Spahni *et al.*, *Science* **310**, 1317 (2005).
6. F. Parrenin *et al.*, *Clim. Past* **3**, 243 (2007).
7. G. Dreyfus *et al.*, *Clim. Past* **3**, 341 (2007).
8. L. Lisiecki, M. E. Raymo, *Paleoceanography* **20**, PA1003 (2005).
9. G. Hoffmann, M. Werner, M. Heimann, *J. Geophys. Res.* **103**, 16871 (1998).
10. J. R. Petit *et al.*, *Nature* **399**, 429 (1999).
11. D. Raynaud *et al.*, *Nature* **436**, 39 (2005).
12. O. Watanabe *et al.*, *Nature* **422**, 509 (2003).
13. W. Dansgaard *et al.*, *Nature* **364**, 218 (1993).
14. P. M. Grootes, M. Stuiver, J. W. C. White, S. J. Johnsen, J. Jouzel, *Nature* **366**, 552 (1993).

15. North Greenland Ice-core project (NorthGRIP), *Nature* **431**, 147 (2004).
16. T. Blunier, E. J. Brook, *Science* **291**, 109 (2001).
17. N. Caillon *et al.*, *Geophys. Res. Lett.* **30**, 1899 (2003).
18. F. Yiou *et al.*, *J. Geophys. Res.* **102**, 26783 (1997).
19. M. Bender, B. Malaizé, J. Orchado, T. Sowers, J. Jouzel, in *Geophys. Monogr. Am. Geophys. Union 112*, P. U. Clark, R. S. Webb, L. D. Keigwin, Eds. (American Geophysical Union, Washington, DC, 1999) pp. 149–164.
20. B. Stenni *et al.*, *Earth Planet. Sci. Lett.* **217**, 183 (2004).
21. A. Landais, J. Jouzel, V. Masson-Delmotte, N. Caillon, *CRAS* **377**, 947 (2005).
22. C. Huber *et al.*, *Earth Planet. Sci. Lett.* **243**, 504 (2006).
23. T. Stocker, S. J. Johnsen, *Paleoceanography* **18**, 1087 (2003).
24. M. Delmotte *et al.*, *J. Geophys. Res.* **109**, D12104 (2004).
25. J. F. McManus, D. W. Oppo, J. L. Cullen, *Science* **283**, 971 (1999).
26. H. Pälike, N. J. Shackleton, U. Röhl, *Earth Planet. Sci. Lett.* **193**, 589 (2001).
27. V. Masson-Delmotte, *Clim. Past* **2**, 145 (2006).
28. A. L. Berger, *J. Atmos. Sci.* **35**, 2362 (1978).
29. M. Medina-Elizalde, D. Lea, *Science* **310**, 1009 (2005).
30. The radiative forcing is calculated using the mathematical formulation described in F. Joos, *PAGES News*, **13**, 11 (2005).
31. X. J. Yuan, D. G. Martinson, *J. Clim.* **13**, 1697 (2000).
32. S. Y. Lee, C. Poulsen, *Earth Planet. Sci. Lett.* **248**, 253 (2006).
33. F. Parrenin, O. Paillard, *Earth Planet. Sci. Lett.* **214**, 243 (2003).
34. P. Huybers, C. Wunsch, *Nature* **434**, 491 (2005).
35. P. Huybers, *Science* **313**, 508 (2006).
36. M. E. Raymo, L. E. Lisiecki, K. H. Nisancioglu, *Science* **313**, 492 (2006).
37. K. G. Schulz, R. E. Zeebe, *Earth Planet. Sci. Lett.* **249**, 326 (2006).
38. J. Jouzel *et al.*, *Geophys. Res. Lett.* **28**, 3199 (2001).
39. D. Paillard, L. Labeyrie, P. Yiou, *Eos Trans. AGU* **77**, 379 (1996).
40. This work is a contribution to EPICA, a joint European Science Foundation/European Commission (EU) scientific program, funded by the EU and by national contributions from Belgium, Denmark, France, Germany, Italy, The Netherlands, Norway, Sweden, Switzerland, and the UK. This is EPICA publication number 181. This work has in particular benefited from the support of EPICA-MIS of the European 6th framework and Agence Nationale de la Recherche (ANR), Integration des Contraintes Paleoclimatiques pour Reduire les Incertitudes sur l'Evolution du Climat pendant les Périodes Chaudes (PICC). The main logistic support was provided by Institut Polaire Français Paul-Emile Victor and Programma Nazionale Ricerche in Antartide (at Dome C and Alfred Wegener Institute (at Dronning Maud Land). We thank the Dome C logistics teams led by late M. Zucchelli and G. Jugie) and the drilling team that made the science possible. This work has benefited from discussions with H. Pälike.

Supporting Online Material

www.sciencemag.org/cgi/content/full/1141038/DC1
SOM Text
Figs. S1 to S8
References

8 February 2007; accepted 11 June 2007
Published online 5 July 2007
10.1126/science.1141038
Include this information when citing this paper.

Improved Surface Temperature Prediction for the Coming Decade from a Global Climate Model

Doug M. Smith,* Stephen Cusack, Andrew W. Colman, Chris K. Folland, Glen R. Harris, James M. Murphy

Previous climate model projections of climate change accounted for external forcing from natural and anthropogenic sources but did not attempt to predict internally generated natural variability. We present a new modeling system that predicts both internal variability and externally forced changes and hence forecasts surface temperature with substantially improved skill throughout a decade, both globally and in many regions. Our system predicts that internal variability will partially offset the anthropogenic global warming signal for the next few years. However, climate will continue to warm, with at least half of the years after 2009 predicted to exceed the warmest year currently on record.

It is very likely that the climate will warm over the coming century in response to changes in radiative forcing arising from anthropogenic emissions of greenhouse gases and aerosols (*1*). There is, however, particular interest in the coming decade, which represents a key planning horizon for infrastructure upgrades, insurance, energy policy, and business development. Over this timescale, climate could be dominated by internal variability (*2*) arising from unforced natural changes in the climate system such as El Niño, fluctuations in the thermohaline circulation, and anomalies of ocean heat content. This could lead to short-term changes, especially regionally, that are quite different from the mean warming (*3*–*5*) expected over the next century in response to anthropogenic forcing. Idealized studies (*6*–*12*) show that some aspects of internal variability could be predictable several years in advance, but actual predictive skill assessed against real observations has not previously been reported beyond a few seasons (*13*).

Global climate models have been used to make predictions of climate change on decadal (*14*, *15*) or longer time scales (*4*, *5*, *16*), but these only accounted for projections of external forcing, neglecting initial condition information needed to predict internal variability. We examined the potential skill of decadal predictions using the newly developed Decadal Climate Prediction System (DePreSys), based on the Hadley Centre Coupled Model, version 3 (HadCM3) (*17*), a dynamical global climate model (GCM). DePreSys (*18*) takes into account the observed state of the atmosphere and ocean in order to predict internal variability, together with plausible changes in anthropogenic sources of greenhouse gases and aerosol concentrations (*19*) and projected changes in solar irradiance and volcanic aerosol (*20*).

We assessed the accuracy of DePreSys in a set of 10-year hindcasts (*21*), starting from the first of March, June, September, and December from 1982 to 2001 (*22*) inclusive (80 start dates in total, although those that project into the future cannot be assessed at all lead times). We also assessed the impact of initial condition information by comparing DePreSys against an additional hindcast set (hereafter referred to as NoAssim), which is identical to DePreSys but does not assimilate the observed state of the atmosphere or ocean. Each NoAssim hindcast consists of four ensemble members, with initial conditions at the same 80 start dates as the DePreSys hindcasts taken from four independent transient integrations (*3*) of HadCM3, which covered the period from 1860 to 2001 (*18*). The NoAssim hindcasts sampled a range of initial states of the atmosphere and ocean that were consistent with the internal variability of HadCM3 but were independent of the observed state. In contrast, the DePreSys hindcasts were initialized by assimilating atmosphere and ocean observations into one of the transient integrations (*18*). In order to sample the effects of error growth arising from imperfect knowledge of the observed state, four DePreSys ensemble members were initialized from consecutive days preceding and including each hindcast start date (*23*). Fig. S1 summarizes our experimental procedure.

We measured the skill of the hindcasts in terms of the root mean square error (RMSE) (*24*) of the ensemble average and tested for differences over our hindcast period between DePreSys and NoAssim that were unlikely to be accounted for by uncertainties arising from a finite ensemble size and a finite number of validation points (*18*). We found that global anomalies (*25*) of annual mean surface temperature (T_a) were predicted with significantly more skill by DePreSys than by NoAssim throughout the range of the hindcasts (compare the solid red curve with the blue shading in Fig. 1A). Averaged over all forecast lead times, the RMSE of global annual mean T_a is 0.132°C for NoAssim as compared with 0.105°C for DePreSys, representing a 20% reduction in RMSE and a 36% reduction in error variance (*E*). Furthermore, the improvement was even greater for multiannual means. For 5-year means, the RMSE was reduced by 38% (a 61% reduction in *E*), from 0.106°C to

Met Office Hadley Centre, FitzRoy Road, Exeter, Ex1 3PB, UK.
*To whom correspondence should be addressed. E-mail: doug.smith@metoffice.gov.uk

0.066°C, and for 9-year means, the RMSE was reduced by 49% (a 74% reduction in E), from 0.090°C to 0.046 C.

Because the internal variability of the atmosphere is essentially unpredictable beyond a couple of weeks (*26*), and the external forcing in DePreSys and NoAssim is identical, differences in predictive skill are very likely to be caused by differences in the initialization and evolution of the ocean. During 600 years of the HadCM3 control integration T_g is highly correlated (correlation $R = 0.89$) with global annual mean ocean heat content in the upper 113 m (H). Furthermore, the correlation is higher when H leads T_g by 1 year ($R = 0.56$) than when T_g leads H by 1 year ($R = 0.32$), providing strong evidence that variations in H can force T_g. We also find that H is predicted with significantly more skill by DePreSys than by NoAssim (Fig. 1B), and we conclude that the improvement of DePreSys over NoAssim in predicting T_g on interannual-to-decadal time scales results mainly from initializing upper ocean heat content.

We now examine the factors that control the predictability of H and T_g on annual-to-decadal time scales. Time series of hindcasts of T_g for 1 year ahead (Fig. 2A) show that both DePreSys and NoAssim capture the observed general warming trend, but the interannual variability of T_g is predicted better by DePreSys (detrended RMSE = 0.066°C) than by NoAssim (detrended RMSE = 0.093°C). A statistical forecast method (*18*) is also able to capture the trend and interannual variability of T_g for the coming year (green triangles in Fig. 2A). The statistical method accounts for interannual variability using predictors based on the state of El Niño and recent volcanic activity. Volcanic activity cannot explain the difference between DePreSys and NoAssim because both include forcing from volcanic aerosol in the same way. We assess the impact of El Niño on the difference between DePreSys and NoAssim as follows. From the transient HadCM3 simulations, we compute linear regression coefficients that relate the state of El Niño, as measured by SST in the Niño3 region (210° to 270°E, 5°S to 5°N), to T_g. Using these coefficients, we compute the contribution to T_g from El Niño for each DePreSys and NoAssim hindcast and remove the difference from the DePreSys hindcasts. We find that the increased skill of DePreSys over NoAssim is consistent with an improved ability to predict El Niño for the first 15 to 18 months, but not at longer lead times (compare the dashed red curve with the blue shading in Fig. 1A).

The hindcasts for year 9 capture the observed mean warming but not the interannual variability (Fig. 2B). This is expected because the main factors governing interannual variability, namely El Niño and volcanic eruptions, are not predictable at this lead time. The 90% confidence limits (*27*) diagnosed from the ensemble spread (red shading) generally capture the observations [supporting online material (SOM) text and fig. S5], apart from the cooling after the eruption of Mount Pinatubo (*28*). This is unavoidable unless volcanic eruptions can be

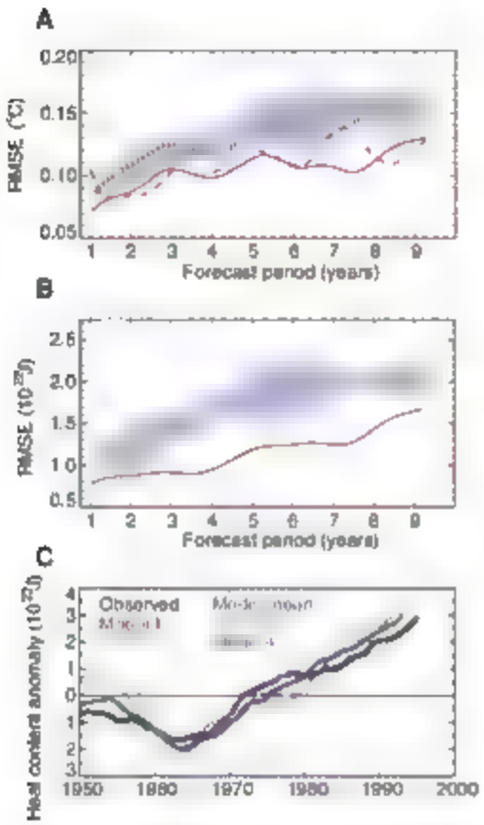

Fig. 1. Impact of initial conditions on hindcast skill. (**A**) RMSE (*24*) of globally averaged annual mean T_g anomalies (relative to 1979–2001) as a function of forecast period. We compare DePreSys (solid red curve) with the NoAssim hindcasts [the blue shading shows the 5 to 95% CI region where differences between DePreSys and NoAssim are not significant (*18*)]. The dashed red curve shows the effect of removing from the DePreSys hindcasts differences between DePreSys and NoAssim that are linearly attributable to the state of El Niño. The dotted red curve shows the effect of removing from the DePreSys hindcasts the mean difference between DePreSys and NoAssim hindcasts of T_g for the coming 9 years. Observations are taken from the HadCRUT2vOA data set (*36*–*38*). (**B**) As (A), but for H (relative to 1941–1996). Observations of H are computed from analyses of ocean temperature observations (*39*). (**C**) Time series of rolling decadal mean global anomalies (relative to 1941–1996) of H from observations (*39*) and the four transient HadCM3 simulations (models 1 to 4) (*3*) that provided initial conditions for the NoAssim hindcasts. Values are plotted annually, with the year representing the mean of the next 10 years.

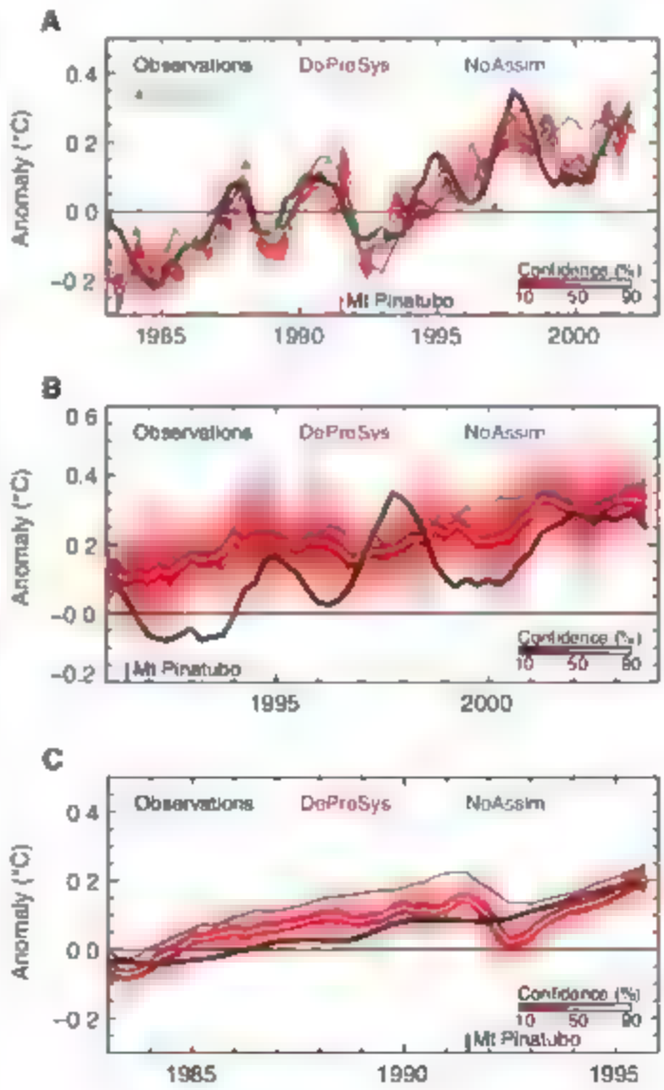

Fig. 2. Time series of hindcast and observed anomalies (relative to 1979–2001) of globally averaged surface temperature. (**A**) Hindcasts of the first annual mean (forecast period of 1 year) compared with observations from HadCRUT2vOA (black curve). Rolling annual mean observations and DePreSys and NoAssim hindcasts are plotted seasonally from March, June, September, and December. Statistical hindcasts are plotted each January. The CI (*27*) (red shading) is diagnosed from the standard deviation of the DePreSys ensemble, assuming a t distribution centered on the ensemble mean (white curve). Only the ensemble mean is shown for the NoAssim hindcasts (blue curve). The mean uncertainty in the observations is ±0.056°C (5 to 95% CI range). (**B**) As (A), but for year 9 of the hindcasts. (**C**) As (A), but for the first 9-year mean of the hindcasts.

predicted, and we note that our decadal forecasts assume that no major volcanic eruptions will occur during the forecast period. We therefore expect both NoAssim and DePreSys hindcasts of periods containing volcanic eruptions to be too warm on average. However, the warm bias is significantly smaller in DePreSys. This is clearly illustrated in hindcasts of 9-year mean T_g (Fig. 2C), for which the DePreSys bias of 0.016°C represents a 79% reduction from the NoAssim bias of 0.075°C. If we remove the difference in these biases (−0.059°C) from the DePreSys hindcasts of annual mean T_g (dotted red curve in Fig. 1A), the RMSE is no longer significantly different from NoAssim at forecast periods greater than 15 months. The cooling of DePreSys relative to NoAssim is consistent with a warm bias of H in the NoAssim initial conditions provided by the transient HadCM3 integrations (Fig. 1C from 1982 onward). Furthermore, the magnitude of this bias is consistent with the level of internal multidecadal variability of H found in both the observations and the individual HadCM3 integrations used to initialize the NoAssim hindcasts (Fig. 1C). We therefore conclude that the increased predictive skill of DePreSys over NoAssim at forecast periods longer than 15 months results mainly from initializing the low-frequency variability of H, thereby removing errors of H from the NoAssim initial conditions (SOM text).

Because forecast errors generally grow with time, differences between the RMSE of NoAssim and DePreSys would be expected to be largest at short lead times. This was not the case in our experiments (Fig. 1, A and B). We investigated this unexpected behavior using a simple energy balance model (EBM) (*29*) to predict the evolution of the average difference in H between the DePreSys and NoAssim initial conditions (SOM text and fig. S2). We found that the detailed evolution of this difference [which increases in magnitude for the first 4 years, decreasing thereafter (fig. S3)] is governed by an atmospheric feedback response to the initial anomaly of H (fig. S4). Furthermore, the RMSE of the trend in global T_g during the first 5 years of the hindcasts is lower in DePreSys than NoAssim (*30*). These results indicate that the evolution of the climate system is predicted better by DePreSys than NoAssim and that some of this improvement results from atmospheric feedbacks simulated by the coupled climate model.

Although global T_g is important for informing greenhouse gas emissions policy, many applications in industry and commerce require regional predictions. We found significant differences between DePreSys and NoAssim RMSE in 9-year mean T_g in many regions (Fig. 3, A to C). Much of the regional improvement in DePreSys relative to NoAssim is coincident with improvements in H (Fig. 3D), particularly in the Indian Ocean and Australasian sector of the Southern Hemisphere [consistent with (*7*)], although there are also some regions where DePreSys gives larger errors than NoAssim. Furthermore, there are significant differences in RMSE over land, the largest improvements occurring in North and South America and eastern Australia (Fig. 3C).

The strong correspondence ($R = 0.75$) between regional differences in T_g and H (Fig. 3, C and D) further supports our conclusion that improvements in DePreSys relative to NoAssim on decadal time scales result mainly from initializing H. Although our hindcast period is limited to 20 years, the existence of natural low-frequency variability of H (*31*) (Fig. 1C) strongly suggests that DePreSys would also improve on NoAssim in other decades, although the regional details could be different. Furthermore, a substantial increase in the number of subsurface ocean observations through the Argo program (*32*) should substantially improve our ability to initialize the ocean in future, thereby leading to further improvements in DePreSys relative to NoAssim both globally and regionally.

Having established the predictive skill of DePreSys, we issued the first GCM-based forecast of global T_g for the coming decade (*33*, *34*) (Fig. 4). The DePreSys forecast is based on 20 ensemble members, 10 starting from consecutive days leading to 1 June 2005, combined with 10 from consecutive days leading to 1 March 2005. We assessed the impact of initial conditions on this forecast by comparing it with a NoAssim forecast, consisting of eight ensemble members. We also compared two eight-member DePreSys and NoAssim hindcasts with observations. The DePreSys hindcast starting from June 1985 correctly predicted a rapid warming during the transition from the weak La Niña of 1985 to the El Niño of 1986–1987 and correctly predicted the warming trend throughout the period until the eruption of Mount Pinatubo.

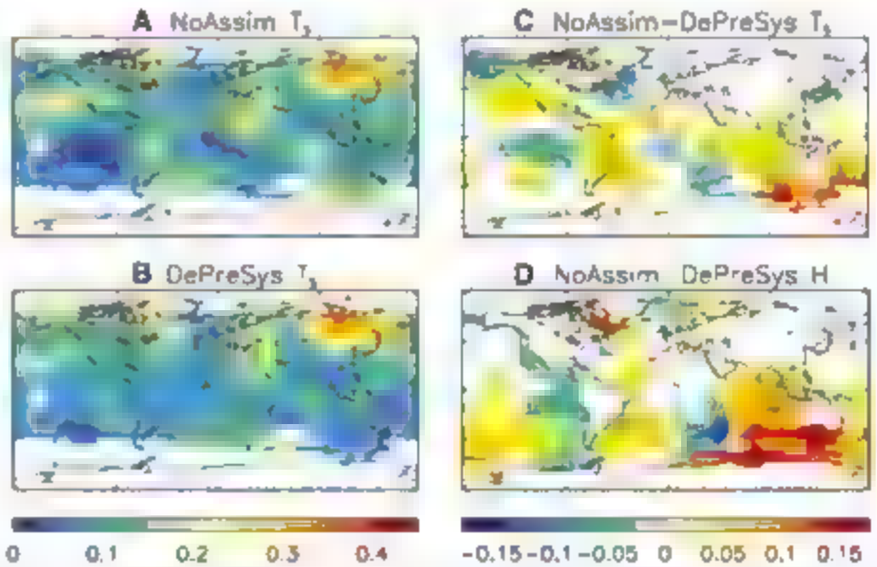

Fig. 3. Impact of initial conditions on regional hindcast skill. (**A**) RMSE of 9-year mean T_g anomalies (relative to 1979–2001) for the ensemble mean NoAssim hindcasts, verified against observations from HadCRUT2v (*36*–*38*). (**B**) As (A), but for DePreSys. (**C**) NoAssim minus DePreSys RMSE of 9-year mean T_g. Differences are shown only where they are significant at the 5% level (*18*). (**D**) As (C), but for 9-year mean H anomalies (relative to 1941–1996). In all panels, each 5° latitude by 5° longitude pixel represents the RMSE for predictions of T_g spatially averaged over the 35° latitude by 35° longitude box centered on that pixel.

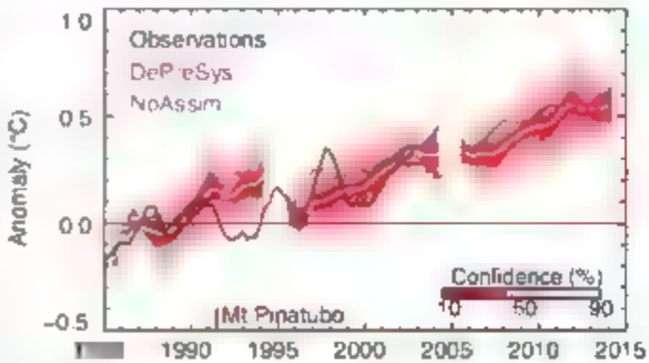

Fig. 4. Globally averaged annual mean surface temperature anomaly (relative to 1979–2001) forecast by DePreSys starting from June 2005. The CI (red shading) is diagnosed from the standard deviation of the DePreSys ensemble, assuming a t distribution centered on the ensemble mean (white curve). Also shown are DePreSys and ensemble mean NoAssim (blue curves) hindcasts starting from June 1985 and June 1995, together with observations from HadCRUT2vGA (black curve). Rolling annual mean values are plotted seasonally from March, June, September, and December. The mean bias as a function of lead time was computed from those DePreSys hindcasts that were unaffected by Mount Pinatubo (SOM text) and removed from the DePreSys forecast (but not the hindcasts).

The DePreSys hindcast starting from June 1995 correctly predicted an initial cooling, followed by a general warming. As expected, the NoAssim hindcasts predicted only the general warming trend, although the NoAssim hindcast from June 1995 is generally too warm. In the DePreSys forecast, internal variability offsets the effects of anthropogenic forcing in the first few years, leading to no net warming before 2008 (Fig. 4). In contrast, the NoAssim forecast warms during this period. Regional assessment to February 2007 (fig. S8) indicates that this initial cooling in DePreSys relative to NoAssim results from the development of cooler anomalies in the tropical Pacific and the persistence of neutral conditions in the Southern Ocean. In both cases, the DePreSys forecast is closer to the verifying changes observed since the forecast start date. Both NoAssim and DePreSys, however, predict further warming during the coming decade, with the year 2014 predicted to be 0.30° ± 0.21°C [5 to 95% confidence interval (CI)] warmer than the observed value for 2004. Furthermore, at least half of the years after 2009 are predicted to be warmer than 1998, the warmest year currently on record.

References and Notes

1. S. Solomon *et al.*, Eds., *Climate Change 2007: The Physical Science Basis. Contribution of Working Group I to the Fourth Assessment Report of the Intergovernmental Panel on Climate Change* (Cambridge Univ. Press, Cambridge, 2007).
2. M. Collins, M. R. Allen, *J. Clim.* **15**, 3104 (2002).
3. P. A. Stott *et al.*, *Science* **290**, 2133 (2000).
4. U. Cubasch *et al.*, in *Climate Change 2001: The Scientific Basis. Contribution of Working Group I to the Third Assessment Report of the Intergovernmental Panel on Climate Change*, J. T. Houghton *et al.*, Eds. (Cambridge Univ. Press, Cambridge, 2001), pp. 525–582.
5. G. A. Meehl *et al.*, in *Climate Change 2007: The Physical Science Basis. Contribution of Working Group I to the Fourth Assessment Report of the Intergovernmental Panel on Climate Change*, S. Solomon *et al.*, Eds. (Cambridge Univ. Press, 2007), pp. 747–845.
6. S. M. Griffies, K. Bryan, *Science* **275**, 181 (1997).
7. A. Grötzner, M. Latif, A. Timmermann, R. Voss, *J. Clim.* **12**, 2607 (1999).
8. M. Collins, B. Sinha, *Geophys. Res. Lett.* **30**, 1306 (2003).
9. M. Latif *et al.*, *J. Clim.* **17**, 1605 (2004).
10. H. Pohlmann *et al.*, *J. Clim.* **17**, 4463 (2004).
11. G. J. Boer, *Clim. Dyn.* **23**, 29 (2004).
12. S. B. Power, R. Colman, X. Wang, P. Hope, *Predictions in Ungauged Basins: International Perspectives on the State of the Art and Pathways Forward*, M. Franks, K. Sivapalan, K. Takeuchi, Y. Tachikawa, Eds. (Publication 301, International Association of Hydrological Science, Wallingford, UK, 2005).
13. T. N. Palmer *et al.*, *Bull. Am. Meteorol. Soc.* **85**, 853 (2004).
14. F. W. Zwiers, *Nature* **416**, 690 (2002).
15. T. C. K. Lee, F. W. Zwiers, X. Zhang, M. Tsao, *J. Clim.* **19**, 5305 (2006).
16. P. A. Stott, J. A. Kettleborough, *Nature* **416**, 723 (2002).
17. C. Gordon *et al.*, *Clim. Dyn.* **16**, 147 (2000).
18. Materials and methods are available as supporting material on *Science* Online.
19. T. C. Johns *et al.*, *Clim. Dyn.* **20**, 583 (2003).
20. Solar irradiance is projected by repeating the previous 11-year solar cycle. Volcanic aerosol is projected as an exponential decay with an *e*-folding time scale of 1 year. Our hindcasts therefore do not use solar or volcanic information that would not have been available at the time.
21. We use the term "hindcast" to refer to a forecast made retrospectively using only data that would have been available at the time.
22. Our hindcast period ends in 2001 because our hindcasts are initialized using the 40-year ECMWF (European Centre for Medium-Range Weather Forecasts) atmosphere reanalysis (*18*), the last complete year of which is 2001.
23. The ensemble size for both DePreSys and NoAssim was further increased by combining with hindcasts from previous seasons. For hindcasts of the coming year, we combine two seasons, giving eight ensemble members. For longer lead times, we combine four seasons, giving [illegible].
24. RMSE $= \sqrt{[\sum_{r=1}^{M} e_r^2]/M}$ where M is the number of hindcasts and e_r is the error of the ensemble mean for each hindcast r averaged over the required spatial region.
25. DePreSys is designed to avoid trends during forecasts caused by systematic model errors. This is achieved by assimilating observed anomalies added to the model climatology and removing the model climatology to produce forecast anomalies. The climatological period is 1979–2001 for the atmosphere and 1941–1996 for the ocean. Further details are given in (*18*).
26. A. J. Simmons, A. Hollingsworth, *Q. J. R. Meteorol. Soc.* **128**, 647 (2002).
27. The confidence interval shown by the red shading in Figs. 2 and 4 should not be confused with the significance limits shown by the blue shading in Fig. 1. The confidence interval is a measure of the uncertainty in a forecast at a single time. The significance limits measure the uncertainty in differences between the skill of NoAssim and DePreSys averaged over all hindcasts.
28. D. E. Parker, H. Wilson, P. D. Jones, J. R. Christy, C. K. Folland, *Int. J. Climatol.* **16**, 487 (1996).
29. G. R. Harris *et al.*, *Clim. Dyn.* **27**, 357 (2006).
30. We computed the RMSE of the linear trend in global T during the first 5 years of each hindcast. The RMSE values are 0.030 and 0.038°C per year for DePreSys and NoAssim respectively, with the difference being significant at the 5% level.
31. S. Levitus, J. Antonov, T. Boyer, *Geophys. Res. Lett.* **32**, L02604 (2005).
32. S. Wilson, *Oceanus* **42**, 17 (2000).
33. Model errors, such as those arising from uncertainties in climate change feedbacks (*35*), are liable to cause biases in predicted changes. We found a modest time-dependent bias in DePreSys hindcasts, unaffected by major volcanic eruptions, rising to 0.07° ± 0.02°C (for year 9 (fig. S6) and removed this from both DePreSys and NoAssim forecasts (Fig. 4).
34. We issue the caveat that any major volcanic eruptions occurring during the forecast period would cool global T, as compared to our forecast.
35. B. J. Soden, I. M. Held, *J. Clim.* **19**, 3354 (2006).
36. C. K. Folland *et al.*, *Geophys. Res. Lett.* **28**, 2621 (2001).
37. D. E. Parker, L. V. Alexander, J. Kennedy, *Weather* **59**, 145 (2004).
38. P. D. Jones, A. Moberg, *J. Clim.* **16**, 206 (2003).
39. D. M. Smith, J. M. Murphy, *J. Geophys. Res.* **112**, C02022 (2007).

40. We thank many colleagues in the Met Office for developing the climate models and for help and advice during the course of this work. This work was supported by the UK Department of the Environment, Food and Rural Affairs, and by the UK Government Meteorological Research Programme.

Supporting Online Material

www.sciencemag.org/cgi/content/full/317/5839/796/DC1
Materials and Methods
SOM Text
Figs. S1 to S8
References

4 January 2007; accepted 19 June 2007
10.1126/science.1139540

Mechanism of Na^+/H^+ Antiporting

Isaiah T. Arkin,[1]* Huafeng Xu,[1] Morten Ø. Jensen,[1] Eyal Arbely,[2] Estelle R. Bennett,[2] Kevin J. Bowers,[1] Edmond Chow,[1] Ron O. Dror,[1] Michael P. Eastwood,[1] Ravenna Flitman-Tene,[2] Brent A. Gregersen,[1] John L. Klepeis,[1] Istvan Kolossvary,[1] Yibing Shan,[1] David E. Shaw[2,3]†

Na^+/H^+ antiporters are central to cellular salt and pH homeostasis. The structure of *Escherichia coli* NhaA was recently determined, but its mechanisms of transport and pH regulation remain elusive. We performed molecular dynamics simulations of NhaA that, with existing experimental data, enabled us to propose an atomically detailed model of antiporter function. Three conserved aspartates are key to our proposed mechanism: Asp^{164} (D164) is the Na^+-binding site. D163 controls the alternating accessibility of this binding site to the cytoplasm or periplasm, and D133 is crucial for pH regulation. Consistent with experimental stoichiometry, two protons are required to transport a single Na^+ ion. D163 protonates to reveal the Na^+-binding site to the periplasm, and subsequent protonation of D164 releases Na^+. Additional mutagenesis experiments further validated the model.

NhaA is the archetypal Na^+/H^+ antiporter and the only member of the family that is absolutely required by *E. coli* for survival in high-salt conditions, under alkaline stress, or in the presence of otherwise toxic Li^+ concentrations (*1*, *2*). It is a membrane protein consisting of 388 residues that traverse the inner membrane 12 times, with both termini ending in the cytoplasm (*3*). The structure of NhaA exhibits a distinctive fold of 10 contiguous transmembrane helices and 2 antiparallel, discontinuous helices (*in* and *inf*) aligned end to end to span the membrane (*3*).

NhaA excretes Na^+ or Li^+ (but not K^+) from the cytoplasm using the energy from the countertransport of protons down their electrochemical gradient into the cell, with a characteristic electrogenic stoichiometry of two protons to one Na^+ or Li^+ (*4*, *5*, *6*). NhaA's activity decreases by three orders of magnitude when shifting from pH 8 to pH 6.5 (*7*), enabling it to regulate cellular acidity in addition to cellular salinity.

[1]D. E. Shaw Research, New York, NY 10036, USA. [2]The Hebrew University of Jerusalem, Department of Biological Chemistry, Jerusalem 91904, Israel. [3]Center for Computational Biology and Bioinformatics, Columbia University, New York, NY 10032, USA.

*On sabbatical leave from The Hebrew University of Jerusalem, Department of Biological Chemistry, Jerusalem, 91904, Israel.

†To whom correspondence should be addressed. E-mail: david@deshaw.com

Using recently developed algorithms for the high-speed, parallel execution of molecular dynamics (MD) simulations (*8*, *11*), we performed simulations of membrane-embedded NhaA with an aggregate length approaching 3 μs, allowing us to examine ion transport, pH regulation, and cation selectivity and to thereby deduce a detailed mechanistic picture of the function of NhaA.

Crystallization of *E. coli* NhaA was performed at pH 4, a state in which the protein is inactive, and accordingly, no Na^+ was seen in the structure (*4*). Hunte *et al.* (*4*) inferred, however, that the Na^+-binding site is near D163 or D164 (*12*), because these have been shown to be the only carboxylic residues absolutely indispensable for transport activity (*13*). Because these residues are likely candidates to undergo protonation state changes that drive Na^+ transport, we simulated NhaA under all four possible combinations of the protonation states of D163 and D164. After equilibration, we initiated MD simulations (12 to 100 ns each) from each of these four configurations, with Na^+ placed adjacent to D163. We then repeated the process, placing Na^+ adjacent to D164.

When Na^+ was placed adjacent to D163, irrespective of the protonation state of D163 or D164, the ion became trapped by the protein and water was unable to penetrate the protein to hydrate it, this finding suggests that D163 is not the Na^+-binding site. The behavior of Na^+ was entirely different when placed adjacent to D164. If D164 was deprotonated, Na^+ remained bound regardless of the protonation state of D163, with water able to reach and hydrate the ion. Placing Na^+ adjacent to protonated D164, however, provided the strongest clues as to how the transporter might function. In this case, the ion was expelled from the protein to the aqueous environment, with the direction of Na^+ release determined by the protonation state of D163. If D163 was protonated, Na^+ was expelled to the periplasm; in contrast, if D163 was deprotonated, Na^+ was expelled to the cytoplasm. (See Fig. 1A.)

We therefore propose that D163 and D164 play different roles in the Na^+ transport mechanism. D164 is the binding site for Na^+. Its protonation state determines whether Na^+ binds to the protein or is released. When D164 is deprotonated and, consequently, negatively charged, Na^+ remains tightly bound as a result of Coulombic attraction. When D164 is protonated, the electrostatic interaction is diminished and Na^+ no longer binds. In contrast, D163 is the accessibility-control site of the protein. Its protonation state is the molecular switch that determines whether the Na^+-binding site (i.e., D164) is accessible to the periplasm or to the cytoplasm. Bound Na^+ can be expelled to the periplasm if D163 is protonated or to the cytoplasm if D163 is deprotonated. In each case, expulsion is accompanied by protonation of D164.

Our simulations provide a structural explanation for how D163 acts as a conformational switch. The carboxylate group of deprotonated D163 makes strong hydrogen bonds with the amide hydrogens of residues M105 and T132 (Fig. 2). Upon protonation, these interactions vanish, and D163 forms a new hydrogen bond between its carboxylic hydrogen and the carbonyl oxygen of M105. This movement causes helix 4 to tilt, which shifts the Na^+-binding site (D164) in the direction of the periplasm.

The local structural changes elicited by D163 protonation lead to global conformational changes (Fig. 2). When D163 is protonated, the cytoplasmic entrance is closed while the periplasmic exit is open. Deprotonation of D163 leads to the closure of the periplasmic Na^+ exit and the opening of the cytoplasmic entrance. Taken together, our data provide a molecular realization of the alternate accessibility mechanism postulated by Jardetzky more than 40 years ago (*14*).

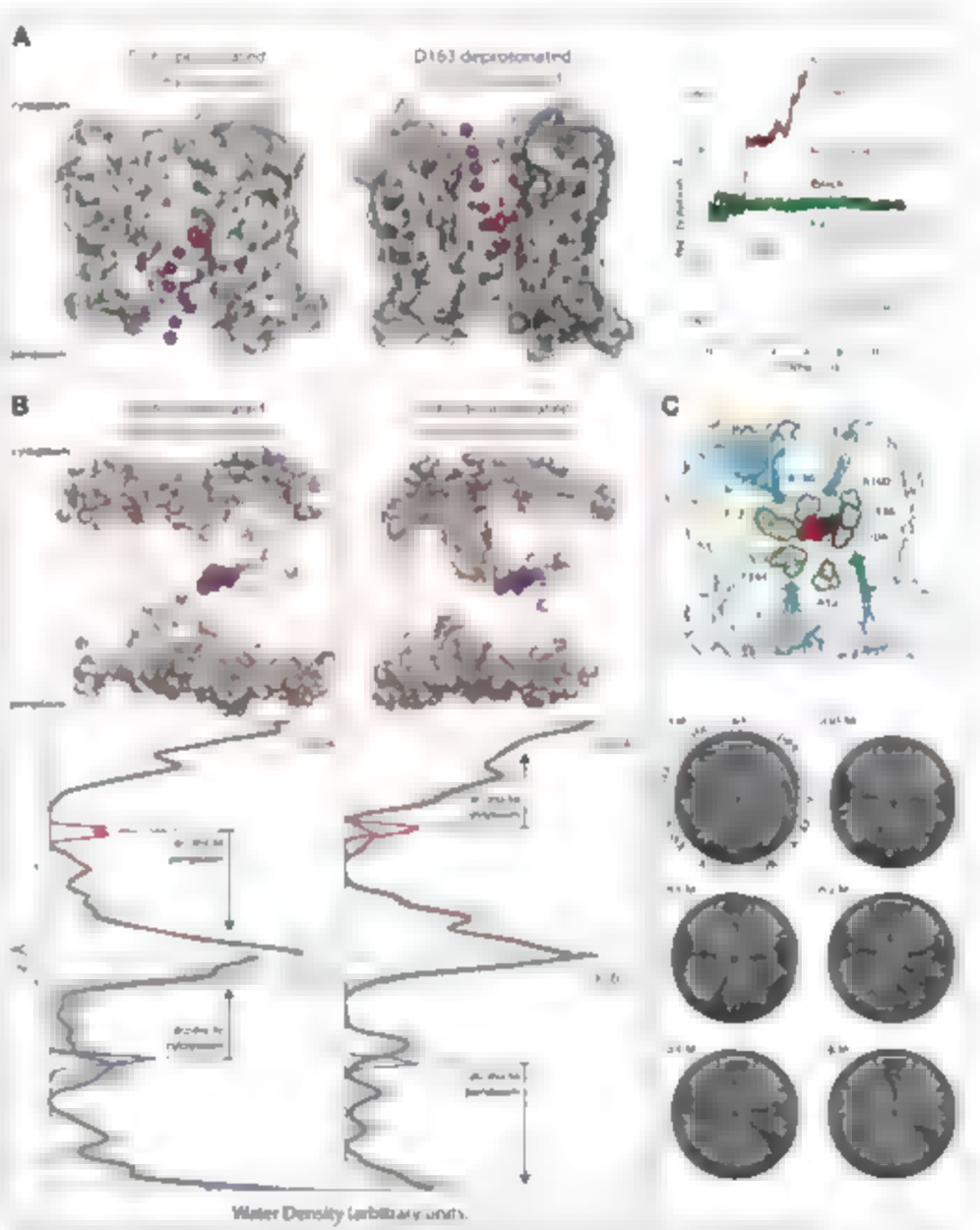

Fig. 1. Na^+ transport and alternating access. D163 and D164 are colored in blue and red, respectively. **(A)** Series of Na^+ (purple) positions when D163 (not shown) is deprotonated or protonated, leading to Na^+ expulsion to the cytoplasm or transport to the periplasm, respectively. The rightmost panel depicts Na^+ position as a function of time in different D163 and D164 protonation states. **(B)** The four graphs show water penetration into the occupied Na^+-binding site at D164 (top graphs) and the regulatory site at D163 (bottom graphs) as a function of position (*z*) across the membrane. The average density and SD were computed from two 60-ns trajectories, with D163 protonated (left) and deprotonated (right). Blue and red lines in graphs represent positions of D163 and D164, respectively. The top panel shows representative snapshots from the simulations, with water molecules shown in pink and white. **(C)** Mutagenesis studies of NhaA. Wild-type (WT) and mutated antiporters were assayed at different NaCl concentrations. Negative control bacteria (pBR) expressed no antiporter. The top panel shows locations of the different mutation sites (green) in the NhaA structure. Substrate pathways from the cytoplasm and periplasm are indicated by blue arrows. Molecular images in Figs. 1, 2, and 4 and Fig. S1 were produced by VMD (*29*), and Fig. 1 and Fig. S3 were generated by PyMOL (*30*).

The hypothesis that the protein contains a Na^+/H^+-binding site at D164 and a H^+-binding site at D163 implies that protons and Na^+ must be able to reach D164 and that protons must be able to reach D163. A putative Na^+ transport pathway, notably blocked in the inactivated x-ray structure, has been suggested (*4*), starting from a large crevice on the cytoplasmic face of the protein, leading to D164, and ending in the periplasm. However, the existence of a pathway to D163 has not been previously considered.

To identify possible ion transport pathways, we determined the water accessibility of the two sites for different protonation states of the protein. Water can reach both D163 and D164 from both sides of the membrane (Fig. 1B), but in no protonation state is there a continuous water density across the protein; such water connectivity might deplete the proton motive force. Instead, when D163 is accessible to the cytoplasm, D164 is accessible to the periplasm (Fig. 1B, left panels), and when D163 is accessible to the periplasm, D164 is accessible to the cytoplasm (Fig. 1B, right panels).

We undertook mutagenesis experiments to substantiate our computational finding of these water pathways to D163. We hypothesized that replacing smaller amino acids with larger ones along these pathways would block access of protons to D163 and thus inhibit the antiporter. Activities of wild-type and mutant antiporters were assayed for their ability to sustain growth of bacteria that do not harbor any of the three native antiporter genes (*15*). Unlike the wild-type antiporters, all mutant antiporters aside from $Ala^{100}\rightarrow Leu^{100}$ (A100L) failed to support growth in elevated concentrations of NaCl (Fig. 1C). Because the G336L mutant protein does not support bacterial growth even in a low concentration of NaCl, it is possible that this protein may be unstable and nonfunctional. The functional comparisons between the mutant antiporters were conducted in vivo, and the concentrations of the different proteins may thus differ despite identical handling.

The inhibitory effects of mutations at A127 and G104 are consistent with blockage of a water-mediated proton pathway to D163 from the periplasm, whereas the inhibitory effect of a mutation of A160 is consistent with blockage of a water-mediated proton entry to D163 from the cytoplasm. Moreover, we explicitly simulated the effect of mutating A127 to leucine (fig. S3) and found that water and, therefore, proton penetration from the periplasm to D163 are indeed blocked. Additional mutagenesis results are reported in the supporting online material (SOM).

Based on these results, we propose a mechanism for the Na^+/H^+ antiporting cycle of NhaA that consists of the following four sequential steps (labeled as in Fig. 3). (A) The accessibility-control site (D163) is deprotonated, resulting in cytoplasmic accessibility of the Na^+-binding site. The Na^+-binding site (D164) therefore releases a H^+ to, and takes up a Na^+ from, the cytoplasm. (B) The accessibility-control site (D163) is protonated by a H^+ that enters from the periplasm. This results in a conformational change (Fig. 2) that exposes the Na^+-binding site to the periplasm. (C) The Na^+-binding site (D164) exchanges the bound Na^+ with a H^+

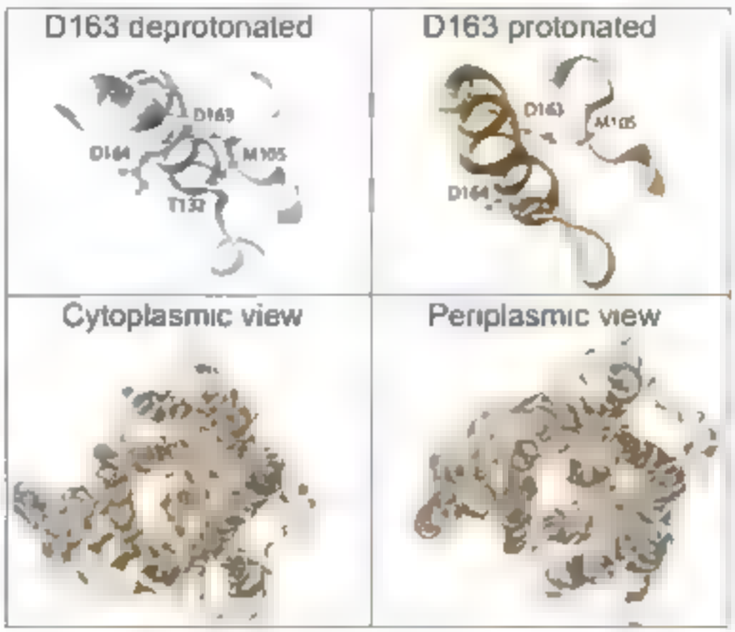

Fig. 2. Effects of D163 protonation state on antiporter conformation. D164 is protonated, such that bound Na^+ would be expelled. The top panels depict the local interaction of D163, whereas the bottom panels illustrate the global conformation of the protein. The structures in which D163 is protonated (orange) and deprotonated (white) are superposed by C_α atoms (D164 is protonated in both structures). The C_α root mean square deviation (RMSD) between the structures is ~2.3 Å when comparing the central helices *iv* to *v*, *ix*, and *xi*.

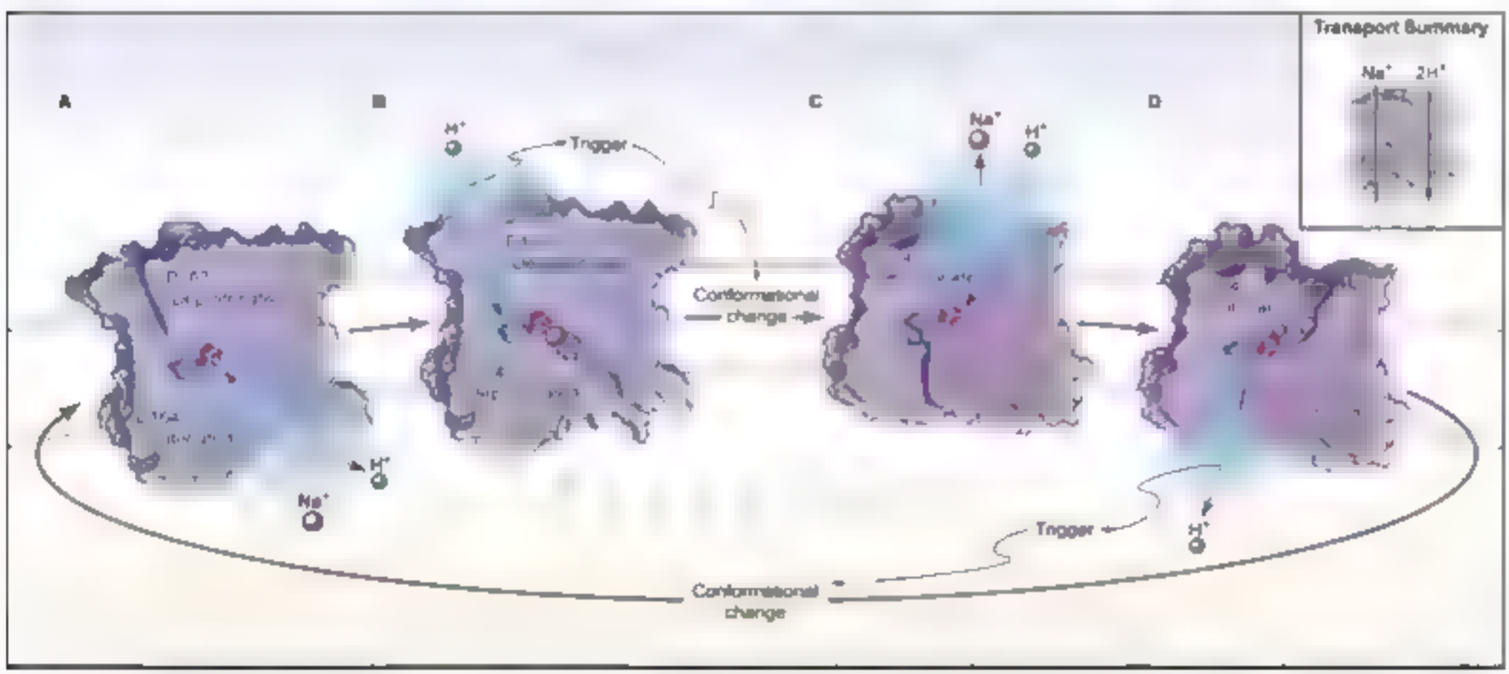

Fig. 3. Schematic representation of the transport model of NhaA. The carboxylic group of D163 in the accessibility-control site is colored blue, and D164 in the Na^+-binding site is red.

from the periplasm. The replacement of bound Na^+ by H^+ could be considered a "knock-on" like mechanism (*16*) acting through electrostatic repulsion (*17*). (D) D163 deprotonates, leading to a protein conformational change that again exposes the Na^+-binding site (D164) to the cytoplasm. Overall, two protons are taken up from the periplasm in panels B and C and released to the cytoplasm in panels A and D (Fig. 3), while a single Na^+ is taken up from the cytoplasm in panel A and then pumped to the periplasm in panel C, which is consistent with NhaA's electrogenic stoichiometry of one Na^+ to two protons (*5*).

Very recent simulations of NhaA (*18*) have explored conformational changes associated with the simultaneous deprotonation of a group of residues (not including D133, discussed below), but a detailed understanding of the mechanism of its pH sensitivity and the identity of its pH sensor has remained elusive. Although the pH activation range of NhaA closely resembles the pK_a of histidine (where K_a is the acid dissociation constant), no single histidine is required for Na^+ transport or is part of the pH sensor (*19*, *20*). We thus focused instead on carboxylic residues as possible pH sensors, because some carboxylic residues are known to have highly elevated pK_a's (*21*, *22*). Recently, pK_a's of all ionizable residues were calculated for acid-inactivated NhaA (*23*). Six carboxylic residues (D78, E82, E124, D133, D163, and D164) were found to have abnormally high pK_a's, with D133 having the highest value. Having already conducted simulations with protonated D163 and D164, we performed four additional simulations (6 ns each): In each of these additional simulations, either D78, E82, E124, or D133 was protonated (with D163 and D164 protonated in all cases). Protonating the "real" pH sensor should lead the protein to adopt a structure similar to the x-ray structure, which was determined at low pH (*4*), conditions under which the pH sensor is presumably protonated.

Our simulations suggest that D133 is a key component of the pH sensor. D133 resides between the N terminus of helix *iv* and helix *m*, thereby neutralizing their opposing helical dipoles (Fig. 4). Upon protonation of D133, the two opposing helices shift such that their dipoles no longer converge on a single point, because a protonated carboxylic group cannot effectively neutralize the opposing dipoles. This conformation is similar to the acid-inactivated x-ray structure (*4*). Moreover, among those carboxylic residues exhibiting elevated pK_a's (*23*), D133 was the only one whose protonation resulted in such a conformational change.

Mechanistically, the shift of the two helical dipoles observed in our simulations upon D133 protonation causes D164 in the Na^+-binding site to face the protein lumen rather than the Na^+ entry and exit pathways (Fig. 4). In this position, D164 is unable to bind Na^+, resulting in an inactive protein. D164 also faces the protein lumen in the low-pH x-ray structure, further pointing to D133 as the pH sensor. Mutation of D133 to the neutral residue asparagine has been shown experimentally (*13*, *24*) to result in nearly complete inhibition of transport, similar to the inactivation caused by lowering of pH. Moreover, mutation of G338K, located at the juncture between the helical dipoles, markedly reduces the pH response of the transporter (*25*).

The antiporter must be, and is (*6*), extremely selective for Na^+ over K^+, and is slightly selective for Li^+ over Na^+ (*26*, *27*). To investigate NhaA's selectivity among different cations, we conducted free-energy perturbation calculations (*28*) and found that NhaA (i) binds Li^+ more strongly than Na^+ (by 16 kJ/mol) and (ii) binds K^+ more weakly than Na^+ (by 14 kJ/mol) (fig. S4A). Potential of mean force analyses (*29*) show that neither Na^+ nor Li^+ encounters a substantial kinetic barrier to binding (fig. S4B). Our results indicate that NhaA's ion selectivity can be explained thermodynamically.

Our combinational approach, based on multiple long time-scale MD simulations, led to the formulation of a model of NhaA's transport mechanism, pH regulation, and cation selectivity that is consistent with both our own and previously reported experimental data. Future studies will be needed to (i) identify the exact source of coupling between Na^+ and proton transport, which is necessary to avoid proton leakage by NhaA, and (ii) determine whether mammalian Na^+/H^+ exchangers, which differ in their Na^+/H^+ stoichiometry and pH response, use a transport mechanism similar to that proposed for NhaA.

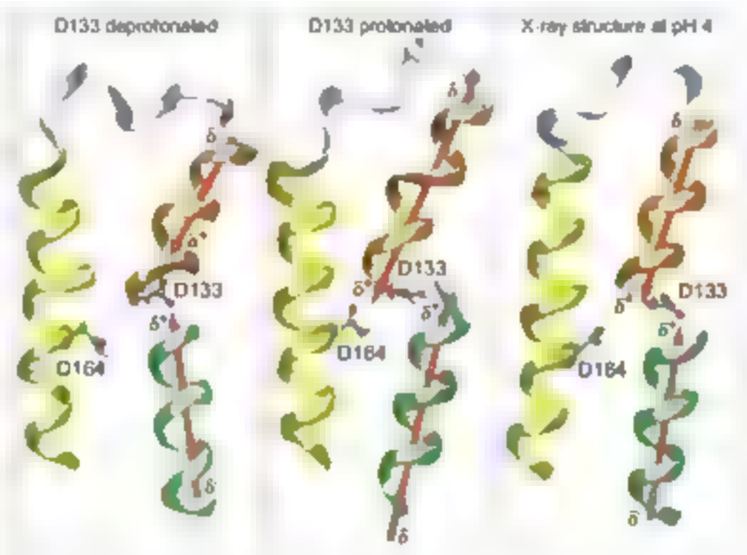

Fig. 4. Effect of D133 protonation on NhaA structure. The leftmost and middle panels display the structures resulting from simulations in which D133 was deprotonated or protonated. The rightmost panel displays the x-ray crystal structure obtained at pH 4 (*4*). Due to the resolution of the x-ray analysis (3.45 Å), no hydrogen is seen in the structure. Red arrows highlight the positions of the helical axes. The helix coloring is as described in fig. S1. The change from the x-ray structure in a simulation with D133 protonated is noticeably smaller than the corresponding change when D133 is deprotonated (C_α RMSD of 2.0 Å versus 2.5 Å when comparing helices *ii*, *iv*, *v*, and *xi*).

References and Notes

1. E. Padan, M. Venturi, Y. Gerchman, N. Dover, *Biochim. Biophys. Acta* **1505**, 144 (2001).
2. E. Padan *et al.*, *Biochim. Biophys. Acta* **1658**, 2 (2004).
3. A. Rothman, E. Padan, S. Schuldiner, *J. Biol. Chem.* **271**, 32288 (1996).
4. C. Hunte *et al.*, *Nature* **435**, 1197 (2005).
5. D. Taglicht, E. Padan, S. Schuldiner, *J. Biol. Chem.* **268**, 5382 (1993).
6. S. Schuldiner, H. Fishkes, *Biochemistry* **17**, 706 (1978).
7. D. Taglicht, E. Padan, S. Schuldiner, *J. Biol. Chem.* **266**, 11289 (1991).
8. D. E. Shaw, *J. Comput. Chem.* **26**, 1318 (2005).
9. K. J. Bowers, R. O. Dror, D. E. Shaw, *J. Comput. Phys.* **221**, 303 (2007).
10. K. J. Bowers, R. O. Dror, D. E. Shaw, *J. Chem. Phys.* **124**, 184109 (2006).
11. K. J. Bowers *et al.*, in *Proceedings of the 2006 Association for Computing Machinery/Institute of Electrical and Electronics Engineers (ACM/IEEE) Conference on Supercomputing (SC06)*, Tampa, FL, 11 to 17 November 2006 (ACM Press, New York, 2006).
12. Single-letter abbreviations for the amino acid residues: A, Ala; C, Cys; D, Asp; E, Glu; F, Phe; G, Gly; H, His; I, Ile; K, Lys; L, Leu; M, Met; N, Asn; P, Pro; Q, Gln; R, Arg; S, Ser; T, Thr; V, Val; W, Trp; and Y, Tyr.
13. H. Inoue, T. Noumi, T. Tsuchiya, H. Kanazawa, *FEBS Lett.* **363**, 264 (1995).
14. O. Jardetzky, *Nature* **211**, 969 (1966).
15. K. Noraki, K. Inaba, T. Kuroda, M. Tsuda, T. Tsuchiya, *Biochem. Biophys. Res. Commun.* **222**, 774 (1996).
16. A. L. Hodgkin, R. D. Keynes, *J. Physiol.* **128**, 61 (1955).
17. S. Berneche, B. Roux, *Nature* **414**, 73 (2001).
18. E. Olkhova, E. Padan, H. Michel, *Biophys. J.* **92**, 3784 (2007).
19. Y. Gerchman *et al.*, *Proc. Natl. Acad. Sci. U.S.A.* **90**, 1212 (1993).
20. A. Rimon, Y. Gerchman, Y. Olami, S. Schuldiner, E. Padan, *J. Biol. Chem.* **270**, 26813 (1995).
21. N. Gutman, S. Steiner-Mordoch, S. Schuldiner, *J. Biol. Chem.* **278**, 16082 (2003).
22. R. Needleman *et al.*, *J. Biol. Chem.* **266**, 11478 (1991).
23. E. Olkhova, C. Hunte, E. Screpanti, E. Padan, H. Michel, *Proc. Natl. Acad. Sci. U.S.A.* **103**, 2629 (2006).
24. L. Galili, A. Rothman, I. Kozachkov, A. Rimon, E. Padan, *Biochemistry* **41**, 609 (2002).
25. A. Rimon, Y. Gerchman, Z. Kariv, E. Padan, *J. Biol. Chem.* **273**, 26470 (1998).
26. E. Padan, N. Marsler, D. Taglicht, R. Karpel, S. Schuldiner, *J. Biol. Chem.* **264**, 20297 (1989).
27. D. Zuber *et al.*, *Biochim. Biophys. Acta* **1709**, 240 (2005).
28. Materials and methods are available as supporting material on *Science* Online.
29. W. Humphrey, A. Dalke, K. Schulten, *J. Mol. Graph.* **14**, 33 (1996).
30. W. L. DeLano, *The PyMOL Molecular Graphics System* (DeLano Scientific, San Carlos, CA, 2002).

31. The authors would like to thank members of the Padan laboratory for helpful discussions, experimental

assistance, and reagents; F. Sacerdoti for invaluable help with computational resources; and A. Weber for editorial assistance. This research was supported in part by a grant from the Israel Science Foundation to I.T.A. A version of Desmond, the software used to perform the simulations described in this article, will be released by the end of 2007. This version will be made available by D. E. Shaw Research for noncommercial research use and by Schrödinger LLC for commercial use. Before release, the current version of Desmond will be available from the authors upon request under conditions described in the SOM. D. E. Shaw Research and Schrödinger have entered into a licensing agreement for the commercial distribution of Desmond by Schrödinger. D.E.S. has a beneficial ownership interest in D. E. Shaw Research, and R.O.D., M.P.E., J.L.K., I.K., Y.S., and D.E.S. have beneficial ownership interests in Schrödinger. Each of these authors may thus benefit financially from any resulting sales of Desmond. D.E.S. is a member of the Board of Directors of the American Association for the Advancement of Science (AAAS), the publisher of *Science*, and serves as treasurer of the AAAS.

Supporting Online Material

www.sciencemag.org/cgi/content/full/317/5839/799/DC1
Materials and Methods
SOM Text
Figs. S1 to S4
Tables S1 to S4
References
Detailed Statement of Software Availability

21 March 2007; accepted 28 June 2007
10.1126/science.1142824

Augmented Wnt Signaling in a Mammalian Model of Accelerated Aging

Hongjun Liu,[1] Maria M. Fergusson,[1]* Rogerio M. Castilho,[2]* Jie Liu,[3] Liu Cao,[1] Jichun Chen,[3] Daniela Malide,[4] Ilsa I. Rovira,[1] Daniel Schimel,[5] Calvin J. Kuo,[6] J. Silvio Gutkind,[2] Paul M. Hwang,[1] Toren Finkel[1]†

The contribution of stem and progenitor cell dysfunction and depletion in normal aging remains incompletely understood. We explored this concept in the Klotho mouse model of accelerated aging. Analysis of various tissues and organs from young Klotho mice revealed a decrease in stem cell number and an increase in progenitor cell senescence. Because Klotho is a secreted protein, we postulated that Klotho might interact with other soluble mediators of stem cells. We found that Klotho bound to various Wnt family members. In a cell culture model, the Wnt-Klotho interaction resulted in the suppression of Wnt biological activity. Tissues and organs from Klotho-deficient animals showed evidence of increased Wnt signaling, and ectopic expression of Klotho antagonized the activity of endogenous and exogenous Wnt. Both in vitro and in vivo, continuous Wnt exposure triggered accelerated cellular senescence. Thus, Klotho appears to be a secreted Wnt antagonist and Wnt proteins have an unexpected role in mammalian aging.

Resident and circulating stem and progenitor cells are critical for long-term tissue maintenance and repair, and it is often postulated that stem and progenitor cell depletion or dysfunction might contribute to aging (*1*). We therefore examined stem cell dynamics in a genetic model of accelerated aging. Mice lacking Klotho expression, henceforth termed Klotho mice, have a shortened life span and exhibit a number of early-onset age-related changes, including arteriosclerosis, decreased fertility, and skin atrophy (*2*). Klotho is a transmembrane protein with a large extracellular domain composed of two repeats (KL1 and KL2 domains) that share similarity to Family 1 glycosidases. In addition to being cell-associated, the extracellular portion of Klotho is secreted and can be detected in the circulation of animals and humans (*3*). It is generally believed that secreted Klotho is the form most likely mediating the protein's longevity effects.

One alteration in Klotho animals is the early appearance of age-related changes in the skin. To assess whether these phenotypic changes were accompanied by alterations in stem cell number, we identified the number of long-term 5-bromo-2′-deoxyuridine (BrdU⁺) retaining cells in the skin of either wild-type or age-matched Klotho animals (*4*). These label-retaining cells (LRCs) are a convenient method to identify stem cells within their niche (*5*). At an age of 2.5 months, Klotho mice had significantly fewer LRCs than their wild-type littermates [wild type: 80 ± 5 LRCs (± SD) per set of three follicles versus Klotho, 35 ± 3 LRCs, $n = 30$, $P < 0.05$ paired t test]. Skin LRCs are confined to a specialized region of the follicle known as the bulge region, and the stem cells contained within this niche are enriched for CD34 expression (*6*). The bulge region in Klotho animals was consistently smaller with reduced CD34 expression (Fig. 1A). Hair follicle epidermal stem cells are also a source of transient amplifying (TA) cells induced by acute wounding (*7*). Consistent with a defect in the number of LRCs, epidermal wounding resulted in a diminished number of TA cells in the Klotho animals (Fig. 1B) and a deficit in wound closure (Fig. 1C).

Age-matched wild-type and Klotho skin sections also exhibited differences in senescence-associated endogenous β-galactosidase (SAβ-gal) activity (Fig. 1D). The observed SAβ-gal staining occurred in the outermost epidermal layer including the acellular stratum corneum. The specificity and physiological significance of this staining is unclear. Examination of numerous random follicles revealed that the Klotho animals also had intense β-galactosidase staining within the follicles, especially within regions known to contain rapidly dividing progenitor cells (*8*). We observed little to no SAβ-gal staining in the intrafollicular regions. Senescent cells often activate the DNA damage response (DDR) pathway, as evidenced by the development of nuclear foci of proteins such as phosphorylated histone (H2AX), ataxia telangiectasia mutated (ATM), and binding protein 1 (53BP1) (*9*). The DDR pathway was activated in multiple random Klotho follicles but not in age-matched wild-type mice (Fig. 1D).

Klotho animals also demonstrated increased SAβ-gal staining in the small intestine, especially within intestinal crypts, an area enriched for stem and progenitor cells (Fig. 1E). Similar analysis of the testis in male animals also demonstrated evidence of increased progenitor cell senescence (fig. S1). In the bone marrow of Klotho mice, there was also a reduction in the population of cells bearing the cell surface phenotype of c-kit⁺ sca-1⁺ lineage negative that encompasses the hematopoietic stem cell (HSC) (Fig. 1F). This reduction of HSC in Klotho animals was accompanied by a marked increase in the percentage of stem cells that were actively dividing (Klotho HSCs: 28.4 ± 3.7% in G_1 versus wild-type HSCs, 10.2 ± 1.1% in G_1, $n = 3$ animal pairs per group, $P < 0.05$ paired t test) (Fig. 1G).

Given that stem cell biology is regulated by a number of secreted factors, we wondered whether there might be a functional interaction between Klotho and one of these known stem cell regulators. In the course of our experiments, we noted that the subcellular distribution of Klotho and Wnt proteins within transfected cells overlapped (fig. S2). Thus, we sought to determine whether Klotho and Wnt3 could form a direct molecular complex. Epitope-tagged Wnt3 and myc-tagged Klotho were readily detectable in transfected cell lysates (Fig. 2A). Klotho associated with immu-

[1]Cardiology Branch, National Heart, Lung, and Blood Institute, NIH, Bethesda, MD 20892, USA. [2]Oral and Pharyngeal Cancer Branch, National Institute of Dental and Craniofacial Research, NIH, Bethesda, MD 20892, USA. [3]Hematology Branch, National Heart, Lung, and Blood Institute, NIH, Bethesda, MD 20892, USA. [4]Light Microscopy Core Facility, National Heart, Lung, and Blood Institute, NIH, Bethesda, MD 20892, USA. [5]Mouse Imaging Facility, NIH, Bethesda, MD 20892, USA. [6]Division of Hematology, Stanford University School of Medicine, Stanford, CA 94305, USA.

*These authors contributed equally to this work.
†To whom correspondence should be addressed. E-mail: finkelt@nih.gov

coprecipitated Wnt3, and the reciprocal immunoprecipitation of klotho contained Wnt3 (Fig. 2A). A single extracellular KL domain was sufficient to mediate the observed interaction with Wnt3 (Fig. 2B). The Wnt binding domain was contained within the amino-terminal portion of klotho's KL1 domain (amino acids 1 to 285) (fig. S3). Full-length klotho also coimmunoprecipitated with a number of other Wnt isoforms including Wnt1, Wnt4, and Wnt5a (fig. S4).

We further analyzed the biological effects of the observed klotho-Wnt interaction. We coexpressed Wnt3 and klotho in human embryonic kidney (HEK) 293 cells along with a Wnt-responsive reporter. The presence of Wnt3 increased reporter activity by approximately 7 times, whereas the addition of increasing amounts of klotho reduced Wnt activity in a dose-dependent fashion (Fig. 2C). Various structural mutants containing a single KL1 domain or altering conserved amino acids believed to be important in klotho's β-glucuronidase activity failed to abrogate klotho-mediated Wnt inhibition (fig. S5). In contrast, klotho constructs that failed to physically interact with Wnt3 also failed to inhibit Wnt activity (fig. S6).

We next asked whether klotho could inhibit Wnt activity in a cell-free system. Conditioned media with and without either klotho or Wnt3a were prepared and mixed in various combinations before being placed on HEK-293 cells transfected with a Wnt reporter construct. These results indicated that secreted klotho could inhibit soluble Wnt activity (Fig. 2D). In contrast, secreted klotho-conditioned medium was ineffective in inhibiting Wnt signaling directly stimulated by intracellular β-catenin expression (fig. S7).

We next tested whether animals lacking klotho expression had increased Wnt activity. We crossed klotho animals with the TOPGAL reporter strain in which the activity of a β-galactosidase reporter is under the control of Wnt-responsive elements (*10*). Analysis of the skin of klotho-TOPGAL animals demonstrated an increase in β-galactosidase reporter activity compared with that of age-matched wild-type TOPGAL controls (Fig. 3A). Quantitative analysis confirmed this augmented Wnt activity in the skin and small intestine of klotho mice and demonstrated that the increased expression of the Wnt-dependent β-galactosidase reporter was similar to that of Axin2, a known Wnt target gene (fig. S8). Other potential transcriptional targets of the Wnt pathway also showed increased transcription in klotho animals (fig. S9).

Whereas normal aging is associated with bone loss, studies in mice and humans have established that augmented Wnt signaling leads to increased bone mass (*11*). We therefore monitored Wnt activity in bones of age-matched wild-type or klotho littermates. Using the TOPGAL reporter, we detected augmented reporter activity in sections obtained from the proximal tibia of 2-week-old klotho mice (Fig. 3B and fig. S10). At this time point, klotho mice lack any discernible phenotype, suggesting that the increase in Wnt activity precedes the apparent onset of accelerated aging. We also analyzed by microcomputerized tomography (μCT) the tibias of 3-month-old wild-type or klotho animals. Klotho mice demonstrated nearly 5 times as much tibial trabecular bone mass (Fig. 3, C to E). An increase in overall tibial and vertebral column trabecular bone density has actually been previously noted but unexplained in klotho mice (*12*). In contrast, other bones in the klotho animals exhibit decreased bone density (*2*). The basis for this regional difference in bone density is unclear but may relate to the complex interplay of klotho's ability both to alter Wnt signaling and to regulate other pathways involved in calcium and vitamin D homeostasis (*13*–*16*).

To test whether augmented klotho expression could inhibit Wnt signaling in vivo, we analyzed TOPGAL reporter mice in the first few weeks of

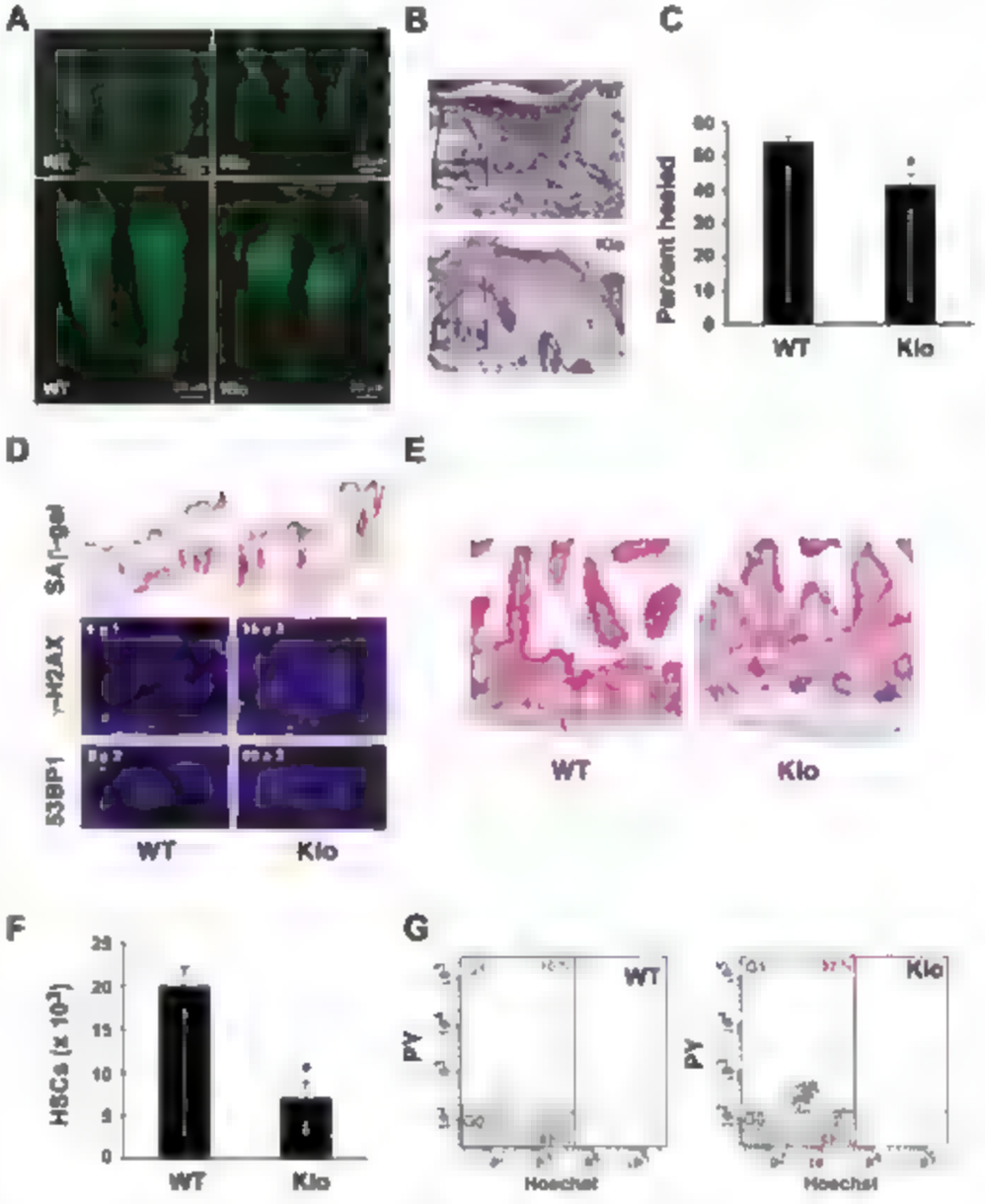

Fig. 1. Altered stem and progenitor cells in klotho mice. (**A**) LRCs within the skin follicles of 80-day-old wild-type (WT) or klotho (Klo) mice (top). Higher magnification of representative bulge regions stained for CD34 (bottom). (**B**) TA cells, identified by positive brown nuclear BrdU staining after skin wounding. (**C**) Assessment of skin closure 4 days after creating a 1-cm wound (n = 4 pairs, $^*P < 0.05$ paired t test). (**D**) Evidence for senescence within the hair follicle of klotho animals as assessed by β-gal staining (SAβ-gal) and nuclear foci of γ-H2AX and 53BP1 (red) in 4′,6-diamidino-2-phenylindole (DAPI)–stained nuclei (blue). Percentage of positive nuclear staining in either wild-type or klotho follicles is shown ± SD. (**E**) SAβ-gal staining of small intestine. (**F**) Determination of the absolute number of c-kit$^+$sca-1$^+$ Lin$^-$ HSCs in bilateral femur and tibias of either wild-type or klotho animals (n = 3 pairs, $^*P < 0.05$ paired t test). (**G**) Representative cell cycle analyses of HSCs from wild-type and klotho animals demonstrating a decrease in HSC quiescence (% G_0) and increased proliferation (% G_1). DNA content is displayed along the x axis, RNA content determined by Pyronin Y (PY) staining is displayed along the y axis.

hair growth kinetics of the hair follicle cycle are synchronized (*17*). On postnatal day 8, mice were injected subcutaneously with one of three different recombinant adenoviruses encoding either klotho (Ad.Klo), the Wnt inhibitor DKK-1 (Ad.DKK-1), or an adenovirus encoding the immunoglobulin G Fc fragment (Ad.FC) that served as a control. Four days after injection (postnatal day 12), we harvested the injected area and assessed Wnt activity in the hair follicle. In control-injected skin, Wnt activity was clearly visible around numerous growing hair follicles, whereas this activity was reduced in both the DKK-1 and klotho injected skin (fig. S11). Assessment of more than 500 random follicles in each condition revealed that klotho was roughly equivalent to DKK-1 in the ability to quantitatively suppress Wnt's biological activity (Fig. 3F).

To assess whether the expression of klotho could also block the effects of pathological Wnt expression, we crossed two strains of mice, one that expressed the tetracycline-inducible transcriptional activator (rtTA) under the control of the cytokeratin 5 promoter (K5rtTA) and another that expressed Wnt1 under the control of multiple *tet*-responsive elements (*tet*-Wnt1) (*18*, *19*). The resultant cross generated the experimental line K5rtTA/*tet*-Wnt1, which provided tetracycline-inducible expression of Wnt1 in the basal layer of stratified epithelium. In our transgenic animals, ectopic expression of Wnt1 from postnatal day 12 to 21 resulted in increased epidermal thickness and marked cutaneous hyperplasia (fig. S12). Both local injection of either DKK-1 or Klotho, but not the control adenovirus, blocked these pathological Wnt-induced skin changes (fig. S13).

To begin to directly assess the role of Wnt proteins in aging, we tested whether continuous Wnt exposure induced cellular senescence. We grew primary mouse embryonic fibroblasts (MEFs) in the presence or absence of Wnt3a conditioned medium. Consistent with Wnt proteins having mitogenic effects, analysis of BrdU

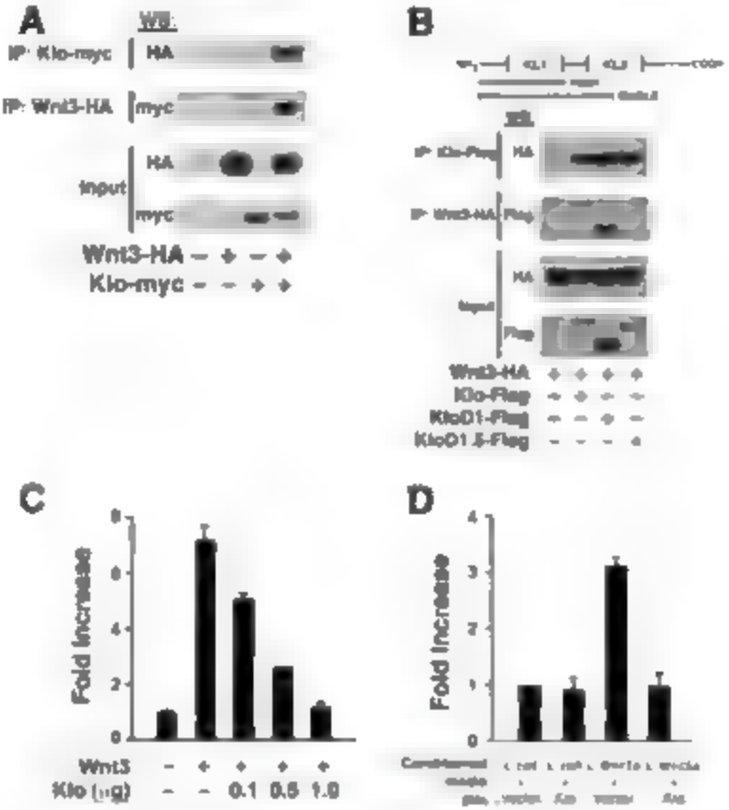

Fig. 2. Interaction of klotho with Wnt and inhibition of Wnt signaling. (**A**) HEK-293 cells were transiently transfected with myc- and hemagglutinin (HA)–tagged expression constructs encoding Wnt3 and murine klotho (Klo). Reciprocal coimmunoprecipitation (IP) of klotho and Wnt3 from cell lysates is also demonstrated. WB, Western blot. (**B**) Schematic diagram of klotho demonstrating the two extracellular klotho repeats (KL1 and KL2) followed by the single-pass transmembrane domain (TM). Flag-tagged full-length klotho (Klo) and truncation mutants were assessed for Wnt binding. (**C**) HEK-293 cells were transfected with a Wnt3 expression construct (100 ng DNA) and the indicated amount of a full-length klotho expression vector along with either an active (TOPFlash) or inactive (FOPFlash) Wnt luciferase reporter. (**D**) Conditioned medium mixes were incubated for 24 hours with HEK 293 cells previously transfected with either the active or inactive Wnt luciferase reporter. All Wnt activity measurements represent the ratio of TOP/FOP activity obtained from a single experiment performed in triplicate and are representative of at least three similar experiments.

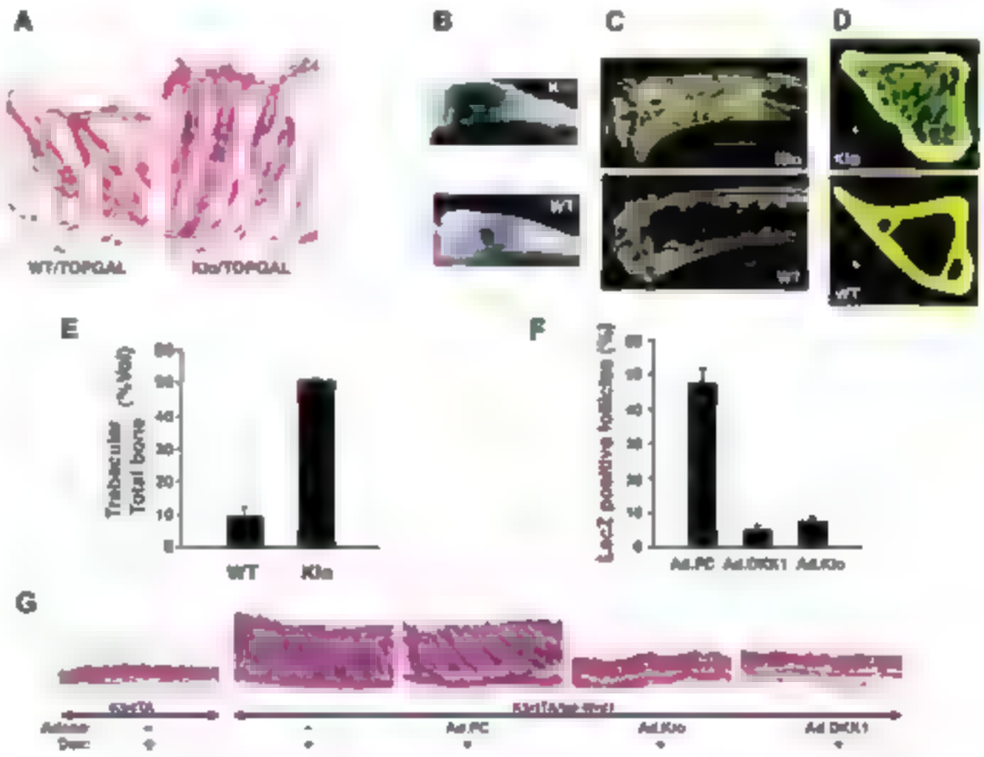

Fig. 3. Inhibition of Wnt signaling by klotho in vivo. (**A**) Endogenous Wnt activity in skin from 14-day-old wild-type or Klotho mice crossed with the TOPGAL reporter strain. (**B**) Wnt activity in tibias of 14-day-old Klotho/TOPGAL or wild-type/TOPGAL mice. (**C**) Longitudinal microcomputerized CT sections from the tibia of 3-month-old Klotho (top) or wild-type (bottom) animals. (**D**) Horizontal three-dimensional reconstruction of cortical bone (yellow) and trabecular bone (green). (**E**) Calculation of the trabecular to total bone volume from the tibia of three pairs of 3-month-old wild-type or Klotho animals. (**F**) Quantification of the percentage of β-galactosidase positive follicles from 12-day-old TOPGAL mice injected 4 days earlier with either a control virus (Ad.FC), an adenovirus encoding the Wnt inhibitor (Ad.DKK1), or an adenovirus encoding klotho (Ad.Klo). Approximately 500 random follicles were assessed per condition. (**G**) Hyperplastic skin phenotype of K5rtTA/*tet*-Wnt1 transgenic mice treated with doxycycline is blocked by prior injection of an adenovirus encoding for either DKK-1 or klotho. Mice were killed on postnatal day 21.

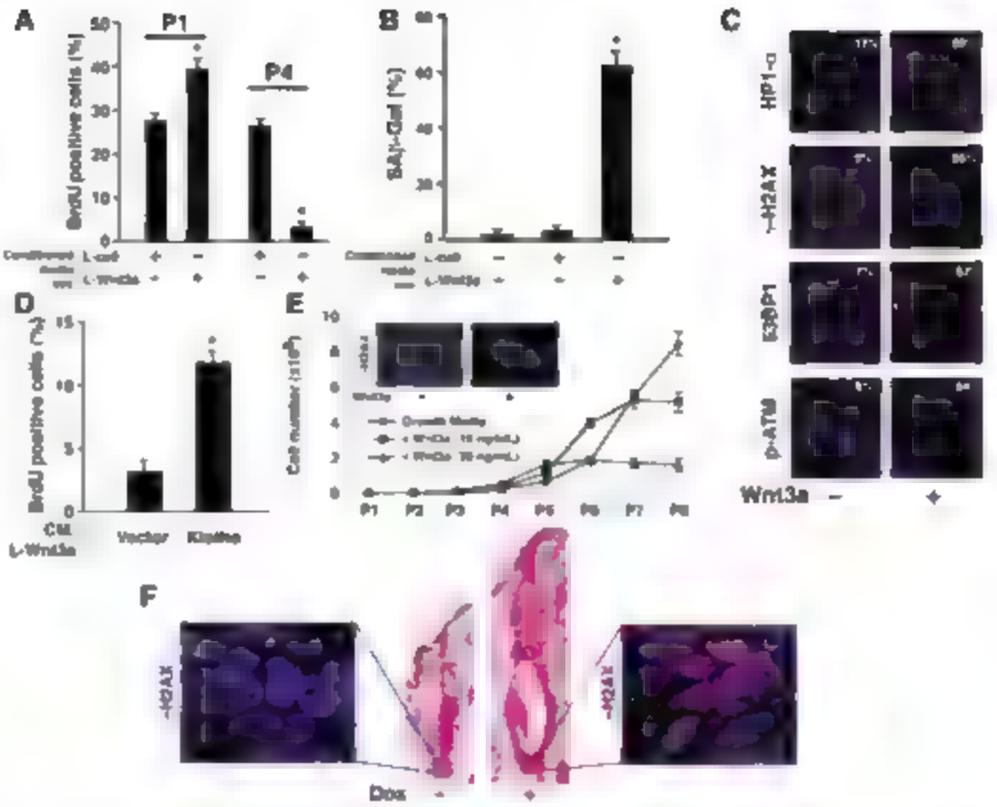

Fig. 4. Senescence induced by increased Wnt activity. (**A**) BrdU incorporation for MEFs grown in the presence or absence of Wnt3a conditioned media. Cells were assayed from passage 1 (P1) through passage 4 (P4). (**B**) Senescence associated β-galactosidase staining (SAβ-gal) for MEFs (P4) grown in standard media (–) or mixed with the indicated L-cell conditioned medium. (**C**) MEFs (P4) with or without continuous Wnt3a exposure were assessed for senescence-associated heterochromatin (HP1-α) and the activation of the DNA damage response. (**D**) Level of BrdU incorporation (P4) for MEF cells continuously treated with L-Wnt3a conditioned media (CM) mixed with either vector-transfected or klotho-transfected conditioned medium. (**E**) Growth of MEFs in standard medium (diamonds), or supplemented with Wnt3a at 10 ng/ml (squares) or 30 ng/ml (triangles). (Inset) P7 cells were stained for activation of H2AX. (**F**) Skin sections obtained from K5rtTA/*tet*-Wnt1 transgenic mice either treated or untreated with doxycycline (Dox) from postnatal days 2 through 21. The senescence-associated marker γ-H2AX is induced in the setting of continuous in vivo Wnt1 (+Dox) exposure.

incorporation revealed that Wnt-conditioned medium initially acted to increase MEF cell proliferation (Fig. 4A). However, over time, continuous Wnt exposure resulted in a marked decrease in proliferation (Fig. 4A and fig. S12). Wnt exposure did not increase the level of apoptosis (fig. S13); rather, assessment of cells grown in the continuous presence of Wnt3a demonstrated a flattened morphology with evidence of increased SAβ-gal activity (Fig. 4B and fig. S14). Similarly, continuous Wnt3a exposure triggered the DDR pathway as well as nuclear foci of HP1-α, a marker of senescence-associated heterochromatin formation (Fig. 4C). The inhibitory effects of long-term Wnt3a-conditioned media on MEF proliferation (fig. S15) and BrdU incorporation (Fig. 4D) were attenuated by the addition of soluble Klotho. Similar results were observed with purified Wnt3a protein rather than Wnt3a-conditioned medium (Fig. 4E and fig. S16) and when using human rather than mouse cells (fig. S17).

Finally, we tested whether Wnt could induce senescence in vivo by analyzing the skin of K5rtTA/*tet*-Wnt1 transgenic animals. Beginning on postnatal day 2, littermate transgenic animals were placed on a diet with or without doxycycline (Dox) and skin samples were collected for study on day 21. Analysis of multiple random follicles ($n > 100$) demonstrated an increase in senescence markers in those animals exposed to continuous Wnt1 expression. On day 21, 70% of the follicles in Wnt1-expressing animals exhibited staining for γ-H2AX, whereas less than 5% of uninduced follicles demonstrated this phenotype (Fig. 4F). Similarly, whereas follicles from young animals without Dox treatment showed little to no evidence of senescence, their Wnt1-induced littermates demonstrated multiple areas of discrete SAβ-gal staining (fig. S18).

We demonstrate that klotho acts as a Wnt antagonist and that chronic Wnt stimulation may contribute to stem cell depletion and aging. During the course of our studies, two other studies appeared demonstrating that forced constitutive Wnt signaling within HSC led to a rapid exhaustion of long-term repopulating stem cells (*20*, *21*). These results, as well as the observations in Brack *et al.* (*22*), are broadly consistent with our observations of klotho mice. Previous attempts to understand the basis of the observed klotho aging phenotype have implicated alterations in insulin signaling as well as, more recently, the fibroblast growth factor 23 pathway (*14*–*16*, *23*). Further analysis is therefore required to fully understand how these various klotho-regulated pathways potentially intersect and whether any biological hierarchy exists. Nonetheless, our results provide an unexpected connection between aging and the well-studied Wnt signaling pathway and suggest that strategies targeting soluble mediators of stem cell function may provide new therapeutic strategies to combat aging and potentially age-related diseases.

References and Notes

1. T. A. Rando, *Nature* **441**, 1080 (2006).
2. M. Kuro-o *et al.*, *Nature* **390**, 45 (1997).
3. H. M. Xiao, Y. M. Zhang, Q. Zheng, J. Gu, *Chin. Med. J. (Engl.)* **117**, 742 (2004).
4. Materials and methods are available as supporting material on *Science* Online.
5. K. M. Braun, F. M. Watt, *J. Invest. Dermatol. Symp. Proc.* **9**, 196 (2004).
6. E. Tumbar *et al.*, *Science* **303**, 359 (2004).
7. M. Ito *et al.*, *Nat. Med.* **11**, 1351 (2005).
8. C. Blanpain, E. Fuchs, *Annu. Rev. Cell Dev. Biol.* **22**, 339 (2006).
9. D. B. Lombard *et al.*, *Cell* **120**, 497 (2005).
10. R. DasGupta, E. Fuchs, *Development* **126**, 4557 (1999).
11. V. Krishnan, H. U. Bryant, O. A. Macdougald, *J. Clin. Invest.* **116**, 1202 (2006).
12. I. Yamashita, Y. Nabeshima, M. Noda, *J. Endocrinol.* **164**, 239 (2000).
13. Q. Chang *et al.*, *Science* **310**, 490 (2005).
14. H. Kurosu *et al.*, *J. Biol. Chem.* **281**, 6120 (2006).
15. M. S. Razzaque, O. Sitara, T. Taguchi, B. St-Arnaud, *FASEB J.* **20**, 720 (2006).
16. I. Urakawa *et al.*, *Nature* **444**, 770 (2006).
17. E. Fuchs, *Nature* **445**, 834 (2007).
18. L. Vitale-Cross, P. Amornphimoltham, G. Fisher, A. A. Molinolo, J. S. Gutkind, *Cancer Res.* **64**, 8804 (2004).
19. E. J. Gunther *et al.*, *Genes Dev.* **17**, 488 (2003).
20. M. Scheller *et al.*, *Nat. Immunol.* **7**, 1037 (2006).
21. P. Kirstetter, K. Anderson, B. T. Porse, S. E. Jacobsen, C. Nerlov, *Nat. Immunol.* **7**, 1048 (2006).
22. A. S. Brack *et al.*, *Science* **317**, 807 (2007).
23. H. Kurosu *et al.*, *Science* **309**, 1829 (2005).

24. We thank R. Moon for the Wnt (TOP/FOP) reporter constructs, M. Kuro-o for generating the *klotho* mice, and H. Dietz for providing the *klotho* mice. The TOPGAL mouse was generated by E. Fuchs and kindly provided by Y. Yang. We also thank J. G. Kang for technical help. This work was supported by intramural NIH funds (T.F.), a grant from the Ellison Medical Foundation (T.F.), and an NIH 1 R01 DK069989-01 to C.J.K.

Supporting Online Material

www.sciencemag.org/cgi/content/full/317/5839/803/DC1
Materials and Methods
Figs. S1 to S18
References

9 April 2007; accepted 9 July 2007
10.1126/science.1143578

Increased Wnt Signaling During Aging Alters Muscle Stem Cell Fate and Increases Fibrosis

Andrew S. Brack,[1] Michael J. Conboy,[1] Sudeep Roy,[1] Mark Lee,[2] Calvin J. Kuo,[2] Charles Keller,[3] Thomas A. Rando[1,4]*

The regenerative potential of skeletal muscle declines with age, and this impairment is associated with an increase in tissue fibrosis. We show that muscle stem cells (satellite cells) from aged mice tend to convert from a myogenic to a fibrogenic lineage as they begin to proliferate and that this conversion is mediated by factors in the systemic environment of the old animals. We also show that this lineage conversion is associated with an activation of the canonical Wnt signaling pathway in aged myogenic progenitors and can be suppressed by Wnt inhibitors. Furthermore, components of serum from aged mice that bind to the Frizzled family of proteins, which are Wnt receptors, may account for the elevated Wnt signaling in aged cells. These results indicate that the Wnt signaling pathway may play a critical role in tissue-specific stem cell aging and an increase in tissue fibrosis with age.

Aging of skeletal muscle is characterized by an increase in fibrous connective tissue (*1*) and an impairment of muscle regenerative potential (*2*, *3*), manifested by a replacement of muscle by fibrous connective tissue and adipose tissue (fig. S1). In the muscular dystrophies, there is also progressive muscle fibrosis with age (*4*). We examined the cellular and molecular mechanisms of this age-dependent increase in skeletal muscle fibrosis.

The regeneration of aged muscle can be enhanced by exposure to a youthful systemic environment, an effect mediated at least in part by restoration of normal signaling of the Delta-Notch pathway (*5*, *6*). Therefore, we tested whether exposure of old tissue to a youthful systemic environment, established by parabiotic pairings of old animals to young animals (heterochronic pairings) (*7*), might also reduce the fibrotic response of old muscle. Indeed, there was a reduction of collagen deposition in regenerating areas in muscles of aged mice in heterochronic pairings compared with that of aged mice in isochronic pairings (pairings of mice of the same age) and this was accompanied by enhanced proliferation of myogenic progenitors (Fig. 1, A and B). Conversely, collagen deposition was increased and progenitor proliferation was reduced in young partners of heterochronic pairings compared with young partners in isochronic pairings. Thus, systemic influences that change with age are important in mediating the fibrotic responses of aged tissues.

We examined cells derived from muscles of young (4-month-old) and aged (24-month-old) mice for any characteristics that might account for the age-related fibrotic response. In single fiber cultures we found 90% of the fiber-associated mononucleated cells appeared to be myogenic as defined by expression of combinations of myogenic markers (Pax7, MyoD, and Desmin) 2 days after fiber isolation from young animals, and 98% of the cells from fibers from aged animals were myogenic (Fig. 2A). After another 1[illegible] days in culture, the percentage of nonmyogenic cells from the young cultures remained 1[illegible], but the percentage from the aged fibers had increased to ~75% and they exhibited morphological changes characteristic of a fibroblastic lineage (Fig. 2B). No loss of cells due to detachment or apoptosis was detected, and the proliferation of nonmyogenic cells from aged muscle was, if anything, lower than that from young muscle (fig. S2). Therefore, the increase in the percentage of fibrogenic cells in cultures from aged mice most likely arose by conversion of previously myogenic cells into nonmyogenic cells.

With age, there is a decline in satellite cell functionality (*5*). That aged muscle regeneration can be enhanced by direct activation of the Notch pathway (*5*) or by exposure to a youthful systemic environment (*6*) indicates that those functional changes are largely reversible. To test for reversibility of the age-related myogenic-to-fibrogenic conversion, we examined satellite cell progeny from young and aged mice in heterochronic parabiotic pairings (*6*). Aged tissues exposed to this heterochronic systemic environment exhibited a reduction in the myogenic-to-fibrogenic conversion (from ~75 to 10%), whereas the youngest tissues exhibited an increase (from ~10 to 50%) (Fig. 2C). We also exposed young and aged cells in vitro to serum from young or aged animals ("young serum" and "aged serum," respectively). Aged serum increased the myogenic-to-fibrogenic conversion of young cells, whereas

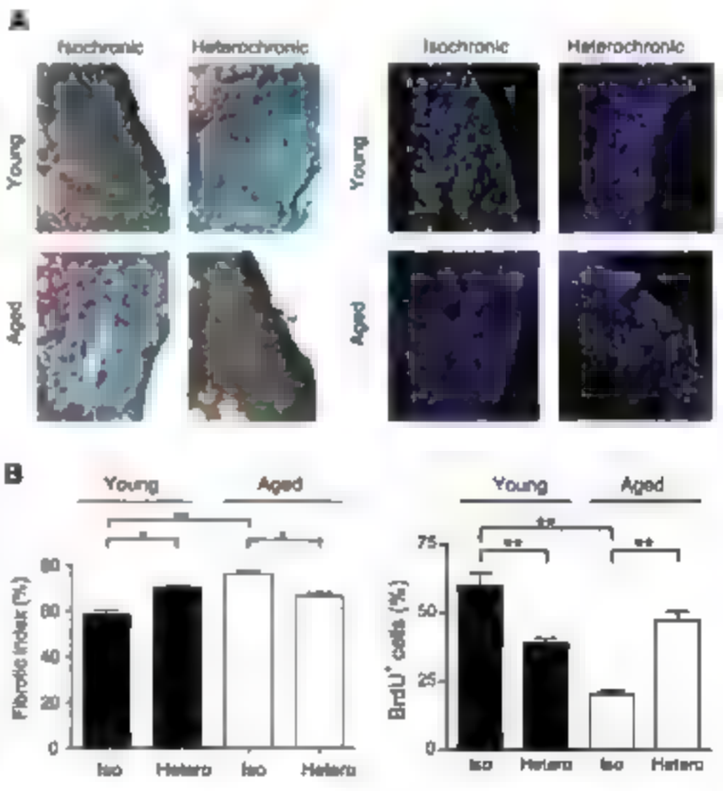

Fig. 1. Prevention of age-related increase in fibrogenesis during muscle regeneration by heterochronic parabiosis. (A) Isochronic or heterochronic parabiotic pairs were established for 4 weeks, and hind limb muscles were subjected to freeze injuries. Bromodeoxyuridine (BrdU) was injected intraperitoneally 2 days after injury. Three days later, muscles were sectioned and (left) stained with Gomori trichrome (red, muscle fibers; green, connective tissue) or (right) immunostained for BrdU (green). 4′,6′-Diamidino-2-phenylindole (DAPI) (blue) labels all nuclei. **(B)** Quantitative analyses of histologic studies as in (A). (Left) Fibrotic index (percentage of the injury area occupied by connective tissue in Gomori-stained sections). (Right) Proliferative response (percentage of DAPI$^+$ mononucleated cells that were also BrdU$^+$). "Young" and "aged" refer to young and aged mice, respectively; "iso" and "hetero" to isochronic and heterochronic pairings, respectively. $^*P < 0.05$, $^{**}P < 0.01$.)

[1]Department of Neurology and Neurological Sciences, Stanford University School of Medicine, Stanford, CA 94305, USA. [2]Department of Medicine, Division of Hematology, Stanford University School of Medicine, Stanford, CA 94305, USA. [3]Department of Cellular and Structural Biology, The University of Texas Health Science Center, San Antonio, TX 78229, USA. [4]Geriatric Research, Education, and Clinical Center (GRECC) and Neurology Service, Veterans Affairs (VA) Palo Alto Health Care System, Palo Alto, CA 94304, USA.

*To whom correspondence should be addressed. E-mail: rando@stanford.edu

young serum had the opposite effect on aged cells (Fig. 2D). Nearly 100% of young cells previously maintained in young serum expressed myosin heavy chain under differentiation conditions, but that declined to ~75% in cultures of young cells previously maintained in aged serum (fig. S3). Together, these results suggest that myogenic progenitors tend to deviate from their myogenic lineage in the aged environment.

We used genetic lineage tracing to confirm that the aged systemic environment promotes a myogenic-to-fibrogenic conversion. To identify fibrogenic cells, we used an antibody to a fibroblast-specific marker (ER-TR7) that was highly specific (0% of Pax7$^+$ or MyoD$^+$ cells were ER-TR7$^+$) and highly sensitive (93% of nonmyogenic cells (Pax7$^-$ and MyoD$^-$) were ER-TR7$^+$) (fig. S4). For myogenic lineage studies, we used Pax7.Cre-ER.ROSA26 mice, a strain in which tamoxifen administration leads to permanent β-galactosidase (β-gal) expression only in myogenic cells in the adult (fig. S5). When myogenic progenitor cultures from these tamoxifen-treated mice were incubated in young serum, all β-gal$^+$ cells had a myogenic phenotype (either MyoD$^+$ or Pax7$^+$, and ER-TR7$^-$). However, in aged serum, 18% of β-gal$^+$ cells were Pax7$^+$ and MyoD$^-$ and 10% were ER-TR7$^+$ (Fig. 2, E and F), which confirmed that the aged environment promotes a myogenic-to-fibrogenic conversion.

Activation of the Wnt pathway can lead to fibrogenic conversion of cells in other lineages (*8*, *9*). Thus, we examined markers of the steady-state activation of the Wnt pathway in muscle and purified satellite cells (fig. S6) from young and aged mice, as well as the effects of modulating Wnt signaling on myogenic-to-fibrogenic conversion and the fibrotic response.

We analyzed a direct downstream target of Wnt signaling, Axin2 (*10*), in uninjured muscle from young and aged mice. Axin2 transcript levels were increased in aged muscle (fig. S7A). Furthermore, purified satellite cells from aged muscle expressed more Axin2 than did such cells from young muscle (Fig. 3A). In addition, analysis of TOPGAL mice (in which β-gal expression is a read-out of Wnt signaling (*11*)) revealed a progressive increase in Wnt signaling in myogenic cells during aging (Fig. 3B).

We also analyzed other components of the canonical Wnt signaling cascade: glycogen synthase kinase 3β (GSK3β) and its substrate β-catenin. In aged satellite cells, fluorescence-activated cell sorting (FACS) analysis demonstrated that the amounts of active GSK3β decreased and active β-catenin increased (Fig. 3C), both changes being indicative of active Wnt signaling (*12*, *13*). Furthermore, these changes were due to Wnt signaling, because systemic adenovirus-mediated expression of Dickkopf-1 (DKK1) (*14*), a Wnt antagonist, decreased the percentage of myogenic progenitors expressing active β-catenin (fig. S7B).

To analyze the Wnt signaling cascade in myogenic progenitors during muscle regenera-

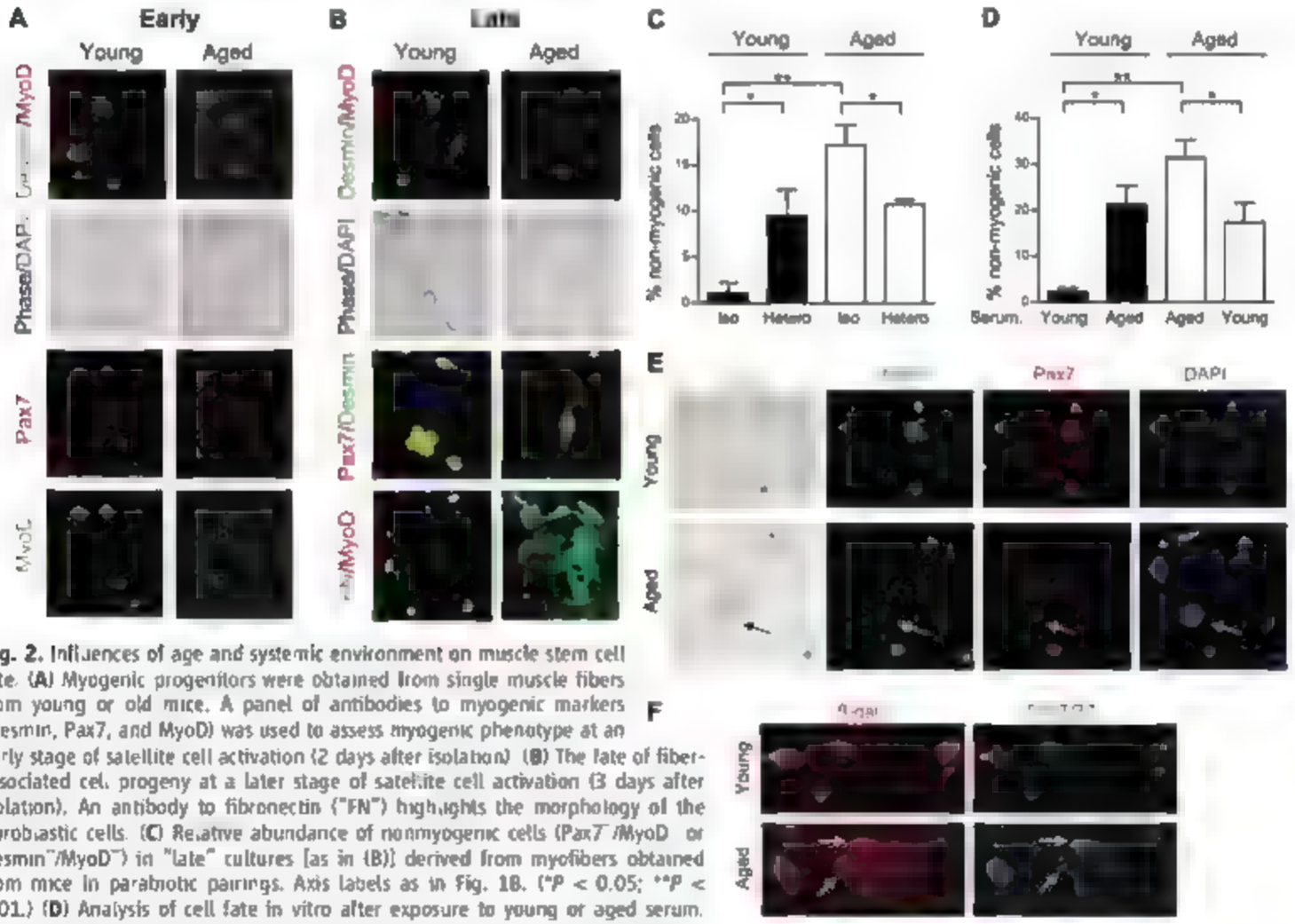

Fig. 2. Influences of age and systemic environment on muscle stem cell fate. (**A**) Myogenic progenitors were obtained from single muscle fibers from young or old mice. A panel of antibodies to myogenic markers (Desmin, Pax7, and MyoD) was used to assess myogenic phenotype at an early stage of satellite cell activation (2 days after isolation). (**B**) The fate of fiber-associated cell progeny at a later stage of satellite cell activation (3 days after isolation). An antibody to fibronectin ("FN") highlights the morphology of the fibroblastic cells. (**C**) Relative abundance of nonmyogenic cells (Pax7$^-$/MyoD$^-$ or Desmin$^-$/MyoD$^-$) in "late" cultures [as in (B)] derived from myofibers obtained from mice in parabiotic pairings. Axis labels as in Fig. 1B. (*$P < 0.05$; **$P < 0.01$.) (**D**) Analysis of cell fate in vitro after exposure to young or aged serum. Pure myogenic progenitor cultures from young or aged mice were incubated in plating media for 1½ days, exposed to young or aged serum for 1½ days, and analyzed for the percentage of nonmyogenic cells. (*$P < 0.05$ **$P < 0.01$.) (**E**) Effect of young or aged serum on myogenic stem cell fate. Myogenic progenitors isolated from Pax7.Cre-ER.ROSA26 mice were incubated in young or aged serum for 2 days. Cells were stained for β-gal, with 5-bromo-4-chloro-3-indolyl β-D-galactopyranoside (X-gal, blue) and with antibodies to MyoD (green) and Pax7 (red). Arrow indicates a cell that has undergone myogenic-to-fibrogenic conversion. (**F**) Myogenic progenitors isolated from Pax7.Cre-ER.ROSA26 mice were incubated in young or aged serum for 2 days. Cells were stained with an antibody to β-gal (red) or to a fibroblast-specific marker, ER-TR7 (green). White arrows in the bottom panel indicate previously myogenic cells showing early fibrogenic phenotype.

(top) (fig. S6). We isolated progenitors 2 days after injury of young and aged muscle and analyzed them by FACS. The percentage of progenitors with detectable levels of active β-catenin was increased in aged myogenic progenitors (fig. S7C). Increased β-gal activity was observed in injured areas of muscle and also in isolated muscle progenitors from aged TOPGAL mice (Fig. 3D and fig. S7, D and E). When we incubated myogenic progenitors from TOPGAL mice in young or aged serum (Fig. 3E), Wnt signaling was increased in progenitors exposed to aged serum, and this increase was prevented by a soluble Wnt inhibitor, Frizzled-related protein 3 (sFRP3).

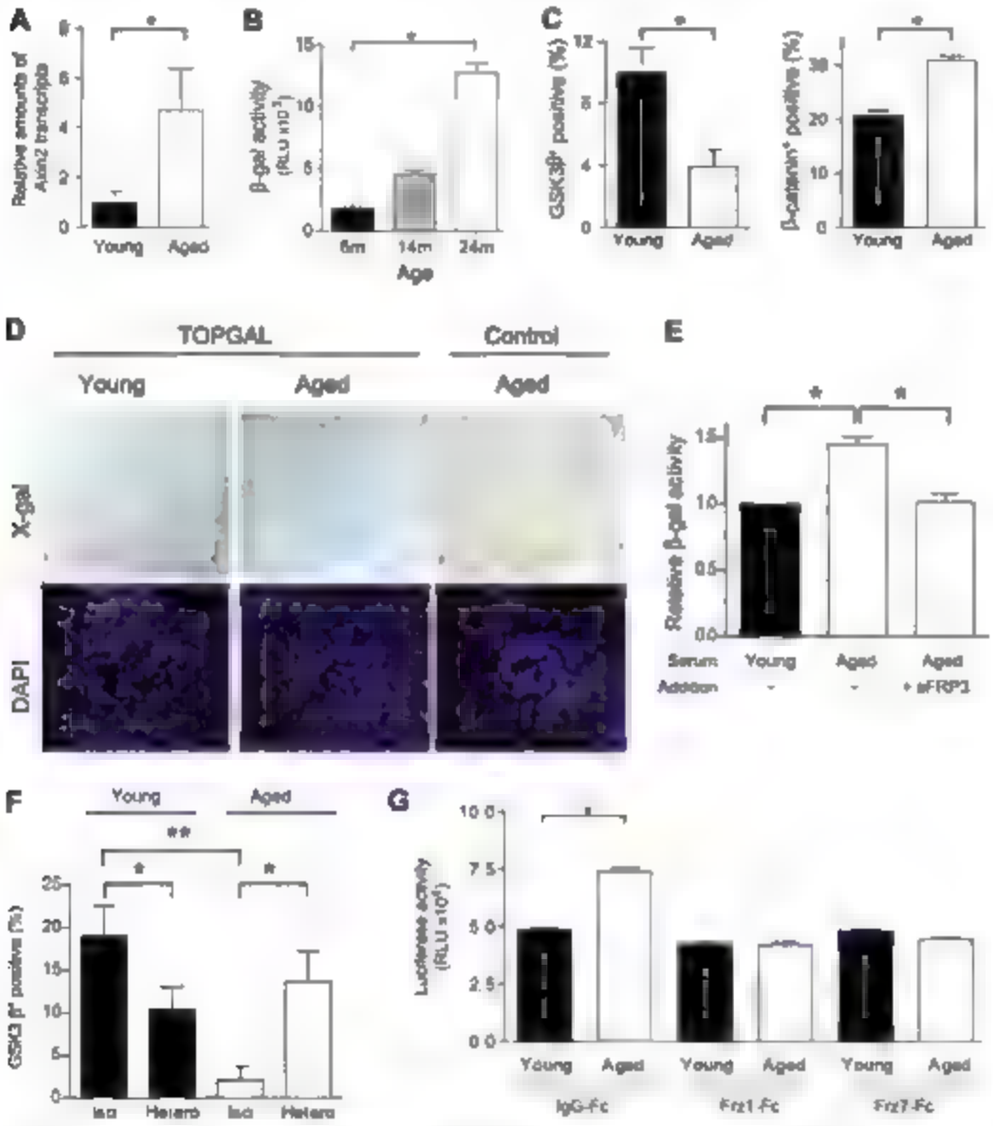

Fig. 3. Enhanced Wnt signaling in aged muscle and in myogenic progenitors exposed to aged serum. **(A)** Axin2 transcript levels assessed by real-time reverse transcription polymerase chain reaction from satellite cells obtained by FACS-sorted Syndecan4⁺ cells (fig. S6) from uninjured muscles of young and aged mice. **(B)** β-Gal activity (normalized to DNA content) in fiber-associated cells isolated from uninjured muscle of TOPGAL mice of different ages. β-Gal activity of aged-matched wild-type controls was subtracted to normalize for any endogenous activity (*$P < 0.05$.) **(C)** FACS analysis of active GSK3β and β-catenin (GSK3β⁺ and β-catenin⁺, respectively) in myogenic progenitors isolated from myofibers cultures from young and aged animals. Graphs show the percentage of all myogenic progenitors (Syn-4⁺) that were also positive for GSK3β⁺ or β-catenin⁺ (*$P < 0.05$.) **(D)** Muscles of young and aged TOPGAL mice were injured, and the muscles were analyzed 2 days later. Cryosections were incubated with a β-gal substrate (X-gal) that is blue after enzymatic conversion (top) and DAPI (bottom). X-gal staining in aged, wild-type littermate showed negligible endogenous β-gal activity. **(E)** Analysis of Wnt signaling activity in myogenic progenitors derived from muscle fibers of TOPGAL mice. Cells were incubated in young or aged serum for 17 hours in the presence or absence of a soluble Wnt inhibitor, sFRP3. The β-gal activity was quantified and normalized to DNA content. The data are presented relative to the levels of β-gal activity in cells exposed to young serum. (*$P < 0.05$.) **(F)** Analysis of GSK3β⁺ in myogenic progenitors isolated from parabiotic pairs. Labeling as in Fig. 1B (*$P < 0.05$, **$P < 0.01$.) **(G)** Wnt reporter gene expression in LSL cells exposed to serum obtained from young and aged mice and incubated with agarose beads conjugated with chimeric Frizzled receptors (Frz1-Fc, Frz7-Fc) or IgG control. Cells were incubated for 24 hours, and luciferase activity was quantified and normalized to β-gal activity (*$P < 0.05$.)

We tested whether the observed heterochronic parabiotic effects (Fig. 1) were associated with corresponding changes in the Wnt signaling pathway. Indeed, in heterochronic pairings, cells from the aged partners exhibited decreased Wnt signaling, and cells from the young partners showed increased Wnt signaling compared with that seen in cells in isochronic controls (Fig. 3F). Thus, circulating factors in aged animals appear to convey signals that result in enhanced Wnt signaling.

To test for the presence of components of serum capable of activating Wnt signaling by binding to Frizzled receptors, we used a chimeric Wnt receptor fusion protein, Frizzled-Fc, to deplete the serum of such activity (fig. S8). Serum was incubated with conjugated Frizzled-Fc or immunoglobulin IgG-Fc control and subsequently tested for its effects on a cell line (LSL) in which luciferase expression is dependent on activation of the Wnt pathway (*15*). When incubated with Frizzled-Fc, the activity in aged serum that promoted Wnt signaling decreased, there was no change in the activity of young serum subjected to the same treatment (Fig. 3G).

We altered Wnt signaling experimentally to test directly for its effects on cell fate and muscle regeneration. Addition of Wnt3A protein to young serum resulted in an increased myogenic-to-fibrogenic conversion of young progenitors in vitro. Conversely, the myogenic-to-fibrogenic conversion by aged serum was abrogated by Wnt inhibitors (Fig. 4A).

In vivo, the injection of Wnt3A into young regenerating muscle 1 day after injury resulted in increased connective tissue deposition (Fig. 4B), phenotypically similar to regenerating aged muscle (fig. S1). Exogenous Wnt also reduced cellular proliferation in young regenerating muscles (fig. S9A). We therefore tested whether inhibiting Wnt signaling in aged muscle would reduce fibrosis and enhance muscle regeneration. Indeed, there was reduced fibrosis in aged regenerating muscle injected with DKK1, whereas no change was observed in young muscle similarly treated (Fig. 4C). Injection of sFRP3 also enhanced myogenic progenitor proliferation in aged muscle (fig. S9, B and C).

These findings demonstrate that with age, the systemic environment is less effective in maintaining the myogenic fate of muscle stem cells and instead facilitates conversion to a fibrogenic fate. In vivo, this is associated with impaired muscle regeneration and an enhanced fibrotic response. These effects are associated with increased Wnt signaling in the myogenic progenitors, possibly resulting from increased amounts of Wnt or Wnt-like molecules in the serum of aged animals. This generalized role of Wnt signaling in promoting an aging phenotype is consistent with the findings of Liu *et al.* from studies of the role of Klotho in tissue aging (*16*). It is clear that Wnts have multiple actions both developmen-

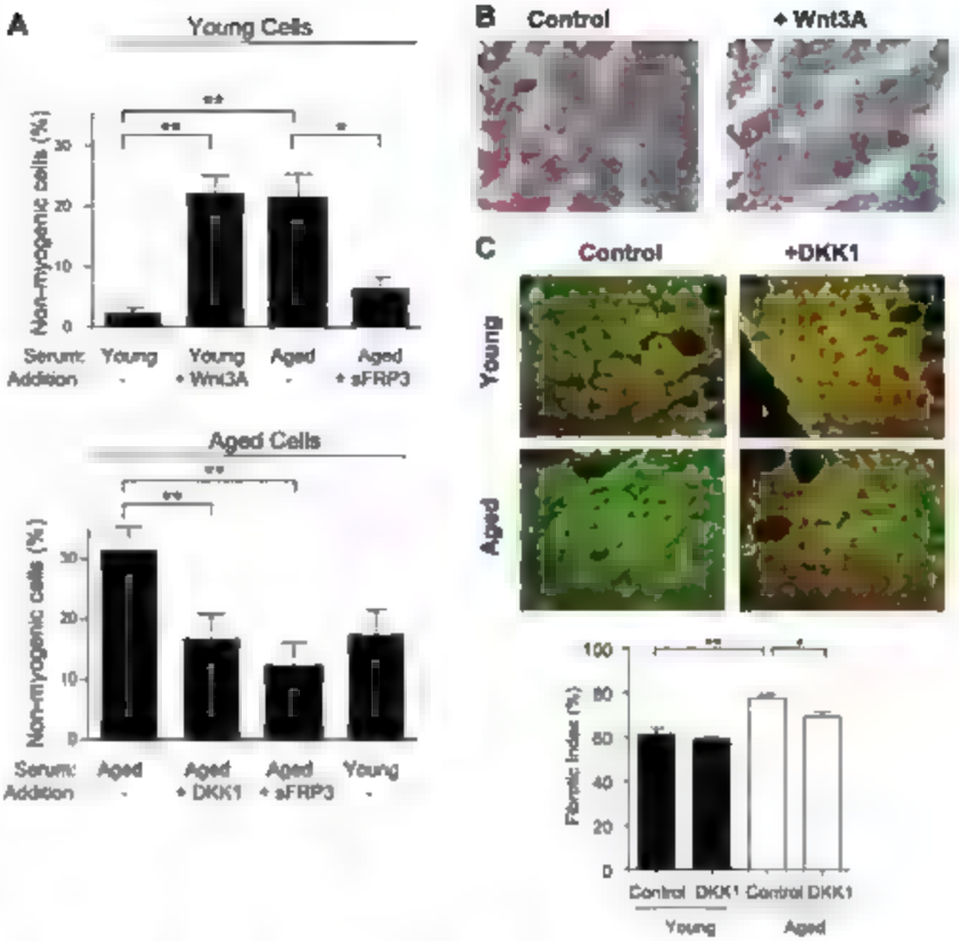

Fig. 4. The effects of the aged environment on myogenic progenitor cell fate and muscle regeneration are mediated by the Wnt signaling pathway. (**A**) (Top) The fate of myogenic progenitors from young mice incubated in young serum, with or without exogenous Wnt3A, or incubated in aged serum, with or without the Wnt inhibitor sFRP3, for 1½ days. (Bottom) Fate of myogenic progenitors from aged mice incubated in young serum or in aged serum, with or without sFRP3 or DKK1, for 1½ days. The percentages of cells that acquired a nonmyogenic cell fate were analyzed morphologically and immunohistochemically as described in Fig. 2 (*$P < 0.05$; **$P < 0.01$.) (**B**) Effects of exogenous Wnt on muscle regeneration. Muscles of young mice were injured, and either Wnt3A (200 ng/10 μl) or control solution [10 μl of 0.1% bovine serum albumin (BSA)] was injected into regenerating tissues 1 day after injury. Cryosections were stained with Gomori stain. (**C**) Effects of Wnt inhibition on fibrosis in regenerating muscle. Muscles of young and aged mice were injured, and either DKK1 (500 ng/10 μl) or control solution (10 μl of 0.1% BSA) was injected into regenerating tissues 1 day after injury. Muscles were analyzed 5 days later. Cryosections were stained with antibodies against collagen VI (green) and embryonic myosin heavy chain (red). The histogram represents the fibrotic index (as in Fig. 1B). (**$P < 0.01$; *$P < 0.05$.)

in vivo and postnatally (*17*). In contrast to the inhibition of myogenesis reported here, Wnt signaling may promote myogenic lineage progression during development (*18*). Such pleiotropic effects may relate to differences in the timing of Wnt signaling with regard to the state of cellular differentiation or to changes in other interacting signaling pathways during development and aging. Our results may provide a strategy to improve tissue repair, particularly under conditions in which regeneration is impaired and fibrosis is favored, such as in aging and muscular dystrophies.

References and Notes

1. G. Goldspink, K. Fernandes, P. E. Williams, D. J. Wells, *Neuromuscul. Disord.* **4**, 183 (1994).
2. M. D. Grounds, *Ann. N Y Acad. Sci.* **854**, 78 (1998).
3. J. M. Conboy, T. A. Rando, *Cell Cycle* **4**, 407 (2005).
4. C. Pastoret, A. Sebille, *J. Neurol. Sci.* **129**, 97 (1995).
5. I. M. Conboy, M. J. Conboy, G. M. Smythe, T. A. Rando, *Science* **302**, 1575 (2003).
6. I. M. Conboy *et al.*, *Nature* **433**, 760 (2005).
7. Materials and methods are available as supporting material on *Science* Online.
8. M. Chiba *et al.*, *Am. J. Pathol.* **162**, 1495 (2003).
9. F. Jiang, C. J. Parsons, B. Stefanovic, *J. Hepatol.* **45**, 401 (2006).
10. E. H. Cho *et al.*, *Mol. Cell. Biol.* **22**, 1172 (2002).
11. R. DasGupta, E. Fuchs, *Development* **126**, 4557 (1999).
12. T. Hagen, E. Di Daniel, A. A. Culbert, A. D. Reith, *J. Biol. Chem.* **277**, 23330 (2002).
13. K. Willert, R. Nusse, *Curr. Opin. Genet. Dev.* **8**, 95 (1998).
14. F. Kuhnert *et al.*, *Proc. Natl. Acad. Sci. U.S.A.* **101**, 266 (2004).
15. J. T. Binder, R. Nusse, *BMC Cell Biol.* **7**, 28 (2006).
16. H. Liu *et al.*, *Science* **317**, 803 (2007).
17. R. Nusse, *Cell Res.* **15**, 28 (2005).
18. P. Holowacz, T. Zeng, A. B. Lassar, *Dev. Dyn.* **235**, 633 (2006).

19. We thank E. Fuchs for TOPGAL mice, R. Nusse for recombinant Wnt3A and L51 cells, and B. Olwin for the Syndecan-4 antibody. Supported by a grant from the NIH (DK069989) to C.J.K. and by grants from the NIH (AG23806), the Department of Veterans Affairs (Merit Review), the Ellison Medical Foundation, and an NIH Director's Pioneer Award to T.A.R.

Supporting Online Material

www.sciencemag.org/cgi/content/full/317/5839/807/DC1
Materials and Methods
Figs. S1 to S9
References

23 April 2007; accepted 9 July 2007
10.1126/science.1144090

International Conservation Policy Delivers Benefits for Birds in Europe

Paul F. Donald,[1]* Fiona J. Sanderson,[2] Ian J. Burfield,[2] Stijn M. Bierman,[3] Richard D. Gregory,[1] Zoltan Waliczky[2]

Conservation of the planet's biodiversity will depend on international policy intervention, yet evidence-based assessment of the success of such intervention is lacking. Poor understanding of the effectiveness of international policy instruments exposes them to criticism or abandonment and reduces opportunities to improve them. Comparative analyses of population trends provide strong evidence for a positive impact of one such instrument, the European Union's Birds Directive, and we identify positive associations between the rate of provision of certain conservation measures through the directive and the response of bird populations. The results suggest that supranational conservation policy can bring measurable conservation benefits, although future assessments will require the setting of quantitative objectives and an increase in the availability of data from monitoring schemes.

Because global threats to biodiversity are largely anthropogenic, already considerable in scale, and accelerating rapidly (*1*), their solutions will depend largely on international policy intervention. This was recognized in the formulation of international agreements

such as the Convention on Biological Diversity (CBD); at least 20 regional or global conservation agreements currently exist, absorbing a high proportion of global conservation resources (*2*). Evaluation of the impact of international conservation policy intervention lags far behind that of most other policy fields (*3*), largely because of a paucity of data on the response of the species to which intervention is targeted (*4*, *5*). This leads to a poor understanding of the cost effectiveness of the relevant policy instruments (*6*), reducing opportunities to improve them (*7*) and exposing them to criticism from both within and outside the conservation lobby (*8*). Although properly implemented conservation legislation can bring measurable benefits to wildlife (*9*–*11*), evaluation has hitherto had its basis either in an assessment of the provision of conservation resources, rather than the population responses of the target species to such provision, or in the responses of a small, possibly unrepresentative proportion of the species or countries to which such legislation was targeted. We assessed the impact of an international bird conservation policy that covers all member states of the European Union (EU) by using data on all the species and countries to which the agreement applies. We aimed to provide an independent assessment of the extent to which a major international policy instrument has resulted in the delivery of measurable conservation outcomes.

Biodiversity conservation legislation in the EU is founded primarily on two directives, Council Directive 79/409/EEC of 2 April 1979 on the conservation of wild birds (the Birds Directive) and Council Directive 92/43/EEC of 21 May 1992 on the conservation of natural habitats and of wild fauna and flora (the Habitats Directive). The Birds Directive set out to establish a framework and objectives for the conservation of all birds throughout the EU, although the precise legal mechanisms for achieving this aim were left to the discretion of individual member states. Central to the directive was a list (Annex I) of species considered to be particularly vulnerable or rare or to require special conservation measures (*12*). Member states are bound by the directive to improve the conservation status of these species by protecting or enhancing their habitats, for example, through the designation of special protection areas (SPAs) (*12*). Furthermore, a number of general measures to protect populations of all bird species was also agreed upon. No quantitative targets were set in the directive, so we developed five expectations that should be met for us to conclude that the directive has had a detectable positive impact. (i) We expected to detect an improvement in the population trajectory of species listed on Annex I after the implementation of the directive, relative to that of non–Annex I species, within the original 15 member states of the EU (EU 15). (ii) We expected any improvement in the population trajectory of Annex I species relative to non–Annex I species in the EU 15 to be significantly greater than that recorded in parts of Europe to which the directive does not apply. (iii) We expected trends of Annex I and non–Annex I species to be more positive within the EU 15 than outside it. (iv) We expected any positive impacts of Annex I listing to be most apparent in species that have been listed for longest. (v) We expected to detect a positive association across participating countries between the extent to which the directive's conservation initiatives were deployed and trends in bird populations. Our analytical approach has its basis in the statistical testing of these five expectations.

Major inventories on the status and population trends of all of Europe's breeding birds, collected at a country level and covering the periods 1970–1990 and 1990–2000 (*13*, *14*), provided the opportunity to evaluate the impact of the Birds Directive. In each period, population trends of each species in each European country were allocated a single population trend score; these have already been published (*13*, *14*) and formed the data we modeled to test the expectations described above. The availability of data from two time periods, and from within and outside the EU, permitted an analysis with serendipitous characteristics of a highly replicated before-after-control-impact (BACI) approach (*15*). This permitted comparison of trends before and after 1990, between Annex I and non–Annex I species within the EU, and between Annex I species in the EU and the same group of species outside the EU (*16*). The use of a semi-experimental design based on both horizontal and longitudinal comparisons and the testing of multiple expectations maximized the likelihood that the observed patterns were causally related to variables identified by the models as having significant explanatory power.

Because the aim of the analysis was to examine the impact of Annex I listing by using trends over the period 1990–2000, we limited comparisons to data from the EU15, all but three of which joined the EU before the start of the 1990–2000 census period (*17*). For the same reason, we restricted our list of Annex I species to those added to the Annex before 1993 (*12*). Because trends were recorded in bands of unequal width (ordered from increasingly negative to increasingly positive population trends), we treated the response variable as ordinal and used the proportional odds model to assess differences between groups of species in the cumulative probabilities of being in higher ordered trend bands (*16*). After controlling for known variation within the database in trends between species using different habitats (*18*), between migrants and nonmigrants (*19*), and for the non-independence of trends within countries and species, we detected a highly significant effect of Annex I listing (Fig. 1). In the EU 15, Annex I species were significantly more likely to be assigned to a lower population trend class than non–Annex I species in 1970–1990. However, this pattern was reversed in 1990–2000, when Annex I species were significantly more likely

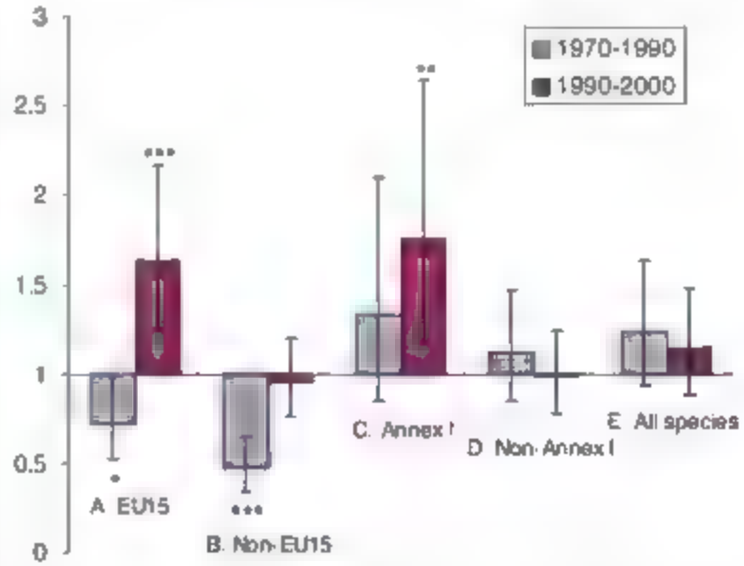

Fig. 1. Odds ratios (±95% confidence limits) from proportional odds models (*16*). Each bar indicates the ratio of two groups of species in their cumulative odds of being in a more positive trend band in one of two time periods, with significant deviations from 1 indicated (*$P < 0.05$, **$P < 0.01$, ***$P < 0.001$). The odds ratios indicate how many times higher the odds were of populations of Annex I species having more positive trends than populations of non–Annex I species in the EU15 (**A**) and outside the EU15 (**B**) in each time period. Significant positive deviation from an odds ratio of 1 indicates a significantly higher probability that Annex I species had more positive trends than non–Annex I species; odds ratios that are significantly smaller than 1 indicate the reverse. The cumulative odds of species in the EU15 having a more positive population trend than those in non-EU15 countries are shown for Annex I species (**C**), non–Annex I species (**D**), and all species combined (**E**). All models controlled for the known effects on trend of each species' habitat and migration strategy and controlled for the non-independence of trends within species across countries.

[1]Royal Society for the Protection of Birds, The Lodge, Sandy, Bedfordshire SG19 2DL, UK. [2]BirdLife International, Wellbrook Court, Girton Road, Cambridge CB3 0NA, UK. [3]Biomathematics and Statistics Scotland, University of Edinburgh, The King's Buildings, Edinburgh EH9 3JZ, UK.

*To whom correspondence should be addressed. E-mail: paul.donald@rspb.org.uk

to be recorded in a higher population trend band than non-Annex I species (Fig. 1A), thus meeting our first expectation. Outside the EU15, although trends of Annex I species improved significantly compared to those of non-Annex I species, they were no more likely to have more positive trends than non-Annex I species in 1990–2000 (Fig. 1B). The difference in trend between Annex I and non-Annex I species did not differ between the EU15 and non-EU15 countries in 1970–1990 [difference in log(odds ratios) −0.17 ± 0.22 SE] but was significantly greater in the EU15 than in non-EU15 countries in 1990–2000 [difference in log(odds ratios) 0.52 ± 0.18 SE]. Thus, our second expectation was met.

There was no significant difference in trends of Annex I species within and outside the EU15 in 1970–1990. However, by 1990–2000, Annex I species in the EU15 were significantly more likely to be recorded in a higher trend band than the same group of species outside the EU15 (Fig. 1C), a pattern that was not apparent in non-Annex I species (Fig. 1D) or across all species combined (Fig. 1E). Our third expectation was therefore partly met.

Between 1990 and 2000, species listed on Annex I of the Birds Directive fared significantly better on average than non-Annex I species within the EU15, a pattern not apparent in the same groups of species outside the EU15. This difference withstood controls for phylogenetic non-independence (*16*) and was due almost entirely to trends of species that had been listed on Annex I for longest (fig. S1), supporting both our fourth expectation and a previous estimate (*9*) that the lag between policy intervention and a detectable population-level response exceeds 10 years. Because the effects of both habitat and migration strategy were controlled in the analyses, this difference could not be ascribed to Annex I species being disproportionately represented in habitat or migration classes that fared better than average. Nor could the difference be accounted for by the deliberate or fortuitous allocation to Annex I of species that were already increasing, because most of these species were listed well before 1990, when their trends were significantly more negative than those of non-Annex I species (Fig. 1A). Lastly, the difference in trends between Annex I and non-Annex I species in the EU could not be explained by a general global increase in Annex I species, for example in response to climate change, because outside the EU15 Annex I trends were no different from those of non-Annex I species.

Evidence for a causal link between policy intervention and species response (our fifth expectation) was found in the positive association across EU15 countries between mean species trend and the proportion of land designated as SPAs (Fig. 2). This pattern was apparent for all species combined, and for Annex I and non-Annex I species separately, and was significantly stronger for Annex I than for non-Annex I species. Parameters of proportional odds models suggested that, for every additional 1% of a country's land area designated as SPAs, the odds of a species being in more-positive population trend classes increased by around 4% across all species and for non-Annex I species and by around 7% for Annex I species (*16*). The significantly stronger response of Annex I species to the provision of SPAs is consistent with a causal link between the delivery of conservation measures through the directive and the response of the target species because SPA designation and management are targeted largely toward Annex I species.

Therefore, four of our five expectations of a positive impact of the Birds Directive were fully met, and the remaining one was partly met (populations of Annex I species, although not of non-Annex I species, had more positive trends in the EU15 than outside it). Furthermore, although trends of non-Annex I species did not differ between the EU15 and other countries, there was evidence that trends of these species were more positive within the EU15 in countries with higher deployment of SPAs. The data are therefore consistent with the hypothesis that the Birds Directive has brought demonstrable benefits to bird populations in the EU, and that international policy intervention can be effective in addressing conservation issues over large geographical areas.

Our results support previous assertions (*4*, *5*, *20*) that relatively simple yet robust population monitoring can play an important role in assessing the success of supragovernmental conservation policies, as it already has in demonstrating the environmentally damaging effects of international policy in other sectors (*21*). Much biodiversity monitoring is undertaken by volunteers (*22*), making it inexpensive relative to the costs of developing and implementing international policy. If such policies were to provide support for monitoring, for example by contributing to a global monitoring network (*23*), their success could be evaluated. Furthermore, setting targets that are both quantitative and measurable would increase the resolution of subsequent assessments. Precise goals and specific measures for monitoring policy effectiveness should be designed and tested at the time that the policy is implemented. Otherwise, quantitative assessments of policy intervention will continue to depend on post hoc, serendipitous analyses of the type presented here. Until policy and monitoring become more integrated, the success of international conservation policies in protecting the planet's biodiversity or in achieving goals such as the CBD's 2010 target to reduce the rate of biodiversity loss (*24*) will be difficult or impossible to quantify. The prognosis for biodiversity is grim because this lack of feedback can only serve to weaken international policy intervention at a time of unprecedented loss.

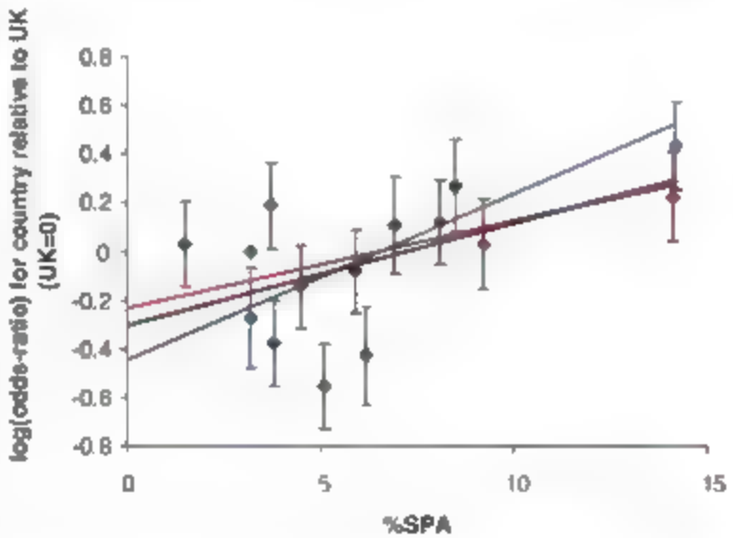

Fig. 2. Plot of country estimates of log(odds ratios) against the percentage of land area designated as SPAs in the EU15 member states for Annex I and non–Annex I species combined (means ± SE and black regression line; slope = 0.042). The odds ratios indicate the extent to which species are more or less likely to appear in more-positive trend classes than species in the reference country (UK), which has a value of zero and no SE. In order to graphically represent this relationship, country effects of odds ratios were extracted from a proportional odds model of trend class, with migration strategy and breeding habitat also fitted as fixed effects and species fitted as a random effect. The regression coefficient differed significantly from zero ($P < 0.02$) and was estimated by fitting percentage of SPA cover directly as a covariate in a proportional odds model and including a random country effect (*16*). A similarly significant positive association was apparent for Annex I (regression line only shown in blue, slope = 0.068) and non-Annex I (regression line only shown in red, slope = 0.036) species separately. A significant ($P < 0.01$) interaction term indicated that the slopes for Annex I and non–Annex I species differed.

References and Notes

1. A. Balmford, W. Bond, *Ecol. Lett.* **8**, 1218 (2005).
2. G. C. Boere, C. G. A. Rubec, in *Conserving Bird Biodiversity: General Principles and their Application*, K. Norris, D. J. Pain, Eds. (Cambridge Univ. Press, Cambridge, 2002), pp. 246–270.
3. P. J. Ferraro, S. K. Pattanayak, *PLoS Biol.* **4**, e105 (2006).
4. R. E. Green *et al.*, *Conserv. Biol.* **19**, 56 (2005).
5. A. Balmford, R. E. Green, M. Jenkins, *Trends Ecol. Evol.* **18**, 326 (2003).

6. F. Watzold, K. Schwerdtner, *Biol. Conserv.* **123**, 327 (2005).
7. D. J. Rohlf, *Conserv. Biol.* **5**, 273 (1991).
8. E. Stokstad, *Science* **309**, 2150 (2005).
9. T. D. Male, M. J. Bean, *Ecol. Lett.* **8**, 986 (2005).
10. D. J. Pain *et al.*, *Anim. Conserv.* **9**, 322 (2006).
11. A. J. Cahill, J. S. Walker, S. J. Marsden, *Orx* **40**, 161 (2006).
12. Further information on the Birds Directive, the suite of conservation measures it introduced, and a list of species classified in the analyses as Annex I species are given in the Supporting Online Material (SOM) text.
13. G. M. Tucker, M. F. Heath, *Birds in Europe: Their Conservation Status* (BirdLife Conservation Series No. 3, BirdLife International, Cambridge, 1994). The raw data underlying this assessment, and used in the present paper, were published in (*25*).
14. BirdLife International, *Birds in Europe: Population Estimates, Trends and Conservation Status* (BirdLife Conservation Series No. 12, BirdLife International, Cambridge, 2004). These data are freely available at www.birdlife.org/action/science/species/birds_in_europe/species_search.html.
15. A. Stewart-Oaten, *The Before-After/Control-Impact-Pairs Design for Environmental Impact Assessment* (Marine Review Committee, San Francisco, 1986).
16. Materials and methods are provided on *Science* Online.
17. Austria, Finland, and Sweden joined on 1 January 1995 and so were member states for 6 of the 11 years of the 1990–2000 census period.
18. P. F. Donald, F. J. Sanderson, I. J. Burfield, F. P. J. van Bommel, *Agric. Ecosyst. Environ.* **116**, 189 (2006).
19. F. J. Sanderson, P. F. Donald, D. J. Pain, I. J. Burfield, F. P. J. van Bommel, *Biol. Conserv.* **131**, 93 (2006).
20. A. Balmford, P. Crane, A. Dobson, R. E. Green, G. M. Mace, *Philos. Trans. R. Soc. London Ser. B* **360**, 221 (2005).
21. P. F. Donald, R. E. Green, M. F. Heath, *Proc. R. Soc. London Ser. B* **268**, 25 (2001).
22. R. D. Gregory *et al.*, *Philos. Trans. R. Soc. London Ser. B* **360**, 269 (2005).
23. H. M. Pereira, H. D. Cooper, *Trends Ecol. Evol.* **21**, 123 (2006).
24. A. Balmford *et al.*, *Science* **307**, 212 (2005).
25. BirdLife International/European Bird Census Council, *European Bird Populations, Estimates and Trends* (BirdLife Conservation Series No. 10, BirdLife International, Cambridge, 2000).

26. We thank R. B. Bradbury, D. J. Cartwright, D. Elston, A. Gammell, D. W. Gibbons, R. E. Green, D. J. Pain, W. J. Sutherland, and two anonymous referees for help and comments and the many observers across Europe who collected the data. The 1970–1990 data set was compiled by G. Tucker and M. Heath, in association with the European Bird Census Council. S.M.B. gratefully acknowledges funding from the EU, contract no. GOCECT-2003-506675.

Supporting Online Material

www.sciencemag.org/cgi/content/full/317/5839/810/DC1
Materials and Methods
SOM Text
Fig. S1
References
Appendix S1

4 June 2007; accepted 18 June 2007
10.1126/science.1146002

Adaptive Mutations in Bacteria: High Rate and Small Effects

Lília Perfeito,[1] Lisete Fernandes,[1,2] Catarina Mota,[1] Isabel Gordo[1]*

Evolution by natural selection is driven by the continuous generation of adaptive mutations. We measured the genomic mutation rate that generates beneficial mutations and their effects on fitness in *Escherichia coli* under conditions in which the effect of competition between lineages carrying different beneficial mutations is minimized. We found a rate on the order of 10^{-5} per genome per generation, which is 1000 times as high as previous estimates, and a mean selective advantage of 1%. Such a high rate of adaptive evolution has implications for the evolution of antibiotic resistance and pathogenicity.

The rate at which new mutations arise in natural populations and their fitness effects are of key importance in evolutionary genetics. Classical mutation accumulation experiments have indisputably shown that among the spontaneous mutations that affect fitness, those that cause deleterious effects are far more common than those that cause increases in fitness. Whereas there are currently several direct and indirect estimates of the deleterious mutation rate in different organisms, data are lacking for beneficial mutations (*1*). The latter are of particular interest because they constitute the driving force of adaptation and survival of populations in new environments.

Several theoretical studies have made some general predictions about the long-term process of adaptation toward an optimum (*2*, *3*). One prediction suggests that the effects of beneficial (advantageous) mutations (s_a) are exponentially distributed, in that many have very small effects and those that cause strong increments in fitness are rare (*3*). These are plausible predictions given that organisms are in general well adapted to their environments, so only small and rare changes lead to fitness increases (*4*–*11*).

The true distribution of newly arising beneficial mutations in an organism in a given environment is difficult to estimate because the probability of fixation of a beneficial mutation that increases fitness by s_a is only $2s_a$, which means that mutations of small effect are not likely to increase in frequency. This implies that the distribution of mutations that escape stochastic loss (become fixed or reach high enough frequencies to be observed) is truncated for small values (*12*, *13*). In addition, clonal interference occurs in large populations with a high beneficial mutation rate (U_a) and no recombination and will slow adaptation (compared to sexual populations of the same size) (*14*). Namely, if multiple beneficial mutations appear in different lineages, they compete with each other for fixation. This translates into an adaptation rate less than that predicted by the mutation rate and population size, and into the fixation only of mutations of large effect (*15*). Recently, there has been a considerable effort to predict the rate and distribution of beneficial mutations and the effect of clonal interference on the adaptation rate (*16*, *17*).

Current estimates for U_a fall around 10^{-9} to 10^{-8} for RNA viruses and *Escherichia coli* (*4*, *5*, *16*). A similar beneficial mutation rate was estimated for *Pseudomonas fluorescens* under adaptation to stressful conditions (*9*). A caveat for all of these estimates is that they were obtained from populations with very large effective population size (N_e) and followed adaptation to a new environment under conditions in which clonal interference had a strong effect. This led to downward biased estimates of U_a. Here, we provide estimates for the genomic mutation rate for beneficial mutations in *E. coli* that are less biased by clonal interference.

In this work, we used populations with an intermediate effective population size: big enough that genetic drift is unlikely to drive slightly deleterious mutations to a high frequency but small enough to minimize the effects of clonal interference between beneficial mutations. To estimate the beneficial mutation rate and the distribution of fitness effects of single mutations, we used a microsatellite marker system pioneered by Imhof and Schlotterer (*4*). Mutations at a microsatellite locus coded by a nonconjugative plasmid can generate neutral allelic diversity in a very short time (*4*, *18*), and selective sweeps, occurring in the bacterial genome, can be identified by following the rapid increase in the frequency of the linked microsatellite allele (*4*).

We allowed populations of *E. coli* to adapt to a given laboratory environment for 1000 generations and followed the allelic distribution of the microsatellite at periodic intervals. From this distribution, the number of mutations that escaped stochastic loss during this period was inferred for populations with a small effective size ($N_e = 2 \times 10^4$) and for populations with a very large effective size ($N_e = 10^7$). The latter allowed us to compare our estimates with those previously published (*4*, *16*, *19*).

The beneficial mutations that escape stochastic loss are expected to follow a gamma distribution with shape parameter 2 and with a mean

[1]Instituto Gulbenkian de Ciência, Rua da Quinta Grande, number 6, 2780-156 Oeiras, Portugal. [2]Escola Superior de Tecnologia da Saúde de Lisboa, Lisboa, Portugal.
*To whom correspondence should be addressed. E-mail: gordo@igc.gulbenkian.pt

equal to twice that of the distribution of the spontaneously arising mutations (*16*). Figure 1 shows the observed distributions of effects of favorable mutations segregating in the populations. In the populations with the smaller effective size ($N_e = 2 \times 10^4$), the mean value of the selection coefficient [$E(s_a)$] measured was 0.013, which is slightly smaller, although close to previous estimates (*4*, *16*). In these populations (Fig. 1A) we find that a gamma distribution with such parameterization provides a good fit to the data (Kolmogorov-Smirnov: not significant, $P = 0.6$). In Fig. 1B, we show the distribution of selective effects measured in the populations with larger effective size ($N_e = 10^7$). As expected, in these populations, the effect of clonal interference was clearly observed in the distributions of microsatellite allele variation [for an example, see fig. S2 (*19*)]. As predicted theoretically (*15*), the effect of interference between clones carrying different beneficial mutations is reflected in an increased value of the mean selective effect of mutations segregating in the population [$E(s_a) = 0.023$, as shown in Fig. 1B]. This is because many newly arising beneficial mutations of small effect are lost in competition with mutations of larger effect.

To measure the rate of spontaneous beneficial mutations, we quantified the total number of mutations that escaped stochastic loss in all the populations with the same effective size during the course of the experiment. We observed 75 such events in the populations with $N_e = 2 \times 10^4$ and 87 in the populations with $N_e = 10^7$. Assuming that the effect of clonal interference is negligible in the populations with larger N_e, we would infer a mutation rate of 2×10^{-8} beneficial mutations per genome, per generation (*20*, *21*). This value is close to those previously measured for this species with the use of populations with similar effective sizes (*4*, *16*). However, with such a large N_e, the effect of clonal interference is very important and leads to an extreme underestimation of the true value of U_a. Indeed, in the populations of smaller effective size, our estimate of the mutation rate was 1000 times as high: $U_a = 2 \times 10^{-5}$ beneficial mutations per genome, per generation (*20*, *21*). Given that clonal interference is much weaker in these populations, we take this value to be a much more accurate measure of the real U_a.

To complement these results, we measured the mean fitness of each evolved population relative to the ancestral one. Mean fitness of an evolved population was assessed by its competitive ability against a reference strain (*19*). As expected in view of the results obtained above, there was an overall increase in fitness in all populations after 1000 generations of adaptation. In the populations with the smaller N_e, this increase was about 17%, which, as expected, was smaller than the one observed for the populations with a larger N_e (overall mean increase in fitness of 40%). We then asked if our estimates of U_a could explain such increments in fitness (*22*). To do this, we compared the results of Monte-Carlo simulations of adaptive evolution, assuming several different values of U_a and $E(s_a)$ with those obtained in the experiments (*19*). In all the simulations, we assumed that the distribution of incoming beneficial mutations is exponential and that mutations interact in a multiplicative way (*2*, *23*). Different combinations of U_a and $E(s_a)$ were consistent with the fitness increase in populations of a given effective size, but the set of parameters that more closely matched the combined data of both population sizes was U_a between 10^{-5} and 10^{-4} and $E(s_a)$ between 1 to 2% (Fig. 2). These parameters agree with the estimates obtained from the microsatellite allelic distribution (small effective size populations in Fig. 1, in which the measured mutation rate was 2×10^{-5}). It is also clear that a mutation rate of about 10^{-9} or 10^{-8} [as inferred in other experiments (*4*, *16*)] cannot explain the fitness increases observed.

Our results show that the mutation rate to new beneficial alleles is 1000 times as high as previously inferred in the same bacterial species (*4*, *16*). The difference in results can be explained by the differences in the effective population size analyzed. If only very large effective sizes are analyzed, and the effect of clonal interference is not accounted for, then our estimates for U_a and $E(s_a)$ for the populations with $N_e = 10^7$ are similar to those previously obtained (Fig. 1B). However, if these estimates were close to the true values, then we would not expect to see the sweeps of beneficial mutations in the populations with lower N_e that we observed (Fig. 1A). Hence, neglecting the effect of clonal interference underestimates the value of U_a. In addition, we showed that clonal interference changes the distribution of segregating mutations. When comparing the distribution of beneficial mutations for the populations with high N_e (strong effect of clonal interference) with that for populations with low N_e (Fig. 1, A and B), a significant difference was observed (Kolmogorov-Smirnov: $P = 0.001$). As predicted theoretically (*15*, *24*), we observed a distribution with a higher mean selection coefficient when the effect of clonal interference was stronger. In the limiting case where the supply of new beneficial mutations per generation ($N_e U_a$) is very high, the speed of adaptation will no longer depend on $N_e U_a$ but on the mutations of largest effect available, be-

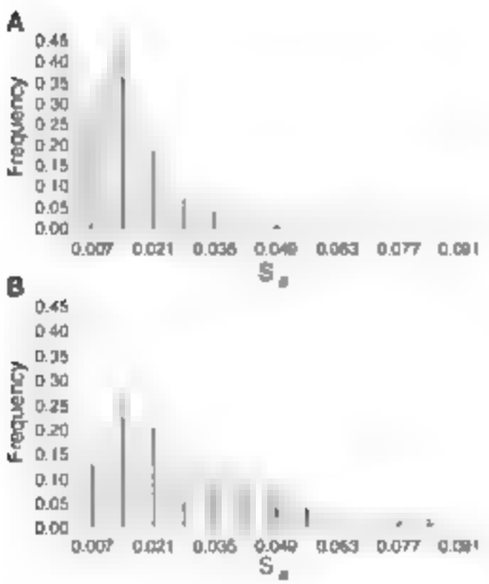

Fig. 1. Distribution of fitness effects of beneficial mutations that escaped stochastic loss, measured in populations of $N_e = 2 \times 10^4$ (**A**) and $N_e = 10^7$ (**B**). The gray bars show the distribution of effects of beneficial mutations inferred in the experimental populations and the white bars correspond to a gamma distribution with shape 2 and scale parameters 158 (A) and 85 (B). Both distributions are supported by the data [Kolmogorov-Smirnov: $P = 0.6$ in (A) and $P = 0.5$ in (B); not significant].

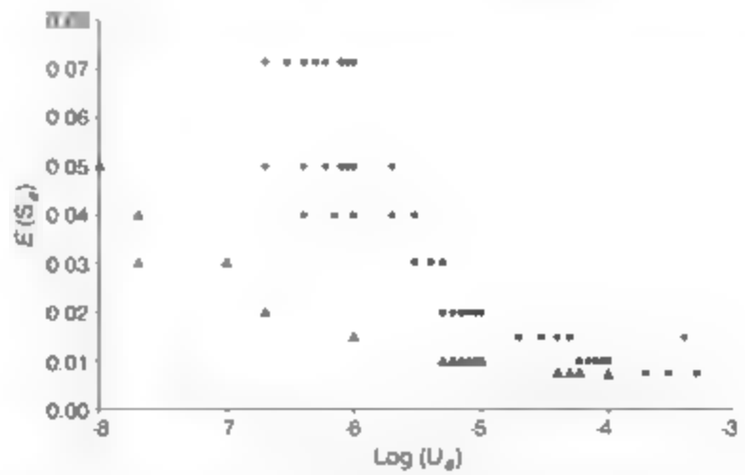

Fig. 2. Mutation rates (U_a) and mean effect of beneficial mutations [$E(s_a)$], used as parameters in Monte Carlo simulations (*19*), which produced mean fitness increases consistent with those observed in the evolved populations (difference was not significant, Student's *t* test $P > 0.05$). The circles show the parameter values consistent with the mean fitness observed in the populations of $N_e = 2 \times 10^4$ and the triangles in the populations of $N_e = 10^7$.

cause these are the only mutations that will fix. This might help explain why similar beneficial mutation rates are estimated in very diverse organisms under very diverse environments. These estimates are obtained in populations with very large effective sizes (*4*, *5*, *9*, *16*), which are likely to produce strong underestimations of U_a.

It is plausible that, in natural habitats, population sizes will be large. If the effective size of a bacterial species is much higher than 10^8 (*25*), then our results imply that clonal interference plays a major role in limiting the adaptation of these asexual organisms. As such, if there is a chance for recombination, clonal interference will be much lower and organisms will adapt faster. This has been predicted theoretically (*14*), although the empirical evidence is still very preliminary (*26*, *27*). Given our results, we anticipate that clonal interference is important in maintaining sexual reproduction in eukaryotes. Notably, mutation accumulation experiments in *Saccharomyces cerevisiae* and *Arabidopsis thaliana* have detected a significantly large number of mutants with increased fitness (*28*, *29*).

Given the estimates for the overall mutation rate in *E. coli* (*30*) and its genomic deleterious mutation rate (*1*), our estimate of U_a implies that 1 in 150 newly arising mutations is beneficial and that 1 in 10 fitness-affecting mutations increases the fitness of the individual carrying it. Hence, an enterobacterium has an enormous potential for adaptation and may help explain how antibiotic resistance and virulence evolve so quickly.

References and Notes

1. T. Bataillon, *Heredity* **84**, 497 (2000).
2. R. A. Fisher, *The Genetical Theory of Natural Selection* (Clarendon Press, Oxford, UK, 1930).
3. H. A. Orr, *Nat. Rev. Genet.* **6**, 119 (2005).
4. M. Imhof, C. Schlotterer, *Proc. Natl. Acad. Sci. U.S.A.* **98**, 1113 (2001).
5. R. Miralles, P. J. Gerrish, A. Moya, S. F. Elena, *Science* **285**, 1745 (1999).
6. C. L. Burch, L. Chao, *Genetics* **151**, 921 (1999).
7. C. Zeyl, *Genetics* **169**, 1825 (2005).
8. S. Estes, M. Lynch, *Evol. Int. J. Org. Evol.* **57**, 1022 (2003).
9. R. D. Barrett, R. C. MacLean, G. Bell, *Biol. Lett.* **2**, 236 (2006).
10. D. R. Rokyta, P. Joyce, S. Caudle, H. Wichman, *Nat. Genet.* **37**, 441 (2005).
11. R. Kassen, T. Bataillon, *Nat. Genet.* **38**, 484 (2006).
12. M. Kimura, *The Neutral Theory of Molecular Evolution* (Cambridge Univ. Press, Cambridge, 1983).
13. A. J. Betancourt, J. P. Bollback, *Curr. Opin. Genet. Dev.* **16**, 638 (2006).
14. W. G. Hill, A. Robertson, *Genet. Res.* **8**, 269 (1966).
15. P. Gerrish, R. Lenski, *Genetica* **102–103**, 127 (1998).
16. D. E. Rozen, J. A. de Visser, P. Gerrish, *Curr. Biol.* **12**, 1040 (2002).
17. M. Hegreness, N. Shoresh, D. Hartl, R. Kishony, *Science* **311**, 1615 (2006).
18. C. Schlotterer, M. Imhof, H. Wang, V. Nolte, B. Harr, *J. Evol. Biol.* **19**, 1671 (2006).
19. Materials and methods are available as supporting material on *Science* Online.
20. J. F. Crow, M. Kimura, *An Introduction to Population Genetics Theory* (Harper & Row, New York, 1970).
21. $U_a = 1-\exp(-\sum_{i=1}^{k} 2E(s_a)\cdot T)$, where k is the number of observed mutations, T is the number of generations and $E(s_a)$ is the mean selection coefficient. This assumes that there is no clonal interference. If its effect is major, the value of U_a will be greatly underestimated. Also, small effect mutations are likely to be missed because the time it takes for a mutation to increase in frequency is $\propto 1/s_a$.
22. The expected fitness increase over 1000 generations without clonal interference is $N_e \cdot 2\,E(s_a)\cdot E(s_a) \cdot 1000 = 0.14$ in the small size populations.
23. H. A. Orr, *Genetics* **163**, 1519 (2003).
24. R. D. H. Barrett, S. P. Otto, L. K. M'gonigle, *Genetics* **174**, 2071 (2006).
25. J. Charlesworth, A. Eyre-Walker, *Mol. Biol. Evol.* **23**, 1348 (2006).
26. B. Gromberg, C. Zeyl, *Evol. Int. J. Org. Evol.* **59**, 431 (2005).
27. M. Colegrave, *Nature* **420**, 664 (2002).
28. S. B. Joseph, D. W. Hall, *Genetics* **168**, 1817 (2004).
29. R. G. Shaw, D. Byers, E. Darmo, *Genetics* **155**, 369 (2000).
30. J. W. Drake, *Proc. Natl. Acad. Sci. U.S.A.* **88**, 7160 (1991).

31. This work was supported by POCTI/BSE/46856/2002 and SFRH/BD/18161/2004 through Fundação para a Ciência e Tecnologia. We thank M. Imhof for help in the initial setup of this work and R. Azevedo, D. Bachtrog, A. Coutinho, F. Dionisio, K. Xavier, and anonymous reviewers for comments on the manuscript.

Supporting Online Material

www.sciencemag.org/cgi/content/full/317/5839/813/DC1
Materials and Methods
SOM Text
Figs. S1 to S4
Table S1
References

8 March 2007; accepted 2 July 2007
10.1126/science.1142284

Divergence of Transcription Factor Binding Sites Across Related Yeast Species

Anthony R. Borneman,[1*] Tara A. Gianoulis,[2] Zhengdong D. Zhang,[3] Haiyuan Yu,[3] Joel Rozowsky,[3] Michael R. Seringhaus,[3] Lu Yong Wang,[4] Mark Gerstein,[2,3,5] Michael Snyder[3,2,3]†

Characterization of interspecies differences in gene regulation is crucial for understanding the molecular basis of both phenotypic diversity and evolution. By means of chromatin immunoprecipitation and DNA microarray analysis, the divergence in the binding sites of the pseudohyphal regulators Ste12 and Tec1 was determined in the yeasts *Saccharomyces cerevisiae*, *S. mikatae*, and *S. bayanus* under pseudohyphal conditions. We have shown that most of these sites have diverged across these species, far exceeding the interspecies variation in orthologous genes. A group of Ste12 targets was shown to be bound only in *S. mikatae* and *S. bayanus* under pseudohyphal conditions. Many of these genes are targets of Ste12 during mating in *S. cerevisiae*, indicating that specialization between the two pathways has occurred in this species. Transcription factor binding sites have therefore diverged substantially faster than ortholog content. Thus, gene regulation resulting from transcription factor binding is likely to be a major cause of divergence between related species.

Differences in related individuals are generally attributed to changes in gene composition and/or alterations in their regulation. Previous efforts to examine divergence of regulatory information have relied on the analysis of conserved sequences in putative promoter regions (*1*, *2*). However, these approaches are limited because transcription factor (TF) binding sites are often short and degenerate, making their computational detection difficult (*3*). In addition, requiring the conservation of motifs across species precludes the detection of sequences that are evolutionarily divergent.

The detection of binding sites with chromatin immunoprecipitation and microarray (ChIP-chip) analysis (*4*, *5*) offers the ability to globally map TF binding locations experimentally rather than computationally. For species such as yeasts, where genome sequences of numerous related species are available (*6*), this approach can allow for the evolutionary comparison of binding sites of conserved TFs across species.

We have used this approach to investigate evolutionary divergence in the targets of two developmental regulators in the *Saccharomyces sensu stricto* yeasts *S. cerevisiae*, *S. mikatae*, and *S. bayanus*. In *S. cerevisiae* diploids, Ste12 and Tec1 act cooperatively to regulate genes during pseudohyphal development (*7*–*9*), whereas in haploid cells, Ste12 regulates mating genes (*10*). The binding sites of Ste12 and Tec1 were mapped in all three species under low-nitrogen

[1]Department of Molecular, Cellular and Developmental Biology, Yale University, New Haven, CT 06511, USA. [2]Program in Computational Biology, Yale University, New Haven, CT 06511, USA. [3]Department of Molecular Biophysics and Biochemistry, Yale University, New Haven, CT 06511, USA. [4]Integrated Data Systems Department, Siemens Corporate Research, Princeton, NJ 08540, USA. [5]Department of Computer Science, Yale University, New Haven, CT 06511, USA.

*Present address: Australian Wine Research Institute, Glen Osmond, Adelaide, SA 5064, Australia.
†To whom correspondence should be addressed. E-mail: michael.snyder@yale.edu.

(pseudohyphal) conditions with the use of triplicate ChIP-chip experiments and species-specific high-density oligonucleotide tiling microarrays (fig. S1) (*11*). Ste12 bound to 380, 167 and 250 discrete sites, whereas Tec1 bound to 348, 185 and 126 sites, in *S. cerevisiae*, *S. mikatae*, and *S. bayanus*, respectively (tables S1 to S6). For each species, the two factors bound to a high proportion of common regions (86, 80, and 87%, for *S. cerevisiae*, *S. mikatae*, and *S. bayanus*, respectively), suggesting that the cooperative interaction observed between Ste12 and Tec1 in *S. cerevisiae* is conserved across the three *Saccharomyces* species.

Analysis of the signal tracks allowed for global comparisons in TF binding to be made among the species, revealing qualitative and quantitative differences in ChIP binding regions (Fig. 1A). To systematically perform interspecies comparisons, we removed regions that were not represented across all three yeast genomes (*12*). Comparison of the overlap in binding across species as a function of rank order revealed significant binding differences throughout the rank order, indicating that even strong targets from one species may not be bound in the others (Fig. 1B). As a control, replicate experiments from *S. cerevisiae* (*12*) displayed >98% concordance in binding.

Overall, three classes of TF binding events were observed: those conserved across all three species, those present in two of the three species, and species-specific binding events (Fig. 1C). Of the 221 and 255 targets bound in total by Ste12 and Tec1, respectively, only 47 (Ste12, 21%) and 50 (Tec1, 20%) targets were conserved across all three species (Figs. 1C and 2A). The conserved binding events were present throughout the rank order, indicating that both highly occupied and less-occupied regions are conserved (tables S7 and S8). To ensure that these binding differences were not due to the scoring threshold used, we calculated signal distributions for unbound orthologs of target regions (*12*). Of the unbound orthologous regions, 80% had signals similar to background, indicating that most will be unaffected by threshold changes (fig. S2). Even when identical binding regions were used, 23% differed in their intensity by at least 1.5 fold between species (0% between *S. cerevisiae* replicates), suggesting that quantitative differences exist in site occupation or binding strength between species (Fig. 2B and tables S9 and S10). Thus, most target genes were bound in only one or two of the three species, indicating considerable divergence in binding sites across

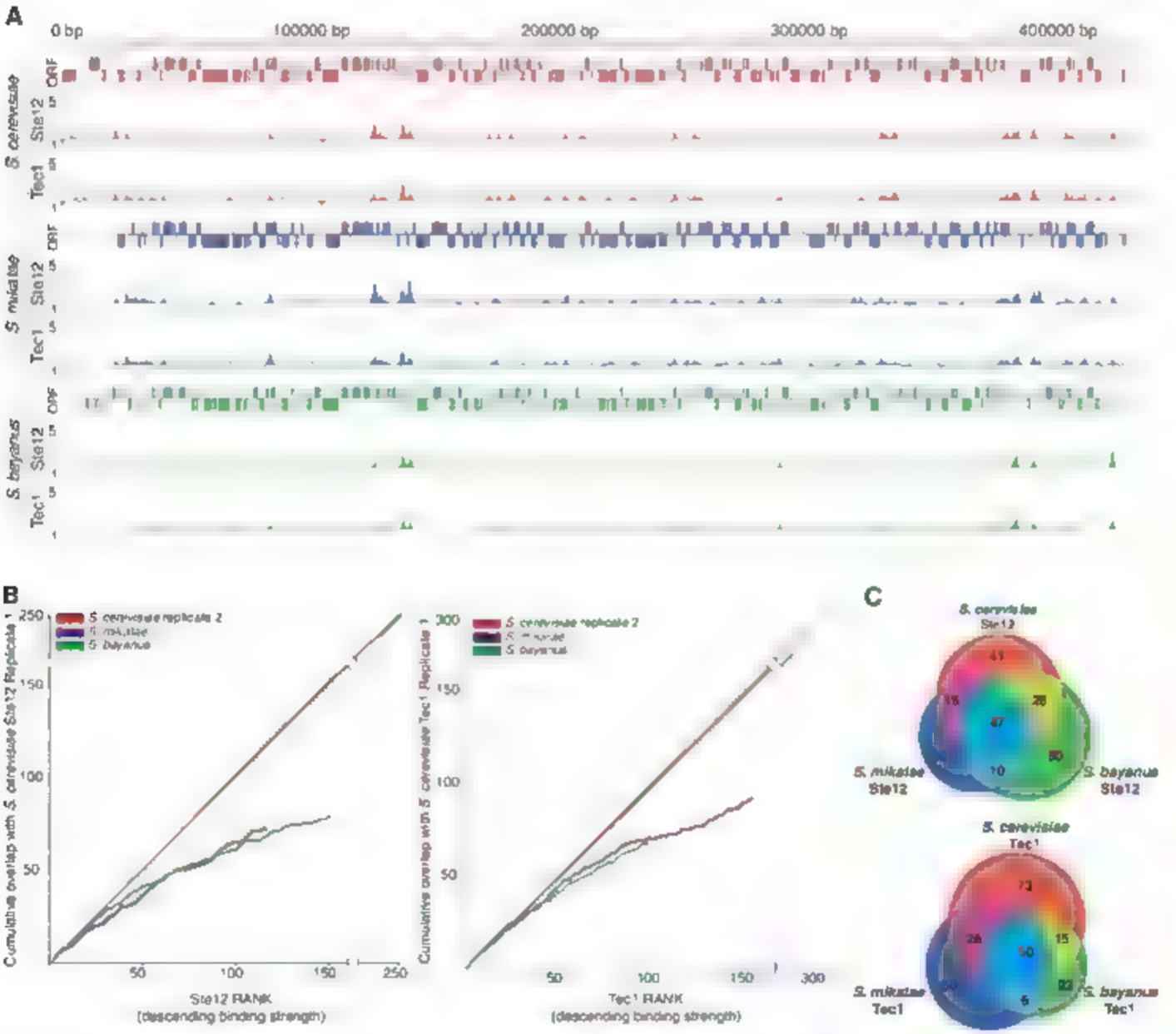

Fig. 1. (**A**) Ste12 and Tec1 bind to discrete regions of chromosome IX of *S. cerevisiae* and to orthologous regions of *S. mikatae* and *S. bayanus*. ChIP-chip enrichment by Tec1 and Ste12 (log 2 ratios) is shown relative to ORFs of *S. cerevisiae* (red), *S. mikatae* (blue), and *S. bayanus* (green). bp, base pairs. (**B**) Rank-order analysis of Ste12 and Tec1 ChIP-chip targets in *S. cerevisiae* (red), *S. mikatae* (blue), and *S. bayanus* (green) (*12*). (**C**) Gene target overlap across the three *Saccharomyces* species.

these yeasts (Fig. 2C). Because the fraction of nonconserved genes among *S. cerevisiae*, *S. mikatae*, and *S. bayanus* is less than 0.05% (*2*), the amount of variation in TF binding is substantially larger than that of gene variation.

One possible cause for the interspecies differences in the ChIP binding locations is divergence in binding site sequences. To examine this possibility, we investigated sequence motifs in both bound and orthologous unbound regions across the three *Saccharomyces* species. Position weight matrices (PWM), representing the putative binding motifs for Ste12 and Tec1, were generated from the ChIP-chip data (*13*). Analysis of the Tec1 targets of the three species revealed an overrepresented sequence motif that matched the known Tec1 consensus (*7*) (Fig. 3A), whereas the targets of Ste12 in *S. cerevisiae* and *S. mikatae* revealed a motif that was similar to the known binding sequence (*14*) (Fig. 3B). This sequence was not overrepresented in *S. bayanus*.

With the use of the PWM sequences, ChIP bound regions and orthologous unbound regions from each species were then scored for the presence of each motif (*15*). There were several significant classes of TF binding events, with those genes bound by all three factors present near the top of both the Tec1 (all bound, motif in all) and Ste12 (all bound, with and without motif) lists (Fig. 3, C and D). For promoter regions that displayed evolutionarily conserved ChIP binding in all three *Saccharomyces* species, 83% (Tec1) and 24% (Ste12) of the regions contained at least one significant occurrence of the PWM motif for that factor in each species (Fig. 3, E and F). In contrast, 2 and 62% of the promoters that displayed conserved ChIP binding did not contain a match to the PWM in at least two of the three species. Thus, the Ste12 motif is not present in a high proportion of pseudohyphal-responsive genes, implying that Tec1 may target Ste12 to these regulatory regions (*16*).

In contrast to the previous results in which experimentally determined binding correlated with the presence of predicted motifs, there were many examples where a species-specific loss of binding and/or a loss of sequence have occurred. There were 48 (Tec1, 14% of total binding events) and 35 (Ste12, 10% of total binding events) experimentally bound regions that contained a PWM match where the orthologous region in at least one other species neither was bound nor contained a motif match. For these loci, loss of ChIP binding is concordant with the loss of the motif for this factor, providing clear examples of regions where network evolution occurred through the gain or loss of regulatory sequences.

Furthermore, there were 45 (Tec1, 17%) and 9 (Ste12, 3%) instances where a PWM match occurred in all three species but where that region was experimentally bound in only two species (Fig. 2D). Either these loci are occupied at other times in the life cycle or they are not functional. Conversely, in 11 (Tec1, 3%) and 22 (Ste12, 6%) instances, genomic regions displayed conserved ChIP binding, but at least one species was missing a PWM motif match (Fig. 2E). Thus, sequence conservation does not readily predict binding.

To further examine the role of conserved versus nonconserved ChIP binding events and motifs, we compared these results with expression microarray studies of pseudohyphal formation in *S. cerevisiae* (*17*). Of the ChIP binding gene targets that had significantly altered expression

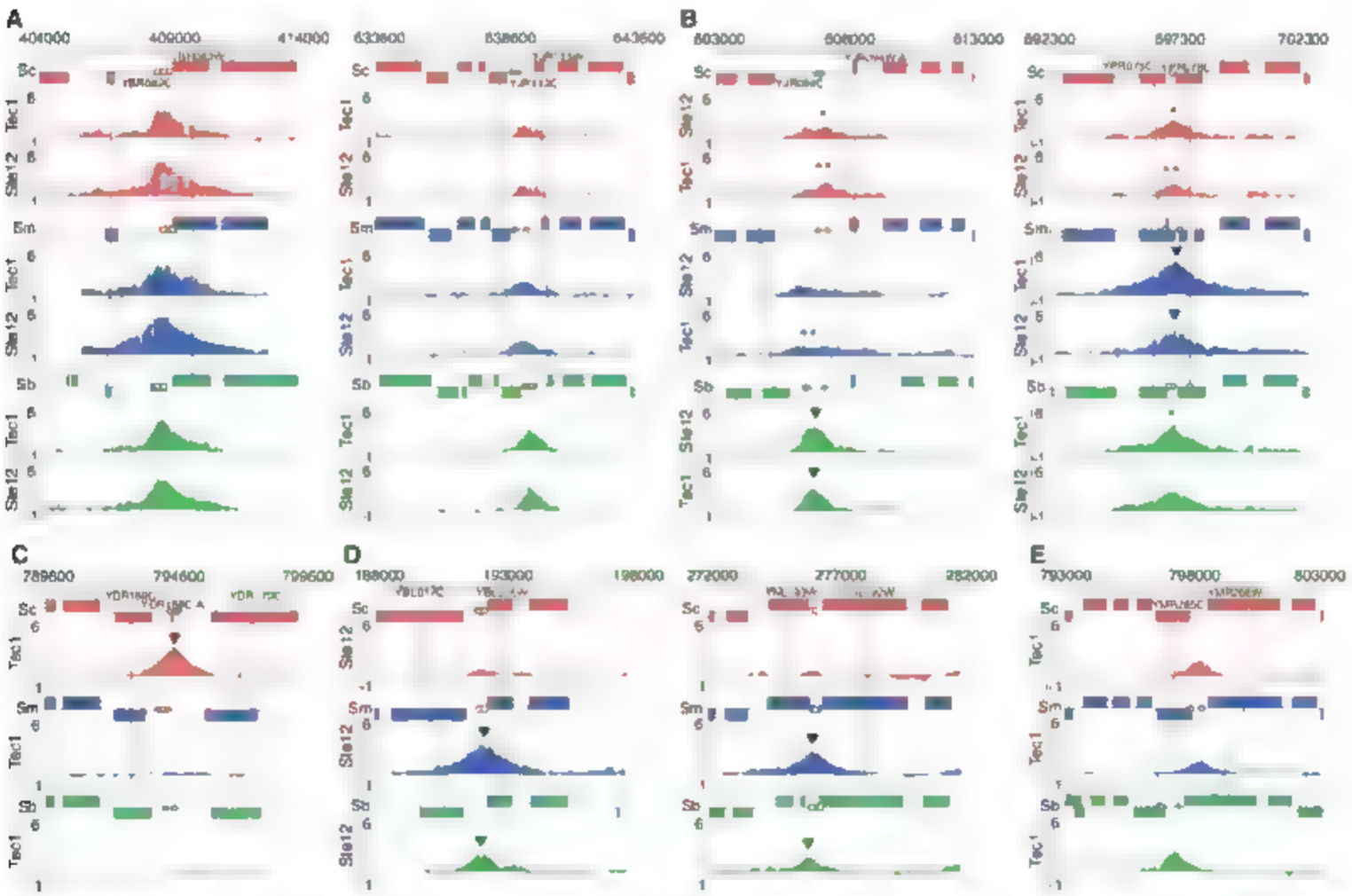

Fig. 2. Comparison of binding by Ste12 and Tec1 across *S. cerevisiae* (red), *S. mikatae* (blue), and *S. bayanus* (green). (**A**) Conserved binding. (**B**) Conserved binding with quantitative signal differences. (**C**) Conserved binding with loss of consensus sequences in one species. (**D**) Species-specific binding despite conserved consensus sequences. (**E**) Binding only in *S. mikatae* and *S. bayanus*. Chip-chip enrichment signals are shown (log 2 ratios). Circles and squares represent matches to Tec1 PWM and Ste12 PWM, respectively. Triangles, nonconserved peaks; **, >2-fold difference in peak signal intensity; *, >1.5-fold difference in peak signal intensity.

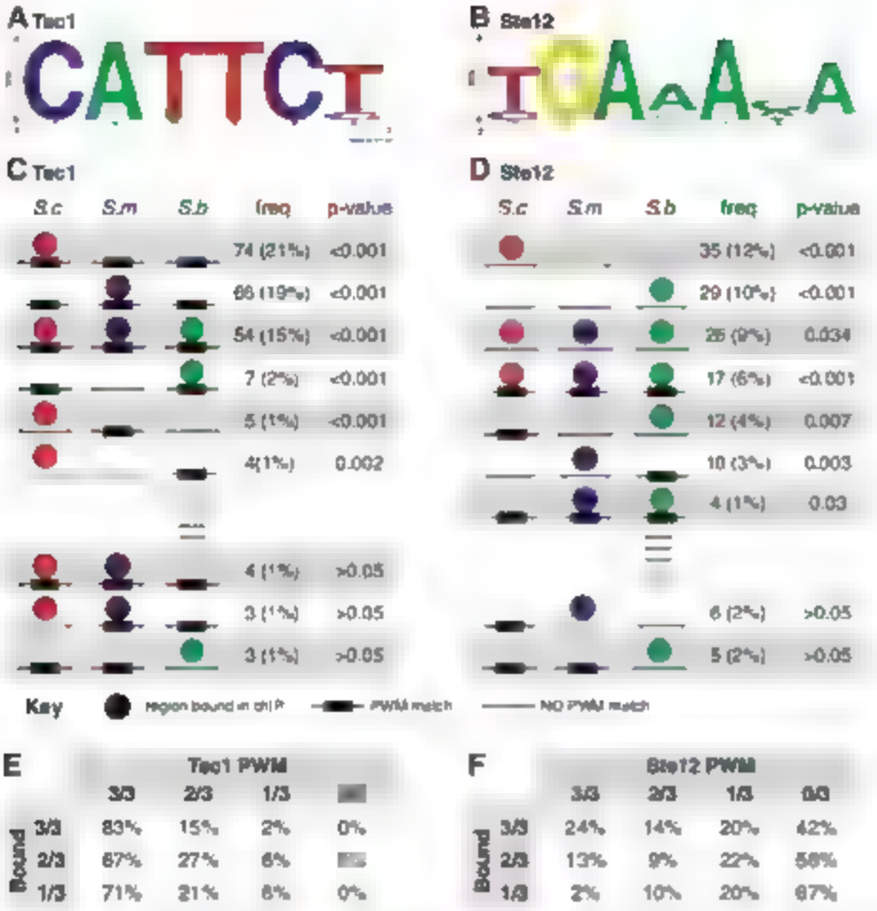

Fig. 3. Motif analysis of ChIP binding targets. Logo representations of the PWM for Tec1 (**A**) and Ste12 (**B**) (*12*). (**C** and **D**) Classes of binding targets after classification by both the conservation of ChIP binding and the presence or absence of consensus motifs. (**E** and **F**) Compiled proportions of binding targets and PWM matches for Tec1 and Ste12.

(~20% of the ChIP targets, a several-fold enrichment), there was no enrichment for genes with conserved binding (11% bound versus 14% unbound) or PWM matches (12% with motif versus 16% without motif) (table S11). Thus, sequence-based motif analyses in the absence of experimentally determined binding data are not sufficient for the accurate prediction of TF binding profiles and gene function. In addition, the presence of nonconserved ChIP targets upstream of pseudohyphal-regulated genes at the same frequency as conserved targets indicates that nonconserved sites are likely to be functional.

To elucidate the biological importance of both the conserved and species-specific gene targets, we mapped each bound region to its downstream target genes by identifying open reading frames (ORFs) that were 3′ of and directly flanking each ChIP binding event (tables S7 and S8). Conserved Ste12 and Tec1 gene targets displayed enrichment for two gene ontology (GO) categories "filamentous growth" and "regulation of transcription from RNA polymerase II promoters" (Fig. 4A). Because most of the genes from within the second category encode TFs, the predicted downstream TF networks of *S. bayanus* and *S. mikatae* were compared to those of *S. cerevisiae* (*19*) to determine which connections had been maintained during the evolution of the *Saccharomyces* sensu stricto group (Fig. 4C). The binding of Ste12 and Tec1 to downstream TFs was shown to be highly conserved (73% across the three species). The network of *S. mikatae* was most diverged and had several key

Fig. 4. (**A**) Ste12 and Tec1 bind to common and distinct sets of genes across the *Saccharomyces* sensu stricto lineage. Overrepresented GO terms are listed for each combinatorial category. (**B**) Mating genes bound specifically by Ste12 in *S. mikatae* and *S. bayanus*. (**C**) TF network conservation in *S. cerevisiae* (red), *S. mikatae* (blue), and *S. bayanus* (green).

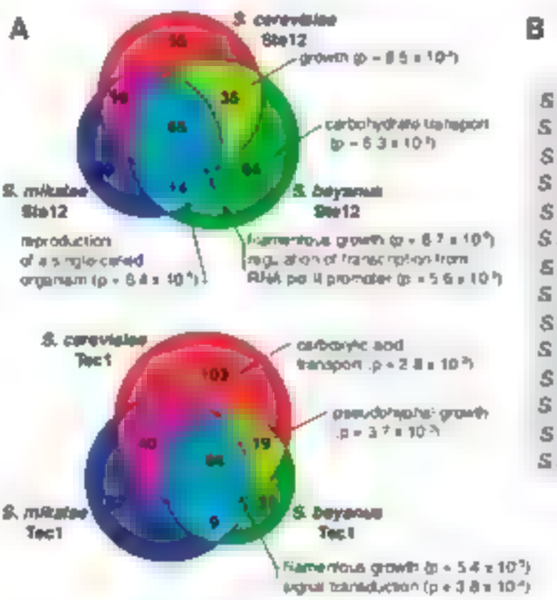

B

Gene	*S. cerevisiae* homologue	$\log_2$ Ratio
S. mikatae ORFN 1359	FUS3	2.29
S. bayanus ORFN 1436	(YBL016C)	2.13
S. mikatae ORFN 18188	CHS1	2.21
S. bayanus ORFN 20364	(YNL192W)	1.70
S. mikatae ORFN 2230	KAR4	2.11
S. bayanus ORFN 2394	(YCL055W)	1.80
S. mikatae ORFN 2120	FUS1	1.79
S. bayanus ORFN 2514	(YCL027W)	1.79
S. mikatae ORFN 7184	MPT5	1.83
S. bayanus ORFN 8405	(YGL178W)	1.31
S. mikatae ORFN 10486	AXL2	1.45
S. bayanus ORFN 11868	(YIL140W)	1.41
S. mikatae ORFN 19760	RRI2	1.26
S. bayanus ORFN 22091	(YDL117W)	1.28

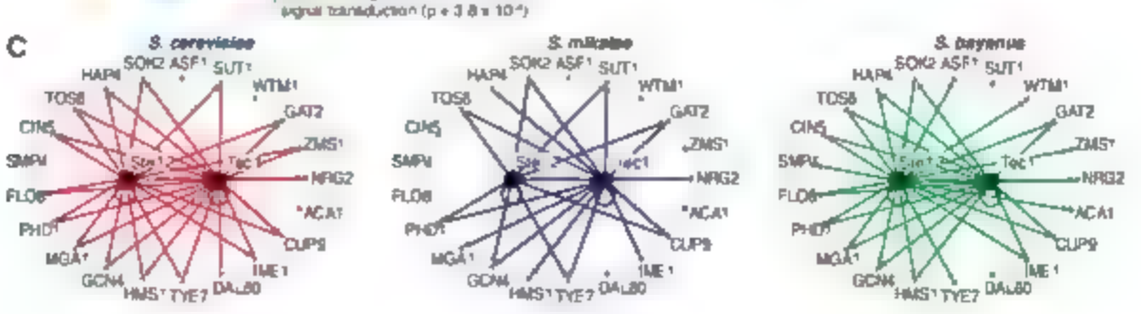

regulatory omissions including Flo8 (not bound by either Ste12 or Tec1) and Mga1 (not bound by Ste12). Thus, although important differences can be found, TF binding to the promoters of other TFs was highly conserved between species relative to the level of conservation observed for other genes.

From those groups of genes that did not display conserved binding across the three species, one notable class was bound by Ste12 specifically in *S. mikatae* and *S. bayanus* and was enriched in genes involved in mating (GO category: "reproduction in single-celled organisms" in *S. cerevisiae* (Fig. 4, A and B). Unlike the gene targets in the diploid cells used in this study, these genes are targets of Ste12 in haploid *S. cerevisiae* cells (*20*, *21*), and this differential binding occurs despite the presence of conserved Ste12 binding motifs (fig. S3). Thus, Ste12 binding targets may be occupied under different conditions across related species. In *S. cerevisiae*, Ste12 binds to these sites only during mating whereas in *S. mikatae* and *S. bayanus*, Ste12 binds to these same regions in diploid cells.

To extend this study outside of *Saccharomyces* yeasts, we also mapped the binding of the *Candida albicans* Ste12 ortholog, Cph1 (*22*). Cph1 functions in the dimorphic switch of this yeast, a process that shares many genetic components with pseudohyphal growth (*23*). A total of 52 significant Cph1 ChIP binding events (table S12) was detected under dimorphic growth conditions, with many residing upstream of known pathogenicity determinants (*24*–*27*). From these gene targets, 33 have recognizable orthologs in *S. cerevisiae*, and of these orthologs, 20, 10, and 13 displayed conserved binding with *S. cerevisiae*, *S. mikatae*, and *S. bayanus*, respectively. Although most gene targets of Cph1 in *C. albicans* are not conserved with the *Saccharomyces* species, the *C. albicans* orthologs bound by Ste12, like those from *S. mikatae* and *S. bayanus*, included a significant number of genes that function during reproduction and mating in *S. cerevisiae* ($P = 4 \times 10^{-3}$) (*28*). Thus, in *C. albicans*, like in *S. mikatae* and *S. bayanus*, the Ste12 ortholog also binds to genes required for mating in *S. cerevisiae* under filamentous growth conditions, raising the possibility that these genes have become more specialized in *S. cerevisiae*.

We find that extensive regulatory changes can exist in closely related species, which is consistent with a recent study that showed that distinct regulatory circuits can produce similar regulatory outcomes in *S. cerevisiae* and *C. albicans* (*29*). Furthermore, although *S. cerevisiae* and *S. mikatae* are quite similar to one another at the nucleotide sequence level, they are equally different to each other and to *S. bayanus* in their TF profiles. We expect that the extensive binding site differences observed in this study reflect the rapid specialization of these organisms for their distinct ecological environments and that differences in transcription regulation between related species may be responsible for rapid evolutionary adaptation to varied ecological niches.

References and Notes

1. P. Clifton *et al.*, *Science* **301**, 71 (2003).
2. M. Kellis, N. Patterson, M. Endrizzi, B. Birren, E. S. Lander, *Nature* **423**, 241 (2003).
3. M. Tompa *et al.*, *Nat. Biotechnol.* **23**, 137 (2005).
4. V. R. Iyer *et al.*, *Nature* **409**, 533 (2001).
5. B. Ren *et al.*, *Science* **290**, 2306 (2000).
6. J. Pinkur, B. B. Langkjaer, *Mol. Microbiol.* **53**, 381 (2004).
7. H. D. Madhani, G. R. Fink, *Science* **275**, 1314 (1997).
8. V. Gavrias, A. Andrianopoulos, C. J. Gimeno, W. E. Timberlake, *Mol. Microbiol.* **19**, 1255 (1996).
9. H. Liu, C. A. Styles, G. R. Fink, *Science* **262**, 1741 (1993).
10. S. Fields, I. Herskowitz, *Cell* **42**, 923 (1985).
11. A. R. Borneman *et al.*, *Funct. Integr. Genomics*, in press; preprint available at www.springerlink.com/content/w6552935420166h.
12. See supporting material on *Science* Online.
13. X. S. Liu, D. L. Brutlag, J. S. Liu, *Nat. Biotechnol.* **20**, 835 (2002).
14. J. W. Dolan, C. Kirkman, S. Fields, *Proc. Natl. Acad. Sci. U.S.A.* **86**, 5703 (1989).
15. T. L. Bailey, M. Gribskov, *Bioinformatics* **14**, 48 (1998).
16. S. Chou, S. Lane, H. Liu, *Mol. Cell. Biol.* **26**, 4794 (2006).
17. S. Prinz *et al.*, *Genome Res.* **14**, 380 (2004).
18. E. I. Boyle *et al.*, *Bioinformatics* **20**, 3710 (2004).
19. A. R. Borneman *et al.*, *Genes Dev.* **20**, 435 (2006).
20. C. T. Harbison *et al.*, *Nature* **431**, 99 (2004).
21. J. Zeitlinger *et al.*, *Cell* **113**, 395 (2003).
22. T. Jones *et al.*, *Proc. Natl. Acad. Sci. U.S.A.* **101**, 7329 (2004).
23. C. Sánchez-Martínez, J. Pérez-Martín, *Curr. Opin. Microbiol.* **4**, 214 (2001).
24. C. E. Birse, M. Y. Irwin, W. A. Fonzi, P. S. Sypherd, *Infect. Immun.* **61**, 3648 (1993).
25. B. R. Braun, W. S. Head, M. X. Wang, A. D. Johnson, *Genetics* **156**, 31 (2000).
26. B. R. Braun, A. D. Johnson, *Genetics* **155**, 57 (2000).
27. T. C. White, S. H. Miyasaki, N. Agabian, *J. Bacteriol.* **175**, 6126 (1993).
28. A. E. Tsong, B. B. Tuch, H. Li, A. D. Johnson, *Nature* **443**, 415 (2006).

29. The authors would like to thank P. Chambers and D. Gelperin for comments on the manuscript. Funding was provided by NIH grants (to M.S. and M.G.) and by the Burroughs Wellcome Foundation. Detailed lists of binding regions, conservation information, and motif scores are available from www.gersteinlab.org/proj/regnetdiverge.

Supporting Online Material

www.sciencemag.org/cgi/content/full/317/5839/815/DC1
Materials and Methods
Fig. S1 to S5
Tables S1 to S14
References

2 February 2007; accepted 20 June 2007
10.1126/science.1140748

High-Speed Imaging Reveals Neurophysiological Links to Behavior in an Animal Model of Depression

Raag D. Airan,[1]* Leslie A. Meltzer,[2]* Madhuri Roy,[1] Yuqing Gong,[1,4] Han Chen,[3] Karl Deisseroth[2,5]†

The hippocampus is one of several brain areas thought to play a central role in affective behaviors, but the underlying local network dynamics are not understood. We used quantitative voltage-sensitive dye imaging to probe hippocampal dynamics with millisecond resolution in brain slices after bidirectional modulation of affective state in rat models of depression. We found that a simple measure of real-time activity—stimulus-evoked percolation of activity through the dentate gyrus relative to the hippocampal output subfield—accounted for induced changes in animal behavior independent of the underlying mechanism of action of the treatments. Our results define a circuit-level, neurophysiological endophenotype for affective behavior and suggest an approach to understanding circuit-level substrates underlying psychiatric disease symptoms.

The hippocampus, as an integral component of the limbic system, is a locus of depression research (*1*), drives other brain regions implicated in depression, and appears to serve as a primary site of action for antidepressants that inhibit pathological hyperactivity (*2*, *3*). Complicating this picture, however, is evidence suggesting that antidepressants can stimulate hippocampal activity. Antidepressant-induced hippocampal neurogenesis is linked to behavioral responses (*4*, *5*). Moreover, excitatory hippocampal neurons are injured by chronic stress (*6*, *7*). Animal models have proven useful in identifying molecular and cellular markers relevant to depression (*8*–*10*) but have not identified neurophysiological final common pathways relevant to behavior. Voltage-sensitive dye imaging (VSDI) could allow analysis of disease-related neural activity on millisecond time scales, with micrometer spatial resolution and a scope spanning entire brain networks (*11*). We applied VSDI to hippocampal physiology in the chronic mild stress (CMS) model, a well-validated rodent

[1]Department of Bioengineering, Stanford University, Stanford, CA 94305, USA. [2]Neuroscience Program, Stanford University, Stanford, CA 94305, USA. [3]Department of Electrical Engineering, Stanford University, Stanford, CA 94305, USA. [4]Department of Statistics, Stanford University, Stanford, CA 94305, USA. [5]Department of Psychiatry and Behavioral Sciences, Stanford University, Stanford, CA 94305, USA.

*These authors contributed equally to this work.
†To whom correspondence should be addressed. E-mail: deissero@stanford.edu

model of core depressive behavioral symptoms (*12*).

Evoked activity was recorded with VSDI in acute horizontal slices prepared from the ventral hippocampus of adult rats (Fig. 1A) (*13*, *14*). Signals reflecting local neuronal network activity were extinguished by 2,3-dihydroxy-6-nitro-7-sulfamoyl-benzo[*f*]quinoxaline-2,3-dione (NBQX) and D-2-amino-5-phosphonopentanoic acid (D-APS), an observation requiring excitatory transmission (Fig. 1B). We used cross-correlation to extract reliable quantitative features of the network response (Fig. 1C and D, and figs. S1 and S2), computing the maximal response amplitude of each pixel (Fig. 1D, top right, and fig. S3, right) and the time at which this maximal amplitude occurred (phase, Fig. 1D, top left, and fig. S3, left). In our experiments, phase distributions were independent of treatment group and coherent in the region responding to stimulation, which was isolated computationally in further analysis (Fig. 1D, bottom, and figs. S4 to S6). A simple metric of circuit response (total activity) defined as the mean amplitude multiplied by the area of the calculated region of interest (*13*) was found to be linear in this study as large and reliable across slices (Fig. 2B).

To quantify behaviorally relevant hippocampal dynamics in a rodent model, we applied CMS (Fig. 2A, left) or delivered one of two chronic antidepressant treatments, the selective serotonin reuptake inhibitor fluoxetine or the tricyclic antidepressant imipramine; the typical antipsychotic haloperidol served as a pharmacological control (Fig. 2A, right). Depression-like behavior was quantified, blind to treatment condition, in terms

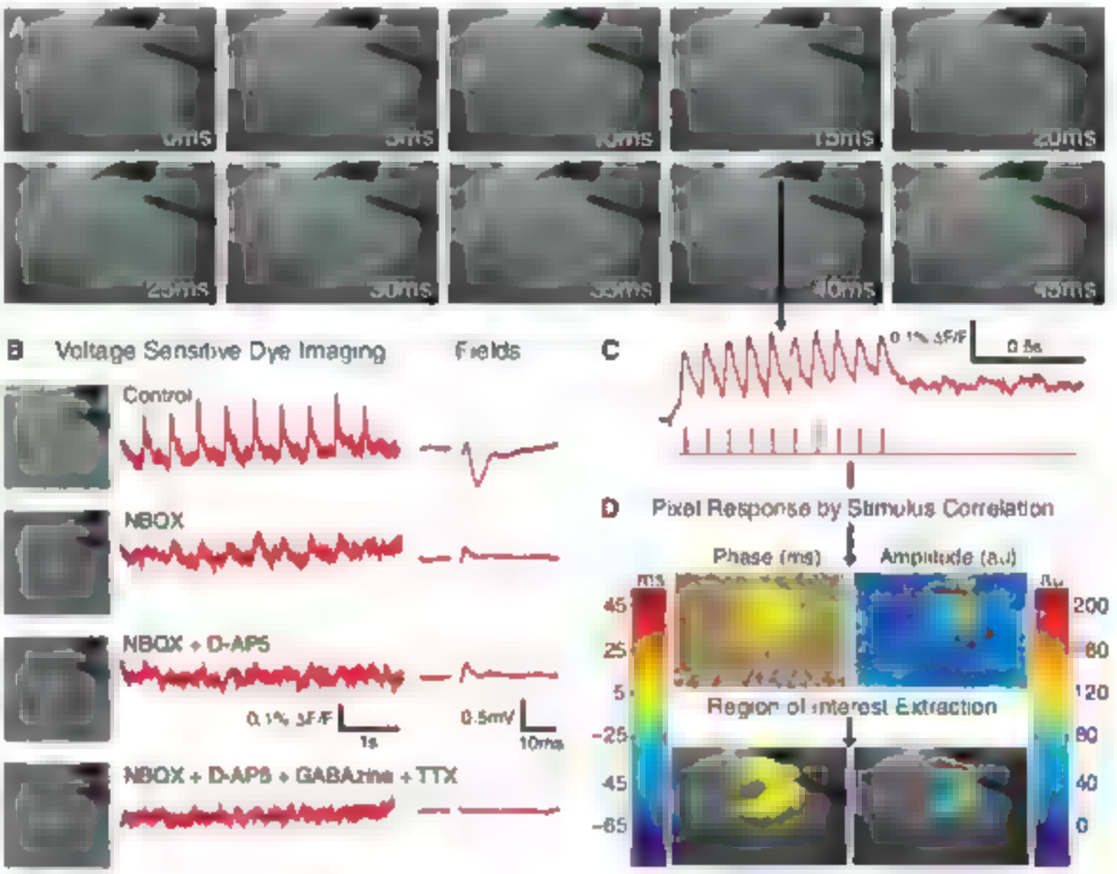

Fig. 1. Voltage-sensitive dye imaging (VSDI) of hippocampal network activity. **(A)** Representative filmstrip acquired using VSDI. Elapsed times are relative to a single stimulus pulse applied to DG; warmer colors indicate greater activity (relative change in VSD fluorescence, $\Delta F/F$). Data represent the average of four individual acquisitions. **(B)** VSDI signal is abolished by blockers of excitatory synaptic transmission (10 μM NBQX and 25 μM D-APS). GABAzine (20 μM) and tetrodotoxin (TTX, 1 μM) application subsequently confirmed signal extinction. **(C)** Single-pixel response ($\Delta F/F$ versus time, top) from the indicated region to the given stimulus train (bottom). **(D)** Phase (top left) and amplitude (top right) of maximal correlation between the stimulus and response at each pixel. The synchronously responding region was extracted computationally, with the same phase criteria applied to all treatment groups, on the basis of similar phase values of responding pixels (bottom). au, arbitrary units.

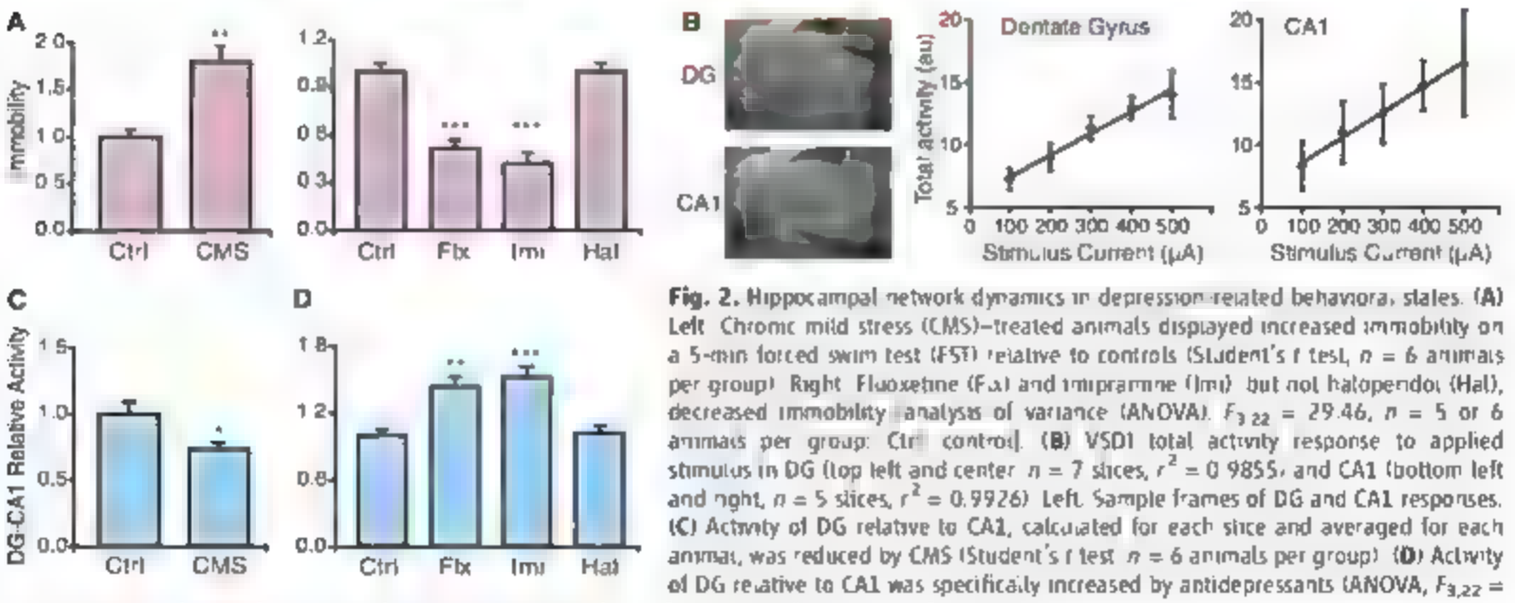

Fig. 2. Hippocampal network dynamics in depression-related behavioral states. **(A)** Left: Chronic mild stress (CMS)–treated animals displayed increased immobility on a 5-min forced swim test (FST) relative to controls (Student's *t* test, $n = 6$ animals per group). Right: Fluoxetine (Fx) and imipramine (Imi), but not haloperidol (Hal), decreased immobility (analysis of variance (ANOVA), $F_{3,22} = 29.46$, $n = 5$ or 6 animals per group; Ctrl, control). **(B)** VSDI total activity response to applied stimulus in DG (top left and center; $n = 7$ slices, $r^2 = 0.9855$) and CA1 (bottom left and right, $n = 5$ slices, $r^2 = 0.9926$). Left: Sample frames of DG and CA1 responses. **(C)** Activity of DG relative to CA1, calculated for each slice and averaged for each animal, was reduced by CMS (Student's *t* test, $n = 6$ animals per group). **(D)** Activity of DG relative to CA1 was specifically increased by antidepressants (ANOVA, $F_{3,22} = 12.74$, $n = 5$ or 6 animals per group). Data are means ± SEM. $^*P < 0.05$, $^{**}P < 0.01$, $^{***}P < 0.001$.

of immobility on the forced swim test (FST); in this test, immobility is increased by CMS and decreased by antidepressants (*15*). In all drug experiments, a 48-hour delay between the last dose and behavioral assessment excluded acute drug effects on behavior that do not have relevant clinical correlates (*16*). Relative to controls, CMS animals were more immobile over a 5-min FST, indicating a depressed-like state (Fig. 2A, left), whereas antidepressant-treated but not antipsychotic-treated animals showed less immobility (Fig. 2A, right).

We then conducted VSDI of evoked activity in ventral hippocampal slices (*14*) from these animals, blind to treatment condition, we probed both the dentate gyrus (DG) and CA1, hypothesizing different effects in the input and output hippocampal subfields (*17*–*20*). We found that activity propagation in DG relative to CA1 provided the most reliable predictor of FST performance on an animal-by-animal basis (Fig. 2C). DG activity was reduced in CMS-treated animals (fig. S7A), whereas CA1 activity was increased (fig. S7B), the CA1 contribution is compatible with results linking depression to elevated hippocampal output (*2*, *3*, *21*), and the DG contribution is consistent with data suggesting reduced hippocampal activity in depression (*4*, *6*).

We found the opposite pattern in antidepressant-treated animals (Fig. 2D and fig. S7), with increased activity propagation in DG (fig. S7C) and reduced activity in CA1 (fig. S7D). These effects were specific to antidepressants; antipsychotic treatment showed no effect on either subfield (fig. S7, C and D). Again, the activity propagation in DG relative to CA1 provided the most reliable (across-individual) indicator of the behavioral phenotype (Fig. 2D; $r^2 = 0.5251$, $P < 10^{-6}$, across CMS and drug groups).

To model clinical use of antidepressants, we next concomitantly administered fluoxetine during the last 2 weeks of 5-week CMS (Fig. 3). FST blinded to treatment condition confirmed that fluoxetine treatment reversed the behavioral effects of CMS (Fig. 3A), and VSDI demonstrated that the activity propagation in DG relative to CA1 significantly accounted for this effect (Fig. 3, B and C). On an individual-animal basis, this measure of activity propagation on the millisecond time scale regressed linearly with the FST scores and explained more than half of the bidirectional behavioral variation (Fig. 3C; $r^2 = 0.5545$, $P < 10^{-6}$) across all four independent treatment arms. Open-field tests (OFTs) from the same animals provided a test of the specificity of the network dynamics phenotype. We observed no significant differences between groups in locomotion or anxiety-related behavior on the OFT (Fig. 3, D and E), and there was no correlation between VSDI physiology and OFT scores (Fig. 3F; $r^2 = 0.0306$, $P > 0.4$), indicating specificity for depression-relevant behavior.

To address the cellular mechanism, we next probed for changes in hippocampal neurogenesis, hypothesized to be relevant to depression (*4*, *5*), but see (*22*)]. In the same animals represented in Fig. 3. In accord with previous observations (*4*, *5*), fluoxetine increased both the number and density of newborn neurons [as assessed by blinded, unbiased stereology of cells positive for 5-bromo-2′-deoxyuridine (BrdU) and Doublecortin (Dcx, immature neuronal marker)] (*13*) in the ventral DG, both in the presence and absence of CMS (Fig. 4, A and B), whereas CMS alone did not significantly alter the production (Fig. 4, A and B) of new neurons despite behavioral and circuit dynamics effects in the same animals (Fig. 3, A to C). Similarly effective CMS did not affect the survival of newborn neurons (Fig. 2 and fig. S12). These data indicate that circuit dynamics changes can account for bidirectional affective state modulation despite fundamental differences in cellular processes occurring during depressed-like state induction and treatment.

To test the capability of a temporally defined cohort of new neurons to modulate behavior and circuit dynamics, we treated animals for 1 week with fluoxetine to up-regulate neurogenesis, followed by a 3-week delay to permit functional integration of neurons born during treatment.

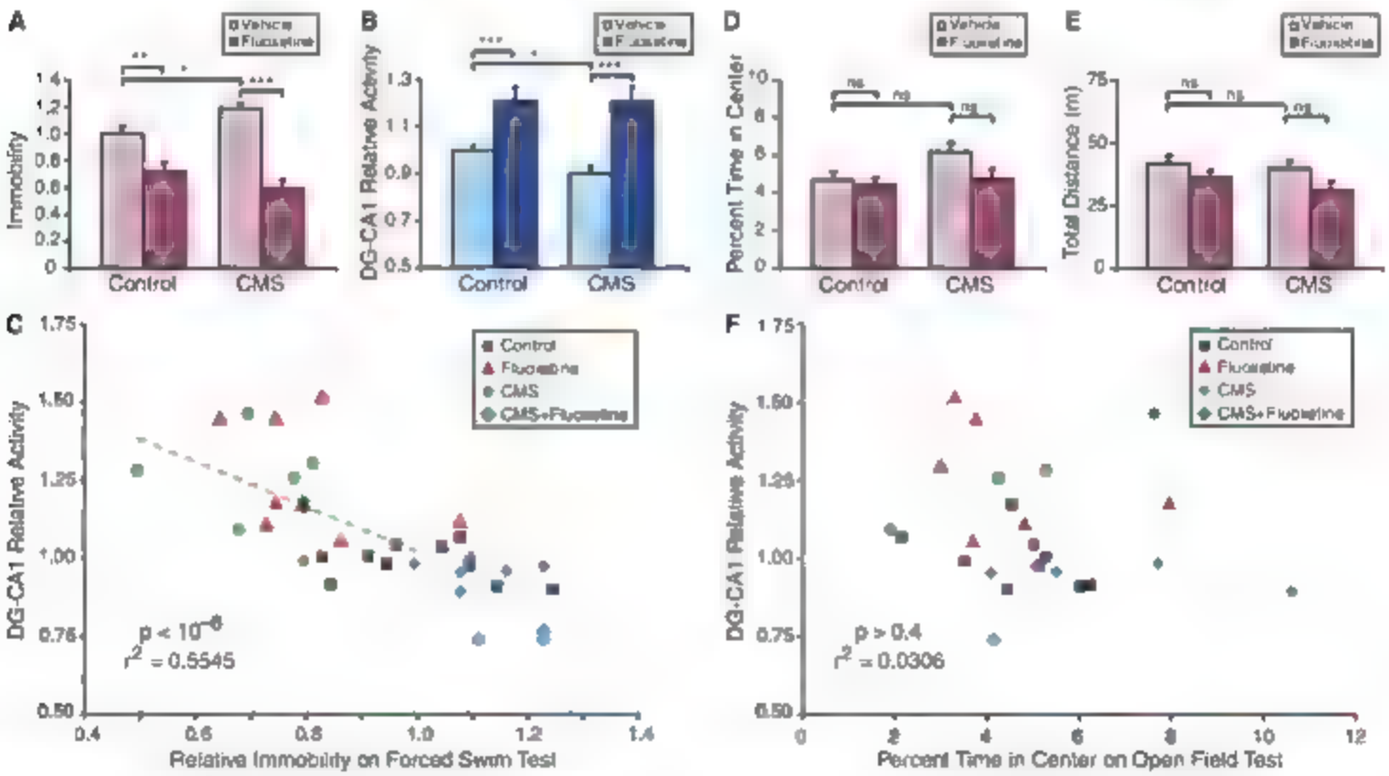

Fig. 3. Hippocampal network dynamics predict antidepressant treatment of depressed-like states. Fluoxetine was concomitantly administered during the last 2 weeks of 5-week CMS. (**A**) CMS increased immobility and fluoxetine decreased immobility in both control and CMS groups (ANOVA, $F_{3,34} = 19.24$, $n = 8$ to 12 animals per group). (**B**) Activity of DG relative to CA1 was decreased in CMS animals and was increased by fluoxetine (ANOVA, $F_{3,34} = 16.17$, $n = 6$ to 12 animals per group). (**C**) Linear regression of activity of DG relative to CA1 against FST scores for each individual animal ($r^2 = 0.5545$, $P < 10^{-6}$, $n = 35$ individual animals). (**D** and **E**) On the open-field test (OFT), no differences were observed in percent time in center [(D); ANOVA, $F_{3,20} = 1.021$, $P > 0.05$, n = 4 to 9 animals per group] or total distance [(E); ANOVA, $F_{3,20} = 1.776$, $P > 0.05$, $n = 4$ to 9 animals per group]. (**F**) Linear regression of activity of DG relative to CA1 against percent time in center for each individual animal ($r^2 = 0.0306$, $P > 0.4$, $n = 25$ individual animals).

(Fig. 4C). In some animals, we ablated hippocampal neurogenesis via irradiation (10 Gy/day for 2 days) 1 month before drug exposure; control experiments revealed no effect of irradiation alone on excitability, network dynamics, or behavior on this time scale (Fig. 4E and figs. S8 and S11). The fluoxetine pulse gave rise to a temporally defined cohort of new neurons (Fig. 4D and figs. S13 and S14) and reduced FST immobility in a manner blocked by irradiation (Fig. 4E, top), indicating that increased neurogenesis indeed is required for these antidepressant behavioral effects (5). However, irradiation alone did not affect behavior (Fig. 4E, top); therefore, inhibition of neurogenesis is neither sufficient (Fig. 4E, top) nor necessary (Fig. 2A, left, Fig. 3A, Fig. 4, A and B, and fig. S12) to induce a depressed-like state.

To quantitatively explore circuit dynamics modulation by the temporally defined cohort of new neurons, we conducted VSDI in the ventral hippocampus from these animals. The activity propagation in DG relative to CA1 was indeed increased (Fig. 4E, bottom), and only the DG effect was neurogenesis-dependent (fig. S8, A and B). Although it may be counterintuitive that a small number of new neurons (*23*) could affect circuit dynamics, simple modeling predicted that rare new neurons can increase the recruited active network area (fig. S9). We therefore analyzed VSDI signal components (area and amplitude) to determine their contribution to the observed changes in DG physiology, and found that the circuit-level effect of a temporally defined cohort of fluoxetine-induced newborn neurons on DG activity is indeed due primarily to increased active DG area (fig. S8), a parameter readily detectable by high-speed VSDI as demonstrated here.

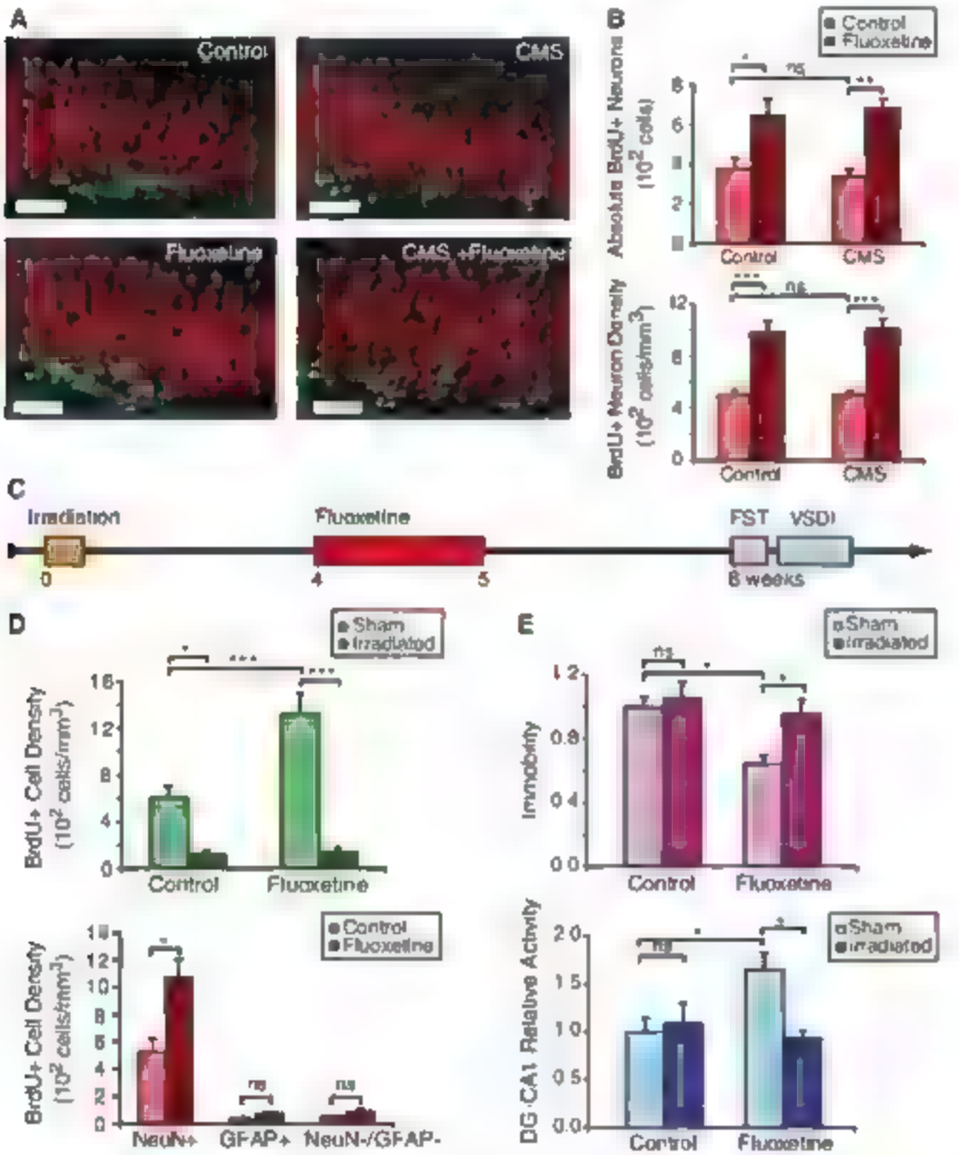

Fig. 4. VSDI resolution of neurogenesis-dependent circuit dynamics changes underlying antidepressant response. (**A**) Representative confocal DG images labeled for BrdU (green), NeuN (mature neuronal marker; red), and Dcx (immature neuronal marker; cyan). Arrowheads indicate BrdU$^+$ neurons. Scale bar, 50 μm. (**B**) New neuron (BrdU$^+$/Dcx$^+$) counts (top) and density (bottom) in ventral hippocampus (same animals as in Fig. 3) were increased with fluoxetine treatment but unchanged with CMS (counts, ANOVA, $F_{3,27} = 9.670$; density, $F_{3,27} = 20.68$; $n = 6$ to 8 animals per group). (**C**) One month after irradiation designed to ablate hippocampal neurogenesis, fluoxetine or vehicle was administered for 1 week, followed by a 3-week delay for newborn neuron incorporation. (**D**) Top: BrdU$^+$ cell density was increased after fluoxetine treatment and substantially decreased with irradiation (ANOVA, $F_{3,24} = 29.72$; $n = 4$ to 8 animals per group). Bottom: Fluoxetine treatment specifically increased the density of newborn neurons (BrdU$^+$/NeuN$^+$) in DG (glial fibrillary acidic protein, GFAP, astrocytic marker; Student's t test, $n = 6$ animals per group). (**E**) Top: Fluoxetine-treated animals showed decreased FST immobility; no effects were observed with irradiation (ANOVA, $F_{3,23} = 7.757$, $n = 6$ animals per group). Bottom: Irradiation blocked increased activity of DG relative to CA1 after fluoxetine treatment (ANOVA, $F_{3,22} = 3.997$, $n = 5$ or 6 animals per group).

These data suggest that behavioral changes can be linked to a common network dynamics phenotype without requiring a common etiology or mechanism such as neurogenesis. Indeed, we propose that genetic or environmental factors with diverse cellular mechanisms (*9, 17, 18, 24*) that are operative in different individuals may exert behavioral effects through a common activity-percolation phenotype. Although many antidepressants are associated with increased seizure risk and therefore could involve increased activity propagation through the DG, other antidepressant treatments clearly do not directly target the hippocampus, such as deep brain stimulation (DBS), which typically targets Cg25 or the nucleus accumbens. However, DBS reduces activity in Cg25 (*25*), which receives excitatory drive from the hippocampus (*2, 3, 21*), suggesting that Cg25 DBS can intervene downstream of an overactive CA1. There had been no obvious way to unify into a single model the hippocampal atrophy seen in depression (*7, 24*) with the likely increased excitatory drive from hippocampus to cortex associated with depression (*2, 25*). Our results suggest that the increased subgenual cingulate activity in depression could result in part from increased CA1 activity, whereas the reduced intrinsic hippocampal function observed in depression is consistent with decreased DG activity.

Hippocampal dysfunction related to mood may be experienced cognitively (e.g., as hopelessness (*26*)), which can manifest clinically as patients' inability to foresee or navigate a reasonable and hopeful plan within the environment. Theoretical models of the dorsal hippocampus have described comparative interactions between DG and CA1 (*19, 20*) in which CA1 activity indicates discrepancies between predictive information from DG and sensory information from the cortex. Depression therefore could be associated with the failure to predict, navigate through, or adapt to environmental changes (experienced as hopelessness) resulting from failed ventral DG associative/predictive activity or increased error signals from CA1. If that is the case, the intensity of the resulting dysphoria may be modulated by anxiety or reward pathways (amygdala, nucleus accumbens, and mesolimbic dopamine projections) or the prefrontal and cingulate cortices (*27*). Indeed, identification of this hippocampal neurophysiological endophenotype may serve as a

starting point in mapping the network-level changes in other brain regions implicated in depression. High-speed, circuit-level optical methods are better suited than single-cell physiology to detect and quantitatively describe spatiotemporal dynamics (such as areal spread of activity) that may be altered in psychiatric disease. These circuit dynamics measures relate to how information propagates rather than to a specific neural code. We propose that depression may depend on changes in the ability of information representations to organize and percolate through sparsely active networks.

References and Notes

1. S. Campbell, G. Macqueen, *J. Psychiatry Neurosci.* **29**, 417 (2004).
2. H. S. Mayberg *et al.*, *Biol. Psychiatry* **48**, 830 (2000).
3. D. A. Seminowicz *et al.*, *Neuroimage* **22**, 409 (2004).
4. J. L. Warner-Schmidt, R. S. Duman, *Hippocampus* **16**, 239 (2006).
5. L. Santarelli *et al.*, *Science* **301**, 805 (2003).
6. C. Mirescu, E. Gould, *Hippocampus* **16**, 233 (2006).
7. R. M. Sapolsky, *Arch. Gen. Psychiatry* **57**, 925 (2000).
8. L. H. Tecott, E. J. Nestler, *Mol. Neurosci.* **7**, 462 (2004).
9. W. M. Cowan, D. H. Harter, E. R. Kandel, *Annu. Rev. Neurosci.* **23**, 343 (2000).
10. J. F. Cryan, A. Holmes, *Nat. Rev. Drug Discov.* **4**, 775 (2005).
11. A. Grinvald, R. Hildesheim, *Nat. Rev. Neurosci.* **5**, 874 (2004).
12. P. Willner, *Neuropsychobiology* **52**, 90 (2005).
13. See supporting material on *Science* Online.
14. D. M. Bannerman *et al.*, *Neurosci. Biobehav. Rev.* **28**, 273 (2004).
15. J. F. Cryan, R. J. Valentino, I. Lucki, *Neurosci. Biobehav. Rev.* **29**, 547 (2005).
16. C. Lopez-Rubalcava, I. Lucki, *Neuropsychopharmacology* **22**, 191 (2000).
17. S. G. Walling, C. W. Harley, *J. Neurosci.* **24**, 596 (2004).
18. S. Bimstiel, T. J. List, S. G. Beck, *Synapse* **20**, 117 (1995).
19. J. E. Lisman, A. A. Grace, *Neuron* **46**, 703 (2005).
20. M. E. Hasselmo, H. Eichenbaum, *Neural Netw.* **18**, 1172 (2005).
21. H. S. Mayberg *et al.*, *Am. J. Psychiatry* **156**, 675 (1999).
22. F. A. Henn, B. Vollmayr, *Biol. Psychiatry* **56**, 146 (2004).
23. H. A. Cameron, R. D. G. McKay, *J. Comp. Neurol.* **435**, [illegible].
24. B. S. McEwen, *Annu. Rev. Neurosci.* **22**, 105 (1999).
25. H. S. Mayberg *et al.*, *Neuron* **45**, 651 (2005).
26. E. J. Nestler *et al.*, *Neuron* **34**, 13 (2002).
27. W. C. Drevets, *Curr. Opin. Neurobiol.* **11**, 240 (2001).

28. We thank the Dessereth lab, J. R. Huguenard, F. D. Palmer, R. C. Malenka, and B. K. Ormerod for helpful discussions. Supported by the National Institute on Drug Abuse, the National Institute of Mental Health the NIH Director's Pioneer Award, NARSAD, the American Psychiatric Institute for Research and Education, and the Snyder, Culpeper, Coulter Klingenstein, Whitehall, McKnight, and Albert Yu and Mary Bechmann Foundations (K.D.), the Stanford Medical Scientist Training Program (R.D.A.); and a Stanford Bio-X predoctoral fellowship (L.A.M.).

Supporting Online Material

www.sciencemag.org/cgi/content/full/1144400/DC1
Materials and Methods
Figs. S1 to S14
References

30 April 2007; accepted 28 June 2007
Published online 5 July 2007
10.1126/science.1144400
Include this information when citing this paper

Characterizing the Limits of Human Visual Awareness

Liqiang Huang,[1]* Anne Treisman,[1] Harold Pashler[2]

Momentary awareness of a visual scene is very limited, however, this limitation has not been formally characterized. We test the hypothesis that awareness reflects a surprisingly impoverished data structure called a labeled Boolean map, defined as a linkage of just one feature value per dimension (for example, the color is green and the motion is rightward) with a spatial pattern. Features compete with each other, whereas multiple locations form a spatial pattern and thus do not compete. Perception of the colors of two objects was significantly improved by successive compared with simultaneous presentation, whereas perception of their locations was not. Moreover, advance information about which objects are relevant aided perception of colors much more than perception of locations. Both results support the Boolean map hypothesis.

Many experiments have explored the process of attentional selection in vision, chiefly through visual search tasks in which observers try to find a single specified target, which may or may not be present in a display (*1*–*4*). Selection sometimes involves sequential checking of different elements, whereas in other search tasks a parallel selection process can exclude all but a single target (*3*, *5*). What has been scarcely investigated at all, however, is an even more fundamental question about human vision: What is the informational content of any single momentary act of conscious perception?

[1]Center for the Study of Brain, Mind, and Behavior, Princeton University, Princeton, NJ 08544, USA. [2]Department of Psychology, University of California, San Diego, La Jolla, CA 92093, USA.

*Present address: Department of Psychology, Chinese University of Hong Kong, Shatin, NT, Hong Kong, China. To whom correspondence should be addressed. E-mail: lghuang@psy.cuhk.edu.hk

Consider, for example, the array of four colored disks shown in Fig. 1A. Can a human observer attend to all four disks and simultaneously be aware of the presence of two blue, one red, and one green disk? A recently proposed theory of attention contends that we cannot (*6*). According to this account, momentary conscious access, although flexibly controlled through voluntary attending, is nonetheless constrained to have the representational content of a data structure termed a labeled Boolean map. There is evidence that visual perception analyzes the scene along a number of different base dimensions, such as color, motion, spatial frequency, and orientation (*3*, *5*, *7*). The data structure of a labeled Boolean map may thus associate at most one value at a time for each of these independent visual dimensions (for example, color is green and motion is rightward) as labels with a spatial pattern (i.e., the set of location values composing the Boolean map) (*6*). Here, we deal only with the case of within-dimension competition, so the claim can be abbreviated for present purposes as awareness of only a single feature value. A choice of three potential Boolean maps could represent either the red, the green, or the blue disk(s) in Fig. 1A. These would afford the observer conscious access to both the location(s) and the color of the attended disk(s). On the other hand, the map could instead encompass disks of more than one color simultaneously, and in that case there would be explicit awareness of all locations but not of the colors. Figure 1B illustrates the representational content of a few (but not all) of the possible percepts that might be elicited by these stimuli according to the present hypothesis.

The claim that conscious access is limited to a "one-feature-multiple-locations" format generates numerous predictions (*6*). Here, we focus on one especially critical and counterintuitive prediction, namely the proposed asymmetry between conscious access to multiple features and to multiple locations. The Boolean map theory predicts that multiple features can only be consciously accessed one by one, whereas multiple locations can be accessed at the same time.

In the first experiment, we presented two objects either at the same time (simultaneous condition) or one by one (successive condition), followed by a single probe (either a color patch or a location marker, to be judged as having been present in the display or not). For any type of visual information (feature or location), if two such values cannot be accessed at the same time, then observers should perform worse in the simultaneous condition. If, however, two such values can be simultaneously accessed without attentional limitation, then observers should perform equally in

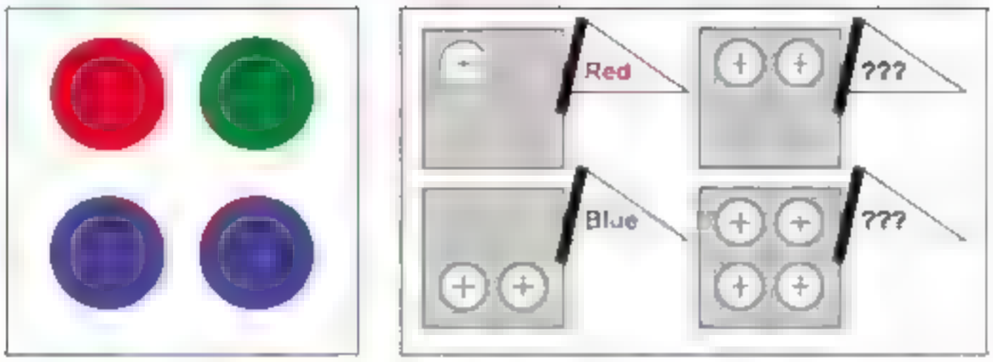

A B

Fig. 1. (**A**) A sample display. (**B**) Some possible states of awareness (possible percepts) when viewing the sample display of (A) in a single brief exposure. When only disks of one color are selected (left two examples), both the locations of the disks and that color value can be consciously accessed. When more than one color is present in the selected disks (right two examples), only the locations of the disks, but not their colors, can be consciously represented. In (B), the regions marked with plus signs stand for the selected regions of the Boolean map, and the flags stand for the color information that is associated with the selected region as a label. The selected region in the map and the color label constitute the only visual information that is consciously accessible at one time.

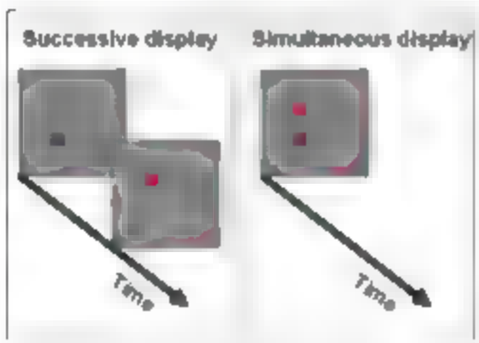

A Method of Experiment 1

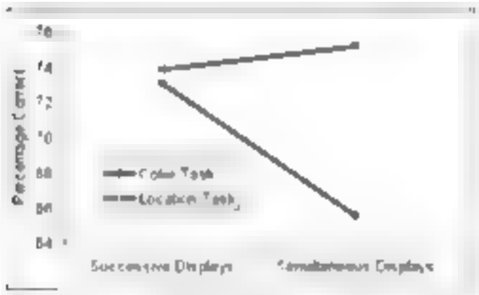

B Results of Experiment 1

Fig. 2. The method (**A**) and results (**B**) of experiment 1. We presented two objects either at the same time or one by one. Each frame was followed by a visual mask to limit processing to a brief exposure. In each trial, the observer had to report whether a probe target color or location, presented at the end of the trial, was present or absent. The performance (as measured by the mean of accuracy over observers) was significantly better for successive than for simultaneous displays in the color task ($P < 0.005$) but not in the location task (interaction significant, $P < 0.02$).

the simultaneous and in the successive conditions (*8*, *9*). Thus, the Boolean map account implies that, for judgments of color, the observers should perform significantly better in the successive than in the simultaneous condition, whereas for judgments of location the observers should perform equally in both conditions. We compared observers' performance in the successive and in the simultaneous conditions for both colors and locations with stimuli like those in Fig. 2A. To ensure a sensitive comparison between accuracies of different conditions in this experiment (and the one below), we always presented the objects very briefly and then masked them. The results are given in Fig. 2B and they confirm the predictions. Moreover, simple quantitative modeling shows that the difference between successive and simultaneous conditions closely fits the prediction from a strictly sequential model [Supporting Online Material (SOM) text)], suggesting that perceiving one color not only causes a moderate decrement in the perception of the second color, but may well prevent the perception of the second color altogether.

In the second experiment, two squares were always presented simultaneously. Square 1 appeared in the top or bottom location and was blue or yellow. Square 2 appeared in the left or right location and was red or green (Fig. 3) (*10*). Some observers were tested on the color and others on the location of one square (the target). The two possible colors (or locations) of the target were shown along with the associated response keys (e.g., "left j right k" would be shown for a location test on square 2 shown in Fig. 3B). In prior-information blocks, the target was either always square 1 or always square 2 across the whole block. Thus as soon as the display appeared, observers knew which square was the target. In no-information blocks, the choice of target varied randomly from trial to trial, although the association between colors and locations remained the same. For any type of visual information (feature or location), if there are attentional limitations on access, then knowing in advance which object will be tested should allow the observer to focus on that object and perceive it significantly better. On the other hand, if two presented values (locations or colors) can be simultaneously accessed without attentional limitation, then advance information would not produce any advantage. Again, the theory claims that access to visual awareness is restricted to one feature at one time, whereas no such restriction should exist for multiple locations. Therefore, for a task on feature values, the observers should perform substantially better with the prior information than without, but no such benefit should be present for a task based on location values.

For the color task, the accuracies were 72.6% for the no-information condition and 80.3% for the prior-information condition (a benefit of 7.7%, $P < 0.00001$). For the location task, the

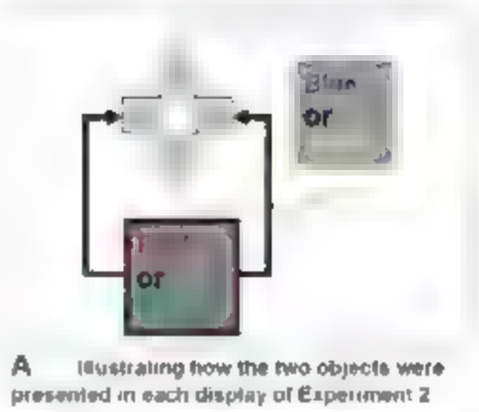

A Illustrating how the two objects were presented in each display of Experiment 2

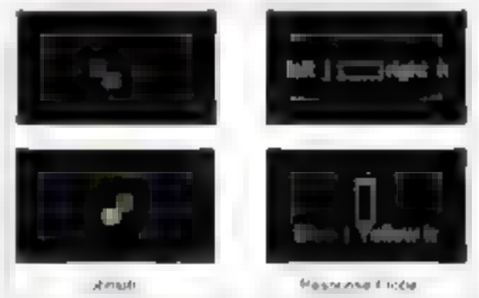

B Two sample trials from Experiment 2

Fig. 3. The method of experiment 2. (**A**) How the two objects were presented in each display. Square 1 (indicated by gray lines) was presented in the top or bottom location, and this object could be blue or yellow. Square 2 (indicated by black lines) was presented on the left or right, and this object could be red or green. (**B**) Two examples of the displays. In this experiment, one group of observers was tested on the color and another on the location of one of the squares. The two possible colors (or locations) of the target were shown along with the associated response keys (e.g., "left j right k"). In the prior-information condition, the tested square was in the prespecified pair (e.g., left-right and red-green) that remained constant across the entire block, so the observers needed only to perceive the relevant object. In the no-information condition, the tested square randomly varied from trial to trial, so the observers had to try to catch both objects to do the tasks.

accuracies were 73.2% for the no-information condition and 75.4% for the prior-information condition (a benefit of 2.2%, significantly smaller than the benefit of 7.7% in color task, $P < 0.001$). The substantial asymmetry of effect of prior information in encoding feature values and location values provides distinctive support for the Boolean map analysis.

Taken together, the experiments reported here, along with other evidence recently presented (*6*), are consistent with the claim that observers have conscious access to only one feature value at one time but have conscious access to more than one location simultaneously. Does the present conclusion—that only one feature can be consciously accessed at any one time—conflict with the well-known evidence for parallel feature processing in the visual search literature (*3*, *5*)? The parallel feature processing demonstrated in that research generally involves the spatially parallel rejection of homogeneous distractors in search of a feature target, a claim that is consistent with the Boolean map hypothesis.

The present results can also be seen as showing that multiple location values can be represented as a holistic pattern or surface (i.e., observers can encode them together as a unit), thus avoiding competition. Feature values, on the contrary, evidently cannot constitute a comparable sort of pattern in feature space (e.g., color space), and thus each needs its own separate visual representation.

The Boolean map format is supported not only by the results of the very austere perceptual tasks investigated here but also by a range of results assessing observers' ability to apprehend complex patterns in relatively rich displays—such as matching, mentally rotating, or judging the symmetry of arrangements of colors or orientations in large grids of elements (*6*, *11*, *12*). In each of these situations, it seems clear that, although people can abstract the spatial distribution of one feature value at a time, even in complex patterns, they are unable to become aware of the distribution of more than one feature value at a time.

This conclusion may seem at odds with ordinary introspection, which may suggest that we can become aware of a heterogeneous world with many feature values at the same time, not the mere spatial distribution of a single feature value. What is to be made of this paradox? The sense that human observers have of being simultaneously aware of varied colors, shapes, directions of motion, and so forth may reflect experiences that are not occurring at any single instant but rather at different times. As some philosophers have noted, our assessment of the content of our awareness may reflect not what we have in mind at one instant, but rather what we can readily fetch with a quick act of will (*13*). Recent studies on change blindness (*14*–*16*) also suggest that visual awareness is starkly limited and that our apparently rich visual experience is likely to be a substantial overestimation of what is actually consciously available.

References and Notes

1. P. T. Quinlan, *Psychol. Bull.* **129**, 643 (2003).
2. J. M. Wolfe, *Psychol. Sci.* **9**, 33 (1998).
3. A. M. Treisman, G. Gelade, *Cognit. Psychol.* **12**, 97 (1980).
4. J. Duncan, G. W. Humphreys, *Psychol. Rev.* **96**, 433 (1989).
5. A. Treisman, S. Gormican, *Psychol. Rev.* **95**, 15 (1988).
6. L. Huang, H. Pashler, *Psychol. Rev.* **114**, 599 (2007).
7. S. M. Zeki, *Nature* **274**, 423 (1978).
8. J. Duncan, *Psychol. Rev.* **87**, 272 (1980).
9. J. Duncan, *Cognit. Psychol.* **12**, 75 (1980).
10. Materials and methods are available on *Science* Online.
11. L. Huang, H. Pashler, *Vision Res.* **42**, 1421 (2002).
12. D. Morales, H. Pashler, *Nature* **399**, 115 (1999).
13. D. C. Dennett, *Consciousness Explained* (Little, Brown, New York, 1991).
14. H. Pashler, *Percept. Psychophys.* **44**, 369 (1988).
15. R. A. Rensink, J. K. O'Regan, J. J. Clark, *Psychol. Sci.* **8**, 368 (1997).
16. R. A. Rensink, *Vision Res.* **40**, 1469 (2000).

17. We thank K. R. Cave, M. M. Chun, H. E. Egeth, J. T. Enns, E. J. Scholl, E. Vul, J. M. Wolfe, and two anonymous reviewers for very useful comments and/or discussion. This research was supported by a grant from the National Institute of Mental Health (H.P.) (R01-MH45584) and a grant from NIH (A.T.) (2004 2R01 MH 058383-04A1).

Supporting Online Material

www.sciencemag.org/cgi/content/full/317/5839/823/DC1
Materials and Methods
SOM Text
Fig. S1

6 April 2007; accepted 3 July 2007
10.1126/science.1143515

Immunization by Avian H5 Influenza Hemagglutinin Mutants with Altered Receptor Binding Specificity

Zhi-Yong Yang,[1]* Chih-Jen Wei,[1]* Wing-Pui Kong,[1] Lan Wu,[1] Ling Xu,[1] David F. Smith,[2] Gary J. Nabel[1]†

Influenza virus entry is mediated by the receptor binding domain (RBD) of its spike, the hemagglutinin (HA). Adaptation of avian viruses to humans is associated with HA specificity for α2,6- rather than α2,3-linked sialic acid (SA) receptors. Here, we define mutations in influenza A subtype H5N1 (avian) HA that alter its specificity for SA either by decreasing α2,3- or increasing α2,6-SA recognition. RBD mutants were used to develop vaccines and monoclonal antibodies that neutralized new variants. Structure-based modification of HA specificity can guide the development of preemptive vaccines and therapeutic monoclonal antibodies that can be evaluated before the emergence of human-adapted H5N1 strains.

The ability of influenza viruses to adapt from animals to humans is determined by several viral gene products [reviewed in (*1*)]. Among them, the viral hemagglutinin (HA) is of particular interest: it binds to specific sialic acid (SA) receptors in the respiratory tract that affect transmission (*1*–*3*). At the same time, it affects sensitivity to neutralizing antibodies, the primary determinant of immune protection (*4*, *5*). The receptor binding domain (RBD) within HA is composed of less than 300 amino acids, situated at the outer surface on top of the viral spike (*6*–*10*). SA binding is mediated by a cavity bordered by two ridges (Fig. 1A), formed by loop 220 (amino acids 221 to 228), loop 130 (amino acids 135 to 138), and a helical domain at amino acids 190 to 197 (numbering based on H3 A/Aichi/2/68) (*10*). The structures of the H1, H5, and H3 HAs have been previously described (*6*–*10*), and the H1 and H5 RBD show greater structural and genetic similarity to one another than to H3 (Fig. 1A).

To define mutations that change receptor recognition, we focused initially on differences between H5 and H1 (A/South Carolina/1/18), which recognizes α2,6-SA linkages, particularly amino acids 190, 193, and 225 (Fig. 1B). Individual or combination mutations to create pseudoviruses were made in which amino acids were replaced at certain positions, described by the single-letter code for the amino acid (*11*), as for example, aspartic acid substituted for glutamic acid at position 190 (E190D). We also used a mutant suggested previously to increase α2,6 recognition, Q226L,G228S (*9*). Surface expression of these HAs was confirmed by flow cytometry (fig. S1A), and pseudotyped lentiviral vectors were produced after cotransfection of neuraminidase (NA). Entry into 293A renal epithelial cells, which ex-

[1]Vaccine Research Center, National Institute of Allergy and Infectious Diseases (NIAID), National Institutes of Health, Building 40, Room 4502, Mailstop Code MSC 3005, 40 Convent Drive, Bethesda, MD 20892, USA. [2]Emory University School of Medicine, 1510 Clifton Road NE, Room 4035, Atlanta, GA 30322, USA.

*These authors contributed equally to this work.
†To whom correspondence should be addressed. E-mail: gnabel@nih.gov

press both α2,3- and α2,6-SAs (fig. S1B), was measured with a luciferase reporter. The E190D,K193S,G225D triple-mutant virus showed entry similar to the wild-type HA (fig. S1C), confirming its functional integrity, however, receptor specificity could not be defined with this assay.

The SA specificity of different HAs was analyzed by a modification of the glycan microarray method (*12*) and by the resialylated HA assay (*13*). For glycan arrays, HAs were coexpressed with NA and purified (*8*). The E190D,K193S,G225D mutation eliminated recognition of most α2,3-linked substrates compared with wild-type protein (Fig. 2, A versus B). The resialylated HA assay confirmed the loss of α2,3-SA recognition in the triple mutant and lack of α2,6 binding (Table 1A), also seen in Q226L,G228S. Analysis of previously described mutants (*14*) also revealed no α2,6-SA recognition (Table 1B). Finally, we identified mutations that increased α2,6-SA recognition (Table 1C), particularly the S137A,T192I variant that alters both the 130 loop and 190 helix. This altered specificity was confirmed in glycan microarrays (table S1). These mutations represent alternatives by which the HA can adapt its substrate recognition; in the last-mentioned instance, it increases α2,6-SA binding to be more similar, although not identical, to human-adapted influenza viruses.

Immunogenic and antigenic differences among HAs with altered receptor specificity were analyzed by vaccination of mice with wild-type or the triple-mutant HA and generation of monoclonal antibodies (mAbs). Each mAb recognized mutant or wild-type HA coexpressed with NA with differential specificity (Fig. 3A). One potent H5-specific mAb, 9E8, neutralized wild-type H5 but showed significantly reduced activity against the triple-mutant pseudovirus (Fig. 3B, left). In contrast, a second such monoclonal, 10D10, neutralized both HAs equivalently at maximal inhibitory concentrations, although smaller differences were observed at intermediate concentrations (Fig. 3B, middle). A third mAb, 9B11, isolated after immunization with the triple-mutant expression vector, showed the converse specificity, inhibiting the triple mutant but not affecting the wild-type H5 pseudovirus (Fig. 3, B and C, right). Finally, although 9E8 more effectively neutralized the wild type than S137A,T192I, another antibody, 11H12, showed comparable activity on both (Fig. 3D), confirming the differential antigenicity of this mutant. Modification of SA binding specificity therefore altered neutralization sensitivity and facilitated the generation of vaccines that elicited effective neutralizing mAbs.

In this report, we have identified mutations in the avian H5 hemagglutinin that alter its specificity for SA receptors and have shown that such mutants can be used to elicit neutralizing monoclonal antibodies that more effectively inhibit these variants. Neutralization sensitivity was determined with a lentiviral entry assay previously shown to define mechanisms of entry for numerous viruses, including HIV, severe acute respiratory syndrome (SARS), Ebola and Marburg hemorrhagic viruses, and, recently, influenza (*15*–*17*). Inhibition by antibodies determined neutralization sensitivity (*18*, *19*) and correlated with hemagglutination inhibition, a traditional marker of immune protection (table S2) (*19*). With this approach, the specificity of the HA was examined, independent of molecular adaptations required to generate replication-competent virus, which allowed identification of several mutants with altered SA specificity. Other mutants have been defined recently whose recognition was assessed with a less-specific assay (*14*), and we find here that they do not gain α2,6-SA recognition in the HA assay.

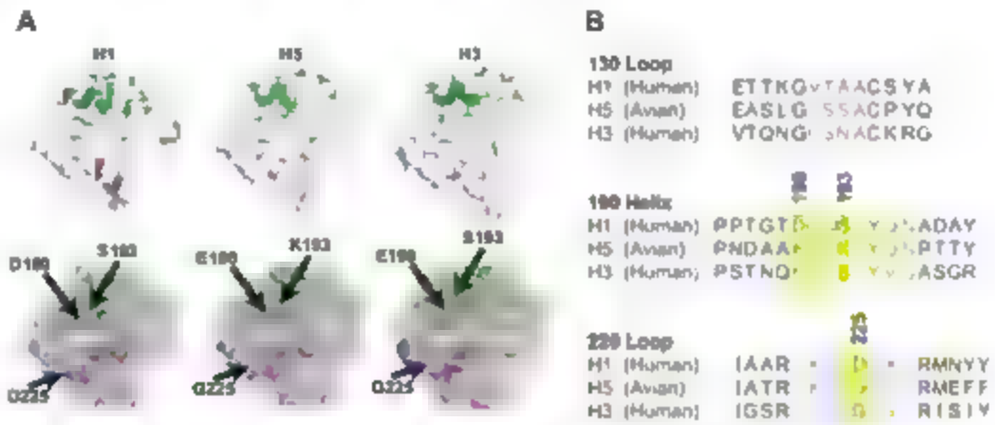

Fig. 1. Structural and genetic basis for hemagglutinin mutations. (**A**) The RBDs of alternative viral hemagglutinins are shown. (**B**) Comparison of amino acid sequences in the major 130 and 220 loops and the 190 helix, color-coded in purple, lavender, and green, respectively.

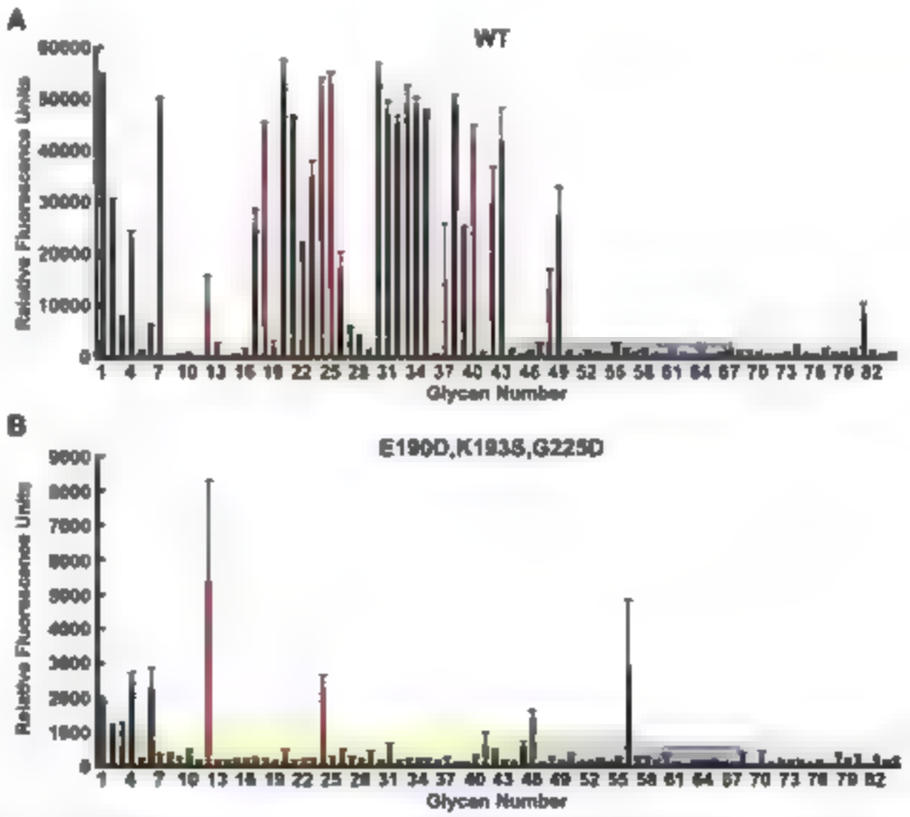

Fig. 2. Altered specificity of the triple-mutant H5 compared with wild-type KAN-1 H5 coexpressed with NA. Glycan microarray analysis of (**A**) wild-type or (**B**) triple-mutant HA purified after coexpression with NA was performed by a modification (*18*) of a previous technique (*12*) performed by Core H, Consortium for Functional Genomics, Emory University. Glycans with related linkages are grouped by color, selected glycoproteins (orange), predominantly α2,3-sialosides (yellow), α2,6-sialosides (green), α2,8 ligands (blue), or others (purple), as previously shown (table S3).

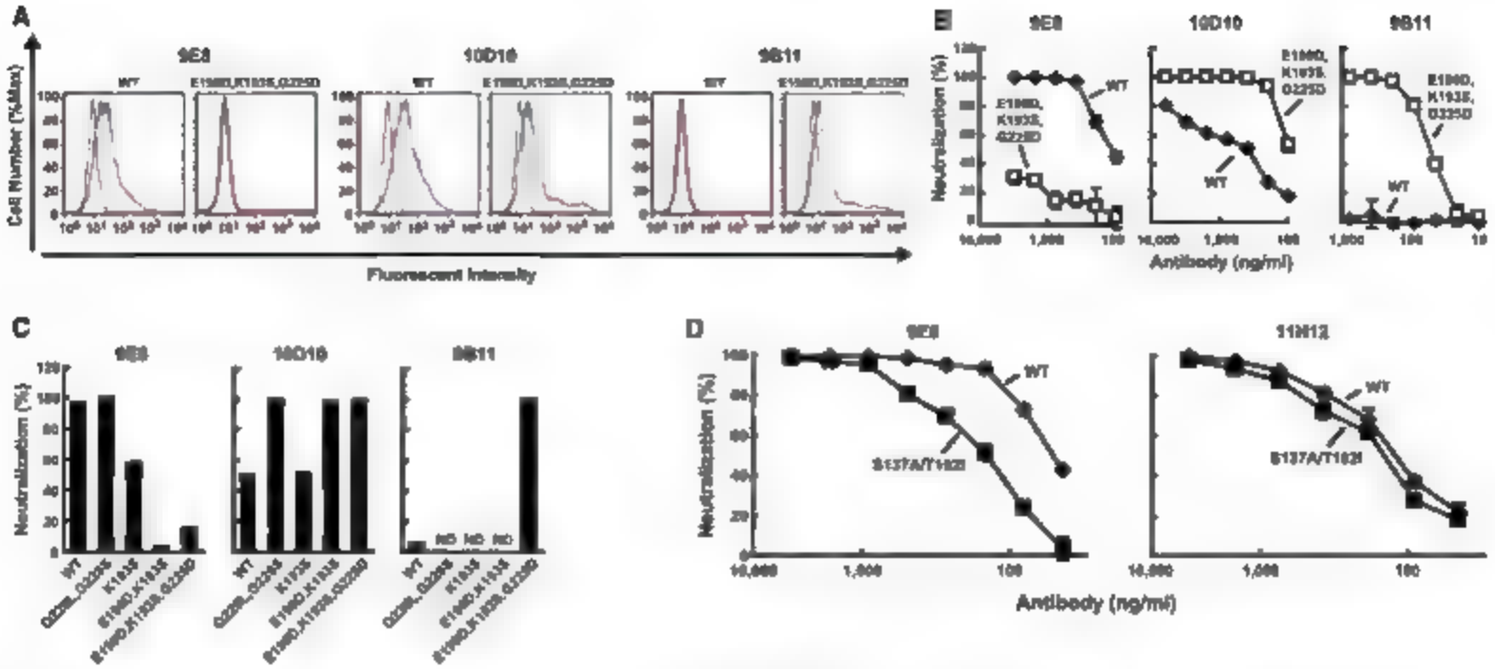

Fig. 3. Altered neutralization sensitivity of mutant H5N1 pseudovirus (**A**) Binding to HA coexpressed with NA in transfected 293T cells was determined by flow cytometry with the indicated mAbs (blue) or isotype control IgG (red). (**B**) Neutralization sensitivities were assessed with the indicated mAbs. (**C**) Neutralization sensitivities of the indicated wild-type and mutant HAs to these mAbs (400 ng/ml) are shown (ND, not done). (**D**) Neutralization sensitivities of wild-type and S137A,T192I mutant to mAb 9E8 and 11H12 are presented.

Table 1. Specificity of glycan recognition and efficacy of entry of wild-type and mutant HAs. H5 mutants KAN-1 from Thailand, or VN1203, and VN1194 from Vietnam were used as described in methods (*18*). The ability of indicated HAs to bind α2,3- and α2,6-SAs was determined by a resialylated hemagglutination assay (*18*) for (**A**) KAN-1 mutants with loss of α2,3-HA activity and relevant controls, (**B**) VN1203 and previously described VN1194 mutants (*14*), and (**C**) KAN-1 mutants with increased α2,6-SA binding. Viral entry of wild-type and mutant pseudotyped lentiviral vectors was measured as described (*18*). The degrees of entry were as follows: + <25% of WT; ++ 25 to 50% of WT; +++, 50 to 75% of WT; ++++ >75% of WT. The H5 (KAN-1) here is identical to the GenBank sequence and differs at amino acids 186(N/K) from Yamada and colleagues (*14*) and the VN1194 mutants are identical to N182K and Q192R (*14*) according to alternative numbering conventions.

Mutation		HA titer			Entry
		CRBC	α2,3	α2,6	
(A)	H5(KAN-1)	80	160	<2	++++
	E190D	<2	<2	<2	+
	G225D	40	<2	<2	++++
	E190,G225D	<2	<2	<2	+
	Q226L	40	<2	<2	+++
	Q226L,G228S	40	<2	<2	+++
	E190D,K193S	20	<2	<2	+++
	K193S,G225D	80	<2	<2	++++
	E190D,K193S,G225D	40	<2	<2	+++
	K193S,Q226L	20	<2	<2	+
	K193S,Q226L,G228S	40	<2	<2	+
	H1N1(1918/SC)	160	<2	160	++++
(B)	H5(VN1203)	20	20	<2	++++
	E190D,K193S,Q226L,G228S	40	<2	<2	+++
	A189K,K193N,Q226L,G228S	40	<2	<2	++++
	H5(VN1194)	320	320	<2	++++
	N186K	320	160	<2	++++
	Q196R	<2	<2	<2	++
(C)	S137A	80	80	80	++++
	T192I	80	160	80	++++
	S137A/T192I	40	40	80	+++

(Table 1B; N186K, Q196R). The previously reported Q226L,G228S mutant (*9*) also showed no α2,6-SA binding (Table 1A). It is therefore unlikely that HA mutants reported previously are human-adapted, although S137A,T192I here may represent a step in this pathway.

Whether acquisition of α2,6-SA specificity would increase H5N1 transmissibility also remains unknown. Recently, HA mutations in the 1918 virus that allowed human SA recognition were shown to enhance transmission in ferrets (*20*), which supports this notion and provides a model to evaluate such H5 mutants. The application of rational design of human-adapted H5-specific vaccines facilitates such analyses, as well as the development of preemptive countermeasures to contain influenza outbreaks. The five major antigenic sites of HA lie on an accessible surface adjacent to the RBD (*7*, *21*, *22*). Although antibodies to this region can affect RBD specificity and neutralization sensitivity (*7*, *23*–*26*), changes solely in the RBD have not been shown to alter immunogenicity. Here, structure-based modification of RBD specificity facilitated the generation of mAbs independent of the major antigenic sites. Directed to a functionally constrained domain, they may less readily evolve resistance and serve as vaccine prototypes that can be developed before human-adapted strains emerge.

References and Notes

1. C. B. Parrish, Y. Kawaoka, *Annu. Rev. Microbiol.* **59**, 553 (2005).
2. W. J. Bean *et al.*, *J. Virol.* **66**, 1129 (1992).
3. A. Vines *et al.*, *J. Virol.* **72**, 7626 (1998).

Gel Documentation System

The compact PhotoDoc-It Imaging System for basic documentation of gels and plates is configured for limited laboratory space and budgets. Attached to the lightweight hood that sits on the transilluminator, the 6.0 megapixel digital camera generates brilliant color images. Transilluminator options include single or multiple ultraviolet wavelengths and filter sizes. A compact color printer connects directly to the camera for low-cost four-inch by six-inch lab-quality prints. In addition, images can be saved to a camera memory card or the instrument can be linked to a computer. Optional software offers additional image enhancement, analysis, and report features.

UVP For information 909-946-3197 www.uvp.com

Vertical Laminar Flow Workstations

The AC600 Series Vertical Laminar Flow Workstations are suitable for applications that are not hazardous to the operator but require a clean work area. The compact, lightweight design allows for multiple "clean zones" within a laboratory. Standard features include microprocessor control, 360° visibility, integral polypropylene base for easy cleaning, all thermoplastic construction, a built-in fluorescent light, and a monitor to indicate when it's time to change the filter. Typical applications include pouring med a plates, assembly of small parts, optic assembly, amplification of DNA and RNA, and trace metal analysis.

AirClean Systems For information 800-849-0472 www.aircleansystems.com

Isolation of Periplasmic Proteins

The presence of a signal sequence is important for the export of certain proteins into the *E. coli* periplasmic space. The PeriPreps Periplasting Kit enables gentle, efficient solubilization of the outer membrane of *E. coli* cells, permitting rapid extraction of proteins from the periplasmic space. This can result in enrichment of certain proteins compared with preparation by lysis of the entire cell. A spheroplast lysis buffer is also provided for isolation of spheroplast proteins.

Epicentre Biotechnologies For information 800-284-8474 www.EpiBio.com/PeriPreps.asp

PCR Workstation

The Combination PCR (polymerase chain reaction) Workstations have a built-in 254 nm ultraviolet light that allows the operator to irradiate tubes, flasks, and pipettes between amplifications. Clean Class 100 laminar flow air prevents outside contaminants from entering into the work area during manipulation. The 254 nm ultraviolet light effectively destroys potentially contaminating DNA and RNA within minutes. A microprocessor controller monitors the life of the bulb to insure proper levels of irradiation. Features include a bi-fold sash with safety interlock to eliminate ultraviolet radiation leaks, an integral polypropylene base for easy cleaning, and an ultraviolet shield with built-in pipettor rack. Low-profile and tall versions are available, as are 32 inch and 48 inch widths. It is available in 110V and 220V models.

AirClean Systems For information 919-255-3220 www.aircleansystems.com

Foam Reduction Agent

GIBCO FoamAway Irradiated is a sterile, ready-to-use reagent that eliminates proteinaceous foam in mammalian and microbial cell cultures. Sterilized through a validated gamma irradiation process, FoamAway Irradiated can be quickly added to a foaming culture without spending time to prepare it. It can also be used to prevent foam formation.

Invitrogen.

For information 617-897-8258 www.invitrogen.com/ivd

Mitotic Assay Kits

The Mitotic Assay Kits make it simple to determine the percentage of cells undergoing mitosis within a specific population. The kits are available in fluorescent, chemiluminescent, and colorimetric formats.

Active Motif For information 877-222-9543 www.activemotif.com

Oligonucleotide Purification

A family of displacers for oligonucleotide purification using anion exchange chromatography, Propell Q displacers and displacement chromatography offer a simple way to convert analytical columns into effective tools for obtaining large volumes of highly purified oligonucleotides. Selectively designed to have the necessary affinity for the targeted chromatography media, these novel displacers drive oligonucleotides off the column at high concentration and high purity, and are easily removed from the column. The purified oligonucleotides can generally be used without additional processing. Intended for use with anion exchange chromatography, Propell Q offers an effective alternative to scaling reverse-phase chromatography, and can isolate large quantities (100+ mg) of purified oligonucleotides in a single run.

Sachem For information 512-421-4945 www.sachem-inc.com

Resolve-It Kit

The Resolve-It Kit is designed to be used in applications such as differential display, in which multiple DNA species of similar size need to be separated before subsequent excision and analysis. The kit contains two ligands: AT Yellow, a bisbenzimide PEG conjugate that binds DNA at AT-rich regions, and GC Red, a phenanthridium PEG conjugate that binds GC-rich regions. One of the ligands is added to the agarose during gel preparation. During electrophoresis, the ligand interacts with AT-rich or GC-rich sequences and retards the mobility of DNA, depending on the amount of ligand bound. Thus, two identically sized DNAs can be resolved.

Vector Laboratories For information 650-697-3600 www.vectorlabs.com

Newly offered instrumentation, apparatus, and laboratory materials of interest to researchers in all disciplines in academic, industrial, and government organizations are featured in this space. Emphasis is given to purpose, chief characteristics, and availability of products and materials. Endorsement by *Science* or AAAS of any products or materials mentioned is not implied. Additional information may be obtained from the manufacturer or supplier.

POSITIONS OPEN

TWO TENURE TRACK FACULTY POSITIONS
Providence College

Applications are invited for two **ASSISTANT PROFESSORS of BIOLOGY** beginning September 2008. Candidates are required to have a Ph.D. (postdoctoral experience preferred) and a sustainable research program that will include undergraduates. Ability to teach electron microscopy will enhance the applications but is not required.

Microbiology: Successful applicant will teach biology major courses such as general biology, microbiology, advanced courses in area of expertise, and nonmajor courses such as human biology and microbes and man. Although emphasis is on molecular/genomic/cellular studies, candidates with backgrounds in systematic or environmental studies are encouraged to apply.

Neurobiology: Successful applicant will teach biology major courses such as general biology, neurobiology, cell and molecular genetics, advanced courses in area of expertise, and nonmajor courses such as human biology. Applicant will be expected to apply for support of a research project that includes undergraduate student training, through the statewide IdeA Network of Biomedical Research Excellence program (**website: http://www.uri.edu/sinbre**).

Send cover letter, curriculum vitae, graduate transcripts, a statement of teaching philosophy and research interests, and three letters of recommendation by October 15, 2007, to **Dr. C.B. Wood, Chair, Biology Department, Providence College, Providence, RI 02918 0001**. For more information on the Department and Providence College see website: **http://www.providence.edu/bio.**

Providence College is a Roman Catholic, four-year liberal arts college conducted under the auspices of the Dominican Friars and seeks candidates who can affirm and contribute to its mission. [illegible] Providence College is an Equal Opportunity Employer. We actively encourage the applications of women and [illegible]

The University of Chicago, Department of Molecular Genetics and Cell Biology is seeking a full time **RESEARCH ASSOCIATE (ASSISTANT PROFESSOR)** to investigate the DNA methylation/chromatin modifier Sam1. Applicants should have Ph.D. degree and at least three years of research experience in molecular, cell, and developmental biology. Qualified applicants should provide current curriculum vitae and bibliography, statement of research interest and goals, and full names, addresses, telephone/fax numbers, and e-mail addresses of at least three scholars who can provide academic references. Application material should be sent to **Robert Sullivan, Executive Administrator, The University of Chicago, Cummings Life Sciences Center, 920 E. 58th Street, Chicago, IL 60637.**
The University of Chicago is an Affirmative Action/Equal Opportunity Employer.

The University of Chicago, Department of Molecular Genetics and Cell Biology is seeking a full time **RESEARCH ASSOCIATE (ASSOCIATE PROFESSOR)** to investigate the role of the cytidine deaminase AID in somatic hypermutation of Ig genes. Applicants should have Ph.D. degree and at least five years of research experience in molecular, cell, and developmental biology. Qualified applicants should provide current curriculum vitae and bibliography, statement of research interest and goals, and full names, addresses, telephone/fax numbers, and e-mail addresses of at least three scholars who can provide academic references. Application material should be sent to: **Robert Sullivan, Executive Administrator, The University of Chicago, Cummings Life Sciences Center, 920 E. 58th Street, Chicago, IL 60637.** *The University of Chicago is an Affirmative Action/Equal Opportunity Employer.*

CHEMISTRY POSITIONS

MULTIPLE POSITIONS
Emory University
Department of Chemistry

Candidates with a proven record of accomplishment in research and scholarship in all areas of chemistry are invited to apply for multiple positions at the level of **ASSISTANT, ASSOCIATE, or FULL PROFESSOR,** as the Department of Chemistry plans a major expansion of its faculty along with its research and teaching space. Outstanding applicants with research interests in organic or physical chemistry, broadly defined, are particularly encouraged. Candidates must have received the Ph.D. or equivalent degree in chemistry or a related discipline. Please submit curriculum vitae, a cover letter, and a summary of research interests (for candidates at the Assistant Professor level, please submit specific research plans) and arrange for three letters of recommendation; all materials and letters should be e-mailed to e-mail: chemsearch@emory.edu, preferably in .PDF format. Review of applications will begin **September 15, 2007.** *Emory University is an Affirmative Action/Equal Opportunity Employer and welcomes applications from women and members of minority groups.*

BIOCHEMISTRY FACULTY POST

Bucknell University seeks outstanding candidates for an entry-level, tenure-track position at the rank of **ASSISTANT PROFESSOR** scheduled to begin in August 2008. The successful applicant will teach biochemistry, lecture, and laboratory, and will also teach introductory organic chemistry, general chemistry, or introductory inorganic chemistry, depending on background and interests. The successful candidate will also have the opportunity to develop advanced course(s) within his/her area(s) of expertise. The development of a vigorous research program in some area of biochemistry (including bioorganic, bioinorganic, and chemical biology) is expected, and this research program will involve undergraduate and Master's students. Ph.D. required, postdoctoral experience preferred. Applications can be submitted at website: **http://www.bucknell.edu/jobs,** and should include curriculum vitae, a detailed description of research interests and plans, and a statement of teaching interests. Additionally, three letters of recommendation are to be sent directly to **Professor Timothy G. Strein, Chair of the Biochemistry Search Committee, Department of Chemistry, Bucknell University, Lewisburg, PA 17837 (e-mail: strein@bucknell.edu).** Review of applications will begin on **October 5, 2007.** *Bucknell University encourages applications from women and members of minority groups as part of its commitment to [illegible] opportunity. Affirmative Action [illegible]*

ASSISTANT PROFESSOR
The University of Chicago
Department of Chemistry

The Department of Chemistry of the University of Chicago invites applications from outstanding individuals for the position of Assistant Professor of Chemistry. This search is in the areas broadly defined as inorganic, organic, and physical chemistry. Applications must include curriculum vitae, a list of publications, and a succinct outline of research plans, and be supported by three letters of recommendation. Submit materials by mail addressed, as appropriate, to: **Inorganic Search Committee, Organic Search Committee, or Physical Search Committee, Department of Chemistry, Office of the Chairman (Gilj 222), The University of Chicago, 5735 S. Ellis Avenue, Chicago, Il 60637.** Review of completed applications will begin October 1, 2007, to ensure full consideration, all material should be submitted by that date. *University of Chicago is an Affirmative Action/Equal Opportunity Employer.*

Constantly Evolving Choices

Leaving the chemistry department behind doesn't have to mean leaving chemistry behind. Chemists have a broad, and broadening, range of career options to choose from, both in and out of the lab. The biggest challenge is looking beyond the more traditional roles, which represent only a fraction of the options available in this fast-growing field.
By Bea Perks

There has always been a far wider range of career opportunities for chemists than the chemists – or at least newly qualified chemists – recognize, according to **Lisa Balbes**, a volunteer careers consultant with the American Chemical Society (ACS). Balbes is a freelance technical writer and consultant, and the author of *Nontraditional Careers for Chemists* (Oxford University Press, 2006).

Chemists do branch out into what she calls nontraditional roles, but they often think this means they have left chemistry behind.

Balbes has a Ph.D. in organic chemistry and spent several years on a postdoc in molecular modeling. Her career evolved following a move to a job "that turned out not to exist," she recalls. She ended up being offered a consulting job by a company whose software she'd been using as a postdoc. She took the job, which led to subsequent consulting contracts and, after about three years, she realized she had become a consultant.

"It was completely accidental. It just worked out really well, and I kept doing it. I've been doing it for 15 years now and I love it," says Balbes.

It's just one example of the career opportunities that chemists might not spot.

Chemistry for Life

Exponential growth in the life sciences arena has led some observers to conclude that employment opportunities for chemistry graduates and postgraduates are on the slide. Far from it. Chemists are central to the success of the biotech and life science industries. While fewer students are choosing to take chemistry Ph.D.s across the US according to a recent news article in *Science* (6 April 2007, p. 35), life science companies are crying out for postgraduate chemists.

The life sciences are in no way an alternative to the chemical sciences. The two are inextricably linked. Career opportunities for chemists haven't decreased with a shift toward the life sciences, they've expanded. There are ever more opportunities to be had, but that means looking beyond more established roles.

Forget straight biology or chemistry; today's successful companies take a multidisciplinary approach. Life scientists kick started the biotech revolution, but it wouldn't have progressed as rapidly without chemical expertise.

Sigma Aldrich, which calls itself a leading life science and high technology company, hires about 45 percent chemists to 55 percent biologists at Ph.D. level, says **Roxanne LaPlante**, recruiting manager at the company's headquarters in St. Louis, Missouri. The spread is even closer to 50/50 at the Bachelor's degree level, she says.

Many of the chemists hired by Sigma Aldrich are medicinal chemists, but the company has a particular challenge recruiting analytical chemists.

"We have difficulty finding Ph.D. level analytical chemists," says LaPlante. "We are in direct competition with big pharma."

Chemists seem to gravitate naturally toward the pharmaceutical industry. It's a career choice future chemists might even make before they start at university. And it's well paid, so why wouldn't they?

"It's a less safe job," offers LaPlante. In LaPlante's opinion, job security in big pharma is not as stable as in other industries, but generally higher salaries attract those willing to make this tradeoff.

continued

Chemists are central to the success of the biotech and life science industries

UPCOMING FEATURES

Postdoc Scientist Survey – August 31

Faculty Positions 2 – September 14

International Careers: Germany – September 21

Careers in Chemistry

"With the growth of our small-molecule program we are looking for chemists with analytical methods development, synthetic organic, medicinal chemistry, and peptide chemistry expertise."
—Holly Butler

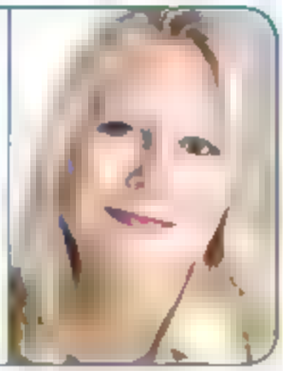

Analyzing Career Options

Analytical chemists carry out qualitative and quantitative analysis they sample, define, isolate, concentrate, and preserve samples. They are responsible for setting error limits, validating and verifying results through calibration and standardization, performing separations based on differential chemical properties, developing new ways of making more precise measurements, interpreting data, and communicating results. Sigma-Aldrich, which serves the pharmaceutical and biotech industries, universities, hospitals, and allied organizations with biochemical and organic chemical products and kits, relies heavily on this skill set among its 6,800 employees worldwide.

Analytical chemistry relies on an ever-increasing array of automated and computerized analytical techniques. To a degree, this has meant that fewer chemists are needed at the bench. hundreds of samples can be prepared and measured at the press of a button, data can be stored and analyzed in minutes. But the demand for increasingly sophisticated analytical techniques, instrumentation, automation, and computerization has opened up options for analytical chemists in other areas. New instrumentation and data management systems have ushered in opportunities for chemists with solid technical and computing skills. At the same time, roles have emerged for quality assurance specialists, whose job it is to ensure that analytical laboratories and the chemists working in them follow documented and approved procedures.

Analytical chemists, regardless of which path they take, need a strong background in chemistry, an eye for detail, good computer skills, and good laboratory and problem-solving skills.

At Agilent Technologies, based in Santa Clara, California, with a worldwide work force of 19,000, the demand for chemists is shifting from analytical to biochemical. "There is a very heavy emphasis, because of the life science focus, on biochemistry," says **Linda Lim**, technical recruiter for the company's life sciences business groups. "Traditionally we had the analytical chemists for our more mature products. For the last 4–5 years we've gravitated toward the biochemistry part of our business."

Think Out Of the Box, Out Of the Lab

Importantly, whichever sort of chemist you are, having those skills should not restrict you to working at the lab bench.

"It's a skill set urgently needed in sales and marketing roles, dealing with products and customers at the pre- and postsale stages," says **Alexis Difirenzi-Swale**, director of worldwide staffing at Agilent. "If you've been in university, often the professors only know about R&D positions, but don't always know about the broader positions that use the same skill sets," says Difirenzi-Swale. Chemists leaving university, she fears, may not know the opportunities that are available, and might see essential marketing roles as somehow less attractive than R&D roles.

All of which could contribute to the fact that Agilent has to give itself a longer lead time when looking for pre- and postsales support. The company's sales activities are concentrated in the UK, says Difirenzi-Swale, while its main manufacturing sites are based in the US, China, and Germany.

Master's and Ph.D.s now represent about 60 percent of Agilent's campus hiring population in the US. It's roughly the same in China, but slightly less in India and Malaysia where there are fewer candidates with higher degrees. In Europe a slightly higher proportion of Agilent's work force has higher degrees.

Agilent recommenced hiring college graduates relatively recently, following a difficult year for the company in 2001, says the company's staffing manager for the Americas, **Mark Bajan**. "The company was actually a lot more focused on Ph.D. hires at that time," he recalls. "That's really switched over the last couple of years; we hire a great deal of Bachelor's and Master's degree candidates to fill our college and intern openings."

Companies that serve life science markets, like Agilent and Sigma-Aldrich, have developed close working relations with universities in order to introduce themselves to, and select, future employees.

Sigma-Aldrich runs internships for university students in the summer. The program involves full time employment for 10 to 12 weeks in the company's analytical services, production, or R&D departments, providing marketable experience in an industrial setting. Likewise, Agilent's university relations programs include research grants, fellowships, equipment grants, and matching of employee gifts to colleges and universities.

California-based Genentech, one of the originators of the biotechnology industry, has always gone to the fall and spring recruiting events for graduate students at the major universities known for their chemistry programs. As well as analytical and computational chemists, the company, with a work force of over 10,000, looks for synthetic organic chemists, medicinal chemists, and combinatorial chemists to join their research teams.

"With the growth of our small-molecule program we are looking for chemists with analytical methods development, synthetic organic, medicinal chemistry, and peptide chemistry expertise," says **Holly Butler**, Genentech's principal staffing consultant for research. "The primary change is that we are hiring more of them now."

Genentech, as with many other biotech companies, preferentially (though not exclusively) recruits graduates in applied chemistry over those studying basic chemistry. The company looks particularly for candidates who have successfully contributed to drug targets going into development and, ideally, for those with experience filing investigational

continued »

CREDIT: SEAWELL PHOTOGRAPHY

"Increasingly in the life sciences, developments are based on an understanding of processes at the molecular level, even where the molecules are large and in complex systems."
—Tony Ashmore

new drug (IND) applications with the US Food and Drug Administration (FDA). "Project leadership experience is important as well," says Butler.

Once they are out of university, "we are more likely to recruit those with work experience in the small-molecule field, often from pharma companies," she says.

Emerging Occupations

There are a growing number of career choices for scientists with degrees in chemistry, agrees **Tony Ashmore**, registrar at the Royal Society of Chemistry in the UK. "Career choice in general has broadened as new occupations emerge," he says.

The traditional generic attributes of chemists, in addition to subject specific skills, include complex numerate problem solving capabilities, particularly for those with backgrounds in physical and theoretical chemistry, notes Ashmore. Chemists tend to share an ability to sift, correlate, evaluate, and manipulate nonquantitative data and solve problems where there is incomplete information, particularly for those with a background in inorganic, organic, and biochemistry, he adds.

"Increasingly in the life sciences, developments are based on an understanding of processes at the molecular level, even where the molecules are large and in complex systems," says Ashmore, "so an increased hiring of folk with a thorough understanding of the fundamentals is taking place."

Multidisciplinary teams are key, he says, where each member is a specialist in a particular field, but also has the ability to work with team members from other fields. This is quite distinct from what might be called an interdisciplinary team, "where everyone knows a little about everything," says Ashmore.

Once a Chemist, Always a Chemist

Consultant Balbes says she became a volunteer careers consultant for the ACS when worried chemists began asking her if there was anything they could do beyond working in a lab.

"I actually have a brochure that was put out by ACS in 1963 talking about all these other careers for chemists – sales, marketing, patent law. All these other things, back in 1963!" she says. But even today, chemists can fail to look beyond academia. "Most university professors train students to become university professors," she says, echoing the concerns of Agilent's Difirenzi-Swale.

In fact, says Balbes, chemists have always found jobs in sales, marketing, and beyond, but they've tended to treat it as a "dirty little secret," as if they have ceased to be chemists. But they still are chemists, she insists. The skills they have developed as chemists are essential in those other roles.

There is a growing school of thought that chemists are trained to approach problems in a certain way. "Analytical is the best word I've come up with," says Balbes. "Chemists know how to ask the right questions."

For the purposes of her recent book, Balbes defined a nontraditional career in chemistry as "non laboratory, non university professor." Such careers, for people with either a Bachelor's or a Ph.D. in chemistry, used to be called alternative careers, but this has ended up sounding relatively unappealing. Perhaps just "non laboratory" would have been best, she suggests.

The big employers of nontraditional chemists include all the science companies—chemical companies, biotech companies, pharmaceutical companies—but also law firms, companies involved in public policy, and companies involved in manufacturing or information technology.

Balbes once met a Ph.D. chemist who had moved into sales and marketing of scientific products, and who gave a talk entitled "A Chemist Moves to the Dark Side." "That's what scientists think," she sighs. "But if nobody sold your products, you wouldn't have a job, would you?"

Selling products to scientists demands a particular skill set, she notes. "It's not used car sales. Scientists want to see the technical merits of products. They want to be able to make their own judgments based on the merits of the product."

Balbes hopes she's starting to see some of the stigma eroding. "For example, people not apologizing for not working in the lab," she says. "I find myself doing it sometimes, and I really have to stop!"

She firmly introduces herself as a chemist, despite not having worked in a lab for 15 years. You have to consider your audience though, she admits. She once spoke to a group of Boy Scouts who, on hearing that she was a chemist who worked from home, wondered if she might be running a methamphetamine lab. Overall, though, the message is getting across, she says.

Balbes has been a volunteer career consultant with the ACS for 15 years. ACS members have access to a list of about 80 such consultants who will help them through a career crisis—if they're about to finish their Ph.D. and don't know what to do next, or if they've just lost their job. Each volunteer provides a short biography, and members can pick the individual they think is most likely to help them—they can then phone or e-mail for tailored assistance. The consultants also attend twice yearly ACS national meetings and run workshops on career-related topics, from CV writing, to interview techniques, to starting up a company.

"You don't get paid, but it's incredibly rewarding," says Balbes. So does she encourage everyone to get a chemistry qualification?

"You should get a chemistry degree if you love chemistry," she says. "If you enjoy it, you're going to be able to find a job that you love. You shouldn't say 'Right now there's a big market for chemists so I should go and become one even though I hate chemistry,' because you'll be miserable," says Balbes. "I'm not trying to talk people into getting a chemistry degree; I'm trying to convince them that if that's what they love, they can make a career out of it."

Bea Perks, deputy editor of the Royal Society of Chemistry's magazine Chemistry World, *writes from Cambridge, UK.*

Each day we invest over $7.5 million in Research, Development and Manufacturing

Research Scientists

Physical or Analytical Chemistry; Chemical Engineering; Materials Science

Cambridge, England

Schlumberger is the world's leading supplier of technology and services to the oil and gas exploration and production industry and has an unwavering commitment to Research and Development

Our chemistry department is comprised of skilled scientists whose specialisation is analytical chemistry, synthetic chemistry, surface science and physical chemistry. By focusing on chemical reaction engineering as well as the development of new chemical measurements and interpretation techniques, we aim to understand and exploit chemical means of measuring, optimising and controlling reservoir and wellbore processes. The work will be varied and multi-disciplinary in nature and strong communication skills and the ability to work within teams is important. You will have a PhD in the field of experimental science or engineering and experience in the development of experimental apparatus and instrumentation would be an advantage. You must also be fluent in spoken and written English.

Several exciting opportunities exist and you will initially find yourself contributing in one of the following areas:

- Membrane/Separation Technologist: Being part of a team developing the next generation of sensors for deployment in the hostile conditions found inside reservoirs, during the exploration and development of hydrocarbon reservoirs. The work involves developing experiments to probe the fundamentals of mass transfer, phase behaviour and material properties as we develop prototype sensors.
- HTHP Experimentalist: Collaborating with different research programs to investigate organic and inorganic chemical reaction pathways and kinetics. Main responsibilities will be to develop experimental equipment and methods and study chemical reactions at high temperatures and pressures (reservoir conditions).
- NMR Spectroscopist: Investigating the chemistry of high performance materials and characterise reaction products. You should have good synthetic chemistry skills to complement your substantial NMR expertise. We are particularly interested in hearing from individuals with solid state NMR, multi-component NMR, pulse sequence design, and NMR protocol design experience.
- Material Scientist: Identifying and investigating chemicals and materials applicable at high temperature, in corrosive brines that maintain their characteristics for prolonged periods. You will have significant experience investigating and enhancing the chemistry of materials.

To apply, please send a detailed CV to Emily Horwich at recruting@cambridge.oilfield.slb.com quoting "Chem_RS" in the subject line. Closing date 30th September 2007

Schlumberger is an Equal Opportunities Employer

Schlumberger

www.slb.com/careers

Success without boundaries

Leave your mark.

Millennium is focused on developing breakthrough treatments in the areas of oncology and inflammation that will make a real difference in patients' lives. We encourage innovation and seek results through collaboration. If you're looking for a dynamic environment where respect and excellence are core values, learn more about us and the possibilities for you at **www.millennium.com**

Millennium has opportunities in the following areas:

Associate Director – Clinical Pharmacology

Scientist – Formulations

Scientist – Molecular Technologies

Sr. Research Associate – Cancer Pharmacology

Research Investigator – Analytical Development

QA Specialist/Manager – Commercial Quality

We are an equal opportunity employer committed to discovering the individual in everyone

MILLENNIUM

FACULTY POSITION IN PLANT BIOLOGY

Section of Plant Biology, College of Biological Sciences, University of California, Davis

The Section of Plant Biology, College of Biological Sciences, at the University of California, Davis invites applications for a tenure-track position at the ASSISTANT PROFESSOR level. Candidates must have a Ph.D. (or equivalent) and have an outstanding record of research achievement. The successful candidate is expected to develop a state-of-the-art research program that will implement quantitative and systems-based approaches to understand fundamental principles underlying the biology of plants. Preference will be given to candidates who use approaches such as analytical and molecular biochemistry with emphasis on metabolomics and metabolic flux analysis, proteomics/interactomics or systems biology. The Section of Plant Biology places a high priority on teaching and the successful candidate will also be expected to contribute to the teaching mission of the Section.

Candidates should submit the following materials, online, at www.plbi.ucdavis.edu: (a) curriculum vitae, (b) summary of research accomplishments, (c) clearly focused description of future research plans (5 years), (d) up to five major publications, (e) statement of teaching experience and/or interest.

Candidates should also arrange for a minimum of three letters of recommendation to be submitted by e-mail to plbscan.bio@ucdavis.edu.

Bo Liu, Chair
Faculty Search Committee
Section of Plant Biology
One Shields Ave
University of California, Davis
Davis, CA 95616

Closing date: open until filled although to assure full consideration, applications should be received on or before Thursday, November 15, 2007.

The Section encourages women and minorities to apply. The University of California, Davis, is an Equal Opportunity/Affirmative Action Employer.

D. E. Shaw Research, LLC

Computational Chemistry and Biology Opportunities

Extraordinarily gifted computational chemists, biologists, and other computational scientists are sought to join a rapidly growing New York–based research group that is pursuing an ambitious, long-term strategy aimed at fundamentally transforming the process of drug discovery.

Candidates should have world-class credentials in computational chemistry, biology, or physics, or in a relevant area of computer science or applied mathematics, and must have unusually strong research skills. Relevant areas of experience might include protein structure prediction, the computation of protein-ligand binding affinities, the study of biologically important systems using molecular dynamics and/or Monte Carlo simulation, and the application of statistical mechanics to biomolecular systems—but specific knowledge of any of these areas is less critical than exceptional intellectual ability and a demonstrated track record of achievement. Current areas of interest within the group include molecular dynamics simulation of functionally significant globular and membrane proteins, the prediction of protein structures and binding free energies, structure- and ligand-based drug design, characterization of protein-protein, protein-nucleic acid, and protein-lipid interactions, and the development of algorithms for biomolecular simulations.

This research effort is being financed by the D. E. Shaw group, a global investment and technology development firm with more than US $25 billion in aggregate investment capital. The project was initiated by the firm's founder, Dr. David E. Shaw, and operates under his direct scientific leadership.

We are eager to add both senior- and junior-level members to our world-class team, and are prepared to offer above-market compensation to candidates of truly exceptional ability.

Please send your curriculum vitae (including list of publications, thesis topic, and advisor if applicable) to *sciencemag-cc@deshawresearch.com*.

D. E. Shaw Research, LLC does not discriminate in employment matters on the basis of race, color, religion, gender, pregnancy, national origin, age, military service eligibility, veteran status, sexual orientation, marital status, disability, or any other protected class.

D E Shaw & Co

Mississippi State University

PROFESSOR and HEAD
Department of Biochemistry and Molecular Biology

Mississippi State University (MSU) invites applications and nominations for the position of Professor and Head of the Department of Biochemistry and Molecular Biology. The Head is the principal representative of the Department with authority and responsibility for administrative decisions. The Department is seeking a dynamic individual with an outstanding record of achievement, an appreciation for the range of disciplines in biochemistry and molecular biology, and an understanding of diverse functions of research, teaching, and service. The selected individual should have a distinguished record of scholarship, as well as significant experience in communication, leadership, and team building, a strong commitment to diversity, and dedication to the land grant mission. Applicants should have a Ph.D. degree in biochemistry or molecular biology or a closely related field and meet eligibility requirements for tenure at the full Professor level and graduate faculty membership at MSU. Review of applications will begin September 30, 2007, and will continue until a suitable candidate is identified. Applicants should submit a letter of interest that discusses qualifications for the position, curriculum vitae, and the names, telephone numbers, and mailing and e-mail addresses of four references. Application may be made online at **website: https://www.jobs.msstate.edu** or by sending the application to: **Dr. Jim Shepard, P.O. Box 9681, Mississippi State, MS 39762, e-mail: jshepard@cfr.msstate.edu, telephone: 662-325-2781.** *Mississippi State University is an Affirmative Action/Equal Opportunity Employer*

DONALD J. CRAM CHAIR in ORGANIC CHEMISTRY
Organic Chemistry at UCLA University of California, Los Angeles (UCLA)

The Department of Chemistry and Biochemistry in the University of California, Los Angeles, is seeking to fill several organic chemistry positions at UCLA, intended to expand the expertise of the Department in synthetic organic chemistry and in materials organic chemistry, in conjunction with the California NanoSystems Institute. The **Donald J. Cram Chair in Organic Chemistry** is to be filled by a very distinguished **ORGANIC CHEMIST;** a Search Committee has been appointed to recommend the most outstanding candidate. The occupant of this Chair will hold a state funded regular faculty position, the income from the endowment is available to the holder as an unrestricted fund for purposes of research and teaching. Positions related to the mission of the California NanoSystems Institute will be considered for joint appointments as Members of the California NanoSystems Institute. Candidates are sought who give evidence of unusual distinction in scholarship and teaching. Curriculum vitae, three letters of recommendation, and brief summaries of research interests should be submitted by October 31, 2007, and directed to:

Chair
Cram Chair Search Committee
Department of Chemistry and Biochemistry
University of California, Los Angeles
P.O. Box 951569
Los Angeles, CA 90095-1569
Fax: 310-206-1843

UCLA is an Equal Opportunity/Affirmative Action Employer. Women and minorities are encouraged to apply.

SYNTHETIC CHEMISTRY FACULTY POSITION at the UNIVERSITY of ARIZONA

The Department of Chemistry at the University of Arizona invites applications for a tenure-track **ASSISTANT PROFESSOR** position in synthetic chemistry beginning fall 2008. Applicants in all areas of modern synthetic chemistry will be considered, but preference will be given to candidates with interests in synthetic inorganic and organometallic chemistry, as well as interdisciplinary areas that interface with these traditional disciplines. The successful applicant will be expected to establish a vigorous, nationally competitive research program and to demonstrate excellence in teaching at both the undergraduate and graduate levels. A Ph.D. in chemistry or a related field is required; postdoctoral experience is preferred. Applicants are encouraged to apply via the University of Arizona Human Resources **website: http://www.uacareertrack.com** (job number 38811). Submit curriculum vitae, a list of publications, and statements of research and teaching interests via the online system. Three letters of recommendation to support your application should be sent to: **Chair, Synthetic Search Committee, Department of Chemistry, University of Arizona, 1306 E. University, Tucson, AZ 85721, e-mail: syntheticsearch@u.arizona.edu.** Review of applicant files will begin October 1, 2007, and will continue until the position is filled. *The University of Arizona is an Equal Employment Opportunity/Affirmative Action Employer. Women and Persons with Disabilities/Veterans. Women and minorities are especially encouraged to apply. The Immigration Reform and Control Act requires proof of authorization to work in the United States upon employment.*

PHYSICAL CHEMISTRY FACULTY POSITION
University of California, Los Angeles (UCLA)

The Department of Chemistry and Biochemistry of the University of California, Los Angeles, intends to make a tenure-track faculty appointment in physical chemistry. The search is open to both **JUNIOR and SENIOR LEVEL** candidates and all areas will be considered, including both experimental and theoretical physical chemistry, biophysical chemistry, and materials. Candidates must give evidence of exceptional promise (for a junior appointment) or great distinction (for a senior appointment) in research and teaching. Applications should include curriculum vitae, a statement of research accomplishments and description of proposed research (not exceeding four pages), reprints of representative publications, and a list of professional references. Junior faculty applicants should arrange to have three letters of recommendation sent at the time of application. To assure consideration, all application materials should be received by October 31, 2007, and directed to:

Chair
Physical Chemistry Search Committee
Department of Chemistry and Biochemistry
University of California, Los Angeles
P.O. Box 951569
Los Angeles, CA 90095-1569
Fax: 310-206-8010

UCLA is an Equal Opportunity/Affirmative Action Employer. Women and minorities are encouraged to apply.

POSTDOCTORAL POSITION is available at the University of Nebraska, Lincoln in the area of redox biology/biochemistry/bioinformatics with emphasis on mechanisms of redox regulation, functional characterization of selenium-containing proteins, bioinformatics and functional genomics of thiol-dependent redox proteins and processes, and their roles in cancer and aging. Additional information is at website: http://genomics.unl.edu/gladyshev. To apply, send curriculum vitae, cover letter of interest and names of three references to **Vadim Gladyshev** at e-mail: vgladyshev1@unl.edu. *The University of Nebraska, Lincoln is an Equal Opportunity, Affirmative Action Employer.*

UNIVERSITY OF WASHINGTON

MANAGING DIRECTOR
Catalysis Center at the University of Washington (Seattle)

The NSF-funded Center for Enabling New Technologies in Catalysis (CENTC) seeks a Managing Director. The Managing Director will be a staff member at University of Washington (UW), based in Seattle. The Managing Director will be the primary Manager and Administrator of this large, technically complex, and continuously evolving Center. Full details of the position will be found at **website: http://www.washington.edu/jobs,** select Staff Jobs and search for Requisition #34179). Priority may be given to applications received by October 1, 2007. Please direct e-mail inquiries to **e-mail: rothen@chem.washington.edu.** *CENTC and UW are committed to building a culturally diverse staff and strongly encourage applications from female and minority candidates. Affirmative Action/Equal Opportunity Employer.*

BIOCHEMISTRY and MOLECULAR BIOLOGY FACULTY POSITION
University of California, Los Angeles (UCLA)

The Biochemistry Division of the Department of Chemistry and Biochemistry (**website: http://www.biochemistry.ucla.edu**), in conjunction with the Molecular Biology Institute, is seeking applications for a tenure-track faculty position at the **ASSISTANT PROFESSOR** level. We invite outstanding candidates in any area of biochemistry, chemical biology, computational biology, or molecular and cellular biology. The new faculty member will be expected to develop a strong and creative research program and contribute to teaching in biochemistry.

Applications should include curriculum vitae, a summary of research accomplishments and future research plans, and two to three reprints of representative publications. Applicants should also arrange to have three letters of reference sent to the address below. To assure consideration, all application materials and letters should be received by October 15, 2007. Please do not send applications by e-mail.

All application materials should be sent to: **Chair, Biochemistry Search Committee, c/o Penny Jennings, Department of Chemistry and Biochemistry, UCLA, P.O. Box 951569, Los Angeles, CA 90095-1569.**

The University of California is an Equal Opportunity/Affirmative Action Employer. Women and minorities are encouraged to apply.

NATIONAL UNIVERSITY of SINGAPORE
Department of Chemical and Biomolecular Engineering

The Department of Chemical and Biomolecular Engineering at National University of Singapore invites applications for **TENURE TRACK FACULTY POSITIONS** at all levels. The Department is one of the largest internationally with excellent in-house infrastructure for experimental and computational research. A Ph.D. in chemical engineering or related areas and a strong research record with excellent publications are required. Please refer to **website: http://www.chbe.nus.edu.sg/** for more information on the areas of interest and for application details. Applicants should send full curriculum vitae (including key publications), a detailed research plan, a statement of teaching interest, and a list of names of at least three references to: **Professor Raj Rajagopalan, Head of Department (attention: Ms. Nancy Chia, e-mail: nancychia@nus.edu.sg).**

Vice President, Biology

R&D China

GSK R&D Shanghai will focus on research into neurodegeneration with the objective of creating new medicines for such severe disorders as multiple sclerosis, Parkinson's disease, and Alzheimer's disease. The site will eventually direct our global discovery and development activities within its therapeutic area, from drug-target identification to late-stage clinical studies, while collaborating with research institutions elsewhere in China and other countries.

We are seeking a PhD educated biologist who is a proven strategic thinker with an established track record (to Proof of Concept) in the development of novel therapeutic agents. It is envisaged that whilst this experience could have been gained in the broad arena of Parkinson's and Alzheimer's research or related fields, the candidate must be recognised as an expert in their field and demonstrate a depth of biology and chemistry understanding commensurate with this influential position. The ability to speak Mandarin would be advantageous in the role together with familiarity of Chinese culture and the willingness to make a long term commitment to live and work in Shanghai.

The candidate will be able to demonstrate strong leadership, visionary skills, determination to succeed and the ability to influence senior management groups, Chemistry, PreClinical and Clinical colleagues to drive both direction and strategy of Biology within the overall strategy of R&D Shanghai. You will have experience in leading/managing large and complex organisations and of being an effective leader in a matrix setting. Proven ability to build and manage an empowered organisation that allows staff to realise their full potential, attract, retain and develop highly talented and diverse contributors.

This role offers an outstanding opportunity to be involved in the first fully integrated R&D facility in Shanghai at its onset, to build a substantial R&D team which is envisaged to be 150 dedicated scientists by the end of 2008. The vision of GSK is unique as the facility will be a Chinese dedicated site for neurodegeneration with full accountability from target to the global healthcare market.

To apply online, please visit www.gsk.com and view vacancies on the UK careers page entering requisition number 44515 in the "Req ID" search box. Alternatively please email your CV and covering letter to RD.ChinaRecruit@gsk.com

Together we can make life better

GSK is proud to promote an open culture encouraging people to be themselves and giving their ideas a chance to flourish. GSK is an equal opportunity employer.

GlaxoSmithKline

HUMAN GENETICIST
Tenure-Track/Tenure Position

The newly formed intramural Laboratory of Translational Genomics (LTG) in the Division of Cancer Epidemiology and Genetics (DCEG), National Cancer Institute (NCI), National Institutes of Health (NIH), Department of Health and Human Services (DHHS), is recruiting two tenure-track/tenured investigators. The mission of the LTG is to investigate the genetic basis of strong association signals identified by candidate gene approaches, linkage analyses in high-risk families, or genome-wide association studies (GWAS), particularly loci identified by the ongoing Cancer Genetic Markers of Susceptibility (CGEMS) program involving GWAS of several major cancers. Investigators in the LTG are expected to develop an independent research portfolio in cancer genomics focused on (1) fine mapping and re-sequencing of loci relevant to cancer susceptibility and/or outcomes, (2) investigation into the causal gene variants that provide biological plausibility for each locus, and (3) bioinformatic analyses of publicly available datasets derived from germline annotation of genetic variation and somatic alterations in cancers. Each investigator is expected to leverage the NCI resources in molecular epidemiology, high-throughput genotyping and whole genome scans, biostatistics and bioinformatics, as well as in basic and clinical sciences. The incumbent will receive research support for developing a state-of-the-art genomics laboratory, and recruiting two post-doctoral fellows, bioinformaticians and a technician.

Applicants must have an M.D. and/or Ph.D. in a relevant field, extensive post-doctoral experience, and a record of publications demonstrating potential for creative independent research in human cancer genetics. Faculty with bioinformatics databases and high dimensional data are highly desirable along with strong communication skills. Interested individuals should send a cover letter, curriculum vitae and a brief summary of research accomplishments and goals, along with copies of three to five publications or preprints, and three letters of reference to:

Ms. Judy Schwadron, Division of Cancer Epidemiology and Genetics, National Cancer Institute, 6120 Executive Blvd. EPS/8073, Bethesda, MD 20892

Recommendations can be included with the package or sent directly by the recommender to Ms. Schwadron. Candidates should submit applications by **October 15, 2007** at this time, the committee will begin to look at suitable candidates. However, the search will continue until qualified scientists are found. Additional information about staff and ongoing research in the NCI Division of Cancer Epidemiology and Genetics is available at **http://www.dceg.cancer.gov**. Please contact **Dr. Stephen Chanock (phone 301-435-7559 at chanocks@mail.nih.gov) or Dr. Peggy Tucker (phone 301-496-8031 at tuckerp@mail.nih.gov)** for questions about the position(s).

Executive Functions Program

The National Institute of Mental Health, National Institutes of Health, Department of Health and Human Services, announces an opening for a Health Sciences Administrator (sometimes referred to as a program officer) at its Rockville, MD site to guide and manage a grants program supporting basic research on the fundamental principles and mechanisms of executive functions in both humans and animals. Attention, cognitive control, planning, decision making, reward, risk analysis, and select aspects of learning and memory are included in the domain of responsibility. In addition, understanding of sophisticated cognitive and behavioral techniques/paradigms to properly assess brain and behavior is expected. The Program Officer will be responsible for maintaining and further developing an innovative program in this research area that includes behavioral and systems neuroscience approaches. Techniques currently employed in the research portfolio cover a wide range, and include but are not limited to: functional neuroimaging (PET, fMRI, EEG, DTI, MEG, fMRI), invasive electrophysiology (LFP, single and multiple unit recording), microdialysis, reversible and irreversible lesions, neuroanatomical tracing, immunocytochemistry, selective use of genetically modified organisms, viral vectors, etc. General responsibilities will include administering and managing an extramural portfolio of research grants, interacting with researchers and program officers for related programs at NIMH, NIH, and other funding agencies, and developing new research initiatives. Candidates must be U.S. citizens and have a Ph.D., M.D., or equivalent degree. Candidates must be able to document relevant research experience in the general field of cognitive and/or systems neuroscience. The position requires working both independently and collaboratively. Strong organizational and oral and written communication skills are also required. Salary will be commensurate with experience. **Applications may be submitted beginning July 31st through September 7th, 2007. Beginning July 31st, official application instructions can be found at the USAJobs Web Site (http://www.usajobs.gov), by searching on Vacancy Announcement NIMH-07-198801-DH or NIMH-07-198801-DE.** For further information about the application process, please contact **Ms. Cindy Grippere (grippere@mail.nih.gov)** at NIH Human Resources. For more details concerning the nature of this position, please contact **Dr. Kevin Quinn (kquinn@mail.nih.gov)**. With nationwide responsibility for improving the health and well being of all Americans, the Department of Health & Human Services oversees the biomedical research programs of the National Institutes of Health (**http://www.os.dhhs.gov**).

WWW.NIH.GOV

Cell Cycle Checkpoint Signaling Mechanisms and ATM Function

NIEHS
National Institute of Environmental Health Sciences
National Institutes of Health

Research Triangle Park, North Carolina

A postdoctoral position is available to investigate signal transduction mechanisms regulating cell cycle checkpoints, with particular interest in the role of the ataxia telangiectasia mutated (ATM) gene product and ATM-interacting proteins. Studies will focus on responses to DNA damage and regulation of cell cycle progression following damage. Current research interests in our group include investigations of the role of ATM in mammary epithelial cell cycle regulation, the interplay of signaling from ATM and ATM-related kinases, as well as ATM signaling in cells from individuals with heritable cancer susceptibility syndromes. Opportunities exist for the incorporation of global gene expression analyses into studies. Candidates should have a Ph.D. or equivalent degree in molecular biology, cell biology, biochemistry or related field. While candidates with five or fewer years of relevant postdoctoral research experience are eligible, recent graduates are encouraged to apply.

TO APPLY: Submit a cover letter, curriculum vitae, bibliography and the names of three references to:

Richard S. Paules, Ph.D.
National Institute of Environmental Health Sciences
Growth Control and Cancer Group
P.O. Box 12233, MD 02-03
Research Triangle Park, NC 27709
FAX: (919) 316-4771
E-mail: paules@niehs.nih.gov

NIEHS and NIH are Equal Opportunity Employers

Technical Laboratory Manager

NIEHS
National Institute of Environmental Health Sciences
National Institutes of Health

Research Triangle Park, North Carolina

Laboratory of Molecular Toxicology – NIEHS Microarray Group

If you would like to work with accomplished scientists in support of environmental health research AND you are skilled in the technical and scientific aspects of microarray technologies, then consider joining the Division of Intramural Research (DIR) at the National Institute of Environmental Health Sciences (NIEHS). NIEHS, a major research component of the National Institutes of Health, is looking for someone who will support an efficient and productive scientific environment and who will work with the Microarray Group Director to provide genomics capabilities to scientists. The research efforts of the NIEHS Microarray Group are designed to apply genomic technologies to elucidate the mechanisms of injury and disease from environmental exposures and to pursue the technical aspects of emerging genomic technologies.

As the Technical Laboratory Manager (Research) for the Microarray Group in the Laboratory of Molecular Toxicology, you will interact closely with scientists from the intramural NIEHS community and extramural collaborators conducting research in microarray-based genomic technologies. You will be relied upon to provide technical and scientific expertise in specialized core areas such as basic research studies, protocol development and coordination, technology transfer, procurement activities, and budget formulation and execution. You will also provide major direction in standard core areas related to resources, management of equipment and personnel, data entry and data compilation. You will lead the technical team in the performance of their duties and have overall day-to-day responsibility for the efficient management and use of laboratory resources as well as other responsibilities as assigned by the Group Director.

Interested candidates should apply online at **www.USAJOBS.gov**. Announcement Number NHSNIH-2007-0438 by **September 7, 2007**. For additional information concerning the position, contact Angela Heard, Office of Human Resources, at hearda@mail.nih.gov or fax 919-541-3026. Applications from women, minorities, and persons with disabilities are strongly encouraged.

NIEHS and NIH are Equal Opportunity Employers

TENURE TRACK POSITION
LABORATORY OF MOLECULAR BIOLOGY

The Laboratory of Molecular Biology (LMB), Center for Cancer Research, of the National Cancer Institute, National Institutes of Health (http://ccr.cancer.gov/labs/lab.asp?labid=99) uses genetics, molecular biology, cell biology, and molecular modeling to examine and solve a broad range of important biological problems. The Laboratory now invites applications for a tenure track position in the Laboratory of Molecular Biology, CCR, NCI for a scientist working in the field of antibody engineering as it relates to cancer therapy. Candidates must have a Ph.D. or M.D. and a proven record of innovative research and productivity in antibody engineering, display of antibody fragments on phage and mammalian cells and cancer therapeutics. The successful candidate will join an active group of translational and clinical investigators in the LMB working on immunotoxins, humanized antibodies, and toxin biology and carrying out clinical trials with immunotoxins and antibodies. Salary will be commensurate with education and experience. *A two-page statement of research interests and goals should be submitted in addition to three letters of recommendation and a curriculum vitae* to **Mrs. Ann Schombert, Executive Secretary, Laboratory of Molecular Biology, CCR, NCI, Building 37, Room 5106, Bethesda, MD 20892-4264, phone: 301-451-8714, Fax: 301-402-1344, email: schombera@mail.nih.gov**. NIH Tenure track investigators with educational debts may be eligible for the NIH Loan Repayment Program. The NCI is an Equal Opportunity Employer. The closing date for applications to be accepted is **September 15, 2007**.

Postdoctoral, Research and Clinical Fellowships at the National Institutes of Health

www.training.nih.gov/pdopenings

www.training.nih.gov/clinopenings

Train at the bench, the bedside, or both

Office of Intramural Training and Education
Bethesda, Maryland 20892-0240
800 - 5 8283

Head, Department of Cellular Biology and Anatomy
Louisiana State University Health Sciences Center in Shreveport

The School of Medicine at LSU Health Sciences Center in Shreveport is seeking applicants for Head of the Department of Cellular Biology and Anatomy from world-class researchers in cardiovascular sciences with an interest in developing a nationally competitive program. Investigators having research interests in the area of cardiovascular complications of metabolic syndrome and diabetes are particularly encouraged to apply.

The salary for this tenured position is fully supported by state funds, with additional compensation possible through an institutional research incentive compensation plan. The position also comes with a $2 million Endowed Chair from the Malcolm Feist Cardiovascular endowment. The new Department Head will receive a generous seed package to support his/her research program and state-of-the art laboratory space. A multi-year strategy and supporting financial resources are in place to substantially enhance the national stature of research and training programs in the Department. This includes the state-funded salary lines, research space, and seed package support to recruit 6 faculty members. In addition, $1 million will be provided to expand the research infrastructure of the Department to complement the new emphasis on cardiovascular sciences.

Successful candidates should have a graduate degree (Ph.D. and/or M.D.), current NIH funding, an outstanding record of achievement in cardiovascular research, and experience mentoring graduate students, postdoctoral fellows, and junior faculty. The responsibilities of the position include development and leadership in departmental Ph.D. and postdoctoral training programs, research activities, and multidisciplinary research endeavors as well as a commitment to maintain strengthen the education obligations of the Department.

The LSU Health Sciences Center-Shreveport, established in 1969, is located in northwest Louisiana and is one of the fastest developing regions within the state. The Shreveport-Bossier City area, with a population of ~325,000, has evolved into a major regional cultural and recreational center, and is in short driving distance to larger metroplexes such as the Dallas-Fort Worth and Houston areas.

Interested applicants and nominations should include a curriculum vitae and a letter of interest. Correspondence should be directed to: **Nicholas Goeders, Ph.D., Professor and Head, Department of Pharmacology, Toxicology and Neuroscience, LSU Health Sciences Center, P.O. Box 33932, Shreveport, LA 71130**. Applications will be accepted by mail or via e-mail (**ngoede@lsuhsc.edu**) until **September 30, 2007**.

LSUHSC is an Affirmative Action Employer

MASSACHUSETTS GENERAL HOSPITAL HARVARD STEM CELL INSTITUTE

The Center for Regenerative Medicine (CRM) at Massachusetts General Hospital invites applications for a tenure-track assistant professor position. Outstanding scientists in the field of stem cell biology who have the demonstrated ability to develop a strong, independent research program will be considered. Successful candidate(s) will be members of the Harvard Stem Cell Institute and faculty of Harvard University. Candidates must hold a PhD and or MD and have a history of innovative, interactive research. Applicants should send an electronic copy of (1) letter of interest (2) research plan and (3) current curriculum vitae to **Dr David Scadden c/o Chris Shambaugh cpasker@partners.org.** Three letters of recommendation should also be sent directly to:

Center for Regenerative Medicine
Search Committee
Attention: Chris Shambaugh
Massachusetts General Hospital
185 Cambridge St., CPZN 4265A
Boston, MA 02114

Women and minority candidates are urged to apply. MGH is an Equal Opportunity Affirmative Action Employer

MICHIGAN STATE UNIVERSITY

Faculty Position in Breast Cancer Biology
Department of Physiology

The Department of Physiology invites applications for a full-time tenure-track appointment at the Assistant/Associate/Full-Professor level.

The successful candidate will be expected to develop an independent research program in a contemporary area of breast cancer biology. Areas of interest include but are not limited to cell or animal models of tumor formation, progression, and metastasis, cancer genetics, breast cancer pathogenesis and molecular pathology, normal and cancer stem cell biology, heterotypic cell interactions in breast cancer and inflammation and breast cancer. Candidates whose experimental approaches include genomics and proteomics, inducible gene targeting in rodent models, as well as live cell or whole animal imaging are especially encouraged to apply.

The successful candidate will join a collegial and highly interactive group of breast cancer investigators whose interests include mammary development, steroid hormones and hormone resistance, cell signaling and cell cycle control, regulation of gene expression, and environmental factors in breast cancer etiology. Opportunities exist to participate in collaborative projects, including a NIEHS/NCI sponsored Research Center on Breast Cancer and the Environment. Candidates must hold a Ph.D., M.D., or equivalent doctoral or professional degree, have postdoctoral experience and be able to demonstrate the potential to develop a vigorous externally funded research program. The successful candidate will be expected to participate in the teaching of graduate and/or professional students.

Interested individuals should submit a complete curriculum vita, a brief statement of research interests, and copies of key publications. Applicants should also request letters of recommendation from three individuals who can evaluate their accomplishments and future potential for research and teaching. Review of applications will begin August 31, 2007 and continue until the position is filled.

Applications should be sent electronically to: **Chair, Breast Cancer Search Committee, Professor Sandra Z. Haslam, Director, Breast Cancer and the Environment Research Center, Department of Physiology, Michigan State University, East Lansing, MI 48824-3320. E-mail: pslofl@msu.edu.**

Michigan State University is committed to achieving excellence through cultural diversity. The university actively encourages applications and/or nominations from women, persons of color, veterans and persons with disabilities.

MSU IS AN AFFIRMATIVE ACTION, EQUAL OPPORTUNITY EMPLOYER.

Two Full Professor Positions at Institute of Development, Aging and Cancer, Tohoku University, Sendai, Japan
http://www.idac.tohoku.ac.jp

The Institute of Development, Aging and Cancer, Tohoku University invites applications for two positions of full professor in the fields of basic medical sciences. We welcome scientists who are motivated in frontier and interdisciplinary research areas to explore a new field of aging, longevity, host defense and their related areas. We also encourage women and foreigners to apply.

The institute, originally founded in 1941, promotes basic and clinical studies on age-related diseases including cancer and degenerative brain diseases. The institute also participates in training programs for PhD and masters students.

Applications should include a CV, a publication list, reprints of major publications (less than 10 papers), summary of scientific activities including future research plans in about 1,000 words, a list of scientific grants awarded, and two recommendation letters. Applications should be submitted via business mail by Oct. 1, 2007 to:

Dr. Hiroshi Fukuda
Director, Institute of Development, Aging and Cancer, Tohoku University
Seiryo-machi 4-1, Aoba-ku Sendai 980-8575, JAPAN

Inquiry to: ida-som@bureau.tohoku.ac.jp

Department of Health and Human Services
National Institutes of Health
National Human Genome Research Institute

CHIEF OF STAFF, IMMEDIATE OFFICE OF THE DIRECTOR

The National Human Genome Research Institute (NHGRI), a major research component of the National Institutes of Health (NIH) and the Department of Health and Human Services (DHHS), has led the groundbreaking enterprise known as the Human Genome Project and is now vigorously exploring the application of advances in genome research to human health. The NHGRI is inviting applications for the career Federal position of Chief of Staff in the immediate Office of the Director, NHGRI. The incumbent will serve as a senior advisor and the Chief of Staff, managing and directing the scientific and administrative activities and priority setting for all tasks occurring within the immediate Office of the Director. The Chief of Staff will have advanced scientific training and maintain an active knowledge of advances in the fields of genetics and genomics and the application of such research to health and disease. Responsibilities will encompass substantive program and policy matters covering the full range of NHGRI's interests and program activities and directing the efficient planning and coordination of operations and staff within the immediate Office of the Director. The NHGRI vacancy announcement for this position contains complex application procedures and lists all mandatory information which must be submitted with your application. To obtain the vacancy announcement for this position, it will be available on **http://www.usajobs.gov** and posted under announcement **#NHGRI-07-203295-CR-DE** or **NHGRI-07-103295-CR-MP** you may also visit the NIH website at: **www.jobs.nih.gov**. Applications must be received no later than **August 24, 2007**.

This is a full-time permanent position offering benefits including health and life insurance, retirement, sick and annual leave. U.S. citizenship is required.

DHHS and NIH are Equal Opportunity Employers

Lecturer/Senior Lecturer in Ecology

Institute of Natural Resources

Auckland

You will lecture in Ecology and will be a member of a multi-disciplinary team teaching and researching ecological issues of national and international importance.

Closing date 26 August 2007

Reference number A217-07L

For further information and to apply online, visit:

http://jobs.massey.ac.nz

www.massey.ac.nz

Massey University

Burnet Institute

Austin Research Institute

Joining together for a healthier world

DIRECTOR

The Burnet Institute, one of Australia's leading infectious diseases, immunology and public health institutes, is seeking to appoint an inspirational leader as Director. This person will possess an international reputation as a researcher and research manager, commanding the respect of peers. The Director will lead the Institute during a growth phase to enhance the Institute's reputation as a significant international research organisation translating discovery to health outcomes. This will require the further development of strategic relationships, collaborative partnerships and commercial ventures.

For a confidential discussion, to find out more about this challenging leadership role and to acquire an information package including selection criteria contact Dr Rachel Lucas or Ms Evie Watt at Heidrick & Struggles, on +61 2 8205 2000 or the Chairman of the Burnet Institute, Mr Alastair Lucas on +61 3 9679 1356 or +61 419 885 594.

Applications including curriculum vitae should be sent in confidence to Dr Rachel Lucas at Heidrick & Struggles, Level 28, 1 Farrer Place, Sydney, NSW 2000, Australia, or email burnetdirector@heidrick.com by 7 September 2007.

For further information on the Burnet visit the following website: http://www.burnet.edu.au/home

GSH751484

CASE WESTERN RESERVE UNIVERSITY
SCHOOL OF MEDICINE

University Hospitals Case Medical Center

Research Faculty Positions in Visual Sciences

The Department of Ophthalmology and Visual Sciences of Case Western Reserve University invites applications for appointments at the junior to senior level ranks to complement the existing major programs include: Immunology and Infectious Diseases, Aging and Diabetes, Molecular Genetics and Retinal Biology. The Department is part of the multi-disciplinary Visual Sciences Research Center, comprising 40 vision researchers in 19 different basic and clinical science departments, which is supported by a P-30 Core Grant and a T-32 Training Grant from the National Eye Institute (**www.case.edu/med/vsrc**). The Core grant facilities and the Department laboratories are centrally located on two floors of newly renovated space.

Successful candidates will have a secondary appointment in a basic science department, and will be expected to participate in graduate education. Applicants should send a curriculum vitae and a one-page description of research interests as a single PDF file to **Eric.Pearlman@case.edu**

CWRU and University Hospitals Case Medical Center are Equal Opportunity Affirmative Action Employers

THE UNIVERSITY of WISCONSIN MADISON

Faculty Position in Systems Neuroscience

The Department of Physiology, University of Wisconsin School of Medicine and Public Health, invites applications for a tenure-track assistant professor position in systems neuroscience. Successful candidates will have outstanding research credentials with interests that complement and extend existing research in the Department (**http://www.physiology.wisc.edu**). We are committed to a strong focus in integrative physiology and especially encourage applications from individuals who study any area of systems neuroscience, broadly construed to include topics such as cognition, perception, action, attention, executive function, and memory. Successful candidates will teach in Departmental courses in undergraduate or medical physiology and participate in Ph.D. and post-doctoral training. The Department features a breadth of inquiry encompassing molecular to systems level research and offers a supportive collegial work environment, and a commitment to collaborative research programs. Excellent opportunities for participation in campus-wide interdisciplinary research and training programs exist. Recruits will participate in faculty governance and service at the department, school and university levels as appropriate to faculty rank.

Interested individuals should submit curriculum vitae, a one to two page summary of research interests and plans, and three letters of reference to **University of Wisconsin–Madison, Department of Physiology, Faculty Search Committee #55370, c/o Alice Puchalski, 1300 University Avenue, Madison, WI 53706**, or electronically to **neuroresearch@physiology.wisc.edu**. To ensure consideration, please submit complete application by **October 4, 2007**. However, applications will be accepted until the position is filled. Unless confidentiality is requested in writing, information regarding applicants and nominees must be released upon request. Finalists cannot be guaranteed confidentiality.

The UW Madison is an Equal Opportunity/Affirmative Action Employer. We promote excellence through diversity and encourage all qualified individuals to apply.

MICHIGAN STATE UNIVERSITY

MSU-DOE PLANT RESEARCH LABORATORY

Michigan State University
East Lansing, MI 48824
http://www.prl.msu.edu

Faculty Position in Plant Biology

The MSU-DOE Plant Research Laboratory (PRL) has a twelve-month tenure-track faculty position available at the Assistant Professor level. We seek to identify individuals who investigate fundamental questions in plant biology that fall in the continuum between photon capture and the deposition of energy-rich molecules, or plant-environment interactions that influence these processes.

The PRL, with core funding from the U.S. Department of Energy, provides an excellent environment for creative research in plant biology. Michigan State University has a history of exceptional breadth and depth in the plant sciences and provides a stimulating atmosphere with excellent colleagues and facilities. PRL faculty members are jointly appointed in an appropriate academic department.

Applicants should have postdoctoral research experience with demonstrated productivity and evidence of potential for independent research. To assure consideration, applications should be submitted electronically to **prlsrch@msu.edu** by **October 1, 2007**. Applications should include curriculum vitae, a summary of research accomplishments, and a brief description of future plans. Candidates should also arrange to have three letters of reference submitted. Questions regarding this position should be directed to **prlsrch@msu.edu**

Michigan State University is an Affirmative Action, Equal Opportunity Employer. MSU is committed to achieving excellence through cultural diversity. The university actively encourages applications and/or nominations of women, persons of color, veterans, and persons with disabilities.

Two Tenure-Track Faculty Positions in Marine Science

The University of Texas at Austin Department of Marine Science and Marine Science Institute invite applications for two faculty positions in marine science. We seek candidates with demonstrated expertise and innovative research in: (1) **Quantitative Ecology**, with a focus on contemporary issues in landscape ecology, benthic-pelagic coupling, conservation biology, or population biology, and (2) **Fish Ecology** in areas that complement our existing strengths in physiology, larval studies, and basic mariculture. The most competitive candidates will make use of the Institute's excellent facilities for experimental work (including 36,000 sq. ft. of mariculture facilities) and proximity to a variety of estuarine and coastal habitats (including the 185,000-acre Mission-Aransas National Estuarine Research Reserve). Candidates must have a Ph.D. degree at the time of appointment and a strong research and publication record. Postdoctoral experience is strongly preferred. The positions, based at the Marine Science Institute (**www.utmsi.utexas.edu**) in Port Aransas, TX, include 9 months of annual salary support. Faculty are expected to maintain a vigorous, externally funded research program, teach graduate and undergraduate courses, and mentor M.S. and Ph.D. students.

Applicants should send an application as a PDF file to **facsearch@utmsi.utexas.edu** and have at least three letters of recommendation mailed to: **Search Committee Chair, The University of Texas Marine Science Institute, 750 Channel View Dr., Port Aransas, Texas 78373-5015**. The application should identify the position of interest and contain a curriculum vitae and a statement of research interests that indicates how the applicant's research activities would take advantage of the Institute's facilities and location (3 pages maximum). Review of applications will start **October 1, 2007**, and will continue until the positions are filled. State law requires a background check on the selected applicant.

The University of Texas at Austin values diversity and is committed to affirmative action and equal opportunity. Women and minorities are encouraged to apply. UT Austin will make every effort to accommodate professional couples.

The Department of Pharmacology & Experimental Therapeutics at Boston University School of Medicine (http://www.bumc.bu.edu/busm/pm) has open faculty positions at the Assistant, Associate or Full Professor levels. Individuals with an interest in neuropharmacology, translational neuroscience, or with research programs bridging to disciplines such as cancer or cardiovascular pharmacology are especially encouraged to apply.

The Department has strengths in a broad range of research areas including gene therapy, learning and memory, neuropeptides, substance abuse, neurodegenerative diseases, neuroinflammation, anxiety, and epilepsy. The Department administers an active university-wide pharmacological sciences training program in Biomolecular Pharmacology that is supported by an NIGMS T32 and awards a combined PhD in Pharmacology-Biomedical Neuroscience or Pharmacology-Cell & Molecular Biology.

Please send a CV, description of future research, and up to three peer-reviewed publications to: **David H. Farb, Ph.D., Chairman, Department of Pharmacology & Experimental Therapeutics, Boston University School of Medicine, 715 Albany Street, L-603, Boston, MA 02118**

An Equal Opportunity/Affirmative Action Employer

U.S. Department of Energy
Office of Science
Deputy for Programs
Announcement #SES-SC-HQ-013 (kd)

The U.S. Department of Energy's (DOE) Office of Science is seeking highly qualified candidates with outstanding scientific achievements to fill the Deputy for Programs position. The Office of Science is the single largest supporter of basic research in the physical sciences in the United States, with a 2007 budget of $3.8 billion. It oversees the Nation's research programs in high-energy and nuclear physics, basic and fusion energy sciences, and biological, environmental and computational sciences. The Office of Science is the Federal Government's largest single funder of materials and chemical sciences, and it supports unique and vital parts of U.S. research in climate change, geophysics, genomics, life sciences, and science education. The Office of Science also manages 10 world-class laboratories and oversees the construction and operation of some of the Nation's most advanced R&D user facilities, located at national laboratories and universities. These include particle and nuclear physics accelerators, synchrotron light sources, nanoscale science research centers, neutron scattering facilities, bio-energy research centers, supercomputers and high-speed computer networks. More information on the Office of Science can be found at **http://science.doe.gov**

The Deputy for Programs provides scientific and management oversight of the six program offices by ensuring program activities are strategically conceived and executed; formulating and defending the Office of Science budget request; establishing policies, plans, and procedures related to the management of the program offices; ensuring the research portfolio is integrated across the program offices with other DOE program offices and other Federal agencies; and representing the organization and making commitments for the Department in discussions and meetings with high-level government and private sector officials. The position is within the ranks of the U.S. government's Senior Executive Service (SES); members of the SES serve in key positions just below the top Presidential appointees.

To apply for this position, please see the announcement and application instructions at **http://jobsearch.usajobs.opm.gov/ses.asp** under the vacancy announcement of **#SES-SC-HQ-013 (kd)**. Qualified candidates are asked to submit their online applications by **August 29, 2007**.

VICE PRESIDENT FOR RESEARCH

NEW ENGLAND

The University of New England (UNE), a private comprehensive institution, seeks an innovative and experienced leader to serve as its new Vice President for Research. UNE has established a research focus in selected fields of health, marine, pharmaceutical, and natural sciences and osteopathic medicine. The Vice President for Research will spearhead the development of a research agenda and infrastructure that will guide the University to a new level of success and national prominence. The successful candidate must be skilled in managing complex programs and will possess a sound knowledge of competitive grant processes, procedures and regulations. The ability to 'lead by example' by maintaining involvement in an active extramurally funded research project is highly desirable.

For more details on this position and the application process visit **www.une.edu/hr/vacancylist.asp**.

Processing of applications will begin immediately and continue until the position is filled. Interested persons should submit a C.V. and cover letter electronically to: **Bill Allen, Human Resources Generalist, at ballen@une.edu.**

The University of New England is an Equal Opportunity / Affirmative Action Employer and welcomes female and minority candidates.

Faculty Positions
Vollum Institute and Jungers Center
Oregon Health & Science University, Portland OR

The Vollum Institute (**http://www.ohsu.edu/vollum**) and the Jungers Center in association with the Department of Neurology announce faculty openings for outstanding scientists. For the **Vollum search**, we are particularly interested in individuals with a research focus in the general areas of *molecular and cellular neuroscience, molecular genetics, development and/or mechanisms of signal transduction*. For the **Jungers search**, we are interested in individuals whose work addresses *neurological diseases, especially the fundamental causes and treatments of neural injury and neurodegeneration as well as mechanisms of neural repair and regeneration*. Laboratory space is available in the Vollum Institute and the adjoining new Biomedical Research Building (**http://www.ohsu.edu/ohsuedu/about/transformation/brb**). It is expected that Jungers faculty will hold appointments in the Vollum Institute and the Department of Neurology. Vollum and Jungers appointments are full-time research positions with minimal teaching or clinical requirements. Ample opportunities are available for collaboration with clinical units within the School of Medicine as well as research units at OHSU (**www.ohsu.edu**).

Applications will be considered at all levels. We offer attractive start-up packages and the opportunity to work in an outstanding scientific environment. Applicants should have a strong record of research and an interest in training graduate students. OHSU is an equal opportunity/affirmative action employer committed to maintaining diversity in its faculty. Candidates with a Ph.D. and/or M.D. and at least several years of postdoctoral experience should apply by sending one paper copy and an electronic copy, of their curriculum vitae, a description of research plans and goals, and three references by **November 1, 2007** to:

Gary L. Westbrook, M.D.
Senior Scientist and Co-Director
Vollum Institute and Jungers Center Search
Vollum Institute, L474
Oregon Health & Science University
3181 SW Sam Jackson Park Road
Portland, OR 97239-3098
volljob@ohsu.edu

OREGON HEALTH & SCIENCE UNIVERSITY

U.S. Department of Energy
Associate Director
Office of Science for
Biological and Environmental Research
Announcement # SES-SC-HQ-014 (kd)

The U.S. Department of Energy's (DOE's) Office of Science is seeking qualified candidates to lead its Biological and Environmental Research (BER) Program. With an annual budget of more than $500 million, the BER Program is the nation's leading program devoted to applications of biology to bio-energy production and use and to environmental remediation. The BER Program supports major research programs in genomics, proteomics, systems biology, and environmental remediation. The Program is also one of the nation's leading contributors to understanding the effects of greenhouse gas emissions, aerosols, and atmospheric particulates on global climate change.

The Director of Biological and Environmental Research is responsible for all strategic program planning in the BER Program, budget formulation and execution, management of the BER office including a federal workforce of more than 70 technical and administrative staff; program integration with other Office of Science activities and with the DOE technology offices; and interagency integration. The position is within the ranks of the U.S. government's Senior Executive Service (SES). members of the SES serve in key positions just below the top Presidential appointees. For more information on the program please go to **http://www.sc.doe.gov/ober/**

For further information about this position and the instructions on how to apply and submit an application, please go to the following website **http://jobsearch.usajobs.opm.gov/getjob.asp?JobID=58520806&AVSDM=2007%2D06%2D06+13%3A44%3A02&Logo=0&q=SES-SC-HQ-014+(kd)&FedEmp=N&sort=rv&vw=d&brd=3876&ss=0&FedPub=Y&SUBMIT1.x=47&SUBMIT1.y=18**. To be considered for this position you must apply online. It is important that you follow the instructions as stated on the announcement **SES-SC-HQ-014 (kd)** located at the website above.

The Wonder of Discovery

Neurocrine Biosciences, Inc., a top-tier biotech company, offers a robust and diversified product pipeline. Our dedicated team of scientists are motivated and poised to bring novel drugs and innovative new treatments through development as rapidly as possible. Neurocrine's strong foundation is built upon great science that starts with great people.

SCIENTIST
(In Vitro Pharmacology)

We are seeking a dynamic, flexible and highly motivated individual with experience in the area of GPCR and/or ion channel biology to join our Research Discovery Group in Neuroscience. As a member of the Neuroscience team, you will be responsible for the design, development, validation and implementation of quantitative in vitro pharmacological assays in support of small molecule drug discovery and lead optimization programs (e.g. binding affinity, cAMP, GTPgamS, calcium imaging). You will be expected to apply these assays to provide rapid and high-quality mechanistic analysis of small molecule drug leads directed against targets in a variety of Neuroscience therapeutic areas. You will also be responsible for interpreting the data and communicating results to members of multidisciplinary drug discovery teams on a regular basis.

Requirements include a Ph.D. in Pharmacology or a related discipline and at least 2 years of postdoctoral experience, preferably in the pharmaceutical industry. Practical experience with a broad range of molecular, cellular, biological or pharmacological techniques ideal. Candidate must be proficient in the use of appropriate data analysis and statistical methodologies and have a proven track record of quality publications and presentations at scientific meetings. Candidate will be expected to work collaboratively with scientists within Neuroscience and other disciplines, and, accordingly, must possess exceptional communication, interpersonal and organizational skills.

To find out more about this exciting opportunity and to apply online, please visit **www.neurocrine.com**. EOE

Neurocrine
Biosciences
Great Science is Our First Priority.

FACULTY POSITION
BIOCHEMISTRY
University of Connecticut, Storrs

The Department of Molecular and Cell Biology at the University of Connecticut invites applications for a tenure-track position at the **ASSISTANT PROFESSOR** level in Biochemistry beginning Fall 2008. The successful candidate will establish a vigorous, extramurally funded research program and will contribute to undergraduate and graduate biochemistry teaching. Research should address significant problems in biochemistry and complement existing strengths in protein export, membrane protein biochemistry, assembly of protein complexes or plant biochemistry. UConn has a strong biochemistry research program (**www.biochemistry.uconn.edu**), as well as a multi-departmental partnership in structural biology (**www.sb.uconn.edu**).

Qualifications: A Ph.D. in biochemistry or a related field; at least two years of postdoctoral experience with an outstanding research record.

Applicants should submit a *curriculum vitae*, a concise description of proposed research, a brief statement of teaching interests, and arrange to have three letters of recommendation sent to: **Biochemistry Search Committee Chair, Department of Molecular and Cell Biology, U-3125, University of Connecticut, Storrs, CT 06269**. Review of applications will begin after publication of this notice and continue until the position is filled.

We encourage members of underrepresented groups including minorities, women, and people with disabilities to apply.

TWO FACULTY POSITIONS
in GENETICS
Department of Molecular and Cell Biology
University of Connecticut

The Genetics and Genomics group of the Department of Molecular and Cell Biology is seeking to appoint **TWO TENURE-TRACK** faculty positions **(one Assistant Professor and one Assistant Associate Professor)** in eukaryote genetics beginning August 2008. Our faculty has interests in developmental genetics, genome evolution, chromosome structure and function, and population, functional and comparative genomics. The ideal candidate will utilize a combination of experimental and computational genomics approaches to address important biological problems in one of these broad areas. Successful candidates will develop an independent research program and participate in the undergraduate and graduate genetics curriculum. The Genetics Field of Study web page is at **http://www.genetics.uconn.edu**. **Qualifications:** a completed Ph.D. in a related field; postdoctoral experience and an outstanding research record. Salary and rank will be determined based on qualifications.

Applicants should submit a *curriculum vitae*, brief statements of research and teaching interests, and arrange to have three letters of recommendation sent to: **Michael O'Neill, Chair, Search Committee, Dept. of Molecular and Cell Biology, U-2131, University of Connecticut, Storrs, CT 06269-2131**. Review of applications will begin after publication of this notice and continue until the positions are filled.

We encourage applications from underrepresented groups including minorities, women, and people with disabilities.

ANIMAL DEVELOPMENTAL BIOLOGIST

The **Department of Biological Sciences at SUNY Brockport** requests applications for a tenure track position at the rank of Assistant Professor starting Fall 2008. The successful candidate will teach an upper-division course in developmental biology and appropriate undergraduate and graduate (M.S. level) courses in his or her area of expertise, and contribute to the teaching mission of the department. The candidate is also expected to develop an active research program in developmental biology, utilizing undergraduates and Master's students and to seek external funding to support the research. We are particularly interested in persons who utilize a combination of cellular, molecular, and genetic approaches in studying development. A Ph.D. is required, and post-doctoral and teaching experience are highly preferred.

Applicants should apply on line at **www.brockportrecruit.org** and submit the following information: letter of application, curriculum vitae, and statements of teaching philosophy and research plans. All positions are subject to final budgetary approval. For full consideration, completed applications should be received by **October 12, 2007**.

Affirmative Action/Equal Opportunity Employer

J. Craig Venter INSTITUTE

Department Head, Bio-Energy
Department Head, Infectious Disease

The [illegible] the public, and the policy makers. JCVI is seeking two distinguished senior scientists with rigorous research [illegible] son, experience, and energy to fill openings for Department Head of Bio-Energy and for Department Head of Infectious Disease.

JCVI is one of the largest independent research institutes in the United States with more than 500 employees. Given our breadth of scientific expertise and multidisciplinary nature of research, scientists are organized in broad research teams that most closely match the core nature of their research. The Bio-Energy Program is a growing area of investigation at the Institute with ongoing research in biohydrogen, cellulosic ethanol, microbial fuel cells, and bacterial nanowires. The Microbial Genomics and Plant Genomics groups within JCVI are working on active components related to Bio-Energy and are available to contribute to the growing Bio-Energy program. The Infectious Disease Program is a vibrant area of investigation at the institute comprising sequencing, functional genomic and proteomics activities across a broad range of microbial pathogenic agents, with much of the research [illegible]

The Department Heads will report to the Executive Vice President for Research and will be expected to [illegible]

[illegible] interests to the JCVI Career Center at www.jcvicareers.org

Tenure-track Faculty Position

The Department of Pharmacology and Bowles Center for Alcohol Studies at the University of North Carolina at Chapel Hill invites applications for a tenure-track faculty position. The faculty rank will be determined at the time of hire based on applicant qualifications. We seek candidates with research interests in neuropharmacology and alcohol studies.

Qualifications include a doctoral degree and a strong record or promise of scholarly achievement and extramural funding. Preference will be given to applicants whose expertise lies in alcohol studies. Salary is competitive and commensurate with experience. An excellent start-up package accompanies this position. The Department of Pharmacology and Center for Alcohol Studies provide an unusually rich opportunity for collegial interaction, research and graduate and post-graduate research training within the UNC School of Medicine.

Applications are encouraged from professionals of all ethnic backgrounds. Candidates should submit a curriculum vitae, a statement of current and future research plans, selected recent publications and three letters of reference to:

Chair of the Neuropharmacology Search Committee
Attn: Amy Mansfield
Bowles Center for Alcohol Studies, CB#7178
The University of North Carolina at Chapel Hill
School of Medicine
Chapel Hill, NC 27599-7178

Application deadline: Open until filled

The University of North Carolina at Chapel Hill is an Equal Opportunity/ADA Employer

Faculty Positions
Institute of Applied Biosciences

NM STATE UNIVERSITY

New Mexico State University invites applications for research-intensive faculty positions AT ANY RANK, to be associated with the newly established Institute of Applied Biosciences. Ideal candidates should demonstrate a willingness to participate in multidisciplinary research proposal development. Applicants are sought from two focus areas: synthetic biology, or emerging infectious diseases. We especially encourage applications from individuals with expertise in pathogenesis and vectors, quantitative modeling, metabolomics, proteomics, and protein engineering.

Successful candidates will have formal appointments in the Institute with tenure or tenure tracks available in one or more of the participating departments belonging to the colleges of Arts and Sciences, Agriculture, Engineering, or Health and Social Services. The candidates will also be expected to teach one course annually and to participate in other scholarly and service activities in line with NMSU's mission and goals. Opportunities are available to participate in graduate training programs sponsored by NIH and undergraduate training programs sponsored by NIH, NSF, and the Howard Hughes Medical Institute. Core facilities include the Molecular Analysis Core Laboratory, the Electron Microscopy Laboratory, and a newly completed BSL-3 facility.

In addition, NMSU collaborates with other leading research facilities, in particular the Los Alamos National Laboratory, Texas Tech Medical School, and the Fred Hutchinson Cancer Research Center. Institute faculty members are encouraged to develop strong collaborative relationships with these and other partners. Applicants should have a Ph. D. in an appropriate field and have a strong record of research productivity and research funding appropriate to rank. They should also have a commitment to mentoring undergraduate and graduate students at an institution with a diverse student body.

Additional information on the position can be found at **http://research.nmsu.edu/iab/**. Send curriculum vitae, statements of research and teaching philosophies, 3 relevant reprints and contact information for three references in a single PDF file to **iabsearch@research.nmsu.edu**. Screening of applicants will begin **September 15th, 2007** and continue until the positions are filled.

NMSU is an EEO/AA Employer

Kumamoto University

Open Recruitment of Young Researchers (1st Stage)

1. Open Recruitment of Researchers (1st stage)
Special project researchers (all given the title of "specially appointed assistant professor")
A maximum of 10 researchers

2. Qualification Requirements
(1) Academic degree, etc., Young researchers who have obtained a PhD degree within approximately the past 10 years (as of April 1, 2008)
(2) Achievements/ability Has outstanding research capabilities and/or research achievements in one of the specialty areas outlined in number 3

3. Arrival
As soon as possible between October 2007 and February 2008

4. Period of Employment
Those hired in stage 1 will be employed through March 2012
(Contracts will be for one year each and will be renewed once a year through March 31, 2012
"Employment contract is based on Article 14 of the Labour Standards Law
(Note: After having gone through career advancement evaluations and after the end of one's term of employment, it is possible for one to be promoted to the position of "Associate Professor" in the Leading Graduate School System. A total of approximately 8 people from stages 1 and 2 will be chosen for these positions.)

5. Application Deadline
Applications must reach the university by no later than September 7, 2007 (Friday)

6. Inquiries
Any inquiries should be made by e-mail to the Research Cooperation Section (person in charge of research strategy) of Kumamoto University at the e-mail address written below
k-senryaku@jimu.kumamoto-u.ac.jp

http://sendou.kuma-u.jp/
Please be sure to allow enough time before the application deadline for a response to be made to you.

Urology, TenureTrack, non-clinical

The Department of Surgery at the University of Pennsylvania's School of Medicine seeks candidates for an Assistant, Associate, and/or Full Professor position in the tenure track. Rank will be commensurate with experience. The successful applicant will have experience in the field of smooth muscle physiology pharmacology and cell molecular biology or neurourology. Responsibilities include targeted research in urothelial biology, smooth muscle physiology, interstitial cystitis and tissue and cell engineering to correct urologic disorders, as well as teaching of medical students and residents doing research rotations in the Urology laboratories. Applicants must have an M.D and/or Ph.D or equivalent degree.

This position, which will be based in the Division of Urology, will include teaching and research duties only, with no patient care responsibilities. The successful candidate will have demonstrated potential for establishing a vigorous independent research program in the cellular/molecular basis of diseases and a willingness to spend 50% or more effort in the study of urologic diseases. He or she will also have a track record of obtaining research grants.

The effective date of appointment will be January 1, 2008. Please submit curriculum vitae, a cover letter, and references to: **Alan J. Wein, MD Chief, Division of Urology, c/o Peter Atherton, Univ. of Pennsylvania Sch. of Med., 3400 Spruce St., 4029 Maloney, Philadelphia, PA 19104-4283; athertop@uphs.upenn.edu.**

The University of Pennsylvania is an Equal Opportunity, Affirmative Action Employer. Women and minority candidates are strongly encouraged to apply.

J. Craig Venter INSTITUTE

Scientist, Plant Genomics
Scientist, Infectious Disease
Scientist, Microbial & Environmental Genomics

[redacted]

[redacted]

- Successful candidates will have a PhD or equivalent in a relevant scientific [redacted]
- **JCVI offers an excellent working environment and a competitive** [redacted] **cover letter outlining research interests to the JCVI Career Center at** www.jcvi.org/jobs.

[redacted]

From physics to nutrition

For careers in science, turn to *Science*
www.ScienceCareers.org

- Search Jobs
- Career Advice
- Job Alerts
- Resume/CV Database
- Career Forum
- Graduate Programs

All features FREE to job seekers.

ScienceCareers
from the journal Science AAAS

ASU ARIZONA STATE UNIVERSITY

The Ira A. Fulton School of Engineering at Arizona State University (ASU) invites applications for the position of **DEPARTMENT CHAIR/PROFESSOR** for the Harrington Department of Bioengineering, one of nine engineering units with ties to leading research centers, liberal arts and science units at ASU, and clinical and external organizations. Deadline: September 30, 2007; if not filled, then the 15th and 30th of each month thereafter until search is closed. For qualifications and application information, refer to job #8940 at **website: http://www.fulton.asu.edu/fulton/departments/business/employment.php.** *Affirmative Action/Equal Opportunity Employer*

The Biology Department at Loyola College is offering a tenure-track **ASSISTANT PROFESSOR** position to begin in the fall of 2008. Applicant should be trained as a **PLANT BIOLOGIST** with expertise in at least one of the following areas: plant molecular biology, plant physiology, plant taxonomy or systematics, or natural history of plants. The successful candidate will teach introductory and upper level courses in biology, be engaged in research involving undergraduate students, participate in departmental and collegewide service, and will receive guidance and mentoring from members of the Department. The successful applicant will be expected to teach at the introductory level (e.g. in cell and molecular biology, organismal biology, and/or ecology, evolution and biodiversity), and also to teach upper level courses in their areas of specialization. Candidates should have a Ph.D. in biology or a related discipline. Postdoctoral training and college teaching experience are preferred.

Loyola College is a selective liberal arts, Jesuit Catholic institution that welcomes applicants from all backgrounds who can contribute to its educational mission. For more information about Loyola, please review our **website: http://www.loyola.edu/** and **website: http://www.loyola.edu./biology/**.

To apply, please apply electronically at **website: http://www.loyola.edu/careers** and include curriculum vitae, statement of teaching and research interests, a teaching philosophy, and contact information for three references. For more information please contact **Monika Matthews, Administrative Assistant to the Biology Department or Dr. Donald Keefer (e-mail: dkeefer@loyola.edu), Chair of the Search Committee.** Applications received by October 1, 2007, will receive full consideration.

Loyola College is an Equal Opportunity Employer, seeking applicants from underrepresented groups.

CORNELIA de LANGE SYNDROME (CdLS) FOUNDATION
Call for Postdoctoral Fellowship Applications

The Cornelia de Lange (CdLS) Foundation announces a Postdoctoral Fellowship to support basic or clinical research on CdLS to start July 1, 2008. CdLS is caused by genetic changes affecting NIPBL, SMC1, or SMC3 proteins involved in sister chromatid cohesion, gene expression, and DNA repair.

The Fellowship provides $60,000 per year for two years to cover salary/benefits for a young investigator who holds a Ph.D. or M.D., and who does not hold a tenure-track faculty position. Topics ranging from molecular functions of the sister chromatid cohesion apparatus in model organisms to diagnostic evaluation and therapeutic management will be considered. The Fellow will present his/her work at the Foundation's national meetings.

For requirements, see **website: http://www.cdlsusa.org/research/index.shtml.** Applications are due December 1, 2007.

POSITIONS OPEN

ASSISTANT/ASSOCIATE PROFESSORS
Bacterial/Viral Pathogenesis

As part of an ongoing recruitment to increase faculty and expand research efforts, the Department of Microbiology and Immunology at the University of Arkansas for Medical Sciences (UAMS) invites applications from qualified individuals (Ph.D., or equivalent) for two tenure-track positions. Applicants with expertise in bacterial or viral pathogenesis are especially preferred. The successful applicants will be expected to develop or expand an active extramurally funded research program, to teach in courses for professional (M.D.) and graduate students, and to participate in routine academic service duties. Competitive startup packages and laboratory space will be provided to successful candidates. Candidates seeking appointment as **ASSOCIATE PROFESSOR** must have current extramural funding and experience commensurate with rank. Additional information about UAMS and the Department of Microbiology and Immunology can be found at **website: http://www.uams.edu/mbim.** Applicants should submit curriculum vitae, statement of research interests and goals, and the names and contact information for three references to **Faculty Search Committee, Department of Microbiology and Immunology, University of Arkansas for Medical Sciences, 4301 W. Markham, Mail Slot 511, Little Rock, AR 72205.** Applications can also be sent by **e-mail: microapp@uams.edu.** Review of applications will begin September 15, 2007, and continue until positions are filled. *UAMS is an Equal Opportunity/Affirmative Action Employer and encourages applications from minorities, women, and other qualified persons.*

IMMUNOLOGY FACULTY POSITION
University of Miami Miller School of Medicine

The Department of Microbiology and Immunology invites applications for a tenure-track/ tenured faculty position at the **ASSISTANT/ASSOCIATE/FULL PROFESSOR** level with research interests in Immunology, particularly in the area of mucosal immunity. Opportunity exists to develop a strong research program and interact with ongoing programs in allergy, autoimmunity, infectious diseases, cancer immunotherapy, aging and development, and transplantation immunology. Applicants must have a Ph.D., M.D., or equivalent degree, at least three to five years of postdoctoral training, a commitment to establish/maintain an externally funded independent research program and an interest to participate in the Department's teaching efforts. Applicants who wish to be considered at the Associate/Full Professor level should have an established funded research program. A highly competitive startup package including research funds and salary support will be provided. Interested applicants should send (1) their curriculum vitae, (2) a statement describing research accomplishments and their future research goals, together with relevant reprints, and (3) the names/contact information of three references preferably by e-mail to: **Immunology Search Committee, c/o Ms. Michelle Perez, Department of Microbiology and Immunology, University of Miami Miller School of Medicine, P.O. Box 016960 (R138), Miami, FL 33101. E-mail: miperez@miami.edu.** *The University of Miami is an Equal Opportunity/Affirmative Action Employer.*

Indiana University, Bloomington and Department of Psychological and Brain Sciences seeks an outstanding faculty to lead and serve as the new **DIRECTOR** for the Imaging Research Facility (**website: http://www.indiana.edu/~imaging/**), a 100 percent research facility located within the Department of Psychological and Brain Sciences. A full position description is available at **website: http://www.indiana.edu/~psych.** Applications will be reviewed as they are received and will continue until the position is filled. A Ph.D. in a relevant field is required. *Indiana University is an Affirmative Action Employer. Applications from women and minority candidates are encouraged.*

ASSISTANT PROFESSOR
University of California, Santa Cruz
Molecular, Cell, and Developmental Biology

We seek candidates for a tenure-track faculty position whose research centers on fundamental problems involving the biological roles of RNA. The position will also be associated with the Center for Molecular Biology of RNA (website: http://rna.ucsc.edu/rnacenter/) in Sinsheimer Laboratories. The successful candidate will be expected to establish a vigorous, externally-funded research program, contribute to the intellectual vitality of the Molecular, Cell, and Developmental Biology Department (website: http://www.biology.ucsc.edu/mcd/), and teach at both the undergraduate and graduate levels. Salary commensurate with qualifications and experience. Minimum qualifications: Ph.D. or equivalent, postdoctoral research experience, and demonstrated potential for university teaching. Position available fall 2008. To apply: See full details at website: http://www2.ucsc.edu/ahr. Closing date: The position will remain open until filled. Screening will begin October 15, 2007. To ensure full consideration, applications must arrive by the initial screening date. Please refer to position #841-08.

The University of California, Santa Cruz is an Affirmative Action, Equal Employment Opportunity Employer, committed to excellence through diversity. We strive to establish a climate that welcomes, celebrates, and promotes respect for the contributions of all students and employees.

LABORATORY MANAGER (Job Number 38464)
Laser Ablation-Inductively Coupled Plasma Mass Spectrometry Arizona LaserChron Center

The University of Arizona seeks a highly motivated scientist to serve as Manager of the Arizona LaserChron Center, which is a multi-user facility that focuses on U-Th-Pb geochronology by laser ablation-multicollector inductively coupled plasma mass spectrometry (LA-MC-ICPMS). Responsibilities would include: (1) directing installation of a new multicollector LA-MC-ICPMS and Excimer laser, (2) developing new analytical techniques and applications using an existing multicollector LA-MC-ICPMS (GVI Isoprobe) and Excimer laser (DUV193), (3) performing minor maintenance and overseeing major repairs of these instruments, (4) supervising visits of research scientists, and (5) conducting independent research. The position is full time and permanent. Applicants should have an M.S. or Ph.D. in earth science or chemistry, and have demonstrated experience with LA-MC-ICPMS instrumentation. Applications will be reviewed beginning 15 August 2007, and will continue until the position is filled. Applications should be submitted at website: https://www.uacareertrack.com for job number 38464. For additional information, please visit the Arizona LaserChron Center website: http://www.geo.arizona.edu/alc and contact George Gehrels (e-mail: ggehrels@e-mail.arizona.edu) or Joaquin Ruiz (e-mail: jruiz@e-mail.arizona.edu).

The University of Arizona is an Equal Opportunity, Affirmative Action Organization.

POSTDOCTORAL POSITION. This Laboratory is interested in hiring a Postdoctoral Fellow with a deep interest in all levels of protein function, structure, dynamics, ground and transition-state structure and energetics, ligand-binding, allostery, the conformational coupling of energetics, and the higher-order organization of catalysis in the cell. Our projects, many of which are structurally grounded, include numerous enzymes that are loosely centered around biomedically relevant issues in sulfur metabolism and isoprenoid biosynthesis. Please send or e-mail your resume and three letters of recommendation to: **Professor Thomas S. Leyh, Department of Biochemistry, The Albert Einstein College of Medicine, Jack and Pearl Resnick Campus, 1300 Morris Park Avenue, Bronx, NY 10461 (e-mail: leyh@aecom.yu.edu).** *Equal Opportunity Employer*

POSITIONS OPEN

THE UNIVERSITY OF IOWA

FACULTY POSITIONS in MEDICINAL and NATURAL PRODUCTS CHEMISTRY
College of Pharmacy

The Division of Medicinal and Natural Products Chemistry (MNPC) invites outstanding candidates for tenure-track **ASSISTANT/ASSOCIATE PROFESSOR** positions. Applicants must have a Ph.D. in medicinal chemistry, pharmacology, chemistry, biochemistry, toxicology, or biological sciences and relevant postdoctoral experience. The new position offers a competitive startup package and salary with expectation of establishing an independent research program and teaching in the graduate and professional programs. Applicants with research interests in medicinal chemistry, receptor pharmacology, chemical biology, enzymology, structural biology, toxicology, cancer research, pharmaceutical biotechnology, or biocatalysis are encouraged to apply. Information about MNPC may be found at website: http://www.pharmacy.uiowa.edu/mnpcphar/index.htm. Applicants should submit curriculum vitae, a concise description of their proposed research, and a list of three references by October 1, 2007, to: **Professor Kevin G. Rice, Chair, Search Committee, Division of Medicinal and Natural Products Chemistry, College of Pharmacy, 115 S. Grand Avenue, University of Iowa, Iowa City, IA 52242 (e-mail: kevin-rice@uiowa.edu).** *The University of Iowa is an Equal Opportunity, Affirmative Action Employer. Women and minorities are encouraged to apply.*

WATERSHED SCIENTIST

The Patrick Center for Environmental Research at the Academy of Natural Sciences invites applications for a career-track research position. Applicants should have a background in hydrology, biosystems engineering, restoration and landscape ecology, or related field, and have research experience in one or more of the following areas: watershed hydrology; watershed influences on water quality, nonpoint source pollution control and modeling, riparian zone processes, and/or application of geographic information systems and remote sensing in natural resource management. For position details, visit website: http://www.ansp.org/about/employment.php#933.

Send curriculum vitae, statement of research interests and representative publications, along with names, addresses, telephone numbers, and e-mail addresses of four references to: **Watershed Scientist Search #933, c/o Maria Eife, Office Manager, Patrick Center for Environmental Research, The Academy of Natural Sciences, 1900 Ben Franklin Parkway, Philadelphia, PA 19103. E-mail: eife@ansp.org.** *An Equal Opportunity Employer*

EVOLUTIONARY/ECOLOGICAL GENOMICS

The Department of Ecology and Evolution and the Institute of Genome and Systems Biology are jointly seeking to fill a faculty position with an individual applying large-scale data approaches to questions in ecology or evolution. The successful candidate will address scientific problems or biological systems with potential to be applied. Rank is open, with a preference for candidates at the level of **ASSISTANT or ASSOCIATE PROFESSOR.** Interested applicants should submit curriculum vitae, selected reprints and preprints, statements of research and teaching interests, and the names and addresses of three references to website: https://genomics.search.uchicago.edu. Applications will be accepted until the position is filled, but applications should be received before 15 October 2007, to ensure full consideration. *The University of Chicago is an Affirmative Action/Equal Opportunity Employer.*

POSITIONS OPEN

GENETICS and PHYSIOLOGY POSITIONS

The Department of Biology at Creighton University invites applications for two tenure-track, **ASSISTANT PROFESSORSHIPS** in (1) genetics and (2) physiology to begin August 2008. Candidates should be qualified to teach genetics with laboratory or physiology with laboratory and a semester course in general biology (cellular or organismal level), in addition to other biology courses in their respective disciplines for introductory, upper-division and/or nonscience undergraduates. Ph.D. required, postdoctoral experience preferred. Candidates should possess a strong desire to teach in a liberal arts environment. Candidates should have a research program in any area within the discipline, amenable to the mentoring of undergraduate research students. Graduate student mentoring is possible through affiliated programs. Normal teaching load is three preparations per semester (for example, two lecture courses, one with laboratory). Tenure and advancement require excellent teaching and development of a sustainable research program leading to peer-reviewed publications. Opportunities exist for research collaboration with faculty in other departments, including those in Creighton's health sciences schools. Additional information on these positions, the Department and the University is available at website: http://biology.creighton.edu/jobs/. To apply, send (1) curriculum vitae, (2) statements of teaching philosophy, research interests and skills, and long-term goals, (3) documentation (if available) of teaching effectiveness; (4) undergraduate and graduate transcripts, and (5) three letters of reference to: **Department of Biology, Creighton University, Omaha, NE 68178-0103, Attention Dr. Charles Brockhouse (Chair, Genetics Search Committee), or Dr. John Schaller (Chair, Physiology Search Committee).** Application review will begin October 1, 2007, and continue until the positions are filled. *Creighton is a Catholic Jesuit institution that seeks qualified applicants from all backgrounds who believe they can contribute to the University's outstanding educational traditions. We are an Equal Opportunity Employer. Affirmative Action Employer. Women and minority candidates are strongly encouraged to apply.*

POSTDOCTORAL POSITIONS
in Urologic Research

Positions available to study molecular and cellular mechanisms of the genitourinary system including bladder differentiation, bladder disease and dysfunction, androgen metabolism, prostate cancer, bladder tissue engineering, and stem cell research. Our state-of-the-art laboratories employ clinical urologists, basic scientists, and bench researchers who investigate basic, translational, and clinical research projects using molecular and cell biology approaches as well as animal models in conjunction with modern molecular, cellular, microarray, and proteomics technologies. For candidates with a Ph.D. degree, the positions provide a robust opportunity to work with urologists in a clinical department and have direct access to surgical specimens to study disease process and development of diagnostic and prognostic markers. Due to nationwide growth in urologic research, those trained in our Program will have tremendous opportunities to become independent investigators in a very reasonable time frame. We invite highly motivated individuals with knowledge and research experience in general molecular and cell biology, or animal research to contact us. Salaries are competitive and commensurate with experience. Submit your curriculum vitae and inquiries to:

H.K. Lin, Ph.D., Urology
University of Oklahoma Health Sciences Center
920 Stanton L. Young Boulevard, WP 3150
Oklahoma City, OK 73104
Telephone: 405-271-6966, extension 46193
Fax: 405 271 3118
E-mail: hk-lin@ouhsc.edu

Oklahoma University Health Science Center is an Equal Opportunity Employer.

launchsymposium

UNIVERSITY OF CAMBRIDGE

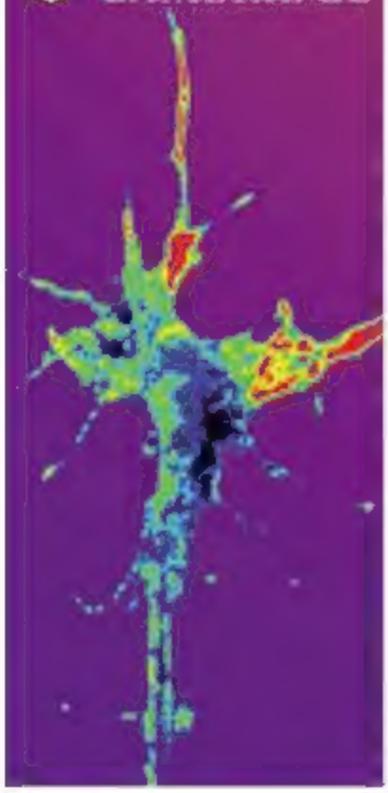

19th-21st September 2007
Cambridge, UK

Keynote speakers

Linda Buck, Antonio Damasio, Tom Jessell

Plenary speakers

Adriano Aguzzi, Earl Miller, Josh Sanes, Mike Shadlen, Daniel Weinberger

CAMBRIDGE NEUROSCIENCE

To register visit www.neuroscience.cam.ac.uk

Sessions in developmental, cellular & molecular, systems & computational, cognitive & behavioural and clinical & veterinary neuroscience

From primates to proteomics

For careers in science, turn to *Science*
www.ScienceCareers.org

- Search Jobs
- Career Advice
- Job Alerts
- Resume/CV Database
- Career Forum
- Graduate Programs

All features FREE to job seekers.

Science Careers
From the journal Science
AAAS

ILMAC

Industry Exhibition for Research and Development, Environmental and Process Technology in Pharmaceuticals, Chemicals and Biotechnology

25 to 28 September 2007 | Exhibition Center Basel | Hall 1 | www.ilmac.ch

Please refer to www.ilmac.ch for further details about the exhibition and accompanying events.

messe schweiz

POSITIONS OPEN

FEINBERG SCHOOL of MEDICINE
Department of Medicine
Division of Hematology/Oncology

The Division of Hematology/Oncology of Northwestern University's Feinberg School of Medicine, is seeking accomplished investigators for full-time, tenure-track positions in basic or translational research. The Division consists of a faculty of over 35 (**website: http://www.medicine.northwestern.edu/divisions/hematology_oncology/**), all members of the NCI-Designated Robert H. Lurie Comprehensive Cancer Center (**website: http://www.lurie.northwestern.edu**). Candidates in the fields of colon cancer, genitourinary cancer, cancer systems biology, cancer genetics, and proteomics are encouraged.

Candidates should have an M.D., Ph.D., or M.D./Ph.D. degree and an established publication record. Faculty rank and salary are negotiable based upon experience. The proposed start date is spring 2008. Interested candidates should submit curriculum vitae by October 15, 2007, to:

Jonathan D. Licht, M.D.
Chief, Division of Hematology/Oncology
Northwestern University Feinberg
School of Medicine
Lurie 5-123
303 East Chicago Avenue
Chicago, IL 60611
E-mail: hemonc@northwestern.edu

The Feinberg School of Medicine is an Affirmative Action/Equal Opportunity Employer. Women and minorities are encouraged to apply. Hiring is contingent upon eligibility to work in the United States.

MICROSCOPIST POSTDOCTORAL or SENIOR RESEARCH TECHNICIAN POSITION
University of Georgia Complex Carbohydrate Research Center

A position is open at either the Postdoctoral or Senior Research Technician level to work on the immunolocalization of carbohydrate structures in the cell walls of agronomically important crop plants using an extensive library of monoclonal antibodies. Demonstrated experience with light (visible and fluorescence) and electron (transmission electron microscope and scanning electron microscopy) microscopy is required; experience with laser confocal microscopy is desirable. All interested applicants should forward curriculum vitae and list of three references to: **Michael Hahn, University of Georgia, Complex Carbohydrate Research Center, 315 Riverbend Road, Athens, GA 30602-4712; e-mail: hahn@ccrc.uga.edu; fax: 706-542-4412.** Review of applications will begin September 15, 2007, and will continue until position is filled. *An Affirmative Action/Equal Employment Opportunity Institution.*

TENURE-TRACK FACULTY POSITIONS
at Ben-Gurion University

The Life Sciences Department (**website: http://www.bgu.ac.il/life**) invites applications from outstanding young scientists for tenure-track positions in the fields of: (1) physiology or cell biology (2) evolutionary and/or molecular ecology. Ben-Gurion University (BGU) provides a dynamic research environment with an emphasis on interdisciplinary research. We offer new laboratory space with modern equipment and startup funding. Teaching ability in Hebrew is required. Send applications, curriculum vitae, publications, research interests, and the names of three references to: **Professor Zvika Abramsky, Chairman, Department of Life Sciences, Ben-Gurion University, P.O.B. 653, Beer-Sheva 84105, Israel. Telephone: 972-8-6461373/6, fax: 972-8-6472992. E-mail: zvika@bgu.ac.il.**

POSITIONS OPEN

QUANTITATIVE/THEORETICAL ECOLOGIST

The Department of Ecology and Evolution is seeking to fill a faculty position with an individual working at the interface of theory and data in ecology. Rank is open, with a preference for **ASSISTANT or ASSOCIATE PROFESSOR.** Interested applicants should submit curriculum vitae, selected reprints and preprints, statements of research and teaching interests, and the names and addresses of three references to **website: https://ecologysearch.uchicago.edu;** letters of reference can be submitted at this site as well. Applications will be accepted until the position is filled, but applications should be received before 15 September 2007, to ensure full consideration. *The University of Chicago is an Affirmative Action/Equal Opportunity Employer.*

POSTDOCTORAL ASSOCIATE/RESEARCH ASSOCIATE/ASSISTANT RESEARCH PROFESSOR POSITIONS are available immediately at Rutgers University to investigate opioid receptor dimerization in immune cells and its impact on NK cell functions and to study the molecular mechanisms governing the circadian control of neuroendocrine functions in fetal alcohol exposed rats. Requirements: Ph.D. in neuroscience or in immunology, expertise in receptor dimerization study and cytolytic activity assay or real-time RT-PCR, immunocytochemistry and rodent surgery. Rutgers New Brunswick Campus is located in a suburban area of central New Jersey with convenient access to New York City. Please send curriculum vitae and the names of three references to **Dr. Dipak K. Sarkar** at **e-mail: sarkar@aesop.rutgers.edu.**

POSTDOCTORAL POSITION available focused on the role of small guanosine triphosate (GTPases) in the transformation of polarized epithelia. Special emphasis is placed on characterizing novel signaling pathways which regulate the activation state of Rho and Arf family GTPases, as well as how these pathways are subverted in cancer. The ideal candidate will be well trained in molecular biology and mammalian cell culture techniques. For further inquiries or to submit an electronic application (statement of research interests, curriculum vitae, and names of three references) please contact: **Dr. Steen H. Hansen (e-mail: steen.hansen@childrens.harvard.edu), Gastrointestinal Cell Biology, Children's Hospital, Boston, MA 02115.**

POSTDOCTORAL FELLOW POSITION, University of Alabama at Birmingham, to study molecular mechanisms of proteinuria and kidney disease (*J. Biol. Chem.* **281:** 39681-39692, 2006; *J. Clin. Investig.* **112:**209-221, 2003). Ph.D. and two years of experience in molecular biology techniques a must. Experience in kidney field not required. E-mail curriculum vitae and summary of research experience to **Sumant S. Chugh, M.D.** at **e-mail: aamoore@uab.edu.**

POSTDOCTORAL POSITION, Philips Laboratory, New York University. Ras regulation of T cells (*Nature Cell Biology* **9:**713, 2007). M.D. and/or Ph.D. degree with strong background in molecular and cellular biology and immunology (transgenic mice and live cell imaging). Salary: Ph.D. $38,000; credentialed M.D. $58,000 with weekly arthritis clinic. Send curriculum vitae and three references to **e-mail: philim01@nyu.edu.**

POSITIONS OPEN

MARKETPLACE

ISI WEB OF KNOWLEDGE℠

The **New Face** of Research

"Perfect...you did exactly what I would have hoped"

"This one just feels right."

"I really like the layout. It's very simple."

...is responsive

You told us what you needed, and mid 2007, *ISI Web of Knowledge* delivers.

See how the new *ISI Web of Knowledge* was built, and what people have to say about it at isiwebofknowledge.com/newface.

Take the next step

isiwebofknowledge.com

THOMSON